Europa Jupiter System Mission (EJSM)

Exploring the emergence of habitable worlds around gas giants

JPL D-67959, Task Order NMO711062

15 November 2010

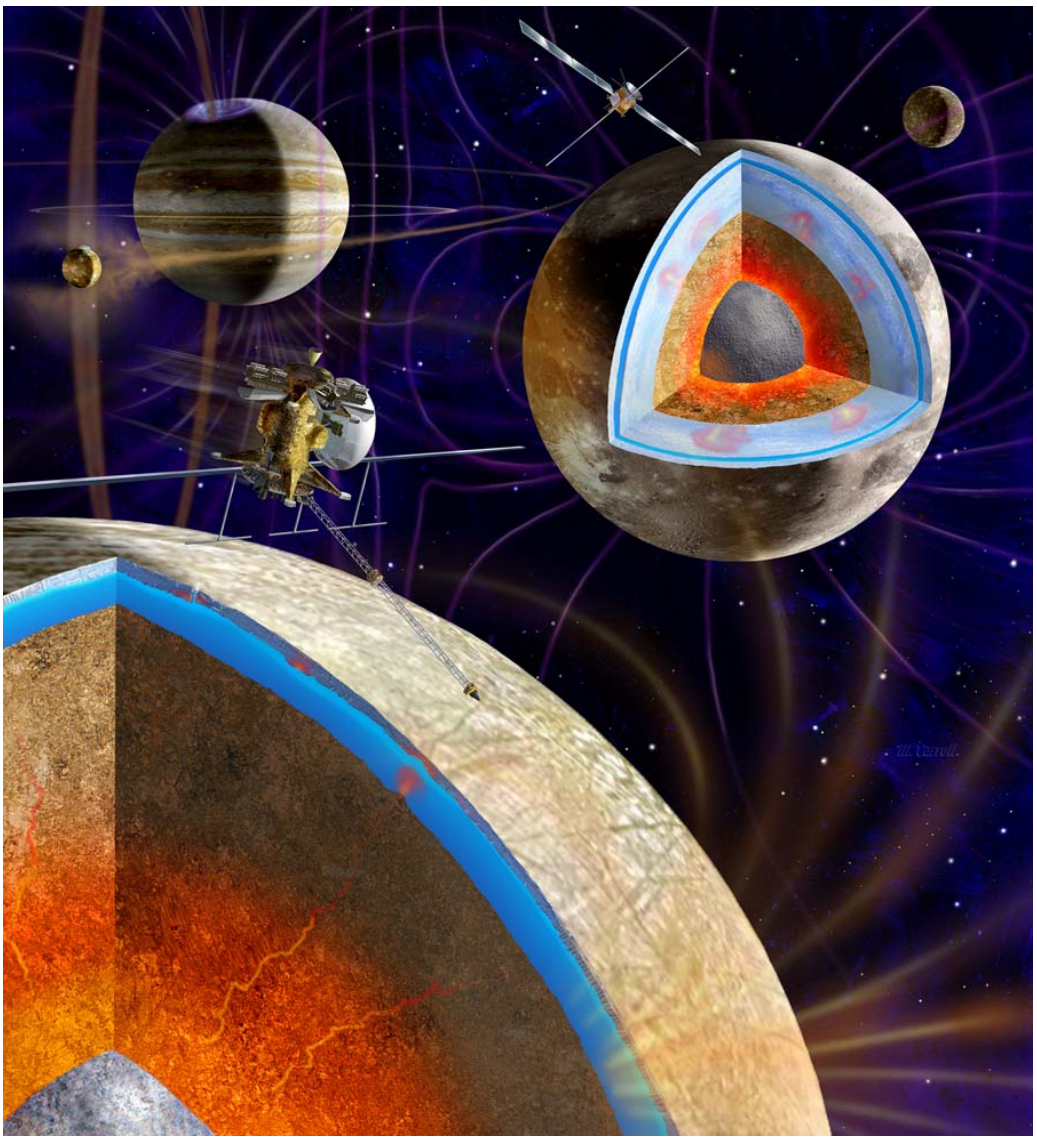

2010 Joint Jupiter Science Definition Team Report to NASA

Part of the research described in this report was carried out at the Jet Propulsion Laboratory, California Institute of Technology, under a contract with the National Aeronautics and Space Administration. Research described in this report was also carried out at the Applied Physics Laboratory, Johns Hopkins University and at the European Space Agency.

2010 Joint Jupiter Science Definition Team Report to NASA

15 November 2010

Ronald Greeley
Co-Chair, Joint Jupiter Science Definition Team
Arizona State University

Michele Dougherty
Co-Chair, Joint Jupiter Science Definition Team
Lead Scientist for ESA Study
Imperial College, United Kingdom

Robert Pappalardo
NASA Study Scientist
California Institute of Technology,
Jet Propulsion Laboratory

Jean-Pierre Lebreton
ESA Study Scientist
European Space Agency
European Space Research & Technology Centre

Table of Contents

1 EXECUTIVE SUMMARY

Figure 1-1. Europa and its parent planet Jupiter.

Some 400 years ago, discovery of the four large moons of Jupiter by Galileo Galilei changed our view of the universe forever. Today Jupiter is the archetype for the giant planets of our solar system, and for the numerous giant planets now known to orbit other stars, and Jupiter's diverse Galilean satellites—three of which are believed to harbor internal oceans—are central to understanding the habitability of icy worlds.

By investigating the Jupiter system, and by unraveling the history of its evolution from initial formation to the emergence of possible habitable environments, insight is gained into to how giant planets and their satellite systems form and evolve. Most important, new light is shed on the potential for the emergence and existence of life in icy satellite oceans.

Europa and Ganymede are believed to be internally active and harbor internal salt-water oceans. Europa (Figure 1-1) is believed to have a saltwater ocean beneath a relatively thin and geodynamically active icy shell. Ganymede is believed to have a liquid ocean sandwiched between a thick ice shell above and high-density ice below, and it is the only satellite known to have an intrinsic magnetic field. These satellites are straddled by Io (the Solar System's most volcanically active body) and Callisto (which may also harbor a deep ocean), key satellite end-members that tell of the origin and evolution of the Jupiter system. Connections to Jupiter's atmosphere and magnetosphere are also key to understanding how gas giant planets and their satellites evolve. A new flagship-class mission to the Jupiter system and its satellites is required to address top priority scientific questions at Europa, Ganymede, and the Jupiter system.

The Europa Jupiter System Mission (EJSM) would be an international mission with an architecture of two independently launched and operated flight elements. Its theme and goals are derived from the US National Research Council's Planetary Science Decadal Survey [*SSB* 2003] and the ESA Cosmic Vision document [*ESA 2005*]. These reports emphasize as key questions for solar system exploration: 1) the origin and evolution of habitable worlds, and 2) processes operating within the solar system.

1.1 Science Theme, Goals, and Objectives

An extensive international effort involving scientists from more than half a dozen countries established the EJSM overarching theme as:

The emergence of habitable worlds around gas giants.

The Joint Jupiter Science Definition Team (JJSDT) was chartered to define the goals and objectives for the EJSM concept. The JJSDT was an international group of US, European, and Japanese scientists, which evaluated the US National Research Council's Planetary Science Decadal Survey [*SSB* 2003], the ESA Cosmic Vision [*ESA 2005*], the NASA 2007 Europa Explorer [*Clark et al. 2007*] and Jupiter System Observer studies [*Kwok et al. 2007*], and the 2007 ESA Laplace Proposal [*Blanc et al. 2007*] to establish a comprehensive and integrated set of goals and objectives for EJSM addressing the nature and origin of the Jupiter system, especially its satellites.

To understand the Galilean satellites as a system, Europa and Ganymede would be singled out for detailed investigation. This pair

of objects provides a natural laboratory for comparative analysis of the nature, evolution, and potential habitability of icy worlds. The primary focus is on in-depth comparative analysis of their internal oceans, current and past environments, surface and near-surface compositions, and geological histories. Moreover, objectives for studying the other two Galilean satellites, Io and Callisto, were also defined. To understand how gas giant planets and their satellites evolve, broader studies of Jupiter's atmosphere and magnetosphere would round out the Jupiter system investigation.

The JJSDT worked with engineering teams to define a two flight element mission to Jupiter and the Galilean satellites, the Jupiter Europa Orbiter (JEO) and the Jupiter Ganymede Orbiter (JGO). Each flight element concludes their prime mission in orbit at a Galilean satellite. The JJSDT and engineering teams developed extraordinary mission concepts that provide extensive Jovian system science as well as focused icy satellite science, with Europa and Ganymede as the primary goals.

Europa is essentially a rocky world with an outer ~100 km layer comprised of a relatively thin icy shell above a saltwater ocean. Its ocean is in direct contact with the rocky mantle below, making it unique among icy satellites in having a plausible chemical energy source to support life (Figure 1-2). However, the details of the processes that shape Europa's ice shell, and the fundamental question of its thickness, are poorly known.

The science goal for the Europa focus portion of EJSM is:

Explore Europa to investigate its habitability.

The objectives developed by the JJSDT to address this goal would be primarily addressed by JEO, with secondary support from JGO:

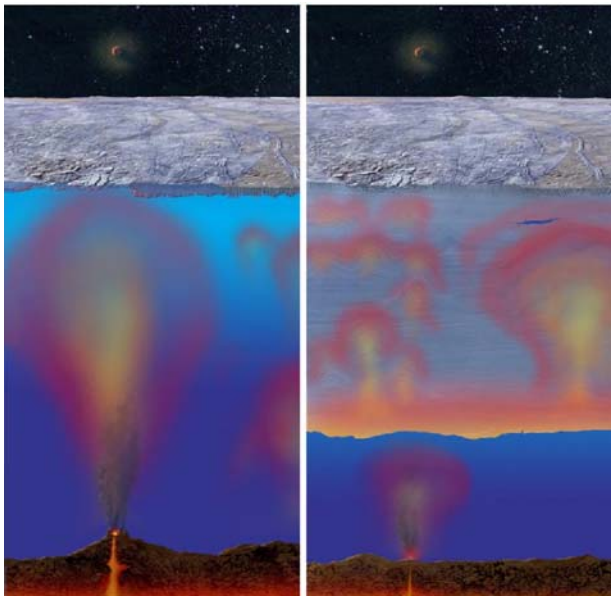

Figure 1-2. The NASA Jupiter Europa Orbiter would address the fundamental issue of whether Europa's ice shell is ~few km (left) or >30 km (right), with different implications for processes and habitability. In either case, the ocean is in direct contact with the rocky mantle below, which can infuse the chemical nutrients necessary for life.

- Characterize the extent of the ocean and its relation to the deeper interior.
- Characterize the ice shell and any subsurface water, including their heterogeneity, and the nature of surface-ice-ocean exchange.
- Determine global composition, distribution, and evolution of surface materials, especially as related to habitability.
- Understand the formation of surface features, including sites of recent or current activity, and identify and characterize candidate sites for potential future *in situ* exploration.
- Characterize the local environment and its interaction with the Jovian magnetosphere.

Ganymede is believed to have a liquid ocean sandwiched between a thick ice shell above and high-density ice polymorphs below, more typical of volatile-rich icy satellites. It is the only satellite known to have an intrinsic magnetic field, which makes the Ganymede-

Jupiter magnetospheric interactions unique in our solar system (Figure 1-3).

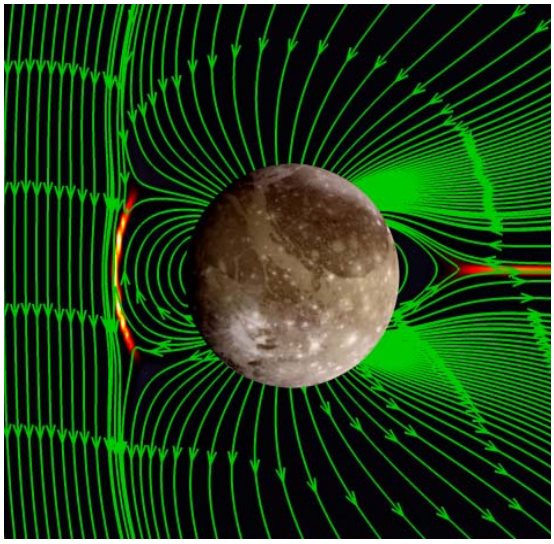

Figure 1-3. The ESA Jupiter Ganymede Orbiter would determine how Ganymede's unique magnetic field interacts with Jupiter's, how the interactions vary with time, and the role of a convecting core and internal ocean.

The science goal for the Ganymede focus of EJSM is:

Characterize Ganymede as a planetary object including its potential habitability.

The objectives to meet this goal would be addressed primarily by JGO, with secondary support from JEO:

- Characterize the extent of the ocean and its relation to the deeper interior.
- Characterize the ice shell.
- Characterize the local environment and its interaction with the Jovian magnetosphere.
- Understand the formation of surface features and search for past and present activity.
- Determine global composition, distribution, and evolution of surface materials.

The jovian system, including Jupiter, its satellites, and the magnetic field and particle environment, constitutes a model for the evolution of planetary systems, including that of our Sun and those being discovered around other stars.

The Galilean satellites formed out of the Jovian circumplanetary disk and have since evolved through complex interactions with the other satellites, Jupiter, and Jupiter's magnetosphere.

Europa and Ganymede cannot be understood in isolation, but must be considered in the context of the entire Jovian system, through study of its parent planet Jupiter, its sibling satellites and the magnetic field and particle environment.

The science goal for the Jupiter system focus of EJSM is:

Explore the Jupiter System as an archetype for gas giants.

The objectives to meet this goal, as categorized into satellites, magnetosphere, and Jupiter objectives, would be addressed by both JEO and JGO:

Satellites objectives:

A. Study Io's active dynamic processes.
B. Study Callisto as a witness of the early Jovian system.
C. Characterize the rings and small satellites.

Magnetosphere objectives:

A. Characterize the magnetosphere as a fast magnetic rotator.
B. Characterize the magnetosphere as a giant accelerator.
C. Understand the moons as sources and sinks of magnetospheric plasma.

Jupiter objectives:

A. Characterize the atmospheric dynamics and circulation.
B. Characterize the atmospheric composition and chemistry.
C. Characterize the atmospheric vertical structure.

The two-spacecraft architecture of EJSM would provide for significant and unique science opportunities for complementary and synergistic science, which could not be accomplished by either spacecraft alone. Details would depend on the mission profiles and instrument complement of the respective spacecraft. Coordinated observations from two locations within the Jupiter system would significantly enhance the science return with respect to both mission elements taken individually. The joint timeline of the two spacecraft would be optimized to offer many opportunities for complementary and synergistic science, for example combining remote sensing with *in situ* measurements, or observations of the same target with different geometries and/or capabilities.

1.2 Science Strategy and Implementation

1.2.1 JEO Science Implementation

To demonstrate that the science objectives of the JEO component of EJSM could be achieved with the types of instruments currently available, the JJSDT performed the exercise to assemble a model payload consisting of ten instruments along with use of the spacecraft X-band and Ka-band telecommunications systems for radio science. JEO's model payload consists of a Laser Altimeter, an Ice Penetrating Radar, a Visible-Infrared Spectrometer, an Ultraviolet Spectrometer, a Thermal Instrument, a Narrow-Angle Camera, a Camera Package containing medium-angle and wide-angle cameras, an Ion and Neutral Mass Spectrometer, a Magnetometer and a Particle and Plasma Instrument.

The reference JEO mission would be 9 months at Europa. As a risk mitigation strategy, and to ensure sufficient time to follow up on discoveries, the primary science hypotheses would be addressed in 100 days in Europa orbit (≈ 28 eurosols ≈ 3 months). The desired orbit is nearly circular, with an orbital inclination of 80° to 85° (or the retrograde equivalent of ~95° to 100°). The optical remote sensing instruments would be nadir-pointed and mutually boresighted. The initial orbital altitude would be 200 km, then reduced to 100 km altitude after 28 eurosols to meet the requirements of gravity, altimetry, magnetometry, and radar. The orbit would not be quite sun-synchronous but precesses slowly, such that the orbit does not exactly repeat the same ground track but allows instrument fields of view to overlap with previous tracks. Thus, the orbit would be near-repeating after several eurosols, within about 1° of longitude at the equator. The solar incidence angle would be nominally 45° (2:30 p.m. orbit) at the start of the Europa orbital science, as the best compromise to the requirements of imaging and spectroscopic optical remote sensing measurements.

Significant Jupiter system science would be enabled by the Jovian tour, which lasts approximately 2.5 years prior to Europa orbit insertion. The model payload would provide the capability for meeting Jupiter system science objectives, tracking Jupiter and the other Galilean satellites to accomplish observations during the Jovian tour phase. However, as a lower priority objective, Jupiter system science generally would not impose strong constraints on the spacecraft itself, with the exception of the addition of an Ultra-Stable Oscillator (USO) to derive the properties of the satellites' atmospheres and ionospheres from radio occultations.

The JEO mission has developed operational scenarios for both the Jovian Tour and the Europa Science mission phases. The preliminary tour scenarios show robust data volume margins and frequent opportunities to conduct the science campaigns defined by the JJSDT. Europa science scenarios are robust to achieve the science objectives with the planning payload.

The long mission duration at Jupiter and especially at Europa would enable significant flexibility of science scenarios to achieve mission science goals and cope with possible radiation based anomalies, and allowed a more diverse set of measurements and investigations in the final Europa science campaigns.

1.2.2 JGO Science Implementation

To show that the science objectives of the JGO component of EJSM could be achieved, the JJSDT identified instrument types that are currently available to assemble a model payload. The JGO model payload would consist of 11 instruments and includes: a Laser Altimeter, a Radio Science Instrument, an Ice Penetrating Radar, a Visible Infrared Hyperspectral Imaging Spectrometer, an Ultraviolet Imaging Spectrometer, a Narrow Angle Camera, a Wide Angle Camera, a Magnetometer, a Plasma Instrument - Ion Neutral Mass Spectrometer, a Sub-millimeter Wave Instrument, and a Radio and Plasma Wave Instrument.

To achieve the science goals, the configuration of the JGO spacecraft is driven by the long distance to Jupiter, the high Δv, the need to protect equipment from the intense radiation field, resulting in grouping of instrument and spacecraft hardware, and by the requirement of using solar electric power generation, resulting in a large area of solar arrays. Furthermore, to optimize the data downlink rate, a large high gain antenna is included in the baseline. Due to its remote sensing and *in situ* exploration requirements, a three-axis stabilized spacecraft is assumed.

The JGO interplanetary trajectory uses gravity assists (Venus-Earth-Earth and Earth-Venus-Earth-Earth for baseline and backup launches, respectively), and following Jupiter Orbit Insertion (JOI), uses the two outer Galilean moons, Callisto and Ganymede for shaping the trajectory within the Jupiter system. Science observations are assumed to be carried out during the flybys of the Jovian moons. In addition, to allow for an extended exploration of Callisto and allowing for extended exploration of the Jupiter magnetosphere in this key region, a series of resonant orbits with Callisto is assumed, which is designed such that at least 9 Callisto flybys would be performed.

Finally the spacecraft would be transferred into an elliptical orbit around Ganymede, which would be circularized and reduced in altitude, until final deposition on Ganymede's surface.

The phases of the mission would include:

- Launch and interplanetary cruise (5.9 years, 7.1 years for the backup launch date);
- Jupiter orbit insertion, and energy reduction for transfer to Callisto (179 days);
- Callisto science phase (388 days);
- Transfer to Ganymede (240 days);
- Ganymede science phase (300 days).

The Ganymede science phase would be comprised of three different types of orbits, which are driven by the requirements of remote sensing at specific illumination conditions, magnetospheric sampling, and the constraint to avoid Ganymede eclipses that would require oversizing the solar panels. The eclipse duration in Ganymede orbit is a consequence of the combination of spacecraft

altitude and sun declination relative to the plane of its orbit resulting at given altitude in longer eclipse durations for smaller sun declination values. For close to polar Ganymede orbits, the orbital plane of the spacecraft would rotate around the pole as a function of inclination due to the influence of Ganymede's oblateness and Jupiter's attraction. This was used to design the orbit such that lower altitudes could be realized later during this phase, while still avoiding sun eclipses, allowing for a sequence of orbits with decreasing altitudes. Due to the high apocenter of the elliptical orbit, perturbation by Jupiter is significant, and would cause the orbit to quickly evolve. The argument of pericenter was chosen such that this evolution leads to a circular orbit within about 20 days, where it would remain at an altitude of 5000 km, which would be maintained for about 80 days, and then the eccentricity would increase until a suitable point for injection into a 500 km altitude circular orbit is reached.

When a suitable altitude is reached, a maneuver would be applied to arrive at a circular 500 km altitude orbit, where the spacecraft would operate for 120 days, and the final orbit of 200 km altitude would be obtained. After nominal operations of at least 60 days, orbit maintenance would be discontinued, and the spacecraft would be left in an orbit with natural growth of eccentricity until final disposition on Ganymede's surface. In this final phase the orbit would be very close to polar (deviation <1°). Mission extension would be possible based on remaining consumables and spacecraft health.

The JGO mission has developed a robust strategy for both the Jovian Tour and the Ganymede science mission phase. Analysis shows adequate flight system capability and tour observation opportunities to perform the science campaigns defined by the JJSDT. The Ganymede observation strategy would provide a means to achieve the science objectives with the planning payload. The mission phases, both at Jupiter and in Ganymede orbit, would enable science scenarios to achieve mission science objectives.

1.3 Conclusion

NASA's Solar System Exploration Decadal Survey and ESA's Cosmic Vision strategic document both emphasize the exploration of the Jupiter system to investigate the emergence of habitable worlds. The NASA-ESA collaborative approach to the exploration of Europa, Ganymede, and the Jupiter system would make possible the next leap in understanding the origin and evolution of habitable worlds and processes operating within the solar system. The exploration of the Jupiter System by EJSM would provide invaluable insights into our own solar system's evolution and into planetary habitability throughout the universe, potentially bringing about paradigm shifts in our knowledge of the emergence of habitable worlds around gas giants.

2 EJSM OVERVIEW

The Joint Jupiter Science Definition Team (JJSDT) was chartered to define the goals and objectives for the EJSM. The JJSDT was an international group of US, European, and Japanese scientists, which evaluated the US National Research Council's Planetary Science Decadal Survey [*SSB* 2003], the ESA Cosmic Vision [*ESA 2005*], the NASA 2007 Europa Explorer [*Clark et al. 2007*] and Jupiter System Observer studies [*Kwok et al. 2007*], and the 2007 ESA Laplace Proposal [*Blanc et al. 2007*] to establish a comprehensive and integrated set of goals and objectives for EJSM addressing the nature and origin of the Jupiter system, especially its satellites.

In 2007, NASA performed two Jupiter mission concept studies: Europa Explorer and Jupiter System Observer. At the same time, an ESA Jupiter proposal, Laplace, was submitted to the Cosmic Vision Programme call. In 2008, the previous 2007 Europa Explorer studt was updated to include Jupiter system science, to begin executing risk reduction activities related to radiation and planetary protection, and to work with ESA. This resulted in the 2008 joint Europa Jupiter System Mission (EJSM), composed of the NASA Jupiter Europa Orbiter (JEO) and the ESA Jupiter Ganymede Orbiter (JGO). In February 2009, NASA and ESA prioritized EJSM as the next Outer Planets Flagship Mission.

In 2010, NASA and ESA chartered the JJSDT with the following tasks, which formed the basis for its work this year:

- Recommend the science content of the EJSM as a whole and the JEO and JGO components in terms of a hierarchy of science goals, objectives, investigations, and measurements;
- Advise on a planning payload for both the notional JEO and JGO spacecraft;
- Produce a traceability matrix linking the science hierarchy, planning payloads, reference science operation scenarios and observation campaigns, and key mission requirements (defined as the baseline science mission);
- Provide a Science Requirements Document describing quantitative, science-derived requirements for the JGO component and aspects of JEO that affect JGO;
- Iterate the science requirements within the constraints and resources emerging from the JGO industrial studies to contain the overall mission cost within an L-Class envelope;
- Improve the definition, fidelity, and realism of JEO-JGO synergistic science;
- Refine the prioritized science requirements for the Jovian-tour phase for a two-spacecraft scenario.

This task list forms the basis for this report, and the companion ESA Assessment Study ("Yellow Book") Report (ESA/SRE 2011).

The architecture of two independently launched and operated flight elements was a result of both the 2007 NASA and ESA studies. All studies of mission architectures performed over the past decade to address investigation of a putative Europan ocean have concluded that a Europa orbiter is an essential element; thus, the NASA component was determined as the JEO. The ESA component, Jupiter Ganymede Orbiter (JGO), was determined by the JJSDT as the most critical complementary component of EJSM, in response to the Cosmic Vision L-Class call.

While the focus of this report is JEO, discussion of the implementation of the ESA element, JGO, is summarized in §5.2. Further details on the integrated EJSM and on specifics JGO mission element are provided in the companion "Yellow Book" JJSDT report to ESA.

The international JJSDT established the EJSM overarching theme as:

The emergence of habitable worlds around gas giants.

To understand the Galilean satellites as a system, Europa and Ganymede are identified for detailed investigation. These objects provide a natural laboratory for comparative analysis of the nature, evolution, and potential habitability of icy worlds. The primary focus is in-depth comparative analysis of their internal oceans, current and past environments, surface and near-surface compositions, and geological histories. Moreover, objectives for studying the other two Galilean satellites, Io and Callisto, were defined. To understand how gas giant planets and their satellites evolve, broader studies of Jupiter's atmosphere and magnetosphere would round out the Jupiter system investigation.

The JJSDT worked with the engineering teams to define a two flight element mission to Jupiter and the Galilean satellites, with each flight element ending their prime mission in orbit at a Galilean satellite, one at Europa and one at Ganymede. The JJSDT and engineering team developed an extraordinary mission concept, which provides extensive Jupiter system science as well as focused icy satellite science.

Europa is essentially a rocky world with an outer layer, about 100 km thick, consisting of a relatively thin icy shell above a saltwater ocean. Its ocean is in direct contact with the rocky mantle below, making it unique among icy satellites in having a plausible chemical energy source to support life. However, the details of the processes that shape Europa's ice shell, and fundamental question of its thickness, are poorly known.

The science goal for the Europa focus portion of EJSM is:

Explore Europa to investigate its habitability.

The objectives developed by the JJSDT to address this goal would be primarily addressed by JEO, with secondary support from JGO:

A. Characterize the extent of the ocean and its relation to the deeper interior;
B. Characterize the ice shell and any subsurface water, including their heterogeneity, and the nature of surface-ice-ocean exchange;
C. Determine global composition, distribution, and evolution of surface materials, especially as related to habitability;
D. Understand the formation of surface features, including sites of recent or current activity, and identify and characterize candidate sites for future *in situ* exploration;
E. Characterize the local environment and its interaction with the Jovian magnetosphere.

Ganymede is believed to have a liquid ocean sandwiched between a thick ice shell above and high-density ice polymorphs below, more typical of volatile-rich icy satellites.

It is the only satellite known to have an intrinsic magnetic field, which makes the Ganymede-Jupiter magnetospheric interactions unique in our solar system.

The science goal for the Ganymede focus of EJSM is:

Characterize Ganymede as a planetary object including its potential habitability.

The objectives to meet this goal are would be primarily addressed by JGO, with secondary support from JEO:

A. Characterize the extent of the ocean and its relation to the deeper interior;
B. Characterize the ice shell;
C. Characterize the local environment and its interaction with the Jovian magnetoshere;
D. Understand the formation of surface features and search for past and present activity;
E. Determine global composition, distribution and evolution of surface materials.

The Jupiter system is the largest coupled planetary system within our solar system, and has been referred to as a "miniature solar system." Within this enormous system exists a multitude of diverse objects: Jupiter itself, more than 60 outer irregular small satellites (1 to 100 km class objects), the four large Galilean satellites, the four inner satellites Metis, Adrastea, Amalthea and Thebe (10-100 km class objects), and the Jovian ring system located in the inner regions. In addition to interest in understanding the physical characteristics of the individual objects described above, there is a strong desire to understand how the components are coupled and continuously interact. The entire system is intricately linked through gravitational and electromagnetic interactions, and atmospheric coupling processes. The electrically conducting sub-surface oceans at the Galilean satellites, for example, interact with the rotating magnetic field of Jupiter to produce induced field signatures, providing vital information on their characteristics.

Active volcanoes on the moon Io interact with the surrounding magnetosphere producing the Io plasma torus and providing the dominant plasma source for the entire magnetospheric system. The electromagnetic effect of the comet-like addition of plasma mass into the system is felt both locally and globally throughout the system. Jupiter's gravitational interaction with the satellites gives rise to tidal heating in the satellites and redistributes rotational and orbital energy between the Galilean moons and Jupiter due to the unique Laplace orbital resonance, in which the orbital periods of Io, Europa, and Ganymede are kept in a ratio of 4:2:1. Gravitational interaction in the Laplace resonance is not only responsible for Io's volcanism but also plays a role in maintaining a subsurface ocean close to the surface of Europa on geological timescales.

The intrinsic magnetic field of Ganymede couples with the surrounding Jovian magnetosphere to form a magnetosphere in miniature within the Jovian system. The Jovian particle environment interacts with the surfaces of the Galilean moons in a variety of ways depending on the shielding (or otherwise) of particles from the surfaces through differing electromagnetic interactions.

The exploration of Jupiter's dynamic atmosphere has played a pivotal role in the development of our understanding of our Solar System, serving as the paradigm for the interpretation of planetary systems around other stars and as a fundamental laboratory for the investigation of large-scale geophysical fluid dynamics and the many physiochemical phenomena evident on the gas giant planets. Our characterization of this archetypal gas giant system remains incomplete, however, with many fundamental questions unanswered.

The science goal for the Jupiter system focus of EJSM is:

Explore the Jupiter system as an archetype for gas giants.

The objectives to meet this goal, as categorized into satellites, magnetosphere, and Jupiter objectives, would be addressed by both JEO and JGO.

Satellites objectives:

A. Study Io's active dynamic processes;
B. Study Callisto as a witness of the early Jovian system;
C. Study the rings and small satellites.

Magnetosphere objectives:

A. Characterize the magnetosphere as a fast magnetic rotator;
B. Characterize the magnetosphere as a giant accelerator;
C. Understand the moons as sources and sinks of magnetospheric plasma.

Jupiter objectives:

A. Characterize the atmospheric dynamics and circulation;
B. Characterize the atmospheric composition and chemistry;
C. Characterize the atmospheric vertical structure.

The two-spacecraft architecture of EJSM would provide significant and unique science opportunities for complementary and synergistic science, which could not be accomplished by either spacecraft alone. Such advances could come in the areas of magnetospheric studies, Jupiter atmosphere monitoring, satellite remote sensing, and rings and small satellite studies. Such unique science includes characterization of the spatial and temporal variability of the magnetic field, Jovian atmospheric and ring studies through spacecraft-to-spacecraft radio occultations, and satellite and Jupiter remote sensing incorporating a range of viewing geometries.

3 JJSDT AND PROCESS

The Joint Jupiter Science Definition Team (JJSDT) was appointed by NASA and ESA to formulate the overarching science theme and goals for the Europa Jupiter System Mission (EJSM). Specific objectives were identified along with the investigations and example measurements that the mission should achieve in order to meet these science goals. To carry out this task, JJSDT members and chairs were appointed from the scientific community to represent the broad range of interests (Table 3-1). Some of the JJSDT members were drawn from the science definition teams from previous Europa and Jupiter system mission studies.

The general approach of the JJSDT included reviews of the current state of scientific knowledge for Europa and the other Jupiter satellites, identification of the key outstanding questions, discussion of how those questions could be answered, and identification of the kinds of experiments that could be carried out via an orbiter. Presentations were heard from JJSDT members, and from other individuals who were invited from the scientific and engineering communities to provide complementary expertise.

The 2009-2010 activities of the JJSDT are summarized by its charter (see §2). Table 3-2 provides overview of the meetings and related activities during the current study phase—from the spring of 2009 through November 2010. Upon submission of this report to NASA and ESA, the JJSDT will be disbanded in preparation for the Announcement of Opportunity for the JEO payload. Throughout the study, NASA and ESA technologists worked closely with the science team; this resulted in a mission concept that was realistic within anticipated resources while preserving the high-level scientific objectives.

For the present phase, the scope and the membership of the JJSDT was expanded and modified from that of the 2008 study. Based on the range of deliverables outlined in the SDT charter, additional scientific members with required expertise from NASA and ESA, including some members of the 2008 Titan Saturn System Mission study, were added to the team. In terms of science activities, emphasis has been on refinement of the combined JEO-JGO investigations for EJSM. Substantial work was conducted to determine the complementary and synergistic science that could be achieved by having two orbiters in operation at the same time in the Jupiter system. This has resulted in a Traceability Matrix (§4.3) that merges the work for JEO and JGO into a single EJSM mission concept.

To perform its tasks, the JJSDT was organized into a leadership group, a core group, and the full JJSDT (Figure 3-1). The Leadership group consisted of the JJSDT Co-chairs, the Study Scientists and their Deputies, and the Study Leads from NASA and ESA. The Core group included the NASA and ESA Co-Chairs from each Discipline Working Group (Table 3-3), and the Leadership group. Some contributions to the Cross-Cutting Working Groups were drawn from the planetary community in

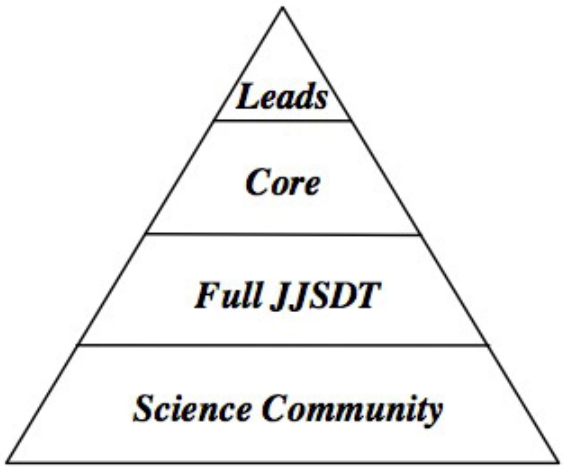

Figure 3-1. Schematic representation of the JJSDT organizational structure.

addition to the JJSDT. The Satellites Working Group was further divided into subgroups to address specific aspects of Europa and Ganymede science.

In addition to the standing groups outlined above, *ad hoc* committees were formed to assess special topics, including the potential science to be gained from "dual-spacecraft" communication between JEO and JGO, the possible science to be gained from a "Gravity Advanced Package" (GAP), and the possibility of JEO accommodating a simple Europa surface element (see Appendix A).

The harsh radiation environment of the Jupiter system, especially near Europa, poses special requirements on spacecraft components and instruments. To inform the scientific community and potential instrument proposers on radiation and other EJSM issues, a series of instrument workshops were held. During 2009-2010, two were held in the United States and one was held in Europe (Table 3-2). These were organized by JPL-APL and ESA technologists, and provided the opportunity for participants to ask specific questions and actively engage both ESA and the JEO pre-project. Workshop materials are posted on-line at:

- http://opfm.jpl.nasa.gov/europajupitersystemmissionejsm/instrumentresources
- http://sci.esa.int/science-e/www/object/index.cfm?fobjectid=46393

Throughout the JJSDT activities, the planetary community was solicited for input and informed of the emerging status of EJSM. This included discussions at meetings of standing organizations (such as the Outer Planet Assessment Group), meetings organized specifically for EJSM science discussions, and "Town-Hall" meetings held in conjunction with other planetary science meetings. In addition, relevant special sessions were arranged at planetary science conferences, to bring attention to the outstanding science issue.

Table 3-1. Joint Jupiter Science Definition Team

Members	Affiliation	Expertise
United States JJSDT Membership		
Ronald Greeley, Co-Chair	Arizona State University	Europa
Robert Pappalardo, Study Scientist	Jet Propulsion Laboratory	Europa and Jupiter System
Ariel Anbar	Arizona State University	Astrobiology
Bruce Bills	Jet Propulsion Laboratory	Geophysics
Diana Blaney	Jet Propulsion Laboratory	Composition
Don Blankenship	University of Texas	Radar/Geophysics
Phillip Christensen	Arizona State University	Composition
Brad Dalton	Jet Propulsion Laboratory	Composition
Jody Deming	University of Washington	Astrobiology
Richard Greenberg	University of Arizona	Geophysics
Kevin Hand	Jet Propulsion Laboratory	Astrobiology
Amanda Hendrix	Jet Propulsion Laboratory	Satellites
Torrence Johnson	Jet Propulsion Laboratory	Satellites
Krishan Khurana	University of California Los Angeles	Fields & Paricles
Ralph Lorenz	Johns Hopkins University—Applied Physics Laboratory	Satellites
Essam Marouf	San Jose State University	Geophysics
Tom McCord	Bear Fight Institute	Composition

Members	Affiliation	Expertise
Melissa McGrath	Marshall Space Flight Center	Satellites
William Moore	National Institute of Aerospace—Hampton University	Geophysics
Jeffrey Moore	Ames Research Center	Geology
Francis Nimmo	University of California Santa Cruz	Geophysics
Chris Paranicas	Johns Hopkins University—Applied Physics Laboratory	Fields & Particles
Louise Prockter	Johns Hopkins University—Applied Physics Laboratory	Geology
Gerald Schubert	University of California Los Angeles	Geophysics & Jupiter
David Senske	Jet Propulsion Laboratory	Satellites
Mark Showalter	SETI Institute	Rings
Adam Showman	University of Arizona	Jupiter
Amy Simon-Miller	Goddard Spaceflight Center	Jupiter Atmosphere
Mitch Sogin	Marine Biological Laboratory	Astrobiology
Christophe Sotin	Jet Propulsion Laboratory	Geophysics
John Spencer	Southwest Research Institute	Satellites
Elizabeth Turtle	Johns Hopkins University—Applied Physics Laboratory	Satellites
Steve Vance	Jet Propulsion Laboratory	Astrobiology
Hunter Waite	Southwest Research Institute	Fields & Particles
Europe JJSDT Membership		
Michele Dougherty—Co-Chair	Imperial College	Fields & Particles
Jean-Pierre Lebreton—Study Scientist	European Space Agency, ESTEC	Plasma Physics
Michel Blanc	Ecole Polytechnique	Magnetospheres
Emma Bunce	University of Leicester	Fields & Particles
Andrew Coates	University College London	Fields & Particles
Angioletta Coradini	Institute for Interplanetary Space Physics	Origins
Athena Coustenis	Paris-Meudon Observatory	Jupiter System
Pierre Drossart	LESIA/Observatory of Paris	Jupiter Atmosphere
Leigh Fletcher	Oxford University	Jupiter Atmosphere
Olivier Grasset	University of Nantes	Satellites
Hauke Hussmann	German Center for Aerospace (DLR)	Geophysics
Ralf Jaumann	German Center for Aerospace (DLR)	Satellites
Norbert Krupp	Max Planck Institute for Solar System Research	Fields & Particles
Olga Prieto-Ballesteros	Center of Astrobiology—INTA-CSIC	Astrobiology
Dima Titov	Max Planck Institute for Solar System Research	Jupiter System
Paolo Tortora	University of Bologna	Radio Science
Federico Tosi	Institute for Interplanetary Space Physics	Composition
Tim Van Hoolst	Royal Observatory of Belgium	Satellites
Japan JJSDT Membership		
Masaki Fujimoto	Institute of Space and Astronautical Science / Japan Space Exploration Agency	Fields & Particles
Yasumasa Kasaba	Tohoku University	Fields & Particles
Sho Sasaki	National Observatory of Japan	Satellites
Yukihiro Takahashi	Tohoku University	Jupiter
Takeshi Takashima	Institute of Space and Astronautical Science / Japan Space Exploration Agency	Fields & Particles

Table 3-2. JJSDT Meetings and Workshops, 2009-2010

Date		Event	Location
2009	2-3 March	ESA JGO downselect briefing and SDT meeting	Paris, France
	25 March	*ad hoc* JJSDT meeting in conjunction with the Lunar and Planetary Science Conference	The Woodlands, Texas, USA
	21-22 April	*ad hoc* JJSDT meeting, in conjunction with the European Geophysical Union conference	Vienna, Austria
	13 July	JJSDT meeting	Columbia, MD, USA
	15-16 July	2nd EJSM Instrument Workshop	Columbia, MD, USA
	18-19 September	*ad hoc* JJSDT meeting, in conjunction with EPSC	Potsdam, Germany
2010	18-20 January	3rd EJSM Instrument Workshop	Noordwijk, The Netherlands
	27-29 January	JJSDT meeting	Monrovia, CA, USA
	5-6 May	*ad hoc* JJSDT meeting, in conjunction with the European Geophysical Union conference	Vienna, Austria
	17-19 May	ESA EJSM Science Open Community Workshop	Noordwijk, The Netherlands
	23-26 June	JJSDT meeting	Noordwijk, The Netherlands
	27-29 July	4th EJSM Instrument Workshop	Los Angeles, CA, USA

Table 3-3. EJSM Working Groups

Working Group	European Co-Chair	US Co-Chair	Japan Co-Chair
Satellites	H. Hussmann	D. Senske	
Geophysics	H. Hussmann	B. Bills	
Composition	F. Tosi	T. McCord Chris Christensen	
Ice	O. Grasset	D. Blankenship	
Geology	R. Jaumann	J. Moore	
Local Environment	A. Coates	M. McGrath	
Jupiter	P. Drossart, L. Fletcher	A. Simon-Miller	
Magnetospheres	N. Krupp	K. Khurana	
Jupiter System	T. Van Holst E. Bunce	M. McGrath M. Showalter	
Origins	A. Coradini	W. Moore H. Waite	
Astrobiology	O. Prieto-Ballesteros	K. Hand	
Cosmic connections and Interdisciplinary links	M. Blanc A. Coustenis		M. Fujimoto
Radio Sciences and Techniques	P. Tortora	E. Marouf	
Education and Outreach	M. Blanc A. Coustenis	R. Greeley L. Prockter	

Note: *ad hoc* JJSDT meetings typically involved a subset of the core group.

4 SCIENCE GOALS AND OBJECTIVES

4.1 Relevance of Europa, Ganymede, and Jupiter System Exploration

Four hundred years after Galileo Galilei's discovery of Jupiter's moons advanced the Copernican revolution, these moons have the potential for discoveries just as profound.

Europa is believed to have a saltwater ocean beneath a relatively thin and geodynamically active icy shell (Figure 4-1). Europa is unique among the large icy satellites because its ocean is in direct contact with its rocky mantle, where the conditions could be similar to those on Earth's biologically rich sea floor. The discovery of hydrothermal zones on Earth's sea floor suggests that such areas are excellent habitats, powered by energy and nutrients that result from reactions between the seawater and silicates. Consequently, Europa is a prime candidate in the search for present-day habitability and life in the solar system.

Figure 4-1. Europa's surface shows a landscape scarred by tectonic and cryomagmatic events. This image of the Conamara Chaos region at 11 m/pixel shows how parts of the surface have been broken up into giant plates. This feature overlies and cuts across other types, indicating that the event happened in Europa's most recent geological epoch.

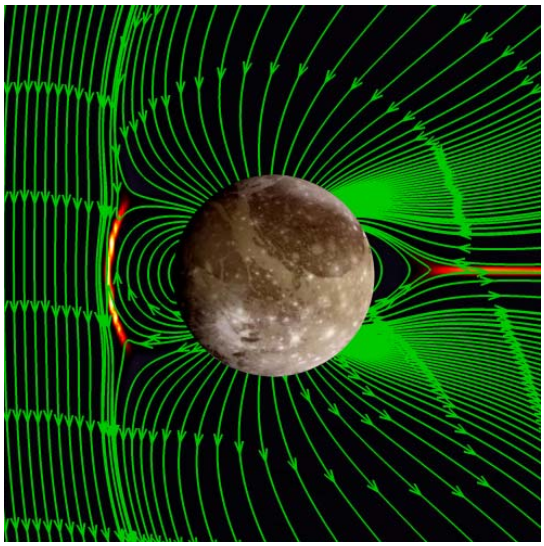

Figure 4-2. JGO would determine how Ganymede's unique magnetic field interacts with Jupiter's, how the interactions vary with time, and the role of a convecting core and internal ocean.

However, the details of the processes that shape Europa's ice shell, and the exchange processes between the surface and ocean, are not well understood.

Ganymede is believed to have a liquid ocean sandwiched between a thick ice shell above and high-density ice polymorphs below, more typical of volatile-rich icy satellites. It is the only satellite known to have an intrinsic magnetic field, which makes the Ganymede-Jupiter magnetospheric interaction unique in the solar system (Figure 4-2).

It is now recognized that oceans probably exist within all three of the icy Galilean moons, and rocky Io may contain a magma ocean (Figure 4-3). Among these ocean worlds, Europa's ocean is believed to be uniquely Earth-like, because its ocean is likely in direct contact with its mantle. This is in contrast to the larger moons Ganymede, Callisto, and Saturn's large moon Titan, which have much greater ice content, meaning that their oceans are sandwiched between ordinary ice above and higher-density ices below.

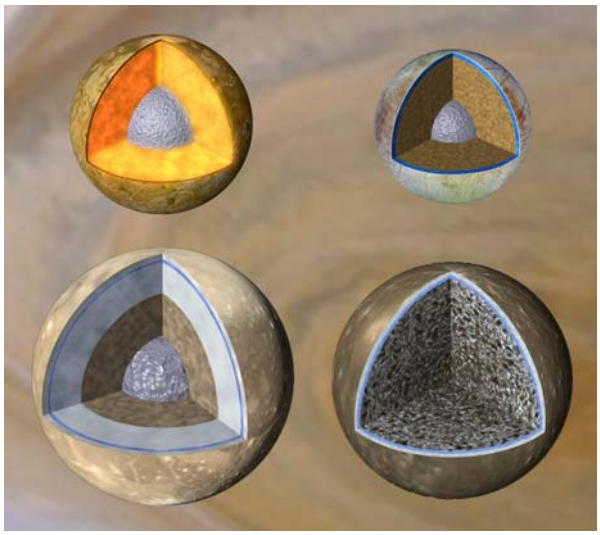

Figure 4-3. Interior models of the Galilean satellites. Io (top left) may possess a magma ocean, with tidal heating creating partially melting interior rock. Europa (top right) is unique in that its ocean (blue) is believed to be in direct contact with the rocky mantle below; thus, Europa's mantle could supply chemical nutrients directly to the water to support life. Ganymede (lower left) is fully differentiated with an iron core, and its probable subsurface ocean is sandwiched between ordinary ice above and higher-density ices below. Callisto (lower right) is also believed to have a subsurface ocean sandwiched between higher density and lower density ices, but its interior may be incompletely differentiated. The satellites are shown to scale, along with the western edge of Jupiter's Great Red Spot (background).

Galileo magnetometer data indicate induced fields at both Ganymede and Callisto, indicating ocean layers tens of kilometers thick beneath about 150 km of ice [*Kivelson et al. 2004*], consistent with the expected depth to the ice-water boundary in these moons. Because Callisto is not tidally heated, it might require a small amount of interior ammonia to maintain an ocean within.

4.1.1 Europa and Ganymede: Investigating Habitability

The contemporary ocean of Europa is believed to provide just the right environment for icy world habitability, so Europa is the natural target for the first focused spacecraft investigation of the habitability of icy worlds. Its candidate sources of chemical energy for life, direct mantle contact, relatively thin ice shell, and potentially active geology that brings oceanic material to the surface make it a recognized top priority for exploration. Moreover, Ganymede and Callisto provide two of the three known examples of oceans "sandwiched" between ice layers. Although less attractive for habitability, investigating these oceans is important to understanding the evolution of large and volatile-rich icy moons. The Europa Jupiter System Mission would be the critical first step in understanding the variety and potential habitability of icy satellite oceans.

Europa's high astrobiological potential and its complex interrelated processes have been previously recognized by a variety of groups, including the National Research Council (NRC) and NASA, which have noted Europa's extremely high priority for future exploration, with Io and Ganymede exploration also given notably high exploration priority.

The likelihood that Europa has a global subsurface ocean hidden beneath a relatively young icy surface has profound implications in the search for past or present life beyond Earth's biosphere. Coupled with the discovery of active microbial life in seemingly extreme environments [e.g. *Rothschild and Mancinelli 2001*], Europa takes on new importance as a primary target for exploring habitable worlds. Life as we know it (Figure 4-4) depends upon liquid water, a photo- or chemical-energy source, complex organics, and inorganic compounds of nitrogen, phosphorus, sulfur, iron and certain trace elements. Europa appears to meet these requirements and is distinguished by the potential presence of enormous volumes of liquid water and geological activity that promotes the exchange of surface materials with the sub-ice environment.

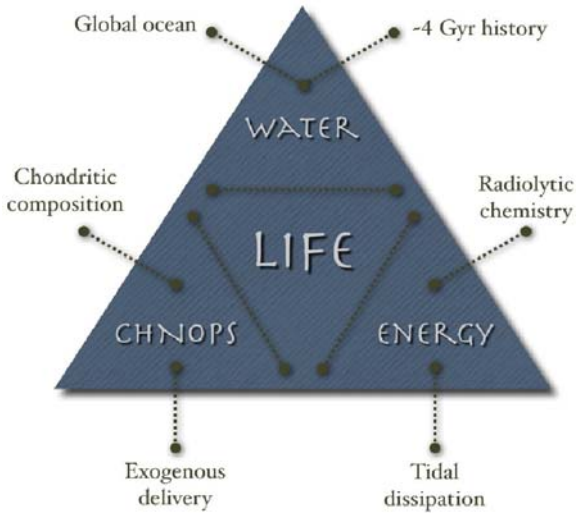

Figure 4-4. Pyramid of habitability. Our present understanding of the conditions for life could be distilled down to three broad requirements: 1) a sustained liquid water environment (internal global oceans, which have likely existed for 4 Gyr), 2) essential elements (*e.g.,* C,H,N,O,P,S) that are critical for building life (derived from primordial chondritic composition of the satellites, plus exogenous delivery over time), and 3) a source of energy that could be utilized by life (surface radiolytic chemistry, and possible hydrothermal activity driven by tidal heating). The cycling of chemical energy into an icy satellite's ocean over geological time scales is key to understanding habitability of the satellite. Courtesy Kevin Hand.

Given current information, we cannot know if life ever existed or persists today at the icy Galilean satellites. However, we could determine whether extant conditions are capable of supporting living organisms. Key to this question is the occurrence of liquid water beneath the icy surface and whether the geological and geophysical properties of the satellites could support the synthesis of organic compounds and provide the energy and nutrients needed to sustain life.

Inferences from Europa's young surface and models suggest that an ocean and hydrothermal system may lie beneath an ice shell a few to tens of kilometers thick. Tidal deformation may drive heating and geological activity within Europa and Ganymede, and there could be brine pockets within the ice associated with impurities, partial melt zones, and clathrates. At Europa, the potential occurrence of hydrothermal systems driven by tidal heating or volcanic activity could serve as a favorable environment for prebiotic chemistry or sustaining microbial chemotrophic organisms. Cycling of water through and within the ice shell, ocean, and the permeable upper rocky mantle could maintain an ocean rich with oxidants and reductants necessary for the chemistry of life. In order to address icy satellite habitability, a better understanding of the ice shells, oceans, and deeper interiors is needed.

Radiolytic chemistry on the surface of Europa is responsible for the production of O_2, H_2O_2, CO_2, SO_2, and other oxidants yet to be discovered. At present, mechanisms and timescales for delivery of these materials to the sub-surface are poorly constrained. Similarly, cycling of the ocean water through seafloor minerals could replenish the water with biologically useful reductants. If much of the tidal energy dissipation occurs in the mantle, then there could be significant cycling between the ocean water and rocky mantle. Conversely, if most of the tidal dissipation occurs in the ice shell, then the ocean water could be depleted in the reductants needed for biochemistry. Chemical cycling of energy on Europa is arguably the greatest uncertainty in the ability to assess its potential habitability.

Geophysical measurements by EJSM would set constraints on the potential habitability of the icy Galilean satellites. A high priority is to characterize the oceans of Europa and Ganymede and their dynamic relationships with the overlying ice shell, including the nature of surface-ice-ocean exchange. Assessments of the geochemical environment would directly address the issue of whether the chemistry of these satellites is compatible with habitability.

Remote sensing measurements could focus on relative terrain ages and chemical composition, and on identifying the youngest regions of direct exchange with the ocean. Chemical analyses of these regions, and those known to be older and more radiolytically processed, would allow distinguishing among the variety of chemical signatures anticipated on the surface. Combined geophysical and compositional results would lead to understanding the processes affecting ocean habitability, and potentially a compelling case for subsurface ocean habitability.

4.1.2 The Jupiter System

The individual objects in the Jupiter system—the giant planet itself, the Galilean Satellites, the small and irregular satellites, the ring system, and the magnetosphere—do not evolve independently. By understanding how the Jupiter System works (*e.g.*, tidal interactions as well as the connection between Jupiter, its magnetosphere and the moons), we understand how the solar system works and whether specific processes and conditions lead to habitable environments. To understand the evolution of the system, we have to study both the individual objects and the processes connecting them. Specifically, the other Galilean satellites afford a window into solar system history by preserving in their cratering records a chronology that dates back nearly 4.5 Gyr. Callisto is a witness plate to the earliest era of solar system history. In a broader context, the Jupiter system is our best analogue to study the evolution of planetary objects on the "system-level," which is of great relevance also for understanding extra-solar systems, including Jupiter-like giant-planets.

Io, Europa, and Ganymede are coupled in a stable resonance that maintains their orbital periods in a ratio of 4:2:1 and forces their orbital eccentricities; Callisto is not included in this resonance. Tidal interaction heats the interior of Io and is responsible for its unparalleled volcanic activity; maintains a liquid ocean within Europa, and causes faulting of its surface and convection within its ice shell; and powers convection within Ganymede's metallic core to produce that satellite's magnetic field. EJSM results would enable detailed comparative studies of how the different conditions with respect to tidal heating have led to different histories and internal structures, surfaces, and dynamic activities among the four Galilean satellites.

A very important aspect of solar system studies is the identification of the processes leading to the formation of gas giant planets, with implications for exoplanets. EJSM would provide new insight into this issue through understanding of the interior structure and properties of the Galilean satellites (especially Europa and Ganymede), derivation of the bombardment history on the Galilean satellites for application to the Jupiter system, and comparative compositional study of the satellites. Along with better understanding of Jupiter's composition, this would improve knowledge of the thermodynamics of the Jovian circumplanetary disk.

Jupiter's magnetosphere is closely coupled to the upper atmosphere and interior by electrodynamic interactions. This giant magnetized environment, driven by the fast rotation of its central spinning zone and populated by ions coming from its moons, is the most accessible and intense environment for direct investigations of general astrophysical processes. EJSM would measure the dynamics of the Jovian magnetodisk (with angular momentum exchange and dissipation of rotational energy), determine the electro-dynamic coupling between the planet and the satellites, and assess the global and continuous acceleration of particles.

Jupiter's internal and atmospheric structures are intimately coupled to the greater Jovian

system environment. EJSM would extend Juno's investigations to the lower latitudes of Jupiter's atmosphere while focusing on complementary scientific questions through measurements of the troposphere, stratosphere, thermosphere, and ionosphere for comparisons with Jupiter's interior and magnetosphere.

4.1.3 Responses to Decadal Survey and Cosmic Vision

EJSM would fully address the high-priority science objectives identified by the NRC's 2003 Decadal Survey and ESA's Cosmic Vision for exploration of the outer solar system. The 2003 Decadal Survey's Steering Group recommended a Europa Orbiter as the outer planet flagship mission and listed six science objectives, each of which would be met by JEO. The Survey also identified a Ganymede mission, such as JGO, as a highly desirable future mission. Moreover, some 20 specific questions were posed for the exploration of large satellites in the outer solar system, and EJSM, through the combined operation of JEO and JEO, would directly investigate all but one.

ESA's Cosmic Vision is structured around various themes and sub-themes, many of which would be addressed by EJSM. For example, one theme relates to understanding solar system processes. Jupiter's "miniature solar system" is ideally suited for this purpose through study and comparison of the diverse Galilean satellites by EJSM, by investigations of the gas giant and its magnetosphere to complement anticipated Juno results, and through analyses of interactions among all the objects, such as the small satellites and the ring system. Thus, the Jupiter system is a natural laboratory for posing and testing hypotheses of planetary processes through spacecraft observations. Another Cosmic Vision theme relates to planetary formation and evolution, which EJSM would address through study of the gas giant, Jupiter. Investigations would include: a) assessing the bulk compositions of the large satellites as critical constraints on formational models, b) observing the irregular satellites and their relations to primitive objects thought to have formed the cores of the giant planets, and c) studying motions in the upper atmosphere in high resolution over long time periods.

Astrobiology is a central theme to both the Decadal Survey and the Cosmic Vision. Determining the habitability of Europa and comparing the results with Ganymede would provide critical clues to habitability and the potential for the emergence of life in the outer solar system. The discovery of life beyond Earth would be profound. Moreover, should niches be found that are apparently habitable, yet do not contain known life forms, such would be equally important.

Operation of two spacecraft in the Jupiter system would provide the unparalleled opportunity to address the high-priority questions posed by the Decadal Survey and Cosmic Vision for exploration of the outer solar system. The EJSM mission concept represents a conservative and robust design approach to successfully answering these high-priority questions and making a major step forward in understanding the emergence of habitable worlds around gas giants.

4.2 Science Background

4.2.1 Europa

4.2.1.1 Europa's Ocean and Interior

Europa is continually flexed as it orbits, tugged and deformed by Jupiter's gravity. The satellite's response of bending, breaking, flowing, heating, and churning, enable the characteristics of its ocean and ice to be inferred. Europa also experiences the varying magnetic field of Jupiter, which generates induction currents in the interior and reveals the conductivity structure through its response. These external influences, in addition to Europa's internal thermal and chemical

properties, create the possibility that Europa's interior is volcanically active. Geophysics both dictates and betrays the characteristics of Europa's ocean, as well as its ice shell and deeper interior.

The surface of Europa suggests recently active processes operating in the ice shell. Jupiter raises gravitational tides on Europa, which contribute to thermal energy in the ice shell and rocky interior [*Ojakangas and Stevenson 1989, Sotin et al. 2009*], produce near-surface stresses responsible for some surface features [*Greeley et al. 2004*], and may drive currents in the ocean. Although relatively little is known about the internal structure, most models include an outer ice shell underlain by liquid water, a silicate mantle, and iron-rich core [*Anderson et al. 1998a, Schubert et al. 2009*]. Means to constrain these models include measurements of the gravitational and magnetic fields, topographic shape, and rotational state of Europa, each of which includes steady-state and time-dependent components. Additionally, the surface heat flux and local thermal anomalies may yield constraints on the satellite's internal heat production and activity. Results could be used to characterize the ocean and the overlying ice shell and to provide constraints on deep interior structure and processes.

Gravity

Observations of the gravitational field of a planetary body provide information about the interior mass distribution. For a spherically symmetric body, all points on the surface would have the same gravitational acceleration, while in those regions with more than average mass, gravity would be greater. Lateral variations in gravitational field strength thus indicate lateral variations in internal density structure.

Within Europa, principal sources of static gravity anomalies could be those due to ice shell thickness variations, or topography on the ocean floor, or internal density variations within the silicate mantle. If the ice shell is isostatically compensated, it would only yield very small anomalies. Gravity anomalies that are not spatially coherent with ice surface topography are presumed to arise from greater depths. Radio Doppler tracking over repeat orbits at 200 km altitude could resolve seamount ridges or other topographic features hundreds of kilometers wide on the ocean floor, though unique determination of their nature would require additional knowledge based on other geophysical measurements (*e.g.*, high-order induced magnetic field measurements)

One of the most diagnostic gravitational features is the amplitude and phase of the time-dependent signal due to tidal deformation [*Moore and Schubert 2000*]. The forcing from Jupiter is well known, and the response would be much larger if a fluid layer decouples the ice from the interior, permitting unambiguous detection of an ocean, and characterization of the ocean and the bulk properties of the overlying ice shell. With an ocean that decouples the surface ice from the rocky interior, the amplitude of the semi-diurnal tide on Europa is roughly 30 m, which is in clear contrast to the ~1 m tide in the absence of an ocean [*Moore and Schubert 2000*]. Because the distance to Jupiter is 430 times the mean radius of Europa, only the lowest degree tides are expected to be detectable. Figure 4-5 illustrates the degree-two tidal potential variations on Europa during a single orbital cycle. The tidal amplitude is directly proportional to this potential.

Topography

Characterizing the topography is important for several reasons. At long wavelengths (hemispheric-scale), topography is mainly a response to tides and possibly shell thickness variations driven by tidal heating [*Ojakangas and Stevenson 1989, Nimmo and Manga 2009*], and is thus diagnostic of internal tidal

processes. At intermediate wavelengths (hundreds of kilometers), the topographic amplitudes and correlation with gravity are diagnostic of the density and thickness of the ice shell. The view of Mars provided by the MOLA laser altimeter [*Zuber et al. 1992*] revolutionized geophysical study of that body, and the same is expected at Europa. The limited topographic information currently available shows Europa to be very smooth on a global scale, but topographically diverse on regional to local scales [*Schenk 2009*]. At the shortest wavelengths (kilometer-scale), small geologic features would tend to have topographic signatures diagnostic of formational processes.

Rotation

Tidal dissipation within Europa probably drives its rotation into equilibrium, with implications for both the direction and rate of rotation. The mean rotation period should almost exactly match the mean orbital period, so that the sub-Jupiter point would librate in longitude, with an amplitude equal to twice the orbital eccentricity. If the body behaves rigidly, the amplitude of this forced libration is expected to be ~100 m [*Comstock and Bills 2003*], but if the ice shell is mechanically decoupled from the silicate interior, then the libration could be three times larger. Similar forced librations in latitude are due to the finite obliquity and are diagnostic of internal structure in the same way. The rate of rotation would also change in response to tidal modulation of the shape of the body, and corresponding changes in the moments of inertia [*Yoder et al. 1981*].

The spin pole is expected to occupy a Cassini state [*Peale 1976*], similar to that of Earth's Moon. The gravitational torque exerted by Jupiter on Europa would cause Europa's spin pole to precess about the orbit pole, while the orbit pole in turn precesses about Jupiter's spin pole, with all three axes remaining coplanar.

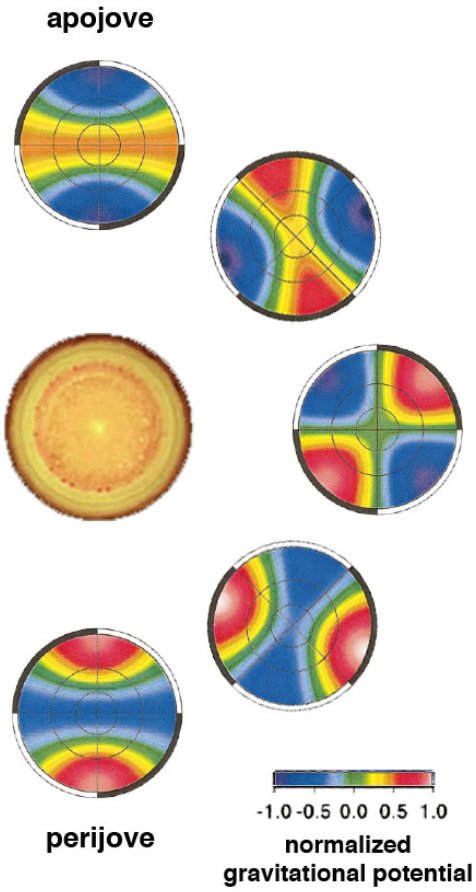

Figure 4-5. Europa experiences a time-varying gravitational potential field as it moves in its eccentric orbit about Jupiter (eccentricity = 0.0094), with a 3.551-day (1 eurosol) period. Europa's tidal amplitude varies proportionally to the gravitational potential, so the satellite flexes measurably as it orbits. In this adaptation of a figure from Moore and Schubert [2000], we look down on the north pole of Jupiter as Europa orbits counterclockwise with its prime meridian pointed approximately toward Jupiter. Measuring the varying gravity field and tidal amplitude simultaneously allows the interior rigidity structure of the satellite to be derived, revealing the properties of its ocean and ice shell.

The obliquity required for Europa to achieve this state is ~0.1 degree, but depends upon the moments of inertia, and is thus diagnostic of internal density structure [*Bills 2005, Bills et al. 2009*].

Obtaining a wide variety of different geophysical observations, all relevant to the internal structure of Europa, reduces the

ambiguity inherent in interpretations of measurements.

Magnetic Field

Magnetic fields interact with conducting matter at length scales ranging from atomic to galactic. Magnetic fields are produced when currents flow in response to electric potential differences between interacting conducting fluids or solids. Many planets generate their own stable internal magnetic fields in convecting cores or inner shells through dynamos powered by internal heat or gravitational settling of the interior. Europa does not generate its own magnetic field, suggesting that its core has either frozen or is still fluid but not convecting.

Europa is known to respond to the rotating magnetic field of Jupiter through electromagnetic induction [*Khurana et al. 1998, 2009*]. In this process, eddy currents are generated on the surface of a conductor to shield its interior from changing external electric and magnetic fields. The eddy currents generate their own magnetic field—called the induction field—external to the conductor. This secondary field is readily measured by a magnetometer located outside the conductor.

The induction technique exploits the fact that the primary alternating magnetic field at Europa is provided by Jupiter, because its rotation and magnetic dipole axes are not aligned. It is now widely believed that the induction signal seen in Galileo magnetometer data [*Khurana et al. 1998*] arises within a subsurface ocean in Europa. The measured signal was shown to remain in phase with the primary field of Jovian origin [*Kivelson et al. 2000*], thus unambiguously proving that the perturbation signal is a response to Jupiter's field.

Although clearly indicative of a Europan ocean, modeling of the measured induction signal suffers from non-uniqueness in the derived parameters because of the limited data. From a short series of measurements, such as those obtained by the Galileo spacecraft, the induction field components cannot be separated uniquely, forcing assumptions that the inducing signal is composed of a single frequency corresponding to the synodic rotation period of Jupiter. Unfortunately, single frequency data cannot be inverted to determine independently both the ocean thickness and the conductivity. Nevertheless, the single frequency analysis of *Zimmer et al.* [*2000*] reveals that the ocean must have a conductivity of at least 0.06 S/m. Work by *Schilling et al.* [*2004*] suggests the ratio of induction field to primary field is 0.97, from which *Hand and Chyba* [*2007*] infer that the ice shell is < 15 km thick and the ocean water conductivity > 6 S/m. [see also *Hand et al.* 2009].

The large uncertainty in the conductivity estimates of the ocean water results from the poor signal-to-noise ratio of the induction signature obtainable from relatively short segments of Galileo flyby data. Observations from a Europa orbiter could improve the S/N ratio of the induction field by several orders of magnitude.

In order to determine the ocean thickness and conductivity, magnetic sounding of the ocean at multiple frequencies is required. The depth to which an electromagnetic wave penetrates is inversely proportional to the square root of its frequency. Thus, longer period waves sound deeper and could provide information on the ocean's thickness, the mantle, and the metallic core. Electromagnetic sounding at multiple frequencies is routinely used to study Earth's mantle and core from surface magnetic data [*Parkinson 1983*]. Recently, it was demonstrated [*Tyler et al. 2003, Constable and Constable 2004*], that data from orbit could be used for electromagnetic induction sounding at multiple frequencies. In the case of Europa,

the two dominant frequencies are those of Jupiter's synodic rotation period (~11 hr) and Europa's orbital period (~85 hr). Observing the induction response at these two frequencies would likely allow determination of both the ocean thickness and the conductivity (see §4.3.1.1).

Some remaining key questions to be addressed regarding Europa's ocean, bulk ice shell properties, and deeper interior include:

- Does Europa undoubtedly have a subsurface ocean?
- What are the salinity and thickness of Europa's ocean?
- Does Europa exhibit kilometer-scale variations in ice shell thickness across the globe?
- Does Europa have a non-zero obliquity and if so, what controls it?
- Does Europa possess an Io-like mantle?

These questions, and how they may be answered by specific measurements, are further discussed in §4.3.1.1.

4.2.1.2 Europa's Ice Shell

Probing the third dimension of Europa's ice shell is essential to understanding the distribution of subsurface water and processes of ice-ocean exchange, which are key to determining Europa's habitability.

A detailed understanding of the internal structure of the ice shell is essential for unraveling the processes that connect the ocean to the surface. The structure and composition of the surface as observed by remote sensing is the result of material transport and chemical exchange through the shell. The thickness of the current ice shell is unknown, but estimates range from relatively thin (~ few km) to relatively thick (tens of km) [*Billings and Kattenhorn 2005*]. The ice shell may have experienced one or more episodes of thickening and thinning [*Hussman and Spohn 2004, Barr and Showman* 2009], directly exchanging material with the ocean at the base. Thermal processing may have also altered the internal structure of the shell through convection or local melting. In addition, geological processes have altered and deformed the surface and transported material horizontally and vertically within the shell. Exogenic processes such as cratering and regolith formation have influenced the surface and deeper structure. Just as a geologist on Earth uses structural information in order to understand the dynamics of the Earth's crust, three-dimensional sounding of the ice shell would reveal the processes connecting the surface to the ocean.

Thermal Processing

The thermal structure of Europa's ice shell (apart from local heat sources) is set by the transport of heat from the interior. Regardless of the properties of the shell or the overall mechanism of heat transport, the uppermost several kilometers are thermally conductive, cold, and stiff. The thickness of this conductive "lid" is set by the total amount of heat that must be transported and thus a measurement of the thickness of the cold and brittle part of the shell is a powerful constraint on the heat production in the interior. The lower, convecting part of the shell (if it exists), is likely to be much cleaner, since regions with impurities should have experienced melting at some point during convective circulation (when the material was brought near the base of the shell) and the melt would segregate downward efficiently, extracting the impurities from the shell [*Pappalardo and Barr 2004*]. Convective instabilities also result in thermal variations in the outer part of the shell that may be associated with features at the surface of Europa (lenticulae and chaos), with scales ranging from ~1–100 km. When warm, relatively pure ice diapirs from the interior approach the surface, they may be far from the pure-ice melting point, but may be above the

eutectic point of some material trapped in the lid. This may create regions of melting within the rigid shell above them as the temperature increases above the flattening diapir (Figure 4-6). The structural horizon associated with these melt regions would provide a good measurement of the thickness of the conductive layer. Other sources of local heating such as friction on faults may lead to similar local melting [*Gaidos and Nimmo 2000*]. High horizontal resolution (a few hundred meters) is required to avoid scale-related biases. The ability to sound through regions of rough large-scale terrain would also be essential. Detection of water lenses would require a vertical resolution of at least a few tens of meters.

Ice-Ocean Exchange

Europa's ice shell has likely experienced one or more phases of thickening and thinning, as its orbital and thermal evolution altered internal heating due to tides [*Hussmann and Spohn 2004, Moore and Hussmann 2009*] The shell may thicken by processes similar to those for ice that accretes beneath the large ice shelves of Antarctica, where frazil ice crystals form directly in the ocean water [*Moore et al. 1994*]. This model is characterized by slow accretion (freezing) or ablation (melting) on the lower side of the icy crust [*Greenberg et al. 1999*]. Impurities present in the ocean tend to be rejected from the ice lattice during the slow freezing process. Temperature gradients in this model are primarily a function of ice thickness and the temperature/depth profile is described by a simple diffusion equation for a conducting ice layer [*Chyba et al. 1998, Blankenship et al.* 2009]. The low temperature gradients at any ice water interface, combined with impurity rejection from accreted ice,

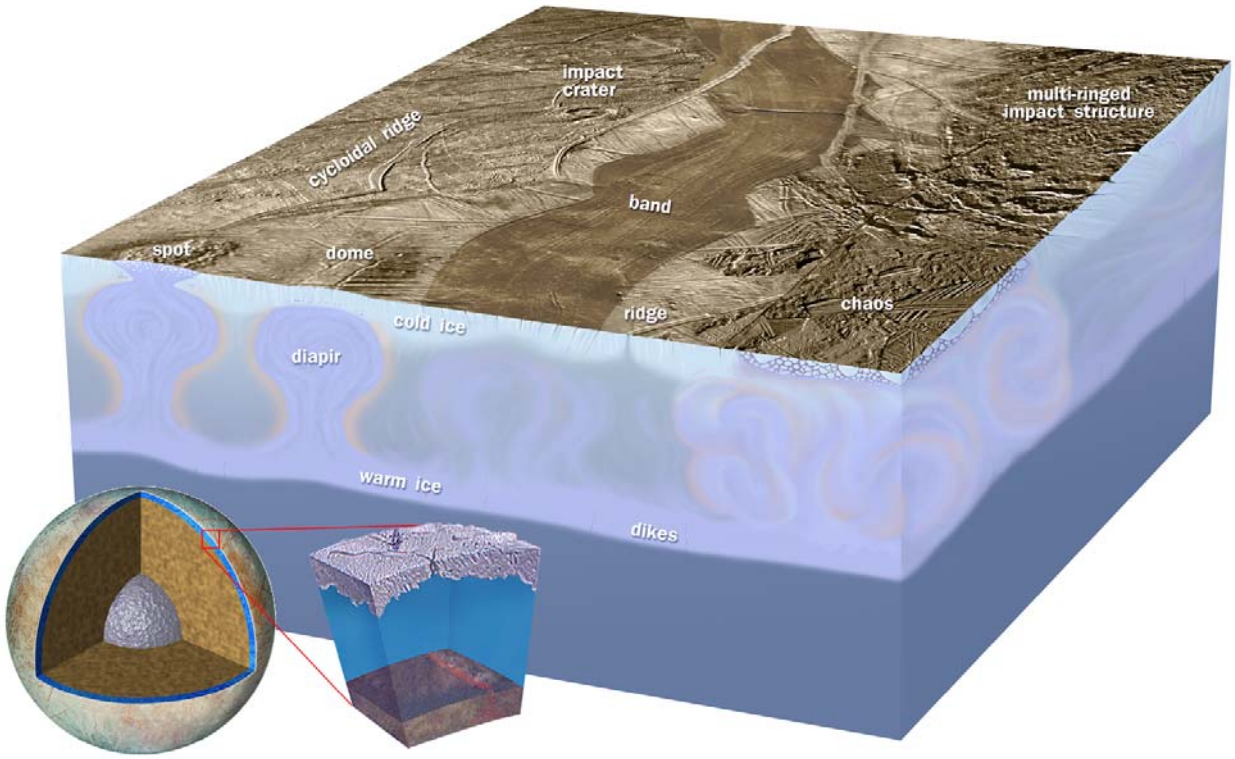

Figure 4-6. Block diagram representation of Europa's ice shell, assuming a thick shell model of possible ice shell processes leading to thermal, compositional, and structural horizons. Hypothesized convective diapirs (front of block diagram) could cause thermal perturbations and partial melting in the overlying rigid ice. Tectonic faulting driven by tidal stresses (upper surface) could result in fault damage and frictional heating. Impact structures (back right) are expected to have central refrozen melt pools and to be surrounded by ejecta.

would likely lead to significant structural horizons resulting from contrasts in ice crystal fabric and composition. Similarly, the melt-through hypothesis for the formation of lenticulae and chaos on Europa's surface implies that ice would accrete beneath the feature after it forms. This process would result in a sharp boundary between old ice (or rapidly frozen surface ice) and the deeper accreted ice. The amount of accreted ice would be directly related to the time since melt-through occurred and could be compared with the amount expected based on the surface age. Testing these hypotheses would require measuring the depth of interfaces to a resolution of a few hundred meters, and horizontal resolutions of a fraction of any lid thickness; *i.e*., a kilometer or so.

Surface and Subsurface Structure

Europa represents a unique tectonic regime in the solar system, and the processes controlling the distribution of strain in Europa's ice shell are uncertain. Tectonic structures could range from sub-horizontal extensional fractures to near-vertical strike-slip features. These would produce structures associated primarily with the faulting process itself, through formation of pervasively fractured ice and zones of deformational melt, injection of water, or preferred orientation of crystalline fabric. Some faults may show local alteration of pre-existing structure, including fluid inclusions, or by juxtaposition of dissimilar regions through motion on the fault. There are many outstanding questions regarding those tectonic features. A measurement of their depth extent and association with thermal anomalies or melt inclusions would strongly constrain models of their origins. In particular, correlation of subsurface structure with surface properties (length, position in the stratigraphic sequence, height and width of the ridges) would test hypotheses for the mechanisms that form the fractures and support the ridges. The observation of melt along the fracture would make these features highly desirable targets for future *in situ* missions.

Extensional structures observed on Europa (gray bands) may be particularly important for understanding material exchange processes. If the analogy with terrestrial spreading centers [*Pappalardo and Sullivan 1996*] is accurate, the material in the band is newly supplied from below and may have a distinct structure. The origin of the material in the bands may thus be constrained by sounding the subsurface. Bands and ridges typically have length scales of a few kilometers. Horizontal resolutions a factor of ten higher than this would be required to discriminate processes. For extensional structures, the ability to image structures sloping more than a few degrees is also necessary. Additionally, tens of meters of vertical resolution would be required to image near surface melt inclusions.

The impact process represents a profound disturbance of the local structure of the shell. Around the impact site, the ice is fractured and heated, and some melt is generated. The surface around the impact is buried to varying degrees with a blanket of ejecta. Finally, the relaxation of the crater creates a zone of tectonism that could include both radial and circumferential faulting. These processes all create subsurface structures that might be probed by sounding.

An outstanding mystery on Europa is the process by which craters are erased from the surface. It may be possible to find the subsurface signature of impacts that are no longer evident at the surface, which would place constraints on the resurfacing processes that operate at Europa. Impact processes affect the structure of the ice shell to different extents depending on the size of the impactor, and it is possible that Europa's subsurface records events which have penetrated the entire thickness of the shell (at the time). Three types

of structural horizons are expected to be derived from impact: the former surface buried beneath an ejecta blanket, solidified eutectic melts in the impact structure itself, and impact related fractures (*e.g.*, a ring graben or radial fractures possibly including injected melt). Vertical resolutions on the scales of a few tens to hundreds of meters would be required to identify ejecta blankets and frozen melt pools. Detection of at least the edges of steep interfaces would aid in the identification of radial dikes, buried crater walls and circumferential fractures.

Remaining outstanding questions to be addressed about Europa's ice shell include:

- Is Europa's ice shell thin and thermally conductive, or thick and convecting?
- Is material transported from the ocean to the near surface or surface, and vice-versa, and if so, what are the transport processes?
- What are the three-dimensional characteristics of Europa's geological structures?

Discussion of how these questions may be addressed using specific measurements is found in §4.3.1.2

4.2.1.3 Europa's Composition

Characterizing the surface organic and inorganic composition and chemistry provides fundamental information about Europa's history and evolution, the properties and habitability of the subsurface and ocean, its interaction with the surface, and the role of exogenic processes. Note that here and in §4.3.1.3, the JJSDT provides expanded discussion regarding composition, in response to requests from NASA for additional information on this topic.

The composition of Europa's surface records its history and evolution. Surface materials may be ancient, derived through time from the ocean, altered by radiation, or exogenic in origin. Europa's bulk density and current understanding of solar and stellar composition suggest the presence of both water and silicates. It is likely that the differentiation of Europa resulted in mixing of water with the silicates and carbonaceous materials that formed the moon and resulted in chemical alteration and redistribution, with interior transport processes bringing a variety of materials from the interior into the ocean and up to the surface. The barrage of high-energy particles from Jupiter's magnetosphere leaves an imprint on the surface composition that provides clues to this environment, but could also complicate efforts to understand the formation, evolution and modification of the surface. Finally, surface materials could be incorporated into the subsurface and react with the ocean, or could be sputtered from the surface to form Europa's tenuous atmosphere.

Icy and Non-Icy Composition

Compositional information from Earth-based telescopic observations and data from the Voyager and Galileo spacecraft [*e.g., Kuiper 1957, Moroz 1965, Clark 1980, Dalton 2000, McCord 2000, Spencer et al. 2005, Alexander et al. 2009*] show that the surface of Europa is composed primarily of water ice in both crystalline and amorphous forms [*Pilcher et al. 1972, Clark and McCord 1980, Hansen and McCord 2004*].

The dark, non-icy materials that make up much of the rest of Europa's surface are of extreme interest for unraveling Europa's geological history, and determining their composition is the key to understanding their origin. The spatial distribution and context of these materials at geologically relevant scales, which could be examined by JEO in far more detail than ever before, allows the processes that have formed the surface and the connection between the surface and the interior to be understood. This link provides important constraints on the nature of the

interior, the potential habitability of sub-surface liquid water environments, and the processes and time scales through which interior materials are transported to the surface. Compositional variations in surface materials may reflect age differences indicative of recent activity, and the discovery of active vents or plumes would show current activity.

The non-ice components are known to include carbon dioxide (CO_2), sulfur dioxide (SO_2), hydrogen peroxide (H_2O_2) and molecular oxygen (O_2) based on comparison of measured spectra with laboratory studies of the relevant compounds [*Lane et al. 1981, Noll et al. 1995, Smythe et al. 1998, Carlson 1999, 2001, Carlson et al. 1999a,b, Spencer and Calvin 2002, Hansen and McCord 2008*]. Spectral observations from the Galileo Near Infrared Mapping Spectrometer (NIMS) instrument of disrupted dark and chaotic terrains on Europa exhibit distorted and asymmetric absorption features indicative of water bound in non-ice hydrates. Hydrated materials observed in regions of surface disruption (Figure 4-7) have been suggested to be magnesium and sodium sulfate minerals (Figure 4-8) that originate from subsurface ocean brines [*McCord et al. 1998b, 1999*]. Alternatively, these materials may be sulfuric acid hydrates created by radiolysis of sulfur from Io, processing of endogenic SO_2, or from ocean-derived sulfates present in these deposits [*Carlson et al. 1999b, 2002, 2005*]. It is also possible that these surfaces are a combination of both hydrated sulfate salts and hydrated sulfuric acid [*Dalton 2000, McCord et al. 2001a,b 2002, Carlson et al. 2005, Orlando et al. 2005, Dalton et al. 2005*], as suggested by linear spectral mixture analyses of disrupted terrains [*Dalton 2007*]. An ultraviolet absorption feature, discovered in Earth-based disk-integrated observations and HST [*Lane et al. 1981, Noll et al. 1995*] on Europa's trailing hemisphere and linked to bombardment by S^+ ions, was found in Galileo UVS high-resolution observations [*Hendrix et al. 1998*] to vary in strength with location on the trailing hemisphere and show a correlation with the NIMS-measured asymmetric water ice bands. An important objective of JEO would be to resolve the compositions and origins of these hydrated materials.

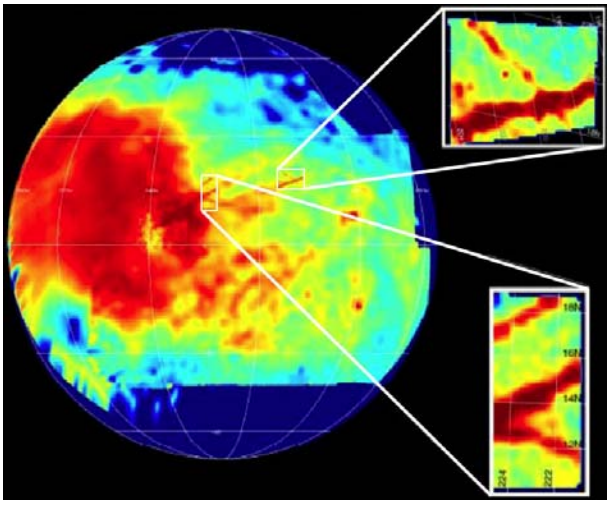

Figure 4-7. The distribution of hydrated materials on Europa (red) reaches its maximum near the apex of the trailing hemisphere, where impinging magnetic radiation flux is highest, and correlates with geologically disrupted terrains and triple bands (insets), and with the trailing hemisphere.

Hydrated material was also reported in dark areas on Ganymede [*McCord et al. 2001b*], which has a much less severe radiation environment than Europa. Such similarities suggest a common origin for these materials. Whether predominantly exogenic or endogenic, the interplay of chemical pathways and physical processes on these worlds could be studied together to better understand each.

Material in the space surrounding Europa also provides compositional clues. *Brown and Hill* [*1996*] first reported a cloud of sodium around Europa, and *Brown* [*2001*] detected a cloud of potassium and reported that the Na/K ratio suggested that endogenic sputtering produced these materials.

A broad suite of additional compounds is predicted for Europa based on observations of

other icy satellites, as well as from experimental studies of irradiated ices, theoretical simulations, and geochemical and cosmochemical arguments. Organic molecular groups, such as CH and CN, have been found on the other icy Galilean satellites [*McCord et al. 1997, 1998b*], and their presence or absence on Europa is important to understanding Europa's potential habitability. Other possible compounds that may be embedded in the ice and detectable by high-resolution spectroscopy include H_2S, OCS, O_3, HCHO, H_2CO_3, SO_3, $MgSO_4$, H_2SO_4, H_3O^+, $NaSO_4$, HCOOH, CH_3OH, CH_3COOH and more complex species [*Moore 1984, Delitsky and Lane 1997, 1998, Hudson and Moore 1998, Moore et al. 2003, Brunetto et al. 2005*].

As molecules become more complex, however, their radiation cross-section also increases and they are more susceptible to alteration by radiation. Radiolysis and photolysis could alter the original surface materials and produce many highly oxidized species that react with other non-ice materials to form a wide array of compounds. Given the extreme radiation environment of Europa, complex organic molecules are not expected in older deposits nor in those exposed to higher levels of irradiation [*Johnson and Quickenden 1997, Cooper et al. 2001*]. However, diagnostic molecular fragments and key carbon, nitrogen, and sulfur products may survive in some locales. Regions of lesser radiation (*i.e.*, the leading hemisphere) and sites of recent or current activity would be the most likely places to seek evidence of organic or derived products.

Improved spectral observations at significantly higher spectral and spatial resolution, together with detailed laboratory analyses under the appropriate temperature and radiation environment, are needed to fully understand Europa's surface chemistry. These data would provide major improvements in the identification of the original and derived compounds and the radiation environment and reaction pathways that create and destroy them.

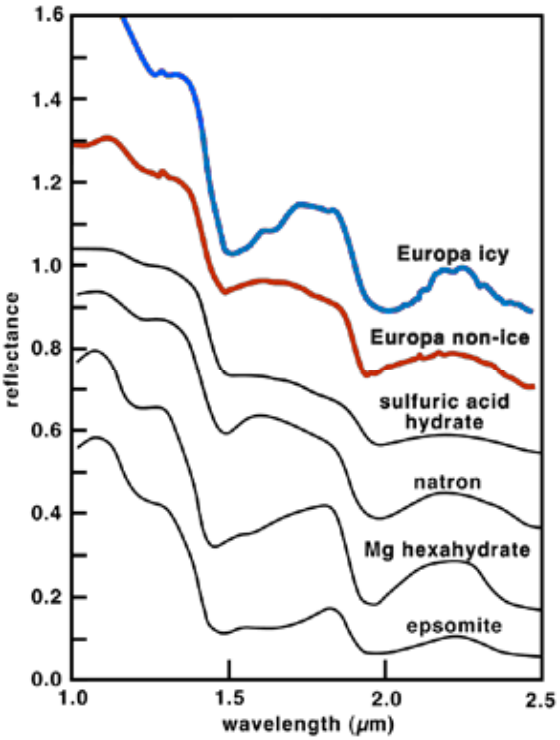

Figure 4-8. Reflectance spectra of hydrated materials on Europa. Candidate materials for Europa's non-ice component include sulfuric acid hydrate (H_2SO_4•nH_2O) and various hydrated sulfate and carbonate salts [*McCord et al. 1999, 2002*].

Isotopic Constraints

The varying degree of preference for the lighter isotopes in many physical and chemical processes is expected to lead to mass fractionation effects that should be evident in isotopic ratios. Ratios of D/H, $^{13}C/^{12}C$, $^{15}N/^{14}N$, ^{18}O /$^{17}O/^{16}O$, $^{34}S/^{32}S$, and $^{40}Ar/^{36}Ar$, and comparison among them, could provide insights into geological, chemical, and possible biological processes such as planetary formation, interior transport, surface evolution, radiolysis, atmospheric escape, and metabolic pathways.

The determination of isotopic ratios would provide a powerful indicator of several

planetary processes. Exchange rates among the Earth's oceans, crust, mantle and atmosphere are closely linked to ratios of radiogenic noble gas isotopes; these have been used at Venus and Mars, for example, to better understand the evolution of their volatile reservoirs. In satellite systems around large gaseous planets such as Jupiter and Saturn, questions about the presence, extent and composition of a primordial circumplanetary disk surrounding the host proto-planet could be addressed by comparing isotope ratios measured at different satellites in the system with those measured in the host planet's atmosphere.

Endogenic processes on Europa and other Galilean satellites may have measurable effects on isotope compositions. Moreover, the exogenic processes of sublimation and sputtering should also cause isotopic fractionation. Differences in solubilities and clathrate dissociation pressures would cause materials and isotopes of interest to freeze or become enclathrated into Europa's ice shell in different proportions than found in the aqueous solution of the ocean. Such differences may be evident from comparison of the predominant ice-rich background terrain on Europa's surface with cracks, chaos regions and other features rich in non-icy material that may have been deposited directly from the ocean.

Relationship of Composition to Processes

Galileo's instruments were designed to study surface compositions at regional scales (Figure 4-8). The association of hydrated and reddish materials with certain geologic terrains, revealed by Galileo, suggests an endogenic source for the emplaced materials, although these may have since been altered by radiolysis. Many surface features with compositionally distinct materials were formed by tectonic processes, suggesting that the associated materials are derived from the subsurface. Major open questions include the links between surface composition and that of the underlying ocean and rocky interior

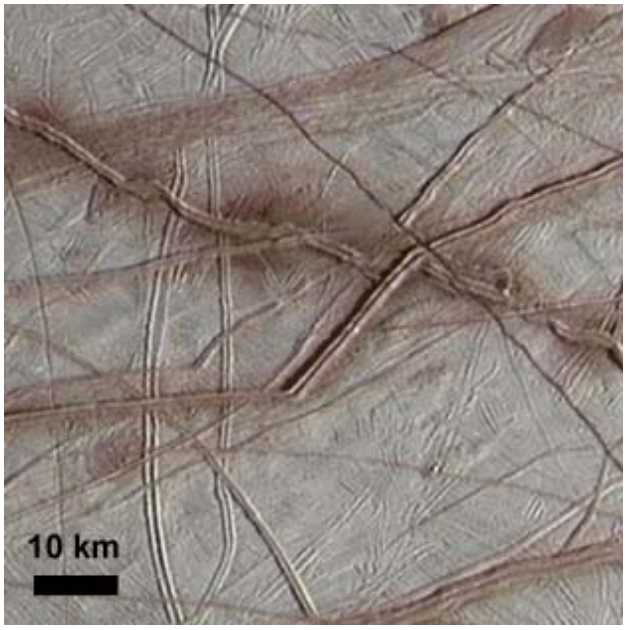

Figure 4-9. This portion of a Galileo image is the size of a typical Galileo NIMS footprint, demonstrating how NIMS sampled multiple terrain types in each spectrum.

[*Fanale et al. 1999, Kargel et al. 2000, McKinnon and Zolensky 2003*], and the relative significance of radiolytic processing [*Johnson and Quickenden 1997, Cooper et al. 2001, Carlson et al. 2002, 2005, Grundy 2007*]. For example, compositional variations associated with surface features such as chaos suggest that material may be derived from an ocean source, either directly through melting or eruptions, or indirectly through processes such as diapirism [*McCord et al. 1998b, 1999, Fanale et al. 1999, Orlando et al. 2005*].

One of the critical limitations of the Galileo NIMS experiment was the low spatial resolution of the high-quality spectra and the limited spatial coverage due to the failure of the spacecraft's high-gain antenna. The spectra used to identify hydrated materials were typically averaged from areas ~75 km by 75 km [*McCord et al. 1998b, Carlson et al. 1999b*] (although a few higher-resolution "postage stamp" data sets were obtained and analyzed). This typical footprint is shown in Figure 4-9**,** illustrating the tremendous mixing

of surface terrain types that occurs within an area of this extent; less than 10% of the NIMS footprint contains materials associated with ridges, bands, or fractures. In order to isolate and identify the young, non-ice materials associated with these structures, and look for spectral variations within geological structures, future observations must be able to resolve the non-ice materials to at least ~100 m scales.

In addition to compositional differences associated with recent geological activity, compositional changes related to exposure age also provide evidence for sites of recent or current activity. The composition of even the icy parts of Europa is variable in space and time. Polar fine-grained deposits suggest frosts formed from ice sputtered or sublimated from other areas [*Clark et al. 1983, Dalton 2000, Hansen and McCord 2004*]. Equatorial ice regions are more amorphous than crystalline, perhaps due to radiation damage. Venting or transient gaseous activity on Europa would indicate present-day surface activity.

Exogenic processes are also a key part of Europa's composition story, but much remains unknown about the chemistry and sources of the materials being implanted. Magnetic field measurements by Galileo of ion-cyclotron waves in the wake of Europa provide evidence of sputtered and recently ionized Cl, O_2, SO_2 and Na ions [*Volwerk et al. 2001*]. Medium energy ions (tens to hundreds of keV) deposit energy in the topmost few tens of microns; heavier ions, such as oxygen and sulfur ions, have an even shorter depth of penetration, while MeV electrons could penetrate and affect the ice to a depth of more than 1 m [*Paranicas et al. 2002, and references therein, Paranicas et al. 2009*]. The energy of these particles breaks bonds to sputter water molecules, molecular oxygen, and any impurities within the ice [*Cheng et al. 1986*], producing the observed atmosphere and contributing to the erosion of surface features.

A major question is the exogenic versus endogenic origin of volatiles such as CO_2 and their behavior in time and space. CO_2 was reported on the surfaces of Callisto and Ganymede [*McCord et al. 1998b*], with hints of SO_2 [*Smythe et al. 1998*] and H_2O_2 [*Carlson et al. 1999a*]. Recent analyses of the NIMS spectra indicate a concentration of CO_2 and other non-ice compounds on the anti-jovian and trailing sides of Europa [*Hansen and McCord 2008*], suggesting an endogenic origin. Radiolysis of CO_2 and H_2O ices is expected to produce additional compounds [*Moore 1984, Delitsky and Lane 1997, 1998, Brunetto et al. 2005*]. Determining the presence and source of organic molecular compounds, such as CH and CN groups detected by IR spectroscopy at Callisto and Ganymede [*McCord et al. 1997, 1998b*] and tentatively identified on Phoebe [*Clark et al. 2005*], would be important to evaluating the astrobiological potential of Europa, especially if there is demonstrable association with the ocean.

Some surface constituents result directly from exogenic sources. For example, sulfur from Io is transported by the magnetosphere and is implanted into Europa's ice. Once there it could form new molecules and may create some of the dark components on the surface. It is important to separate surface materials formed by implantation from those that are endogenic., and this could be done by quantitative analysis. For example, the detected Na/K ratio is supportive of an endogenic origin—and perhaps an ocean source—for sodium and potassium [*Brown 2001, Johnson et al. 2002, McCord et al. 2002, Orlando et al. 2005*].

Spatial variations could also help separate exogenic and endogenic processes. For

example, comparison of spectra of disrupted terrain on the leading and trailing hemispheres, which encounter far different radiolytic fluxes, would help to isolate the effects of the radiation environment and unravel the endogenic and exogenic chemical processes that led Europa to its present state.

Regardless of origin, surface composition results from combinations of all these processes, and materials emplaced at the surface are subsequently processed by radiation to produce the observed composition [*Dalton 2000*]. For example, material derived from the ocean could be a mixture of dominantly Mg and Na salts. Na sulfates would be more vulnerable to radiative disassociation, producing sulfuric acid (H_2SO_4) [*Dalton 2000, 2007, McCord et al. 2001b, 2002, Orlando et al. 2005*]. Such a mixture would allow for both indigenous salts and sulfuric acid, and could account for the origin of Na and K around Europa.

Some key outstanding questions to be addressed regarding Europa's composition include:

- Are there endogenic organic materials on Europa's surface?
- Is chemical material from depth carried to the surface?
- Is irradiation the principal cause of alteration of Europa's surface materials through time?
- Do materials formed from ion implantation play a major role in Europa's surface chemistry?

Specific measurements that could be made to address these questions are discussed in §4.3.1.3.

4.2.1.4 Europa's Geology

By understanding Europa's varied and complex geology, the moon's past and present processes are deciphered, along with implications for habitability. An understanding of Europa's geology provides clues about geological processes on other icy satellites with similar surface features, such as Miranda, Triton, and Enceladus.

The relative youth of Europa's surface is inherently linked to the ocean and the effects of gravitational tides, which trigger processes that include cracking of the ice shell, resurfacing, and possibly release of materials from the interior. Clues to these and other processes are provided by spectacular surface features such as linear fractures and ridges, chaotic terrain, and impact craters.

Linear Features

Europa's unusual surface is dominated by tectonic features in the form of linear ridges, bands, and fractures (Figure 4-10). The class of linear features includes simple troughs and scarps (*e.g.*, Figure 4-10g), double ridges separated by a trough, and intertwining ridge-complexes. Whether these represent different processes or stages of the same process is unknown. Ridges are the most common feature type on Europa and appear to have formed throughout the satellite's visible history (Figure 4-10j and l). They range from 0.1 to > 500 km long, are as wide as 2 km, and could be several hundred meters high. Cycloidal ridges are similar to double ridges, but form chains of linked arcs.

Most models of linear feature formation involve fracturing in response to processes within the ice shell [*Greeley et al. 2004, Kattenhorn and Hurford 2009, Prockter and Patterson 2009*]. Some models suggest that liquid oceanic material or warm mobile subsurface ice squeezes through fractures to form the ridge, while others suggest that ridges form by frictional heating and possibly melting along the fracture shear zone. Thus, ridges might represent regions of material exchange between the surface, ice shell, and ocean,

plausibly providing a means for surface oxidants to enter the ocean. Some features, such as cycloidal ridges, appear to initiate as a direct result of Europa's tidal cycle [*Hoppa et al. 1999*].

Bands reflect fracturing and lithospheric separation, much like sea-floor spreading on Earth, and most display bilateral symmetry [*e.g., Sullivan et al. 1998*] (Figure 4-10b and d). Their surfaces vary from relatively smooth to heavily fractured. The youngest bands tend to be dark, while older bands are bright, suggesting that they brighten with time. Geometric reconstruction of bands suggests that a spreading model is appropriate, indicating extension in these areas and possible contact with the ocean [*Tufts et al. 2000, Prockter et al. 2002*].

The accommodation of extensional features remains a significant outstanding question regarding Europa's geology. A small number of contractional folds were found on the

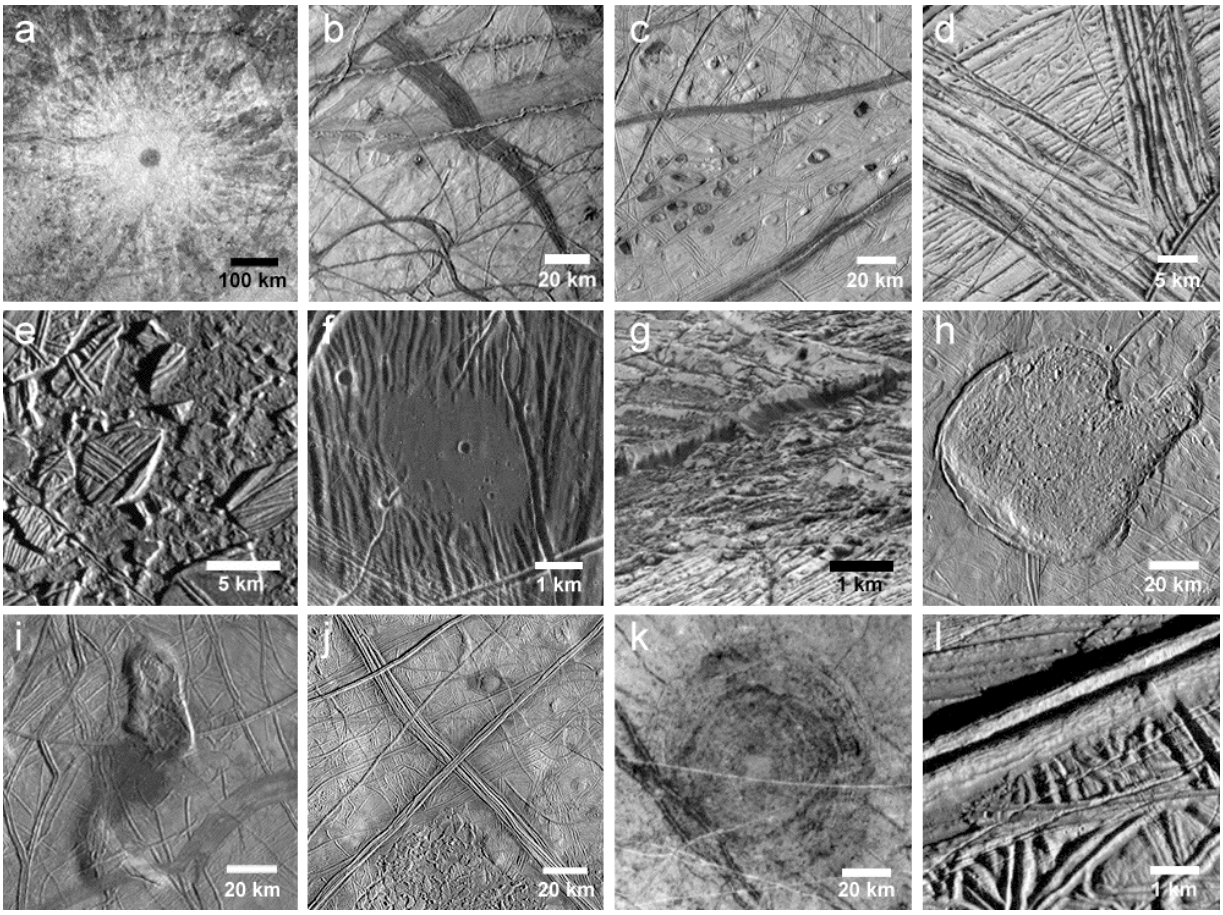

Figure 4-10. Europa is a cryological wonderland, with a wide variety of surface features. Many appear to be unique to this icy moon. While much was learned from Galileo, it is still not understood how many of these features form, or their implications for Europa's evolution. Shown here are: (a) The impact crater Pwyll, the youngest large crater on Europa; (b) Pull-apart bands; (c) Lenticulae; (d) Pull-apart band at high resolution; (e) Conamara Chaos; (f) Dark plains material in a topographic low, (g) Very high resolution image of a cliff, showing evidence of mass wasting; (h) Murias Chaos, a cryovolcanic feature which has appears to have flowed a short distance across the surface; (i) The Castalia Macula region, in which the northernmost dome contains chaos and is ~900 m high; (j) Regional view of two very large ridge complexes in the Conamara region; (k) Tyre impact feature, showing multiple rings; and (l) One of Europa's ubiquitous ridges, at high resolution.

surface [*Prockter and Pappalardo 2000*] and some sites of apparent convergence within bands have been suggested [*Sarid et al. 2002*], but these are insufficient to accommodate the extension documented across Europa's surface. Some models suggest that ridges and local folds could reflect such contraction, but the present lack of global images, topographic information, and knowledge of subsurface structure precludes testing these ideas.

Fractures are narrow (from hundreds of meters to the ~10 m limit of image resolution) and some exceed 1000 km in length. Some fractures cut across nearly all surface features, indicating that the ice shell is subject to deformation on the most recent time-scales. The youngest ridges and fractures could be active today in response to tidal flexing. Subsurface sounding and surface thermal mapping could help identify zones of warm ice coinciding with current or recent activity. Young ridges may be places where there has material exchange between the ocean and the surface, and would be prime targets as potential habitable niches.

Chaotic Terrain

Europa's surface has been disrupted to form regions of chaotic terrain, as subcircular features termed lenticulae, and irregular-shaped, generally larger chaos zones [*Collins and Nimmo 2009*]. Lenticulae include pits, spots of dark material, and domes where the surface is upwarped and commonly broken (Figure 4-10c and f). *Pappalardo et al.* [*1998a, 1999*] argued that these features are typically ~10 km across and possibly formed by upwelling of compositionally or thermally buoyant ice diapirs through the ice shell. In such a case, their size distribution would imply the thickness of the ice shell to be at least 10–20 km at the time of formation.

An alternative model suggests that there is no dominant size distribution and that lenticulae are small members of chaos [*Greenberg et al. 1999*], formed through either direct material exchange (through melting) or indirect exchange (through convection) between the ocean and surface [*e.g., Carr et al. 1998a*]. Thus, global mapping of the size distribution of these features could address their origin.

Chaos is generally characterized by fractured plates of ice that have been shifted into new positions within a background matrix (Figure 4-10e). Much like a jigsaw puzzle, many plates could be fit back together, and some ice blocks appear to have disaggregated and "foundered" into the surrounding finer-textured matrix. Some chaos areas stand higher than the surrounding terrain (Figure 4-10h and i). Models of chaos formation suggest whole or partial melting of the ice shell, perhaps enhanced by local pockets of brine [*Head and Pappalardo 1999*]. Chaos and lenticulae commonly have associated dark, reddish zones thought to be material derived from the subsurface, possibly from the ocean. However, these and related models are poorly constrained because the total energy partitioning within Europa is not known, nor are details of the composition of non-ice components. Subsurface sounding, surface imaging, and topographic mapping [*e.g., Schenk and Pappalardo 2004*] are required to understand the formation of chaotic terrain, and its implications for habitability.

Impact Features

Only 24 impact craters $\geq$ 10 km have been identified on Europa [*Schenk et al. 2004*], reflecting the youth of the surface. This is remarkable in comparison to Earth's Moon, which is only slightly larger but far more heavily cratered. The youngest Europan crater is thought to be the 24 km-diameter Pwyll, (Figure 4-10a) which still retains its bright rays, and likely formed less than 5 Myr ago [*Zahnle et al. 1998, Bierhaus et al.* 2009]. Complete global imaging would provide a full crater inventory, allowing a more

comprehensive determination of the age of Europa's surface, and helping to identify the very youngest areas.

Crater morphology and topography provide insight into ice layer thickness at the time of the impact. Morphologies vary from bowl-shaped depressions with crisp rims, to shallow depressions with smaller depth-to-diameter ratios. Craters up to 25–30 km in diameter have morphologies consistent with formation in a warm but solid ice shell, while the two largest impacts [Tyre (Figure 4-10k) and Callanish] might have punched through brittle ice about 20 km deep into a liquid zone [*Moore et al. 2001, Schenk et al. 2004, Schenk and E. P. Turtle* 2009].

Geological History

Determining the geological histories of planetary surfaces requires identifying and mapping surface units and structures and placing them into a time-sequence.

In the absence of absolute ages derived from isotopic measurements of rocks, planetary surface ages are commonly assessed from impact crater distributions, with more heavily cratered regions reflecting greater ages. The paucity of impact craters on Europa limits this technique. Thus, superposition (*i.e.*, younger materials burying older materials) and cross-cutting relations are used to assess sequences of formation [*Figueredo and Greeley 2004, Doggett et al.* 2009]. Unfortunately, only 10% of Europa has been imaged at a sufficient resolution to understand temporal relationships among surface features; for most of Europa, imaging data is both incomplete and disconnected from region to region, making the global surface history difficult to decipher.

Where images of sufficient resolution (better than 200 m/pixel) exist, it appears that the style of deformation evolved through time from ridge and band formation to chaotic terrain [*Greeley et al. 2004*], although there are areas of the surface where this sequence is less certain [*e.g., Riley et al. 2000*]. The mechanism for the change in geological style is uncertain, but a plausible mechanism for the change is one in which Europa's ocean is slowly cooling and freezing out as the ice above it is thickening. Once the ice shell reaches a critical thickness, solid-state convection may be initiated, allowing diapiric material to be convected toward the surface. A thickening ice shell could be related to a waning intensity of geological activity.

Given the relative youth of Europa's surface, such a fundamental change in style might seem unlikely over the last ~1% of the satellite's history, and its activity over the rest of its ~4.5 billion year existence could only be speculated. Four possible scenarios have been proposed (Figure 4-11):

(a) Europa resurfaces itself in a steady-state and relatively constant, but patchy style;
(b) Europa is at a unique time in its history, having undergone a recent major resurfacing event;

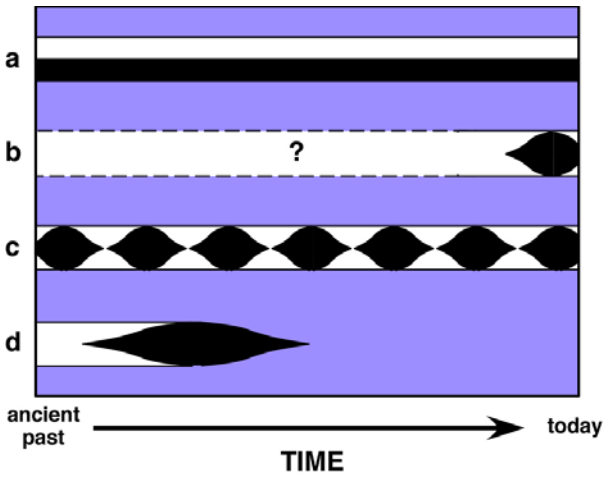

Figure 4-11. Possible evolutionary scenarios for Europa's surface. (a) Steady-state, relatively constant resurfacing; (b) Unique time in history with recent major resurfacing event; (c) Global resurfacing is episodic or sporadic; (d) Surface is older than cratering models suggest. Mapping data from JEO when related to system data as a whole, would help to distinguish among these models. After Pappalardo et al. [*1999*].

(c) Global resurfacing is episodic or sporadic;
(d) Europa's surface is actually much older than current cratering models suggest [*Zahnle et al. 2003*].

From the standpoint of the dynamical evolution of the Galilean satellite system, there is good reason to believe that Europa's surface evolution could be cyclical. If so, Europa could experience cyclical variations in its orbital characteristics and tidal heating on time scales of perhaps 100 million years [*Hussman and Spohn 2004*].

Global monochrome and color imaging, coupled with topography and subsurface sounding, would enable these evolutionary models to be tested. Europa's surface features generally brighten and become less red through time, so albedo and color could serve as a proxy for age [*Geissler et al. 1998, Moore et al. 2009*]. Quantitative topographic data [*Schenk and Pappalardo 2004*] could provide information on the origin of geologic features and may show trends with age. Profiles across ridges, bands, and various chaotic terrains would aid in constraining their modes of origin. Moreover, flexural signatures are expected to be indicative of local elastic lithosphere thickness at the time of their formation, and may provide evidence of topographic relaxation [*e.g., Nimmo et al. 2003, Billings and Kattenhorn 2005*].

Characterizing Potential Future Landing Sites

A capable lander has been identified as a high priority follow-up to a Europa Orbiter if Europa is found to have habitable environments at present with active material exchange between subsurface water and the near surface [*SSB 2003*, *NASA 2006*]. Soft landed missions would require high-resolution images (~1 m/pixel or better) to assess the surface on scales needed for safe surface access. The roughness and overall safety of potential landing sites could also be characterized through radar scattering properties, photometric properties, spectral analysis, thermal inertia, and detailed altimetry. Such data would also illuminate fine-scale processes that create and affect the regolith, including mass wasting, sputter erosion, sublimation, impact gardening, and frost deposition. Along with corresponding high-resolution subsurface sounding, these observations would help to assess possible mechanisms and likely sites of recent material exchange with the subsurface ocean. Characterizing the global radiation environment would also greatly aid in the choice of a landing site. These datasets would provide for hazard assessment, while imaging, radar, compositional, and thermal mapping would identify sites of greatest scientific interest and would yield data vital for the coupled engineering and scientific assessment of possible future landing sites.

Some remaining outstanding questions related to Europa's geology include:

- Do Europa's ridges, bands, chaos, and/or multi-ringed structures require the presence of near-surface liquid water to form?
- Where are Europa's youngest regions?
- Is current geological activity sufficiently intense that heat flow from Europa's interior is measurable at the surface?

Questions such as these regarding Europa's geology could be answered using specific measurements, as discussed in §4.3.1.4.

4.2.1.5 Europa's Local Environment

Europa is immersed in a complex local environment that is the interface between Jupiter's magnetosphere and Europa's surface. Its tenuous atmosphere could provide important clues to its potential habitability. The intense flux of electrons and ions from the Jovian magnetosphere alters the surface by

radiation-induced chemistry, and erodes surface material by ion sputtering to produce a tenuous atmosphere. The radiation induced surface chemistry may have important consequences for life. In the near-surface ice, the particle radiation produces many highly oxidized species that react with other non-ice materials to form a wide array of compounds. Such compounds, if transported to the ocean, would provide an important source of chemical energy. At the surface, radiation processing alters any compounds that may have come from below, including any organics. To understand Europa's surface chemistry and thus its habitability, it is critical to understand how the local environment interacts with the surface.

Composed principally of molecular oxygen derived from the water ice surface, Europa's sputter-produced atmosphere has a surface pressure of just ~$2x10^{-12}$ bar [*Hall et al. 1995*]. The abundance and distribution of the atmospheric constituents are indicative of surface processes and provide a direct link to surface composition. Sputtering could eject water molecules, molecular oxygen, and any impurities within the ice, contributing to the erosion of surface features. Some of these molecules are ejected fast enough to escape Europa, some add to the satellite's atmosphere, while others return to the surface, potentially brightening the surface through time. Sputtering also has the potential to expose subsurface material that had not been in equilibrium with the atmosphere. Once released from the surface, some atmospheric constituents, such as Na and K, are more readily observed in their gas phase. Their abundance relative to that on Io provides a strong discriminator between endogenic and exogenic origin for these species, which has been used to argue for the presence of an ocean on Europa [*Johnson et al. 2002*]. Thus, probing the sputter-produced atmosphere of Europa is a means of studying surface constituents, from which parent molecules could be inferred.

The very plasma that produces the tenuous atmosphere also ionizes it to produce an ionosphere [*Kliore et al. 2001a*]. Existing observations of both the atmosphere (Figure 4-12) and ionosphere (Figure 4-13) exhibit considerable heterogeneity and complexity [*McGrath et al. 2009*], which is currently poorly understood [*Cassidy et al. 2007, 2008*]. A possible source of this heterogeneity might be active geysers [*Nimmo et al. 2007a,b*], the discovery of which would provide clues to subsurface processes and interior structure.

Close to Europa, an interaction region is formed in which the plasma, electric, and magnetic fields are perturbed from their background values. For example, the plasma slows in the upstream region approaching the satellite, enhancing the magnetic field strength in that region. The nature and strength of this

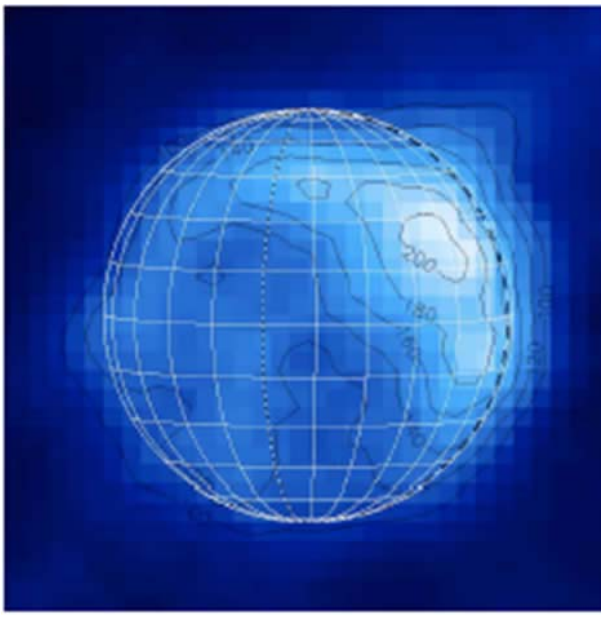

Figure 4-12. Oxygen emission from Europa's atmosphere, observed in ultraviolet wavelengths (1356 angstroms) with the Hubble Space Telescope [*McGrath et al. 2004*]. This image shows emissions to be bright in the anti-Jovian hemisphere, suggesting significant heterogeneity and complexity.

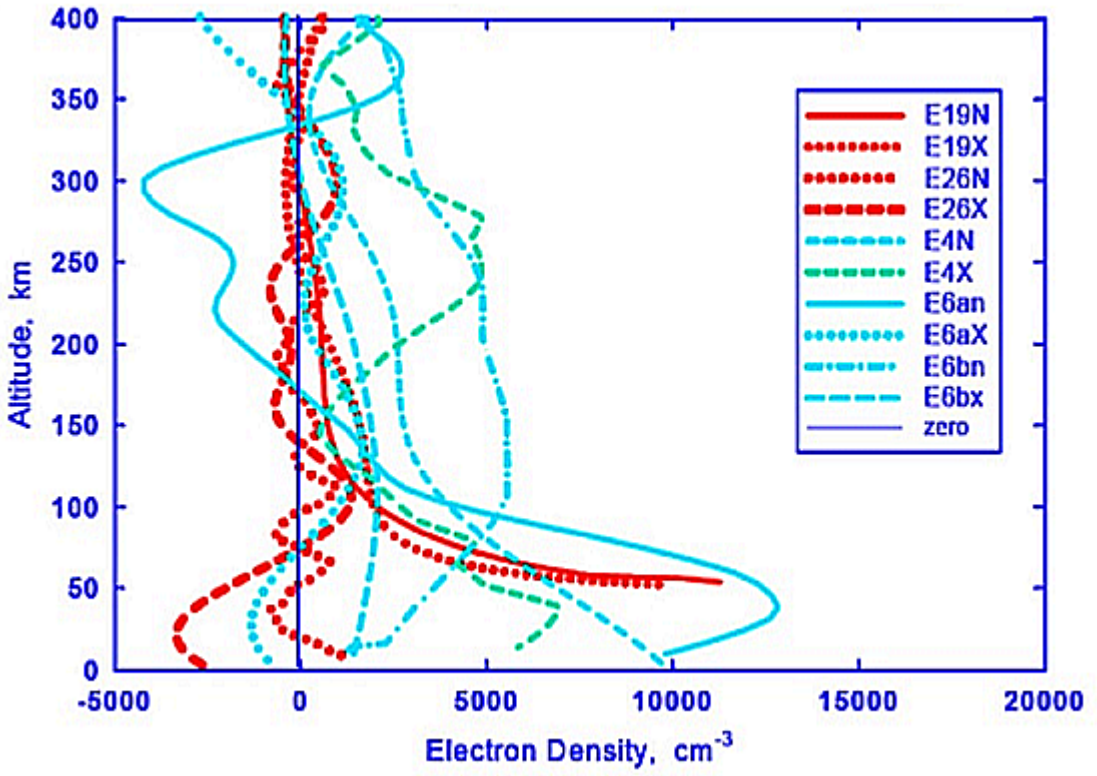

Figure 4-13. Compilation of all the Galileo radio occultation and near-occultation results illustrating the nonuniformity of Europa's ionosphere. Figure from *McGrath et al. [2009]*, courtesy of A. Kliore.

interaction field provides information on ionospheric conductivity, the scale height of the atmosphere, and the plasma pick-up rate. Because Europa also produces its own induced magnetic field, which implies the existence of an ocean, the interaction region would reflect those contributions as well. Characterizing the perturbations from plasma near Europa is critical for studies of the ocean electromagnetic induction. Because surface, atmospheric, ionospheric, and field and particle environments are intimately interconnected, an integrated set of magnetic field, plasma, energetic particle, and neutral atmosphere investigations are required to unravel the numerous processes involved.

- Are trace species that reveal properties of Europa's interior driven into the atmosphere in sufficient quantities to be detected?
- Is Europa's atmosphere produced chiefly by the interaction of magnetospheric particles with the surface?

Questions such as these regarding Europa's environment could be answered using specific measurements, as discussed in §4.3.1.5.

4.2.2 Ganymede

Ganymede is the solar system's largest satellite and the only one known to have an intrinsic magnetic field. Its surface could be broadly separated into two geologically distinct terrains: ancient densely cratered terrain and younger heavily-tectonized terrain. Ganymede's surface composition is dominated by water ice [*McKinnon and Parmentier*

1986]. The edge of the bright polar "caps" appears to follow the magnetospheric boundary between open and closed field lines [*Khurana et al. 2007*], which provides an opportunity to examine differences in space weathering processes on the same surface under different conditions. Beyond the polar caps toward equatorial regions, are found dark non-ice materials, which may be hydrated frozen brines similar to those inferred for Europa; other minor constituents of Ganymede's surface include CO_2, SO_2, and some sort of tholin material exhibiting CH and CN bonds [*McCord et al. 1998b*]. There is also evidence for trapped O_2 and O_3 in the surface, as well as a thin molecular oxygen atmosphere, and auroral emissions that are concentrated near the polar cap boundaries [*McGrath et al. 2004*].

It is not clear how active Ganymede is today. Its internal dynamo implies a hot convecting iron core that is cooling today from a heating event that occurred only about 1 Gyr ago [*Showman et al. 1997*]. Based on crater counts and models of impactor flux, Ganymede's bright grooved terrain has a nominal age of ~2 Gyr; however, large uncertainties in the impact flux through time imply that grooved terrain may have been emplaced any time from ~400 Myr to >4 Gyr ago [*Zahnle et al. 2003*]. The level of activity is an important outstanding question.

4.2.2.1 Ganymede's Ocean and Interior

Gravity: Ganymede's bulk density is 1.94g/cm^3, implying a bulk composition that is about 40% ice and 60% rock. Analysis of Galileo data from several close flybys indicates that Ganymede's moment of inertia is 0.31 MR^2. The factor of 0.31 is the smallest measured value for any solid body in the solar system, implying a strongly differentiated interior [*Anderson et al. 1996*]. Three-layer models, constrained by plausible compositions, indicate that Ganymede is strongly differentiated into an outermost ~800 km thick ice layer and an underlying silicate mantle of density 3000–4000 kg/m^3. A central iron core is allowed, but not required, by the gravity data. The existence of Ganymede's magnetic field, however, supports the presence of such a metallic core, and implies that it is hot enough (>1300 K, *Anderson et al. 1996*) to be at least partially molten today. Galileo gravity data also indicate that Ganymede has internal mass anomalies, possibly related to topography on the ice-rock interface or internal density contrasts [*Anderson et al. 2004, Palguta et al. 2006*].

Ocean

Galileo magnetometer data provide tentative evidence for an inductive response at Ganymede, which again suggests the presence of a salty internal ocean tens of kilometers thick at a nominal depth of 170 km. However, the inference is less robust Europa and Callisto, because the existing flyby data are equally well explained by an intrinsic quadrupole magnetic field (superposed on the intrinsic dipole), with an orientation that remains fixed in time [*Kivelson et al. 2002*]. The tidal response of a satellite's icy shell strongly depends on the presence of an ocean. Theoretically predicted tidal amplitudes on Ganymede are about 7 to 8 m if an ocean is present, and a few tens of cm if there is no ocean [e.g. *Moore and Schubert 2000*].

Magnetic field

Magnetometer data acquired during several close flybys show that Ganymede has an intrinsic magnetic field strong enough to generate a mini-magnetosphere embedded within the Jovian magnetosphere [*Kivelson et al. 1996*]. A model with a fixed Ganymede-centered dipole superposed on the ambient Jovian field provides a good first-order match to the data and suggests equatorial and polar field strengths of ~719 and 1438 nT, respectively; these values are 6–10 times the 120 nT ambient Jovian field at Ganymede's

orbit. Detection of numerous electromagnetic and electrostatic waves and measurements of energetic particles close to Ganymede confirm the inference of a magnetosphere. The most plausible mechanism for generation of Ganymede's intrinsic field is dynamo action in a liquid-iron core [*Schubert et al. 1996*].

Some of the remaining outstanding questions related to Ganymede's interior structure include:

- What are the characteristics of Ganymede's magnetic field and how is it generated?
- Is Ganymede in hydrostatic equilibrium?
- What is the role of tidal heating in Ganymede evolution?

4.2.2.2 Ganymede's Ice Shell

Ganymede's outer Ice I shell is believed to be ~100 km thick above the internal ocean. [*Spohn and Schubert 2003*]. A thermal gradient steep enough to induce melting implies an internal structure of ice phases I, III, V and VI with increasing depth, comprising the remainder of Ganymede's ~800 km thick H_2O layer. The minimum melting temperature of the ocean (near 250K) occurs at the phase boundary between ice I and ice III. A cooler ocean and a thinner ice shell would be possible if alkali and halide salts were present.

Little is known of the internal structure of the ice shell, and how it relates to surface geology (§4.2.2.4.). The uppermost several kilometers of the ice shell is expected to behave as a cold brittle-plastic material that undergoes faulting, while the warmer lower portion is expected to flow on geological time scales. Models of grooved terrain formation involve stretching and faulting of the upper brittle ice lithosphere, with associated regular pinching and swelling [*Pappalardo et al. 1998b, Dombard and McKinnon 2001*]. Grooved terrain formation may have involved cryovolcanism, creating horizontal layering in the shallow subsurface. It has been suggested that convective ice plumes might well up through the ice shell during the emplacement of bright grooved terrain [*Kirk and Stevenson 1987*]. If Ganymede's ice shell is still geologically active today, then thermal heterogeneities should exist within the ice shell.

A key outstanding question related to Ganymede's ice shell is:

- Has there been material exchange between the deep interior, the ocean, ice shell and surface?

4.2.2.3 Ganymede's Composition

The relationship between ice and non-ice materials and their distribution is a crucial point to understand the origin and evolution of the surfaces of the Galilean satellites, as surface material could be a link to the interior of the moons and provides constraints about the environment in which these bodies were formed and currently exist.

High-resolution NIMS spectra of Ganymede show absorption bands interpreted to be hydrated salt minerals [*McCord et al. 2001a*], very similar to the possible hydrated salts found on Europa. This implies that some briny liquid has modified the surface, possibly erupted from the subsurface. The organic material may be formed in situ from radiolysis and chemical reactions within the contaminated icy crust, and from exogenic material falling onto Ganymede's surface. Bright terrain contains less CO_2 than dark terrains, i.e. CO_2 is concentrated in the non-ice material(s) present, not in the fraction that is ice, and there does not appear to be any leading/trailing hemisphere asymmetry in the distribution of CO_2 nor do impact craters tend to be CO_2 rich [*Hibbitts et al. 2003*], while CO_2 is occasionally enriched in terrain

containing larger grained ice in comparison with adjacent terrain of similar morphology and ice abundance.

Ganymede shows evidence of the presence of oxygen species, particularly solid O_2 and O_3 [*Noll et al. 1996, Hendrix et al. 1999*] in the trailing hemisphere, consistent with the preferential orientation of that side of the satellite with Jupiter's magnetosphere. Both of these species are trapped within the ice, and probably originate from ionic bombardment of the icy surface. In addition, the interaction with the Jovian magnetosphere causes spectral differences with respect to the crystallinity and particle size of H_2O ice between the equatorial and the polar regions of Ganymede [*Hansen and McCord 2004, Stephan 2006, Stephan et al. 2009*]. O_3 abundance varies with latitude, with the strongest absorption measured at higher latitudes. This is caused by the configuration of Ganymede's own magnetic field that at least partly protects surface regions between ±40° latitude from impacting magnetospheric particles.

Questions remain about the composition of Ganymede's surface and interior, including:

- What is the chemical composition of visually dark, non-water-ice materials on Ganymede, and how do they correlate with surface geology?
- How are the compositions and physical states of materials on Ganymede altered by radiation weathering effects?
- What is the temporal cycle of the oxygen species on Ganymede?

4.2.2.4 Ganymede's Geology

With its mix of old and young terrain, ancient impact basins and fresh craters, and landscapes dominated by tectonics, icy volcanism, or slow degradation by space weathering, Ganymede serves as a "type example" for understanding many icy satellite processes throughout the outer solar system. Understanding the surface of this largest example of an icy satellite would provide insight into how this entire class of worlds evolves differently from the terrestrial planets.

Dark terrain

Dark terrain covers 1/3 of the surface and is dominated by impact craters with a variety of morphologies. It is ancient (perhaps essentially primordial), and appears grossly similar to the surface of Callisto [*Prockter et al. 1998*]. In addition to craters, dark terrain also displays hemisphere-scale sets of concentric troughs termed furrows, which are probably the remnants of vast multi-ring impact basins, now disrupted by subsequent bright terrain tectonism. This type of terrain appears dark due to the addition of a non-ice contaminant that appears to be concentrated at the surface by a variety of processes including sublimation, sputtering and mass wasting [*Spencer et al., 1987,; Prockter et al. 1998*].

Bright terrain

Bright terrain separates the dark units in broad, up to several hundred kilometers wide, linear or curved parallel, closely spaced grooves, termed sulci (Figure 4-14). The grooves are

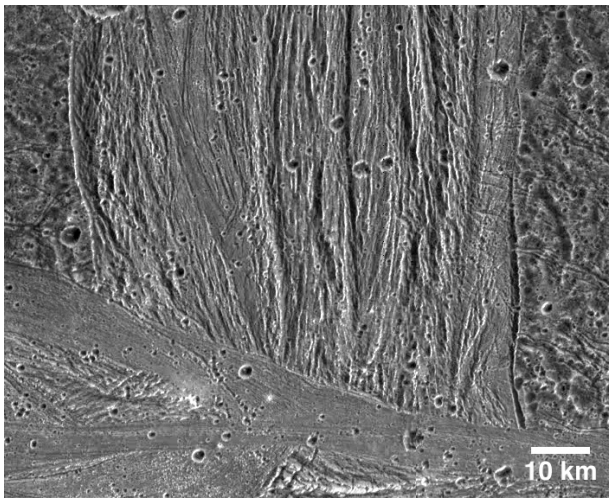

Figure 4-14. Bright grooved terrain of Erech Sulcus is cut by smooth bright terrain of Sippar Sulcus (bottom) on Ganymede. Both are younger than the dark terrain that straddles Erech Sulcus.

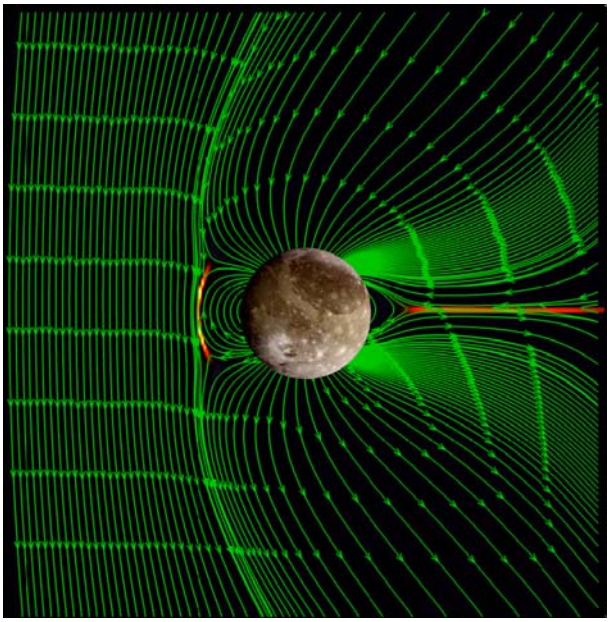

Figure 4-15. Ganymede's magnetosphere, simulated by *X. Jia, UCLA, 2007*. Field lines are green; current perpendicular to B is represented by color variation. Note intense currents flow both upstream on the boundary between Jupiter's field and the field lines that close on Ganymede, and downstream in the reconnecting magnetotail region.

dominated by extensional tectonic features, and morphologically and genetically have much in common with terrestrial rift zones [*Parmentier et al. 1982, Pappalardo et al. 1998b*]. Bright terrain exhibits the full range of extensional tectonic behavior, from wide rifting, to narrow rifting, to possible examples of crustal spreading (much like the smooth bands on Europa). The bright terrain units formed predominantly at the expense of dark terrain through a process termed tectonic resurfacing, causing the partial or total transformation of dark terrain into bright terrain by tectonism [e.g. *Pappalardo et al. 1998b*]. Generally, grooved terrain represents rifts created by extensional stress [*Pappalardo et al. 2004*].

Several caldera-like, scalloped depressions termed paterae are found in the bright terrain represent probable volcanic vents [*Pappalardo et al. 2004*] and ridged deposits in one of the largest of such paterae were interpreted as cryovolcanic flows [*Head et al. 1998*]. The smoothest units as found in a number of localities in bright terrain could have been created by extrusion of low viscosity cryomagmatic materials [*Giese et al. 2001*, *Schenk et al. 2001*]. The smoothest units also exhibit some degree of tectonics, suggesting that cryovolcanism and tectonic deformation are closely linked [*Head et al. 2002*].

Although the ultimate driving mechanism for groove formation is uncertain, it may be tied to the internal evolution of Ganymede and the history of orbital evolution of the Galilean satellite system [*Showman et al. 1997*].

Impact features

The impact features on Ganymede exhibit a wider range of diversity than those on any other planetary surface. They include vast multi-ring structures, low-relief ancient impact scars called palimpsests, craters with central pits and domes, pedestal craters, dark floor craters, and craters with dark or bright rays (see review in *Schenk et al. 2004*). The largest structures have been dissected by the formation of grooved terrain into partial systems termed furrow systems. The original multi-ring basins are interpreted to have formed by impact into a very thin lithosphere [*McKinnon and Melosh 1980*]. The subdued character of Ganymede's oldest impact craters imply a steep thermal gradient in Ganymede's early history, with more recent impact structures reflecting a thicker and stiffer elastic lithosphere [*Passey and Shoemaker 1982, Shoemaker 1982*]. Such an interpretation indicates a much warmer shallow subsurface early in Ganymede's history than at present.

Many questions remain about the origin and evolution of Ganymede's surface features, such as:

- What are the origins and ages of Ganymede's surface features, and what could they tell us about the moon's evolution?
- What is the role of cryovolcanism in the formation of surface features?

4.2.2.5 Ganymede's Local Environment

Ganymede is unique among planetary moons: it has an intrinsic magnetic field, which couples with the surrounding Jovian magnetosphere to form a magnetosphere in miniature within the Jovian system (Figure 4-15). The magnetic field permits plasma access to the surface most easily at the poles, resulting in brightening of the polar caps [*Khurana et al. 2007*]. Ganymede's surface is bombarded by particles from Jupiter's radiation belt, creating a weak exosphere, an ionosphere, and aurorae. The aurorae represent "maps" of these interactions, although the details of the processes causing them are not well understood. Ganymede's hydrogen exosphere, measured by the Galileo UVS in a limb scan [*Barth et al. 1996*] is produced by sputtering processes and sublimation of the surface materials. Exospheric properties are thus indicative of processes at and composition of the surfaces. Ganymede also has a thin O_2 atmosphere, inferred from measurements of UV emissions [*McGrath et al. 2004*].

Outstanding questions about Ganymede's local environment include:

- What are the major exogenic surface alteration processes?
- What are the sources and sinks of the atmospheric constituents?
- How does Ganymede's magnetosphere interact with the Jovian magnetosphere?

4.2.3 Jupiter System

4.2.3.1 Jovian Satellites

The Jovian system, including Jupiter, its satellites, and the magnetic field and particle environment, constitutes a model for the evolution of planetary systems, including that of our Sun and those being discovered around other stars.

The Galilean satellites formed out of the Jovian circumplanetary disk and have since evolved through complex interactions with the other satellites, Jupiter, and Jupiter's magnetosphere.

Europa and Ganymede cannot be understood in isolation, but must be considered in the context of the entire Jovian system. Europa and Ganymede formed out of the Jovian circumplanetary disk and have since evolved through complex interactions with the other satellites, Jupiter, and Jupiter's magnetosphere. In order to understand the potential habitability of Europa and Ganymede, and icy moons in general, it is critical to understand how the intricately related components of the Jovian system originated and evolved, and how they currently operate and interact. This requires observations of the other Galilean satellites, the Jovian magnetosphere and particle environment, the planet Jupiter itself, and the minor satellites and ring system. The Jupiter system science background section that follows emphasizes connections to Europa and its potential habitability, while touching on additional important Jupiter system science. The discussion is organized into five themes: satellite surfaces and interiors, satellite atmospheres, plasma and magnetospheres, Jupiter atmosphere, and rings, dust and small moons.

Satellite Surfaces and Interiors

The present environment of Europa depends in part on how it formed and evolved. Europa itself does not record its early surface history. However, its neighboring satellites—Io, Ganymede and Callisto—provide clues to Europa's origin, evolution, and potential habitability, through studies of their surfaces

and interiors (Figure 4-3). They are also of great scientific interest on their own.

Io. The innermost of the Galilean satellites, Io, is undergoing intense tidally driven volcanism. Io is important for understanding Europa because it illuminates Europa's own tidal heat engine and provides a window on Europa's silicate interior. Moreover, Io is potentially a major source of contamination of Europa's surface. But Io is also fascinating in its own right as an extreme example of interior, volcanic, atmospheric, and plasma processes that are important throughout the solar system.

Io's density of 3530 kg m^{-3} suggests a primarily silicate interior [*Keszthelyl et al. 2004*]. A 4:2:1 Laplace resonance between Io, Europa, and Ganymede as they orbit Jupiter leads to tidal flexing of the order of ~100 m at Io's surface, generating the heat that powers global volcanism [*Yoder and Peale 1981*].

Galileo data indicate the presence of extensive moon-plasma interactions near Io but appear to rule out a strong intrinsic dipolar magnetic field. Io's moment of inertia inferred from Galileo of 0.377 MR^2 (M and R = satellite mass and mean radius, respectively), suggests that the satellite is differentiated into a metallic core and silicate mantle [*Anderson et al. 2001*]. Io is thought to have a large Fe-FeS core. The apparent lack of an intrinsic magnetic field suggests that the silicate mantle is currently experiencing sufficiently strong tidal heating to prevent cooling and, therefore, there is no convective dynamo in the putative iron core [*Wienbruch and Spohn 1995*].

Io's mantle appears to undergo a high degree of partial melting (~5–20% molten [*Moore 2001*]) that produces mafic to ultramafic lavas dominated by Mg-rich orthopyroxene, suggesting a compositionally undifferentiated mantle. Silicate volcanism appears to be dominant, although secondary sulfur volcanism may be locally important. The heat flux inferred from long-term thermal monitoring of Io exceeds 2 W/m^2, making Io by far the most volcanically active solid body in the solar system (Figure 4-17) [*Nash et al. 1986, Veeder et al. 2004, McEwen et al. 2004, Lopes and Spencer 2007*]. This heat flow is probably higher than could be supported by steady-state tidal heating.

Despite the high heat flux, the existence of numerous mountains up to 18 km high indicates that the lithosphere is at least 20–30 km thick, rigid, and composed mostly of silicates with possibly some sulfur and sulfur dioxide (SO_2) components [*e.g., Carr et al. 1998, Schenk and Bulmer 1998, Turtle et al. 2001, Jaeger et al. 2003*]. The thick lithosphere could only conduct a small fraction of Io's total heat flux, and Io may lose its heat primarily by magmatic transport through the lithosphere [*O'Reilly and Davies 1981, Carr et al. 1998, Moore 2001*]. Io's rapid resurfacing rate (Io has no known impact craters) requires a gradual subsidence of its lithosphere, which could cause a compressional lithospheric environment that may help to explain the formation of Io's numerous mountains [*Schenk and Bulmer 1998*].

High-temperature volcanism (≥1300°C) suggests superheated mafic to slightly ultramafic magmas, though these temperatures are lower limits and higher temperatures are possible. Silicate lavas, sulfur, and sulfur dioxide materials interact in a complex and intimate way, and volcanic styles include massive inflating lava flow fields; major, explosive, high-temperature outbursts; and overturning lava lakes. Volcanic plumes erupt both from central vents and lava flow fronts (Figure 4-16) where surface volatiles are remobilized. Volcanism and sputtering on Io feed a unique patchy and variable atmosphere, in which sulfur, oxygen, and sodium become ionized to form Io's plasma torus, neutral

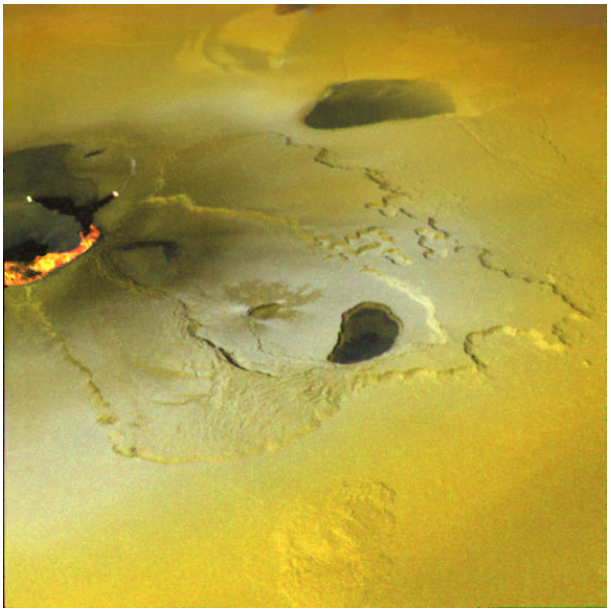

Figure 4-16. In the Tvashtar region of Io, active glowing volcanic flows (left) were observed by the Galileo spacecraft. A series of volcanic calderas were observed over several years by Galileo in this region. At one time, a 25 km long, 1–2 km high curtain of lava was erupted, followed by a plume of gas that rose 385 km above the surface, blanketing areas as far as 700 km away.

clouds, and aurorae. Their abundance relative to that on Europa provides a strong discriminator between endogenic and exogenic origin for these species, which has been used to argue for the presence of an ocean on Europa [*Johnson et al. 2002*]. Sublimation of SO_2 frost is also a source of Io's thin atmosphere; the relative contributions of sublimation and volcanism to the atmosphere are not well understood. Because material from Io is transported to and implanted in the surface of Europa, it is important to understand the nature of the Io atmosphere, the ultimate source of the exogenic material that contaminates Europa. Electrical current flows between Io and Jupiter and produce auroral footprints in the Jovian atmosphere. Near the ionospheric end of the Io flux tube, accelerated electrons interact with the Jovian magnetic field and generate decametric radio emissions [*Lopes and Williams 2005*].

There is an apparent paradox between Io's putative ultramafic volcanism and the widespread intensity of the volcanism on Io, which might be expected to produce extreme differentiation and thus silica-rich eruptions (at the current rate, Io would have produced a volume of lava ~40 times its global volume over the last 4.5 Gyr). The resolution of this paradox requires either that Io only recently entered the tidal resonance and became volcanically active, or that wholesale recycling of Io's lithosphere is sufficient to prevent extreme differentiation [*McEwen et al. 2004*].

Galileo's study of Io's dynamic processes was severely hampered by its low data rate. Major volcanic events were missed entirely or seen only in disconnected snapshots, and only a small sample of its diverse landforms was studied in any detail (for instance, the 2001 Surt eruption seen from Earth [*Marchis et al. 2002*] was 20 times brighter than anything seen by Galileo).

Outstanding science issues for Io include: understanding the mechanisms responsible for the formation of its surface features, determining the surface compositions, and investigating the implications for the origin and evolution and transport of surface materials. Specific issues relate to these science areas: a) understanding Io's heat balance and tidal dissipation, and their relationship to Europa's tidal evolution; b) Io's active volcanism for insight into rare, major volcanic events and their effect on the surface and atmosphere; c) the relationships among volcanism, tectonism, erosion and deposition; d) the silicate and volatile components of Io's crust; and e) the composition of material escaping from Io which would help to distinguish endogenic and Io-derived materials on the surface of Europa.

Additional gravity data during Io flybys would place more stringent constraints on interior structure. New discoveries are likely, e.g., gravity anomalies similar to that detected by Galileo on a Ganymede flyby [*Palguta et al. 2006*]. Determination of Io's pole position and changes in the location of the pole with time might be possible with high resolution imaging; these observations would also place constraints on the satellite's shape and, thus, internal structure. It might also be possible to determine any secular acceleration of Io in its orbit through the combination of Doppler tracking and high-resolution imaging, thus constraining the orbital and tidal evolution of the system. Heat flow mapping would place important constraints on theories of tidal dissipation in Io and on the satellite's internal structure and thermal and orbital evolution and those of its sibling Galilean satellites.

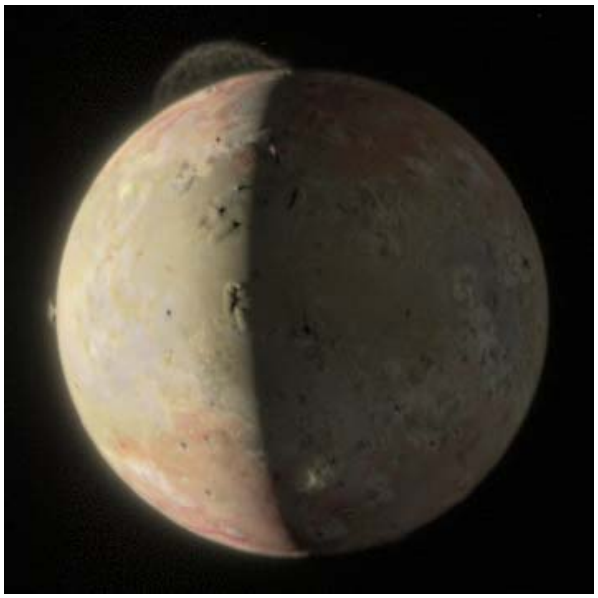

Figure 4-17. Volcanic plumes on Io, as imaged by the LORRI instrument on the New Horizons spacecraft at a distance of 2.5 million km (35 Rj). A 290 km high plume from the volcano Tvashtar (top) shows detailed structure. A 60-km high symmetrical plume from the volcano Prometheus (left) has been active during all spacecraft flybys since Voyager. Long-term observations and flybys with JEO would provide unprecedented detail of Io's dynamic volcanism.

Callisto. As the outermost large satellite of Jupiter, Callisto is the least affected by tidal heating and the least differentiated, thus offering an "endmember" example of satellite evolution for the Jovian system [see reviews in *McKinnon and Parmentier 1986, Showman and Malhotra 1999,* and *Moore et al. 2004*]. Accordingly, assessing its internal structure, geologic history, compositional evolution, impact cratering history, and radiolysis of its surface are important to understanding the evolution of the Jovian satellites.

Galileo gravity data plus the assumption of hydrostatic equilibrium suggest that Callisto's moment of inertia is $0.355\ MR^2$, suggesting that it has a partially differentiated structure containing an ice-rich outer layer less than 500 km thick, an intermediate ice-rock mixture with a density near 2000 kg/m^3, and a central rock/metal core [*Anderson et al. 1998*]. However, if Callisto's degree-2 gravity structure is not hydrostatically balanced, then Callisto could be more or less differentiated than the moment of inertia suggests. This could have major implications for understanding satellite formation. Pre-Galileo models suggested that Ganymede and Callisto formed from debris in a proto-Jovian disk in ~10^4 years; however, for Callisto to be undifferentiated, its formation time must have exceeded 10^6 years [*Canup and Ward 2002, Mosqueira and Estrada 2003*].

Galileo magnetometer data indicate that Callisto has an inductive magnetic response that is best explained by a salty ocean within 200 km of the surface [*Khurana et al. 1998, Kivelson et al. 1999, Zimmer et al. 2000*]; properties of the ice phase diagram strongly suggest that the ocean on Callisto (and Ganymede) lies ~160 km below the surface. Maintaining an ocean in Callisto today either requires stiffer ice rheology than is generally assumed (to slow down the convective heat

loss) or existence of antifreeze (ammonia or salts) in the ocean. However, reconciling partial differentiation with the existence of the ocean is difficult: some part of the uppermost ice layer must remain at the melting temperature to the present day, while the mixed ice-rock layer must never have attained the melting temperature.

Along with the discovery of Callisto's conducting, probably fluid sub-surface layer, major Galileo discoveries about Callisto include the absence of cryovolcanic resurfacing and the inference of surface erosion by sublimation. Callisto's landscape at decameter scales, and particularly its lack of small craters, is unique among the Galilean satellites, and might be akin to that of cometary nuclei. The process of sublimation degradation is recognized as a key surface modification process on Callisto (Figure 4-18).

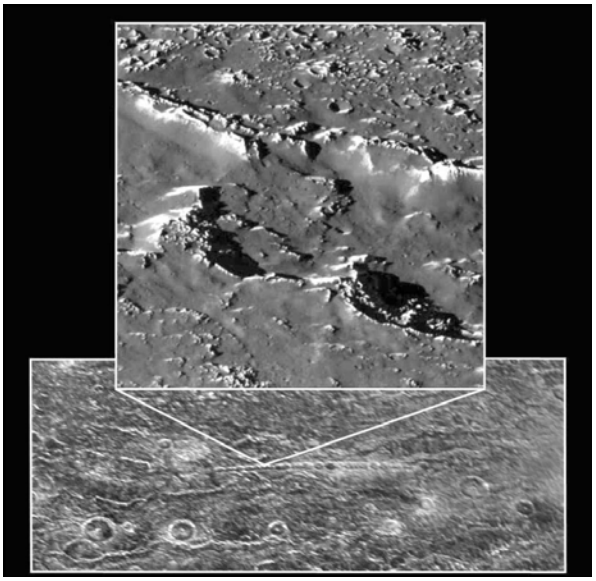

Figure 4-18. Galileo images of a catena (crater chain) on Callisto. Note the dearth of small craters in the inset, which shows an area 8 km across.

The primary surface composition of Callisto is bimodal (water ice and an unidentified non-ice material), with trace constituents detected in the non-ice material. The visible color of the non-ice material is similar to C-type asteroids and carbonaceous chondrites. The trace materials detected in the non-ice material include CO_2, SO_2, and substances containing C-H, C-N, and possibly S-H functional groups, and they may be present in the ice as well [*McCord et al. 1998, Carlson et al. 1999*]. Carbon dioxide is detected as an atmosphere and is nonuniformly dispersed over the surface, but concentrated on the trailing hemisphere and more abundant in fresh impact craters [*Hibbitts et al. 2002*]. This hemispheric asymmetry is similar to that for sulfate hydrates on Europa and is also suggestive of externally induced effects by corotating magnetospheric plasma [*Cooper et al. 2001*]. Callisto is thought—like Europa and Ganymede—to have a predominantly O_2 atmosphere, but lacks oxygen emissions like those detected from Europa, Io, and Ganymede [*Strobel et al. 2002*]. Instead, Callisto has CO_2 emission above the limb, detected by the Galileo NIMS [*Carlson 1999*]. IR limb scans at Europa were not performed by NIMS. Small amounts of CO_2 may well be present in Europa's atmosphere, by analogy with Callisto. Callisto's atmosphere may be thicker than either Europa's or Ganymede's [*McGrath et al. 2004, Liang et al. 2005*], which is reflected by its relatively dense ionosphere [*Kliore et al. 2002*].

Outstanding questions remaining in Callisto studies include:

- What is the configuration of its interior and is there a rock core?
- What is the composition and structure of the upper "crust?"
- What controls impactor populations, and what are the retention ages represented by crater counts?
- What does Callisto reveal about Galilean satellite formation and evolution? Is the reason Callisto and Ganymede had divergent histories solely the consequence of the role of tidal heating, or are there

viable alternative explanations (such as accretion dynamics)?

4.2.3.2 Small Satellites and Rings

A system of small moons and faint rings encircles Jupiter (Figure 4-19) within Io's orbit. Although Saturn's ring system is more familiar, faint and dusty rings are much more common in the outer solar system, encircling all four of the giant planets, and may represent the end result of the evolution of a much denser ring system such as Saturn's. Dusty rings are of interest because they reveal a variety of non-gravitational processes that are masked within more massive disks. For example, fine dust grains become electrically charged by solar photons and by interactions with Jupiter's plasma. Their orbits are perturbed by solar radiation pressure and by Jupiter's magnetic field [*e.g., Burns et al. 2004*]. Therefore, a better description of dust dynamics and properties has the potential to provide valuable information about Jupiter's plasma and magnetic field within regions that cannot be easily probed by spacecraft.

Jupiter's dusty rings may serve as a source of exogenic material on the surfaces of the Galilean satellites. Most ring dust evolves inward, but Galileo images show a very faint stream of material moving outward from Thebe [*Burns et al. 1999*, *Showalter et al. 2008*]. Little is known about this material, but *Hamilton and Krueger* [*2008*] attribute it to grains trapped in a particular orbital resonance with Jupiter's shadow. Furthermore, *Horanyi et al.* [*1993*] have found that ring dust could contribute to dust streams emanating outward from Jupiter (although they regard Io as the dominant source).

Over relatively brief time scales, dust grains are swept from the system by drag forces or destroyed in place by impacts. They must therefore be continuously replenished from some reservoir. The inner moons clearly play a role—Amalthea and Thebe bound the especially faint "gossamer" rings [*Burns et al. 1999*], and these moons orbit near the edge of Jupiter's main ring. However, images indicate a family of additional bodies inside the main ring, which could contribute most of the main ring's dust [*Showalter 2007*]. However, New Horizons searched for kilometer-sized moons and found none, indicating a peculiar break in the size distribution below 8 km, the radius of Adrastea. Perhaps this is the result of a balance between accretion and disruption for small bodies orbiting at the edge of Jupiter's Roche zone.

With typical optical depths of 10^{-6} to 10^{-8}, small injections of new dust could produce noticeable changes in the ring. Recent impacts might explain a variety of changes observed in the ring system over the years, including the appearances of arcs, clumps and other asymmetries. With regular monitoring over a long time baseline than currently possible, one could potentially use the rings to place new constraints on the present flux of meteoroids into the Jovian system. This result would have implications for the ages of all satellite surfaces.

Jupiter's rings share many of their properties with protoplanetary disks. In both systems,

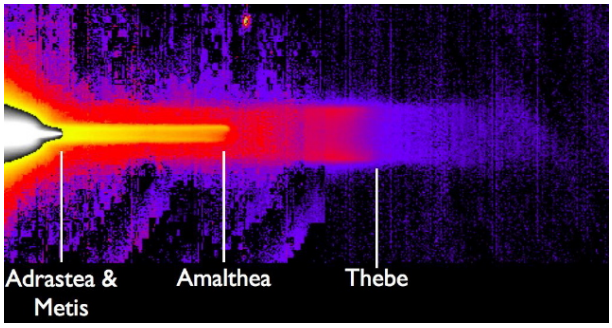

Figure 4-19. This edge-on color-coded mosaic of the ring system from Galileo shows the connection between the dust and inner satellites. Adrastea and Metis bound the main ring and its thick interior halo (white, left). Amalthea and Thebe each produce fainter rings (yellow and red), which are shaped like "tuna cans." The very faint outward extension to Thebe's ring (blue) is unexplained.

dust and larger bodies commingle and interact through a variety of processes: gravitational, collisional, and other. Thus, the ring system provides a dynamical laboratory for understanding the formation of the broader Jovian system.

4.2.3.3 Jovian Magnetosphere

To understand the Jovian system as a whole as well as to investigate the exchange processes between the moons and their environment it is fundamentally important to study the Jovian magnetosphere. Understanding the physics which drives the global configuration and the dynamic processes affecting the largest magnetosphere of our solar system is one of the outstanding goals in planetary magnetospheric science. Those processes occur on spatial scales ranging from several kilometers up to the size of the entire magnetosphere (hundreds of Jovian radii); temporal scales range from several tens of minutes up to long-term variations of several days.

Previous missions to Jupiter significantly enhanced our knowledge of the Jovian magnetosphere. However, the single-point measurements along flybys provided only snapshots of the configuration at a given time. Eight missions thus far have made measurements close to Jupiter. Only Galileo orbited the planet for an extended period and was hence able to study physical phenomena on spatial and temporal scales from orbit, which is simply not possible during a spacecraft flyby.

In addition to the required strong internal magnetic field which is necessary to hold off the solar wind, the other two main ingredients of Jupiter's magnetosphere are the planet's fast rotation as the energy driving source, and the Galilean moon Io as the major source of plasma residing deep inside the magnetosphere. Neutral material preferentially in the form of SO_2-molecules from Io's active volcanoes are dissociated and charged into oxygen and sulphur ions. The picked-up plasma populates a torus region between 5 and 10 R_J. Low-energy charged particles are transported radially outward due to centrifugal forces stretching the magnetic field lines into a magnetodisc-like configuration around the magnetic equator. Since the magnetic dipole axis and the rotation axis of Jupiter are displaced by 9.7 degrees relative to each other, the magnetodisc wobbles up and down by +/- 9.7 degrees around the rotational equator.

The population of plasma and charged particles rigidly corotates with the planet in this confined magnetodisc up to a certain distance until the forces in the disc are too strong to maintain the rotation speed of the planet. As a result of the planet's attempt to speed the disc in this location, current systems build coupling the magnetosphere and the upper atmosphere of the planet. As a result field-aligned electrons penetrating into Jupiter's ionosphere/atmosphere create auroral emissions. Beyond that distance the entire magnetosphere continues to rotate but with a significantly slower speed than that of the planet. Deep in the magnetotail reconnection of magnetic field lines occur and plasmoids are released periodically every few days.

Between the inner, middle and outer part of the Jovian magnetosphere transport processes occur, such as interchange motion in the inner magnetosphere where cold low-energy flux tubes are moved radially outward, while hot high-beta plasma is injected from the outer and middle magnetosphere into the inner region. Coupling processes between the magnetosphere and the ionosphere of the planet, e.g. field-aligned current systems, are also important tin order to aid understanding how the entire system reacts to dynamic changes.

All of these processes in the Jovian magnetosphere are far from being understood in detail. They are important for magnetospheric science in terms of Jupiter as a prototype for exoplanetary systems, and they are important to better understand how the moons inside the magnetosphere are affected by their local environment, *e.g.*, surface sputtering, space weathering, and radiation effects. Without a continuous monitoring of the various magnetospheric parameters it would be much more difficult to study the interaction and exchange processes which affect the moons.

EJSM would have the capability to shed light on most of the unanswered questions concerning Jupiter's magnetosphere via multi-point measurements with both remote sensing and in-situ instrumentation as well exploration of new regions of the magnetosphere not yet visited by spacecraft, or investigated by Juno.

4.2.3.4 Jovian Atmosphere

The exploration of Jupiter's dynamic atmosphere (Figure 4-20) has played a pivotal role in our understanding of the Solar System, serving as the paradigm for the interpretation of planetary systems around other stars. It serves as a fundamental laboratory for the investigation of large-scale geophysical fluid dynamics and the many physiochemical phenomena evident on the gas giants. However, despite decades of intense investigation, our characterization of this archetypal giant planet remains incomplete, with many fundamental questions about its nature unanswered. While the thin atmospheric "weather-layer," the only region accessible to direct investigation by remote sensing, is only a tiny fraction of Jupiter's total mass, it provides vital insights to the interior structure, bulk composition, and formation history of most of our solar system. The EJSM dual-spacecraft mission offers an unprecedented opportunity to study Jupiter's atmosphere over long temporal baselines of 2 years or more, and complementary spectral and imaging coverage from the far-UV to the sub-millimeter and radio wavelengths.

Jupiter's atmospheric structure and composition is the end product of energetic accretion processes, thermochemistry, photochemistry, condensation processes, planetary-scale turbulence and gravitational differentiation. Its atmosphere is characterized by distinct latitudinal bands of differing cloud colors, vertical motions, temperatures and vertical mixing strengths separated by strong zonal winds and perturbed by long-lived vortices, storms, polar circulations, convective outbreaks, wave activity and variable large-scale circulation patterns [*Rogers 1995, Ingersoll et al. 2004, West et al. 2004*]. Although primarily composed of hydrogen and helium, Jupiter also contains small amounts of

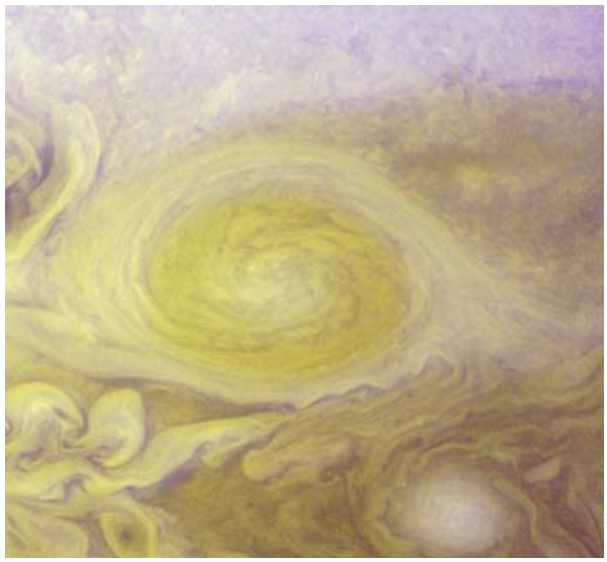

Figure 4-20. Image of Jupiter's "Little Red Spot" (LRS) from the LORRI instrument on the New Horizons spacecraft in February 2007, colorized using Hubble Space Telescope images [*Cheng et al. 2008*]. The spot formed from the merger of three white ovals in 1998–2000, and visibly reddened in late 2005. The LRS is approximately 4000 km in width half the size of the Great Red Spot. Image resolution is about 15 km/pixel, 10 times better than Hubble's. Images such as these permit an understanding of the development and dynamics of Jupiter's atmospheric storms.

heavier elements found in their fully reduced forms (CH_4, PH_3, NH_3, H_2S, H_2O), providing source material for complex photochemical pathways powered by UV irradiation [*Taylor et al, 2004, Moses et al. 2004*]. The abundances of most of these heavy elements are enriched over the solar composition, providing a window into the evolution of the primordial nebula material incorporated into the gas giants during their formation [*Lunine et al. 2004*]. Jupiter's vertical atmospheric structure is governed by a delicate balance between solar, chemical and internal energy sources, and its layers are coupled by poorly understood dynamical processes which transport energy, momentum and material [*Vasavada and Showman 2005*]. Finally, Jupiter's atmosphere is intricately connected to the charged-particle environments of the ionosphere and magnetosphere [*e.g., Yelle and Miller 2004*] and the local Jovian environment of the rings and icy satellites.

Atmospheric science goals are grouped into three categories, designed to address the open questions and mysteries raised by previous missions to the gas giant, and to complement Juno's studies of the deep interior.

Atmospheric Dynamics and Circulation

The plethora of dynamical and chemical phenomena of Jupiter's "visible" upper atmosphere (the "weather-layer") are thought to be governed by a balance between solar energy deposition and forcing from deeper internal processes. Moist convection, eddies, turbulence, vertical wave propagation and frictional damping are all believed to play a role in shaping and maintaining atmospheric circulation, and transporting energy, momentum and material tracers both horizontally and vertically [*e.g., Vasavada and Showman 2005, Salyk et al. 2006*]. Furthermore, Jupiter's atmosphere exhibits a wealth of time-variable phenomena that would be studied by both spacecraft, ranging from short-lived thunderstorms and lightning, formation and interaction of giant vortices, episodic plumes and outbursts, waves and turbulence to multi-year-long, quasi-periodic variations in the banded cloud patterns and storms ("upheavals"). An ongoing global upheaval of the banded structure occurred throughout 2007-2010 [*Sanchez-Lavega et al. 2008*], as well as the formation and reddening of new anticyclonic ovals in 2006 and 2008 [*Simon-Miller et al. 2006, Cheng et al. 2008*]. Asteroidal and cometary impacts influence the atmosphere over time scales from minutes to months and may be quite common. From EJSM, wave activity would be studied over a range of spatial scales, from sporadic equatorial mesoscale waves; to planetary-scale Rossby waves and the forcing of the Quasi-Quadrennial Oscillation [*Leovy et al. 1991*]; and gravity waves in the middle and upper atmosphere, which are thought to play an important role in energy transfer between different layers, particularly as a dominant source of heating in the thermosphere. EJSM would provide a comprehensive four-dimensional climate database of Jupiter to reveal the underlying physical processes at work in giant planet atmospheres.

Composition and Chemistry

Jupiter is the product of a myriad of thermochemical and photochemical pathways resulting from its bulk composition [*Atreya et al. 2003*]. Atmospheric composition determines the structures of the cloud decks; radiative energy balance influences the troposphere and middle atmosphere; and condensation processes could provide the energy required for convective dynamics. Furthermore, Jupiter's bulk composition provides a window on the formation and evolution of the gas giant, and connects it directly to the nature of the extensive satellite system. EJSM would: (a) use the spatial distribution of volatiles to understand the importance of moist convection in cloud formation, lightning and chemistry; (b) study localized and non-equilibrium composition

associated with discrete atmospheric features like storms and instabilities; (c) determine the 3D spatial distribution and variability of stratospheric hydrocarbons and exogenic oxygen-bearing species; and (d) assess the composition (especially hydrocarbons) in the mesosphere and thermosphere.

Vertical Structure of the Atmosphere and Interior

EJSM would characterize the vertical structure of Jupiter's atmosphere and the nature of coupling processes from the deep interior to the charged upper atmosphere, including wave propagation (transporting energy and momentum between layers), as well as ion drag and meridional circulation in the upper atmosphere. EJSM aims to globally map the vertical structure and optical properties of clouds and hazes from the millibar level to approximately 5 bar [*e.g., West et al. 2004*] to reveal the mechanisms responsible for aerosol production – photochemical production and sedimentation, condensation and uplift of NH_3 and NH_4SH ices, shock chemistry in lightning. In particular, we hope to discover the chromophores responsible for the differences in cloud coloration on Jupiter. Finally, EJSM would study the unique physiochemical processes occurring at high latitudes (e.g., auroral energy deposition and associated haze production, circumpolar waves, north/south asymmetry and high-latitude vortices) as a vital counterpoint to the seasonal asymmetries observed on Saturn by Cassini.

The objectives for Jupiter were developed to address big-picture questions about how Jupiter's atmosphere works as a coupled system, connected to both the deep interior and the immediate planetary environment. EJSM would provide the first four-dimensional climate database for the study of Jovian meteorology and chemistry, and would investigate the atmospheric structure, clouds and composition from the thermosphere down to the lower troposphere. The fundamental insights into Jupiter's origin, formation, and physiochemical processes would serve as the paradigm for the interpretation of gas giants in our solar system and beyond for decades to come.

4.3 EJSM Theme, Goals, and Traceability to Objectives and Investigations

The Galileo mission revealed the dynamic nature of the Jovian satellite system. Europa is probably an active world—and is potentially habitable. Ganymede resembles a planet in many respects, including the presence of an intrinsic magnetic field. However, many fundamental questions remain unanswered. The production, presence and transport of materials among the moons' surfaces, ice shells, and oceans are unknown; the thicknesses of their ice shells is uncertain by more than an order of magnitude; and the origins of most surface landforms remain mysterious. The influence of the Jovian environment is poorly understood, including the interplay among the jovian and satellite magnetospheres, plasma sources, and surface chemistry. In this section these open science issues are placed within the overall context of EJSM, and details are provided on how they would be addressed.

By understanding the Jupiter system and unraveling its history from origin to the possible emergence of habitats, we could understand better how gas giant planets and their satellites form and evolve. Most importantly, new light would be shed on the potential for the emergence of life in the galactic neighborhood and beyond. Thus, the overarching theme for EJSM has been formulated as:

The emergence of habitable worlds around gas giants.

To address this theme, the Jupiter system would be explored and the processes leading to the diversity of its associated components

and their interactions would be studied. The focus would be to characterize the conditions that might have led to the emergence of habitable environments among its satellites, with special emphasis on the two geologically active ocean-bearing worlds: Europa and Ganymede.

To understand the Galilean satellites as a system, Europa and Ganymede are singled out for detailed investigation. This pair of moons provides a natural laboratory for examining the nature, evolution, and potential habitability of icy worlds. The primary focus is on an in-depth comparative analysis of their internal oceans, current and past environments, surface and near-surface compositions, and geologic histories. Objectives for studying the other two Galilean satellites, Io and Callisto, are also defined, in order to understand their place in the Galilean satellite system and how their evolution has varied from that of the two innermost moons. To understand how gas giant planets and their satellites evolve, broader studies of Jupiter's atmosphere and magnetosphere would round out the Jupiter system investigation.

The fundamental theme for the EJSM is refined into science goals relating to habitability (focusing on Europa and Ganymede) and processes at work within the Jupiter system and the system's origin.

The traceability from the EJSM goal to objectives to investigations is summarized in Table 4-1. The complete traceability to example measurements and the generic instruments which could accomplish them is compiled in Foldout 1. These example measurements and generic instruments that could accomplish them are meant as a proof-of-concept to demonstrate the types of measurements that could address the investigations, objectives, and goals. These are not meant to be exclusive of other measurements and instruments that might be able to address the investigations and objectives in other ways. Moreover, it is understood and acceptable that the model payloads of JEO and JGO (§5.1.1 and §5.2.1, respectively) could not accomplish each example measurement of the Traceability Matrix, but the model payloads do address all of the highest priority investigations.

The Traceability Matrix (Table 4-1 and Foldout 1) is divided into the three goals:

1. Explore Europa to investigate its habitability
2. Characterize Ganymede as a planetary object including its potential habitability
3. Explore the Jupiter System as an archetype for gas giants

Each goal has specific objectives (listed in priority order), and each objective has specific investigations (listed in priority order).

In the detailed Traceability Matrix (Foldout 1), the example measurements that could address each investigation are also in priority order for each investigation. It is important to note that each investigation and objective requires multiple instruments to be fully accomplished. Thus, it is anticipated that data from multiple instruments will be obtained and analyzed collaboratively in order to fulfill the EJSM science objectives and goals.

Each objective and its investigations are described in sections §4.3.1 through §4.3.3, along with the corresponding example measurements that could address them. The right-hand colored columns of the matrix (Foldout 1) are ratings of the EJSM science value matrix, which is discussed in §5.3.

Table 4-1. EJSM High-Level Traceability Matrix

EUROPA				
Goal	**Science Objective**		**Science Investigation**	
Explore Europa to investigate its habitability.	**EA. Ocean**	Characterize the extent of the ocean and its relation to the deeper interior.	EA.1	Determine the amplitude and phase of the gravitational tides.
			EA.2	Determine the magnetic induction response from the ocean and characterize the influence of the space plasma environment on this response.
			EA.3	Characterize surface motion over the tidal cycle.
			EA.4	Determine the satellite's dynamical rotation state (forced libration, obliquity and nutation).
			EA.5	Investigate the core, rocky mantle, rock-ocean interface, and compensation of the ice shell.
	EB. Ice Shell	Characterize the ice shell and any subsurface water, including their heterogeneity, and the nature of surface-ice-ocean exchange.	EB.1	Characterize the distribution of any shallow subsurface water and the structure of the icy shell including its subsurface properties.
			EB.2	Search for an ice-ocean interface.
			EB.3	Correlate surface features and subsurface structure to investigate processes governing material exchange among the surface, ice shell, and ocean.
			EB.4	Characterize regional and global heat flow variations.
	EC. Composition	Determine global composition, distribution and evolution of surface materials, especially as related to habitability.	EC.1	Characterize surface organic and inorganic chemistry, including abundances and distributions of materials, with emphasis on indicators of habitability and potential biosignatures.
			EC.2	Relate material composition and distribution to geological processes, especially material exchange with the interior.
			EC.3	Investigate the effects of radiation on surface composition, including organics, and regional structure.
			EC.4	Characterize the nature of exogenic (e.g., Io) materials.
			EC.5	Determine volatile content to constrain satellite origin and evolution.
	ED. Geology	Understand the formation of surface features, including sites of recent or current activity, and identify and characterize candidate sites for potential future *in situ* exploration.	ED.1	Determine the formation and three-dimensional characteristics of magmatic, tectonic, and impact landforms.
			ED.2	Determine sites of most recent geological activity, and evaluate future potential landing sites.
			ED.3	Constrain global and regional surface ages.
			ED.4	Investigate processes of erosion and deposition and their effects on the physical properties of the surface.
	EE. Local Environ-ment	Characterize the local environment and its interaction with the jovian magnetosphere.	EE.1	Characterize the composition, structure, dynamics and variability of the bound and escaping neutral atmosphere.
			EE.2	Characterize the composition, structure, dynamics and variability of the ionosphere and local (within the Hill sphere) charged particle population.

GANYMEDE				
Goal	**Science Objective**		**Science Investigation**	
Characterize Ganymede as a planetary object including its potential habitability.	**GA. Ocean**	Characterize the extent of the ocean and its relation to the deeper interior.	GA.1	Determine the amplitude and phase of the gravitational tides.
			GA.2	Characterize the space plasma environment to determine the magnetic induction response from the ocean.
			GA.3	Characterize surface motion over Ganymede's tidal cycle.
			GA.4	Determine the satellite's dynamical rotation state (forced libration, obliquity, and nutation).
			GA.5	Investigate the core and rocky mantle.
	GB. Ice Shell	Characterize the ice shell.	GB.1	Characterize the structure of the icy shell including its properties and the distribution of any shallow subsurface water.
			GB.2	Correlate surface features and subsurface structure to investigate near-surface and interior processes.
	GC. Local Environment	Characterize the local environment and its interaction with the jovian magnetosphere.	GC.1	Globally characterize Ganymede's intrinsic and induced magnetic fields, with implications for the deep interior.
			GC.2	Characterize the particle population within Ganymede's magnetosphere and its interaction with Jupiter's magnetosphere.
			GC.3	Investigate the generation of Ganymede's aurorae.
			GC.4	Determine the sources and sinks of the ionosphere and exosphere.
	GD. Geology	Understand the formation of surface features and search for past and present activity.	GD.1	Determine the formation mechanisms and characteristics of magmatic, tectonic, and impact landforms.
			GD.2	Constrain global and regional surface ages.
			GD.3	Investigate processes of erosion and deposition and their effects on the physical properties of the surface.
	GE. Composition	Determine global composition, distribution and evolution of surface materials.	GE.1	Characterize surface organic and inorganic chemistry, including abundances and distributions of materials.
			GE.2	Relate compositions and properties and their distributions to geology.
			GE.3	Investigate surface composition and structure on open vs. closed field line regions.
			GE.4	Determine volatile content to constrain satellite origin and evolution.

JUPITER SYSTEM				
Goal	**Science Objective**		**Science Investigation**	
Explore the Jupiter system as an archetype for gas giants.	**SATELLITE SYSTEM**			
	S. Study the Jovian satellite and ring system	SA. Study Io's active dynamic processes.	SA.1	Investigate the nature, distribution and magnitude of tidal dissipation and heat loss on Io.
			SA.2	Investigate Io's composition and active volcanism for insight into its origin, evolution and geological history (particularly of its silicate crust).
			SA.3	Determine Io's dynamical rotation state (forced libration, obliquity and nutation).
			SA.4	Investigate the interior of Io.
			SA.5	Understand satellite origin and evolution by assessing sources and sinks of Io's crustal volatiles and atmosphere.
		SB. Study Callisto as a witness of the early jovian system.	SB.1	Investigate the interior of Callisto.
			SB.2	Characterize the space plasma environment to determine the magnetic induction response from Callisto's ocean.
			SB.3	Characterize the structure and properties of Callisto's icy shell.
			SB.4	Constrain the tidally varying potential and shape of Callisto.
			SB.5	Determine Callisto's dynamical rotation state (forced libration, obliquity and nutation).
			SB.6	Characterize surface organic and inorganic chemistry, including abundances and distributions of materials and volatile outgassing.
			SB.7	Characterize the ionosphere and exosphere of Callisto.
			SB.8	Relate material composition and distribution to geological and magnetospheric processes.
			SB.9	Constrain global and regional surface ages.
			SB.10	Determine the formation and characteristics of magmatic, tectonic, and impact landforms.
		SC. Characterize the rings and small satellites.	SC.1	Conduct a comprehensive survey of all the components of the Jovian ring-moon system.
			SC.2	Identify the processes that define the origin and dynamics of the ring dust, source bodies, and small moons.
			SC.3	Characterize the physical properties of the inner small moons, ring source bodies and dust.
			SC.4	Remotely characterize the composition, properties and dynamical groupings of the outer, irregular moons.
			SC.5	Perform disk-resolved and local characterization of one or more outer, irregular moons.

JUPITER SYSTEM				
Goal	**Science Objective**		**Science Investigation**	
Explore the Jupiter system as an archetype for gas giants.	**MAGNETOSPHERE**			
	M. Jovian magnetosphere	MA. Characterize the magnetosphere as a fast magnetic rotator.	MA.1	Understand the structure and stress balance of Jupiter's magnetosphere.
			MA.2	Investigate the plasma processes, sources, sinks, composition and transport (including transport of magnetic flux) in the magnetosphere and characterize their variability in space and time.
			MA.3	Characterize the large-scale coupling processes between the magnetosphere, ionosphere and thermosphere, including footprints of the Jovian moons.
			MA.4	Characterize the magnetospheric response to solar wind variability and planetary rotation effects.
		MB. Characterize the magnetosphere as a giant accelerator.	MB.1	Detail the particle acceleration processes.
			MB.2	Study the loss processes of charged energetic particles.
			MB.3	Measure the time evolving electron synchrotron emissions.
		MC. Understand the moons as sources and sinks of magnetospheric plasma.	MC.1	Study the pickup and charge exchange processes in the Jupiter system plasma and neutral tori.
			MC.2	Study the interactions between Jupiter's magnetosphere and Io, Europa, Ganymede, and Callisto.
			MC.3	Study the interactions between Jupiter's magnetosphere and small satellites.
	JUPITER			
	J. Jovian atmosphere	JA. Characterize the atmospheric dynamics and circulation.	JA.1	Investigate the dynamics of Jupiter's weather layer.
			JA.2	Determine the thermodynamics of atmospheric phenomena.
			JA.3	Quantify the roles of wave propagation and atmospheric coupling.
			JA.4	Investigate auroral structure and energy transport.
			JA.5	Understand the interrelationships of the ionosphere and thermosphere.
		JB. Characterize the atmospheric composition and chemistry.	JB.1	Determine Jupiter's bulk elemental abundances.
			JB.2	Measure the composition from the stratosphere to low thermosphere in three dimensions.
			JB.3	Study localized and non-equilibrium composition.
			JB.4	Determine the importance of moist convection in meteorology, cloud formation, and chemistry.
		JC. Characterize the atmospheric vertical structure.	JC.1	Determine the three-dimensional structure from Jupiter's upper troposphere to lower thermosphere.
			JC.2	Explore Jupiter's interior density structure and dynamics below the upper troposphere.
			JC.3	Study coupling across atmospheric layers.

Foldout 1. EJSM Traceability Matrix

EUROPA									
Goal	**Science Objective**		**Science Investigation**		**Example Measurements**	**JEO Example Instruments**	**JGO Example Instruments**	**JEO**	**JGO**
Explore Europa to investigate its habitability	**EA. Ocean**	Characterize the extent of the ocean and its relation to the deeper interior.	EA.1	Determine the amplitude and phase of the gravitational tides.	EA.1a. Measure spacecraft accelerations to resolve 2nd degree gravity field time dependence to recover k_2 at the orbital frequency to 0.0005 absolute accuracy and the phase to 1 degree, by means of range-rate measurements with an accuracy better than 0.1 mm/s at 60 sec integration time to determine spacecraft orbit to better than 1-meter (rms) over several tidal cycles.	Radio Subsystem (Multi-frequency communication (e.g., Ka & X) is best, but X is sufficient)	Radio Science Instrument & USO (Multi-frequency communication (e.g., Ka & X) is best, but X is sufficient)		
					EA.1b. Determine topographic differences from globally distributed repeat measurements, to recover spacecraft altitude at crossover points to 1-meter vertical accuracy, by means of contiguous global ranging to the surface with 10-cm accuracy.	Laser Altimeter	Laser Altimeter		
					EA.1c. Determine the position of Europa's center of mass relative to Jupiter during the lifetime of the mission to better than 10 meters, by means of range-rate measurements with an accuracy better than 0.1 mm/s at 60 sec integration time to determine spacecraft orbit to better than 1-meter (rms) throughout the lifetime of the orbiter.	Radio Subsystem	Radio Science Instrument		
			EA.2	Determine the magnetic induction response from the ocean and characterize the influence of the space plasma environment on this response.	EA.2a. Measure three-axis magnetic field components at 32 Hz, 8 vectors/s, and a sensitivity of 0.1 nT, near-continuously for at least one month at multiple frequencies to determine the induction response at multiple frequencies (orbital as well as Jupiter rotation time scales) to an accuracy of 0.1 nT.	Magnetometer	Magnetometer		
					EA.2b. Characterize the local plasma distribution function (ions, electrons) and its moments, and constrain contribution from currents not related to the surface and ocean, by determining the three-dimensional distribution functions for electrons and ions (first order mass resolution) over 4π and an energy range of few eV to few MeV, along with cold plasma density and velocity.	Particle and Plasma Instrument, Ion and Neutral Mass Spectrometer	Particle and Plasma Instrument–Ion Neutral Mass Spectrometer		
					EA.2c. Determine electric field vectors (near DC to 3 MHz), and measure electron and ion density, as well as electron temperature, for local conductivity and electrical currents determination.	Radio and Plasma Wave Instrument	Radio and Plasma Wave Instrument		
			EA.3	Characterize surface motion over the tidal cycle.	EA.3a. Determine topographic differences from globally distributed repeat measurements at varying orbital phases, with better than or equal to 1-meter vertical accuracy, to recover h_2 to 0.01 (at the orbital frequency). Example: Contiguous global ranging to the surface with 10-cm accuracy.	Laser Altimeter	Laser Altimeter		
					EA.3b. Measure spacecraft accelerations to resolve the position of the spacecraft to better than 1-meter (rms), by means of range-rate measurements with an accuracy better than 0.1 mm/s at 60 sec integration time over several tidal cycles.	Radio Subsystem	Radio Science Instrument & USO		
			EA.4	Determine the satellite's dynamical rotation state (forced libration, obliquity and nutation).	EA.4a. Determine the mean spin pole direction (obliquity) to better than or equal 10-meters, through development of an altimetry corrected geodetic control network (~100 points) at better than or equal 100-m/pixel.	Wide Angle Camera, Laser Altimeter, Radio Subsystem	Wide Angle Camera, Laser Altimeter, Radio Science Instrument		
					EA.4b. Determine the forced nutation of the spin pole at the orbital period to better than or equal to 1-meter, through development of an altimetry corrected geodetic control network at better than or equal to 10-m/pixel at multiple tidal phases.	Narrow Angle Camera, Laser Altimeter, Radio Subsystem	Narrow Angle Camera, Laser Altimeter, Radio Science Instrument		
					EA.4c. Determine the amplitude of the forced libration at the orbital period to better than 1-meter, through development of an altimetry corrected geodetic control network at better than or equal to 10-m/pixel at multiple tidal phases.	Narrow Angle Camera, Laser Altimeter, Radio Subsystem	Narrow Angle Camera, Laser Altimeter, Radio Science Instrument		
			EA.5	Investigate the core, rocky mantle, rock-ocean interface, and compensation of the ice shell.	EA.5a. Resolve the gravity field to degree and order 30 or better, through range-rate measurements with an accuracy better than 0.1 mm/s at 60 sec integration time to determine spacecraft orbit to better than 1-meter (rms).	Radio Subsystem	Radio Science Instrument & USO		

Science Value Rating Criteria					
Significant contribution or achieves the measurement (75% to 100%)	Major contribution to achieving the measurement (50% to 75%)	Moderate contribution to achieving the measurement (25% to 50%)	Litte or no contribution to achieving the measurement (less than 25%)	Tour trajectory does not provide a suitable opportunity to make observations	Example instrument not in model payload

EUROPA									
Goal	**Science Objective**		**Science Investigation**		**Example Measurements**	**JEO Example Instruments**	**JGO Example Instruments**	**JEO**	**JGO**
Explore Europa to investigate its habitability	**EA. Ocean**	Characterize the extent of the ocean and its relation to the deeper interior.	EA.5	Investigate the core, rocky mantle, rock-ocean interface, and compensation of the ice shell.	EA.5b. Make topographic measurements to resolve coherence with gravity to degree 30 or better, with better than or equal to 1-meter vertical accuracy, through contiguous global ranging to the surface with 10-cm accuracy.	Laser Altimeter	Laser Altimeter		
					EA.5c. Identify deep thermal, compositional, or structural horizons by obtaining profiles of subsurface dielectric horizons, with better than 50-km profile spacing over more than 80% of the surface, at depths of 1- to 30-km at 100-meter vertical resolution.	Ice Penetrating Radar (nominally ~5 or 50 MHz, with ~1 MHz bandwidth)	Ice Penetrating Radar (nominally ~5 or 50 MHz, with ~1 MHz bandwidth)		
					EA.5d. Characterize the three-dimensional distribution functions for electrons and ions (first order mass resolution) over 4π and an energy range of a few eV to a few MeV, along with cold plasma density and velocity.	Particle and Plasma Instrument	Particle and Plasma Instrument–Ion Neutral Mass Spectrometer		
					EA.5e. Measure three-axis magnetic field components at 32 Hz with a sensitivity of 0.1 nT.	Magnetometer	Magnetometer		
	EB. Ice Shell	Characterize the ice shell and any subsurface water, including their heterogeneity, and the nature of surface-ice-ocean exchange.	EB.1	Characterize the distribution of any shallow subsurface water and the structure of the icy shell including its subsurface properties.	EB.1a. Identify and locally characterize subsurface thermal or compositional horizons and structures related to the current or recent presence of water or brine, by obtaining profiles of subsurface dielectric horizons and structures, with better than 50-km profile spacing over more than 80% of the surface, at depths of 100-meters to 3-km at 10-meter vertical resolution, and performing targeted subsurface characterization of selected sites at least 30-km in length with estimations of subsurface dielectric properties and the density of buried scatterers.	Ice Penetrating Radar (nominally ~50 MHz, with ~10 MHz bandwidth)	Ice Penetrating Radar (nominally ~50 MHz, with ~10 MHz bandwidth)		
					EB.1b. Measure topography on the order of 250-meter horizontal scale and better than or equal to 20-meters vertical resolution and accuracy, over more than 80% of the surface, co-located with subsurface profiles.	Wide Angle Camera (stereo), Laser Altimeter, Ice Penetrating Radar	Wide Angle Camera, Laser Altimeter, Ice Penetrating Radar		
			EB.2	Search for an ice-ocean interface.	EB.2a. Identify deep thermal, compositional, or structural horizons by obtaining profiles of subsurface dielectric horizons and structures, with better than 50-km profile spacing over more than 80% of the surface, at depths of 1- to 30-km at 100-meter vertical resolution.	Ice Penetrating Radar (nominally ~5 or 50 MHz, with ~1 MHz bandwidth)	Ice Penetrating Radar (nominally ~5 or 50 MHz, with ~1 MHz bandwidth)		
					EB.2b. Measure topography on the order of 250-meter horizontal scale and better than or equal to 20-meter vertical resolution, over more than 80% of the surface, co-located with subsurface profiles.	Wide Angle Camera (stereo), Laser Altimeter	Wide Angle Camera, Laser Altimeter		
			EB.3	Correlate surface features and subsurface structure to investigate processes governing material exchange among the surface, ice shell, and ocean.	EB.3a. Globally identify and locally characterize subsurface dielectric horizons and structures, at depths of 1- to 30-km at 100-meter vertical resolution and depths of 100-meters to 3-km at 10-meter vertical resolution, by obtaining subsurface profiles with better than 50-km spacing over more than 80% of the surface, plus targeted characterization of selected sites at least 30-km in length.	Ice Penetrating Radar (dual-frequency, nominally ~5 & ~50 MHz, with ~1 and ~10 MHz bandwidth)	Ice Penetrating Radar (dual-frequency, nominally ~5 & ~50 MHz, with ~1 and ~10 MHz bandwidth)		
					EB.3b. Characterize the detailed three-dimensional surface morphology of targeted features at better than or equal 25-meter horizontal scale and 1-meter vertical accuracy across the target, co-located with subsurface profiles.	Medium Angle Camera (stereo), Laser Altimeter	Laser Altimeter		
					EB.3c. Map endogenic thermal emission from the surface by measuring the albedo over more than 80% of the surface at spatial resolution of better than or equal to 250-m/pixel to 10% radiometric accuracy, and making targeted night-time and day-time thermal and albedo observations at better than 250-m/pixel spatial resolution and temperature accuracy better than 2 K.	Thermal Instrument	Thermal Instrument		
					EB.3d. Measure surface reflectance along profiles with less than or equal to 25-km spacing over more than 80% of the surface, at a spatial resolution of better than or equal 100 m/pixel, from 0.4- to 2.5-μm with a spectral resolution of better than or equal to 5 nm, and from 2.5 μm to greater than or equal to 5 μm and with a spectral resolution better than or equal to 10 nm, along with targeted characterization of selected sites at ~25 m/pixel spatial resolution.	Vis-IR Spectrometer	Visible InfraRed Hyperspectral Imaging Spectrometer		

Science Value Rating Criteria						
Significant contribution or achieves the measurement (75% to 100%)	Major contribution to achieving the measurement (50% to 75%)	Moderate contribution to achieving the measurement (25% to 50%)	Litte or no contribution to achieving the measurement (less than 25%)	Tour trajectory does not provide a suitable opportunity to make observations	Example instrument not in model payload

EUROPA									
Goal	**Science Objective**		**Science Investigation**		**Example Measurements**	**JEO Example Instruments**	**JGO Example Instruments**	**JEO**	**JGO**
Explore Europa to investigate its habitability	**EB. Ice Shell**	Characterize the ice shell and any subsurface water, including their heterogeneity, and the nature of surface-ice-ocean exchange.	EB.3	Correlate surface features and subsurface structure to investigate processes governing material exchange among the surface, ice shell, and ocean.	EB.3e. Measure surface reflectance along profiles with less than or equal to 25-km spacing over more than 80% of the surface, at a spatial resolution of better than or equal 100 m/pixel, through a spectral range of at least 100- to 350-nm, with better than or equal to 13-nm spectral resolution.	UV Spectrometer	UltraViolet Imaging Spectrometer		
					EB.3f. Measure topography at better than or equal to 250-meter horizontal scale and better than or equal to 20-meter vertical resolution and accuracy over more than 80% of the surface, co-located with subsurface profiles.	Wide Angle Camera (stereo), Laser Altimeter	Wide Angle Camera, Laser Altimeter		
					EB.3g. Determine surface color characteristics at ~100 m/pixel scale in at least 3 colors (e.g., 0.99, 0.76 & 0.56 μm), over more than 80% of the surface.	Wide Angle Camera (color)	Wide Angle Camera		
			EB.4	Characterize regional and global heat flow variations.	EB.4a. Identify and map subsurface thermal horizons, by obtaining profiles of subsurface dielectric horizons, with better than 50-km profile spacing over more than 80% of the surface, at depths of 1- to 30-km at 100-meter vertical resolution.	Ice Penetrating Radar	Ice Penetrating Radar		
					EB.4b. Map endogenic thermal emissions from the surface by measuring the albedo over more than 80% of the surface at a spatial resolution of better than or equal to 250-m/pixel to 10% radiometric accuracy, and making targeted night-time and day-time thermal observations at better than or equal to 250-m/pixel spatial resolution and temperature accuracy better than 2 K at 100 K.	Thermal Instrument	Thermal Instrument		
	EC. Composition	Determine global composition, distribution and evolution of surface materials, especially as related to habitability.	EC.1	Characterize surface organic and inorganic chemistry, including abundances and distributions of materials, with emphasis on indicators of habitability and potential biosignatures.	EC.1a. Measure surface reflectance along profiles with less than or equal to 25-km spacing over more than 80% of the surface, at a spatial resolution of better than or equal 100 m/pixel, from 0.4- to 2.5-μm with a spectral resolution of better than or equal to 5 nm, and from 2.5 μm to greater than or equal to 5 μm and with a spectral resolution better than or equal to 10 nm, along with targeted characterization of selected sites at ~25 m/pixel spatial resolution.	Vis-IR Spectrometer	Visible InfraRed Hyperspectral Imaging Spectrometer		
					EC.1b. Characterize the composition of sputtered surface products over a mass range better than 300 Daltons, mass resolution better than 500, with sensitivity that allows measurement of partial pressures as low as 10^{-17} mbar.	Ion and Neutral Mass Spectrometer	Ion and Neutral Mass Spectrometer		
					EC.1c. Measure surface reflectance along profiles with less than or equal to 25-km spacing over more than 80% of the surface, at a spatial resolution of better than or equal 100 m/pixel, through a spectral range of at least 100- to 350-nm, with better than or equal to 3-nm spectral resolution, along with targeted characterization of selected sites.	UV Spectrometer	UltraViolet Imaging Spectrometer		
					EC.1d. Correlate surface composition and physical characteristics (e.g., grain size) with geologic features through global 3-color mapping at resolution of 100-m/pixel over at least 80% of the surface.	Narrow Angle Camera, Wide Angle Camera	Narrow Angle Camera, Wide Angle Camera		
			EC.2	Relate material composition and distribution to geological processes, especially material exchange with the interior.	EC.2a. Measure surface reflectance along profiles with less than or equal to 25-km spacing over more than 80% of the surface, at a spatial resolution of better than or equal 100 m/pixel, at 0.4- to 2.5-μm with a spectral resolution of better than or equal to 5 nm, and from 2.5 μm to greater than or equal to 5 μm and with a spectral resolution better than or equal to 10 nm, and characterize selected sites at ~25 m/pixel spatial resolution.	Vis-IR Spectrometer	Visible InfraRed Hyperspectral Imaging Spectrometer		
					EC.2b. Measure surface reflectance along profiles with less than or equal to 25-km spacing over more than 80% of the surface, at better than or equal to 100-m/pixel spatial resolution over the spectral range of 100- to at least 350 nm with better than or equal to 3-nm spectral resolution.	UV Spectrometer	UltraViolet Imaging Spectrometer		
					EC.2c. Globally identify and locally characterize subsurface dielectric horizons and structures, at depths of 1- to 30-km at 100-m vertical resolution and depths of 100-m to 3-km at 10-meter vertical resolution, by means of subsurface profiles with better than 50-km spacing over more than 80% of the surface, along with targeted characterization of selected sites at least 30-km in length.	Ice Penetrating Radar (dual-frequency, nominally ~5 & ~50 MHz, with ~1 and ~10 MHz bandwidth)	Ice Penetrating Radar (dual-frequency, nominally ~5 & ~50 MHz, with ~1 and ~10 MHz bandwidth)		

Science Value Rating Criteria						
Significant contribution or achieves the measurement (75% to 100%)	Major contribution to achieving the measurement (50% to 75%)	Moderate contribution to achieving the measurement (25% to 50%)	Litte or no contribution to achieving the measurement (less than 25%)	Tour trajectory does not provide a suitable opportunity to make observations	Example instrument not in model payload

EUROPA									
Goal	**Science Objective**		**Science Investigation**		**Example Measurements**	**JEO Example Instruments**	**JGO Example Instruments**	**JEO**	**JGO**
Explore Europa to investigate its habitability	**EC. Composition**	Determine global composition, distribution and evolution of surface materials, especially as related to habitability.	EC.2	Relate material composition and distribution to geological processes, especially material exchange with the interior.	EC.2d. Determine the distributions and morphologies of surface landforms at regional and local scales, through monochromatic imaging with resolution better to or equal 10-m/pixel using at least 20-km wide swaths. Constrain regional and global stratigraphic relationships by determining surface color characteristics at ~100-m/pixel scale in at least 3 colors (e.g., 0.99, 0.76 & 0.56 μm) with near-uniform lighting conditions and solar phase angles less than or equal to 45 degrees, over more than 80% of the surface.	Wide Angle Camera (color), Medium Angle Camera	Wide Angle Camera		
					EC.2e. Characterize topography of targeted features at better than 25-m/pixel scale and better than or equal to 1-m vertical resolution and accuracy.	Medium or Narrow Angle Camera (stereo), Laser Altimeter	Narrow Angle Camera, Laser Altimeter		
					EC.2f. Map endogenic thermal emission from the surface by making daytime and nighttime thermal observations at spatial resolution better than or equal to 250-m/pixel and temperature accuracy better than 2 K, over more than 80% of the surface, and measure albedo to 10% radiometric accuracy at spatial resolution better than or equal to 250-m/pixel.	Thermal Instrument	Thermal Instrument		
					EC.2g. Measure the volatile content of potential outgassing sources from the shallow subsurface or deeper interior and relate them to the origin and evolution of the satellite, over a mass range better than 300 Daltons, mass resolution better than 500, with sensitivity that allows measurement of partial pressures as low as 10^{-17} mbar.	Ion and Neutral Mass Spectrometer	Ion and Neutral Mass Spectrometer		
					EC.2h. Measure topography at better than or equal to 250-m/pixel spatial scale and better than or equal to 20-meter vertical resolution, over more than 80% of the surface, in regions that are co-located with subsurface profiles.	Wide Angle Camera (stereo), Laser Altimeter	Wide Angle Camera, Laser Altimeter		
			EC.3	Investigate the effects of radiation on surface composition, including organics, and regional structure.	EC.3a. Measure surface reflectance along profiles with less than or equal to 25-km spacing over more than 80% of the surface, at a spatial resolution of better than or equal 100 m/pixel, at 0.4- to 2.5-μm with a spectral resolution of better than or equal to 5 nm, and from 2.5 μm to greater than or equal to 5 μm and with a spectral resolution better than or equal to 10 nm, and characterize selected sites at ~25 m/pixel spatial resolution.	Vis-IR Spectrometer	Visible InfraRed Hyperspectral Imaging Spectrometer		
					EC.3b. Measure surface reflectance along profiles with less than or equal to 25-km spacing over more than 80% of the surface, at better than or equal to 100-m/pixel spatial resolution over the spectral range of 100- to at least 350 nm with better than or equal to 3-nm spectral resolution.	UV Spectrometer	UltraViolet Imaging Spectrometer		
					EC.3c. Determine three-dimensional distribution functions for electrons and ions (first order mass resolution) over 4π and an energy range of a few eV to a few MeV, along with cold plasma density and velocity.	Particle and Plasma Instrument, Ion and Neutral Mass Spectrometer	Particle and Plasma Instrument–Ion Neutral Mass Spectrometer		
					EC.3d Measure three-axis magnetic field components at 32 Hz to 128 Hz at 8 vectors/s and a sensitivity of 0.1 nT, near-continuously for at least one month at multiple frequencies to determine the induction response at multiple frequencies (orbital as well as Jupiter rotation time scales) to an accuracy of 0.1 nT.	Magnetometer	Magnetometer		
					EC.3e. Characterize the composition of sputtered surface products over a mass range better than 300 Daltons, mass resolution better than 500, with sensitivity that allows measurement of partial pressures as low as 10^{-17} mbar.	Particle and Plasma Instrument, Ion and Neutral Mass Spectrometer	Particle and Plasma Instrument–Ion Neutral Mass Spectrometer		
					EC.3f. Characterize the structure of the sputter-produced atmosphere using stellar occultations, and by measuring atmospheric emissions, in the wavelength range of at least 100- to 200-nm at better than or equal to 0.5-nm spectral resolution and 100-m/pixel scale.	UV Spectrometer	UltraViolet Imaging Spectrometer		
					EC.3g. Determine the flux of trapped and precipitating ions (with composition) and electrons in the energy range 10 eV to 10 MeV at 15° angular resolution and ΔE/E = 0.1 and a time resolution of at least 1 minute.	Particle and plasma instrument, Ion and Neutral Mass Spectrometer	Particle and Plasma Instrument–Ion Neutral Mass Spectrometer		

Science Value Rating Criteria					
Significant contribution or achieves the measurement (75% to 100%)	Major contribution to achieving the measurement (50% to 75%)	Moderate contribution to achieving the measurement (25% to 50%)	Litte or no contribution to achieving the measurement (less than 25%)	Tour trajectory does not provide a suitable opportunity to make observations	Example instrument not in model payload

EUROPA									
Goal	**Science Objective**		**Science Investigation**		**Example Measurements**	**JEO Example Instruments**	**JGO Example Instruments**	**JEO**	**JGO**
Explore Europa to investigate its habitability	**EC. Composition**	Determine global composition, distribution and evolution of surface materials, especially as related to habitability.	EC.3	Investigate the effects of radiation on surface composition, including organics, and regional structure.	EC.3h. Determine the distributions and morphologies of surface landforms at regional and local scales, through monochromatic imaging with resolution better to or equal 10-m/pixel using at least 20-km wide swaths. Constrain regional and global stratigraphic relationships by determining surface color characteristics at ~100-m/pixel scale in at least 3 colors (e.g., 0.99, 0.76 & 0.56 μm) with near-uniform lighting conditions and solar phase angles less than or equal to 45 degrees, over more than 80% of the surface.	Wide Angle Camera (color), Medium Angle Camera	Wide Angle Camera		
					EC.3i. Map the thermal inertia of the surface by making daytime and nighttime thermal observations at a spatial resolution better than or equal to 250-m/pixel and temperature accuracy better than 2 K, over more than 80% of the surface. Measure albedo to 10% radiometric accuracy at spatial resolution better than or equal to 250-m/pixel.	Thermal Instrument	Thermal Instrument		
					EC.3j. Detailed morphological characterization of targeted features at better than or equal to 1-m/pixel spatial scale, and solar incidence angles between 50° and 70°, ideally with stereo.	Narrow Angle Camera	Narrow Angle Camera		
					EC.3k. Measure ion composition with the mass resolution M/δM better than or equal to 20; determine three-dimensional ion and electron distribution functions over the range of a few keV to MeV; characterize the spatial and energy distribution of sputtered neutrals in the energy range of eV to keV, with high mass resolution mode; image (with less than or equal to 5 degrees angular resolution) ion-sputtered and back-scattered energetic neutrals (eV to keV range) from Europa's surface.	Particle and Plasma Instrument, Ion and Neutral Mass Spectrometer	Particle and Plasma Instrument–Ion Neutral Mass Spectrometer		
					EC.3l. Measure electron and ion density (0.001- to $10^4/cm^3$) and electron temperature (0- to 100-eV), and constrain the ion temperature (0- to 20-eV); image the temporal, spatial, and spectral evolution of large-scale acceleration and injection events in energetic neutral atoms (10- to 300-keV) for H, He, O, S; detect dust and determine its mass and size distribution with electric field (near DC to 45 MHz); measure electric field vectors (near DC to 3 MHz) that accelerate charged dust and plasma toward Europa's surface.	Particle and Plasma Instrument	Radio and Plasma Wave Instrument		
			EC.4	Characterize the nature of exogenic (e.g., Io) materials.	EC.4a. Determine the ion and electron precipitation flux with ion composition at energies of 10 eV to 10 MeV at 15° angular resolution and ΔE/E = 0.1 and a time resolution of at least 1 minute.	Particle and Plasma Instrument	Particle and Plasma Instrument–Ion Neutral Mass Spectrometer		
					EC.4b. Measure ions and neutrals over a mass range better than 300 Daltons, mass resolution better than 500, with sensitivity that allows measurement of partial pressures as low as 10^{-17} mbar.	Ion and Neutral Mass Spectrometer	Ion and Neutral Mass Spectrometer		
					EC.4c. Measure surface reflectance along profiles with less than or equal to 25-km spacing over more than 80% of the surface, at a spatial resolution of better than or equal 100 m/pixel, at 0.4- to 2.5-μm with a spectral resolution of better than or equal to 5 nm, and from 2.5 μm to greater than or equal to 5 μm and with a spectral resolution better than or equal to 10 nm, and characterize selected sites at ~25 m/pixel spatial resolution.	Vis-IR Spectrometer	Visible InfraRed Hyperspectral Imaging Spectrometer		
					EC.4d. Measure surface reflectance along profiles with less than or equal to 25-km spacing over more than 80% of the surface, at better than or equal to 100-m/pixel spatial resolution over the spectral range of 100- to at least 350 nm with better than or equal to 3-nm spectral resolution.	UV Spectrometer	UltraViolet Imaging Spectrometer		
					EC.4e. Determine surface color at ~100-m/pixel scale in at least 3 colors (e.g., 0.99, 0.76 & 0.56 μm), over at least 80% of the surface.	Wide Angle Camera (color)	Wide Angle Camera		
			EC.5	Determine volatile content to constrain satellite origin and evolution.	EC.5a. Measure the stable isotopes of C, H, O, and N in the major volatiles (e.g., H_2O, CH_4, NH_3, CO, CO_2, SO_2), and measure the noble gases Ar, Kr, and Xe, with mass resolution better than 500 and sensitivity that allows measurement of partial pressures as low as 10^{-17} mbar, and characterize the composition of sputtered desorbed volatiles over a mass range better than 300 Daltons and mass resolution better than 500.	Ion and Neutral Mass Spectrometer	Ion and Neutral Mass Spectrometer		
					EC.5b. Characterize the structure of the sputter-produced atmosphere using stellar occultations, and by measuring atmospheric emissions in the wavelength range of at least 100- to 200-nm at better than or equal to 0.5-nm spectral resolution and 100-m/pixel spatial resolution.	UV Spectrometer	UltraViolet Imaging Spectrometer		

Science Value Rating Criteria						
Significant contribution or achieves the measurement (75% to 100%)	Major contribution to achieving the measurement (50% to 75%)	Moderate contribution to achieving the measurement (25% to 50%)	Litte or no contribution to achieving the measurement (less than 25%)	Tour trajectory does not provide a suitable opportunity to make observations	Example instrument not in model payload

EUROPA									
Goal	**Science Objective**		**Science Investigation**		**Example Measurements**	**JEO Example Instruments**	**JGO Example Instruments**	**JEO**	**JGO**
Explore Europa to investigate its habitability	**EC. Composition**	Determine global composition, distribution and evolution of surface materials, especially as related to habitability.	EC.5	Determine volatile content to constrain satellite origin and evolution.	EC.5c. Measure surface reflectance along profiles with less than or equal to 25-km spacing over more than 80% of the surface, at a spatial resolution of better than or equal 100 m/pixel, at 0.4- to 2.5-µm with a spectral resolution of better than or equal to 5 nm, and from 2.5 µm to greater than or equal to 5 µm and with a spectral resolution better than or equal to 10 nm, and characterize selected sites at ~25 m/pixel spatial resolution.	Vis-IR Spectrometer	Visible InfraRed Hyperspectral Imaging Spectrometer		
					EC.5d. Measure surface reflectance along profiles with less than or equal to 25-km spacing over more than 80% of the surface, at better than or equal to 100-m/pixel spatial resolution over the spectral range of 100- to at least 350 nm with better than or equal to 3-nm spectral resolution.	UV Spectrometer	UltraViolet Imaging Spectrometer		
	ED. Geology	Understand the formation of surface features, including sites of recent or current activity, and identify and characterize candidate sites for potential future *in situ* exploration.	ED.1	Determine the formation and three-dimensional characteristics of magmatic, tectonic, and impact landforms.	ED.1a. Determine the distributions and morphologies of surface landforms at regional and local scales, through monochromatic imaging with resolution better to or equal 10-m/pixel using at least 20-km wide swaths. Constrain regional and global stratigraphic relationships by determining surface color characteristics at ~100-m/pixel scale in at least 3 colors (e.g., 0.99, 0.76 & 0.56 µm) with near-uniform lighting conditions and solar phase angles less than or equal to 45 degrees, over more than 80% of the surface.	Wide Angle Camera (color), Medium Angle Camera	Wide Angle Camera		
					ED.1b. Measure topography at better than or equal to 250-m/pixel spatial scale and better than or equal to 20-meter vertical resolution, over more than 80% of the surface, co-located with subsurface profiles.	Wide Angle Camera (stereo), Laser Altimeter	Wide Angle Camera, Laser Altimeter		
					ED.1c Characterize topography at better than 25-m/pixel scale and better than or equal to 1-meter vertical resolution and accuracy for selected features.	Medium or Narrow Angle Camera (stereo), Laser Altimeter	Narrow Angle Camera, Laser Altimeter		
					ED.1d. Globally identify and locally characterize physical and dielectric subsurface horizons, at depths of 1- to 30-km at 100-meter vertical resolution and depths of 100-meters to 3-km at 10-meter vertical resolution, by obtaining subsurface profiles with better than 50-km spacing over more than 80% of the surface, plus targeted characterization of selected sites.	Ice Penetrating Radar (dual-frequency, nominally ~5 & ~50 MHz, with ~1 and ~10 MHz bandwidth)	Ice Penetrating Radar (dual-frequency, nominally ~5 & ~50 MHz, with ~1 and ~10 MHz bandwidth)		
					ED.1e. Characterize small-scale three-dimensional surface morphology at ~1- to 10-m/pixel over targeted high-priority sites. Co-located with imaging at approximately 10 times wider swath and not worse than 10 times coarser resolution, and co-located with topographic profiles.	Narrow Angle Camera	Narrow Angle Camera		
					ED.1f. Measure surface reflectance along profiles with less than or equal to 25-km spacing over more than 80% of the surface, at a spatial resolution of better than or equal 100 m/pixel, at 0.4- to 2.5-µm with a spectral resolution of better than or equal to 5 nm, and from 2.5 µm to greater than or equal to 5 µm and with a spectral resolution better than or equal to 10 nm, and characterize selected sites at ~25 m/pixel spatial resolution.	Vis-IR Spectrometer	Visible InfraRed Hyperspectral Imaging Spectrometer		
					ED.1g. Measure surface reflectance along profiles with less than or equal to 25-km spacing over more than 80% of the surface, at better than or equal to 100-m/pixel spatial resolution over the spectral range of 100- to at least 350 nm with better than or equal to 3-nm spectral resolution.	UV Spectrometer	UltraViolet Imaging Spectrometer		
					ED.1h. Map endogenic thermal emission from the surface by making daytime and nighttime thermal observations at spatial resolution better than or equal to 250-m/pixel and temperature accuracy better than 2 K, over more than 80% of the surface. Measure albedo to 10% radiometric accuracy at spatial resolution better than or equal to 250-m/pixel.	Thermal Instrument	Thermal Instrument		
					ED.1i. Detailed morphological characterization of targeted features at better than or equal to 1-m/pixel spatial scale, and solar incidence angles between 50° and 70°, ideally with stereo. Co-located with imaging at approximately 10 times wider swath and not worse than 10 times coarser resolution, and co-located with topographic profiles.	Narrow Angle Camera	Narrow Angle Camera		

Science Value Rating Criteria					
Significant contribution or achieves the measurement (75% to 100%)	Major contribution to achieving the measurement (50% to 75%)	Moderate contribution to achieving the measurement (25% to 50%)	Litte or no contribution to achieving the measurement (less than 25%)	Tour trajectory does not provide a suitable opportunity to make observations	Example instrument not in model payload

EUROPA									
Goal	**Science Objective**		**Science Investigation**		**Example Measurements**	**JEO Example Instruments**	**JGO Example Instruments**	**JEO**	**JGO**
Explore Europa to investigate its habitability	**ED. Geology**	Understand the formation of surface features, including sites of recent or current activity, and identify and characterize candidate sites for potential future *in situ* exploration.	ED.2	Determine sites of most recent geological activity, and evaluate future potential landing sites.	ED.2a. Map endogenic thermal emission from the surface to by making daytime and nighttime thermal observations at spatial resolution better than or equal to 250-m/pixel and temperature accuracy better than 2 K, over more than 80% of the surface. Measure albedo to 10% radiometric accuracy at spatial resolution better than or equal to 250-m/pixel.	Thermal Instrument	Thermal Instrument		
					ED.2b. Perform stellar occultations and measure surface reflectance at better than or equal to 100-m/pixel spatial resolution in the wavelength range of 100- to 200-nm with better than 1 nm spectral resolution. Obtain limb views for stellar occultations, and obtain surface profiles with less than or equal to 25-km spacing over more than 80% of the surface.	UV Spectrometer	UltraViolet Imaging Spectrometer		
					ED.2c. Characterize topography at better than 25-m/pixel scale and better than or equal to 1-meter vertical resolution and accuracy for selected features.	Medium or Narrow Angle Camera (stereo), Laser Altimeter	Narrow Angle Camera, Laser Altimeter		
					ED.2d. Detailed morphological characterization of targeted features at better than or equal to 1-m/pixel spatial scale, and solar incidence angles between 50° and 70°, ideally with stereo. Co-located with imaging at approximately 10 times wider swath and not worse than 10 times coarser resolution, and co-located with topographic profiles.	Narrow Angle Camera	Narrow Angle Camera		
					ED.2e. Measure surface reflectance along profiles with less than or equal to 25-km spacing over more than 80% of the surface, at a spatial resolution of better than or equal 100 m/pixel, at 0.4- to 2.5-µm with a spectral resolution of better than or equal to 5 nm, and from 2.5 µm to greater than or equal to 5 µm and with a spectral resolution better than or equal to 10 nm, and characterize selected sites at ~25 m/pixel spatial resolution.	Vis-IR Spectrometer	Visible InfraRed Hyperspectral Imaging Spectrometer		
					ED.2f. Measure surface reflectance along profiles with less than or equal to 25-km spacing over more than 80% of the surface, at better than or equal to 100-m/pixel spatial resolution over the spectral range of 100- to at least 350 nm with better than or equal to 3-nm spectral resolution.	UV Spectrometer	UltraViolet Imaging Spectrometer		
					ED.2g. Measure the volatile content of potential outgassing sources from the shallow subsurface or deeper interior over a mass range better than 300 Daltons, mass resolution better than 500, with sensitivity that allows measurement of partial pressures as low as 10^{-17} mbar.	Ion and Neutral Mass Spectrometer	Particle and Plasma Instrument–Ion Neutral Mass Spectrometer		
					ED.2h. Characterize the interaction between the surface and plasma by measuring the depth and temperature of the diagnostic 1.65-micron water band, in addition to measurements at 2.0, 3.1- and 4.53-microns.	Vis-IR Spectrometer	Visible InfraRed Hyperspectral Imaging Spectrometer		
					ED.2i. Characterize the interaction between the surface and plasma by determining the ion and electron precipitation flux with ion composition for energies of 1 eV to 1 MeV.	Particle and Plasma Instrument, Ion and Neutral Mass Spectrometer	Particle and Plasma Instrument–Ion Neutral Mass Spectrometer		
					ED.2j. Determine the ion and electron precipitation flux with ion composition at energies of 10 eV to 10 MeV at 15° angular resolution and $\Delta E/E = 0.1$ and a time resolution of at least 1 minute.	Particle and Plasma Instrument	Particle and Plasma Instrument–Ion Neutral Mass Spectrometer		
			ED.3	Constrain global and regional surface ages.	ED.3a. Determine the distributions and morphologies of surface landforms at regional and local scales, through monochromatic imaging with resolution better to or equal 10-m/pixel using at least 20-km wide swaths. Constrain regional and global stratigraphic relationships by determining surface color characteristics at ~100-m/pixel scale in at least 3 colors (e.g., 0.99, 0.76 & 0.56 µm) with near-uniform lighting conditions and solar phase angles less than or equal to 45 degrees, over more than 80% of the surface.	Narrow Angle Camera, Wide Angle Camera	Narrow Angle Camera, Wide Angle Camera		

Science Value Rating Criteria						
Significant contribution or achieves the measurement (75% to 100%)	Major contribution to achieving the measurement (50% to 75%)	Moderate contribution to achieving the measurement (25% to 50%)	Litte or no contribution to achieving the measurement (less than 25%)	Tour trajectory does not provide a suitable opportunity to make observations	Example instrument not in model payload

EUROPA									
Goal	**Science Objective**		**Science Investigation**		**Example Measurements**	**JEO Example Instruments**	**JGO Example Instruments**	**JEO**	**JGO**
Explore Europa to investigate its habitability	**ED. Geology**	Understand the formation of surface features, including sites of recent or current activity, and identify and characterize candidate sites for potential future *in situ* exploration.	ED.3	Constrain global and regional surface ages.	ED.3b. Detailed morphological characterization of targeted features at better than or equal to 1-m/pixel spatial scale, and solar incidence angles between 50° and 70°, ideally with stereo. Co-located with imaging at approximately 10 times wider swath and not worse than 10 times coarser resolution, and co-located with topographic profiles.	Narrow Angle Camera	Narrow Angle Camera		
					ED.3c. Measure surface reflectance along profiles with less than or equal to 25-km spacing over more than 80% of the surface, at a spatial resolution of better than or equal 100 m/pixel, at 0.4- to 2.5-µm with a spectral resolution of better than or equal to 5 nm, and from 2.5 µm to greater than or equal to 5 µm and with a spectral resolution better than or equal to 10 nm, and characterize selected sites at ~25 m/pixel spatial resolution.	Vis-IR Spectrometer	Visible InfraRed Hyperspectral Imaging Spectrometer		
					ED.3d. Measure surface reflectance along profiles with less than or equal to 25-km spacing over more than 80% of the surface, at better than or equal to 100-m/pixel spatial resolution over the spectral range of 100- to at least 350 nm with better than or equal to 3-nm spectral resolution.	UV Spectrometer	UltraViolet Imaging Spectrometer		
					ED.3e. Measure topography at better than or equal to 250-m/pixel spatial scale and better than or equal to 20-meter vertical resolution, over more than 80% of the surface, co-located with subsurface profiles.	Wide Angle Camera (stereo), Laser Altimeter	Wide Angle Camera, Laser Altimeter		
					ED.3f. Globally identify and locally characterize subsurface dielectric horizons and structures, at depths of 1- to 30-km at 100-meter vertical resolution and depths of 100-meters to 3-km at 10-meter vertical resolution, by obtaining subsurface profiles with better than 50-km spacing over more than 80% of the surface, plus targeted characterization of selected sites at least 30-km in length.	Ice Penetrating Radar (dual-frequency, nominally ~5 & ~50 MHz, with ~1 and ~10 MHz bandwidth)	Ice Penetrating Radar (dual-frequency, nominally ~5 & ~50 MHz, with ~1 and ~10 MHz bandwidth)		
			ED.4	Investigate processes of erosion and deposition and their effects on the physical properties of the surface.	ED.4a. Map surface temperatures better than or equal to 250-m/pixel spatial resolution and temperature accuracy better than 2 K, and albedo measurements to 10% radiometric accuracy, over more than 80% of the surface, with the same regions observed in both the day and night.	Thermal Instrument	Thermal Instrument		
					ED.4b. Detailed morphological characterization of targeted features at better than or equal to 1-m/pixel spatial scale, and solar incidence angles between 50° and 70°, ideally with stereo. Co-located with imaging at approximately 10 times wider swath and not worse than 10 times coarser resolution, and co-located with topographic profiles.	Narrow Angle Camera	Narrow Angle Camera		
					ED.4c. Measure water ice bands at 1.65, 2.0, 3.1, and 4.53 µm along profiles with less than or equal to 25-km spacing over more than 80% of the surface, with a spectral resolution better than or equal to 5 nm and a spatial resolution of better than 1 km to characterize water ice bands (e.g., grain size), hydrated salts, and sulfuric acid hydrate.	Vis-IR Spectrometer	Visible InfraRed Hyperspectral Imaging Spectrometer		
					ED.4d. Determine the precipitation flux of electrons and ions (with composition) in the eV to few MeV energy range, and characterize the composition of sputtered surface products over a mass range better than 300 Daltons, mass resolution better than 500, with sensitivity that allows measurement of partial pressures as low as 10^{-17} mbar.	Particle and Plasma Instrument, Ion and Neutral Mass Spectrometer	Particle and Plasma Instrument–Ion Neutral Mass Spectrometer		
					ED.4e. Measure ion-cyclotron waves and relate to plasma-pickup and erosion by magnetic field sampling at 32 vectors/s and a sensitivity of 0.1 nT, to constrain sputtering rates.	Magnetometer	Magnetometer		
	EE. Local environment	Characterize the local environment and its interaction with the jovian magnetosphere.	EE.1	Characterize the composition, structure, dynamics and variability of the bound and escaping neutral atmosphere.	EE.1a. Perform stellar occultations to search for absorption signatures and derive densities of atmospheric species (e.g., water and oxygen), globally distributed with a sampling at the equator of better than 30° of arc, in the wavelength range 100- to 200-nm at better than or equal to 0.5 nm resolution, in the wavelength range of 1.0- to 2.5-µm with a spectral resolution of better than or equal to 5 nm, and from 2.5 µm to greater than or equal to 5 µm and with a spectral resolution better than or equal to 10 nm.	UV Spectrometer, Vis-IR Spectrometer	UltraViolet Imaging Spectrometer, Visible InfraRed Hyperspectral Imaging Spectrometer		
					EE.1b. Characterize the neutral atmosphere and ionosphere through radio occultations.	Radio Subsystem	Radio Science Instrument & USO		

Science Value Rating Criteria						
Significant contribution or achieves the measurement (75% to 100%)	Major contribution to achieving the measurement (50% to 75%)	Moderate contribution to achieving the measurement (25% to 50%)	Litte or no contribution to achieving the measurement (less than 25%)	Tour trajectory does not provide a suitable opportunity to make observations	Example instrument not in model payload

EUROPA									
Goal	**Science Objective**		**Science Investigation**		**Example Measurements**	**JEO Example Instruments**	**JGO Example Instruments**	**JEO**	**JGO**
Explore Europa to investigate its habitability	**EE. Local environment**	Characterize the local environment and its interaction with the jovian magnetosphere.	EE.1	Characterize the composition, structure, dynamics and variability of the bound and escaping neutral atmosphere.	EE.1c. Perform globally distributed limb observations to measure atmospheric emissions at better than or equal to 1 km spatial resolution, by means of: observations in the wavelength range of 100- to 320-nm with a spectral resolution better than 1 nm to measure or search for emission from O (135.6 nm); observations in the wavelength range of 0.4- to 2.5-μm with a spectral resolution better than or equal to 5 nm to measure or search for emission from O_2 (1.27 microns); and observations in the wavelength range of 2.5- to greater than or equal to 5.0-μm with spectral resolution better than or equal to 10 nm to measure or search for emission from H_2O, CO_2 (4.26 microns).	UV Spectrometer, Vis-IR Spectrometer	UltraViolet Imaging Spectrometer, Visible InfraRed Hyperspectral Imaging Spectrometer		
					EE.1d. Obtain two-dimensional spectral-spatial images at ~120 to 300 nm wavelengths covering emissions from OI (135.6 nm, 130.4 nm), H Ly alpha, OH, Na, Ca, etc. at spectral resolution of at least 0.5 nm in the range 120 to 300 nm and better than 1 nm in the range 200 to 300 nm, and better than 48 hr temporal resolution, including through the synodic cycle to measure atmospheric emissions.	UV Spectrometer	UltraViolet Imaging Spectrometer		
					EE.1e. Obtain local thermal maps over a range of representative terrains, latitudes, longitudes, and local times, especially near noon, with better than 1 km/pixel resolution, at two well-separated wavelengths for sensitivity to sub-pixel thermal inhomogenities, in order to determine the temperature of surface volatiles that are a source of the exosphere.	Thermal Instrument	Thermal Instrument		
			EE.2	Characterize the composition, structure, dynamics and variability of the ionosphere and local (within the Hill sphere) charged particle population.	EE.2a. Determine the flux and composition of the impacting charged particles (ions and electrons) between energies of 10 eV to 10 MeV at 15° angular resolution and ΔE/E = 0.1 and a time resolution of at least 1 minute.	Particle and Plasma Instrument	Particle and Plasma Instrument–Ion Neutral Mass Spectrometer		
					EE.2b. Measure three-axis magnetic field components at equal to or better than 32 Hz to 128 Hz at 8 vectors/s and a sensitivity of 0.1 nT with multiple flybys at different orbital phases and closest approach of less than 0.5 planetary radii.	Magnetometer	Magnetometer		
					EE.2c. Determine the fluxes of positive ions and neutral particles over a mass range equal to or better than 300 Daltons, mass resolution of better than 500, and pressure range of 10^{-6} to 10^{-17} mbar, and energy resolution of 10%.	Ion and Neutral Mass Spectrometer	Ion and Neutral Mass Spectrometer		
					EE.2d. Determine the three-dimensional distribution function of electrons and ions in the energy range of 10 eV to a few MeV; acquire energetic neutral atom images in the energy range 10 eV to a few keV; measure ion mass composition with M/δM better than or equal to 20; measure the open source positive ion spectrum to determine the sputtered ions; measure the open source neutral spectrum to determine the composition of sputtered neutrals and evaporated species; and measure the closed source neutral spectrum to determine minor species.	Particle and Plasma Instrument and Ion and Neutral Mass Spectrometer	Particle and Plasma Instrument–Ion Neutral Mass Spectrometer		
					EE.2e. Measure the electron and ion density (0.001-10^4/cm^3) and electron temperature (0- to 100-eV), as well as the ion ram speed (0- to 200-km); constrain ion temperature (0- to 20-eV); determine the ionizing EUV flux; determine electric field vectors (near DC to 3 MHz); determine the presence of suprathermal electrons and plasma inhomogenities (δn/n, 0- to 10-kHz).	Radio and Plasma Wave Instrument	Radio and Plasma Wave Instrument		
					EE.2f. Measure the distribution of bulk plasma and bulk ion drift speed with 10 s resolution; determine electron and ion density 0.001- to 10^4/cm^3, electron temperature (0.01- to 100-eV), bulk ion drift speed (0- to 200-km/s), and suprathermal electrons (non-Maxwellian distribution); constrain ion temperature (0.01- to 20-eV).	Particle and Plasma Instrument	Particle and Plasma Instrument–Ion Neutral Mass Spectrometer		
					EE.2g. Determine the three-dimensional distribution function of electrons and ions in the energy range of 10 eV to a few MeV with 4π coverage, with a 10 second resolution and first order mass analysis; determine plasma composition with the mass resolution M/δM better than or equal to 20; measure the open source positive ion spectrum, negative ion spectrum, and neutral spectrum; measure the closed source neutral spectrum with high mass resolution mode; determine the spatial (less than 5 degrees angular resolution and 30 minute time resolution) and energy characteristics of the sputtered and backscattered neutrals (H and heavies in the 10- to 300-keV energy range).	Particle and Plasma Instrument, Ion and Neutral Mass Spectrometer	Particle and Plasma Instrument–Ion Neutral Mass Spectrometer		

Science Value Rating Criteria					
Significant contribution or achieves the measurement (75% to 100%)	Major contribution to achieving the measurement (50% to 75%)	Moderate contribution to achieving the measurement (25% to 50%)	Litte or no contribution to achieving the measurement (less than 25%)	Tour trajectory does not provide a suitable opportunity to make observations	Example instrument not in model payload

GANYMEDE								
Goal	**Science Objective**		**Science Investigation**		**Example Measurements**	**JEO Example Instruments**	**JGO Example Instruments**	**JEO**	**JGO**
Characterize Ganymede as a planetary object including its potential habitability	**GA. Ocean**	Characterize the extent of the ocean and its relation to the deeper interior.	GA.1	Determine the amplitude and phase of the gravitational tides.	GA.1a. Measure spacecraft acceleration to resolve 2nd degree gravity field time dependence. Recover k_2 at the orbital frequency to 0.01 absolute accuracy and the phase to 10 degrees by performing range-rate measurements with an accuracy better than 0.01 mm/s at 60 sec integration time to determine spacecraft orbit to better than 1-meter (rms) over several tidal cycles.	Radio Subsystem	Radio Science Instrument & USO		
					GA.1b. Measure topographic differences from globally distributed repeat ranging measurements, to recover spacecraft altitude at crossover points to 1-meter vertical accuracy by contiguous global ranging to the surface with 10-cm accuracy.	Laser Altimeter	Laser Altimeter		
					GA.1c. Determine the position of Ganymede's center of mass relative to Jupiter during the lifetime of the mission to better than 10 meters, by performing range-rate measurements with an accuracy better than 0.1 mm/s at 60 sec integration time to determine spacecraft orbit to better than 1-meter (rms) throughout the lifetime of the orbiter.	Radio Subsystem	Radio Science Instrument & USO		
			GA.2	Characterize the space plasma environment to determine the magnetic induction response from the ocean.	GA.2a. Measure three-axis magnetic field components at 8- to 32-Hz to determine the induction response at multiple frequencies to an accuracy of 0.1 nT.	Magnetometer	Magnetometer		
					GA.2b. Determine three-dimensional distribution functions for electrons and ions (first order mass resolution) over 4p and an energy range of a few eV to a few tens keV and cold plasma density and velocity to measure local plasma distribution function (ions, electrons) and its moments and to constrain contributions from currents not related to the surface and ocean. Identify open and closed field lines and magnetic field at the surface by measuring electrons over wide energy range.	Particle and Plasma Instrument, Ion and Neutral Mass Spectrometer	Particle and Plasma Instrument–Ion Neutral Mass Spectrometer		
					GA.2c. Determine electric field vectors (near DC to 3 MHz), electron and ion density, electron temperature for local conductivity, and electrical currents.	Radio and Plasma Wave Instrument (including Langmuir probe)	Radio and Plasma Wave Instrument (including Langmuir probe)		
			GA.3	Characterize surface motion over Ganymede's tidal cycle.	GA.3a. Measure topographic differences from globally distributed repeat measurements at varying orbital phase, with better than or equal to 1-meter vertical accuracy, to recover h_2 to 0.01 (at the orbital frequency) by contiguous global ranging to the surface with 10-cm accuracy.	Laser Altimeter	Laser Altimeter		
					GA.3b. Measure spacecraft acceleration to resolve the position of the spacecraft to better than 1-meter (rms) by performing range-rate measurements with an accuracy better than 0.01 mm/s at 60 sec integration time to determine spacecraft orbit to better than 1-meter (rms) over several tidal cycles.	Radio Subsystem	Radio Science Instrument & USO		
			GA.4	Determine the satellite's dynamical rotation state (forced libration, obliquity and nutation).	GA.4a. Determine the mean spin pole direction (obliquity) to better than 10 meters by developing an altimetry-corrected geodetic control network (~100 points) at a resolution better than 100 meter/pixel.	Wide Angle Camera, Laser Altimeter, Radio Subsystem	Wide Angle Camera, Laser Altimeter, Radio Science Instrument & USO		
					GA.4b. Determine forced nutation of the spin pole at the orbital period to better than 1 meter by developing an altimetry corrected geodetic control network at a resolution better than 10 meter/pixel at multiple tidal phases.	Narrow Angle Camera, Laser Altimeter, Radio Subsystem	Narrow Angle Camera, Laser Altimeter, Radio Science Instrument & USO		
					GA.4c. Determine the amplitude of the forced libration at the orbital period to better than 1 meter by developing an altimetry corrected geodetic control network at a resolution better than 10 meter/pixel at multiple tidal phases.	Narrow Angle Camera, Laser Altimeter, Radio Subsystem	Narrow Angle Camera, Laser Altimeter, Radio Science Instrument & USO		
			GA.5	Investigate the core and rocky mantle.	GA.5a. Resolve the gravity field to degree and order 12 or better by performing range-rate measurements with an accuracy better than 0.01 mm/s at 60 sec integration time to determine spacecraft orbit to better than 1-meter (rms).	Radio Subsystem	Radio Science Instrument & USO		
					GA.5b. Perform topographic measurements to resolve coherence with gravity to degree and order 12 or better, with better than or equal to 1-meter vertical accuracy, by contiguous global ranging to the surface with 10-cm accuracy.	Laser Altimeter	Laser Altimeter		

Science Value Rating Criteria						
Significant contribution or achieves the measurement (75% to 100%)	Major contribution to achieving the measurement (50% to 75%)	Moderate contribution to achieving the measurement (25% to 50%)	Litte or no contribution to achieving the measurement (less than 25%)	Tour trajectory does not provide a suitable opportunity to make observations	Example instrument not in model payload

GANYMEDE									
Goal	**Science Objective**		**Science Investigation**		**Example Measurements**	**JEO Example Instruments**	**JGO Example Instruments**	**JEO**	**JGO**
Characterize Ganymede as a planetary object including its potential habitability	**GA. Ocean**	Characterize the extent of the ocean and its relation to the deeper interior.	GA.5	Investigate the core and rocky mantle.	GA.5c. Measure three-axis magnetic field components at 32 Hz to 128 Hz with a sensitivity of 0.1 nT.	Magnetometer	Magnetometer		
					GA.5d. Determine the distribution function of the plasma ions and electrons with continuous observations over several months.	Particle and Plasma Instrument	Particle and Plasma Instrument–Ion Neutral Mass Spectrometer		
	GB. Ice Shell	Characterize the ice shell.	GB.1	Characterize the structure of the icy shell including its properties and the distribution of any shallow subsurface water.	GB.1a. Identify and locally characterize subsurface compositional horizons and structures by obtaining profiles of subsurface dielectric horizons and structures, with better than 50-km profile spacing over more than 80% of the surface, at depths of 100 meters to 6- to 9-km and vertical resolution ranging from a minimum of 10 meters to one percent of the target depth; estimate subsurface dielectric properties and the density of buried scatterers in targeted regions.	Ice Penetrating Radar (~50 MHz with up to ~10 MHz bandwidth)	Ice Penetrating Radar (~50 MHz with up to ~10 MHz bandwidth)		
					GB.1b. Perform globally distributed profiling with better than 50-km profile spacing of subsurface thermal, compositional and structural horizons at depths of 1- to 30-km at 100 meter vertical resolution, and obtain simultaneous topography at better than or equal to 1 km/pixel spatial scale and better than or equal to 10 meter range accuracy.	Ice Penetrating Radar, Laser Altimeter	Ice Penetrating Radar, Laser Altimeter		
					GB.1c. Perform surface reflectance measurements in the wavelength range from 0.1 to greater than or equal to 5 microns of targeted features at better than or equal to 100 m/pixel spatial resolution, with spectral resolution sufficient to distinguish sulfuric acid hydrate from Mg- and Na-enriched salt hydrates (better than 2 nm from 0.1 to 0.32 microns, better than 5 nm from 0.4 to 2.5 microns and better than 10 nm from 2.5 to greater than or equal to 5 microns).	Vis-IR Spectrometer, UV Spectrometer	Visible InfraRed Hyperspectral Imaging Spectrometer, UltraViolet Imaging Spectrometers		
			GB.2	Correlate surface features and subsurface structure to investigate near-surface and interior processes.	GB.2a. Identify and locally characterize subsurface compositional horizons and structures by obtaining profiles of subsurface dielectric horizons and structures, with better than 50-km profile spacing over more than 80% of the surface, at depths of 100 meters to 6- to 9-km and vertical resolution ranging from a minimum of 10 meters to one percent of the target depth; estimate subsurface dielectric properties and the density of buried scatterers in targeted regions.	Ice Penetrating Radar (~50 MHz with up to ~10 MHz bandwidth)	Ice Penetrating Radar (~50 MHz with up to ~10 MHz bandwidth)		
					GB.2b. Measure topography at better than or equal to 1-km horizontal scale and better than or equal to 20-meter vertical resolution and accuracy, over more than 80% of the surface, co-located with subsurface profiles sounding data.	Wide Angle Camera, Laser Altimeter	Wide Angle Camera, Laser Altimeter		
					GB.2c. Measure surface reflectance in the wavelength range from 0.1 to greater than or equal to 5 microns of targeted features at better than or equal to 100 m/pixel spatial resolution, with spectral resolution sufficient to distinguish sulfuric acid hydrate from Mg- and Na-enriched salt hydrates (better than 2 nm from 0.1 to 0.32 microns; better than 5 nm from 0.4 to 2.5 microns and better than 10 nm from 2.5 to greater than or equal to 5 microns).	Vis-IR Spectrometer, UV Spectrometer	Visible InfraRed Hyperspectral Imaging Spectrometer, UltraViolet Imaging Spectrometer		
					GB.2d. Perform radiometric-polarized measurements in 2 bands from 600- to 500-µm and 270- to 230-µm with spatial resolution of 200- to 400-meters and under different off-nadir angles in order to constrain the thermophysical properties of the ice, regolith and ice-regolith mixtures down to a depths of a few cm.	Sub-millimeter Wave Instrument	Sub-millimeter Wave Instrument		
					GB.2e. Perform detailed three-dimensional surface morphological characterization of targeted features through imaging at better than or equal to 25-meter horizontal scale and 10-meter vertical accuracy across selected targets co-located with subsurface profiles.	Narrow Angle Camera, Laser Altimeter	Narrow Angle Camera, Laser Altimeter		
					GB.2f. Perform globally distributed profiling of subsurface thermal, compositional and structural horizons to depths from 1-km up to 30-km with 100 meter vertical resolution.	Ice Penetrating Radar (~5 or 50 MHz with 1 MHz bandwidth)	Ice Penetrating Radar (~5 or 50 MHz with 1 MHz bandwidth)		

Science Value Rating Criteria						
Significant contribution or achieves the measurement (75% to 100%)	Major contribution to achieving the measurement (50% to 75%)	Moderate contribution to achieving the measurement (25% to 50%)	Litte or no contribution to achieving the measurement (less than 25%)	Tour trajectory does not provide a suitable opportunity to make observations	Example instrument not in model payload

GANYMEDE									
Goal	**Science Objective**		**Science Investigation**		**Example Measurements**	**JEO Example Instruments**	**JGO Example Instruments**	**JEO**	**JGO**
Characterize Ganymede as a planetary object including its potential habitability	**GB. Ice Shell**	Characterize the ice shell.	GB.2	Correlate surface features and subsurface structure to investigate near-surface and interior processes.	GB.2g. Determine the thermal emission flux by: 1) measuring global surface thermal emission at a spatial resolution of 5 km/pixel to 10% radiometric accuracy at least two thermal wavelengths; 2) identifying thermally-controlled subsurface horizons within the ice shell at depths of 1- to 30-km at 100 meter vertical resolution.	Thermal Instrument, Ice Penetrating Radar	Ice Penetrating Radar, Sub-millimeter Wave Instrument, Visible InfraRed Hyper-spectral Imaging Spectrometer		
	GC. Local environment	Characterize the local environment and its interaction with the jovian magnetosphere.	GC.1	Globally characterize Ganymede's intrinsic and induced magnetic fields, with implications for the deep interior.	GC.1a. Measure three-axis magnetic field components at 32 Hz (required rate depends on the expected orbital velocity such that the magnetic field vector is sampled at least once per 300 km) to an accuracy of 0.1 nT.	Magnetometer	Magnetometer		
					GC.1b. Measure three-dimensional distribution functions for electrons and ions (first order mass resolution) over 4p and an energy range of a few eV to a few tens keV and cold plasma density and velocity. Requires imaging (better than 5 degrees angular resolution) of tens eV to a few keV neutrals from the surface.	Particle and Plasma Instrument, Ion and Neutral Mass Spectrometer	Particle and Plasma Instrument–Ion Neutral Mass Spectrometer		
					GC.1c. Determine electric Field Vectors (near DC to 3 MHz), electron/ion density, electron temperature for local conductivity, and electrical currents.	Radio and Plasma Wave Instrument (including Langmuir probe)	Radio and Plasma Wave Instrument (including Langmuir probe)		
			GC.2	Characterize the particle population within Ganymede's magnetosphere and its interaction with Jupiter's magnetosphere.	GC.2a. Measure three-axis magnetic field components at 32 Hz (required rate depends on the expected orbital velocity such that the magnetic field vector is sampled at least once per 300 km).	Magnetometer	Magnetometer		
					GC.2b. Measure the distribution of bulk plasma and bulk ion drift speed with 10 second resolution; Determine electron and ion density 0.001- to 10^4/cm^3, electron temperature (0.01- to 100-eV), bulk ion drift speed (0- to 200-km/s), as well as suprathermal electrons (non-Maxwellian distribution). Constrain ion temperature (0.01- to 20 eV)	Radio and Plasma Wave Instrument (including Langmuir probe)	Radio and Plasma Wave Instrument (including Langmuir probe)		
					GC.2c. Measure three-dimensional distribution functions of electrons and ions in the energy range of 10 eV to a few MeV with 4p coverage with a 10 second resolution and first order mass analysis. Determine plasma composition with the mass resolution M/dM greater than 20. Measure open source positive ion spectrum, negative ion spectrum, neutral spectrum, and closed source neutral spectrum. Spatial (less than 5 degree angular resolution and 30 minute time resolution) and energy characterization of the sputtered/backscattered neutrals (H and heavies in the 10- to 300-keV)	Particle and Plasma Instrument, Ion and Neutral Mass Spectrometer	Particle and Plasma Instrument–Ion Neutral Mass Spectrometer		
					GC.2d. Measure Ganymede's aurora emissions with sufficient spatial resolution to characterize the variability of the atmosphere and provide a complementary observation of the open/closed field line boundary through two-dimensional spectral-spatial images. Perform observations in the wavelength range of 120- to 200-nm to measure OI (135.6 nm, 130.4 nm) and H Ly alpha with a spectral resolution of at least 0.5 nm to derive information on the energy and energy flux of the incoming particles.	UV Spectrometer	UltraViolet Imaging Spectrometer		
			GC.3	Investigate the generation of Ganymede's aurorae.	GC.3a. Measure the three-dimensional distribution function of electrons and ions in the energy range of tens eV to a few keV with the 4p coverage and time resolution tens of seconds. Obtain Energetic Neutral Atom (ENA) images in the energy range of 10 eV to a few keV. Measure the open source neutral spectrum and the closed source neutral spectrum.	Particle and Plasma Instrument, Ion and Neutral Mass Spectrometer	Particle and Plasma Instrument–Ion Neutral Mass Spectrometer		
					GC.3b. Measure three-axis magnetic field components at 32 Hz (required rate depends on the expected orbital velocity such that the magnetic field vector is sampled at least once per 300 km).	Magnetometer	Magnetometer		
					GC.3c. Perform multi-wavelength spectral and monochromatic imaging of Ganymede's aurora in the wavelength range of 0.1- to 5.2-microns with a spectral resolution of 0.5 nm for wavelengths of 120- to 350-nm. Requires a temporal resolution of 1-minute and a spatial resolution better than 1-km/pixel.	UV Spectrometer, Vis-IR Spectrometer	UltraViolet Imaging Spectrometer, Visible InfraRed Hyper-spectral Imaging Spectrometer		

Science Value Rating Criteria					
Significant contribution or achieves the measurement (75% to 100%)	Major contribution to achieving the measurement (50% to 75%)	Moderate contribution to achieving the measurement (25% to 50%)	Litte or no contribution to achieving the measurement (less than 25%)	Tour trajectory does not provide a suitable opportunity to make observations	Example instrument not in model payload

GANYMEDE									
Goal	**Science Objective**		**Science Investigation**		**Example Measurements**	**JEO Example Instruments**	**JGO Example Instruments**	**JEO**	**JGO**
Characterize Ganymede as a planetary object including its potential habitability	**GC. Local environment**	Characterize the local environment and its interaction with the jovian magnetosphere.	GC.3	Investigate the generation of Ganymede's aurorae.	GC.3d. Determine electric field vectors/polarization (near DC to 45 MHz). Determine electron and ion density (0.001- to $10^4/cm^3$), bulk ion drift speed (0- to 200-km/s), as well as suprathermal electrons. Measure small scale density perturbations (δn/n, near DC to 10 kHz). Determine the presence of electrostatic and electromagnetic wave emissions of importance for the auroral energy transfer (near DC to 20 kHz).	Radio and Plasma Wave Instrument (including Langmuir probe)	Radio and Plasma Wave Instrument (including Langmuir probe)		
			GC.4	Determine the sources and sinks of the ionosphere and exosphere.	GC.4a. Global measurements in the wavelength range of 0.1- to 5-microns to determine column densities of atmospheric species at better than or equal to 1 km/pixel spatial resolution. Spectral resolution: better than 1 nm resolution in the range from 100- to 320-nm; better than or equal to 5 nm from 400- to 2500-nm; better than or equal to 10 nm from 2500 to greater than or equal to 5000 nm; 0.1 micron in the sub-mm range. Perform long-term and high-temporal-resolution monitoring in context of magnetospheric variations.	UV Spectrometer, Vis-IR Spectrometer	UltraViolet Imaging Spectrometer, Visible InfraRed Hyper-spectral Imaging Spectrometer, Sub-millimeter Wave Instrument		
					GC.4b. Determine the composition, distribution and physical characteristics (grain-size, crystallinity, physical state) of volatile materials on the surface in the overall spectral range 100 to greater than or equal to 5.0-microns, including measurements of water ice, O_2, O_3, H_2O_2, carbon dioxide ices and other species. Spectral resolution: better than or equal to 2 nm from 100- to 320-nm, better than or equal to 10 nm from 1.0 to 5.0 microns. Determination of the oxygen and hydrogen isotopic composition of surface water ice along sub-solar longitudes with about 2 km × 4 km spatial resolution through observations in two far infrared bands in the 500- to 600-μm and 230- to 270-μm wavelength range.	UV Spectrometer, Vis-IR Spectrometer	UltraViolet Imaging Spectrometer, Vis-IR Imaging Spectrometer, and Submillimeter Wave Instrument		
					GC.4c. Perform stellar occultations in the wavelength range of 100-nm to 5.0 microns to search for absorption and/or emission signatures of atmospheric species (*e.g.*, water and oxygen). Cover 100- to 200-nm at better than or equal to 0.5 nm resolution, and latitude/longitude resolution of better than 30 deg.	UV Spectrometer, Vis-IR Spectrometer	UltraViolet Imaging Spectrometer, Visible InfraRed Hyper-spectral Imaging Spectrometer		
					GC.4d. Perform scans perpendicular to the limb from ~5 km above the surface to the surface of the satellite in the wavelength range of 100-nm to greater than 5.0-microns (spectral resolution of 2 nm from 100- to 200-nm, better than or equal to 5 nm from 1.0- to 2.5-microns and better than or equal to 10 nm from 2.5- to greater than or equal to 5.0 microns) to measure or search for emission from O (135.6 nm), O_2 (1.27 microns), H_2O, CO_2 (4.26 microns) and other species in the atmosphere. Determine the concentration of water vapor and its three-dimensional distribution by observations of the 557 GHz rotational transition of water.	UV Spectrometer, Vis-IR Spectrometer	UltraViolet Imaging Spectrometer, Vis-IR Imaging Spectrometer, Submillimeter Wave Instrument		
					GC.4e.Obtain two-dimensional spectral-spatial images at in the wavelength range of 120- to 300-nm covering emissions from OI (135.6 nm, 130.4 nm), H Ly alpha, OH, Na, Ca, etc. at spectral resolution of at least 0.5 nm in the wavelength range of 120- to 200-nm and better than 1 nm in the wavelength range of 200- to 300-nm.	UV Spectrometer	UltraViolet Imaging Spectrometer		
					GC.4f. Perform radio occultations to measure the neutral atmosphere and ionosphere.	Radio Subsystem	Radio Science Instrument & USO		
					GC.4g. Measure neutrals coming off Ganymede with a mass range up to 300 Daltons and a mass resolution of up to 500.	Ion and Neutral Mass Spectrometer	Particle and Plasma Instrument–Ion Neutral Mass Spectrometer		
					GC.4h. Measure three-axis magnetic field components at 32 Hz (required rate depends on the expected orbital velocity such that the magnetic field vector is sampled at least once per 300 km).	Magnetometer	Magnetometer		

Science Value Rating Criteria						
	Significant contribution or achieves the measurement (75% to 100%)	Major contribution to achieving the measurement (50% to 75%)	Moderate contribution to achieving the measurement (25% to 50%)	Litte or no contribution to achieving the measurement (less than 25%)	Tour trajectory does not provide a suitable opportunity to make observations	Example instrument not in model payload

GANYMEDE									
Goal	**Science Objective**		**Science Investigation**		**Example Measurements**	**JEO Example Instruments**	**JGO Example Instruments**	**JEO**	**JGO**
Characterize Ganymede as a planetary object including its potential habitability	**GC. Local environment**	Characterize the local environment and its interaction with the jovian magnetosphere.	GC.4	Determine the sources and sinks of the ionosphere and exosphere.	GC.4i. Measure the phase space distribution function of ions in the energy range ~1 eV to ~1 MeV with 4p coverage. The mass resolution should be sufficient to distinguish between key magnetospheric and ionospheric pickup ions. Measure neutral exospheric composition with sufficient sensitivity and to sufficient mass resolution to identify major volatile species with mixing ratios better than 1%. Map directly the backscattering neutral flux from the surface in the energy range to 10 eV to 10 keV at a velocity resolution better than 30% and angular resolution less than 7 degrees.	Particle and Plasma Instrument, Ion and Neutral Mass Spectrometer	Particle and Plasma Instrument–Ion Neutral Mass Spectrometer		
					GC.4j. Determine the plasma density and temperature of the ionosphere, ion drift speeds (dynamics) in the ionosphere, and the electric field vector. Measure electron and ion density (0.001- to $10^4/cm^3$) and electron temperature (0- to 100-eV), as well as the ion ram speed (0- to 200-km/s). Constrain ion temperature (0- to 20- eV). Determine the ionizing Extreme Ultraviolet flux. Determine the electric field vectors (near DC to 3 MHz). Determine the presence of suprathermal electrons and plasma inhomogenities (δn/n, 0-10 kHz).	Particle and Plasma Instrument	Radio and Plasma Wave Instrument (including Langmuir probe)		
					GC.4k. Determine the vertical temperature profile from the ground to 300- to 400-km altitude with about 5 km vertical resolution by multiple water line observations in the 500- to 600-μm and 230- to 270-μm wavelength range. Determine the ortho-para ratio in water ice by simultaneous observations of ortho- and para- water lines in the 230- to 270-μm wavelength range.	Submillimeter Wave Instrument	Submillimeter Wave Instrument		
					GC.4l. Obtain local thermal maps over a range of representative terrains, latitudes, longitudes, and local times, especially near noon with better than 1 km/pixel resolution, at two well-separated thermal wavelengths for sensitivity to sub-pixel thermal inhomogenities.	Thermal Instrument, Vis-IR Spectrometer	Visible InfraRed Hyperspectral Imaging Spectrometer		
	GD. Geology	Understand the formation of surface features and search for past and present activity.	GD.1	Determine the formation mechanisms and characteristics of magmatic, tectonic, and impact landforms.	GD.1a. Determine the distributions and morphologies of surface landforms at regional and local scales. In addition, constrain the regional and global stratigraphic relationships among them, by determining surface color characteristics at ~100-m/pixel scale in at least 3 colors with near-uniform lighting conditions and solar phase angles less than or equal to 45 degrees, over more than 80% of the surface. Characterize selected 20-km × 20-km (or larger) areas at 10m/pixel.	Narrow Angle Camera, Wide Angle Camera	Narrow Angle Camera, Wide Angle Camera		
					GD.1b. Characterize small-scale three-dimensional surface morphology, at ~1- to 10-m/pixel over targeted sites, with vertical resolution of better than or equal to 1-meter. Requires context coverage at 10× greater scale and not worse than 10× coarser resolution.	Narrow Angle Camera	Narrow Angle Camera		
					GD.1c. Acquire imaging at 2- to 10-m/pixel of high science interest targets with at least 2- to 20-km wide swaths and with simultaneous altimetric profiles to at least 10-meter vertical resolution and better than 1 km horizontal resolution (at least 100 meter horizontal resolution preferable and at least along specific spacecraft tracks if not globally).	Narrow Angle Camera, Laser Altimeter	Narrow Angle Camera, Laser Altimeter		
					GD.1d. Globally characterize at least the 400 m/pixel (desired 100 m/pixel) to provide context for higher resolution data. Targeted imaging at 2- to 10-m/pixel with repeat pass for stereo coverage for ~2% of the surface.	Narrow Angle Camera, Wide Angle Camera	Narrow Angle Camera, Wide Angle Camera		
					GD.1e. Constrain heat flow by making thermal measurements in the 8- to 100-micron range with a spectral resolution of 2K and spatial resolution better than 30 km/pixel. Requires that observations be made several times of day and at night.	Thermal Instrument	Thermal Instrument		
			GD.2	Constrain global and regional surface ages.	GD.2a. Determine the distributions and morphologies of surface landforms at regional and local scales. In addition, constrain the regional and global stratigraphic relationships among them, by imaging at ~100-m/pixel in at least 3 colors (e.g., 0.4-mm, 0.7-mm, 0.9-mm) with near-uniform lighting conditions and solar phase angles less than or equal to 45 degrees, over more than 80% of the surface.	Narrow Angle Camera, Wide Angle Camera	Narrow Angle Camera, Wide Angle Camera		
					GD.2b. Characterize the morphology of targeted features through imaging at better than or equal 1 m/pixel spatial scale.	Narrow Angle Camera	Narrow Angle Camera		

Science Value Rating Criteria						
Significant contribution or achieves the measurement (75% to 100%)	Major contribution to achieving the measurement (50% to 75%)	Moderate contribution to achieving the measurement (25% to 50%)	Litte or no contribution to achieving the measurement (less than 25%)	Tour trajectory does not provide a suitable opportunity to make observations	Example instrument not in model payload

GANYMEDE									
Goal	**Science Objective**		**Science Investigation**		**Example Measurements**	**JEO Example Instruments**	**JGO Example Instruments**	**JEO**	**JGO**
Characterize Ganymede as a planetary object including its potential habitability	**GD. Geology**	Understand the formation of surface features and search for past and present activity.	GD.2	Constrain global and regional surface ages.	GD.2c. Acquire high spatial resolution observations (better than or equal to 100 m/pixel) from 100-nm to greater than or equal to 5.0-microns (spectral resolution: better than or equal to 2 nm from 100- to 320-nm; better than or equal to 5 nm from 400-nm to 2.5 microns; better than or equal to 10 nm from 2.5 to greater than or equal to 5.0 microns) on the leading hemisphere, particularly on the subjovian quadrant, with emphasis on the spectral differences between geologic features and the surrounding areas. Medium spatial resolution (better than or equal to 5 km/pixel) on large areas to map leading/trailing asymmetries due to contamination by exogenic material.	Vis-IR Spectrometer, UV Spectrometer	Visible InfraRed Hyperspectral Imaging Spectrometer, UltraViolet Imaging Spectrometer		
					GD.2d. Globally identify and locally characterize physical and dielectric subsurface horizons, at depths of 1- to 30-km at 100-meter vertical resolution and depths of 100-meters to 3-km at 10-meter vertical resolution, by obtaining subsurface sounding profiles with better than 50-km spacing over more than 80% of the surface, plus targeted characterization of selected sites.	Ice Penetrating Radar	Ice Penetrating Radar		
			GD.3	Investigate processes of erosion and deposition and their effects on the physical properties of the surface.	GD.3a. Perform thermal mapping at better than or equal to 250-m/pixel spatial resolution with temperature accuracy better than 2 K, and albedo measurements to 10% radiometric accuracy. Requires covering more than 80% of the surface with the same regions observed in both the day and night.	Thermal Instrument	Thermal Instrument		
					GD.3b. Characterize the morphology of targeted features through imaging at better than or equal 1 m/pixel spatial scale.	Narrow Angle Camera	Narrow Angle Camera		
					GD.3c. Determine the precipitation flux of electrons and ions (with composition) in the eV to few MeV energy range. Measure sputtered exospheric products. Perform measurements in the wavelength range of 1000-nm to 5000-nm with a spectral resolution better than or equal to 5 nm to characterize water ice bands at 1650 nm, 2000 nm, 3100 nm and 4530 nm (e.g., grain size), and hydrated salts and sulfuric acid hydrate at a spatial resolution better than 1 km.	Particle and Plasma Instrument, Ion and Neutral Mass Spectrometer, Vis-IR Spectrometer	Particle and Plasma Instrument–Ion Neutral Mass Spectrometer, Visible InfraRed Hyper-spectral Imaging Spectrometer		
					GD.3d. Measure ion-cyclotron waves and relate to plasma-pickup and erosion by magnetic field sampling at 32 vectors/s and a sensitivity of 0.1 nT, to constrain sputtering rates.	Magnetometer	Magnetometer		
	GE. Composition	Determine global composition, distribution and evolution of surface materials.	GE.1	Characterize surface organic and inorganic chemistry, including abundances and distributions of materials.	GE.1a. Identify and map non-water-ice materials (including organic compounds and radiolytic materials) over a wide range of spatial scales (from 5 km/pixel to 100 m/pixel or better), in the overall spectral range of 100 to greater than or equal to 5.0-microns and with a spectral resolution better than or equal to 1 nm from 100- to 320-nm; better than or equal to 5 nm from 400-nm to 2.5 microns and better than or equal to 10 nm from 2.5 to greater than or equal to 5.0 microns. At least 50% coverage with spatial resolution better than or equal to 2 km/pixel.	Vis-IR Spectrometer, UV Spectrometer.	Visible InfraRed Hyperspectral Imaging Spectrometer, UltraViolet Imaging Spectrometer.		
					GE.1b. Identify globally distributed bulk material composition by measuring grain size, porosity, crystallinity, and physical state of water ice in the spectral range from 1.0- to 4.0-microns with a spectral resolution better than or equal to 10 nm and over a wide range of spatial scales (from 10 km/pixel to 100 m/pixel or better), and from polarized continuum observations of the surface in the 500- to 600-μm and 230- to 270-μm wavelength ranges under different off-nadir angles. Constrain the dielectric permittivity of the surface material by bistatic radar observations.	Vis-IR Spectrometer, Radio Subsystem	Visible InfraRed Hyperspectral Imaging Spectrometer, Sub-millimeter Wave Instrument, Radio Science Instrument		
					GE.1c. Image at resolution of ~5 m/pixel with an image width of ~2-km. Obtain repeat coverage to facilitate stereo analysis of targeted features.	Narrow Angle Camera	Narrow Angle Camera		
			GE.2	Relate compositions and properties and their distributions to geology.	GE.2a. Acquire global imaging at 400 m/pixel in four colors (e.g., 0.4-mm, 0.5-mm, 0.7-mm, 0.9-mm). Obtain three-color (e.g., 0.4-mm, 0.7-mm, 0.9-mm) coverage for selected large areas at up to or better than 100 m/pixel. Acquire image mosaics at a uniform spatial resolution and viewing angle (e.g., mid-morning/mid-afternoon).	Narrow Angle Camera, Wide Angle Camera	Narrow Angle Camera, Wide Angle Camera		

Science Value Rating Criteria					
Significant contribution or achieves the measurement (75% to 100%)	Major contribution to achieving the measurement (50% to 75%)	Moderate contribution to achieving the measurement (25% to 50%)	Litte or no contribution to achieving the measurement (less than 25%)	Tour trajectory does not provide a suitable opportunity to make observations	Example instrument not in model payload

GANYMEDE									
Goal	**Science Objective**		**Science Investigation**		**Example Measurements**	**JEO Example Instruments**	**JGO Example Instruments**	**JEO**	**JGO**
Characterize Ganymede as a planetary object including its potential habitability	**GE. Composition**	Determine global composition, distribution and evolution of surface materials.	GE.2	Relate compositions and properties and their distributions to geology.	GE.2b. Measure three-dimensional distribution function of ions in the energy range ~1 eV to ~1 MeV with the 4p coverage. Mass resolution should be sufficient to distinguish between key magnetospheric and ionospheric pickup ions. Measure neutral exospheric composition with sufficient sensitivity and to sufficient mass resolution to identify major volatile species with mixing ratios better than 1%. Map directly the backscattering neutral flux from the surface in the energy range 10 eV to 10 keV at a velocity resolution better than 30% and angular resolution less than 7 degrees.	Particle and Plasma Instrument	Particle and Plasma Instrument–Ion Neutral Mass Spectrometer		
					GE.2c. Detect dust and determine its mass and size distribution with electric field (near DC to 45 MHz). Measure electric field vectors (near DC to 3 MHz) that accelerate charged dust and plasma near the surface.	Radio and Plasma Wave Instrument (including Langmuir probe)	Radio and Plasma Wave Instrument (including Langmuir probe)		
					GE.2d. Map daytime and nighttime temperatures to identify variations in regolith properties and thermal skin depth with latitude and longitude. Perform measurements in the 8- to 100-micron range with a spectral resolution of 2K and spatial resolution better than 30 km/pixel.	Thermal Instrument	Submillimeter Wave Instrument		
					GE.2e. Identify and locally characterize subsurface compositional horizons and structures by obtaining profiles of subsurface dielectric horizons and structures, with better than 50-km profile spacing over more than 80% of the surface, at depths of 100 meters to 6- to 9-km and vertical resolution ranging from a minimum of 10-meters to one percent of the target depth; estimate subsurface dielectric properties and the density of buried scatterers in targeted regions.	Ice Penetrating Radar (~50 MHz with up to ~10 MHz bandwidth)	Ice Penetrating Radar (~50 MHz with up to ~10 MHz bandwidth)		
					GE.2f. Measure topography at better than or equal to 1-km horizontal scale and better than or equal to 20-m vertical resolution and accuracy, over more than 80% of the surface, co-located with subsurface profiles.	Wide Angle Camera, Laser Altimeter	Wide Angle Camera, Laser Altimeter		
					GE.2g. Map non-water-ice materials (including organics and products of radiolysis and ion bombardment, e.g., H_2O_2, O_3, H_2CO, H_2CO_3) and their association with known geologic features over the wavelength range of 100- to 320-nm with spectral resolution better than or equal to 1 nm and over the wavelength range of 400-nm to greater than or equal to 5.0-microns with spectral resolution better than or equal to 5 nm from 400-nm to 2.5-microns; better than or equal to 10 nm from 2.5 to greater than or equal to 5.0-microns. Requires at least 50% coverage with spatial resolution better than or equal to 2 km/pixel.	UV Spectrometer, Vis-IR Spectrometer	UltraViolet Imaging Spectrometer, Visible InfraRed Hyper-spectral Imaging Spectrometer		
					GE.2h. Determine the origin and evolution of non-water-ice materials by making measurements in the wavelength range of 0.8- to greater than or equal to 5.0-microns with a spectral resolution better than or equal to 10 nm and a spatial resolution better than or equal to 1 km/pixel of representative features. Co-register with higher-resolution monochromatic images at better than or equal to 100 m/pixel.	Vis-IR Spectrometer, Narrow Angle Camera	Visible InfraRed Hyperspectral Imaging Spectrometer, Narrow Angle Camera		
			GE.3	Investigate surface composition and structure on open vs. closed field line regions.	GE.3a. Map several known or expected tracer species of weathering effects induced by the magnetosphere (e.g., H_2O, CO_2, NH_3, O_3, H_2O_2, H_2SO_4 hydrate, etc.) over the wavelength range of 100- to 320-nm with spectral resolution better than or equal to 4 nm and over the wavelength range of 1.0- to 2.5-µm with a spectral resolution better than or equal to 5 nm and 2.5- to 5-µm with a spectral resolution less than or equal to 10 nm. Requires at least 50% coverage with spatial resolution better than or equal to 2 km/pixel.	UV Spectrometer, Vis-IR Spectrometer	UltraViolet Imaging Spectrometer, Visible InfraRed Hyper-spectral Imaging Spectrometer		
					GE.3b. Map the distribution of the state of water ice (crystalline vs. amorphous) as a function of the latitude, in the spectral range from 1.0- to 4.0-µm with spectral resolution less than or equal to 10 nm. Map targeted features to assess local conditions (albedo) in the 0.4- to 1.0-µm range. Requires at least 50% coverage with spatial resolution better than or equal to 2 km/pixel.	Vis-IR Spectrometer	Visible InfraRed Hyperspectral Imaging Spectrometer		
					GE.3c. Measure three-axis magnetic field components at 8- to 128 Hz at a sensitivity of 0.1 nT at different orbital phases and closest approach of less than 0.5 planetary radii.	Magnetometer	Magnetometer		
					GE.3d. Global monochromatic imaging at 400 m/pixel with selected features mapped in 4 colors (e.g., 0.4-mm, 0.5-mm, 0.7-mm, 0.9-mm) at 100 m/pixel. Targeted imaging at a resolution of better than 20 m/pixel with an image width of ~ 2 km.	Narrow Angle Camera, Wide Angle Camera	Narrow Angle Camera, Wide Angle Camera		

Science Value Rating Criteria						
Significant contribution or achieves the measurement (75% to 100%)	Major contribution to achieving the measurement (50% to 75%)	Moderate contribution to achieving the measurement (25% to 50%)	Litte or no contribution to achieving the measurement (less than 25%)	Tour trajectory does not provide a suitable opportunity to make observations	Example instrument not in model payload

GANYMEDE									
Goal	**Science Objective**		**Science Investigation**		**Example Measurements**	**JEO Example Instruments**	**JGO Example Instruments**	**JEO**	**JGO**
Characterize Ganymede as a planetary object including its potential habitability	**GE. Composition**	Determine global composition, distribution and evolution of surface materials.	GE.3	Investigate surface composition and structure on open vs. closed field line regions.	GE.3e. Measure phase space distribution function of ions in the energy range ~1 eV to ~1 MeV with the 4p coverage. Requires mass resolution sufficient to distinguish between key magnetospheric and ionospheric pickup ions. Measure neutral exospheric composition with sufficient sensitivity and to sufficient mass resolution to identify major volatile species with mixing ratios better than 1%. Measure phase space distribution of electrons from 10 eV to ~1MeV.	Particle and Plasma Instrument, Ion and Neutral Mass Spectrometer	Particle and Plasma Instrument–Ion Neutral Mass Spectrometer		
					GE.3f. Measure electron and ion density and electron temperature (0- to 100- eV), as well as constrain ion temperature (0- to 20-eV). Detect dust and determine its mass/size distribution with electric field (near DC to 45 MHz). Measure electric field vectors (near DC to 3 MHz) that accelerate charged dust and plasma toward the surface.	Radio and Plasma Wave Instrument (including Langmuir probe)	Radio and Plasma Wave Instrument (including Langmuir probe)		
					GE.3g. Map directly the backscattering neutral flux from the surface in the energy range 10 eV to 10 keV at a velocity resolution better than 30% and angular resolution less than 7 degrees.	Particle and Plasma Instrument, Neutral Mass Spectrometer	Particle and Plasma Instrument–Ion Neutral Mass Spectrometer		
			GE.4	Determine volatile content to constrain satellite origin and evolution.	GE.4a. Measure the stable isotopes of C, H, O, and N in the major volatiles (e.g., H_2O, CH_4, NH_3, CO, CO_2, SO_2), and measure the noble gases Ar, Kr, and Xe, with mass resolution better than 500 and sensitivity to measure partial pressures as low as 10^{-17} mbar. Characterize the composition of sputtered desorbed volatiles over a mass range better than 300 Daltons with mass resolution better than 500.	Ion and Neutral Mass Spectrometer	Ion and Neutral Mass Spectrometer		
					GE.4b. Determine the D/H ratio in water ice from simultaneous limb observations of HDO and H_2O spectra in the tangential point above the surface	Submillimeter Wave Instrument	Submillimeter Wave Instrument		
					GE.4c. Identify and map non-water-ice materials over a wide range of spatial scales (from 5 km/pixel to 100 m/pixel or better), in the overall spectral range 0.1 to greater than or equal to 5 μm and with a spectral resolution (better than or equal to 1 nm from 100- to 320-nm; better than or equal to 5 nm from 0.4 to 2.5 μm and better than or equal to 10 nm from 2.5 to greater than or equal to 5 μm) suitable to discriminate various volatiles known or expected to exist on the surface. Requires at least 50% coverage with spatial resolution better than or equal to 2 km/pixel.	Vis-IR Spectrometer, UV Spectrometer.	Visible InfraRed Hyperspectral Imaging Spectrometer, UltraViolet Imaging Spectrometer.		
					GE.4d. Identify globally distributed bulk material composition in the spectral range from 1.0- to 4.0-μm with a spectral resolution better than or equal to 10 nm and over a wide range of spatial scales (from 10 km/pixel to 100 m/pixel or better), and from polarized continuum observations of the surface in the 500- to 600-μm and 230- to 270-μm wavelengths ranges under different off-nadir angles.	Vis-IR Spectrometer	Visible InfraRed Hyperspectral Imaging Spectrometer, Sub-millimeter Wave Instrument		

Science Value Rating Criteria						
Significant contribution or achieves the measurement (75% to 100%)	Major contribution to achieving the measurement (50% to 75%)	Moderate contribution to achieving the measurement (25% to 50%)	Litte or no contribution to achieving the measurement (less than 25%)	Tour trajectory does not provide a suitable opportunity to make observations	Example instrument not in model payload

JUPITER SYSTEM

SATELLITE SYSTEM

Goal		Science Objectives	Science Investigation		Example Measurements	JEO Example Instruments	JGO Example Instruments	JEO	JGO
Explore the Jupiter system as an archetype for gas giants	S. Study the Jovian satellite and ring system	SA. Study Io's active dynamic processes.	SA.1	Investigate the nature, distribution and magnitude of tidal dissipation and heat loss on Io.	SA.1a. Determine regional and global heat flow by measuring global surface thermal emission at spatial resolution of 5 km/pixel to 10% radiometric accuracy at two or more thermal wavelengths.	Thermal Instrument	Thermal Instrument		
					SA.1b. Globally map surface temperatures to 2K absolute accuracy, from ~80K to greater than 160K, with spatial resolution better than 10 km/pixel and selected targets at better than 500 m/pixel within 30 degrees of the noon meridian and at night.	Thermal Instrument	Thermal Instrument		
					SA.1c. Perform astrometric determination of the rate of change of Io's orbit by obtaining multiple full disk images of Io including background stars with a position accuracy of at least 1 km.	Narrow Angle Camera	Narrow Angle Camera		
					SA.1d. Determine the time-varying gravity of Io by measuring the range-rate from spacecraft tracking during multiple flybys at different orbital phase to resolve 2nd degree gravity field time dependence. Requires Doppler velocity of 0.1 mm/s over 60 s accuracy.	Radio Subsystem	Radio Science Instrument & USO		
			SA.2	Investigate Io's composition and active volcanism for insight into its origin, evolution and geological history (particularly of its silicate crust).	SA.2a. Perform repeated (daily to monthly) monochromatic imaging of selected active volcanic features at ~1 km/pixel spatial resolution along with global broadband characterization at ~10-km/pixel scale and color (e.g., green, red, violet, near-IR) at ~250 km/pixel scale.	Narrow Angle Camera, Wide Angle Camera	Narrow Angle Camera, Wide Angle Camera		
					SA.2b. Identify and map of sulphur species (including SO_2 frost) and silicates over a wide range of spatial scales (from 10 km/pixel to 100 m/pixel or better), with a spectral resolution (better than or equal to 5 nm from 0.4- to 2.5-μm and better than or equal to 10 nm from 2.5 to greater than or equal to 5 μm) suitable to discriminate among different compounds known or expected to exist on the surface.	Vis-IR Spectrometer	Visible InfraRed Hyperspectral Imaging Spectrometer		
					SA.2c. Measure the chemical constituents of the atmosphere as an indicator of surface and subsurface composition. Measurements over a mass range better than 300 Daltons and mass resolution better than 500 (high sensitivity and sufficient mass resolution to determine stable isotope ratios are highly desirable).	Ion and Neutral Mass Spectrometer	Particle and Plasma Instrument–Ion Neutral Mass Spectrometer		
					SA.2d. Perform repeated multispectral global mapping (minimum 3 colors; e.g., violet, green and NIR) at better than or equal to 10 km/pixel over a range of temporal scales (e.g., hourly, daily, weekly, monthly).	Narrow Angle Camera	Narrow Angle Camera		
					SA.2e. Perform high-resolution visible imaging (better than 100 m/pixel spatial resolution) of selected volcanic features for change detection (e.g., compare to Galileo and Voyager data).	Narrow Angle Camera	Narrow Angle Camera		
					SA.2f. Perform global (greater than 80%) monochromatic imaging at ~1 km/pixel spatial resolution.	Narrow Angle Camera	Narrow Angle Camera		
					SA.2g. Map volcanic thermal emissions at better than 100 km/pixel spatial scale in the wavelength range of 1- to 20-μm with absolute accuracy of 2K, sufficient to measure silicate melt temperatures, over a broad range of temporal scales (e.g., hours to years). Desire better than 20 km/pixel spatial resolution. Monochromatic imaging at a spatial scale of 10s of km/pixel.	Vis-IR Spectrometer, Narrow Angle Camera, Thermal Instrument	Visible InfraRed Hyperspectral Imaging Spectrometer, Narrow Angle Camera		
					SA.2h. Monitor plumes over a wavelength range of ~200-nm to 1-μm at high phase angle (for dust and gas emissions) and low phase angle (for gas absorptions) over a range of temporal scales (hours to weeks). Spatial resolution better than 20-km/pixel at visible wavelengths and better than 50-km/pixel at UV wavelengths.	UV Spectrometer, Narrow Angle Camera	UltraViolet Imaging Spectrometer, Narrow Angle Camera		
					SA.2i. Global thermal observations at least two well-separated wavelengths with a spatial resolution of 100s of km/pixel over periods of days to weeks.	Thermal Instrument	Thermal Instrument		
			SA.3	Determine Io's dynamical rotation state (forced libration, obliquity and nutation).	SA.3a. Determine the mean spin pole direction (obliquity) to at least 100 meters through globally distributed imaging at a resolution less than 500 meters/pixel to produce a geodetic control network (~20 points).	Narrow Angle Camera	Narrow Angle Camera		
					SA.3b. Determine forced nutation of the spin pole at the orbital period to at least 100 meters. Requires imaging at a resolution of better than 500 m/pixel at multiple tidal phases.	Narrow Angle Camera	Narrow Angle Camera		
					SA.3c. Determine the amplitude of the forced libration at the orbital period to better than 100 meters by generating a geodetic control network at a resolution better than 500 m/pixel at multiple tidal phases.	Narrow Angle Camera	Narrow Angle Camera		

Science Value Rating Criteria

Significant contribution or achieves the measurement (75% to 100%)	Major contribution to achieving the measurement (50% to 75%)	Moderate contribution to achieving the measurement (25% to 50%)	Litte or no contribution to achieving the measurement (less than 25%)	Tour trajectory does not provide a suitable opportunity to make observations	Example instrument not in model payload

JUPITER SYSTEM

SATELLITE SYSTEM

Goal		Science Objectives	Science Investigation		Example Measurements	JEO Example Instruments	JGO Example Instruments	JEO	JGO
Explore the Jupiter system as an archetype for gas giants	S. Study the Jovian satellite and ring system	SA. Study Io's active dynamic processes.	SA.4	Investigate the interior of Io.	SA.4a. Derive the static low-degree shape by measuring globally distribute topographic profiles with a vertical accuracy better than 1 meter and a 50 meter or better footprint (per elevation posting).	Laser Altimeter	Laser Altimeter		
					SA.4b. Image the limb for shape determination. Requires multiple images at better than 1 km/pixel resolution.	Wide Angle Camera	Wide Angle Camera		
					SA.4c. Determine the static gravity field at low order using range-rate from spacecraft tracking during multiple flybys at different latitudes and longitudes to resolve 2nd degree gravity field and local potential anomalies. Requires Doppler velocity of 0.1 mm/s over 60 s accuracy.	Radio Subsystem	Radio Science Instrument & USO		
			SA.5	Understand satellite origin and evolution by assessing sources and sinks of Io's crustal volatiles and atmosphere.	SA.5a. Characterize the volatile cycle, including composition, physical state, distribution, and transport of surface volatiles by global mapping of the surface at multiple wavelengths (e.g., for SO_2 frost variations) on a range of temporal scales (~days). Requires measurements at: (1) 0.2- to 0.35-µm with better than 20 nm spectral resolution and better than 100 km/pixel spatial resolution; (2) 0.35- to 1-µm at 2 nm resolution; and (3) 1- to 5-µm at 20 nm spectral resolution and ~10- to 500-km/pixel. Identify features in absorption including, H_2O, CO_2, NH_3 (at 120- to 200-nm), O_3, H_2O_2, SO_2 (at 200-nm to 300-nm) along with additional features in emissions (O, CO_2) and absorption (O_2, CO_2, O_3, H_2O).	UV Spectrometer, Vis-IR Spectrometer	UltraViolet Imaging Spectrometer, Visible InfraRed Hyper-spectral Imaging Spectrometer		
					SA.5b. Perform dayside, nightside, and eclipse observations in the wavelength range of ~100- to 350-nm including two-dimensional spectral-spatial images to detect emissions for S, O, Cl and SO2 and other gas density. Requires a spectral resolution of 0.5-nm for ~100- to 200-nm and better than 1-nm for 200- to 350-nm with better than 500-km/pixel spatial resolution.	UV Spectrometer	UltraViolet Imaging Spectrometer		
					SA.5c. Determine roles and rates of sublimation, sputtering, and radiation darkening by global mapping of the surface over a wide range of longitudes (i.e., to facilitate comparisons between leading and trailing hemispheres, especially in non-plume regions). Requires measurements at 0.1- to 1-microns with a spectral resolution of ~2 nm and from 1- to 5-microns at 10 nm spectral resolution over spatial scales of ~10- to 500-km/pixel along with 8- to 20-µm mapping with spatial resolution better than 10 km/pixel, including polar coverage.	UV Spectrometer, Vis-IR Spectrometer, Thermal Instrument	UltraViolet Imaging Spectrometer, Visible InfraRed Hyper-spectral Imaging Spectrometer		
					SA.5d. Measure the volatile content of potential outgassing sources from the near subsurface or deeper interior. Perform measurements over a mass range better than 300 Daltons and mass resolution better than 500 with sensitivity that allows the measurement of partial pressures as low as 10^{-17} mbar.	Ion and Neutral Mass Spectrometer	Particle and Plasma Instrument–Ion Neutral Mass Spectrometer		
					SA.5e. Determine column densities of atmospheric/plume species across the globe and document correlations with plumes, geologic features and local albedo variations. Perform global surface and limb observations in the wavelength range from 60- to 350-nm at a spectral resolution of 0.3 nm and spatial scale of better than 500 km/pixel and from 0.4- to 5-microns with a spectral resolution better than 10-nm and better than 50 km/pixel spatial resolution. Acquire visible (e.g., 390- to 800-nm) images of Io in eclipse.	UV Spectrometer, Vis-IR Spectrometer, Narrow Angle Camera	UltraViolet Imaging Spectrometer, Visible InfraRed Hyper-spectral Imaging Spectrometer Narrow Angle Camera		
					SA.5f. Perform stellar occultations in the wavelength range of 0.1- to 0.25-microns with a spectral resolution of 0.5 nm to measure SO_2, S_2, SO in absorption over a range of latitudes and longitudes. Requires coverage at a range of temporal scales periodically throughout the mission with resolution of 1 second.	UV Spectrometer	UltraViolet Imaging Spectrometer		
					SA.5g. Perform long-term and high-temporal-resolution monitoring of the atmosphere, plumes and limb-glow via 0.06- to 1-micron limb imaging observations over a range of temporal scales (e.g., hourly, daily, weekly, monthly). Requires measurements at 0.06- to 0.4-microns with a spectral resolution of 0.5 nm and a spatial resolution of better than 500 km/pixel and from 0.4- to 1.0-microns with a spectral resolution of better than or equal to 5 nm and spatial coverage at better than 10 km/pixel.	UV Spectrometer, Vis-IR Spectrometer	UltraViolet Imaging Spectrometer, Visible InfraRed Hyper-spectral Imaging Spectrometer		

Science Value Rating Criteria						
Significant contribution or achieves the measurement (75% to 100%)	Major contribution to achieving the measurement (50% to 75%)	Moderate contribution to achieving the measurement (25% to 50%)	Litte or no contribution to achieving the measurement (less than 25%)	Tour trajectory does not provide a suitable opportunity to make observations	Example instrument not in model payload

JUPITER SYSTEM

SATELLITE SYSTEM

Goal		Science Objectives	Science Investigation		Example Measurements	JEO Example Instruments	JGO Example Instruments	JEO	JGO
Explore the Jupiter system as an archetype for gas giants	S. Study the Jovian satellite and ring system	SA. Study Io's active dynamic processes.	SA.5	Understand satellite origin and evolution by assessing sources and sinks of Io's crustal volatiles and atmosphere.	SA.5h. Determine the composition, distribution and physical characteristics (grain-size, crystallinity) of volatile materials on the surface, including SO_2 frost by 0.4- to 5-micron imaging of selected yellow and gray targets at better than 10 km/pixel and selected green and red targets at ~1 km/pixel.	Vis-IR Spectrometer	Visible InfraRed Hyperspectral Imaging Spectrometer		
					SA.5i. Monitor H, O, and S in the 10- to 300-keV range, separating H from heavies (O, S) with 5 degree angular resolution and better than 60 min time resolution to assess long-term signatures of Io's extended neutral sulfur cloud by monitoring the extent of Energetic Neutral Atom (ENA) emissions from Jupiter's magnetosphere	Particle and Plasma Instrument, Ion and Neutral Mass Spectrometer	Particle and Plasma Instrument–Ion Neutral Mass Spectrometer		
					SA.5j. Monitor emissions from 1 kHz to 45 MHz from the Io environment including the Io tori	Radio and Plasma Wave Instrument	Radio and Plasma Wave Instrument		
					SA.5k. Perform radio occultation measurements to determine ionosphere electron density profiles.	Radio Subsystem	Radio Science Instrument & USO		
		SB. Study Callisto as a witness of the early jovian system.	SB.1	Investigate the interior of Callisto.	SB.1a. Derive the static shape by measuring range to the surface during multiple fly-bys. Requires topographic profiles distributed globally.	Laser Altimeter	Laser Altimeter		
					SB.1b. Image the limb for shape determination by acquiring multiple images at better than 1 km/pixel resolution.	Wide Angle Camera	Wide Angle Camera		
					SB.1c. Determine the static gravity field at low order by measuring the range-rate from spacecraft tracking during multiple flybys at a range of latitudes and longitudes to derive the 2nd degree gravity field and local potential anomalies. Requires Doppler velocity of 0.01 mm/s over 60 s accuracy.	Radio Subsystem	Radio Science Instrument & USO		
			SB.2	Characterize the space plasma environment to determine the magnetic induction response from Callisto's ocean.	SB.2a. Measure three-axis magnetic field components at 32 Hz to 128 Hz. Measure the magnetic field at 8 vectors/s and a sensitivity of 0.1 nT with multiple flybys at different orbital phases and closest approach of less than 0.5 planetary radii.	Magnetometer	Magnetometer		
					SB.2b. Measure three-dimensional distribution functions for electrons and ions (first order mass resolution) over 4π and an energy range of a few eV to a few tens keV and cold plasma density and velocity. Use energetic particle (greater than 10 keV) measurements to obtain flow anisotropies during cases when the plasma measurements cannot be obtained.	Particle and Plasma Instrument, Ion and Neutral Mass Spectrometer	Particle and Plasma Instrument–Ion Neutral Mass Spectrometer		
					SB.2c. Determine electric field vectors (near DC to 3 MHz). Measure electron and ion density (0.001- to 10^4/cm^3), and electron temperature (0.01- to 20-eV) for local conductivity and electrical currents determination.	Particle and Plasma Instrument	Radio and Plasma Wave Instrument		
			SB.3	Characterize the structure and properties of Callisto's icy shell.	SB.3a. Identify and locally characterize subsurface compositional horizons and structures by obtaining globally distributed profiles of subsurface dielectric horizons and structures, at depths of 100 meter to 30-km and vertical resolution ranging from a minimum of 100 meters to one percent of the target depth to estimate subsurface dielectric properties and the density of buried scatterers in targeted regions.	Ice Penetrating Radar (~5 to 50 MHz with 1 MHz bandwidth)	Ice Penetrating Radar (~5 to 50 MHz with 1 MHz bandwidth)		
			SB.4	Constrain the tidally varying potential and shape of Callisto.	SB.4a. Determine degree 2 time-varying gravity of Callisto by measuring the range-rate from spacecraft tracking during multiple flybys at different latitudes and longitudes to determine k_2 to 0.03 absolute error. Requires Doppler velocity of 0.01 mm/s over 60 s accuracy.	Radio Subsystem	Radio Science Instrument & USO		
					SB.4b. Determine the time-varying shape of Callisto to an accuracy of 1 meter by performing repeat altimetry profiles during multiple flybys at differing tidal phases.	Laser Altimeter	Laser Altimeter		
					SB.4c. Perform astrometric determination of the rate of change of Callisto's orbit by acquiring multiple images of Callisto from a distance including background stars with a position accuracy of at least 1 km.	Narrow Angle Camera	Narrow Angle Camera		
			SB.5	Determine Callisto's dynamical rotation state (forced libration, obliquity and nutation).	SB.5a. Determine the mean spin pole direction (obliquity) to better than 1 km by developing a geodetic control network (~20 points) at a resolution better than 500 m/pixel.	Narrow Angle Camera	Narrow Angle Camera		
					SB.5b. Determine the forced nutation of the spin pole at the orbital period to better than 100 meters by developing a geodetic control network at better than 500 m/pixel at multiple tidal phases.	Narrow Angle Camera	Narrow Angle Camera		

Science Value Rating Criteria					
Significant contribution or achieves the measurement (75% to 100%)	Major contribution to achieving the measurement (50% to 75%)	Moderate contribution to achieving the measurement (25% to 50%)	Litte or no contribution to achieving the measurement (less than 25%)	Tour trajectory does not provide a suitable opportunity to make observations	Example instrument not in model payload

JUPITER SYSTEM									
SATELLITE SYSTEM									
Goal		**Science Objectives**	**Science Investigation**		**Example Measurements**	**JEO Example Instruments**	**JGO Example Instruments**	**JEO**	**JGO**
Explore the Jupiter system as an archetype for gas giants	**S. Study the Jovian satellite and ring system**	SB. Study Callisto as a witness of the early jovian system.	SB.5	Determine Callisto's dynamical rotation state (forced libration, obliquity and nutation).	SB.5c. Determine the amplitude of the forced libration at the orbital period to better than 100 meters by developing a geodetic control network at a resolution better than 500 m/pixel at multiple tidal phases.	Narrow Angle Camera	Narrow Angle Camera		
			SB.6	Characterize surface organic and inorganic chemistry, including abundances and distributions of materials and volatile outgassing.	SB.6a. Identify and map non-water-ice materials (including organic compounds and radiolytic materials) over a wide range of spatial scales (from 5 km/pixel to 100 m/pixel or better), with a spectral resolution (better than or equal to 5 nm from 0.4- to 2.5-µm and better than or equal to 10 nm from 2.5 to greater than or equal to 5 µm) suitable to discriminate various compounds known or expected to exist on the surface. Acquire two-dimensional spectral-spatial images in the range 100- to 320-nm with a spectral resolution better than or equal to 1 nm.	Vis-IR Spectrometer, UV Spectrometer	Visible InfraRed Hyperspectral Imaging Spectrometer, UltraViolet Imaging Spectrometer		
					SB.6b. Determine globally distributed bulk material composition, grain size, porosity, crystallinity, and physical state of water ice in the spectral range from 1- to 4-microns with a spectral resolution better than or equal to 10 nm over a wide range of spatial scales (from 10 km/pixel to 100 m/pixel or better). Perform thermal observations with 2K absolute accuracy, from ~80K to greater than 160K and spatial resolution better than or equal to 10 km/pixel.	Vis-IR Spectrometer, Thermal Instrument	Visible InfraRed Hyperspectral Imaging Spectrometer		
					SB.6c. Determine the composition, distribution and physical characteristics (grain-size, crystallinity, physical state) of volatile materials on the surface, including measurements in the wavelength range of 100- to 320-nm at 2 nm spectral resolution to identify O_3, H_2O_2 and other species.	UV Spectrometer, Vis-IR Spectrometer	UltraViolet Imaging Spectrometer, Visible InfraRed Hyper-spectral Imaging Spectrometer		
					SB.6d. Measure the volatile content (i.e., water, carbon dioxide, methane, ammonia, and noble gases) of potential outgassing sources from the near subsurface or deeper interior over a mass range better than 300 Daltons with a mass resolution better than 500 and sensitivity that allows measurement of partial pressures as low as 10^{-17} mbar.	Ion and Neutral Mass Spectrometer	Particle and Plasma Instrument–Ion Neutral Mass Spectrometer		
					SB.6e. Image at medium-resolution (~100s m/pixel) for global surface characterization in four spectral band passes (e.g., 0.4µm, 0.67 µm, 0.76 µm, 1.0 µm) in the wavelength range of 350-nm to 1.0-µm including multiphase coverage for measurements of surface physical properties. Acquire high-resolution (better than 10 m/pixel) imaging of selected targets covering at least 30% of the surface. Requires repeat pass coverage of areas of interest to assess temporal variations.	Narrow Angle Camera, Wide Angle Camera	Narrow Angle Camera, Wide Angle Camera		
					SB.6f. Determine the origin and geologic evolution of non-water-ice materials, including the role of geologic processes by making observations in the wavelength range of 0.8 to greater than or equal to 5 µm with a spectral resolution better than or equal to 10 nm and spatial resolution better than or equal to 1 km/pixel of representative features. Observations need to be co-registered with higher-resolution panchromatic images.	Vis-IR Spectrometer, Narrow Angle Camera	Visible InfraRed Hyperspectral Imaging Spectrometer, Narrow Angle Camera		
					SB.6g. Characterize the charged and neutral particle populations in the ionosphere related to sputtering processes from the surface. Measure the D/H ratio in the proximity of the target if any emission is present. Measure open source positive ion spectrum for ionospheric plasma ion composition, open source neutral spectrum and closed source neutral spectrum. Map the ion-sputtering product and the ion backscattering neutral flux from the surface in the energy range 10 eV to 10 keV at a velocity resolution less than 30% and angular resolution less than 7 degrees.	Particle and Plasma Instrument, Ion and Neutral Mass Spectrometer	Particle and Plasma Instrument–Ion Neutral Mass Spectrometer		
			SB.7	Characterize the ionosphere and exosphere of Callisto.	SB.7a. Identify and determine column densities of atmospheric species across the globe at better than 1 km spatial resolution using stellar occultations. Requires coverage in the wavelength ranges of 100- to 200 nm at 0.5 nm spectral resolution, 0.4- to 2.5 µm with spectral resolution better than or equal to 5 nm and 2.5- to 5.0 µm with a spectral resolution better than or equal to 10 nm.	UV Spectrometer, Vis-IR Spectrometer	UltraViolet Imaging Spectrometer, Visible InfraRed Hyper-spectral Imaging Spectrometer		

Science Value Rating Criteria						
Significant contribution or achieves the measurement (75% to 100%)	Major contribution to achieving the measurement (50% to 75%)	Moderate contribution to achieving the measurement (25% to 50%)	Litte or no contribution to achieving the measurement (less than 25%)	Tour trajectory does not provide a suitable opportunity to make observations	Example instrument not in model payload

JUPITER SYSTEM

SATELLITE SYSTEM

Goal		Science Objectives	Science Investigation		Example Measurements	JEO Example Instruments	JGO Example Instruments	JEO	JGO
Explore the Jupiter system as an archetype for gas giants	**S. Study the Jovian satellite and ring system**	SB. Study Callisto as a witness of the early jovian system.	SB.7	Characterize the ionosphere and exosphere of Callisto.	SB.7b. Obtain global, two-dimensional, spectral-spatial images at better than 50 km/pixel spatial resolution in the wavelength range of 0.1- to 5-microns to measure CO_2, C, O, CO, O^+ and other species in absorption and/or emission. Requires spectral resolution of 0.5 nm for wavelengths less than 120 nm; spectral resolution of at least 0.5 nm for wavelengths from 120- to 200-nm; spectral resolution of better than 1 nm for wavelengths from 200- to 300-nm; spectral resolution better than 10 nm for wavelengths greater than 1.0-micron.	UV Spectrometer, Vis-IR Spectrometer	UltraViolet Imaging Spectrometer, Visible InfraRed Hyper-spectral Imaging Spectrometer		
					SB.7c. Map atmospheric emissions by scanning perpendicular to the limb from ~300 km above the surface to the surface of the satellite (at steps of 5 km). Requires measurements in the wavelength range of 100- to 200-nm at 0.5 nm spectral resolution, 1.0- to 2.5-μm at better than or equal to 5 nm from and 2.5- to 5-μm at better than or equal to 10 nm.	UV Spectrometer, Vis-IR Spectrometer	Visible InfraRed Hyperspectral Imaging Spectrometer		
					SB.7d. Determine local plasma distribution functions including ion composition and characterize the ion precipitation. Requires ion composition measurements with M/δM greater than 20 to measure sputtered/backscattered neutral and charged particle population. Determine the temperature of surface volatiles that support the exospheres, ion drift speeds, the D/H ratio in the proximity of the target if any emission is present. Energetic neutral imaging of the particle precipitation regions in the energy range tens eV to keV, open source positive ion spectrum of the sputtered ions, open source neutral spectrum of sputtered and evaporated (thermal) species, closed source neutral spectrum, density profiles of evaporated species. Measure three-dimensional distribution functions of ions in the energy range 10 eV to MeV with the 4π coverage. Measure spatial (less than 5 degrees angular resolution) and energy characterization of energetic neutral atoms from the surface in the energy range of 10 eV to a few keV).	Particle and Plasma Instrument, Ion and Neutral Mass Spectrometer	Particle and Plasma Instrument–Ion Neutral Mass Spectrometer		
					SB.7e. Measure the electron and ion density (0.001- to $10^4/cm^3$) and electron temperature (0- to 100-eV), as well as the ion ram speed (0- to 200 km/s) and constrain ion temperature (0- to 20-eV). Determine the ionizing EUV flux. Determine electric field vectors (near DC to 3 MHz), allowing assessment of local generated currents and conductivities. Determine the presence of suprathermal electrons. Determine plasma inhomogenities (δn/n, 0- to 10-kHz).	Particle and Plasma Instrument	Radio and Plasma Wave Instrument		
					SB.7f. Determine the temperature of surface volatiles that support the exosphere by mapping over a range of representative terrains, latitudes, longitudes, and local times, especially near noon with better than 1 km/pixel resolution, at two well-separated wavelengths for sensitivity to sub-pixel thermal inhomogenities.	Thermal Instrument	Thermal Instrument		
					SB.7g. Characterize and map the ionosphere by performing radio occultations over as wide a range of longitude space as possible.	Radio Subsystem (Two-band radio communication system with USO)	Radio Science Transponder and USO (Two-band radio communication system with USO)		
			SB.8	Relate material composition and distribution to geological and magnetospheric processes.	SB.8a. Map the surface globally at medium resolution (~100s m/pixel) in four spectral band passes (e.g., 0.4 μm, 0.67 μm, 0.76 μm, 1.0 μm) in the wavelength range of 350-nm to 1.0-μm. Requires solar illumination at mid-morning to mid-afternoon local times.	Narrow Angle Camera, Wide Angle Camera	Narrow Angle Camera, Wide Angle Camera		
					SB.8b. Measure the three-dimensional distribution function of ions in the energy range of a few keV to a few MeV with the 4π coverage, Energetic Neutral Atom (ENA) images in the energy range of 10 eV to a few keV. Spatial (less than 5 degrees angular resolution) and energy characterization of energetic neutral atoms from the surface in the energy range of 10 eV to a few keV. Requires open source positive ion spectrum to characterize the composition of ionospheric plasma, open source neutral spectrum for density profiles of sputtered species, and closed source neutral spectrum.	Particle and Plasma Instrument, Ion and Neutral Mass Spectrometer	Particle and Plasma Instrument–Ion Neutral Mass Spectrometer		

Science Value Rating Criteria						
Significant contribution or achieves the measurement (75% to 100%)	Major contribution to achieving the measurement (50% to 75%)	Moderate contribution to achieving the measurement (25% to 50%)	Litte or no contribution to achieving the measurement (less than 25%)	Tour trajectory does not provide a suitable opportunity to make observations	Example instrument not in model payload

JUPITER SYSTEM

SATELLITE SYSTEM

Goal		Science Objectives	Science Investigation		Example Measurements	JEO Example Instruments	JGO Example Instruments	JEO	JGO
Explore the Jupiter system as an archetype for gas giants	S. Study the Jovian satellite and ring system	SB. Study Callisto as a witness of the early jovian system.	SB.8	Relate material composition and distribution to geological and magnetospheric processes.	SB.8c. Measure the surface reflectance in the wavelength range from 0.1- to 5-µm to identify surface composition and relate it to geologic units and weathering processes. Identify and map the distribution of products of radiolysis and ion bombardment (e.g., H_2O_2, O_3, H_2CO, H_2CO_3) over the wavelength range of 100- to 320-nm with spectral resolution better than or equal to 2 nm, from 1.0- to 2.5-µm at better than or equal to 5 nm spectral resolution and from 2.5 to greater than or equal to 5 µm at better than or equal to 10 nm spectral resolution.	UV Spectrometer, Vis-IR Spectrometer	UltraViolet Imaging Spectrometer, Visible InfraRed Hyper-spectral Imaging Spectrometer		
					SB.8d. Identify variations in regolith properties with latitude and longitude as constrained by thermal inertia Map thermal emission from the surface by measuring albedo to 10% radiometric accuracy at a spatial resolution better than or equal to 1 km/pixel, and by making daytime and nighttime thermal observations at a spatial resolution better than or equal to 1 km/pixel and temperature accuracy better than 2 K, over more than 50% of the surface.	Thermal Instrument	Thermal Instrument		
			SB.9	Constrain global and regional surface ages.	SB.9a. Determine the distribution and morphology of impact craters by mapping in four colors (visible to near-IR) for large areas at global scales (~400 m/pixel) and in a single color at regional scales (~100 m/pixel) with near-uniform lighting conditions and solar phase angles less than or equal to 45 degrees, over more than 60% of the surface.	Narrow Angle Camera, Wide Angle Camera	Narrow Angle Camera, Wide Angle Camera		
					SB.9b. Perform detailed morphological characterization of selected features through imaging at better than or equal 2 m/pixel spatial scale.	Narrow Angle Camera	Narrow Angle Camera		
					SB.9c. Acquire globally distributed topography to 1 meter vertical resolution and better than 1 km horizontal resolution with selected targets at 100-meter horizontal resolution.	Laser Altimeter	Laser Altimeter		
					SB.9d. High spatial resolution observations (better than or equal to 1 km/pixel) from 0.1- to 5-µm (spectral resolution: better than or equal to 2 nm from 100- to 320-nm, better than or equal to 5 nm from 0.4- to 2.5-µm, better than or equal to 10 nm from 2.5 to greater than or equal to 5 µm), with emphasis on the spectral differences between geologic features (multi-ring basins, craters) and the surrounding areas. Medium spatial resolution (better than or equal to 10 km/pixel) on large areas to map leading/trailing asymmetries.	UV Spectrometer, Vis-IR Spectrometer	UltraViolet Imaging Spectrometer, Visible InfraRed Hyper-spectral Imaging Spectrometer		
					SB.9e. Identify young surfaces by searching for immature surface regolith, which may produce unusually high or low thermal inertias. Map thermal emission from the surface by measuring albedo to 10% radiometric accuracy at a spatial resolution better than or equal to 1 km/pixel, and by making daytime and nighttime thermal observations at a spatial resolution better than or equal to 1 km/pixel and temperature accuracy better than 2 K, over more than 50% of the surface.	Thermal Instrument	Thermal Instrument		
					SB.9f. Identify and locally characterize subsurface compositional horizons and structures by obtaining globally distributed profiles of subsurface dielectric horizons and structures, at depths of 100 meters to 30-km and vertical resolution ranging from a minimum of 100 meters to one percent of the target depth to estimate subsurface dielectric properties and the density of buried scatterers in targeted regions.	Ice Penetrating Radar (~5 to 50 MHz with 1 MHz bandwidth)	Ice Penetrating Radar (~5 to 50 MHz with 1 MHz bandwidth)		
			SB.10	Determine the formation and characteristics of magmatic, tectonic, and impact landforms.	SB.10a. Acquire globally distributed topography to 1 meter vertical resolution and better than 1 km horizontal resolution with selected targets at 100-meter horizontal resolution.	Laser Altimeter	Laser Altimeter		
					SB.10b. Globally characterize the surface at medium resolution (~100s m/pixel) in four spectral band passes (e.g., 0.4 µm, 0.67 µm, 0.76 µm, 1.0 µm) in the wavelength range of 350-nm to 1.0-µm. Requires solar illumination at mid-morning to mid-afternoon local times. Acquire high-resolution (better than 10 m/pixel) imaging of selected targets covering at least 30% of the surface with ~60% overlap and sufficient parallax between the different data sets to facilitate stereo analysis.	Narrow Angle Camera, Wide Angle Camera	Narrow Angle Camera, Wide Angle Camera		
					SB.10c. Measure surface reflectance in the wavelength range from 0.4 to greater than or equal to 5 µm with spectral resolution better than or equal to 5 nm from 0.4- to 2.5-µm and better than or equal to 10 nm from 2.5 to greater than or equal to 5 µm and spatial resolution better than or equal to 20 km/pixel. Requires targeted high spatial/high spectral observations of important geologic units and terrain types.	Vis-IR Spectrometer	Visible InfraRed Hyperspectral Imaging Spectrometer		

Science Value Rating Criteria					
Significant contribution or achieves the measurement (75% to 100%)	Major contribution to achieving the measurement (50% to 75%)	Moderate contribution to achieving the measurement (25% to 50%)	Litte or no contribution to achieving the measurement (less than 25%)	Tour trajectory does not provide a suitable opportunity to make observations	Example instrument not in model payload

JUPITER SYSTEM

SATELLITE SYSTEM

Goal		Science Objectives	Science Investigation		Example Measurements	JEO Example Instruments	JGO Example Instruments	JEO	JGO
Explore the Jupiter system as an archetype for gas giants	S. Study the Jovian satellite and ring system	SB. Study Callisto as a witness of the early jovian system.	SB.10	Determine the formation and characteristics of magmatic, tectonic, and impact landforms.	SB.10d. Identify and locally characterize subsurface compositional horizons and structures by obtaining globally distributed profiles of subsurface dielectric horizons and structures, at depths of 100 meters to 30-km and vertical resolution ranging from a minimum of 100 meters to one percent of the target depth to estimate subsurface dielectric properties and the density of buried scatterers in targeted regions.	Ice Penetrating Radar (~5 to 50 MHz with 1 MHz bandwidth)	Ice Penetrating Radar (~5 to 50 MHz with 1 MHz bandwidth)		
					SB.10e. Perform topographic characterization at better than 10 m/pixel scale and better than or equal to 10 meter vertical resolution and accuracy for targeted features, co-located with subsurface profiles.	Laser Altimeter	Laser Altimeter		
					SB.10f. Measure and constrain upper limit on heat flow using measurements in the 8- to 100-micron range with a spectral resolution of 2K and spatial resolution better than 30 km/pixel. Perform observation several times during the day and at night.	Thermal Instrument	Thermal Instrument		
		SC. Characterize the rings and small satellites.	SC.1	Conduct a comprehensive survey of all the components of the Jovian ring-moon system.	SC.1a. Conduct a comprehensive search for embedded moons within the ring system via imaging, down to a limiting size of ~100 meters (~14th magnitude). Conduct ~3 complete surveys of the ring region at low phase angles (less than 30 degrees), with at least two occurring early in the tour. For any objects found, determine the orbit via additional imaging with astrometric precision of better than 30 km/pixel, distributed over a period of ~1 year.	Narrow Angle Camera	Narrow Angle Camera		
					SC.1b. Search for dust belts throughout the Jovian system (from the rings to beyond the orbit of Callisto) using imaging down to optical depths of ~10^{-9} (or reflectivities of ~10^{-8} depending on viewing geometry). Emphasize high phase angles and edge-on viewing geometry to achieve the most stringent detection limits. Study any belts detected from at least 10 phase angles, ranging from less than 10 degrees to greater than 170 degrees, to constrain particle sizes.	Narrow Angle Camera, Wide Angle Camera (especially broadband visual & CH_4 filters)	Narrow Angle Camera and Wide Angle Camera (especially broadband visual & CH_4 filters)		
					SC.1c. Search for km-sized moons throughout the Jovian system (from the rings to beyond the orbit of Callisto) with a detection threshold of ~1 km (~10th magnitude). This requires repeated, complete image mosaics of the system taken at low phase angles. For any objects found, determine the orbit via additional imaging with astrometric precision of better than 30 km/pixel, distributed over a period of ~1 year.	Narrow Angle Camera, Wide Angle Camera	Narrow Angle Camera, Wide Angle Camera		
					SC.1d. Search for plasma effects associated with dust particles and energetic neutral fluxes associated with the ring-magnetosphere interactions. Look for microsignatures in energetic ions and electrons. Measure the three-dimensional distribution function of ions in the energy range of 10 eV to MeV with 4π coverage, Energetic Neutral Atom (ENA) images in the energy range few keV to tens of keV and ion composition with the mass resolution M/δM greater than 20.	Particle and Plasma Instrument, Ion and Neutral Mass Spectrometer	Particle and Plasma Instrument–Ion Neutral Mass Spectrometer		
			SC.2	Identify the processes that define the origin and dynamics of the ring dust, source bodies, and small moons.	SC.2a. Determine the rings' three-dimensional structure, including the vertical structure of the halo and gossamer rings, via imaging from a variety of viewing geometries. Requires complete mosaics of the system from Jupiter out to beyond the orbit of Thebe, with resolution of finer than 100 km/pixel globally and finer than 10 km/pixel on the main ring. Images of the faintest ring components must be sensitive to reflectivities below 10^{-8}. Images must be obtained at a variety of opening angles and phase angles in order to decouple the rings' variations depending on radius, vertical distance from the ring plane, and phase angle. Imaging of the halo along the boundary of Jupiter's shadow provides optimal vertical resolution.	Narrow Angle Camera, Wide Angle Camera (broadband visual & CH_4 filters)	Narrow Angle Camera, Wide Angle Camera (broadband visual & CH_4 filters)		
					SC.2b. Identify and characterize time-variable phenomena, including clump formation and evolution, via repeated, complete rotational profiles of the main ring with a resolution of finer than 100 km/pixel. Obtain at least 20 complete profiles, sampling a wide variety of time scales from ~days to ~1 year.	Narrow Angle Camera, Wide Angle Camera (broadband visual & CH_4 filters)	Narrow Angle Camera, Wide Angle Camera (broadband visual & CH_4 filters)		
					SC.2c. Search for warps and asymmetries on scales of 10- to 30-km via imaging of the system from nearly and exactly edge-on perspectives. Encompass the entire region from the halo out to beyond the orbit of Thebe.	Narrow Angle Camera, Wide Angle Camera (broadband visual & CH_4 filters)	Narrow Angle Camera, Wide Angle Camera (broadband visual & CH_4 filters)		

Science Value Rating Criteria					
Significant contribution or achieves the measurement (75% to 100%)	Major contribution to achieving the measurement (50% to 75%)	Moderate contribution to achieving the measurement (25% to 50%)	Litte or no contribution to achieving the measurement (less than 25%)	Tour trajectory does not provide a suitable opportunity to make observations	Example instrument not in model payload

JUPITER SYSTEM

SATELLITE SYSTEM

Goal		Science Objectives	Science Investigation		Example Measurements	JEO Example Instruments	JGO Example Instruments	JEO	JGO
Explore the Jupiter system as an archetype for gas giants	S. Study the Jovian satellite and ring system	SC. Characterize the rings and small satellites.	SC.2	Identify the processes that define the origin and dynamics of the ring dust, source bodies, and small moons.	SC.2d. Determine radial and vertical structure of the main ring on scales of ~1 km. Emphasize the region around and between the orbits of Metis and Adrastea.	Radio Subsystem	Radio Science Instrument & USO		
					SC.2e. Refine the orbits of the small moons to derive masses and to detect possible ongoing secular acceleration. Requires observations of each body against star backgrounds, with resolution of finer than 30 km/pixel, spanning ~1 year. Also requires timing of ~40 mutual events with precision of finer than 0.1 second.	Narrow Angle Camera, UV Spectrometer	Narrow Angle Camera, UltraViolet Imaging Spectrometer		
			SC.3	Characterize the physical properties of the inner small moons, ring source bodies and dust.	SC.3a. Determine the phase function and color of the entire ring system (from the inner halo to beyond the orbit of Thebe) with a resolution of finer than ~100 km/pixel and a sensitivity to reflectivities of 10^{-8}. Obtain images at least 10 phase angles from less than 10 degrees to greater than 170 degrees, and use several visual and near-IR images in broad-band filters. Requires viewpoints of at least a few degrees out of the ring plane.	Narrow Angle Camera, Wide Angle Camera (especially broadband visual & CH_4 filters)	Narrow Angle Camera, Wide Angle Camera (especially broadband visual & CH_4 filters)		
					SC.3b. Determine the size distribution of ring parent bodies in the centimeter to meter size range through dual spacecraft occultations. Emphasize the region around and between the orbits of Metis and Adrastea.	Radio Subsystem	Radio Science Instrument & USO		
					SC.3c. Determine ring and inner moon surface composition with a sensitivity to reflectivities of ~10^{-7}. Obtain this level of sensitivity in each of more than 200 spectral bands from 0.4- to beyond ~5 microns. Observe near backscatter to emphasize the surface composition of the larger embedded bodies in the system. At wavelengths from 70- to more than 200-nm, observe H_2O, H, OH in absorption with rings in front of atmosphere (or other sources (*e.g.*, interplanetary background)). In all spectral ranges, ensure coverage of a wide range of phase angles (including less than 10° and greater than 170°). Observe near backscatter to emphasize the surface composition of the larger embedded bodies in the system. Ensure sampling of the evolution of composition over different timescales.	Vis-IR Spectrometer, UV Spectrometer	Visible InfraRed Hyperspectral Imaging Spectrometer, UltraViolet Imaging Spectrometer		
					SC.3d. Improve the determination of each satellite's size, shape and cratering history, study of the surface photometric and thermophysical parameters through phase and light curves.	Narrow Angle Camera	Narrow Angle Camera		
			SC.4	Remotely characterize the composition, properties and dynamical groupings of the outer, irregular moons.	SC.4a. Study the shapes and gross surface topography via low-resolution imaging of at least 3 distinct targets. Requires resolution of at least ~6 pixels across the disk. Bodies should be observed at least 4 different rotational phases.	Narrow Angle Camera	Narrow Angle Camera		
					SC.4b. Determine surface photometric parameters and study weathering processes on at least 3 distinct targets by obtaining disk-integrated phase and light curves and color measurements (visible to near-IR). Include observations at least 4 higher phase angles inaccessible from Earth.	Narrow Angle Camera, Wide Angle Camera	Narrow Angle Camera, Wide Angle Camera		
					SC.4c. Measure surface reflectance in the wavelength range from 0.1- to 5-μm to identify surface composition with spectral resolution better than or equal to 2 nm from 100- to 320-nm, better than or equal to 5 nm from 0.4- to 2.5-μm and better than or equal to 10 nm from 2.5- to 5-μm. From a close flyby or ~1,000,000 km distance, acquire long-duration exposure, disk-integrated spectra, of at least 3 distinct targets.	Vis-IR Spectrometer, UV Spectrometer	Vis-IR Imaging Spectrometer, UltraViolet Imaging Spectrometer		
					SC.4d. Constrain the orbits of outer irregular moons via imaging against star backgrounds. Requires at least 5 images of each target over a ~1 year period.	Narrow Angle Camera	Narrow Angle Camera		
			SC.5	Perform disk-resolved and local characterization of one or more outer, irregular moons.	SC.5a. Determine the mass of irregular satellites from Doppler tracking. Measure the range-rate between the spacecraft and ground station from Doppler tracking with ~0.01 mm/s at 60 sec integration time	Radio Subsystem	Radio Science Instrument & USO		
					SC.5b. Derive the shape, topography and spatially resolved composition of the surface. Requires at least 10 pixels across the disk and wavelength coverage from the visual to at least ~3 microns.	Narrow Angle Camera, Medium Angle Camera, Wide Angle Camera, Vis-IR Spectrometer	Narrow Angle Camera, Wide Angle Camera, Visible InfraRed Hyperspectral Imaging Spectrometer		
					SC.5c. Obtain a global map of daytime and nighttime thermal emission with at least 10 pixels across the target	Thermal Instrument	Thermal Instrument		

Science Value Rating Criteria					
Significant contribution or achieves the measurement (75% to 100%)	Major contribution to achieving the measurement (50% to 75%)	Moderate contribution to achieving the measurement (25% to 50%)	Litte or no contribution to achieving the measurement (less than 25%)	Tour trajectory does not provide a suitable opportunity to make observations	Example instrument not in model payload

JUPITER SYSTEM									
SATELLITE SYSTEM									
Goal		**Science Objectives**	**Science Investigation**		**Example Measurements**	**JEO Example Instruments**	**JGO Example Instruments**	**JEO**	**JGO**
Explore the Jupiter system as an archetype for gas giants	**S. Study the Jovian satellite & ring system**	SC. Characterize the rings and small satellites.	SC.5	Perform disk-resolved and local characterization of one or more outer, irregular moons.	SC.5d. Acquire two-dimensional spectral-spatial images in the wavelength range of ~120- to 300-nm with a spectral resolution of 0.5 nm for ~120- to 200-nm and 1 nm for 200- to 300-nm to identify absorption features associated with H_2O, CO_2, NH_3, O_3, H_2O_2.	UV Spectrometer	UltraViolet Imaging Spectrometer		
					SC.5e. Measure the neutral and charged particles sputtered off the surface. Measure the D/H ratio in the proximity of the target if any emission is present. Measure open source positive ion spectrum of sputtered ions, open source neutral spectrum of sputtered neutral species, closed source neutral spectrum, high cadence mode, spatial (less than 5 degrees angular resolution) and energy characterization of energetic neutral atoms from the surface in the energy range 10 eV to a few keV).	Particle and Plasma Instrument, Ion and Neutral Mass Spectrometer	Particle and Plasma Instrument–Ion Neutral Mass Spectrometer		
					SC.5f. Measure three-axis magnetic field components at 1Hz.	Magnetometer	Magnetometer		
					SC.5g. Measure three-dimensional distribution functions for electrons and ions (first order mass resolution) over 4π and an energy range of a few eV to a few tens keV and cold plasma density and velocity. Energetic Neutral Atom (ENA) images of backscattered ENAs in the footprint in the energy range of 10 eV to a few keV. Measure open source neutral spectrum and closed source neutral spectrum.	Particle and Plasma Instrument, Ion and Neutral Mass Spectrometer	Particle and Plasma Instrument–Ion Neutral Mass Spectrometer		
					SC.5h. Measure plasma density (0.001- to $10^4/cm^3$), Electric Field Vectors determination (near DC to 3 MHz), bulk ion drift speeds (0- to 200-km/s). Search for mass-loading effects.	Particle and Plasma Instrument	Radio and Plasma Wave Instrument		

Science Value Rating Criteria						
	Significant contribution or achieves the measurement (75% to 100%)	Major contribution to achieving the measurement (50% to 75%)	Moderate contribution to achieving the measurement (25% to 50%)	Litte or no contribution to achieving the measurement (less than 25%)	Tour trajectory does not provide a suitable opportunity to make observations	Example instrument not in model payload

JUPITER SYSTEM

MAGNETOSPHERE

Goal	Science Objective		Science Investigation		Example Measurements	JEO Example Instruments	JGO Example Instruments	JEO	JGO
Explore the Jupiter system as an archetype for gas giants	M. Jovian magnetosphere	MA. Characterize the magnetosphere as a fast magnetic rotator.	MA.1	Understand the structure and stress balance of Jupiter's magnetosphere.	MA.1a. Measure three-axis magnetic field components at 8 Hz or less to near-continuously monitor the configuration of the global magnetic field, and to determine the pitch angle, throughout the magnetosphere.	Magnetometer	Magnetometer		
					MA.1b. In situ measurements of ions and electrons from eV to MeV at 1 min resolution or better with 4π coverage, along with imaging of energetic neutral atoms to study large-scale evolution of ion distributions.	Particle and Plasma Instrument, Ion and Neutral Mass Spectrometer	Particle and Plasma Instrument–Ion Neutral Mass Spectrometer		
			MA.2	Investigate the plasma processes, sources, sinks, composition and transport (including transport of magnetic flux) in the magnetosphere and characterize their variability in space and time.	MA.2a. Measure three-axis magnetic field components at 32 Hz (to study the ion cyclotron waves) near-continuously, to characterize the properties of the magnetodisk at small scale.	Magnetometer	Magnetometer		
					MA.2b. Measure the plasma density and electron temperature (0.1- to 100-eV), the bulk ion drift speed, particle pressure, and the electric field vector (near DC to 3 MHz); measure plasma wave and electromagnetic emissions in the magnetodisk (electric DC to 45 MHz and magnetic 0.1- to 20-kHz); and measure possible presence of dust in the magnetodisk.	Radio and Plasma Wave Instrument (including Langmuir probe)	Radio and Plasma Wave Instrument (including Langmuir probe)		
					MA.2c. Measure the three-dimensional distribution functions of ions and electrons, mass spectra of ions and neutrals (eV to MeV), and determine the spectrum (eV to keV range) and image (at better than or equal 5 degrees angular resolution) energetic neutral atoms at 1 minute resolution or better.	Particle and Plasma Instrument, Ion and Neutral Mass Spectrometer	Particle and Plasma Instrument–Ion Neutral Mass Spectrometer		
					MA.2d. Acquire hyperspectral images in the range ~100-nm to 5.0-μm to monitor and characterize emissions in the Io and Europa tori, on a range of temporal scales from daily to monthly.	Vis-IR Spectrometer, UV Spectrometer	Visible InfraRed Hyperspectral Imaging Spectrometer, UltraViolet Imaging Spectrometer		
					MA.2e. Perform observations in the spectral range ~100-nm to 5.0-μm at a spatial scale of 10s to 100s of km/pixel, to monitor and characterize Io's volcanic activity, on a range of temporal scales from daily to monthly.	Narrow Angle Camera, Wide Angle Camera, UV Spectrometer, Vis-IR Spectrometer	Narrow Angle Camera, Wide Angle Camera, UltraViolet Imaging Spectrometer, Visible InfraRed Hyper-spectral Imaging Spectrometer		
			MA.3	Characterize the large-scale coupling processes between the magnetosphere, ionosphere and thermosphere, including footprints of the Jovian moons.	MA.3a. Monitor the variability of global and localized jovian auroral emissions in the spectral range ~100 nm to 5.0-μm with ~100 km/pixel spatial resolution and ~1 to 10 min time resolution, on a range of temporal scales from daily to monthly.	Narrow Angle Camera, Vis-IR Spectrometer, UV Spectrometer	Narrow Angle Camera, Visible InfraRed Hyperspectral Imaging Spectrometer, UltraViolet Imaging Spectrometer		
					MA.3b. Acquire two-dimensional spectral-spatial images of the jovian auroral regions at high spatial and temporal resolution, in the spectral range 90- to 110 nm (soft electron component) and 110- to 170 nm (hard electron component), covering H_2 Lyman and Werner bands and H Ly α emissions, at a spectral resolution of better than 0.5 nm, and spatial resolution of ~100 km/pixel (for the moon footprints), with ~10 min time resolution.	UV Spectrometer	UltraViolet Imaging Spectrometer		
					MA.3c. Measure the vector electric field (near DC to 45 MHz), the magnetic field vector (0.1 to 20 kHz), plasma density inhomogenities (near DC to 10 kHz), plasma density, and the bulk ion drift speed, near-continuously throughout the magnetosphere.	Radio and Plasma Wave Instrument (including Langmuir probe)	Radio and Plasma Wave Instrument (including Langmuir probe)		

Science Value Rating Criteria						
Significant contribution or achieves the measurement (75% to 100%)	Major contribution to achieving the measurement (50% to 75%)	Moderate contribution to achieving the measurement (25% to 50%)	Litte or no contribution to achieving the measurement (less than 25%)	Tour trajectory does not provide a suitable opportunity to make observations	Example instrument not in model payload

JUPITER SYSTEM

MAGNETOSPHERE

Goal	Science Objective		Science Investigation		Example Measurements	JEO Example Instruments	JGO Example Instruments	JEO	JGO
Explore the Jupiter system as an archetype for gas giants	M. Jovian magnetosphere	MA. Characterize the magnetosphere as a fast magnetic rotator.	MA.3	Characterize the large-scale coupling processes between the magnetosphere, ionosphere and thermosphere, including footprints of the Jovian moons.	MA.3d. Measure three-axis magnetic field components at 1 Hz at 1 min resolution in the middle magnetosphere region where corotation breaks-down, to monitor dynamics and general configuration of the magnetic field.	Magnetometer	Magnetometer		
					MA.3e. Measure the three-dimensional distribution functions of ions and electrons, with ion composition, at a mass resolution M/δM better than or equal to 20, and obtain images of energetic neutral atoms (H and heavy neutrals) from 10- to 300-keV with better than or equal 5 degree angular resolution.	Particle and Plasma Instrument, Ion and Neutral Mass Spectrometer	Particle and Plasma Instrument–Ion Neutral Mass Spectrometer		
			MA.4	Characterize the magnetospheric response to solar wind variability and planetary rotation effects.	MA.4a. Measure three-axis magnetic field components near-continuously at 1- to 8 Hz for the global characterization of the magnetospheric field, and its variability, throughout the magnetosphere.	Magnetometer	Magnetometer		
					MA.4b. Measure the vector electric field (near DC to 45 MHz), the magnetic field vector (0.1 to 20 kHz), plasma density inhomogenities (near DC to 10 kHz), plasma density, and the bulk ion drift speed, near-continuously throughout the magnetosphere.	Radio and Plasma Wave Instrument (including Langmuir probe)	Radio and Plasma Wave Instrument (including Langmuir probe)		
					MA.4c. Monitor the variability of the global jovian auroral emissions at multiple wavelengths (UV, IR, and visible) with ~100 km/pixel spatial resolution and ~1- to 10-min time resolution	UV Spectrometer, Vis-IR Spectrometer, Narrow Angle Camera, Wide Angle Camera	UltraViolet Imaging Spectrometer, Visible InfraRed Hyper-spectral Imaging Spectrometer, Narrow Angle Camera, Wide Angle Camera		
					MA.4d. Determine the three-dimensional distribution function of electrons and ions from 10 eV to a few MeV with 4π coverage, and image energetic neutral atoms of the magnetosphere in the energy range keV-hundreds of keV with better than or equal 5 degree angular resolution..	Particle and Plasma Instrument, Ion and Neutral Mass Spectrometer	Particle and Plasma Instrument–Ion Neutral Mass Spectrometer		
		MB. Characterize the magnetosphere as a giant accelerator.	MB.1	Detail the particle acceleration processes.	MB.1a. Measure the vector electric field (near DC to 45 MHz), the magnetic field vector (0.1- to 20-kHz), plasma density inhomogenities (near DC to 10 kHz), plasma density, and the bulk ion drift speed, near-continuously throughout the magnetosphere.	Radio and Plasma Wave Instrument (including Langmuir probe)	Radio and Plasma Wave Instrument (including Langmuir probe)		
					MB.1b. Measure the three-dimensional distribution functions of ions and electrons in the energy range tens of eV to tens of keV with 4π coverage, and their spectral evolution during acceleration events; and image the temporal, spatial and spectral evolution of large-scale acceleration and injection events in energetic neutral atoms (10- to 300-keV) for H, He,O., S, with better than or equal to 5 degrees angular resolution, on time scales of days to months.	Particle and Plasma Instrument, Ion and Neutral Mass Spectrometer	Particle and Plasma Instrument–Ion Neutral Mass Spectrometer		
					MB.1c. Measure three axis magnetic field components near-continuously to determine the characteristics of field-aligned currents at 32 Hz to 128 Hz, throughout the magnetosphere.	Magnetometer	Magnetometer		
					MB.1d. Measure the brightness of jovian auroral emissions with two-dimensional spectral-spatial images, in the spectral range 90- to 110 nm (soft electron component) and 110- to 170 nm (hard electron component), covering H_2 Lyman and Werner bands and H Ly α emissions, at a spectral resolution of better than 0.5 nm, to indirectly infer particle energy from auroral emissions with a spatial resolution of ~100 km/pixel.	UV Spectrometer	UltraViolet Imaging Spectrometer		
			MB.2	Study the loss processes of charged energetic particles.	MB.2a. Measure three-axis magnetic field components at 32 Hz to look for evidence of tail reconnection signatures, plasmoid ejections, and other events, near-continuously deep in the magnetotail.	Magnetometer	Magnetometer		
					MB.2b. Measure the three-dimensional distribution functions of ions and electrons in the energy range of tens of kev to MeV with 4π coverage, and image energetic neutral atoms at 10- to 300-keV (H, He, O, S) with 30 min time resolution and 0.5 R_J spatial resolution, deep in the magnetotail.	Particle and Plasma Instrument, Ion and Neutral Mass Spectrometer	Particle and Plasma Instrument–Ion Neutral Mass Spectrometer		

Science Value Rating Criteria					
Significant contribution or achieves the measurement (75% to 100%)	Major contribution to achieving the measurement (50% to 75%)	Moderate contribution to achieving the measurement (25% to 50%)	Litte or no contribution to achieving the measurement (less than 25%)	Tour trajectory does not provide a suitable opportunity to make observations	Example instrument not in model payload

JUPITER SYSTEM

MAGNETOSPHERE

Goal	Science Objective		Science Investigation		Example Measurements	JEO Example Instruments	JGO Example Instruments	JEO	JGO
Explore the Jupiter system as an archetype for gas giants	M. Jovian magnetosphere	MB. Characterize the magnetosphere as a giant accelerator.	MB.2	Study the loss processes of charged energetic particles.	MB.2c. Monitor the variability of the global jovian auroral emissions in the spectral range ~100 nm to 5.0-μm with ~100 km/pixel spatial resolution and ~1 to 10 min time resolution, on a range of temporal scales from daily to monthly.	UV Spectrometer, Vis-IR Spectrometer, Narrow Angle Camera, Wide Angle Camera	UltraViolet Imaging Spectrometer, Visible InfraRed Hyper-spectral Imaging Spectrometer, Narrow Angle Camera, Wide Angle Camera		
			MB.3	Measure the time evolving electron synchrotron emissions.	MB.3a. Measure three-axis magnetic field components at 32 Hz near-continuously to determine pitch angles, throughout the magnetosphere.	Magnetometer	Magnetometer		
					MB.3b. Measure the three-dimensional distribution functions of electrons in the energy range of tens of kev to MeV with 4π coverage, near-continuously throughout the magnetosphere.	Particle and Plasma Instrument, Ion and Neutral Mass Spectrometer	Particle and Plasma Instrument–Ion Neutral Mass Spectrometer		
					MB.3c. Map the synchrotron radiation of the inner magnetosphere at GHz radio wavelengths.	Radio Subsystem	Radio Science Instrument & USO		
					MB.3d. Measure radio waves from the synchrotron radiation of the inner magnetosphere in the frequency range 1 kHz to 45 MHz.	Radio and Plasma Wave Instrument (including Langmuir probe)	Radio and Plasma Wave Instrument (including Langmuir probe)		
		MC. Understand the moons as sources and sinks of magnetospheric plasma.	MC.1	Study the pickup and charge exchange processes in the Jupiter system plasma and neutral tori.	MC.1a. Determine Io's interaction with the magnetosphere through imaging of airglow emissions in eclipse at ~10 km/pixel, in multiple colors from 390- to 800-nm.	Narrow Angle Camera, Wide Angle Camera	Narrow Angle Camera, Wide Angle Camera		
					MC.1b. Observe the three-dimensional distribution of the neutral tori (e.g., H, O, S) on a time scale of several months, by means of high-phase scans in the wavelength range 400-nm to 2.5-μm with a spectral resolution of better than or equal to 5 nm, and from 2.5 μm to 5 μm and with a spectral resolution better than or equal to 10 nm.	Vis-IR spectrometer	Visible InfraRed Hyperspectral Imaging Spectrometer		
					MC.1c. Two-dimensional spectral-spatial images of the Io plasma torus through a wavelength range of 30- to 300-nm at a spatial resolution of better than or equal 0.1 Rj/pixel and a spectral resolution of better than 0.5 nm over a range of timescales (hourly through monthly), with emphasis on daily monitoring for at least 30 days.	UV spectrometer	UltraViolet Imaging Spectrometer		
					MC.1d. Measure the three-dimensional distribution function, flux and composition of electrons and ions in the energy range of 10 eV to a few MeV with 4π coverage and better than or equal 15° angular resolution, $\Delta E/E = 0.1$ and a time resolution of better than or equal 1 minute; image energetic neutral atoms in the energy range of keV to tens of keV; and measure ion composition with the mass resolution $M/\delta M$ better than or equal to 20, including the ion and neutral mass spectrum.	Particle and Plasma Instrument, Ion and Neutral Mass Spectrometer	Particle and Plasma Instrument–Ion Neutral Mass Spectrometer		
					MC.1e Measure radio waves (1 kHz to 45 MHz), in situ electric field vector (near DC to 3 MHz), plasma density, and bulk ion drift speed throughout the magnetosphere and from the neutral tori.	Radio and Plasma Wave Instrument (including Langmuir probe)	Radio and Plasma Wave Instrument (including Langmuir probe)		
					MC.1f. Measure 3 axis magnetic field components near-continuously at 32 to 128 Hz, to study ion cyclotron waves generated by the pick-up plasma throughout the magnetosphere and from the neutral tori.	Magnetometer	Magnetometer		

Science Value Rating Criteria						
Significant contribution or achieves the measurement (75% to 100%)	Major contribution to achieving the measurement (50% to 75%)	Moderate contribution to achieving the measurement (25% to 50%)	Litte or no contribution to achieving the measurement (less than 25%)	Tour trajectory does not provide a suitable opportunity to make observations	Example instrument not in model payload

JUPITER SYSTEM

MAGNETOSPHERE

Goal	Science Objective		Science Investigation		Example Measurements	JEO Example Instruments	JGO Example Instruments	JEO	JGO
Explore the Jupiter system as an archetype for gas giants	M. Jovian magnetosphere	MC. Understand the moons as sources and sinks of magnetospheric plasma.	MC.1	Study the pickup and charge exchange processes in the Jupiter system plasma and neutral tori.	MC.1g. Image energetic neutral tori (e.g., H, O, S) in the range of eV to hundreds of keV, near the orbits of each of the Galilean satellites, with better than or equal 5° angular resolution.	UV spectrometer, Particle and Plasma Instrument	UltraViolet Imaging Spectrometer, Particle and Plasma Instrument–Ion Neutral Mass Spectrometer (including ENA)		
			MC.2	Study the interactions between Jupiter's magnetosphere and Io, Europa, Ganymede, and Callisto.	MC.2a. Determine the trapped and/or precipitating fluxes of ions and electrons with energies between 10 eV and 10 MeV, better than or equal 15° angular resolution with δE/E=0.1, and time resolution of better than or equal 1 minute.	Particle and Plasma Instrument, Ion and Neutral Mass Spectrometer	Particle and Plasma Instrument–Ion Neutral Mass Spectrometer		
					MC.2b. Observe the tori at: 55- to 110 nm (for O and S ion emissions) to infer the electron temperature in the Io torus with spectral resolution of better than or equal to 0.3 nm; 110- to 170-nm (for H Ly alpha). Observe the satellite footprints at: 90- to 110 nm (for the soft electron component) and 110- to 170-nm (for the hard electron component), covering H_2 Lyman and Werner bands and H Ly α emissions, with a spectral resolution of at least 0.5 nm and a spatial resolution of ~100 km/pixel.	UV spectrometer	UltraViolet Imaging Spectrometer		
					MC.2c. Image auroral footprints of the satellites in the Jovian atmosphere in the spectral range ~100 nm to 5.0-µm, with ~100 km/pixel spatial resolution and with ~1-min temporal resolution, on a range of temporal scales from daily to monthly..	UV Spectrometer, Vis-IR Spectrometer, Narrow Angle Camera	UltraViolet Imaging Spectrometer, Visible InfraRed Hyper-spectral Imaging Spectrometer, Narrow Angle Camera		
					MC.2d. Obtain images of energetic neutral atoms of the flux tubes of the satellites, with better than or equal 5 degrees angular resolution, in the energy range of 10 eV to a few keV, to measure back-scattering and ion-sputtered energetic neutral atoms from the precipitating ions.	Particle and Plasma Instrument, Ion and Neutral Mass Spectrometer	Particle and Plasma Instrument–Ion Neutral Mass Spectrometer		
					MC.2e. Measure radio waves from the auroral footprint regions of each of the Galilean satellites in the frequency range 1 kHz to 45 MHz, and measure electric field vectors (near DC to 3 MHz).	Radio and Plasma Wave Instrument (including Langmuir probe)	Radio and Plasma Wave Instrument (including Langmuir probe)		
					MC.2f. Measure three-axis magnetic field components at 8 and 32 Hz to characterize Alfven wings of the Galilean satellites, and to look for signatures of the electrodynamic coupling between the moons and Jupiter, such as field-aligned currents and Alfven waves, near-continuously in the vicinity of the Galilean satellites.	Magnetometer	Magnetometer		
			MC.3	Study the interactions between Jupiter's magnetosphere and small satellites.	MC.3a. Measure three-axis magnetic field components at 1 Hz, near-continuously in the vicinity of small satellites.	Magnetometer	Magnetometer		
					MC.3b. Measure the three-dimensional distribution functions for electrons and ions (first-order mass resolution) over 4π and an energy range of a few eV to a few tens of keV, including cold plasma density and velocity, near-continuously in the vicinity of small satellites.	Particle and Plasma Instrument, Ion and Neutral Mass Spectrometer	Particle and Plasma Instrument–Ion Neutral Mass Spectrometer		
					MC.3c. Measure plasma density, electric field vectors, and bulk ion drift speeds, and search for mass-loading effects, near-continuously in the vicinity of small satellites.	Radio and Plasma Wave Instrument (including Langmuir probe)	Radio and Plasma Wave Instrument (including Langmuir probe)		

Science Value Rating Criteria						
Significant contribution or achieves the measurement (75% to 100%)	Major contribution to achieving the measurement (50% to 75%)	Moderate contribution to achieving the measurement (25% to 50%)	Litte or no contribution to achieving the measurement (less than 25%)	Tour trajectory does not provide a suitable opportunity to make observations	Example instrument not in model payload

JUPITER SYSTEM

JUPITER

Goal	Science Objective		Science Investigation		Example Measurements	JEO Example Instruments	JGO Example Instruments	JEO	JGO
Explore the Jupiter system as an archetype for gas giants	J. Study the jovian atmosphere	JA. Characterize the atmospheric dynamics and circulation.	JA.1	Investigate the dynamics of Jupiter's weather layer.	JA.1a. Image the dayside with ~15-km/pixel resolution to determine cloud-top windspeeds (zonal and meridional) and eddy momentum fluxes. Imaging should include repeated coverage of the same regions at ~2 hour intervals for cloud tracking (necessary to obtain winds, divergence and vorticity) with 2-m/s accuracy. Wavelengths should include visible and/or near-IR continuum (e.g., 3.7 micron) as well as one or more methane absorption band (e.g., 889 nm and another near-IR, e.g., 2.3 micron). Characterize behavior over a range of timescales, including short (1- to 3-days), medium (~1 month), and long (~1 year) variability. Global or near-global daily coverage for periods of weeks-to-months is desired.	Narrow Angle Camera, Medium Angle Camera, Wide Angle Camera, Vis-IR Spectrometer	Narrow Angle Camera, Wide Angle Camera, Visible InfraRed Hyperspectral Imaging Spectrometer		
					JA.1b. Measure Doppler broadening of molecular lines at a wide range of latitudes and times to derive 5- to 300-mbar temperatures and stratospheric wind speeds with high vertical resolution (10- to 20-km/pixel, R>1E6 for line shape, 2- to 10-m/s accuracy).	Submillimeter Wave Instrument	Submillimeter Wave Instrument		
					JA.1c. Global view of velocity fields at the cloud level through Doppler shift of reflected visible solar lines, with a precision of about 2 m/s and a resolution of 100 km/pixel.	Doppler instrument	Doppler instrument		
					JA.1d. Generate global maps of material tracers of tropospheric dynamics (NH_3, H_2O, PH_3, AsH_3, GeH_4) in the 1- to 5-bar region at wavelengths from 1.0- to 5.2-microns, R> 400 with 100-km/pixel spatial resolution.	Vis-IR Spectrometer	Visible InfraRed Hyperspectral Imaging Spectrometer		
					JA.1e. Image (15- to 100-km/pixel) lightning flashes at visible wavelengths on the nightside of Jupiter and combine with imaging of discrete thunderstorms on the dayside at the same resolution. Obtain multiple views of all latitudes on the nightside with clear filter imaging combined with imaging of discrete thunderstorms on the dayside. Acquire repeated imaging while tracking a feature (usually near 90° phase). Combine with complementary plasma and fields measurements to understand global distribution.	Narrow Angle Camera, Wide Angle Camera, Particle and Plasma Instrument	Narrow Angle Camera, Wide Angle Camera, Radio and Plasma Wave Instrument		
			JA.2	Determine the thermodynamics of atmospheric phenomena.	JA.2a. Repeated thermal observations in the 7- to 250-micron spectral range to globally map the three-dimensional temperature structure, horizontal gradients (thermal windshear) and potential vorticity. Perform nadir mapping in the 80- to 700-mbar region (troposphere) and 0.5- to 20-mbar region (stratosphere) to an absolute accuracy of 1.0 K, relative accuracy of 0.4 K with spatial resolution of 100-km/pixel. Requires limb viewing geometry to achieve 10- to 20-km altitude resolution at a wide range of latitudes. Track discrete features (e.g., storms, waves) over a range of timescales (days to months).	Thermal Instrument (need Thermal-IR Spectrometer—not in current model payload)	Thermal-IR Spectrometer		
					JA.2b. Perform repeated radio occultations closely spaced in latitude and time (e.g., at the same latitude +/-10 degrees, once every 2 weeks and at a similar longitude where possible), retrieving pressure as a function of altitude to relate to zonal winds.	Radio Subsystem (Radio doppler tracking in one-way mode at X-band and Ka-band frequencies driven by the USO)	Radio Science Instrument & USO (Radio doppler tracking in one-way mode at X-band and Ka-band frequencies driven by the USO)		
					JA.2c. Perform stellar and solar occultations in the near-IR and UV for high vertical resolution temperature (and methane profile) to sub-scale height resolution sounding over a wide range of latitudes in the upper stratosphere.	UV Spectrometer, Vis-IR Spectrometer	UltraViolet Imaging Spectrometer, Visible InfraRed Hyper-spectral Imaging Spectrometer		
					JA.2d. Determine the three-dimensional temperatures of selected atmospheric species (HCN, H_2O and CH_4) between 400 mbars and 1 microbar.	Submillimeter Wave Instrument	Submillimeter Wave Instrument		
			JA.3	Quantify the roles of wave propagation and atmospheric coupling.	JA.3a. Multispectral imaging in the 0.4- to 1.0 micron and 4.0- to 5.0-micron spectral range to determine the depth and shears on the zonal wind fields and the vertical structure of vortices and plumes between 2- to 3-bar and the 0.5- to 1.0-bar levels (50- to 200-km/pixel). Acquire multiple high-resolution images of mesoscale waves and cloud structure on a timescale of hours, days, months, and years.	Vis-IR Spectrometer, Narrow Angle Camera, Wide Angle Camera	Visible InfraRed Hyperspectral Imaging Spectrometer, Narrow Angle Camera, Wide Angle Camera		

Science Value Rating Criteria					
Significant contribution or achieves the measurement (75% to 100%)	Major contribution to achieving the measurement (50% to 75%)	Moderate contribution to achieving the measurement (25% to 50%)	Litte or no contribution to achieving the measurement (less than 25%)	Tour trajectory does not provide a suitable opportunity to make observations	Example instrument not in model payload

JUPITER SYSTEM

JUPITER

Goal	Science Objective		Science Investigation		Example Measurements	JEO Example Instruments	JGO Example Instruments	JEO	JGO
Explore the Jupiter system as an archetype for gas giants	J. Study the jovian atmosphere	JA. Characterize the atmospheric dynamics and circulation.	JA.3	Quantify the roles of wave propagation and atmospheric coupling.	JA.3b. Perform radio occultations repeated closely in space and time (e.g., at the same latitude +/-10 degrees, once every 2 weeks) to determine pressure, density and temperature profiles perturbed by vertically-propagating waves which couple the troposphere and middle-atmosphere	Radio Subsystem	Radio Science Instrument & USO		
					JA.3c. Determine the vertical temperature structure and thermal wave activity at high spatial resolution between 1-microbar and 400-mbars from molecular lineshapes (R>1E6, 20- to 40-km vertical resolution depending upon altitude). In addition, perform limb observations in the thermal-IR (e.g., methane/hydrocarbon emission at 7.7 and 12- to 13-μm) to determine stratospheric temperature oscillations (20-km vertical resolution), with particular focus on the equatorial QQO.	Thermal Instrument (need Thermal-IR Spectrometer—not in model payload)	Submillimeter Wave Instrument		
					JA.3d. Near-IR and UV stellar occultations to obtain high-resolution stratospheric temperatures and study wave forcing from below the thermosphere. Near-IR imaging of multiple altitude levels to determine vertical structure of horizontally propagating waves. Observations of dayside (0.4- to 5.2-micron range) or nightside (2.5- to 5.2-micron range), including coverage of equatorial regions and polar vortices.	Vis-IR Spectrometer, UV Spectrometer	Visible InfraRed Hyperspectral Imaging Spectrometer, UltraViolet Imaging Spectrometer		
					JA.3e. Image from 7- to 250-microns for tropospheric and stratospheric temperatures and wind shears at regular (2 week) intervals, with 200- to 400-km/pixel spatial resolution to determine the latitudes, amplitudes and periodicities of zonal thermal wave activity, and to track oscillations of equatorial temperature field associated with the Quasi-Quadrennial Oscillation (QQO).	Thermal Instrument (need Thermal-IR Spectrometer—not in model payload)	Thermal-IR Spectrometer		
			JA.4	Investigate auroral structure and energy transport.	JA.4a. Imaging and polar spectral scans (70- to 90-degrees latitude, both hemispheres) and measure H^{3+} emission in the 2- to 5-micron range at regular intervals with 100 km/pixel spatial resolution. Sample from less than an hour (for solar flares) to days to study the internal structure of the aurora and identify satellite footprints.	Vis-IR Spectrometer	Visible InfraRed Hyperspectral Imaging Spectrometer		
					JA.4b. Acquire images and scans of the polar H_2 glow, morphology and the composition of the polar vortices (aerosols, exotic chemicals) in the 70- to 200-nm range. Obtain H Lyman alpha spectral line profiles with milliAngstrom resolution. Spectral analysis of H_2 Lyman and Werner bands and H Ly alpha for inferring information on the auroral precipitating electrons. Perform stellar and solar occultations over the poles in the upper atmosphere (90- to 200-nm).	UV Spectrometer	UltraViolet Imaging Spectrometer		
					JA.4c. Perform high spatial resolution (30-km vertical resolution) limb observations to determine the three-dimensional morphology of the Jovian aurora (200- to 500-km/pixel spatial resolution), and the nature of energy deposition and transport processes. Perform imaging in the wavelength ranges of 50- to 320-nm and 0.4- to 1.0-μm with a resolution of 150 km/pixel of the polar regions, dayside and nightside.	UV Spectrometer, Narrow Angle Camera	UltraViolet Imaging Spectrometer, Narrow Angle Camera		
			JA.5	Understand the interrelationships of the ionosphere and thermosphere.	JA.5a. Perform repeated radio occultations to study the relation between vertically propagating waves and the heating mechanisms for the thermosphere. Derive both neutral density and electron/ion density profiles in the ionosphere. Monitor variability with local time at multiple different latitudes/longitudes.	Radio Subsystem	Radio Science Instrument		
					JA.5b. Perform stellar occultations in the wavelength ranges of 200- to 320-nm to sample the stratosphere, 90- to 160-nm to sample H_2 above the homopause, and near 2 microns to measure the vertical structure of the thermosphere with 10- to 15-km vertical resolution.	UV Spectrometer, Vis-IR Spectrometer	UltraViolet Imaging Spectrometer, Visible InfraRed Hyper-spectral Imaging Spectrometer		
					JA.5c. Perform limb observations of H^{3+} ionic species and tracers, intensity modulation by gravity waves in the upper atmosphere (3.3- to 3.6-microns, Resolution > 10,000). Requires vertical resolution of half a scale height, coverage of mid and low latitudes with 300 km/pixel spatial resolution. Short and continuous time coverage (1 rotation or more) is required.	Vis-IR Spectrometer	Visible InfraRed Hyperspectral Imaging Spectrometer		

Science Value Rating Criteria						
Significant contribution or achieves the measurement (75% to 100%)	Major contribution to achieving the measurement (50% to 75%)	Moderate contribution to achieving the measurement (25% to 50%)	Litte or no contribution to achieving the measurement (less than 25%)	Tour trajectory does not provide a suitable opportunity to make observations	Example instrument not in model payload

JUPITER SYSTEM

JUPITER

Goal	Science Objective		Science Investigation		Example Measurements	JEO Example Instruments	JGO Example Instruments	JEO	JGO
Explore the Jupiter system as an archetype for gas giants	J. Study the jovian atmosphere	JA. Characterize the atmospheric dynamics and circulation.	JA.5	Understand the interrelationships of the ionosphere and thermosphere.	JA.5d. Acquire two-dimensional spectral-spatial images in the wavelength range of 90- to 230-nm for $H_{2\ and}$ Lyman alpha (121.6 nm) and from 100- to 200-nm for O and S ions/neutrals to study the latitudinal morphology of the thermosphere; the H Ly alpha bulge and H_2 emissions (from nadir viewing). Determine the origin of the H bulge and the possible connection to auroral activity and thermospheric circulation.	UV Spectrometer	UltraViolet Imaging Spectrometer		
					JA.5e. Measure the thermospheric circulation and winds, both zonally and meridionally, and determine the importance of wave acceleration and ion drag at these altitudes from high spectral resolution near-IR observations and UV line Doppler shifts (e.g., H^{3+}at 3.4 μm, 2.1 μm; Lyman alpha at 121.6 nm with high SNR and 1 km/s accuracy). Perform measurements in the wavelength range of 90- to 160-nm to determine the latitudinal morphology of H_2 band brightnesses for thermospheric winds.	UV Spectrometer, Vis-IR Spectrometer	UltraViolet Imaging Spectrometer, Visible InfraRed Hyper-spectral Imaging Spectrometer		
					JA.5f. Measure molecular lines to determine atmospheric temperatures, neutral density profiles and three-dimensional distribution of atmospheric species between 1-microbar and 400-mbars.	Submillimeter Wave Instrument	Submillimeter Wave Instrument		
		JB. Characterize the atmospheric composition and chemistry.	JB.1	Determine Jupiter's bulk elemental abundances.	JB.1a. Perform high spectral resolution observations (R>10000 at 5-microns) to determine bulk abundances of NH_3, CH_4, H_2O, PH_3, AsH_3, GeH_4 to 5 to 10% in the upper troposphere (1- to 6-bars). Measure at 4- to 5-micron wavelengths (R> 4000-10000) for D/H.	Vis-IR Spectrometer	Visible InfraRed Hyperspectral Imaging Spectrometer		
					JB.1b. Measurements in the Mid-IR and far-IR (R> 1000 at 7- to 1000-microns) to determine the distributions of PH_3, CH_4, CH_3D, NH_3 at 0.1- to 0.8-bar, D/H ratio at 1-mbar pressure level; (R>2500 to 10000 at 10-micron) for the $^{15}N/^{14}N$ ratio in the upper troposphere. Limb observations at 7- to 8-micron for $^{13}C/^{12}C$ ratio.	Thermal Instrument (need Thermal-IR Spectrometer—not in model payload)	Thermal-IR Spectrometer		
					JB.1c. Perform near-simultaneous radio occultations and measurements in the wavelength range from 20- to 50-μm to obtain helium abundance. Carry out dual spacecraft radio occultations at low frequencies to probe to 40-bars.	Far-IR Spectrometer (not in model payload), Radio Subsystem	Far-IR Spectrometer (not in model payload), Radio Science Instrument		
					JB.1d. Observe H_2O and CO at 250 μm (R> 10^6) for $^{18}O/^{17}O$ ratio.	Submillimeter Wave Instrument	Submillimeter Wave Instrument		
			JB.2	Measure the composition from the stratosphere to low thermosphere in three dimensions.	JB.2a. Perform measurements in the 70- to 200-nm range to study the 1- to 1000-microbar pressure level distributions of H_2, methane, acetylene, ethylene and ethane. Perform occultation measurements to detect stratospheric hydrocarbons in absorption and haze scattering properties.	UV Spectrometer	UltraViolet Imaging Spectrometer		
					JB.2b. Perform measurements in the 7- to 14-micron region to sample 1-mbar pressure level methane, ethane and acetylene distributions (R>2000), 7- to 9-micron to study the D/H ratio in the stratosphere (1-mbar pressure level), 13- to 14- micron region for HCN. Limb and nadir viewing required.	Thermal Instrument (need Thermal-IR Spectrometer—not in model payload), Vis-IR Spectrometer	Thermal-IR Spectrometer (not in model payload), Visible InfraRed Hyperspectral Imaging Spectrometer		
					JB.2c. Sounding at high spectral resolution of H_2O lines in the 100- to 3000- GHz range with R>1E6, 1-mbar to 10- μbar and above, CO_2, CO, HCN, and/or CS abundance. Map spatial variations at 1000-km/pixel resolution, vertical resolution of 25-km, absolute abundances to within a factor of 2. Acquire vertical profiles with approximate scale height resolution.	Submillimeter Wave Instrument	Submillimeter Wave Instrument		
					JB.2d. Measurements in the 30- to 80- micron range (R>1000) for stratospheric emission lines or water (exogenic origin), with simultaneous derivations of atmospheric temperature from line width. Mapping for spatial variations at 1000-km/pixel resolution, vertical resolution of 100-km or better.	Far IR spectrometer	Far IR spectrometer		

Science Value Rating Criteria						
	Significant contribution or achieves the measurement (75% to 100%)	Major contribution to achieving the measurement (50% to 75%)	Moderate contribution to achieving the measurement (25% to 50%)	Litte or no contribution to achieving the measurement (less than 25%)	Tour trajectory does not provide a suitable opportunity to make observations	Example instrument not in model payload

JUPITER SYSTEM

JUPITER

Goal	Science Objective		Science Investigation		Example Measurements	JEO Example Instruments	JGO Example Instruments	JEO	JGO
Explore the Jupiter system as an archetype for gas giants	J. Study the jovian atmosphere	JB. Characterize the atmospheric composition and chemistry.	JB.2	Measure the composition from the stratosphere to low thermosphere in three dimensions.	JB.2e. Perform repeat sounding, mapping in the wavelength range of 6- to 100-µm, and imaging from 110- to 230-nm (Lyman alpha, 121.6-nm), and radio occultation studies of the same latitudes 6- to 12-months apart to study long term evolution of the stratospheric temperature structure in response to seasonal variations.	Radio Subsystem, Thermal Instrument, UV Spectrometer	Radio Science Instrument & USO, Submillimeter Wave Instrument, UltraViolet Imaging Spectrometer		
			JB.3	Study localized and non-equilibrium composition.	JB.3a. Perform observations at regular intervals of evolving discrete features (*e.g.*, plumes, vortices, Great Red Spot Wake) at 160- to 230-nm wavelengths to determine the PH_3 distribution at altitudes higher than p <400 mbar.	UV Spectrometer	UltraViolet Imaging Spectrometer		
					JB.3b. Determine the distribution of disequilibrium species in the upper troposphere, particularly associated with lightning locations and discrete atmospheric features (repeated 10-hour separation views to study ice feature lifetimes, regular intervals for other discrete features) at spatial resolution of ~100-km/pixel (spectral resolutions R > 500 required to resolve lines of H_2O, NH_3 (ice and gas) and PH_3; R>2000 for AsH_3, GeH_4 and CO) all present in the 4.5- to 5.5-µm region. Both regional high-resolution hyperspectral maps, and low resolution global maps are required.	Vis-IR Spectrometer	Visible InfraRed Hyperspectral Imaging Spectrometer		
					JB.3c. Perform 8- to 12-micron, measurements at 200-km/pixel spatial resolution to determine the distribution of PH_3 in the 0.1- to 0.8-bar region. Far-IR measurements (15- to 250-microns) to determine the ortho/para-H_2 ratio, methane distribution.	Mid to Far IR Spectrometer, Thermal IR Spectrometer	Mid to Far IR Spectrometer, Thermal IR Spectrometer		
			JB.4	Determine the importance of moist convection in meteorology, cloud formation, and chemistry.	JB.4a. Perform measurements (1.0- to 5.2-microns, R> 400) with 100-km/pixel spatial resolution to determine aerosol properties (optical depth, cloud heights, number density, scattering properties) and related ice distributions (NH_3, H_2O) over a range of timescales (days to months).	Vis-IR Spectrometer	Visible InfraRed Hyperspectral Imaging Spectrometer		
					JB.4b. Perform measurements in the 8- to 12-micron region with 200-km/pixel spatial resolution to study long-wave aerosol extinction properties and relation to NH_3/PH_3 distribution (200- to 800-mbar).	Thermal Instrument (need Thermal-IR Spectrometer—not in model payload)	Thermal-IR Spectrometer		
					JB.4c. Measure NH_3 distribution in the photochemical depletion region (pressures less than 400 mbar) in the 160- to 230-nm wavelength range.	UV Spectrometer	UltraViolet Imaging Spectrometer		
					JB.4d. Perform radio occultations to probe upper atmosphere down to a minimum of 1-bar, and vertical resolution of 1- to 4-km. Determine the vertical and horizontal distribution of radio opacity sources (NH_3, H_2S, H_2O) below the cloud-tops.	Radio Subsystem (Dual X/Ka-band—Unmodulated 3.6-cm [X-band] and 0.94-cm [Ka-band])	Radio Science Instrument & USO (Dual X/Ka-band—Unmodulated 3.6-cm [X-band] and 0.94-cm [Ka-band])		
					JB.4e. Nightside imaging of lightning to determine the spatial distribution and power of lightning sources.	Vis-IR Spectrometer	Visible InfraRed Hyperspectral Imaging Spectrometer		
		JC. Characterize the atmospheric vertical structure.	JC.1	Determine the three-dimensional structure from Jupiter's upper troposphere to lower thermosphere.	JC.1a. Perform multispectral mapping in the wavelength range from 0.4- to 5.5 µm at 100-km/pixel resolution of the clouds composition and particle size distribution, both globally and regionally (within discrete atmospheric features) on the dayside and nightside. Multiple phase angle coverage to constrain scattering properties and cloud altitude. Strong and weak CH_4 absorption band imaging to investigate the vertical cloud structure to a spatial resolution of 30 km/pixel. Constrain composition, size and altitude of particulates.	Narrow Angle Camera, Wide Angle Camera, Vis-IR Spectrometer	Narrow Angle Camera, Wide Angle Camera, Visible InfraRed Hyperspectral Imaging Spectrometer		

Science Value Rating Criteria					
Significant contribution or achieves the measurement (75% to 100%)	Major contribution to achieving the measurement (50% to 75%)	Moderate contribution to achieving the measurement (25% to 50%)	Litte or no contribution to achieving the measurement (less than 25%)	Tour trajectory does not provide a suitable opportunity to make observations	Example instrument not in model payload

JUPITER SYSTEM										
JUPITER										
Goal	**Science Objective**		**Science Investigation**		**Example Measurements**	**JEO Example Instruments**	**JGO Example Instruments**	**JEO**	**JGO**
Explore the Jupiter system as an archetype for gas giants	**J. Study the jovian atmosphere**	JC. Characterize the atmospheric vertical structure.	JC.1	Determine the three-dimensional structure from Jupiter's upper troposphere to lower thermosphere.	JC.1b. Observations across the wavelength range of 200- to 300-nm at a spatial resolution of 100- to 200-km/pixel, to determine the distribution and densities of high altitude UV-absorbent hazes. Repeated latitude mapping with spatial resolution of 5- to 10-degrees of latitude. Requires multiple phase angle views.	Narrow Angle Camera, Wide Angle Camera, UV Spectrometer	Narrow Angle Camera, Wide Angle Camera, UltraViolet Imaging Spectrometer		
					JC.1c. Perform thermal observations to determine the tropospheric and stratospheric temperature structure, and to study the physiochemical environment in which clouds and aerosols form, 200-km/pixel spatial resolution.	Thermal Instrument (need Thermal-IR Spectrometer—not in model payload)	Thermal-IR Spectrometer		
					JC.1d. Track discrete features at high-resolution (15-km/pixel) using latitudinal (center to limb) scans, with time separations of hours over multiple rotations for storm evolution from 0.25- to 5.2-microns.	Narrow Angle Camera, Wide Angle Camera, Vis-IR Spectrometer	Narrow Angle Camera, Wide Angle Camera, Visible InfraRed Hyperspectral Imaging Spectrometer		
					JC.1e. Perform multiple radio science occultations for vertical temperature, pressure and neutral density profiles.	Radio Subsystem	Radio Science Instrument		
					JC.1f. Identify the location of the homopause by performing multiple UV stellar occultations at a range of latitudes and local times (e.g., use CH_4 absorption and aerosol scattering below 145 nm).	UV Spectrometer	UltraViolet Imaging Spectrometer		
					JC.1g. Determine the vertical temperature structure at a range of well-separated latitudes from the upper troposphere to the lower thermosphere via occultations at UV, radio and near-IR wavelengths in combination with thermal-IR and sub-mm measurements. Regular repetition to study wave phenomena and seasonal variability.	UV Spectrometer, Vis-IR Spectrometer, Thermal Instrument, Radio Subsystem	UltraViolet Imaging Spectrometer, Visible InfraRed Hyper-spectral Imaging Spectrometer, Sub-millimeter Wave Instrument, Radio Science Instrument		
			JC.2	Explore Jupiter's interior density structure and dynamics below the upper troposphere.	JC.2a. Measure frequencies of the global acoustic modes of the planet, up to degree l=50 (goal) to 100 (target) in the range 0.3- to 3-mHz. Global radial velocity maps monitored continuously for weeks, up to 6 months (target), at 1 frame/mn sampling rate, with a duty cycle higher than 70%. Spatial resolution 700-km/pixel at 40 R_J. Radial velocity noise level < 1 $cm^2/s^2/\mu Hz$. Precision on frequency measurement <0.3 μHz	Doppler Spectro-imager	Doppler Spectro-imager		
			JC.3	Study coupling across atmospheric layers.	JC.3a. Perform multispectral imaging in the visible and 4- to 5-micron spectral range to determine the depth and shears on the zonal wind fields and the vertical structure of vortices and plumes between 2- to 3-bar and the 0.5- to 1.0-bar levels (50- to 200- km/pixel). Acquire multiple high-resolution images of cloud structure on a timescale of hours, days, months, and years.	Vis-IR Spectrometer	Visible InfraRed Hyperspectral Imaging Spectrometer		
					JC.3b. Perform radio occultations closely spaced in space and time (e.g., at the same latitude +/-10 degrees, once every 2 weeks) to determine pressure, density and temperature profiles perturbed by vertically-propagating waves which couple the troposphere and middle-atmosphere.	Radio Subsystem	Radio Science Instrument & USO		
					JC.3c. Determine the vertical temperature structure and wave activity at high spatial resolution between 1-microbar and 400-mbars from molecular lineshapes (R>1E6). Perform limb observations in the thermal-IR to determine stratospheric temperature oscillations (20-km vertical resolution), with particular focus on the equatorial QQO.	Thermal Instrument (need Thermal-IR Spectrometer—not in model payload)	Submillimeter Wave Instrument, Thermal-IR Spectrometer (not in model payload)		

Science Value Rating Criteria						
Significant contribution or achieves the measurement (75% to 100%)	Major contribution to achieving the measurement (50% to 75%)	Moderate contribution to achieving the measurement (25% to 50%)	Litte or no contribution to achieving the measurement (less than 25%)	Tour trajectory does not provide a suitable opportunity to make observations	Example instrument not in model payload

JUPITER SYSTEM									
JUPITER									
Goal	**Science Objective**		**Science Investigation**		**Example Measurements**	**JEO Example Instruments**	**JGO Example Instruments**	**JEO**	**JGO**
Explore the Jupiter system as an archetype for gas giants	**J. Study the jovian atmosphere**	JC. Characterize the atmospheric vertical structure.	JC.3	Study coupling across atmospheric layers.	JC.3d. Perform stellar occultations to obtain high-resolution stratospheric temperatures and study wave forcing from below the thermosphere. Imaging of multiple altitude levels required to determine vertical structure of horizontally propagating waves. Perform observations of dayside (0.4- to 5.2-micron range) or nightside (2.5- to 5.2-micron range), including coverage of equatorial regions and polar vortices.	Vis-IR Spectrometer, UV Spectrometer	Visible InfraRed Hyperspectral Imaging Spectrometer, UltraViolet Imaging Spectrometer		
					JC.3e. Nadir imaging (7- to 250-microns for tropospheric and stratospheric temperatures and wind shears) at regular (2-week) intervals, with 200- to 400 km/pixel spatial resolution to determine the latitudes, amplitudes and periodicities of zonal thermal wave activity, and to track oscillations of equatorial temperature field associated with the QQO.	Thermal Instrument (need Thermal-IR Spectrometer—not in model payload)	Thermal-IR Spectrometer		

Science Value Rating Criteria						
	Significant contribution or achieves the measurement (75% to 100%)	Major contribution to achieving the measurement (50% to 75%)	Moderate contribution to achieving the measurement (25% to 50%)	Litte or no contribution to achieving the measurement (less than 25%)	Tour trajectory does not provide a suitable opportunity to make observations	Example instrument not in model payload

As stated in the 2006 Solar System Exploration Roadmap [*NASA 2006*], "By studying the Jupiter system as a whole, we could better understand the 'type example' for habitable planetary systems within and beyond our Solar System." The top priority objectives in the EJSM Traceability Matrix relate directly to Europa and its potential habitability. Moreover, many aspects of Jupiter System science relate closely to understanding Europa and its potential habitability. For example: Ganymede and Callisto are believed to possess subsurface oceans which would provide comparisons to Europa; Io holds clues to the fundamentals of tidal heating and interactions with the Jovian magnetospheric environment; and Jupiter's composition sheds light on the initial conditions of the Galilean satellite system.

The JJSDT also recognizes the importance of Jupiter System science in its own right, as it relates to the overall theme of: The emergence of habitable worlds around gas giants. Moreover, EJSM presents important synergistic and complementary science opportunities for Jupiter system science through the two spacecraft.

4.3.1 Goal 1: Europa Objectives and Investigations

The Cosmic Vision document states: "Europa is a high-priority target in the search for habitability in the Solar System." The Planetary Decadal Survey summarizes the inherent motivation for Europa exploration as a fundamental science question: "Where are the habitable zones for life in the solar system, and what are the planetary processes responsible for producing and sustaining habitable worlds?" Both processes and habitability are key drivers for Europa exploration, as are the focus areas of origin, evolution, and habitability. Thus, the goal adopted for the Europa aspect of EJSM is:

Explore Europa to investigate its habitability.

This goal implies understanding processes, origin, and evolution. These include testing the numerous scientific questions described in §4.2. It also allows for "discovery" science—unpredicted findings of the type that have often reshaped the very foundations of planetary science, especially in the surprises uncovered in the outer solar system by the Voyager, Galileo, and Cassini missions. "Investigate its habitability" recognizes the significance of Europa's astrobiological potential. "Habitability" includes confirming the existence and determining the characteristics of water below Europa's icy surface, understanding the possible sources, sinks and cycling of chemical and thermal energy, investigating the evolution and chemical composition of the surface and ocean, and evaluating the processes that have affected Europa through time.

The Europa objectives are categorized in priority order as:

EA. Europa's Ocean
EB. Europa's Ice Shell
EC. Europa's Composition
ED. Europa's Geology
EE. Europa's Local Environment.

These are primarily met by the JEO. Dual instrument support and additional context are provided by the JGO.

4.3.1.1 EA. Europa's Ocean

Characterize the extent of the ocean and its relation to the deeper interior.

Galileo observations, in particular the magnetometer data (§4.2.1.1), provide evidence that the presence of a sub-surface ocean is very likely. Given the critical importance of such an ocean to Europa's

astrobiological potential, it is important to first confirm its existence.

In the likely instance that an ocean exists, several geophysical measurements (Foldout 2) would place constraints on its depth, extent, and physical state (e.g., salinity). Several of these techniques would also help to characterize the deeper interior structure of Europa (the mantle and core). Doing so is important because of the coupling that takes place between the near-surface and deeper layers: for instance, an Io-like mantle implies a vigorously convecting ocean and a relatively thin ice shell. In priority order, the investigations and corresponding measurement techniques are as follows.

Investigation EA1: Determine the amplitude and phase of the gravitational tides.

Perhaps the most direct way of confirming the presence of an ocean is to measure the time-variable gravity and topography due to the tides raised by Jupiter. In the absence of an ocean, Europa's ice shell would be coupled directly to the rocky core, and the time-dependent tidal surface displacement would be a few meters [*Moore and Schubert 2000*]. On the other hand, if Europa has a liquid water ocean beneath a relatively thin ice shell, the displacement amplitude would be 30 m over one orbit (Figure 4-21). The surface displacement would also cause a measurable periodic gravity signal. Thus, measurement of the tidally driven time-variable topography or gravity (described by the Love numbers h_2 and k_2, respectively) would provide a simple and definitive test of the existence of a sub-ice ocean.

The Love number k_2 is estimated from the time-variable gravitational field of Europa. Simulations show that measurements of the Doppler shift of the spacecraft radio signal could be used to estimate k_2, the mantle and ice shell libration amplitudes and phase lag angle, and the static gravitational field parameters, which are estimated along with the spacecraft trajectory information [*Wu et al. 2001*]. Simulations adding altimetry measurements shows that the tidal Love number h_2 could also be estimated [*Wahr et al. 2006*].

Multiple orbits are required to estimate the body gravity field, including the tidal response, because the spacecraft orbit has to be determined at the same time. Orbit determination is improved by crossover analysis using the laser altimeter. If the spacecraft measures different distances to the same spot on the surface during different orbits, then (neglecting tides) the change must be due to the changing spacecraft altitude. In this manner, the spacecraft position could be accurately determined as at Mars [*Neumann et al. 2001*]. This approach could also take into account the fact that the surface undergoes periodic displacements, due to tides and librations (see §4.2.1.1).

To detect the radio Doppler shift caused by the spacecraft motion in the line-of-sight to Earth, two frequency bands have been considered. X-band (near 8 GHz) would be used for spacecraft commanding and Ka-band (near 32 GHz) is used for transmission of spacecraft data to Earth. With the X-band uplink, Doppler measurement accuracy is limited by fluctuations in the solar plasma. An accuracy of 0.1 mm/s for 60 s integration times is typical but varies as a function of solar elongation. To reduce the effect of solar plasma, an auxiliary Ka-band receiver is included in the baseline payload. By using Ka-band on both Earth-to-spacecraft and vice versa, the Doppler measurement accuracy is improved by a factor of 10 except for times near solar conjunction. At Ka-band the dominant noise for most observing times is due to Earth troposphere calibration accuracy.

Can JEO determine the thickness of Europa's ice shell?

On Thick or Thin Ice?

Despite more than a decade of study of the Galileo data, the fundamental issues of the thickness of Europa's ice shell remain uncertain to over an order in magnitude [*Kattenhorn and Billings 2005*]. Estimates range from just a few kilometers [*e.g. Greenberg et al. 2000*] to several tens of kilometers, or more [*Pappalardo et al. 1999*]. The thickness of the ice shell is important to understanding Europa's potential habitability, for example, in controlling the types of geological processes that affect material exchange between the ice shell and ocean.

Galileo gravity data suggest that Europa is differentiated into an iron core, rocky mantle, and an H_2O-rich outer shell ~100 km thick, consisting of an ice shell and a liquid ocean. Galileo imaging data reveal a wide variety of enigmatic surface features.

In a thin ice shell interpretation (near right), ridges are sites where liquid water has squeezed out onto the surface, and chaotic terrains form by melt-through of the ice shell from strong hydrothermal plumes below [*Greenberg et al. 2000*]. In a thick ice shell interpretation (far right), Europa's ice shell is convecting and localized partial melting can occur [*Pappalardo et al. 1999*].

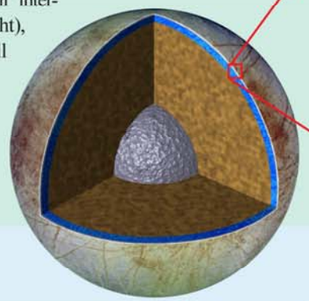

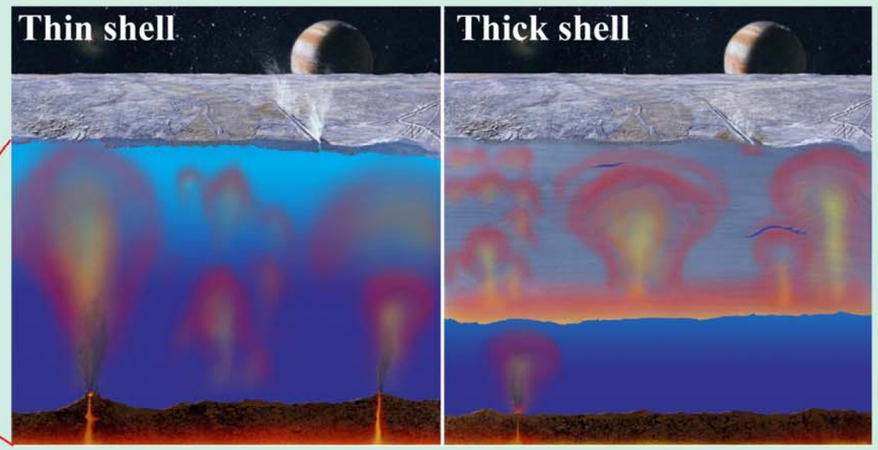

A hypothetical example using geophysical techniques

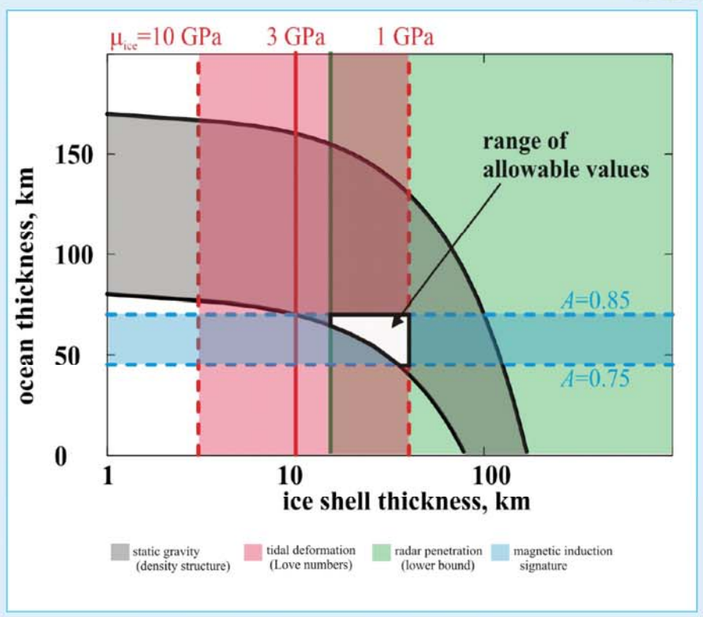

Geophysical measurements are non-unique. Nevertheless, using a combination of carefully planned geophysical techniques, JEO can constrain the thickness of Europa's ice shell.

Here is presented an example of how a combination of (hypothetical) JEO measurements can be used to constrain the ice shell thickness. Based on the bulk density and moment of inertia of the satellite (derived from flybys by JEO and previous spacecraft), the thickness of the water + ice layer may be obtained (gray shading) [*Anderson et al. 1997*]. The uncertainties arise mainly from our lack of knowledge of the density of the rocky interior (the bulk density is already well known).

Gravity and topography measurements

Measuring the time-variable gravity and topography gives the k_2 and h_2 Love numbers, respectively. Hypothetical Love number constraints here (red shading) assume observed h_2 and k_2 of 1.202 and 0.245, respectively, and constrain shell thickness as a function of rigidity μ_{ice} [*Moore and Schubert 2000*]. The hypothetical values assumed here are characteristic of a moderately thick ice shell.

In the example shown, the ice shell deformation is sufficiently large that a shell thickness in excess of 40 km is prohibited. Determining both k_2 and h_2 constrains the thickness significantly more than either value can alone. The ratio of h_2/k_2 is quite different depending on whether a subsurface ocean exists or not, and provides an additional test of the ocean's existence.

Radar Sounding

A lower bound on the ice shell thickness may be derived using ice-penetrating radar observations. The base of the ice shell is hard to image because warm ice is radar absorptive; however, even a non-detection of the ice-water interface allows a lower bound to be placed on the shell thickness. Here, a tectonic model of ice shell properties is assumed [*Moore 2000*], resulting in a radar penetration depth (and lower bound on shell thickness) of 15 km (green shading).

Magnetometer data

Multiple-frequency magnetic induction signatures (blue shading) constrain ocean thickness [*Khurana et al. 2002*]; here a hypothetical dimensionless induction signal A = 0.75–0.85 and an ocean conductivity of 2 S/m are assumed, resulting in an ocean thickness in the range 45-70 km.

This particular (hypothetical) set of observations results in a range of acceptable ice shell thicknesses (15 to 40 km) and a range of acceptable ocean thicknesses (45-70 km). A different set of observations would result in different constraints, but the main point is that the combined constraints are more rigorous than could be achieved by any one technique alone. JEO will provide the measurements needed to constrain the thickness of Europa's ice shell.

Foldout 2. Ice Shell Thickness.

Doppler-only simulations [*Wu et al. 2001*] show that the Love number k_2 could be determined with an accuracy of about 0.0005, or 0.25%, using either X/X or X/Ka Doppler tracking over 15 days when fit simultaneously with the Europa gravity field, librations, and spacecraft trajectory. In the same estimation the radial position of the spacecraft could be determined with accuracy 2 m, close to the desired orbit reconstruction accuracy, but about 10 times worse than currently being achieved with Mars orbiting spacecraft using much longer data arcs [*Konopliv et al. 2006*]. The expected accuracy in determining k_2 is easily sufficient to distinguish between an ocean-bearing and ocean-free Europa. The addition of Ka/Ka tracking reduces the radial orbit error below 1 m and would permit definitive testing of the ocean hypothesis based on the tidal response as measured by h_2.

Range-rate measurements would also permit precise determination of the position of Europa's center of mass relative to Jupiter during the lifetime of the mission. This is necessary for determining the spacecraft orbit to better than 1-meter (rms) throughout the orbiter lifetime.

In addition to testing the ocean hypothesis, h_2 and k_2 could be used to investigate the ice shell thickness (Foldout 2). Figure 4-21 shows how these quantities vary with ice shell thickness and rigidity. Based on simulations of plausible internal structures, measurement uncertainties of ±0.0005 for k_2 and ±0.01 for h_2 would permit the actual k_2 and h_2 of Europa to be inferred with sufficient accuracy such that the combination places bounds on the depth of the ocean and the thickness of the ice shell [*Wu et al. 2001, Wahr et al. 2006*].

Investigation EA2: Determine the magnetic induction response from the ocean and characterize the influence of the space plasma environment on this response.

The strongest current evidence for Europa's ocean is the induction signature apparently generated by Jupiter's time-dependent magnetic field interacting with a shallow conductive layer, presumably a salty ocean (§4.2.1.1). However, because the Galileo

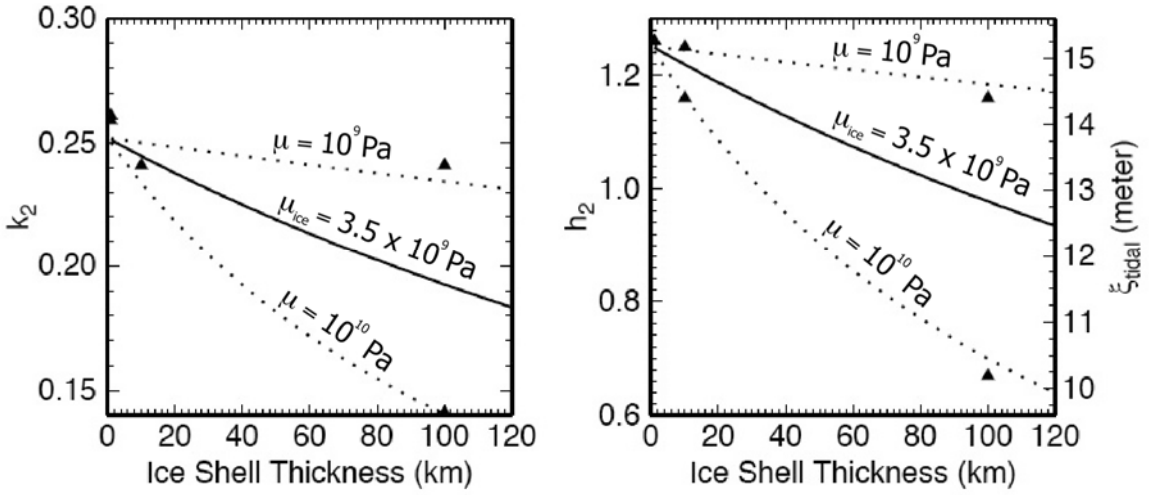

Figure 4-21. Sensitivity of Love numbers k_2 (left) and h_2 (right) to ice shell thickness and rigidity, with the assumption of a subsurface ocean. For the same curves which depict h_2, the right-hand axis shows the amplitude ζ_{tidal} (which is half of the total measurable tide) as a function of ice shell thickness. For a relatively thin ice shell above an ocean, the tidal amplitude is ζ_{tidal} ~ 15 m (total measureable tide ~30 m), while in the absence of an ocean ζ_{tidal} ~1 m [*Moore and Schubert* 2000]. Solid curves show the h_2 and corresponding ζ_{tidal} for an ice shell rigidity of $\mu_{ice} = 3.5 \times 10^9$ Pa, while the dotted lines bound a plausible range for ice rigidity). A rocky core is assumed, with a radius 1449 km and rigidity $\mu_{rock} = 10^{11}$ Pa, and the assumed ice + ocean thickness = 120 km. Triangles show the reported values from *Moore and Schubert* [*2000*], which did not include a core. Figure courtesy Amy Barr.

spacecraft was effectively measuring the induction response at a single frequency during its flybys, only the product of the layer thickness and conductivity could be established. By contrast, an orbiter could determine both thickness and conductivity by measuring the induction response at multiple frequencies.

Europa is immersed in various low-frequency waves that could be used for magnetic sounding, some of which arise from Io's torus at the outer edge of Europa's orbit. Waves of different frequencies penetrate to different depths within the satellite, and exhibit different induction responses. Dominant frequencies occur at the synodic rotation period of Jupiter (period ~ 11 hr) and the orbital period of Europa (period = 3.55 days = 85.2 hr). Over a broad range of parameter space, the induction curves at two frequencies intersect [*Khurana et al. 2002*]. In this range, the ocean thickness and conductivity (which constrains the salinity) could be determined uniquely. In order to sound the ocean at these two frequencies, continuous data are required from low altitude over times of at least one month.

Further constraints on the ocean, mantle, and core would be provided by the broadband (but weak) signal excited by Io's torus for which continuous observations of at least months are desirable. This latter requirement drives the required sensitivity of the magnetometery measurements to 0.1 nT. Magnetometry requires near-continuous observations from Europa orbit for at least 8–10 eurosols, i.e. at least one month. A high cadence of 8 vectors/s is required to remove the effects of moon-plasma interactions from the data and knowledge of spacecraft orientation is required to 0.1°. In addition, measurements of plasma density, temperature, and flows are required to quantify the currents generated in Europa's vicinity by the moon-plasma interaction and remove their contribution from the measured magnetic field. Near the surface of Europa, at the synodic rotational period of Jupiter, the interaction currents contribute to the internal and external harmonics of first degree (uniform external field and dipolar internal field) at a level of 10–20 nT [*Schilling et al. 2007*]. The requirement to determine interaction currents could be met by measuring fluxes of charged particles (ions and electrons) over a broad energy range (tens of eV to several MeV) over a solid angle of 2π. Because the energies of the sputtering particles is very high (E $\geq$100 keV) and the energies of the recently picked-up ions is quite low (a few keV), measurements over a broad energy range are desired to quantify the plasma interaction.

Investigation EA3: Characterize surface motion over the tidal cycle.

The time-dependent tidal deformation of Europa's surface, characterized by the Love number h_2, provides a strong test for the existence of an ocean (§4.2.1.1). It could also be used in conjunction with the k_2 Love number to constrain the ice shell thickness (Foldout 2).

The Love number h_2 is derived by measuring the time-variable topography of Europa, specifically by measuring topography with the laser altimeter at cross-over points (Figure 4-22), a technique which has been demonstrated for Earth [*Luthcke et al. 2002 2005*] and Mars [*Rowlands et al. 1999, Neumann et al. 2001*]. After ~60 days in orbit about Europa the sub-spacecraft track would form a reasonably dense grid, comprised of a number N of (~700) great circle segments over the surface of Europa. Each of the N arcs intersects each of the remaining N-1 arcs at two roughly antipodal locations, and at these cross-over locations, the static components of gravity and topography should agree. As illustrated in Figure 4-22, differences in the measured values at cross-over points are equal to the sum of actual change in radius caused

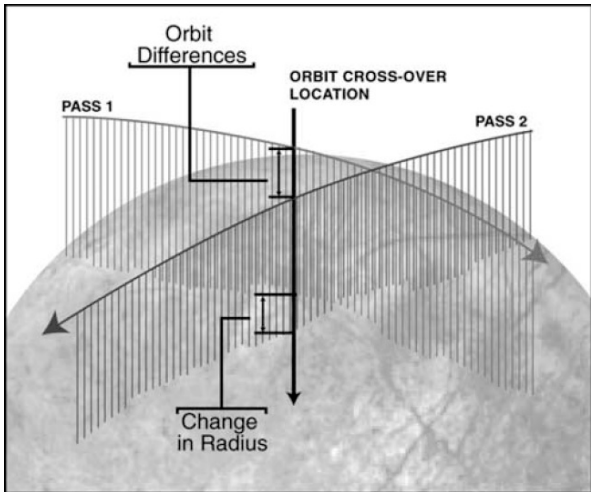

Figure 4-22. Illustration of the cross-over technique. Actual change in radius of Europa due to tidal and librational motions is determined by measuring altitude from the spacecraft to the surface, and by accounting for the distance of the spacecraft from the center of mass by means of Doppler tracking [*Wahr et al. 2006*].

by tides and libration, combined with the difference in orbital altitude, along with any errors in range to the center of the body or orbital position. The errors are dominated by long wavelength effects and could be represented by 4 sine and cosine terms in each orbital component (radial, along track, and cross track). The tidal effects in gravity and topography have known spatial and temporal patterns and could each be represented globally by two parameters, an amplitude and phase. The librations are effectively periodic rigid rotations with specified axes and periods, and again an amplitude and phase parameter.

Investigation EA4: Determine the satellite's dynamical rotation state (forced libration, obliquity and nutation).

As part of the orbit determination and crossover analysis necessary to determine h_2 and k_2 (§4.3.1.1), Europa's rotation pole position and its librations in both longitude and latitude would be determined. These quantities all depend on Europa's internal structure; thus, they provide additional, largely independent, constraints on the presence or absence of an ocean and the polar moment of inertia C. This latter quantity contains information about the distribution of mass within the satellite.

Librations in longitude and latitude are driven by the non-zero eccentricity and obliquity of the satellite, respectively. The amplitude of forced librations in longitude gives the combination (B-A)/C for the principal moments of inertia $A < B < C$, as has been done for Earth's Moon [*Newhall and Williams 1997*]. The quantity (B-A) depends on the degree-two static gravity coefficients, which would be determined to high accuracy, and thus the polar moment of inertia C may be determined. If the ice shell is decoupled from the interior by an ocean, the libration amplitude would be a factor of three larger than for a solid Europa [*Comstock and Bills 2003*]. Similar constraints would be provided by determination of the latitudinal libration amplitude.

If there is an ocean, there may be two librational signals, one from the ice shell and another from the deeper interior. The shell's signal would be revealed in both gravity and topography data, whereas the deeper signal would appear only in the gravity.

Europa's obliquity—the angular separation between its spin and orbit poles—provides another constraint on its polar moment of inertia C. If its spin state is tidally damped, the obliquity is expected to be ~0.1^o [*Bills 2005*], with the exact amplitude depending on C [*Ward 1975, Bills and Nimmo 2008*].

The dynamical rotational state (spin rate and orientation, libration amplitudes) of Europa would be determined using Doppler tracking data and a laser altimetry crossover technique. Initially assuming both steady rotation and zero obliquity, the cross-over analysis described above would be used to adjust the spacecraft orbit estimate and to determine the

dynamical rotation as well as the tidal flexing of Europa.

Investigation EA5: Investigate the core, rocky mantle, rock-ocean interface, and compensation of the ice shell.

Whether Europa's silicate interior is Io-like and dissipative, or cold and inactive, has important consequences for the likely thickness of the shell and for silicate-ocean interchange. Clues to the nature of the deeper interior could be obtained from gravity, topographic, and magnetic observations.

Static gravity observations, made using the same techniques as outlined above, may be used to investigate the topography at the silicate-ocean interface. Figure 4-23 illustrates the estimated gravitational spectrum for Europa, with separate contributions from an ice shell and a silicate interior, along with simulated error spectra for 30 days of tracking at each of three representative orbital altitudes [*cf. Wu et al. 2001*]. To be conservative, only the X-band error estimate has been used. The recovered gravity errors are smaller at lower altitudes because the spacecraft is closer to the anomalies and thus experiences larger perturbations.

At long wavelengths, the gravity signal is dominated by the silicates. Because the water-

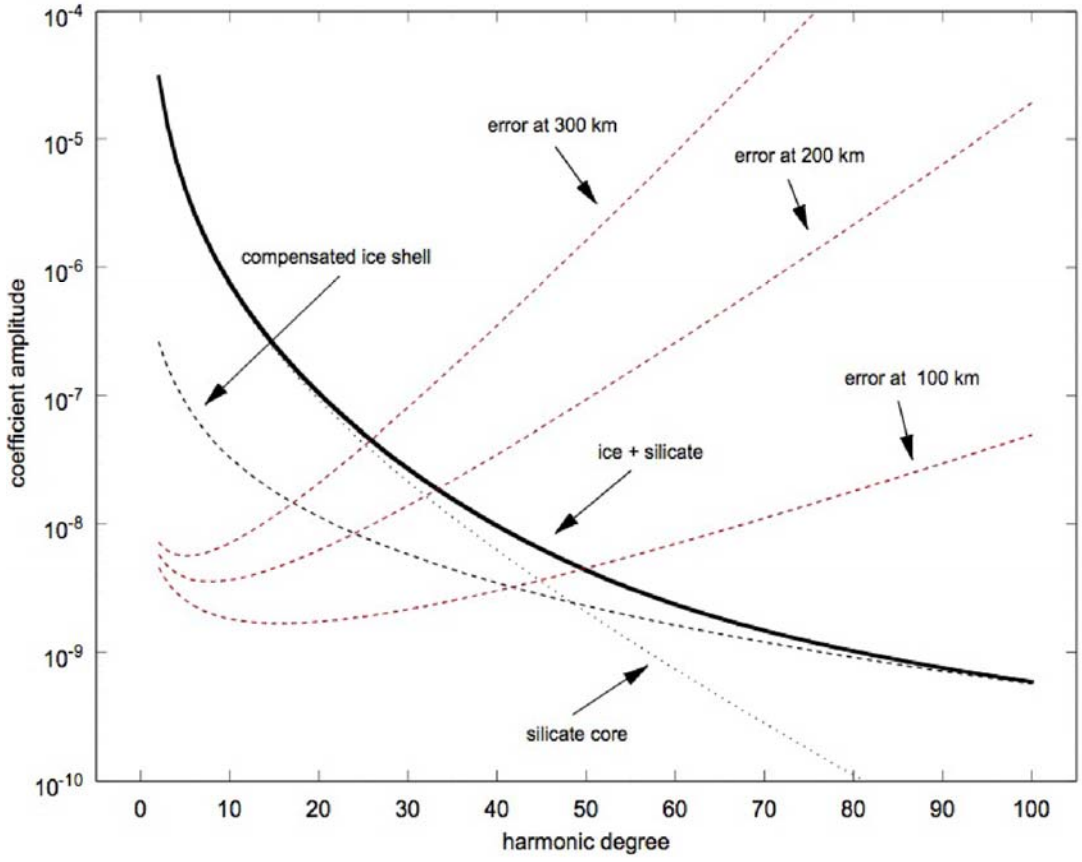

Figure 4-23. Models of Europa's gravity spectrum, assuming an ice shell 10 km thick with isostatically compensated topography above an ocean, and a silicate interior with a mean surface 100 km below the ice surface. The variance spectra of the ice topography and silicate gravity are assumed similar to those seen on terrestrial planets [*Bills and Lemoine 1995*]. The signal has contributions from the silicate mantle and ice shell. The error spectra represent 30 days at fixed altitude, and reflect variations in sensitivity with altitude. The error spectra at different orbital altitudes do not have the same shape because the longer wavelength anomalies are attenuated less at higher altitudes. During a few days at these altitudes, the improvement is linear with time; for longer times, repeat sampling leads to improvement proportional to square root of time.

silicate density contrast likely greatly exceeds density variations within the mantle, long-wavelength gravity anomalies would provide evidence for seafloor topography and may point to the existence of seamounts or volcanic rises. Such long-wavelength gravity anomalies may also result in potentially measurable surface topographic variations (as with the sea surface on Earth).

At shorter wavelengths, the signal is dominated by shallower ice-shell contributions, and the topography and gravity should be spatially coherent [*Luttrell and Sandwell 2006*]. Isostatically supported topography in the ice shell produces a gravity anomaly which is larger for thicker shells. If the wavelength at which the transition from silicate-dominated to ice-dominated signals could be determined, this would provide a constraint on the thickness of the ice shell (assuming isostatic compensation). Such a transition is potentially detectable at 100 km orbit altitude.

Ice penetrating radar may be able to detect the ice-ocean interface, as discussed in §4.3.1.2. Mapping the ice-ocean interface would provide a direct indication of ice shell thickness and how it varies spatially across the satellite. Measurements that determine the ice shell thickness only locally could be combined with the global gravity measurements as mentioned above, which would permit extrapolation of ice shell thickness to other regions of the satellite.

Time-dependent gravity measurements may also provide constraints on Europa's deep interior: for instance, a fluid-like Love number (k_2 ~2.5) would imply a low-rigidity mantle and core, as well as a subsurface ocean.

Magnetometer measurements of very low-frequency magnetic variations (periods of several weeks) would shed light on the magnetic properties of the deep interior, including the core. For instance, a partially molten, Io-like mantle is expected to have a higher conductivity than a cold, inactive interior. Such measurements need to be taken over a period of several months. Simultaneous plasma measurements are necessary to remove the effects of moon-plasma interactions from the data.

The key outstanding questions relating to Europa's ocean (2.1.1) could be linked to and addressed by the Objective EA investigations described above, as summarized in Table 4-2.

4.3.1.2 EB. Europa's Ice Shell

Characterize the ice shell and any subsurface water, including their heterogeneity, and the nature of surface-ice-ocean exchange.

There are strong scientific reasons for studying the subsurface structure of Europa's shell, especially as it relates to subsurface water and the nature of the surface-ice-ocean exchange (see §4.2.1.2). Dielectric losses in very cold ice are low, yet highly sensitive to increasing temperature, water, and impurity content; therefore, much could be learned through orbital electromagnetic sounding of the ice shell. This is especially true when subsurface profiling is coupled to observations of the topography and morphology of surface landforms and placed in the context of both surface composition and subsurface density distribution. Because of Jupiter's strong radio emissions and the unknown size of volume scatterers within Europa's ice shell, the range of sounding frequencies must be carefully matched to the science objectives.

The thickness of Europa's ice shell is one of the most important questions left unanswered by the Galileo mission. Determining the ice shell thickness is of fundamental astrobiological significance: it constrains the

Table 4-2. Hypothesis Tests to Address Selected Key Questions Regarding Europa's Ocean and Interior.

Example Hypothesis Questions		Example Hypothesis Tests
EA.1	Does Europa undoubtedly have a subsurface ocean?	Measure the gravity field at Europa over the diurnal cycle.
EA.2	What are the salinity and thickness of Europa's ocean?	Determine the magnetic induction signal over multiple frequencies to derive ocean salinity and thickness.
EA.3	What is the internal structure of Europa's outermost H_2O-rich layers?	Use measurements of the time-variable topography to derive the Love number h_2, to relate the ice shell and ocean layer thicknesses.
EA.4	Does Europa have a non-zero obliquity and if so, what controls it?	Use gravitational and topographic measurements of the tides to infer obliquity, which in turn constrains moments of inertia especially in combination with libration amplitude(s).
EA.5	Does Europa possess an Io-like mantle?	Radar, magnetic and/or gravitational inferences of the ice shell thickness constrain how much heat the silicate interior is producing; magnetometer inferences of ocean salinity constrain the rate of chemical exchange between silicates and water, and the conductivity structure of the deep interior; local thinning of the ice shell (identified by radar) could be linked to hydrothermal plumes; time-variable gravity place bounds on the rigidity of the silicate interior.

tidal heat the satellite is generating; whether the silicate interior is Io-like or not; and the extent to which the ocean and near-surface ice are likely to exchange material.

Investigation EB1: Characterize the distribution of any shallow subsurface water and the structure of the icy shell including its subsurface properties.

The subsurface signatures from near-global ice-penetrating radar surveys at high depth resolution combined with surface topography of similar vertical resolution would identify regions of possible ongoing or relatively recent upwelling of liquid water or brines. Orbital subsurface profiling of the top 3 km of Europa's ice shell should be feasible [*Chyba 1998, Moore 2000*] and is recommended at frequencies slightly above the upper end of Jupiter's radio noise spectrum (i.e., about 50 MHz) to establish the geometry of various thermal, compositional, and structural horizons to a depth resolution of about 10 m (requiring a bandwidth of about 10 MHz). This high-resolution search for shallow water would produce data analogous to that of the Shallow Subsurface Radar (SHARAD) instrument onboard the Mars Reconnaissance Orbiter (Figure 4-24).

This profiling should be done in conjunction with co-located stereo imaging and laser altimetry which could be used to register photogrammetric topography to vertical resolution of better than 10 m, permitting surface clutter effects to be removed from the radar data. Stereo imaging is susceptible to relative errors, and stereo vertical accuracy may vary across a scene. However, significantly higher vertical resolutions could be extracted using photoclinometry that is controlled by stereo imaging and laser altimetry profiles. By tying this high horizontal-resolution relief to the high absolute vertical resolution of a laser altimeter, substantially improved digital elevation models with vertical resolution <10 meters could be generated, which could be used to attribute radar clutter. Ultimately, shallow subsurface profiles should extend over at least 80% of Europa's surface utilizing profiles with spacings no more than twice the hypothesized maximum ice shell thicknesses (i.e., about 50 km).

Investigation EB2: Search for an ice-ocean interface. Subsurface signatures from lower resolution but more deeply penetrating radar surveys might reveal the ice-ocean interface, which could be validated over a region by carefully correlating ice thickness and surface topography. An unequivocally thin ice shell, even within a limited region, would have significant implications for understanding direct exchange between the ocean and the overlying ice. Similarly, the detection of deep subsurface interfaces in these surveys and the presence or absence of shallower interfaces above them could validate hypotheses regarding the convective upwelling of deep ductile ice into the cold brittle shell implying indirect exchange with any ocean. Additional orbital profiling of the subsurface of Europa to depths of 30 km with a vertical resolution of about 100 m would establish the geometry of any deeper geophysical interfaces such as an ice-ocean interface. Although warm ice is very attenuating [*Chyba et al. 1998*], thick ice in a regime of steady-state thermal conduction could be sounded on Europa to depths of 25 to 40 km if it is essentially free of impurities [*Moore 2000*]. Although impurities are almost certainly present, the non-steady-state convective thermal regime could generate "windows" of very cold downwelling material within the ice shell, allowing local penetration to great depth [*McKinnon 2005*]. Moreover, while the presence of meter-scale voids within the ice shell would confound sounding measurements at higher frequencies (> 15 MHz) [*Eluszkiewicz 2004*], the presence of such large voids is probably unrealistic [*Lee et al. 2005*].

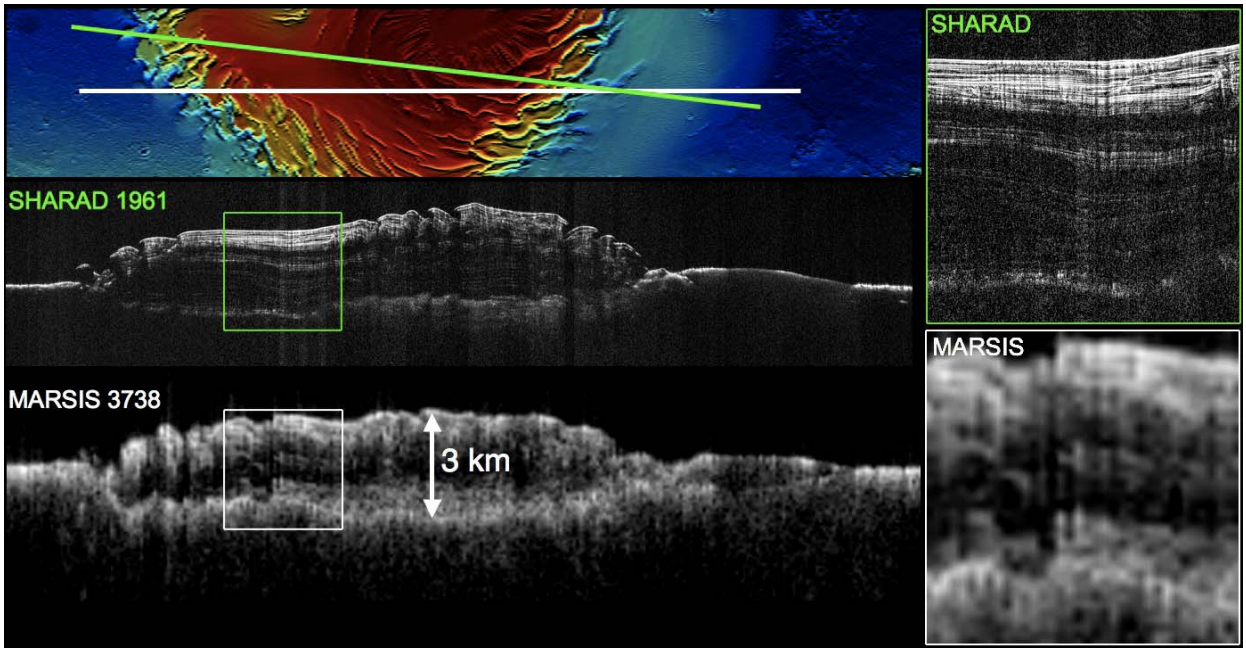

Figure 4-24. Orbital Subsurface Profiling of Mars North Polar Cap. These nearly co-linear profiles across the Mars North Polar Cap (MOLA data at top left) demonstrate the value of the complementary perspectives provided by the high-center frequency and high bandwidth profiling of the SHARAD instrument (20 MHz and 10 MHz, respectively), and the low-center frequency and low bandwidth profiling of MARSIS (5 MHz and 1 MHz, respectively). In particular, note the clarity of shallow horizons revealed by SHARAD (detail at top right) and the prominence of deep interfaces revealed in the MARSIS results (detail at bottom right). The value of a multi-frequency approach to subsurface profiling on Europa would be significantly enhanced in the presence of strong volume scattering. (MARSIS data courtesy of Picardi, Plaut and the MARSIS Team; SHARAD data courtesy of Seu, Phillips, and the SHARAD Team.)

Table 4-3. Hypothesis Tests to Address Selected Key Questions Regarding Europa's Ice Shell

Example Hypothesis Questions		Example Hypothesis Tests
EB.1	Is Europa's ice shell very thin and conductive or thick and convecting?	Sound Europa's ice shell for a strong water reflector at shallow depth, or to observe a gradual absorption of the signal with depth which may reveal diapiric structures.
EB.2	Is there fluid transport from the ocean to the near-surface or surface, and vice versa?	Sound Europa's ice at shallow and greater depths for liquid water, and correlate to surface morphology, compositional and thermal data.
EB.3	What are the three-dimensional characteristics of Europa's geological structures?	Combine ice-penetrating radar and topographic measurements, with high-resolution imaging to investigate the 3D structure of geological features.
EB.4	Are there regional variations in the thickness of Europa's thermally conductive layer?	Sound Europa's ice shell to map dielectric horizons near-globally.

Deep ocean searches would produce data analogous to those of the Mars Advanced Radar for Subsurface and Ionosphere Sounding (MARSIS) instrument on the Mars Express spacecraft (Figure 4-24). This profiling should establish the geometry of any deeper geophysical interfaces that may correspond to an ice-ocean boundary, to a vertical resolution of about 100 m (requiring a bandwidth of about 1 MHz).

Frequencies significantly less sensitive to any volume scattering that may be present in the shallow subsurface profiling detailed above (i.e., about 5 MHz) should be used on the anti-jovian side of Europa, which is substantially shadowed from Jupiter's radio emissions. This low-frequency low-resolution profiling should be complemented by high-frequency low-resolution profiling over Europa's sub-jovian surface (where Jupiter's radio noise is an issue for low-frequency sounding). Combined, the deep low-resolution profiling should also cover at least 80% of Europa's surface with a minimum profile separation of about 50 km. Profiling should be performed along with co-located stereo imaging and laser altimetry of better than 100 m topographic resolution, permitting surface clutter effects to be removed from the radar data.

Investigation EB3: Correlate surface features and subsurface structure to investigate processes governing material exchange among the surface, ice shell, and ocean.

Targeted radar observations would lead to understanding the processes controlling the distribution of any shallow subsurface water and either the direct or indirect exchange of materials between the ice shell and its underlying ocean. Fractures, topographic and compositional data correlated with subsurface structures could provide information on tidal response and its role in subsurface fluid migration. Similarly, differences in the physical and compositional properties of the near-surface ice may arise due to age differences, tectonic deformation, mass wasting, or impact gardening. Knowledge of surface properties gained from spectroscopy and high resolution topographic data would be essential for integrated interpretation of subsurface structure, as well as understanding liquid water or ductile ice migration within Europa's ice shell.

Because of the complex geometries expected for subsurface structures, subsurface radar images should be obtained along profiles ~30 km long in targeted regions, either to a depth of 3 km for high resolution imaging of shallow targets or to a depth of 30 km for lower resolution imaging of deeper features, in conjunction with co-located topographic data.

These targeted subsurface studies should be considered a necessary prerequisite for any future *in situ* astrobiological exploration.

Investigation EB4: Characterize regional and global heat flow variations.

The thermal structure of the shell (apart from local heat sources) is set by the transport of heat from the interior. Regardless of the properties of the shell or the overall mechanism of heat transport, the uppermost few kilometers at least are thermally conductive, cold, and stiff. The thickness of this conductive "lid" is set by the total amount of heat that must be transported; thus, a measurement of the thickness of the cold and brittle part of the shell would provide a constraint on the heat production in the interior. For a thin ice shell, the ice-ocean interface forms a significant dielectric horizon at the base of the thermally conductive layer. However, when warm pure-ice diapirs from the interior of a thicker convective shell approach the surface, they may be different from the pure-ice melting point and above the eutectic of many substances; this could create regions of melting within the rigid shell above them as the temperature increases above the flattening diapir. Any dielectric horizon associated with these melt regions would also provide a good measurement of the thickness of the conductive layer. Global radar profiles of the subsurface thermal horizons to depths of 30 km at a vertical resolution of 100 m combined with global maps of thermal emissions at the surface enable characterization of regional and global heat flow variations in Europa's ice shell.

The key outstanding questions relating to Europa's ice shell (§4.2.1.2) could be related to and addressed by the Objective EB investigations described above, as summarized in Table 4-3.

4.3.1.3 EC. Europa's Composition

Determine global surface composition, distribution and evolution of surface materials, especially as related to habitability.

Composition forms the linkages that enable understanding Europa's potential habitability in the context of geologic processes. Composition is also a probe of the interior and records the evolution of the surface under the influence of internal and external processes. Investigations regarding Europa's chemistry and composition require synergistic, coordinated observations of targeted geological features, along with synoptic near-global remote-sensing data, including multi-spectral imaging, stereo imaging, radar sounding, and thermal mapping.

There are two basic approaches to determining the composition of Europa's surface; materials could be measured on the surface using remote optical (ultraviolet through infrared) spectroscopy, or the surface composition could be inferred by measuring materials sputtered or ejected from the surface into an atmosphere using both direct sampling and remote observations. Optical measurements of the surface could determine the composition and distribution of materials at geologically relevant scales (10 s to 100 s of meters). However, the spectroscopy of solids is complicated by the physical properties of the material (i.e., grain size, temperature, etc.) and by material mixing, and high-quality spectra of specific surface units are required to identify minor components. Materials with strong, narrow, isolated absorption features could be accurately identified with detection limits of ~1%, and much greater sensitivity (~0.1%) could be achieved for strongly absorbing components intimately mixed with a less-absorbing component such as water ice. Materials with broad, shallow features may have detection limits of ≥10%, and their identification may be limited to the mineral or

functional group of material present (e.g., phyllosilicates). Some materials (e.g., NaCl) are optically inactive through much of the visible and infrared and are difficult to detect remotely. Detection and identification of atmospheric components could be very precise using mass spectroscopy or UV through millimeter wavelength spectroscopy, with detection limits that could be several orders of magnitude more sensitive than surface spectroscopy. However, materials in an atmosphere would be derived from an area approximately equal to the height at which the measurement is made [*e.g., Hartle and Killen 2006*], so only regional surface compositions could be inferred. In addition, the surface composition must be inferred from measurements of daughter products that have been derived from the surface by sputtering and radiation-induced chemistry.

Various measurement techniques are appropriate for the investigation of Europa's composition and were considered by the JJSDT during its deliberations, including UV, visible, infrared, microwave, and mass spectroscopy. Examples of the capabilities of these techniques are summarized in Table 4-4.

Table 4-4. Composition Measurements and Candidate Instruments

	VIS/NIR Imaging Spectrometer	UV Spectrometer	INMS	IR or Millimeter Spectrometer
Europa science measurements (From Traceability Matrix, Foldout 1)	Composition of organic and inorganic materials (EC.1a) Relationship of surface materials to geologic processes (EB.3d; EC.2a, EC.5c, ED.4c) Effects of radiation environment (EC.3a) Nature of exogenic materials (EC.4c) Exposure age (ED.1f) Recent activity (ED.2e, ED.2h, ED.3c)	Plume composition and regional mapping to surface vents (EC.1c) Current activity through spatial and temporal variability of venting (ED.2f) Effects of radiation, sputtering (EC.3b, EC.3f) Relationship of surface materials to geologic processes (Imager; EB.3e, EC.2b, EC.5d, ED.3d) Exposure age (Imager; ED.1g) Nature of exogenic materials (Imager; EC.4d)	Composition of organic and inorganic surface materials (EC.1b, EC.5a) Effects of radiation, sputtering (EC.3e) Nature of exogenic materials (EC.4b) Relationship of surface materials to geologic processes (EC.2g, ED.2g)	Composition of organic and inorganic surface materials (EC.1b) Effects of radiation, sputtering (EC.3e) Nature of exogenic materials (EC.4b) Recent activity (ED.2g)
Species of interest				
Identified	H_2O; CO_2, SO_2, H_2O_2, sulfate hydrates, CH compounds, CN compounds, O_2	H, O (gas emission) H_2O_2, SO_2 (solids)	O_2 (~10^6 cm^{-3}); H_2; Na (~300 cm^{-3}); K; Cl+ (Atmosphere) SO_2 (~1600 cm^{-3}); CO_2 (~700 cm^{-3}); H_2O (~10^5 cm^{-3}) (Surface)	H_2O

	VIS/NIR Imaging Spectrometer	UV Spectrometer	INMS	IR or Millimeter Spectrometer
Expected	HC, SH, SO, Fe^{2+}, S_8, HCHO, H_2S, $MgSO_4$, H_2SO_4, H_3O^+, $NaSO_4$, Na_2MgSO_4, CH_3OH, CH_3COOH	OH, C, CO (gas emission) H_2O (gas absorption)		OH, C, CO (atmosphere) H_2O (atmosphere)
Possible	NaHCO, $NaCO_3$, H_2CO_3, $MgCO_3$, $MgCl_2$, NaCl, OCS, HCN, OCN-, KOH, K_2O, SO_3, CH_2CO	S, Cl, N (gas emission) CO_2, SO_2, SO, O_3, hydrocarbons (gas absorption) Water ice, salts, sulfates, acids, Tholins (solids)	H_2O_2 (~200 cm^{-3}); sulfur, sulfate, carbon, carbonate, CN, organics, minerals	CO_2, SO_2, SO, O_3, hydrocarbons salts, sulfates, acids, tholins Sputtered species: e.g., Mg-sulfate ⇒ $MgSO_3$, MgO_2, MgS, MgO, Mg
Detection Limits	Surface: 0.1 to 10% abundance, varying with species and environmental conditions	Atmosphere: $1x10^{15}$ cm^{-2} H_2O column	~ 200 cm^{-3}	Atmosphere: Column abundance 10^{-3} to 30% relative to H_2O vapor for many possible species
Measurement requirements				
Spectral/mass range	0.4 - >5 μm (desired) ~1.2 - 4.8 μm (minimum)	EUV (60-110 nm); FUV (110-200 nm); NUV (200-350 nm) (desired); FUV (110-200) (minimum)	1 to ≥300 amu	IR: 5-50 μm mm: 110 ±20 GHz; 560 ±30 GHz,
Spectral/mass resolution	(Grating) 0.4-2.5 μm: 5 nm; 2.5-≥5 μm: 10 nm (desired) 1.2-4.8 μm: 10 nm (minimum)	0.5 nm EUV, FUV; 3 nm NUV	Mass resolution: Dm/m ≥500 Pressure range: 10^{-6}-10^{-17} mbar Sensitivity: 10^{-5} A/mbar	IR: 1-5 cm^{-1} mm: 100-250 kHz
Spatial resolution	25 m/pixel from 100 km (0.25 mrad) (desired) 100 m/pixel (1 mrad) (minimum)	1 mrad/pixel (imager)	100-200 km (comparable to orbital altitude)	100-500 m
SNR	≥128 (0.4-2.6 microns), ≥32 (2.6-5 microns)	≥5	N/A	>50
Coverage	Global	Occultation profiles at ≤25 km spacing over >80% of surface	Regional	Regional
Heritage	(Grating) NIMS, VIMS, Hyperion, CRISM, ARTEMIS, M3, Rosetta VIRTIS, Mars Express OMEGA, Dawn VIR	Cassini UVIS; New Horizons Alice	Cassini INMS; Rosetta ROSINA	CloudSat, EOS-MLS, MIRO, and Herschel-HIFI

Ultraviolet through infrared imaging spectroscopy could detect a broad suite of surface ices, hydrates, organics, and mineral compounds and map these globally at a spatial scale of tens of meters. UV through microwave spectroscopy would investigate the composition and temporal and spatial variability of atmospheric components such as oxygen, hydrogen, organics and sulfur-bearing compounds. An ion and neutral mass spectrometer (INMS) could detect ions and neutrals that are sputtered, outgassed, and sublimated from the surface, with a significant fraction of these molecules reaching 100 km altitude [*Johnson et al. 1998, Paranicas et al. 2007*]. Both remote UV and long-wavelength observations and *in situ* INMS sampling could provide sensitive detection of gaseous plumes, if present, as demonstrated by the Cassini UVIS and INMS instruments at Enceladus [*Hansen et al. 2006, Waite et al. 2006*].

Surface spectroscopy. The best means to map the surface composition at the spatial scales relevant to geologic processes is through near-UV to infrared imaging spectroscopy. Data obtained by the Galileo NIMS of Europa and observations by the Cassini VIMS of the Saturnian system demonstrate the existence of a wealth of spectral features throughout this spectral range [*e.g., McCord et al. 1998, Carlson et al. 1999a,b, Clark et al. 2005, Cruikshank et al. 2007*]. Of the materials studied thus far in the laboratory, the hydrated sulfates appear to most closely reproduce the asymmetric and distorted H_2O spectral features observed at Europa. In these compounds, hydration shells around anions and/or cations contain water molecules in various configurations, held in place by hydrogen bonds. Each configuration corresponds to a particular vibrational state, resulting in complex spectral behavior that is diagnostic of composition. These bands become particularly pronounced at temperatures below 150 K as the reduced intermolecular coupling causes the individual absorptions that make up these spectral features to become more discrete [*Crowley 1991, Dalton and Clark 1998, Carlson et al. 1999b, 2005, McCord et al. 2001a, 2002, Orlando et al. 2005, Dalton et al. 2003, 2005, Dalton 2000, 2007*]. As a result, the spectra of low-temperature materials provide highly diagnostic, narrow features ranging from 10 to 50 nm wide (Figure 4-25).

Cryogenic spectra for all of the hydrated sulfates and brines in Figure 4-26 display the diagnostic absorption features near 1.0, 1.25, 1.5, and 2.0 µm that are endemic to water-bearing compounds. These features generally align with those in water ice and with the features observed in the Europa spectrum. Other spectral features arising from the presence of water occur in many of the spectra, including features of moderate

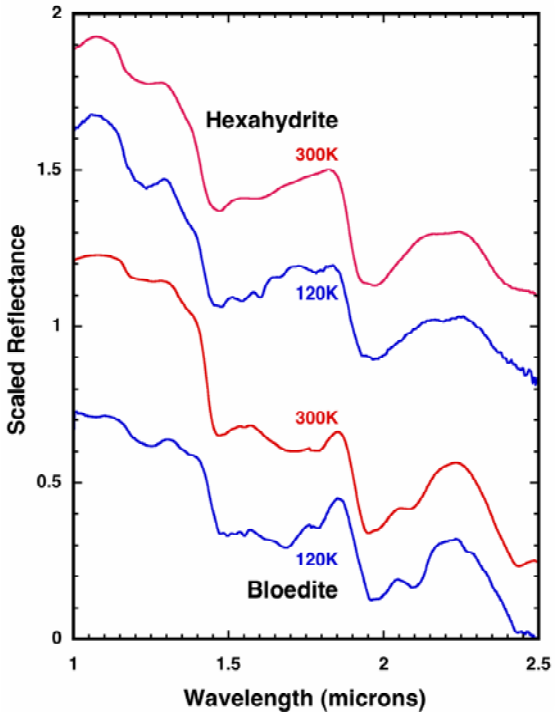

Figure 4-25. Reflectance spectra of two hydrated salts at room temperature and at 120 K, as expected at the surface of Europa. The fine spectral structure apparent at high (~5 nm) spectral resolution could be exploited to discriminate between hydrates. From *Dalton et al.* [*2003*].

strength near 1.65, 1.8, and 2.2 µm (Figure 4-27). An additional absorption common to the hydrates at 1.35 µm arises from the combination of low frequency lattice modes with the asymmetric O-H stretching mode [*Hunt et al. 1971a,b, Crowley 1991, Dalton and Clark 1999*]. Although weak, this feature is usually present in hydrates and has been used to place upper limits on abundances of hydrates in prior studies [*Dalton and Clark 1999, Dalton 2000, et al. 2003*].

Cassini Visual and Infrared Mapping Spectrometer (VIMS) observations of Phoebe provide additional examples of the wealth of

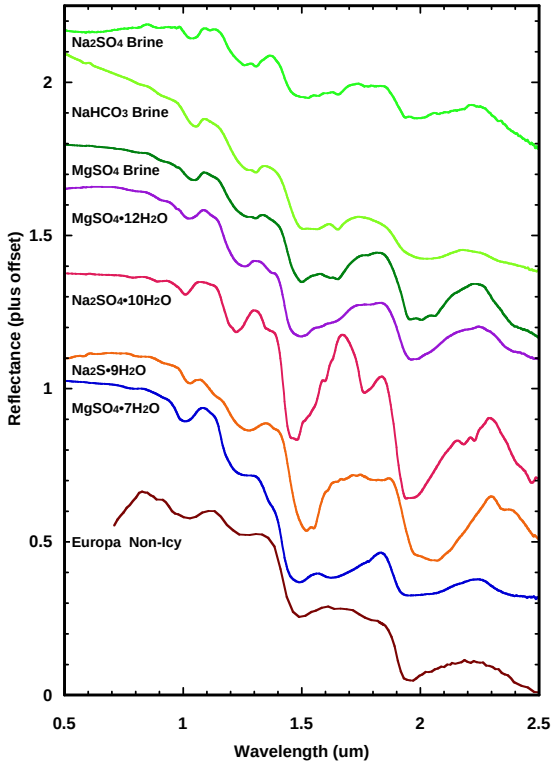

Figure 4-26. Cryogenic reflectance spectra of hydrated sulfates and brines, compared to Europa. Spectra of epsomite ($MgSO_4$•$7H_2O$), hexahydrite ($MgSO_4$•$6H_2O$) and bloedite ($Na_2Mg(SO_4)_2$•$4H_2O$ were measured at 100, 120, and 120 K, respectively [Dalton 2000, 2003]. Spectra of sodium sulfide nonahydrate (Na_2S•$9H_2O$), mirabilite (Na_2SO_4•$10H_2O$) magnesium sulfate dodecahydrate ($MgSO_4$•$12H_2O$) and $MgSO_4$, $NaHCO_3$, and Na_2SO_4 brines were measured at 100 K [*Dalton et al. 2005*].

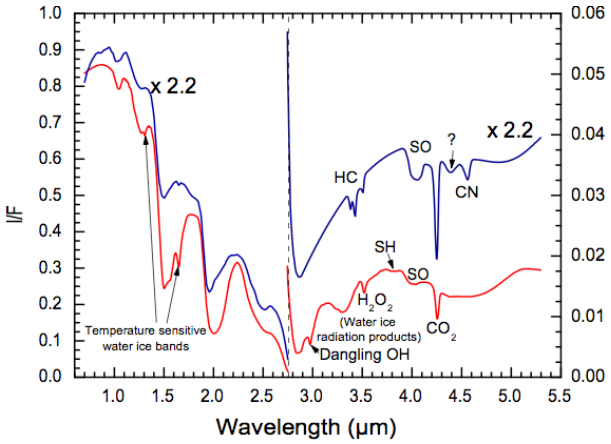

Figure 4-27. Notional reflectance spectra for icy (lower) and non-ice (upper) regions on Europa (based on observations of compounds observed on other Jovian and Saturnian satellites) at 6 nm spectral resolution in the 1–5 µm spectral range. A variety of materials and molecules have been identified or inferred from the Galileo results. The spectra shown here are composites to illustrate the types and variety of features found or expected. The detailed spectral structure observed in hydrates at high spectral resolution (e.g., Figure 4-25 Figure 4-27) is not fully represented here. The non-ice spectrum is scaled by 2.2 from the ice spectrum, and the 2.8–5 µm range spectra are scaled by 10 over the shorter wavelength range. Figure courtesy Tom McCord.

information available in infrared spectra. *Clark et al.* [*2005*] reported 27 individual spectral features (Table 4-5) indicating a complex surface containing a rich array of ices including H_2O and CO_2, and organic species including CN-bearing ices. The 3–5 µm portion of the Phoebe spectrum include absorptions tentatively interpreted as nitrile and hydrocarbon compounds. This spectral range is useful for detecting numerous organic and inorganic species anticipated at Europa.

Unexpectedly, the diagnostic spectral features of hydrated minerals are not seen in high spectral resolution 1.45–1.75 µm Keck telescopic spectra collected from regions of dark terrain that are several 100 km in extent, suggesting that hydrated materials may be non-crystalline (glassy) because of radiation damage or flash freezing [*Spencer et al. 2006*]. Although these regions are dominated by dark materials, ice-rich materials probably occur

within the observed area, and significant spatial mixing and dilution of the spectra of the optically active species may occur. It is also possible that the various hydrated species are mixed in such proportions that their diagnostic features overlap. It is expected that there would be smaller regions (perhaps the youngest ones) on Europa in which diagnostic spectral features could be found if observed at high spatial resolution. An excellent example of the importance of spatial resolution is observed for Martian dark region spectra, in which telescopic spectra in both the thermal and short-wave infrared [*e.g., Bell 1992, Moersch et al. 1997*] did not reveal the mineralogic components that have been detected once high spatial resolution spectra were acquired from orbit [*e.g., Christensen et al. 2001*, *Bibring et al. 2005, Ehlmann et al. 2008, Mustard et al. 2008*].

Laboratory studies have shown that at Europa's surface temperature, anticipated materials, in particular hydrates, exhibit fine structure, with the full width at half maximum (FWHM) of spectral features ranging from 7–50 μm [*Carlson et al. 1999b, 2005, Dalton 2000, Dalton et al. 2003, Orlando et al. 2005*]. Analysis shows that to detect materials in relatively low abundance, or in mixtures with dark materials, signal-to-noise ratio (S/N) > 128 is desirable in the wavelength range 0.4–2.6 μm, and S/N > 32 is desirable in the wavelength range 2.6–5.0 μm (Figure 4-28). An ideal spectral resolution of 2 nm per channel would be sufficient to identify all of the features observed in the laboratory hydrates thus far [*Dalton et al. 2003, Dalton et al. 2005*]. This would ensure multiple channels across each known feature of interest. However, at Jupiter's distance from the Sun, the reflected near-infrared radiance limits the achievable spectral resolution for high spatial resolution mapping. The signal-to-noise performance is further complicated by the severe radiation noise effects at Europa's orbit.

Table 4-5. Carbon and Nitrogen Compound Absorption Bands Observed at Saturn's Moon Phoebe by Cassini VIMS [*Clark at al. 2005*]

Feature	Wavelength (μm)	Width (μm)	Origin
f1	1.0	1.1	Probable Fe^{2+}
f2	1.04	~0.05	H_2O ice overtone
f3	1.2	~0.02	OH stretch, CH combination, or artifact
f4	1.3	~0.02	OH stretch, CH combination, or artifact
f5	1.4	~0.02	OH stretch, CH combination, or artifact
f6	1.5	~0.2	H_2O ice overtone
f7	1.7	Variable	CH stretch overtone
f8	1.95	~0.1	Bound H_2O
f9	2.02	~0.2	H_2O ice combination
f10	2.16	~0.03	Probable metal-OH combination
f11	2.42	~0.07	Probable CN combination
f12	2.95	~0.7	H_2O ice and/or bound H_2O
f13	3.1	~0.05	H_2O ice Fresnel peak
f14	3.2–3.3	Variable	CH stretch fundamentals
f15	3.55	~0.06	Probable CH
f16	3.9	~0.2	Perhaps CH, CN or H_2O
f17	4.26	~0.03	Trapped CO_2 (gaseous / fluid inclusion)
f18	4.50	~0.03	CN in a nitrile
f19	4.8–5.0	~0.05	Probable CN fundamental
f20	5.1	??	not determined
f21	4.3	0.7	H_2O ice and/or bound water
f22	2.05	0.17	H_2O ice
f23	2.3	~0.08	Probable metal-OH combination
f24	2.72	~0.05	OH stretch fundamental
f25	1.25	~0.1	H_2O ice
f26	3.62	~0.07	Probable CH or CN
f27	2.54	~0.016	Probable CH

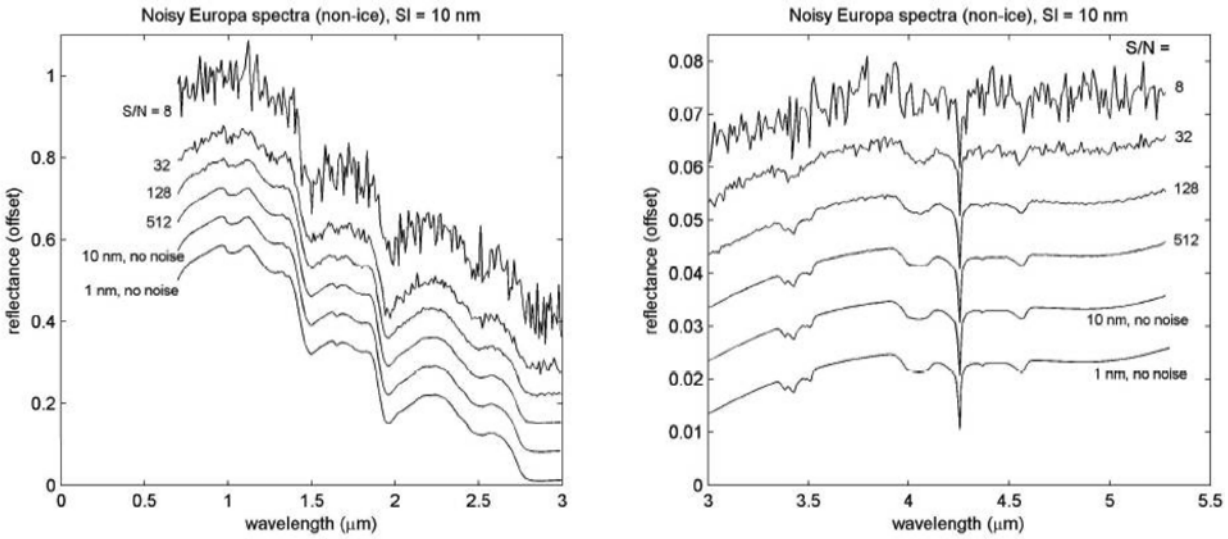

Figure 4-28. Infrared reflectance spectra for a range of signal-to-noise ratios (S/N) show that to detect absorption bands of materials in relatively low abundance, or in mixtures with dark materials, S/N > 128 is desirable in the shorter wavelength range 0.4-2.6 μm, and S/N > 32 is desirable in the longer wavelength range 2.6-5.0 μm [*Tom McCord, personal communication*].

Obtaining infrared spectra at wavelengths beyond 5 μm might enhance the capability to map and characterize organic chemistry and potential biosignatures. In particular, carbon and nitrogen compounds, which are essential to the chemistry of known life, have numerous absorption bands associated with C-O, C-C and C-N bonds in the 5–7 μm region. The strong carbonyl and amide bands at ~5.9 μm might be detected at concentrations of tens of ppm using sufficiently long integration times and large spatial averages. However, Figure 4-29 shows that the flux of reflected sunlight decreases markedly as wavelength increases through this spectral region, while thermal emission simultaneously increases. Therefore, the interpretation of spectra in this region is hindered by both low SNR resulting from the low fluxes, and by the complex and variable intermingling of reflected and thermal emission. Nevertheless, it is plausible that the blackbody thermal radiation of Europa in warmer regions at ~130 K might be detected using a combination of spectral integration made possible by being in orbit around Europa, spectroscopic techniques such as Fourier transform spectroscopy that significantly enhance signal throughput, and reduced spatial resolution "point spectroscopy" approaches.

In summary, the multiple spectral features and fine (10–50 nm) structure of materials of interest in the 1 to ≥5 μm range in low temperature spectra are sufficiently unique to

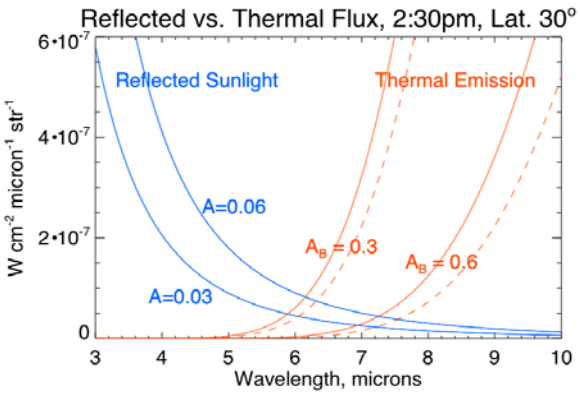

Figure 4-29. Expected reflected and thermal flux from Europa for an example mid-afternoon, mid-latitude location. The relative proportions of reflected and thermal emission in the 5–7 μm region depend very strongly on both the surface albedo at the wavelength of interest, A, and the surface temperature, which is controlled by the bolometric albedo A_B and the thermal inertia. Solid and dashed thermal emission curves are for plausible thermal inertias of 40 and 80 W m^{-2} s$^{-1/2}$ K^{-1} respectively.

allow these materials to be identified even in mixtures of only 5–10 weight percent [*Dalton 2007, Hand 2007*]. The ability to fully resolve these features through high-spectral, high-spatial resolution observations would permit determination of the relative abundances of the astrobiologically relevant molecules at the surface of Europa (Figure 4-27).

Atmospheric spectroscopy. Remote UV through millimeter spectroscopy of the atmosphere would enhance the study of surface composition and the search for current activity at Europa, with ties to the subsurface ocean and habitability.

Venting or transient gaseous activity on Europa could arise from present-day activity. UV measurements would provide high sensitivity to very low column gas abundances using stellar occultations, as demonstrated in the detection of the Enceladus gas plume [*Spencer et al. 2006, Hansen et al. 2006*]. UV imaging of Europa could measure atmospheric density, distribution, and temporal and spatial variations of the atmosphere that could be related to surface composition on regional scales. A stellar occultation instrument operating in the FUV could provide information on the derived atmospheric constituents.

Long wavelength (IR through millimeter) observations could detect, definitively identify, and determine the abundance of atmospheric species. The rotational-vibrational absorption lines of gases are extremely diagnostic of specific composition, and could provide total column abundances at ppm levels [*Fink and Sill, 1982*]. These observations would provide sensitive detection of plumes at low opacities. They would also have the capability to determine the isotopic composition and abundance of the major components (e.g., C, O, and N). Millimeter /sub-millimeter observations have been modeled to have detection sensitivities of 2%, 3%, 12%, and 36% for NaCl, MgS, NaO, and CH_3CN relative to water vapor for an assumed water column abundance of 5×10^{13} molecules/cm^3 in nadir observations [*Herzberg 1991*]. Improvements by factors of several hundred are possible for limb emission and solar occultation observations respectively. Long wavelength observations could provide insight into the physical processes that have led to the creation of the atmospheres of Europa and the other icy satellites and the processes that underlie the formation of any plumes. These observations could also provide measurements of the temperature of the solid surfaces of the moons. As with the UV measurements, an IR or millimeter instrument operating remotely would be less sensitive to distance from target, and would be effective at making composition measurements for all targets within the Jovian system.

Europa's tenuous atmosphere, first postulated to exist in the 1970s, has four observed components: O [*Hall et al. 1995, 1998*] near the surface, Na and K in the region from ~3.5 to 50 R_E [*Brown and Hill 1996, Brown 2001, Leblanc et al. 2002, Leblanc et al. 2005*] and H_2 in Europa's co-orbiting gas torus [*Smyth and Marconi 2006*]. The robust plasma bombardment of Europa's surface is expected to produce many other components [*e.g., Johnson et al. 1998*]. To date there have been so few measurements of the Europan atmosphere that models must be relied upon to draw inferences about the its vertical structure, and especially the abundances of species other than those already detected (O, Na, and K). Figure 4-30 shows one such model [*Smyth and Marconi 2006*] of Europa's atmosphere.

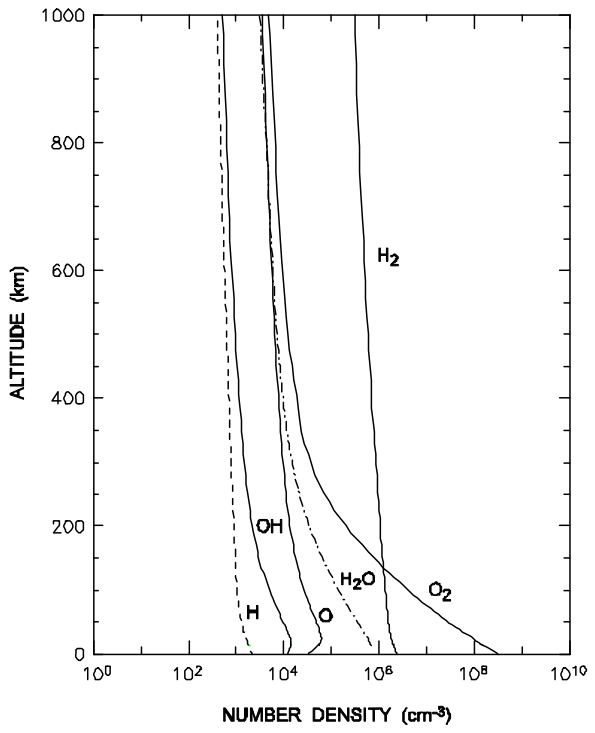

Figure 4-30. Vertical distribution of the modeled abundance, globally averaged density of potential atmospheric components. The O_2 rate was set to reproduce the 135.6 nm O brightness of 37 ± 15 Rayleigh observation of *Hall et al.* [*1995*]. Sublimation was taken into account but is unimportant except in the sub-solar region. In both simulations, the ejecta energy distributions discussed in the text were used for H_2O and O_2 and thermalization of returning H_2 and O_2 in the regolith is assumed. From *Smyth and Marconi* [*2006*].

An INMS would provide a highly-sensitive means to measure ions and neutrals present in Europa's atmosphere that are derived from the surface by sputtering, outgassing, and sublimation. Most of the postulated atmospheric constituents could be detected by an orbiting instrument at 100 km based on the proposed detection limit of 200 cm^{-3} from the ROSINA reflectron type time-of-flight (RTOF) mass spectrometer, which is flying on the Rosetta mission.

An important contribution from an INMS would be the capability of measuring isotopic ratios. As a key example, the stable isotopes of oxygen in water could be determined, as shown in Table 4-6. The variations in the $^{17}O/^{16}O$ and $^{18}O/^{16}O$ ratios in water vapor are the most useful system for distinguishing different planetary materials. For example, it has been argued that two gaseous reservoirs, one terrestrial and one ^{16}O rich, are required to explain O-isotopic variations in meteorites. The terrestrial fractionation line is due to mass fractionation of the O isotopes in terrestrial materials and the carbonaceous chondrite fractionation line represents mixing between different components. Obtaining similar isotope information for Europa would provide important constraints on the origin of water ice in the Galilean satellites.

The sensitivity for ions is much higher than for neutrals, and based on experience at Enceladus and Titan [*Waite et al. 2006*], ionization would occur by electron impact, photo-ionization, charge exchange, and electron attachment. Predicted ionization rates for several of these molecules are: O_2: 2×10^{-6}/s; H_2O: 3×10^{-6}/s; O: 2×10^{-7}/s; Na: 5×10^{-6}/s; CO_2: 5×10^{-6}/s; and SO_2: 10^{-5}/s.

The trace materials detected from surface spectroscopy (SO_2, CO_2) should be readily detected using INMS [*Johnson et al. 2004*]. Further characterization of the hydrate and associated dark materials could also be accomplished. For example Mg should be

Table 4-6. Water Vapor Components, Including Isotopes, in Europa's Atmosphere Expected To Be Measurable by an INMS

Species	Mass	Expected partial pressure (mbar) at 200 km
H_2	2.01	$>10^{-10}$
O_2	31.99	10^{-10}
O	15.9	10^{-12}
H_2O	18.0	5×10^{-13}
$^{18}O^{16}O$	33.9	2×10^{-13}
$^{17}O^{16}O$	32.9	7×10^{-14}
HD	3.02	$>10^{-14}$?
HDO	19.0	2×10^{-16}

present in the atmosphere if $MgSO_4$ is present at the surface. Atmospheric emission measurements have confirmed a surface source for Na and K [*Johnson et al. 2002, LeBlanc et al. 2002*], with some evidence that the Na and K originate in dark regions [*LeBlanc et al. 2005, Potter et al. 2005, Cassidy et al. 2008*]. However, these have not yet been detected in surface spectral measurements. Vented material or materials from flows that are emplaced on the surface are rapidly degraded by the incident radiation. However, this degradation process also produces sputtered products that could be detected and interpreted. Trace organics would also be sputtered with the ice from the surface. Some calculated densities for these various classes of compounds at an orbital altitude of 100 km are shown in Table 4-7. The range of values indicates various assumptions about the interaction with the regolith.

Using a modeled atmosphere and some assumptions about trace surface salts and organics and the Monte Carlo sputtering model of *Cassidy et al.* [*2008*] predicted atmospheric composition models at 100 km could be generated. These models could be used to generate simulated mass spectra, shown in Figure 4-31. Predicited isotopic abundances are shown in the blow-out figure. Ratios of $^{13}C/^{12}C$ could be inferred over the course of the mission given sufficiently long integration times.

Table 4-7. Calculated Densities of Sputtered Europa Surface Materials at 100 km

Species	Predicted Densities @ 100 km
Na	60–1600 cm^{-3}
CO_2	170–580 cm^{-3}
SO_2	290–1800 cm^{-3}
H_2O_2	150–3000 cm^{-3}
L-Leucine (Mass 131)	3×10^6F cm^{-3} where F is number fraction at surface

Ionospheric model results are shown in Figure 4-32 and are expected to be within INMS detection limits. From this analysis it is apparent that an INMS could detect vapor from an active vent, sublimation from a warm region, the sputter products during the degradation process, and ions that are in all of these processes.

Investigation EC1: Characterize surface organic and inorganic chemistry, including abundances and distributions of materials, with emphasis on indicators of habitability and potential biosignatures.

The first priority investigation for Europa's surface composition and chemistry is to identify the surface organic and inorganic constituents, with emphasis on materials relevant to Europa's habitability, and to map their distribution and association with geologic features. The search for organic materials, including compounds with CH, CO, CC, and CN, is especially relevant to understanding Europa's potential habitability.

Moreover, identifying specific salts and/or acids may constrain the composition, physical environment, and origin of Europa's ocean [*Kargel et al. 2000, McKinnon and Zolensky 2003, Zolotov and Kargel 2009*]. Additional compounds of interest include species that could be detected at UV wavelengths, such as water ice (crystalline and amorphous phases), products of irradiation (e.g., H_2O_2), compounds formed by implantation of sulfur and other ions, and other as yet unknown materials.

A spectral sampling of ~5 nm through the visible and near-IR wavelengths of 0.4 to ~2.5 μm, and ~10 nm from ~2.5 to ≥5 μm would provide the required SNR while maximizing spectral separability (Figures 4-25, 4-26, and 4-27) [*Dalton et al. 2003, 2007*].

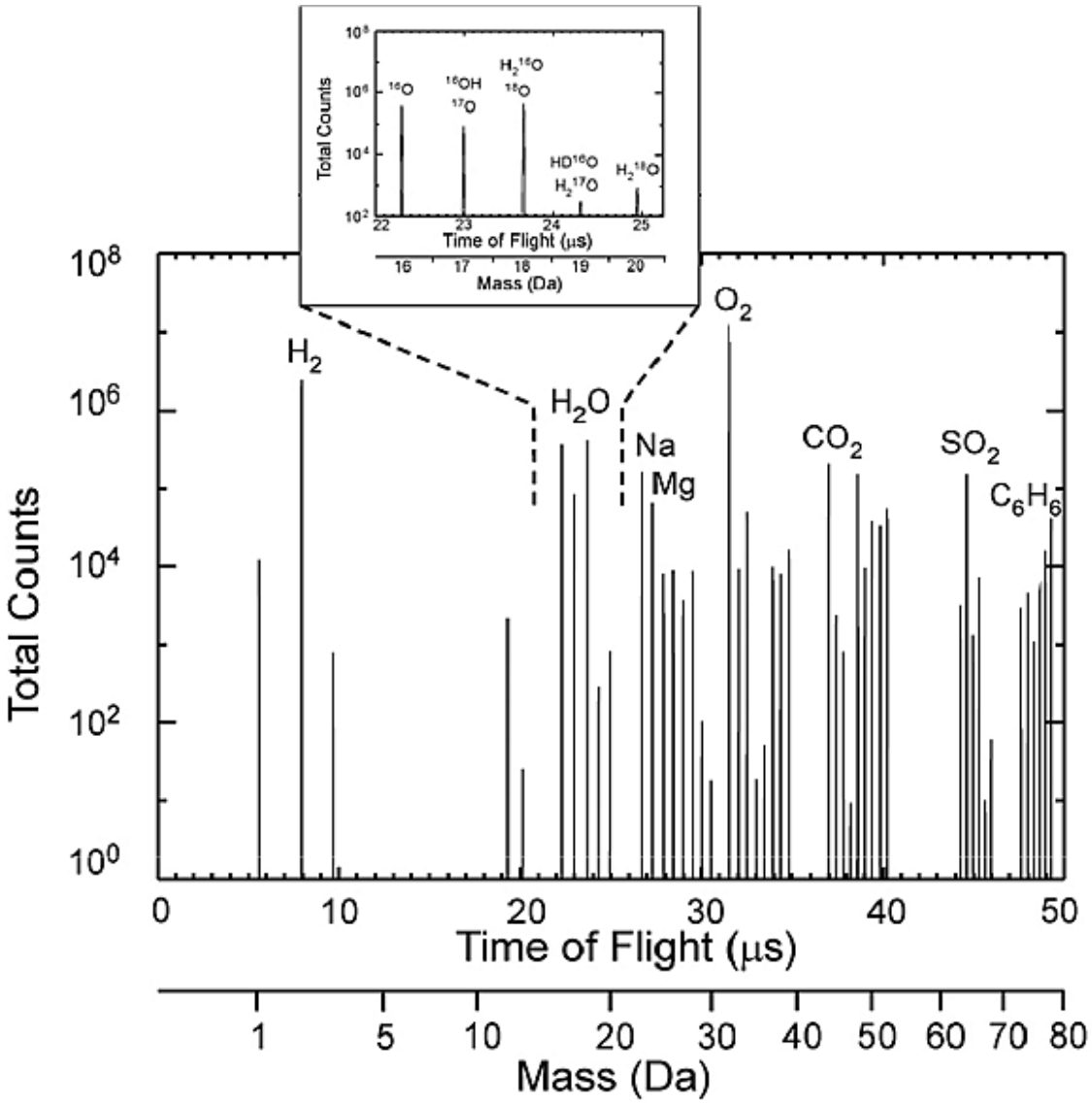

Figure 4-31. Simulated mass spectrum of the anticipated Europa Ion Neutral Mass Spectrometer (INMS) results for neutral species at an orbit altitude of 100 km. The simulation is based on a surface composition given by 60% sulfuric acid hydrate: $H_2SO_4 \cdot 8H_2O$, 20% mirabilite: $Na_2SO_4 \cdot 10H_2O$, 10% hexahydrite: $MgSO_4 \cdot 6H_2O$, 5% epsomite: $MgSO_4 \cdot 7H_2O$, and 4% CO_2 combined with the modeled atmospheric composition and 1% heavy organic represented in this case by benzene (but similar for any heavy organic that may be present). This surface composition has been used as an input into a Monte Carlo ion sputtering/thermal desorbtion model based on the work of *Cassidy et al.* [*2008*] the output of which was then introduced into an instrument model of the ROSINA Reflectron Time-of-Flight (RTOF) mass spectrometer to produce the simulated spectrum. The plot assumes a background noise of 1.

Observations should sample across at least 80% of the globe, with targeted imaging observations having better than 100 m/pixel spatial resolution in order to resolve small geologic features, map compositional variations, and search for locations with distinctive compositions. By comparison, the Galileo NIMS observations of Europa had a spectral sampling of 26 nm, a spatial resolution of 2 to >40 km, and an SNR which varied from 5 to 50 in individual spectra. Linear spectral modeling using Galileo NIMS data with cryogenic measurements of hydrate spectra displayed sensitivities to abundances at the 3-5% level [*Dalton 2007, Shirley et al. 2010*]. High spectral resolution, coupled with high spatial resolution that could permit sampling of distinct compositional units at 25–100 m scales, would allow identification and quantification of the contributions of hydrated salts, sulfuric acid, sulfur polymers, CO_2, organics, and other compounds anticipated at the surface of Europa.

Ultraviolet measurements should be made in the 0.1-0.35 µm range, with at least 3 nm spectral resolution, to measure water ice abundances and radiolytic products such as H_2O_2 and SO_2.

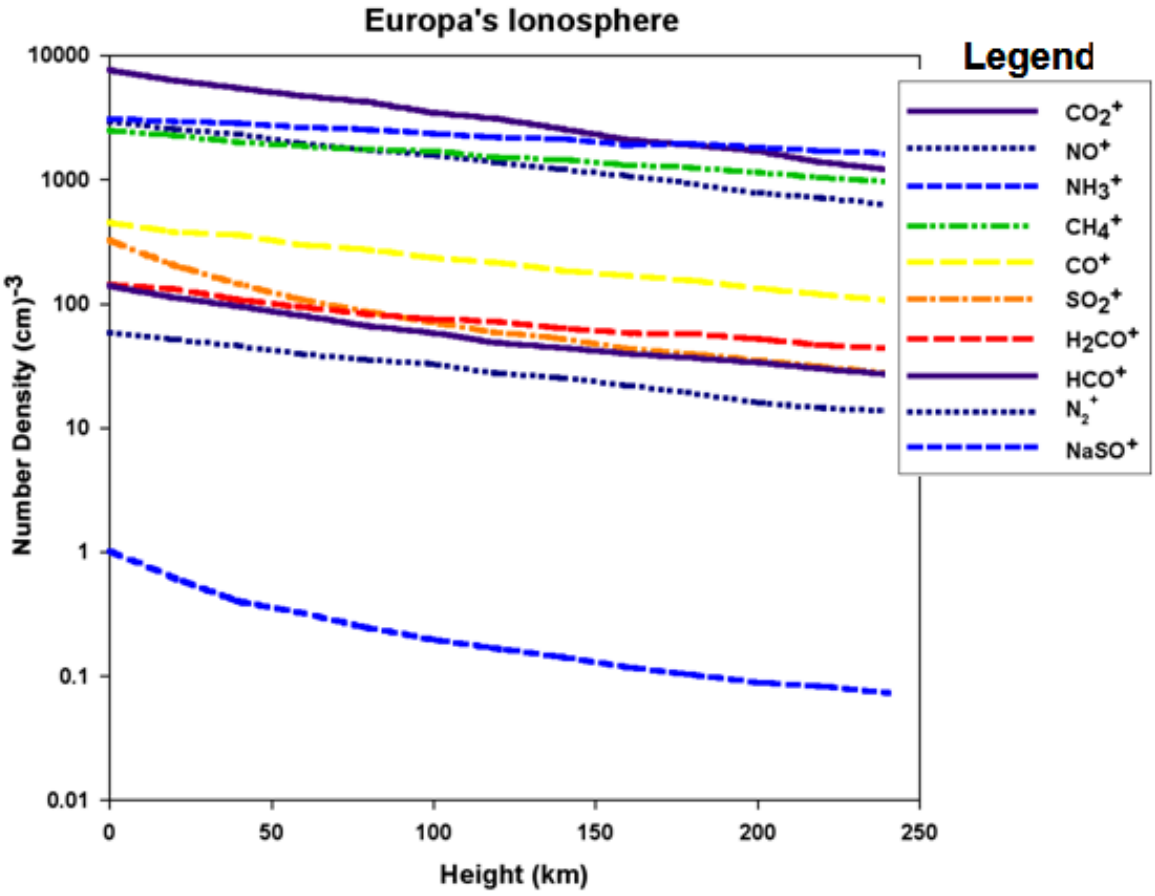

Figure 4-32. Ionosphere densities vs. altitude, determined as discussed in *Johnson et al.* [*1998*] for molecules sputtered from the Europa's surface based on suggested surface materials. All densities exceed the detection limit (10^{-3} cm^{-3}; Y-axis) of a modern time-of-flight mass spectrometer, such as the Cassini INMS instrument.

INMS observations should be performed to determine the composition of sputtered products. Such measurements should be made in the mass range from 1 to > 300 amu, with a mass resolution (m/Δm) of ≥ 500 and pressure range of 10^{-6} to 10^{-17} mbar.

Investigation EC2: Relate material composition and distribution to geological processes, especially material exchange with the interior

The spatial resolution required for compositional mapping is determined by the scale of critical landforms such as bands, lenticulae, chaos, and craters. Europa displays albedo and morphological heterogeneity at scales of 25–100 m, suggesting that compositional variations also exist at this scale. However, the composition of these features remains unknown because Galileo NIMS observations are averages of light reflected from large areas containing both icy and "non-icy" terrain units [*e.g., McCord et al. 1999, Fanale et al. 1999*] (Figure 4-9, Figure 4-33). Spectra of adjacent regions within an instrument field of view combine to produce an average spectrum, with spectral features from all the materials. However, these composite spectra have potential overlap of spectral features and reduced spectral contrast relative to the spectra of the individual surface units. This spectral mixing and reduced contrast results in an attendant decrease in detectability, and eventually a given material could no longer be distinguished from its surroundings. For this reason it is desirable to resolve regions of uniform composition in order to map distinct surface units. While these in turn may be mixtures, spatially resolving dark terrains that have fewer components and are free of the strong and complex absorption features of water ice would greatly facilitate identification of the non-ice materials. For reasonable statistical sampling, it is also desirable to have multiple pixels within a given surface unit. Adjacent measurements could then be compared with each other and averaged together to improve the signal and reduce noise.

An example illustrating the importance of spatial resolution is shown in Figure 4-33. This image has a nominal resolution of 12 m/pixel and shows a variety of small-scale features, including linea with central troughs filled with dark material. The troughs are ~100 m wide and present an opportunity for spectral measurements of contiguous deposits of dark material. Dark material may be linked to interior processes, or may result from radiolytic processing, or a combination of both, while the bright icy material may be water frost. Spectral imaging of these units at a spatial resolution of ≤ 100 m/pixel would allow the composition of the bright and dark materials to be independently determined.

Galileo images of Europa suggest geologically recent formation ages for ridges, chaos, and other features. The images also show abundant evidence for much younger materials exposed by mass wasting of faces and scarps [*Sullivan et al. 1999*]. These post-formational modification processes have likely affected many surfaces, potentially exposing fresh materials that are less altered than their surroundings. Spectroscopy at a resolution better than 100 m would isolate these surfaces and provide an opportunity to determine the composition of primary materials. Such spectroscopic measurements should be made in the 0.4–2.5 μm region with a resolution of 5 nm, and in the 2.5–5 μm regions at 10 nm resolution, in addition to the UV range of 0.1–0.35 μm with of spectral resolution better than 3 nm. Color imaging will also aid compositional interpretations.

Additional important compositional information could come from an INMS instrument, which could measure sputtered materials. Integration of results from spectroscopic analysis and *in situ* INMS

measurements would be key to identifying the non-ice materials on Europa's surface.

In order to relate composition to geological processes, especially material exchange with the interior, composition interpretations need to be considered in the context of geophysical and morphological measurements. Specifically, compositional maps should be compared to detections of subsurface dielectric horizons obtained using ice penetrating radar, any detections of endogenic thermal emission derived from a thermal instrument, and to morphology and topography derived from stereo imaging and laser altimetry data.

Investigation EC3: Investigate the effects of radiation on surface composition, including organics, and regional structure.

In order to understand the surface, it is important to determine separately the effects of weathering, as by photons, neutral and charged particles, and micrometeoroids. In particular, radiolytic processes may alter the chemical signature over time, complicating efforts to understand the original composition of the surface. Assessing these relationships requires a detailed sampling of the surface with ultraviolet through infrared spectroscopy, using global and targeted observations. Ultraviolet measurements of the surface should cover the 0.1–0.35 μm spectral range, with spectral resolution of better than 3 nm. Visible-near IR measurements should cover the 0.4–2.5 μm spectral range with better than 5 nm spectral resolution, and the 2.5–5 μm range at better than 10 nm spectral resolution. It is also critical to populate, to the greatest extent possible, a precipitation map of ion and electron flux into the surface as a function of species and energy. Efforts to separate the primary and alteration surface composition would be aided by the acquisition of high spatial resolution spectra on both leading and trailing hemispheres, in which younger, less altered materials may be exposed by magmatic, tectonic, or mass-wasting processes.

Characterization of the sputter-produced atmosphere with UV observations of Europa's atmosphere would allow for the measurement of species, abundances, and ion implantation rates. Atmospheric measurements could be accomplished with far-ultraviolet stellar occultations and ultraviolet imaging of atmospheric emissions. These UV measurements should cover the 0.1–0.2 μm range with a spectral resolution of better than 0.5 nm.

An INMS would provide a highly sensitive means to directly measure species sputtered off the surface, which may include organic fragments. An INMS should operate in the mass range from 1 to > 300 amu, with a mass resolution (m/Δm) of ≥ 500, and pressure

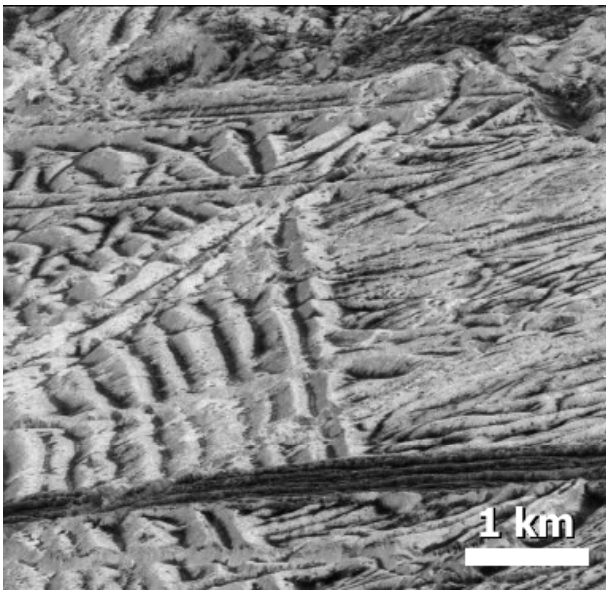

Figure 4-33. Galileo image of ridged plains on Europa at 6 m/pixel horizontal resolution. The lineae in the central portion of the image have central troughs with deposits of dark material ~100 m wide, but with bright, presumably icy ridges and walls close by. Spectral observations with at least 100 m spatial resolution would be needed to independently measure the bright and dark materials. Such measurements would address outstanding questions regarding the composition and origins of the dark material.

range of 10^{-6} to 10^{-17} mbar. To understand sputtering sources, it is important to measure ions from the plasma energies to about 10 MeV, along with simultaneous magnetic field measurements. The number of sputtered molecules is the product of the precipitating ion flux and the neutral yield per ion. For heavy ions, the yield peaks in the few MeV energy range, so it is important to measure ion fluxes into the MeV. Additional collaborative observations would allow determination of how Europa's surface materials evolve in the radiation environment. Specifically, such observations include: color imaging to produce geological maps, high resolution imaging to show possible surface modification effects, and thermal observations to reveal thermal inertia effects.

Investigation EC4: Characterize the nature of exogenic (e.g. Io) materials

The nature of exogenically-implanted materials could be elucidated by measuring ions. Each ion energy and species has a specific penetration depth in ice. If they do have access to the surface, cold plasma ions are deposited in the most processed layer. Energetic charged particles could penetrate more deeply into surfaces and therefore would not be removed as readily by processes such as sublimation. A 1 MeV proton has a range of 24 μm depth and 1 MeV electron has a range of 4.2 mm in water. In addition to sputtering by ions, which adds molecules to the atmosphere of a satellite, electron radiolysis could also create neutral species in the material (e.g., H_2O_2). Such molecules could dissociate in the ice and the lighter byproducts could escape from the surface and enter the atmosphere with a small amount of energy. To constrain the exogenic materials, the flux of the precipitating charged particles over the entire surface should be determined for the energy range between the eV and few MeV, with resolutions $\Delta E/E \sim 0.1$, 15° angular resolution, and basic ion mass discrimination. This is accomplished with a plasma sensor and an energetic charged particle sensor, both with the capacity to measure the upstream flux at the satellite orbits and to view in the precipitating direction at all points in Europa orbit.

These measurements should be synthesized with globally distributed infrared and ultraviolet spectroscopic measurements, as described in other composition investigations above, along with global multi-spectral visible color images. These data would allow materials to be traced from their magnetospheric sources, to the surface, and into the sputter-produced atmosphere. The atmosphere is then measured directly *in situ* (such as with an INMS as described above) and remotely.

The key outstanding questions relating to Europa composition (§4.3.1.3) can be addressed by the Objective C investigations described above, as summarized in Table 4-8.

Investigation EC5: Determine volatile content to constrain satellite origin and evolution

Satellite formation and the subsequent evolution is an important issue, and the composition and abundance of volatiles within a satellite is key to addressing this. Two possibilities must be considered: 1) satellites were made from building blocks formed in and little altered from the solar nebula, or 2) satellites were made from building blocks formed in a circumplanetary nebula, distinct from the solar nebula. The former appears to be more representative of the satellite formation process in the Saturn system [*Mousis et al., 2009, Waite et al. 2009*] (and in comets) and it is uncertain which is more appropriate for the Galilean satellites, considering the lack of measurements of volatiles and their stable isotopes in the Galilean satellites [*Mousis and Alibert 2006*]. Determining which of the two is more likely for a given set of satellites provides insight into the physical processes of satellite

Table 4-8. Hypothesis Tests to Address Selected Key Questions Regarding Europa's Composition

Example Hypothesis Questions		Example Hypothesis Tests
EC.1	Are there endogenic organic materials on Europa's surface?	Examine surface and sputtered materials for absorptions and masses consistent with organic materials, especially in regions most protected from radiation, and correlate distributions to likely endogenic materials.
EC.2	Is chemical material from depth carried to the surface?	Determine whether hydrates and other minerals that may be indicative of a subsurface ocean are concentrated in specific geologic features, and correlate with evidence for subsurface liquid water at these locations.
EC.3	Is irradiation the principal cause of alteration of Europa's surface materials through time?	Determine the suite of compounds observable on Europa's surface, correlating to the local radiation environment and to the relative age of associated surface features.
EC.4	Do materials formed from ion implantation play a major role in Europa's surface chemistry?	Determine the distribution of sulfur-rich and other compounds and correlate to inferred implantation rates and the chemistry of material escaping from Io.

formation through constraints on the temperature and pressure conditions adjacent to the giant planet itself. This information is complementary to what could be gleaned directly from the Galileo probe, which suggested that very cold planetesimals from the outer solar system contributed to the Jovian heavy element abundance. However, this information is incomplete because the molecular state of the material in Jupiter has been completely altered in the deep, hot interior.

Reconstructing the formation conditions of planetesimals and determining the extent of their subsequent evolution requires that we benefit from thermodynamic markers that are sensitive indicators of physical conditions within the regions of satellite formation. The noble gases are key because they serve as traces of the condensation temperatures reached in the region where satellite planetesimals formed, without the chemical complexity associated with nitrogen- and carbon-bearing compounds.

Noble gases could be paired to major carbon- and nitrogen-bearing compounds of similar volatility such that the resulting ratio provides temperature constraints [*cf. Owen and Niemann 2009*]. Important information about the thermodynamic state of the initial condensation process could be determined from "stable isotope thermometers," such as the deuterium-to-hydrogen ratio derived from water ice.

Measurement of the ratios of the noble gases, particularly Ne, Ar, Kr, would allow comparison to demonstrably solar nebula material such as comets, and thereby constrain whether the material from which the icy satellites formed. The deuterium-to-hydrogen ratio in water, compared to that of the well-determined primordial value and that in terrestrial ocean water, gives an indication of the extent to which water in planetesimals experienced elevated temperatures for durations sufficient for re-equilibration with the surrounding hydrogen-rich gas. Measurement of the ratio of Kr to CH_4 and the $^{12}C/^{13}C$ ratio provides constraints on the origin of any methane that might be present either primordial or a product of serpentinization in the ocean of Europa, which was thought to have been in contact with a rocky mantle. The

origin of methane as primordial or a later product of internal processing would shed light on the temperature history of the circumplanetary disk. We expect the disk to have been too warm for methane, but the mass spectrometric results from the Galileo probe forced consideration of the possibility of low temperature planetesimals being important for the assembly of Jupiter and, therefore, its satellites. INMS measurements should be made with a mass resolution better than 500 and sensitivity that allows measurement of partial pressures as low as 10^{-17} mbar, along with characterization of the composition of sputtered desorbed volatiles over a mass range better than 300 Daltons and mass resolution better than 500.

In the UV, stellar occultations can also be used to measure the sputter-produced atmosphere, and atmospheric emissions can be observed in the wavelength range of at least 100- to 200-nm, at better than or equal to 0.5-nm spectral resolution and 100-m/pixel spatial resolution. Supporting measurements to measure volatile content can come from surface spectroscopy at IR and UV wavelengths.

4.3.1.4 ED. Europa's Geology

Understand the formation of surface features, including sites of recent or current activity, and identify and characterize candidate sites for potential future *in situ* exploration.

Europa's landforms are enigmatic and have a wide variety of hypotheses for formation. The search for geologic activity is especially significant for understanding Europa's potential for habitability. Identification and characterization of astrobiologically promising sites would guide future *in situ* exploration.

Investigation ED1: Determine the formation and three-dimensional characteristics of magmatic, tectonic, and impact landforms

Of first order importance is characterization of surface features—their distribution, morphologies, and topography—at regional and local scales, to understand the processes by which they formed. Galileo images demonstrate that regional-scale data (~100 m/pixel especially as aided by 3-color coverage), is excellent for geologic study of Europa, yet less than 10% of the surface was imaged at better than 250 m/pixel (Figure 4-34). Near-global coverage (> 80% of the surface) in at least 3 colors at 100 m/pixel would ensure characterization of landforms across the satellite. Galileo images (e.g., Figure 4-33) also show the great promise of targeted high-resolution (~10 m/pixel) monochromatic imaging for detailed characterization of selected landforms.

Topographic mapping through stereo images at regional scale can permit construction of digital elevation models with vertical resolution of ~20 m and horizontal resolution of ~250 m, which would greatly aid morphologic characterization and geological interpretation. Stereo imaging could be achieved through horizontal overlap of adjacent medium-angle camera image tracks, resulting in approximately 20 m vertical height accuracy with 100 m/pixel wide-angle camera images. Height accuracy further improves by $\approx\sqrt{N}$ by averaging of N overlapping stereo pairs. For example, if each equatorial patch of Europa is imaged about 12 times in 9 months, height accuracy improves by ~3 times.

It is also valuable to determine topographic signatures at higher resolution through stereo imaging and altimetric profiling across targeted representative features, with vertical accuracy of 1 m or better. Subsurface profiling (discussed above) would greatly illuminate subsurface structure and the role of liquid water. Europa's surface is quite heterogeneous

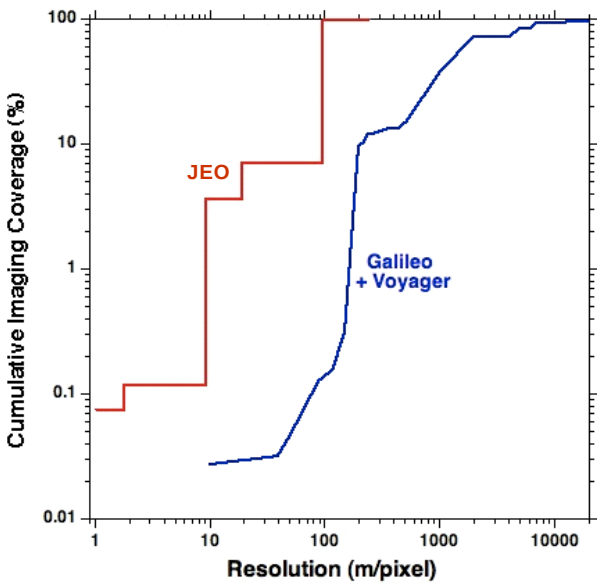

Figure 4-34. Cumulative imaging coverage of Europa's surface as a function of imaging resolution, illustrating the 1–2 orders of magnitude improvement of planned JEO imaging coverage relative to that from Voyager and Galileo combined. Unlike the opportunistic coverage obtained from earlier flybys, JEO's deliberate imaging coverage from orbit would be in discrete resolution steps.

and rough at the decameter scale (Figure 4-33), and the same may be true at smaller scales. Very high-resolution monochromatic imaging (1 m/pixel; <0.1% of the satellite) would reveal the detailed character of landforms, the properties of the regolith, and erosion and deposition processes. Moreover, imaging at this scale would be critical in characterizing potential future landing sites.

It would be important to correlate surface morphology and topography to thermal observations that could potentially reveal endogenic heat sources, and to surface spectroscopic data obtained in the ultraviolet and infrared. Thermal and multispectral signatures can aid interpretation of the formation mechanisms of Europa's endogenic landforms.

Investigation ED2: Determine sites of most recent geological activity, and evaluate future potential landing sites

Geologically active sites are the most promising for astrobiology, and it would be important to identify and characterize them in preparation for future landers. Active processes typically involve elevated heat flow and may involve plumes detectable by imaging, laser altimetry, or ultraviolet occultations. These would also be the most likely locations for near-surface liquid water. Recently or currently active regions also best illustrate the processes involved in the formation of some surface structures, showing pristine morphologies and geologic relationships and perhaps associated thermal and/or plume activity as seen on Enceladus.

Modeling predicts that liquid water brought to the surface of Europa could maintain >5 K nighttime thermal anomalies over hundreds of years, with younger spots being warmer [*van Cleve et al. 1999*, *Abramov and Spencer 2008*]. Regions of anomalously high heat flow should be identified through thermal mapping, with a 2 K measurement temperature accuracy to permit a robust search for elevated temperatures due to thermal anomalies when combined with albedo information. Such measurements require observing the same features during the day and at night, ideally near maximum and minimum temperatures, but with no strict requirement on the relative times between the measurements. A resolution of 250 m/pixel is sufficient to resolve Europa's larger cracks and ridge axial valleys, and observations should be made over at least 80% of the surface.

Searching for regions of outgassing is a powerful method of locating currently active regions, best accomplished by observing stellar occultations in the ultraviolet, since vented water vapor and other gases would absorb starlight. Ultraviolet stellar occultation experiments were fundamental to the

discovery of plumes on Enceladus [*Hansen et al. 2006*] (Figure 4-35). Moreover, observing the surface and the tenuous atmosphere at ultraviolet wavelengths could reveal patchy regions of absorption that might be related to recent venting or other internal activity. An ultraviolet wavelength range of 0.1–0.35 μm and spatial resolution of better than 100 m/pixel are recommended, with capability to observe the sunlit surface, stellar occultations over Europa's limb, and atmospheric emissions.

Discoveries of any active regions would be followed by visible and other remote sensing of the inferred source. It may be possible to observe surface changes within the orbital lifetime of JEO; moreover, the most recently active landforms are expected to show the freshest morphologies and display the least superposed impact craters. Imaging at high resolution (10 m/pixel) in stereo, coupled with very high resolution (~1 m/pixel) images, thermal and compositional measurements, would be used to characterize features that are suspected candidates for recent activity. If age-sensitive chemical or physical indicators could be identified, such as H_2O frost, ice crystallinity, sulfate hydrates, SO_2, or H_2O_2, then mapping their distribution may reveal currently or recently active regions.

Constraining the global and local heat flow of Europa is of great importance. High heat fluxes (~1 W/m^2) would be necessary for detection of uniform conductive heat flow [*Spencer et al. 1999*], but lower levels of endogenic heat flow could be detected if locally concentrated, as on Enceladus [*Spencer et al. 2006*]. A high heat flow could indicate that significant tidal heating and likely volcanic activity is occurring in the mantle. This would have important implications for astrobiology, as on Earth where it is hypothesized that life may have developed at hot hydrothermal vents on the ocean floor.

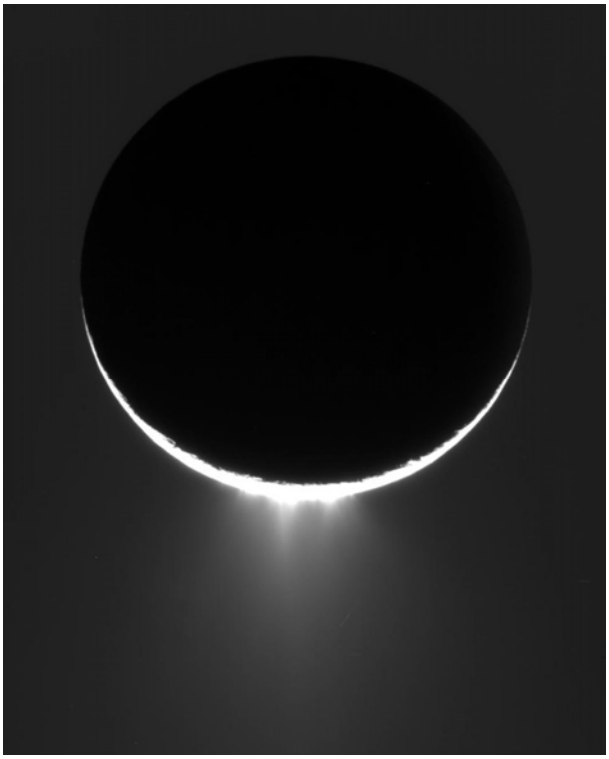

Figure 4-35. The plumes of Enceladus dramatically illustrate that satellite to be geologically active today, as revealed by a combination of Cassini high-phase imaging (shown here), plus thermal, UV, and fields and particles observations [*Porco et al. 2006*]. Analogous plumes would be ~70 km tall when scaled to Europa's gravity [*Nimmo et al. 2007a*], so similar activity could be plentiful yet undiscovered on Europa, and might contribute to Europa's recently discovered torus [*Mauk et al. 2003*]. A combination of thermal and UV observations would permit a thorough search and characterization of active regions on Europa.

Thermal emission from the surface could be appropriately mapped by measuring albedo to 10% radiometric accuracy at spatial resolution of ~250 m/pixel in two thermal wavelength bands with temperature accuracy <2 K, over > 80% of the surface.

Constraints on global heat flow would also come from subsurface ice temperatures derived from ice penetrating radar, and estimates of ice shell thickness derived from gravity or radar data (Foldout 2).

To understand links between surface properties and relative age, we must

understand the ion and electron precipitation flux onto Europa across the satellite. Thus, INMS plasma measurements are valuable to contraining surface age, examining energy ranges of 1 eV to 1 MeV and 10 eV to 10 MeV.

Investigation ED3: Constrain global and regional surface ages.

Determining the relative ages of Europa's surface features allows the evolution of the surface to be unraveled. Indication of relative age comes from the stratigraphy, derived from cross-cutting and embayment relationships, and the relative density of small primary impact craters. These relationships enable a time history to be assembled within regions, for global extrapolation. Without a global map, the relative ages of different regions cannot be determined, because they cannot be linked; this is the current problem in understanding Europa's stratigraphy based on Galileo imaging.

Galileo 3-color imaging at low phase angle showed the great advantage of color in stratigraphic studies, because features generally brighten and become less red with age [*Geissler et al. 1998*]. Global color imaging (> 80% of the surface) at resolution better than ~100 m/pixel, with near-uniform lighting conditions and phase angle $\leq 45°$, would allow Europa's global stratigraphic sequence to be derived.

Relative surface ages also could be derived by identifying regions of anomalously high heat flow, by assessing surface morphology and topography, and by mapping age-sensitive chemical and physical indicators. Moreover, correlation of surface morphology to subsurface structure would be valuable to understanding surface ages. For example, it would be exciting to find correlation between the presence of water or warm ice at relatively shallow depths and surface regions that have youthful characteristics.

Investigation ED4: Investigate processes of erosion and deposition and their effects on the physical properties of the surface.

Europa's regolith provides information about modification processes occurring on very small scales. Modification occurs by mass wasting, sputtering, impact gardening, and thermal redistribution of material. Investigation of regolith characteristics and processes would be important in characterizing high-priority sites for future landed missions, and in understanding means of material exchange between the oxidant-rich upper meter of the surface and the subsurface. Regolith processes could be investigated by imaging at ~1 m/pixel resolution, which would reveal the small-scale morphology of targeted sites, shedding light on erosional processes and material deposition. Meter-scale imaging is critical to understanding the nature and safety of potential future landing sites.

Variations in daytime temperatures seen by the Galileo Photopolarimeter Radiometer (PPR) show 5 K temperature variations that could have been caused by variations in thermal inertia when corrected for albedo [*Spencer et al. 1999*]. Thermal measurements would investigate the regolith by mapping surface thermal inertia, with the same measurement requirements as for investigation of possible thermal anomalies. This would follow up on the mysterious nighttime thermal anomalies identified by Galileo.

Magnetometry data are important for understanding sputtering and its effects on regolith evolution; thus, it is valuable to measure ion-cyclotron waves, which could be related to plasma-pickup and erosion processes. Measuring these high-frequency waves requires magnetic field sampling at 32 vectors/s at a sensitivity of 0.1 nT, with knowledge of spacecraft orientation to 0.1°.

The key outstanding questions relating to Europa's geology (§4.2.1.4) could be addressed by the Objective D investigations described above, as summarized in Table 4-9.

Table 4-9. Hypothesis Tests to Address Selected Key Questions Regarding Europa's Geology

Example Hypothesis Questions		Example Hypothesis Tests
ED.1	Do Europa's ridges, bands, chaos, and multi-ringed structures require the presence of near-surface liquid water to form?	Combine high-resolution imaging, compositional, subsurface, and thermal data sets to determine the style of surface deformation and the links to interior structure and water.
ED.2	Where are the youngest regions on Europa and how old are they?	Use repeat imaging, sputtering measurements, vapor transport observations and thermal data to determine absolute age ranges.
ED.3	What is the roughness and thickness of the regolith?	Use thermal measurements and imaging, combined with plasma measurements, to characterize the uppermost surface.

4.3.1.5 EE. Europa's Local Environment

Characterize the local environment and its instructions with the jovian magnetosphere.

The rapidly rotating magnetosphere of Jupiter is continuously overtaking Europa in its orbit. Charged particles impact the surface and atmosphere and could liberate and redistribute material. Energetic particles could deliver energy deep into the ice, and could form radiolytic products such as oxidants. Because surface, atmospheric, ionospheric, and field and particle environments are intimately interconnected, an integrated set of magnetic field, plasma, energetic particle, and neutral atmosphere investigations are required to unravel the numerous processes involved.

Investigation EE.1 Characterize the composition, structure, dynamics and variability of the bound and escaping neutral atmosphere.

The surface of Europa continuously exchanges material with the atmosphere, and direct measurements of the atmosphere are of prime interest. The measurement of major and minor constituents of the neutral atmosphere would greatly aid geological, compositional, and exospheric studies. Current knowledge of the atmosphere is largely based on isolated observations of spectral emission features that depend on the local plasma environment, and which provide little information on minor species chemistry and temporal variations. In addition to water ice, heavy molecules and molecular fragments could be sputtered and subsequently detected by UV spectroscopy (including UV spectral images and stellar occultations), IR spectroscopy (including limb scans such as those used to detect the CO_2 atmosphere of Callisto [*Carlson 1999*]), and in situ by an INMS. UV stellar occultations provide stringent constraints on the extent and structure of the atmosphere. A non-uniform atmosphere is anticipated, and could be examined with *in situ* INMS measurements. Because the atmosphere may have episodic sources such as geysers or plumes, a frequent cadence of observations of the neutral species is required.

Investigation EE.2 Characterize the composition, structure, dynamics and variability of the ionosphere and local (within the Hill sphere) charged particle population.

Understanding the ionosphere of Europa is critical to disentangling the higher order magnetic moments for interpretation of Europa's induced magnetic field. Radio occultations provide a proven technique with which to sound the ionosphere [*Kliore et al. 1997*]. During the Europa Science orbital phase of the mission, *in situ* measurements of the ionosphere could be made by both an INMS and a plasma and particle instrument.

Table 4-10. Hypothesis Tests to Address Selected Key Questions Regarding Europa's Local Environment

Example Hypothesis Questions		Example Hypothesis Tests
EE.1	Are trace species that reveal properties of Europa's interior driven into the atmosphere in sufficient quantities to be detected?	Use stellar and radio occultations through UV spectroscopy and radio science to search for absorption signatures and characterize the neutral atmosphere and ionosphere
EE.2	Is Europa's atmosphere produced chiefly by the interaction of magnetospheric particles with the surface?	Determine the flux and composition of impacting charged particles and measure the magnetic field components along with plasma measurements, mass spectroscopy, magnetic field measurements, and visible imaging.

It is of great importance to understand how Jupiter's magnetic field is perturbed the satellite. Magnetic field measurements complement direct particle measurements by other instruments. The shielding of the electric field around Europa is affected by the strength and configuration of the local magnetic field and the scale height of the atmosphere. The magnetic field must be measured with an accuracy of at least 0.1 nT and requires near-continuous measurements with a cadence of 8 vectors/s to resolve sharp currents sheets created by the moon-plasma interaction.

The magnetic environment is profoundly affected by the local production of charged particles and by currents generated when plasma interacts with Europa; thus, plasma ions (tens of eV to few keV range) are linked to perturbations in the magnetic field near the satellite. To determine the plasma flow around the body and the relationship between plasma and the magnetic field, ions with energies 50 eV to 10 keV need to be detected with good energy resolution ($\Delta E/E = 0.15$) and angular resolution (~15 degrees) to properly understand their fluxes. The goal is to assemble a consistent scenario of magnetic field, plasma flow, and currents near the Europa.

The key outstanding questions relating to Europa's local environment (§4.2.1.5) could be addressed by the Objective E investigations described above, as summarized in Table 4-10.

4.3.2 Goal 2: Ganymede

The Planetary Decadal Survey points out the uniqueness and relevance of Ganymede in possessing intriguing surface geology, a strongly differentiated interior, and an internally generated magnetic field. The Cosmic Vision points out the relevance of Jupiter exploration for permitting "the first fundamental advances in understanding the structure and dynamics of this fascinating plasma environment"; the space plasma interactions between Ganymede and Jupiter are unique among the solar system's planets and satellites. Ganymede provides a fundamental comparison to Europa in understanding the potential habitability of ocean-bearing icy worlds. These high-level drivers lead to the goal for the Ganymede aspect of EJSM:

Characterize Ganymede as a planetary object including its potential habitability.

This goal emphasizes the importance of understanding Ganymede's processes and its implications for the Jupiter system, especially its unique space plasma environment. It also recognizes that Ganymede's ocean and internal activity suggest the potential for habitability: although there is less potential for life than Europa, it is feasible that Ganymede possesses the "ingredients" for life (§4.1.1). Ganymede is central to understanding

planetary processes and habitability in the Jupiter system.

One of the themes of ESA's Cosmic Vision document [*ESA 2005*] relates to understanding solar system processes. Jupiter's "miniature-solar system" is ideally suited for this purpose, through study and comparison of the diverse Galilean satellites by EJSM. In particular, the comparison of Ganymede to Europa would further elucidate the requirements for habitable worlds, while the comparison of Ganymede to Callisto would help to answer questions as to why one moon differentiated and the other did not. Of particular significance is the study of Ganymede's magnetosphere and its interactions with the Jovian magnetosphere.

The Ganymede objectives are categorized in priority order as:

- GA. Ganymede's Ocean
- GB. Ganymede's Ice Shell
- GC. Ganymede's Local Environment
- GD. Ganymede's Geology
- GE. Ganymede's Composition.

4.3.2.1 GA. Ganymede's Ocean

Characterize the extent of the ocean and its relation to the deeper interior.

Measurements of the time-variable gravity and topography of tides raised on Ganymede by Jupiter could confirm the presence of an ocean. If a liquid water ocean exists on Ganymede, surface displacement of several meters is expected over one orbit, whereas if no ocean is present, only a few tens of centimeters of displacement is expected. A measurable periodic gravity signal would also be caused by tidal displacement. Measurement of the tidally driven time-variable topography or gravity from orbit, as described by the Love numbers h_2 and k_2, respectively, would test the existence of a sub-surface ocean (see Figure 4-36.

EJSM would investigate the Ganymede intrinsic magnetic field in detail and would characterize the interplay between this intrinsic field, induced magnetic fields generated in the subsurface ocean, and the Jovian magnetosphere. Ocean currents would be sought in the induced magnetic signal. The induction response would be determined at multiple frequencies by measuring the magnetic field. The local plasma distribution function (ions and electrons) and moments would be measured in three dimensions in order to constrain contributions from currents that are not related to the surface and ocean. The magnetic field at the surface, along with the locations of open and closed field lines, would be identified by measuring over a wide range of electron and ion densities, and electron temperatures would be determined. These measurements would establish the dimensions of the magnetosphere and the regions in which particles are trapped or transported.

Whether a planet generates a magnetic field depends on the presence of a metallic core and its structure. Lateral variations in density could provide constraints on the differentiation history and on alternative dynamo models. EJSM would carry out a detailed investigation of the magnetic field of Ganymede, which would provide important inputs to dynamo theories that, combined with thermal-evolution models, would inform as to what conditions are required for generating and maintaining dynamo activity.

The Galilean moons are locked in a stable 1:1 spin-orbit coupling. However, slight periodic variations in the rotation rate (physical librations) and the amplitudes associated with these librations could provide further evidence for subsurface oceans. EJSM would measure the rotation rates, pole-positions, obliquities, and libration amplitudes of Ganymede. This

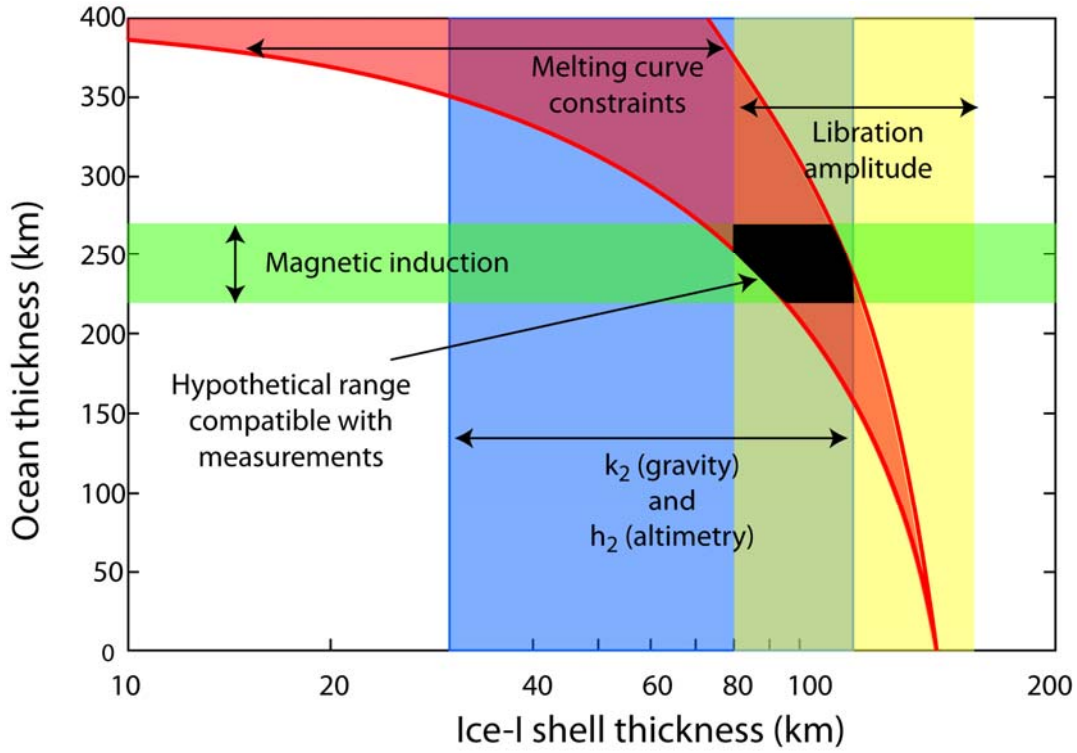

Figure 4-36. Schematic view of the strategy to characterize Ganymede's ice crust and liquid layer by using combined techniques on JGO. The parameter space (ice-I shell thickness and ocean thickness) is bounded by the domain of stability of ices (red curves), but not fully constrained due to our poor knowledge of the temperature profile and the volatile content. JGO will put the required additional constraints (resulting black area) by determining (a) the Love numbers h_2 and k_2 (main ambiguity: rigidity of ice-I), (b) the libration amplitude (main ambiguity: density contrast between ice-I and ocean), and (c) the magnetic induction signal (main ambiguity: electrical conductivity of the ocean).

would further constrain the dynamical history of the satellite, e.g., de-spinning, resonance capture, or non-synchronous rotation of the icy shell.

EJSM would verify whether a hydrostatic state is obtained by measuring the low-order gravity field to quantify mass anomalies, asymmetries in the mass distribution and other non-hydrostatic contributions to the satellites' gravity fields. Combining gravity data with shape measurements would allow any offset between the center of mass and center of figure to be determined, since the finite strength of planetary material and dynamic processes in the interior cause deviations of the surface from the equilibrium surface. EJSM would perform global topographic measurements of Ganymede, thus providing the reference for local and regional high-degree topography. The time-varying tidal deformations would be related to the equilibrium shape. Interpretation of the gravity and shape measurements would significantly improve the interior structure models of Europa and Ganymede, thus providing constraints on evolution models of these moons.

In the objective to characterize the extent of the ocean and its relation to the ice crust, the investigations are:

- GA.1: Determine the amplitude and phase of the gravitational tides.
- GA.2: Characterize the space plasma environment to determine the magnetic induction response from the ocean
- GA.3: Characterize surface motion over the tidal cycle.

- GA.4: Determine the satellite's dynamical rotation state (forced libration, obliquity and nutation).
- GA.5: Investigate the core and rocky mantle.

4.3.2.2 GB. Ganymede's Ice Shell

Characterize the ice shell.

Subsurface sounding would be used to locate liquid water in the ice shell and to identify stratigraphic and structural horizons. Hypotheses could be tested related the origin of structures on the surface and in the shallow surface. Structural boundaries would help to distinguish among processes such as convection, tectonism, impacts and marine processes such as brine channels.

Ganymede's near-surface environment would be investigated using a combination of sounding, topography, and thermal measurements. Compositional, phase, and tectonic boundaries within the ice would be characterized in order to understand how surface features, particularly grooved terrain, formed and evolved. The relative roles of cryovolcanism and tectonism would be investigated using a combination of techniques, including imaging, topographic mapping and sounding.

In the objective to characterize Ganymede's ice shell, the investigations are:

- GB.1: Characterize the structure of the icy shell including its properties and the distribution of any shallow subsurface water.
- GB.2: Correlate surface features and subsurface structure to investigate near-surface and interior processes

4.3.2.3 GC. Ganymede's Local Environment

Characterize the local environment and its interaction with the jovian magnetosphere.

Ganymede possesses a thin exosphere, an ionosphere, and aurorae, created by surface bombardment by particles from Jupiter's radiation belt. Exospheric properties are indicative of processes at and composition of the surfaces.

EJSM would characterize Ganymede's magnetosphere and investigate particle trapping and transport along flux tubes connecting the poles of Jupiter and Ganymede.

EJSM would investigate Ganymede's intrinsic magnetic field in detail to characterize the interplay between the intrinsic field, induced magnetic fields generated in the subsurface ocean, and the Jovian magnetosphere (Figure 4-37). The mission would establish the dimensions of Ganymede's magnetosphere, as well as regions of open/closed field lines where particles are either trapped or transported, field-aligned, between the polar regions of Jupiter and Ganymede along the flux tubes connecting both bodies. Ocean currents would be sought in the induced magnetic signal. Long-term changes in the magnetic field may also be detected by comparison with Galileo data.

Many crucial parameters of the satellite/magnetosphere coupling would be investigated, including processes associated with sputtering of surfaces and exospheres, and with resurfacing due to intense bombardment by energetic particles. Given the complex composition of the environment of Jupiter, understanding plasma resurfacing is a necessity for the interpretation of the spectral signatures of Ganymede's surfaces. It is currently unknown whether noble gases and nitrogen- and carbon-bearing species would be present in sputtered or geyser-emitted material from Europa or Ganymede; their presence would be of extremely high value for understanding the origin of the Jovian

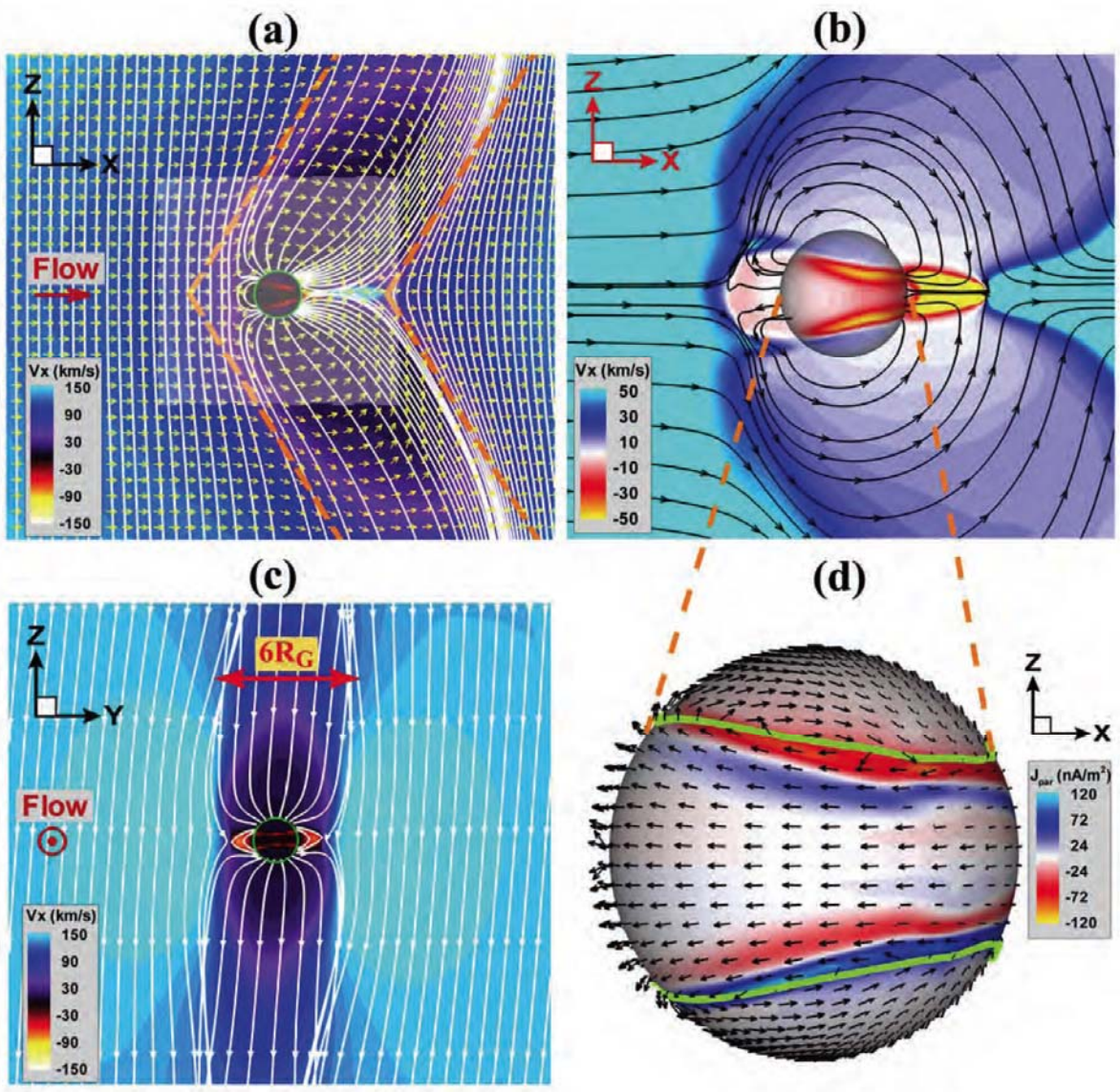

Figure 4-37. (a) Flows and the projection of field lines (white solid lines) in the XZ plane at Y = 0. Color represents the V_x contours, and unit flow vectors in yellow show the flow direction. A theoretical prediction of the Alfvení' characteristics (orange dashed lines) is shown for reference. The projection of the ionospheric flow is also shown as color contours on a circular disk of r = 1.08 R_G in the center. (b) A zoomed-in view of the light area in (a). Flow streamlines are superimposed on color contours of V_x. Note that the color bar differs in order to illustrate the relatively weak flow within the magnetosphere. (c) Same as (a) but in the YZ plane at X = 0. (d) Field-aligned current density along with unit flow vectors shown on a sphere of radius r = 1.08 R_G. (From *Jia et al., 2009*.)

satellites. It is also clear that energetic ions and electrons are the principal chemical agents in layers close to the surface of moons. The actual importance of these effects depends on the magnetic environment.

Ganymede possesses an internal dipolar magnetic field which interacts with the jovian magnetic field, thus permitting the plasma to impact the surface at specific regions, resulting in a specific albedo distribution, with the polar regions being brighter than the equatorial belt [*Khurana et al. 2007*]. EJSM would identify the particles near the moons and their interaction with Jupiter's magnetosphere, would measure the velocity space distribution

of thermal plasma and energetic particles from eV to MeV, as well as plasma and radio waves, and neutral imaging of the impacting and ejected plasma from eV to keV.

How Ganymede's mini-magnetosphere interacts with the giant magnetosphere of Jupiter is a mystery; it is only known that this interaction is powerful enough to create an auroral footprint in Jupiter's aurora. The mission would also study Ganymede's exosphere through remote measurements, multi-wavelength limb scans and stellar occultations, imaging of the aurorae, and in-situ charged and neutral particle measurements from low orbits and fly-bys. EJSM would study the aurorae using close-up imaging and the *in situ* measurements of the particles producing them. The location and intensity of the footprints in the aurora of Jupiter would be measured remotely, in combination with *in situ* measurements of particles and fields in the field – aligned current systems.

In the objective to characterize Ganymede's space plasma environment and its interaction with the Jovian magnetosphere, the investigations are:

- GC.1: Globally characterize Ganymede's intrinsic and induced magnetic fields, with implications for the deep interior.
- GC.2: Characterize the particle population within Ganymede's magnetosphere and its interaction with Jupiter's magnetosphere.
- GC.3: Investigate the generation of Ganymede's aurorae.
- GC.4: Determine the sources and sinks of the ionosphere and exosphere.

4.3.2.4 GD. Ganymede's Geology

Understand the formation of surface features and search for past and present activity.

EJSM would study the geological history of Ganymede using global, regional, and local mapping at different levels of resolution, and topographic mapping on regional and local scales. EJSM would image Ganymede at regional resolutions and acquire high resolution imaging of selected targets. Combined with spectral mapping and heat flow measurements, these observations would reveal details of Ganymede's geological evolution, constrain the role of cryovolcanism and tectonics in the satellite's geological history, and provide information on the satellite's origin. EJSM would acquire detailed topographic profiles of surface features including grooved terrain, craters, and candidate cryovolcanic features. This information would help elucidate the dynamical processes that cause near-surface tectonics.

EJSM would also probe the upper ice shell of Ganymede, investigating the processes linking the ocean to the surface, and the dynamics of the near-surface ice layers, by detecting compositional or phase boundaries between different ice sheets and unconformities. Inferences from topographic and thermal data would be combined with stratigraphic and structural data to provide information on processes responsible for the formation and destruction of the lithosphere.

EJSM would significantly improve the current estimate of Ganymede's surface age by providing crater distributions based on almost complete global imaging at regional resolutions, and by identifying craters with a range of morphological degradation states. Subsurface sounding may identify hidden crater populations, such as might be expected if cryovolcanic flooding had occurred on the surface.

In the objective to understand the formation of surface features and search for past and present activity, the investigations are:

- GD.1: Determine the formation mechanisms and characteristics of magmatic, tectonic, and impact landforms.
- GD.2: Constrain global and regional surface ages.
- GD.3: Investigate processes of erosion and deposition and their effects on the physical properties of the surface.

4.3.2.5 GE. Ganymede's Composition

Determine global composition, distribution and evolution of surface materials on Ganymede.

As revealed by results from the Galileo spacecraft, there are substantial amounts of non-water-ice components present at the H_2O-ice dominated surface of Ganymede (Figure 4-38). These species may have been derived from a subsurface briny layer of fluid, and their nature and origin are still debated. The detection and distribution of biologically essential elements (C, H, O, N, P, S) is critical in assessing habitability. EJSM would survey the surface composition and chemistry of Ganymede by nearly global, multi-wavelength spectral mapping, mass spectroscopy, and high-resolution spectral imaging of selected targets.

The relationship of ice and non-ice materials and their distribution is crucial for understanding the origin and evolution of the surface of Ganymede. Surface material

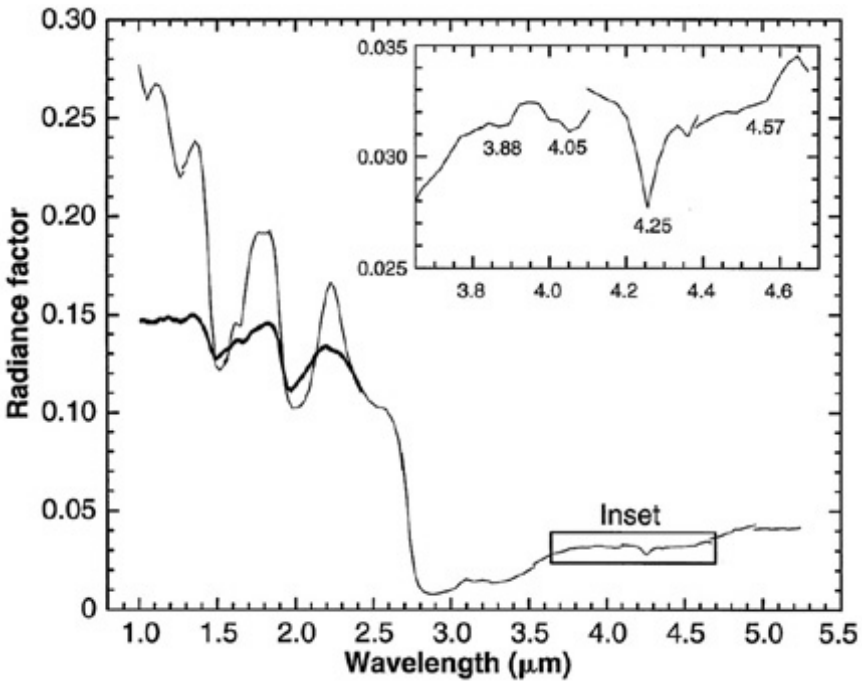

Figure 4-38. NIMS spectra of Ganymede. Thin curve is an average of 3000 pixels from a global observation covering 110° to 230°W. The strong absorption near 3 μm is the fundamental O–H stretching transition active in water ice and in hydrated and hydroxylated minerals; other bands evident in the 1 to 3 μm region are due to combination and overtone transitions in water ice. Bold spectrum is for a dark terrain region near 3°N, 274°W with ice absorptions removed, revealing asymmetric absorption bands characteristic of hydrated minerals. Inset shows details of absorptions inferred to be from minor constituents S-H (3.88 μm), SO_2 (4.05 μm), CO_2 (4.25 μm), and organic materials such as those containing C-N (4.57 μm). After *McCord et al.* [1997, 2001a].

distribution could be linked to the internal activity of the moons but also to external processes (e.g., the effect of the Ganymede's intrinsic field shielding high-energetic particles at equatorial to mid-latitudes or precipitation of particles at high latitudes). On Ganymede, various non-ice materials have been identified, but a reliable identification of non-ice compounds is still missing. EJSM would have the ability to map a significant portion of Ganymede's surface with high spectral resolution and good signal-to-noise ratio. High-resolution spectral imaging of selected targets would allow reliable identification of the non-ice material. EJSM would correlate the distribution of non-water-ice material with geologic units over a wide range of spatial scales, revealing sites where material has been exchanged between the surface and subsurface.

Surface composition could also be inferred by measuring materials sputtered or ejected from the surface into an atmosphere using direct sampling, which is not affected by the physical properties of the material. Models predict that large molecules such as hydrated Mg and Na sulfates and organics may be sputtered to orbital altitudes at levels detectable for sub-millimeter wave or INMS-type instruments.

Results from EJSM are expected to significantly enhance understanding of ion bombardment processes and the dynamical response of Ganymede's surface, as well as physical processes that give rise to the cycle of oxygen species. EJSM would study neutrals produced by plasma-surface interactions and would provide 2D imaging of impacting plasma. The oxygen species O_2 and O_3, found on Ganymede's trailing hemisphere, appear to be trapped within the ice matrix and probably originate from ionic bombardment of the icy surface. The abundance of ozone varies with latitude, with the strongest absorption measured at higher latitudes, interpreted to be the result of plasma bombardment creating O_3 in the ice matrix and photodissociation destroying it, on a continual basis.

In the objective to determine global composition, distribution and evolution of surface materials on Ganymede, the investigations are:

- GE.1: Characterize surface organic and inorganic chemistry, including abundances and distributions of materials.
- GE.2: Relate compositions and properties and their distributions to geology.
- GE.3: Investigate surface composition and structure on open vs. closed field line regions.
- GE.4: Determine volatile content to constrain satellite origin and evolution.

4.3.3 Goal 3: Jupiter System

The scientific exploration of Europa and Ganymede must be placed in the context of the Jovian System as a whole. As such, an overarching motivation from the Planetary Decadal Survey provides the context for Jupiter system exploration by EJSM through the specific questions, "How do the processes that shape the contemporary character of planetary bodies operate and interact?" and "What does the solar system tell us about the development and evolution of extrasolar planetary system, and vice versa?" As the largest and arguably the most influential planet in the Solar system, Jupiter's complex environment is key to understanding processes, origins, and evolution in other planetary systems. EJSM would address in depth two of the four themes of ESA's Cosmic Vision Programme:

- What are the conditions for planet formation and the emergence of life?
- How does the solar system work?

Thus, the goal adopted for the Jupiter System Science aspect of EJSM is:

Explore the Jupiter system as an archetype for gas giants.

This includes testing the scientific issues described in §4.2, and allows for "discovery" science that responds to unexpected findings that so often occur in planetary exploration.

Jupiter system science for EJSM falls into four overarching objective categories: (1) The Jovian satellite system (2) Rings and small satellites, (3) The Jovian magnetosphere and (4) The Jovian Atmosphere. Each contains it own set of specific objectives. The corresponding investigations and measurements are prioritized within each category, with the lower priorities generally having less relevance to the Europa and Ganymede goals; yet they allow application to the overarching theme of EJSM. Jupiter system science would be the principal focus of the Jovian Tour phase of the mission, which has takes place during the ~2–2.5 years prior to orbit insertion around Europa (JEO) and Ganymede (JGO).

The Jupiter objectives are categorized as:

S. Jovian Satellite and Ring System
M. Jovian Magnetosphere
J. Jovian Atmosphere.

4.3.3.1 S: Jovian Satellite and Ring System Objectives and Investigations

Study the Jovian satellite and ring system.

The four Galilean Satellites, Io, Europa, Ganymede, and Callisto are diverse with respect to their chemical composition, the geology of their surfaces, their internal structure and evolution, and their degree of tidal interaction with Jupiter (Figure 4-39). The bulk density decreases with increasing distance from Jupiter, indicating differing chemical compositions ranging from silicate rock + iron at Io to a 40% ice and 60% rock + metal mixture at Callisto. This trend reflects the conditions (mainly temperature) within the circumJovian disc at the time the satellites formed. However, this stands in contrast to the Saturn system, which is lacking such clear-cut trends. By studying all four Galilean Satellites we seek to understand the evolution of such a regular satellite system from its origin to the present diverse surfaces and internal structures of the Galilean Moons related to their different energy budgets and evolutionary histories.

By studying Io, Callisto, and small bodies and rings, in addition to Ganymede and Europa, a broad range of processes and their interrelationships would be explored by EJSM. This would permit understanding of processes in the Jovian system and would place Europa and Ganymede in their planetological context.

All four Galilean satellites probably formed in a similar environment, while the inner three affected each other through tidal interaction as their orbits and interiors evolved. The outer three satellites share analogous surface materials, altered to differing extents by external and internal processes. Within the overarching theme of studying the Jovian satellite and ring system, three principle objectives are defined: (1) Understand Io's active dynamic processes; (2) Characterize Callisto as a witness of the early Jovian system; and (3) characterize the rings and small satellites.

Io

Understand Io's active dynamic processes.

- SA.1 Investigate the nature, distribution and magnitude, of tidal dissipation and heat loss on Io.
- SA.2 Investigate Io's composition and active volcanism for insight into its origin, evolution and geological history (particularly of its silicate crust).

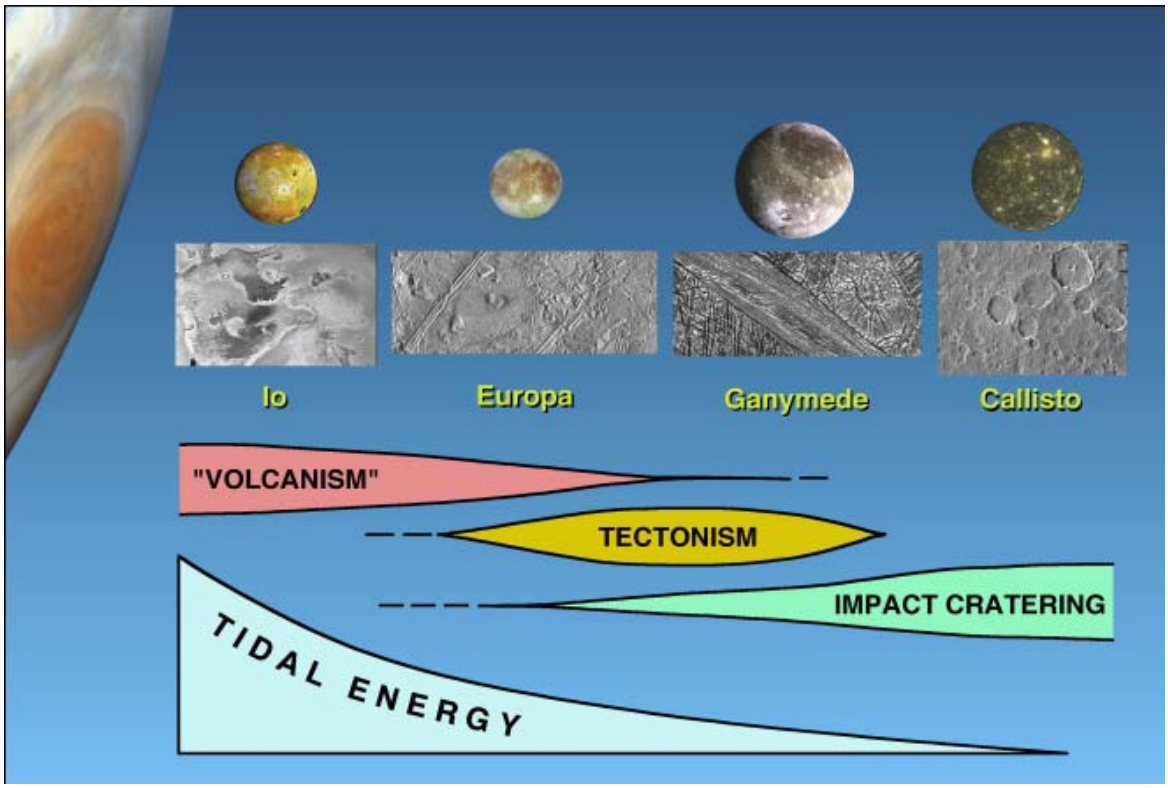

Figure 4-39. Schematic illustration of the relative importance of processes and tidal energy for the Galilean satellites.

- SA.3 Determine Io's dynamical rotation state (forced libration, obliquity, and nutation). SA.4 Investigate the interior of Io.
- SA.5 Understand satellite origin and evolution by assessing sources and sinks of Io's crustal volatiles and atmosphere. change from italics to regular text.

Tidal heating has shaped the evolution of all four Galilean satellites, but the details remain poorly understood. Tidal heating is most readily studied on Io, where the spatially and temporally variable surface temperature and heat flow. As the tidal engine of the Laplace resonance, variations in Io's heat flow and orbital eccentricity could drive changes in these parameters in the resonant satellites Europa and Ganymede.

Thermal measurements would characterize the different styles of volcanic activity and their controlling factors, with contributions from high-resolution images, stereo- and altimeter-derived topography, and visible/NIR observations of high-temperature volcanic thermal emissions. Visible and IR mapping may be used to determine the compositional variability, spatial and temporal distribution, and geologic associations of both silicates and volatiles at Io.

Various techniques are required to understand Io's unusual atmosphere, which is produced by a combination of sources. Its reservoir of surface volatiles, especially SO_2, has a major impact on the Jovian system. The Io plasma torus is a key link in the transfer of material from Io to Europa. Understanding the sources and sinks of the volatiles, both on the surface and in the atmosphere, is a key undertaking of the Jupiter system science program. Eclipse imaging, plume monitoring, far- and mid-UV and IR spectroscopy of the surface and atmosphere with high spatial and temporal resolution, as well as stellar occultations,

would provide critical constraints on the flux of materials escaping Io. Monitoring the neutral clouds and plasma torus, together with measurements of dust and neutral and charged particles, would help determine how these materials are dispersed throughout the Jovian system and beyond.

The JEO Io campaign would include multiple Io flybys, allowing *in situ* particles and fields measurements, and high-resolution remote sensing of the surface. Whether plumes could be flown through safely, and thus sampled directly, would require further study.

Callisto

Study Callisto as a witness of the early Jovian system.

- SB.1 Investigate the interior of Callisto.
- SB.2 Characterize the space plasma environment to determine the magnetic induction response from Callisto's ocean.
- SB.3 Characterize the structure and properties of Callisto's icy shell.
- SB.4 Constrain the tidally varying potential and shape of Callisto.
- SB.5 Determine Callisto's dynamical rotation state (forced libration, obliquity and nutation).
- SB.6 Characterize surface organic and inorganic chemistry, including abundances and distributions of materials and volatile outgassing.
- SB.7 Characterize the ionosphere and exosphere of Callisto.
- SB.8 Relate material composition and distribution to geological and magnetospheric processes.
- SB.9 Constrain global and regional surface ages.
- SB.10 Determine the formation and characteristics of magmatic, tectonic, and impact landforms.

Callisto is inferred to possess an ocean sandwiched between two layers of ice, yet gravity data from Galileo suggest that it is incompletely differentiated. Its cratered surface is ancient, yet erosive processes appear to be ongoing today. Callisto serves as a witness to 4.6 Gyr of Jovian system history, and it provides an important linchpin in the comparative evolution of the Galilean satellites.

The presence of a Callisto ocean could in principle be confirmed by measuring the time-dependent (tidally-driven) gravity field or surface topography; these measurements would also help determine the amount of tidal heating. Magnetometer observations would place bounds on the depth, thickness, and salinity of the ocean. The deeper structure of this satellite, and in particular the extent to which Callisto is differentiated, may be determined by Doppler-tracking during equatorial and especially high-latitude flybys. Galileo was not able to perform a high-latitude Callisto fly-by, which is critical in understanding whether the satellite is hydrostatic, and thus whether it is differentiated. Combining regional images taken at different times would establish the spin pole orientation, and potentially show librations, both of which depend on the internal structure.

Characterizing surface materials on Callisto would help disentangle the origin of similar materials on Europa. IR and UV spectroscopy would be used to identify individual compounds and map their distribution (e.g., hydrated non-ice material and trace constituents such as CO_2). Combined with high-resolution color images, correlations between particular species and geologic features may be tested. Repeat measurements would allow characterization of any surface changes. (e.g., mass wasting or sublimation).

At Callisto, sublimation may be more significant than charged particle sputtering.

Current knowledge of the atmosphere is largely based on isolated observations, derived largely from observations of spectral emission features that are reliant on the local plasma environment, which provide little information on minor species chemistry and temporal variations.

Measurements at Callisto would reveal information about the sources and sinks of the atmosphere, and the measurement of major and minor constituents of Callisto's neutral atmosphere would greatly aid geological, compositional, and exospheric studies. In addition to water ice, heavy molecules and molecular fragments could be sputtered and subsequently detected by UV spectroscopy, IR spectroscopy (including limb scans such as those used by Galileo to detect the CO_2 atmosphere of Callisto [*Carlson 1999*]), and *in situ* by an INMS. UV stellar occultations provide stringent constraints on the extent and structure of the atmosphere. Any atmospheric non-uniformity atmospheres could be examined with *in situ* INMS measurements.

Rings and Small Satellites

Characterize the rings and small satellites.

- SC.1 Conduct a comprehensive survey of all the components of the Jovian ring-moon system.
- SC.2 Identify the processes that define the origin and dynamics of the ring dust, source bodies, and small moons.
- SC.3 Characterize the physical properties of the inner small moons, ring source bodies and dust.
- SC.4 Remotely characterize the composition, properties and dynamical groupings of the outer, irregular moons.
- SC.5 Perform disk-resolved and local characterization of one or more outer, irregular moons.

The "skeleton" that holds together the Jovian ring system is its collection of source bodies. Four inner moons are known, but it is clear that the ring also contains a large number of embedded meter- to kilometer-sized bodies. Learning the nature and properties of these bodies is critical to understanding origin, evolution and the long-term stability of the system.

At a certain point, the distinction between a "moon" and a "ring body" should become moot, because the ring contains a continuum of sizes. However, imaging at low phase angles is needed to characterize the radial distribution of the bodies and to identify its largest members. New Horizons achieved a detection threshold of 500 m in radius; future imaging should reduce this threshold to ~100 m (assuming albedos of ~0.1, comparable to those of Adrastea and Metis) to ensure detection of the largest bodies. High-quality ring detection requires sensitivity to reflectivities in the range of 10^{-8}. Searches for the source bodies must be conducted primarily at low phase angles.

The composition of the Jovian ring or its ring-moons is as-yet unknown, beyond the fact that they are very dark and red. Spectrophotometry in visible and near-IR wavelengths is needed for precise information about the molecular makeup of their surfaces.

The dust component of the system should also be characterized. The size distribution of ring dust probably varies with location, and could be derived from light phase curves and spectra. Imaging of all the ring components should be carried out at a full range of phase angles, up to and including within a few degrees of exact forward-scatter. This is where diffraction by the dust particles dominates, yielding the most precise size constraints. Such imaging could only be obtained when passing through the Jovian shadow. Measurements should be sensitive to rings with optical depths as low as

$\sim 10^{-9}$, the approximate value for a faint outward extension to Thebe's "gossamer" ring.

To assess any role that ring dust might have in contributing to the surfaces of the Galilean satellites, more information is required about its composition. This could be accomplished via IR spectroscopy of the dust grains and their parent bodies, particularly Amalthea and Thebe. A match of specific spectral signatures between the rings and the Galilean surfaces would provide strong circumstantial evidence that this process is occurring. It is also important to understand better the dynamics of the faint outward stream of ring dust, which requires imaging the outermost ring components with fine sensitivity. This is most readily at very high phase angles, where diffraction by the fine dust grains makes the rings much easier to observe.

The search for Jovian dust and moons should not end at the ring boundary. Trojan moons are a commonplace feature of the Saturnian system, but a deep, systematic search for small moons orbiting among the Galilean satellites has never been conducted. Any bodies that are found would surely have interesting dynamical histories and place new constraints on how the entire system formed. The detection threshold should be less than 1 km. At higher phase angles, the system should be searched for faint dust belts, which might be indicators of unseen small bodies in the system.

In addition to precise measurements of the particle properties, a better understanding is needed of the dust grains' motion. The grains are known to respond to solar radiation pressure and magnetic forces. These produce the "Lorentz resonances" that distribute so much of the dust well out of the ring plane. However, the three-dimensional structure of the system's faint inner "halo" and its outer gossamer rings have never been mapped out in detail. This requires imaging at a large variety of viewing and lighting geometries, with sensitivity to I/F $\sim 10^{-8}$ and resolution of finer than 100 km. Such observations may illuminate the dynamics behind some of system's more peculiar features, such as vertical ripples found in some Galileo images [*Ockert-Bell et al. 1999*] but not reported in images from New Horizons.

Because the system has shown clumps and other time-variable phenomena, repeated observations of the system throughout the tour are required. The most rapid phenomena are likely to change in periods of days to months. To understand the phenomena at work, it is critical to obtain reliable constraints on their time scales.

To complete our understanding of the entire Jovian system, attempts should also be made to study the distant, outer "irregular" satellites. As at the other planets, these are presumably captured bodies, with properties very different from the inner Jovian system. Should the opportunity present itself during tour design, a close flyby of one such object could provide unique details of its surface properties, shape, size, and possibly its mass.

4.3.3.2 M. Jovian Magnetosphere Objectives and Investigations

The extremely strong internal magnetic field of Jupiter (equatorial surface intensity of 4 Gauss) creates the largest and fastest rotating magnetosphere in the solar system. With an average subsolar magnetopause distance of 75 R_J, the magnetosphere rotates in less than 10 hours about its rotation axis. It is driven by the fast rotation of its central spinning object, Jupiter.

The magnetosphere's major plasma source is the volcanic moon Io, deep inside the magnetosphere, which releases about 1 ton/s of oxygen and sulphur and feeds with this plasma an equatorial magneto-disc extending

out over hundreds of planetary radii. The Jovian magnetosphere is the most accessible environment for direct *in-situ* investigations of processes regarding: (i) the stability and dynamics of magneto-discs, and more generally, angular momentum exchange and dissipation of rotational energy (the "fast rotator" theme), (ii) the electro-dynamical coupling between a central body and its satellites (the "binary system" theme) including plasma/surface interactions, transport processes and turbulence in partly ionized media. Jupiter is also a powerful particle accelerator, its inner magnetosphere being the most severe radiation environment in the Solar System.

EJSM, providing for the first time the opportunity to conduct dual measurements in the Jovian system (Figure 4-40), would measure the dynamics of the Jovian magnetodisk (with angular momentum exchange and dissipation of rotational energy), determine the electro-dynamic coupling between the planet and the satellites, and assess the global and continuous acceleration of particles.

The three main science objectives of EJSM relating to the Jovian magnetosphere focus on several key investigations that are derived from open questions from previous missions, and the Cosmic Vision themes of ESA. The investigation of Jupiter's magnetosphere is a key element in the study of the "plasma universe" since a large fraction of the Universe is filled with plasma composed of charged particles, and carrying magnetic fields. Nearly all of the exoplanets that have been discovered beyond our solar system are so-called "Jupiter-like" gas giants, and they would most likely possess plasma environments similar to Jupiter's. It is therefore imperative to investigate the Jovian magnetospheric environment *in situ* to further our understanding of planetary plasma environments in general.

The investigation of Jupiter's magnetosphere has three major aspects:

- *The astrophysical aspect*: Jupiter's magnetosphere as an example of a rotating astrophysical object generating a rotating magnetodisc filled with neutral and charged particles.
- *The solar system aspect*: Jupiter's magnetosphere as the most extreme plasma laboratory in our solar system where processes *i.e.* magnetic coupling, and acceleration processes etc. could be studied *in situ*.
- *The binary system aspect*: Jupiter's magnetosphere as an interlinked environment where the moons, rings, and plasma tori of the Jovian system interact with each other on a variety of spatial and temporal scales.

These top-level topics have been summarized in three magnetospheric science objectives and their corresponding investigations.

Characterize the magnetosphere as a fast magnetic rotator.

- MA.1 Understand the structure and stress balance of Jupiter's magnetosphere
- MA.2 Investigate the plasma processes, sources, sinks, composition and transport (including transport of magnetic flux) in the magnetosphere and characterize their variability in space and time.
- MA.3 Characterize the large-scale coupling processes between the magnetosphere, ionosphere and thermosphere, including footprints of the Jovian moons.
- MA.4 Characterize the magnetospheric response to solar wind variability and planetary rotation effects.

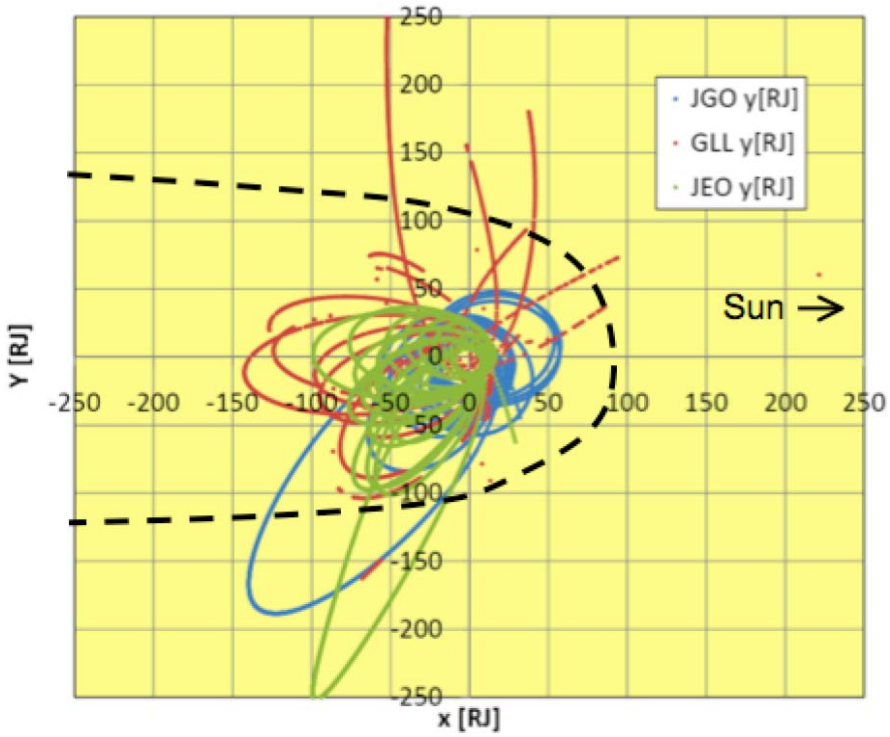

Figure 4-40. Schematic of Jupiter's magnetosphere showing the equatorial cross-section and the trajectories of JEO (green), JGO (blue) in comparison with Galileo orbits where particle data exist (red).

In this objective, Jupiter's magnetosphere is studied as a fundamental astrophysical object. The magnetosphere system provides energy and momentum through rotation and mass-loaded by internal sources, particularly the volcanic moon Io. As such the magnetosphere operates as a "fast magnetic rotator." The goal is to understand the three-dimensional structure of the magnetodisc, its sources and sinks, and its dynamic variability in both time and space.

Characterize the magnetosphere as a giant accelerator.

- MB.1 Detail the particle acceleration processes.
- MB.2 Study the loss processes of charged energetic particles.
- MB.3 Measure the time evolving electron synchrotron emissions.

This objective looks at Jupiter's magnetosphere as an important region in our solar system where charged particles originating from internal sources are accelerated to very high energies. The accelerated particles reach energies up to MeV, and this material is circulating between the inner and the outer parts of the magnetosphere trapped by the intense magnetic field in the radiation belt regions. Jupiter's magnetosphere would also be investigated as a source of high-energy charged particles in interplanetary space.

Understand the moons as sources and sinks of magnetospheric plasma.

- MC.1 Study the pickup and charge exchange processes in the Jupiter system plasma and neutral tori.

- MC.2 Study the interactions between Jupiter's magnetosphere and Io, Europa, Ganymede, and Callisto.
- MC.3 Study the interactions between Jupiter's magnetosphere and small satellites.

This final magnetosphere objective focuses on studies of Jupiter's variable magnetospheric environment in the locality of the moons, and how this changing local environment interacts with the moons in the system. The satellites could act as sources and sinks of magnetospheric plasma caused by sputtering of surface material (or by geological activity—Io) and by implanting of magnetospheric particles into the moons' surfaces. Depending on the presence of an internal magnetic field, or induced fields associated with sub-surface oceans, the Jovian magnetosphere-moon interaction would be different.

4.3.3.3 J. Jovian Atmosphere Objectives and Investigations

The exploration of Jupiter's dynamic atmosphere has played a pivotal role in the development of our understanding of the Solar System, serving as the paradigm for the interpretation of planetary systems around other stars and as a fundamental laboratory for the investigation of large-scale geophysical fluid dynamics and physiochemical phenomena. However, our characterization of this archetypal giant planet remains incomplete, with many fundamental questions about its nature unanswered. While the thin atmospheric "weather-layer"—the only region accessible to direct investigation by remote sensing—is only a tiny fraction of Jupiter's total mass, it provides vital insights to the interior structure, bulk composition, and formation history of our solar system. The EJSM dual spacecraft mission would offer an unprecedented opportunity for study of Jupiter's atmosphere over long temporal baselines of 2 years or more.

Jupiter is the end product of energetic accretion processes, thermochemistry, photochemistry, condensation processes, planetary-scale turbulence and gravitational differentiation. Its atmosphere is characterized by distinct latitudinal bands of differing cloud colors, vertical motions, temperatures and vertical mixing strengths separated by strong zonal winds and perturbed by long-lived vortices, storms, polar circulations, convective outbreaks, wave activity and variable large-scale circulation patterns [*Rogers 1995, Ingersoll et al. 2004, West et al. 2004*]. Although primarily composed of hydrogen and helium, Jupiter also contains small amounts of heavier elements found in their fully reduced forms (CH_4, PH_3, NH_3, H_2S, H_2O), providing source material for complex photochemical pathways powered by UV irradiation [*Taylor et al. 2004, Moses et al. 2004*]. The abundances of most of these heavy elements are enriched over the solar composition, providing a window into the evolution of the primordial nebula material incorporated into the gas giants during their formation [*Lunine et al. 2004*]. Jupiter's vertical atmospheric structure is governed by a delicate balance between solar, chemical and internal energy sources, and its layers are coupled by poorly understood dynamical processes which transport energy, momentum and material [*Vasavada and Showman 2005*]. Finally, Jupiter's atmosphere is intricately connected to the charged-particle environments of the ionosphere and magnetosphere [*e.g., Yelle and Miller 2004*], and the local Jovian environment of the rings and icy satellites.

EJSM would study the plethora of atmospheric phenomena described in §4.4 as a three-dimensional, highly coupled, system that varies over a range of timescales, from hours to years (Figure 4-41). As a Flagship-class mission, EJSM would have several advantages over previous missions to the outer planets that would enable both new discoveries and a

comprehensive survey of the physical and chemical processes at work on the outer planets: (a) broad spectral coverage for imaging, spectroscopy and occultations from the far-UV to the radio; (b) advanced instrumentation with improved sensitivity and resolution, both spectral and spatial; (c) synergistic science opportunities from the dual-spacecraft system (see §4.2.3.4); (d) long temporal baseline, combined with a large data volumes, for regular monitoring of the dynamic atmosphere from long approaches on the sunlit side of Jupiter (phase angles 70-75° on approach) and greater than two year orbital tours prior to satellite orbit insertion. The orbital tours are envisioned to sample a wide range of viewing geometries and allow frequent global mapping over a broad wavelength range. Taken together, JEO and JGO would offer a significant potential for Jupiter atmospheric science. In this section we describe the investigations, and how they contribute to the three Jupiter atmosphere objectives in §4.2.3.3.

Characterize the atmospheric dynamics and circulation of the Jupiter atmosphere.

- JA.1 Investigate the dynamics of Jupiter's weather layer.
- JA.2 Determine the thermodynamics of atmospheric phenomena.
- JA.3 Quantify the roles of wave propagation and atmospheric coupling.
- JA.4 Investigate auroral structure and energy transport.
- JA.5 Understand the interrelationships of the ionosphere and thermosphere.

Jovian dynamical studies require characterization of fluid flow through a variety of techniques. Discrete cloud tracers need to be tracked in the UV, visible and near infrared to measure tropospheric zonal and meridional

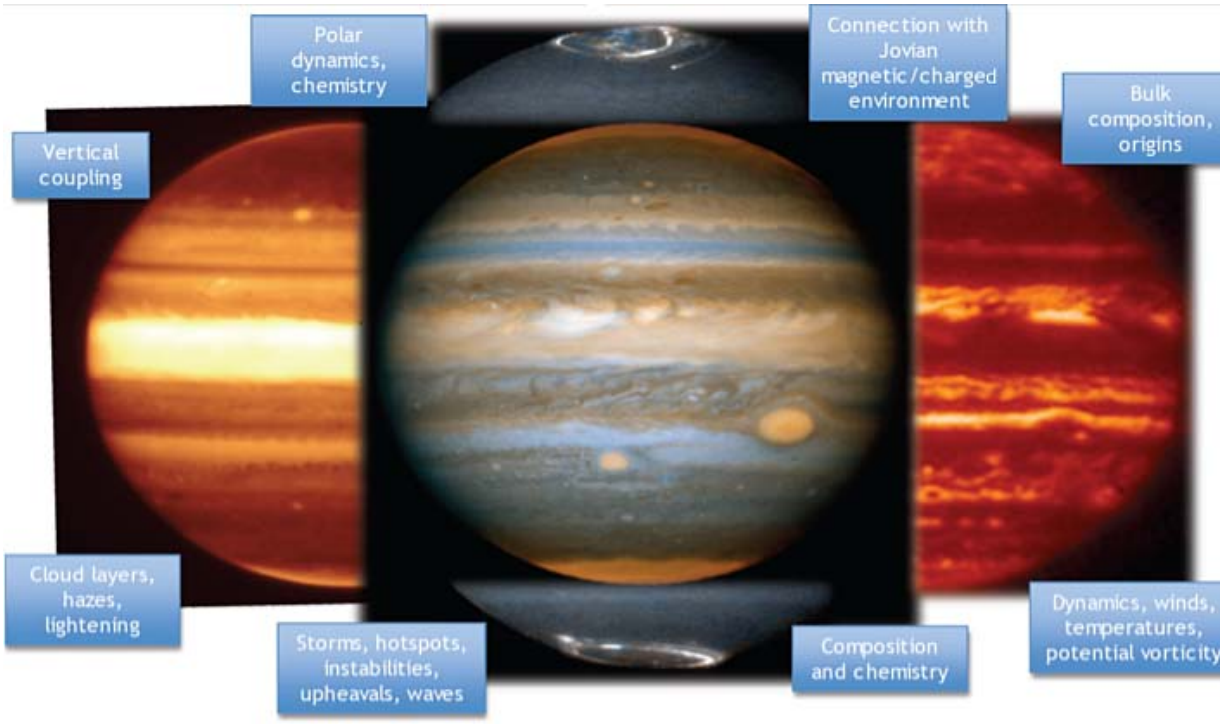

Figure 4-41. Examples of data needed to achieve Jupiter science objectives. Each image shows Jupiter's appearance at a range of different wavelengths, from visible for wind tracking (center, HST, credit: NASA/ESA/A. Simon-Miller/I. de Pater) to cloud properties in the near-IR (left, Gemini/NIRI image, credit: Gemini Observatory/AURA/L.N. Fletcher); thermal structure and chemistry in the mid-IR (right, credit: NASA/IRTF/G.S. Orton, 5 μm image) and auroral properties in the UV (top and bottom, credit: NASA/ESA/J. Clarke).

velocities, vorticity and eddy fluxes over a range of timescales. To determine the thermodynamic properties of the flow, it would be necessary to couple measured velocities with thermal-infrared characterization of the temperature and para-hydrogen distributions, vertical wind shear and potential vorticity (a quasi-conserved tracer of motion). Vertical and meridional transport of material could be assessed by mapping the distribution of dynamical tracers (cloud composition, volatiles and disequilibrium species like PH_3, AsH_3 and GeH_4 in the troposphere, hydrocarbons in the upper atmosphere), and by assessing vertically propagating wave activity. EJSM's high spatial resolution would also permit detailed mapping in the UV to IR of dynamical tracers in association with discrete features like thunderclouds, giant vortices, waves, instabilities and plumes. The spatiotemporal variability of these tracers could reveal the underlying mechanisms responsible for these features.

Measurements of lightning (spatial distribution, spectral energy distribution of the flashes, lightning temperature and global discharge rate) in individual convective cells enable constraining the energetics of the atmosphere at depth [*Little et al. 1999, Gierasch et al. 2000*], helping to distinguish between "shallow" and "deep" models for the origins of eddies, vortices and zonal jets. Furthermore, if the depth of the discharges is confirmed to be within the water cloud or below [*Little et al. 1999*] then tracking the motion and lifetimes of the lightning storms would provide an additional method of determining zonal wind speeds at depth. These investigations of Jupiter as a fundamental fluid dynamics laboratory would benefit from the long baseline and broad spectral range offered by EJSM.

Characterize the atmospheric composition and chemistry of the Jupiter atmosphere.

- JB.1 Determine Jupiter's bulk elemental abundances.
- JB.2 Measure the composition from the stratosphere to low thermosphere in three dimensions.
- JB.3 Study localized and non-equilibrium composition.
- JB.4 Determine the importance of moist convection in meteorology, cloud formation, and chemistry.

Spectroscopic observations in the UV, visible, near-IR, thermal-IR and sub-millimeter (JGO) are sensitive to a multitude of species (condensable volatiles, disequilibrium species, photochemical products) throughout the Jovian atmosphere. Near-IR (1- to 5-μm) spectroscopy would allow the mapping of compositional variability (NH_3, H_2O, PH_3, etc.) associated with discrete dynamical phenomena and evolving cloud structures to determine the importance of moist convection in cloud formation, lightning and chemistry. UV occultations could probe hydrocarbon distributions in the high atmosphere as a tracer of the circulation. Measurements at Sub-millimeter wavelengths could constrain the distribution of oxygenated species in the stratosphere (e.g., CO, H_2O) to measure the influx of exogenic material (e.g., from Io, interplanetary dust particles, asteroidal/cometary collisions). Thermal imaging would provide a means to study the distribution of tropospheric NH_3, para-hydrogen and, possibly, stratospheric ethane and acetylene. Finally, radio occultations would be sensitive to the vertical distribution of opacity sources (NH_3, H_2S) in the lower troposphere to the 2-3 bar level.

Characterize the atmospheric vertical structure.

- JC.1 Determine the three-dimensional structure from Jupiter's upper troposphere to lower thermosphere.
- JC.2 Explore Jupiter's interior density structure and dynamics below the upper troposphere.
- JC.3 Study coupling across atmospheric layers.

Jupiter's atmospheric structure from the lower troposphere to the ionosphere and thermosphere could be characterized by occultation studies and by exploiting the range of observational geometries (phase angles, emission angles) offered by the extensive tours. UV, visible, near-IR and thermal imaging and spectroscopy provide a means to study the vertical distribution of cloud and haze material. Measurements at radio, sub-millimeter and UV wavelengths could provide insight into the vertical wave activity at a wide range of latitudes and local times, to investigate their importance in the transport of energy between different levels (*e.g.,* is wave propagation the dominant cause of thermospheric heating?) and the relationship between gravity waves and the Quasi-quadrennial oscillation (QQO [*Leovy et al. 1991*]). Radio occultations would also allow the study of the vertical distribution of charged particles (electrons, ions) in Jupiter's ionosphere, to assess the interrelationship between the charged and neutral atmosphere and the connection with the magnetospheric environment (*e.g.* satellite footprints in the aurora). Energy transport mechanisms and aurora in Jupiter's polar regions would be studied via UV and IR imaging (*e.g.,* H_3^+ emission). Each of these measurements would help to reveal how Jupiter's dynamic atmosphere works as a coupled system, connecting the deep interior to the immediate planetary environment.

In summary, EJSM's Jupiter investigations have been designed to advance our understanding of three scientific themes—dynamics, chemistry and the vertical structure of the atmosphere. The results obtained by EJSM's could have far reaching astrophysical implications, serving as a paradigm for the processes at work in gas giant atmospheres in our solar system and beyond.

4.4 Dual Platform (JEO/JGO) Complementary and Synergistic Measurements

The simultaneous presence of the two EJSM spacecraft in the Jupiter system (Figure 4-42) creates opportunities for rich complementary and synergistic scientific investigations. Details of these would depend on the mission profiles and instrument complement of the respective spacecraft. Coordinated observations from two locations within the Jupiter system would significantly enhance the science return with respect to both mission elements taken individually. The joint timeline of the two spacecraft would be optimized to offer many opportunities of these kinds, combining remote sensing with *in-situ* measurements, or observations of the same target from different angles, wavelengths and resolutions. In this section, we discuss specific possibilities with respect to satellite science, structure and dynamics of dust and rings, magnetospheric processes and structure and dynamics of Jupiter's atmosphere.

4.4.1 Satellite Science

While the JEO concept is tailored for in-depth close orbital study of Europa, it would also perform several close fly-by observations of Io and the other Galilean satellites. JEO would cover the two inner satellites and their environments in greatest detail. In a complementary way, JGO is tailored for in-depth orbital study of Ganymede, providing a basis for detailed comparisons between Ganymede and Europa. It would also conduct a detailed study of Callisto during a series of

quasi-resonant orbits, providing multiple encounters with this satellite. JGO would cover the two outermost Galilean satellites, and the middle magnetosphere within which they are embedded.

During the initial phases of their missions—approach to Jupiter, orbital insertion, and a long Jovian orbital phase—both JEO and JGO would navigate inside the Jupiter system. Separate coverage of the system by the two platforms could be orchestrated in such a way as to maximize the total coverage.

Specific details of unique opportunities for satellite science using both spacecraft are described in the following sub-sections.

4.4.1.1 Satellite Mapping, Surface Properties, and Active processes

The ability to obtain global maps of the icy Galilean satellites is greatly enhanced by the presence of two spacecraft performing separated tours of the Jovian system. As an example, Figure 4-43 shows the potential for complementary science between JEO and JGO at Callisto. Imaging opportunities and coverage as a function of resolution are shown for each mission component on the same map. Each spacecraft would have similar remote sensing instrument capabilities but would have limited viewing geometries at various times in the Tour. Taken together, high and moderate resolution observing opportunities are uniformly spread across Callisto. The combined data set provides nearly full uniform coverage, which could only be achieved by both spacecraft working together.

The trajectories of the two EJSM spacecraft would provide the opportunity for JGO to obtain distant observations of Europa and Io. In a similar manner, JEO would view Callisto and Ganymede from a distance along with performing a number of close fly-bys. These would be valuable for enhancing overall EJSM science. For instance, low-spatial-resolution photometric and solar phase angle coverage should improve knowledge of the bolometric albedos of the satellites, thus improving understanding of their internal heat flow. Depending on instrumentation, JGO could improve the temporal resolution and spatial coverage for monitoring Io volcanism: large hot spots and plumes could be seen even with very low spatial resolution. Stereo imaging of plumes would provide a valuable constraint on plume dynamics. Outbursts on Io could be monitored by both spacecraft for increased coverage, as could plasma exchanges between

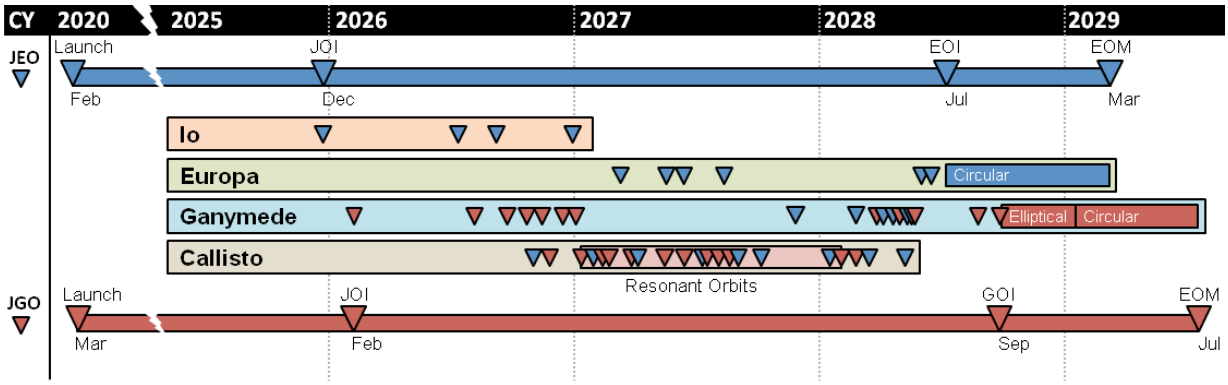

Figure 4-42. Notional timeline for the EJSM, assuming launches one month apart in calendar year 2020. JEO events are indicated by blue triangles, and JGO events by red triangles. Jupiter Orbit Insertion (JOI) is staggered in the depicted scenario. Satellite orbital phases and the JGO resonant orbits at Callisto are indicated by bars. The nominal End of Mission (EOM) is also indicated for both missions.

Jupiter and its four largest satellites.

4.4.1.2 Properties and Composition of Satellite Atmospheres

The combined JEO and JGO suite of instruments could enhance the spatial and spectral coverage of atmospheric measurements. Many diagnostic gaseous emission and absorption features are present in the UV, but several important features are present in the visible and IR as well. Synergistic measurements from the two spacecraft would allow for simultaneous observations in different wavelength regimes, providing unprecedented spectral coverage of the satellite atmospheres. Because isolated flybys of the moons would likely not provide full spatial coverage of the atmospheres, observations using the two spacecraft would enable greater coverage to understand atmospheric asymmetries.

For Io monitoring to investigate correlations between volcanic activity and atmospheric species, observation coverage and density are critical. Io is an ever-changing world, so the overall duration of EJSM would allow for increased temporal coverage in monitoring this volcanic world. Simultaneous imaging of Io in eclipse from the two spacecraft could provide unique information on the three-dimensional plasma interaction.

Temporal resolution is also important at Ganymede, which auroral emissions vary spatially and temporally. Shared observations of this unique phenomenon would probe both the atmospheric and magnetic characteristics of Ganymede.

The presence of two spacecraft in the Jovian system would allow the unprecedented opportunity for dual-spacecraft radio occultations of satellite ionospheres, to infer atmospheric conditions and study plasma interactions at a wide range of local times. Radio occultations involving the Earth are, in contrast, restricted to local times near 6 a.m. and 6 p.m., limiting study of the diurnal variability of the satellite atmospheres.

Deployment of two spacecraft in the Jupiter system simultaneously would also enable rapid follow-up on discoveries by one spacecraft with observations by the second spacecraft. For instance, if JEO were to discover outbursts in activity at Europa or Io, JGO could provide backup support with additional observational coverage, perhaps using a complementary set of instruments.

4.4.1.3 Geophysics

Several of EJSM's geophysical investigations would be enhanced by the presence of multiple spacecraft. These investigations would be particularly valuable for Ganymede and Callisto, which would have multiple flybys from both JEO and JGO. The most direct application is determination of gravity fields by Doppler tracking of flybys. Multiple spacecraft could improve coverage by distributing closest approach positions more widely over the satellite and by altering the geometry of flybys, depending on the orbit geometries of the spacecraft. This could help to break degeneracies in the inversion process, potentially allowing the determination of gravity coefficients at degrees larger than 2. Multiple flybys of satellites at different orbital phases may also measure the tidal response, thereby constraining the internal rheological structure and possibly confirming the presence of liquid water oceans. Accurate determination of the rotational state and, potentially, measurement of the rotational dynamics could be achieved through tracking and geodetic (control network) measurements through observations of the same locations on the surface at multiple times.

Multi-point magnetic field measurements between the Europa and Ganymede orbiters could help to separate the influence of Jovian

magnetospheric dynamics from the magnetic response of Europa. Phase coverage of induced magnetic field measurements in the other satellites could also be increased by multiple spacecraft encountering the satellite at different phases of Jupiter's magnetic field, potentially allowing the determination of the induced response at multiple periods. Similarly, JEO flybys of Ganymede during JGO orbit would aid in assessing the interaction of the Jovian field with the intrinsic Ganymede field.

Another synergy that could be achieved from the presence of multiple spacecraft in the system is the potential for extremely accurate spacecraft-to-spacecraft positioning by single-beam interferometry. This technique has the potential to improve satellite ephemerides, though it requires significant antenna resources on the ground.

4.4.1.4 Structure and Dynamics of Dust and Rings

A key aspect to understanding the Jovian ring system is to determine the nature of the embedded population of "parent bodies." The main ring is dominated by dust grains, which have brief lifetimes due to solar radiation pressure and interactions with the Jovian plasma and magnetosphere. The grains must be replenished continuously from larger bodies, which contain most of the system's mass. The tiny ring-moons Adrastea and Metis surely contribute to the dust, but probably only at the level of ~10%. Based on photometry, an additional population of parent bodies, must be distributed throughout the system. We would never understand the origin of the Jovian ring system without knowing further details of the ring's reservoir of mass.

Photometry provides a crude measure of the total cross-sectional area of the parent bodies, but not their sizes. Imaging may reveal the largest parent bodies, but only radio occultations could characterize the population as a whole, owing to its lack of interaction with the dust.

The only prior radio occultation of the Jovian ring, by Voyager 1 [*Tyler et al. 1981*], returned negative results. With an optical

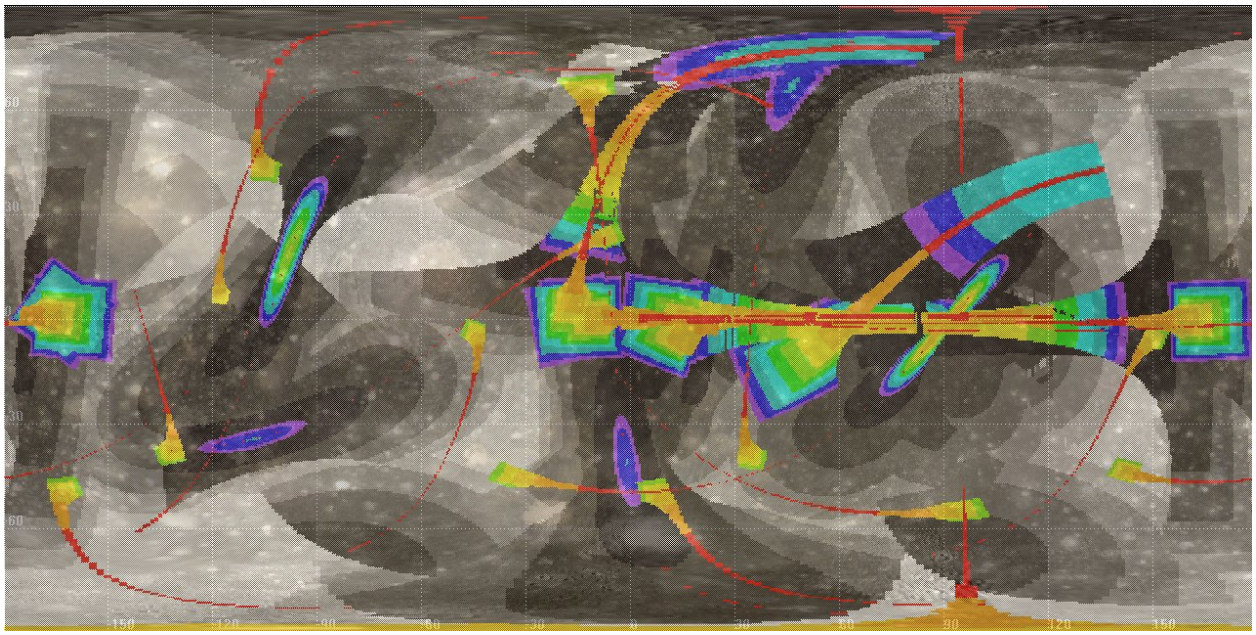

Figure 4-43. Example camera coverage opportunity on Callisto from JEO and JGO.

depth ~10^{-6}, the ring is too faint for detection in spacecraft-to-earth occultations. However, dual radio occultation capabilities of JEO and JGO make this detection possible. Using two or more wavelengths, the size distribution of the parent population could be determined. Radio occultations would also provide details of the ring structure, including possible vertical bending, with precision at least 100 times finer than imaging.

To characterize the system fully, several occultations would be required. The ideal occultation track crosses the ring ansa slowly, radially, and at a small opening angle (to enhance the optical depth along the line of sight). Occultations at several different times and opening angles would be needed to study packing density, microstructure, and possible temporal variations within the system. Most occultations need only cover the range of a few thousand kilometers around the orbits of Adrastea and Metis, because this is where most parent bodies appear to reside. However additional occultations, covering portions of the halo and gossamer rings, would be desirable to search for any bands of parent bodies orbiting at unexpected locations.

4.4.2 Magnetospheric Processes

In the Jupiter system, a wealth of opportunities exists for exciting synergistic observations in the field of magnetospheric science. A major problem in understanding the structure and dynamics of the Jovian magnetosphere is a general lack of simultaneous field and plasma measurements from multiple spacecraft. With observations from a single spacecraft, it is not possible to distinguish between temporal and spatial gradients in the magnetosphere. Temporal changes in the structure, shape and size of the magnetosphere occur in response to the variable buffeting by the solar wind and variable input of mass from interior sources such as Io's torus maintained by its volcanic activity and small but appreciable mass-loading near Europa from surface/plasma interaction. Magnetospheric spatial gradients are known to occur naturally in plasma density, current sheet thickness and electrical current density over local time and radial distance.

Simultaneous measurements from two spacecraft would help distinguish between spatial and temporal changes and would help to better understand the complex processes in the magnetosphere of Jupiter (Figure 4-44). Here, a number of different synergistic strategies are discussed for improved understanding of the structure and dynamics of Jupiter's magnetosphere.

EJSM would perform multi-point measurements

One synergistic opportunity is to investigate how disturbances in the solar wind affect the Jovian magnetosphere. For example, shock passage over the Jovian magnetosphere would influence plasma flow, boundaries, and aurora. A synergistic scenario exists whereby one spacecraft in the solar wind (on approach to Jupiter) would detect the shock and measure its properties, while the other spacecraft, in orbit about the planet, measures the Jovian aurora and the effects of the IMF and solar wind dynamic pressure changes on the middle and outer magnetosphere.

The presence of two spacecraft in the Jovian system would enable observations of the dynamic coupling between different magnetospheric regions (e.g., injections, reconnection) and could provide a global perspective on 3-day and other system periodicities. Simultaneous two point monitoring of reconnection in Jupiter's magnetotail by dual spacecraft, located in the pre-midnight and post-midnight sectors, would help in understanding whether magnetotail reconnection is global or local in scope, and whether, as some models predict, the reconnection line is slanted in such a way that it occurs close to Jupiter in the dawn sector but recedes away from the planet in the dusk

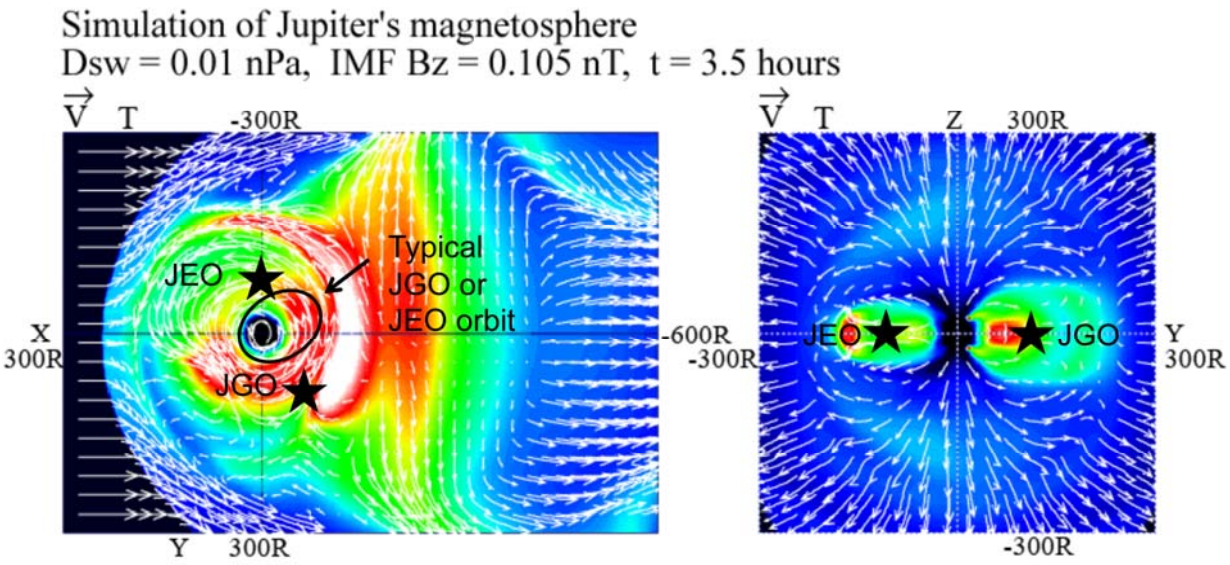

Figure 4-44. Temperature per AMU and plasma flow vectors in the dawn-dusk meridian plane (right) and equatorial plane (left). The figure shows the results for a solar wind dynamic pressure of 0.01 nPa and 0.105 nT IMF. The color ranges refer to increasing temperature values in KeV (blue through to red). The white lines are flow streamlines. Superposed are example trajectories for the JGO or JEO spacecraft. Example locations of the individual spacecraft (shown by stars) emphasise the importance of dual-spacecraft measurements, given the difference in the environment sampled simultaneously by each spacecraft at different local times. Adapted from *Fukazawa et al.* [2005].

sector. Similarly, if one spacecraft is in the outer part of the magnetosphere while the other is in the inner magnetosphere, it would be easier to study transport processes between different regions.

Synergistic opportunities for studying Ganymede's magnetosphere would occur with JGO in orbit around Ganymede while JEO performs Ganymede flybys (outside in the Jovian magnetosphere) (Figure 4-45). Such a scenario would allow simultaneous internal and external observations of Ganymede's magnetosphere (e.g., boundaries, convection, reconnection conditions) and would enable the study of the response of the small magnetosphere of Ganymede to changes happening in the Huge Jovian magnetosphere. Connections could also be made between in-situ observations of the plasma environment and changes in the Ganymede aurora.

EJSM would provide enhanced capability to address magnetospheric dynamics

Transport processes in Jupiter's magnetosphere are complex. Simultaneous measurements in parallel from different locations in local time and/or distance would help to study particle drifts, diffusion processes, interchange motion, flux tube interchange or acceleration processes during magnetospheric reconfiguration events.

Dynamics in plasma and energetic particle fluxes in the vicinity of the moons and the visible response in Jupiter's atmosphere could be studied and would significantly enhance our understanding of the dynamics.

EJSM would provide local and global views of Jupiter's magnetosphere with remote-sensing and in-situ measurements in parallel

A local view of the magnetosphere in the vicinity of a moon is provided through the study of plasma transport between the moon and the magnetosphere while both spacecraft orbit their respective moons. The global view

of the magnetosphere includes the investigation of magnetodisc dynamics and large-scale transport while both spacecraft travel through the Jovian magnetosphere during Jupiter orbit.

A combination of local and global views would be possible by studying auroral processes where the coupling processes are investigated, through remote sensing of auroral emissions in parallel with particle and field measurements, between Jupiter and the satellite (moon's footprints), Jupiter and the magnetodisc (main oval caused by corotation breakdown of the magnetodisc).

Multispacecraft views could also entail JEO investigating the Io and Europa tori through in situ particle and field measurements while JGO measures perturbations to the system through remote sensing.

EJSM would have the capability to study the entire electromagnetic environment of Jupiter

The ability to sense particles, fields and plasma waves would enable studies of all aspects of radio emission: UV aurora, ionospheric currents, magnetic field, auroral footprints, torus emissions, as well as emissions from the mini-magnetosphere of Ganymede, the internal inductive layers of Europa and Ganymede. Dual-platform measurements would enable direct observation

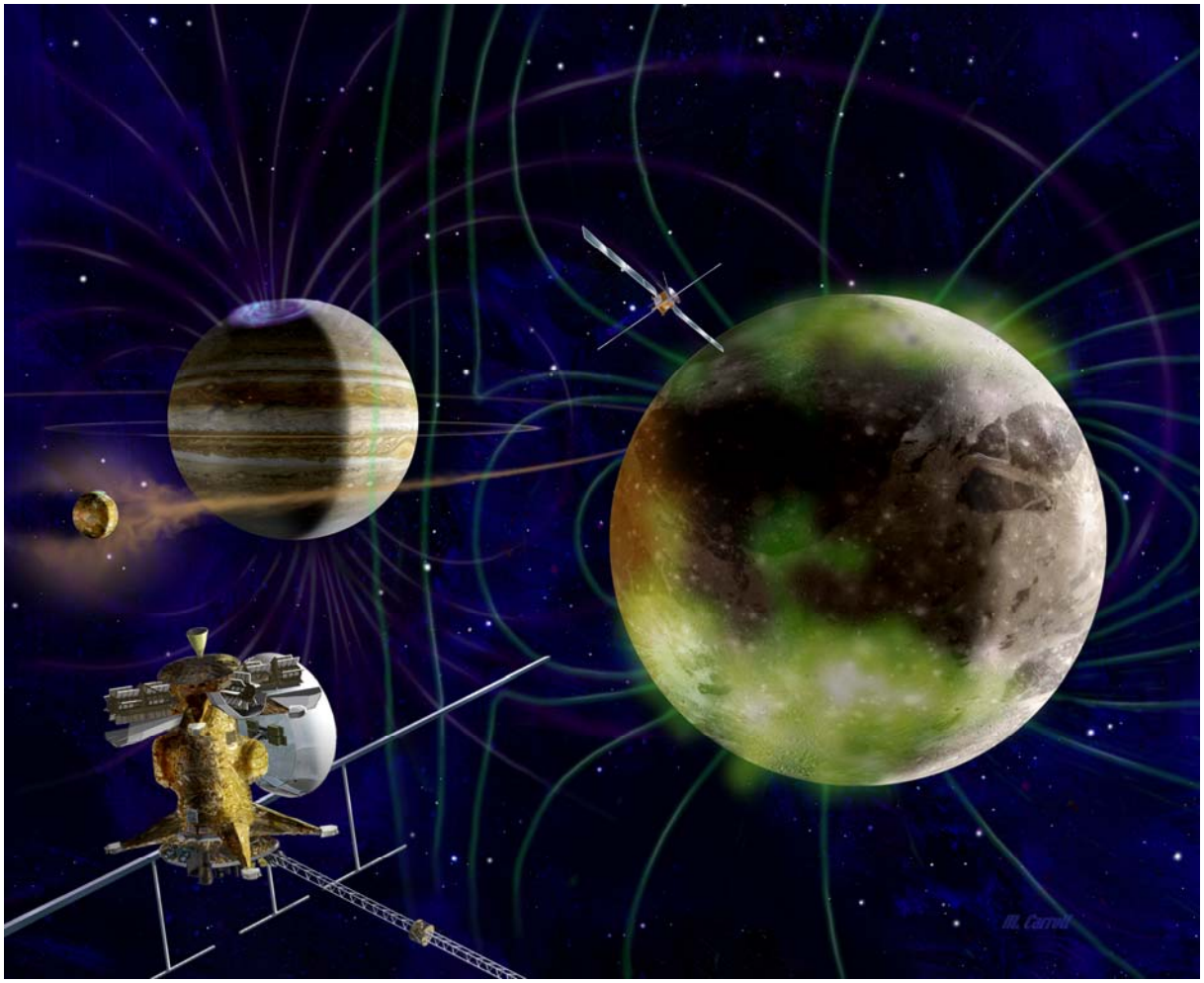

Figure 4-45. Synergistic measurements of Ganymede's magnetic field and aurora are enabled by the two EJSM flight systems: JGO could acquire data while within the magnetosphere of Ganymede, as JEO would measure the influence of the Jovian magnetic field.

of satellite-magnetosphere interactions through simultaneous radio emission measurements at multiple locations.

4.4.3 Structure and Dynamics of the Jupiter Atmosphere

The presence of two spacecraft in the Jovian system would provide an unprecedented opportunity to study Jupiter's atmosphere and local environment from multiple vantage points. For almost all of the Jupiter scientific objectives, the dual spacecraft system permits both synergistic and complementary atmospheric studies.

4.4.3.1 Structure of the Neutral Atmosphere, Gases and Ionosphere

The temperature, pressure, and density structure of the neutral atmosphere, the abundance of microwave absorbing gases, as well as the energetic electron distribution of the ionosphere, are typically probed through Earth-based monitoring of attenuation and frequency changes of a spacecraft signal as it passes behind the limb of a planet. For the outer planets, this means that spacecraft-to-Earth occultations only sample the dawn and dusk terminators, and only a narrow range of local times has ever been sampled. The neutral atmosphere is not expected to respond quickly to these local changes in insolation, but the charged ionosphere may exhibit significant variability as a function of local time. EJSM would provide the capability for spacecraft-to-spacecraft occultations, permitting sampling of the full range of local times on Jupiter for the first time, from orbital geometries that are unique to EJSM (Figure 4-46).

The presence of two spacecraft performing Earth and spacecraft occultations would dramatically increase the number of possible occultations in the 2+ year nominal tours of JGO and JEO. Frequent sampling of the same latitude at regular intervals would reveal the temporal variability of the atmospheric structure from the deep troposphere to the thermosphere. In particular, vertically propagating waves that evolve with time are thought to dominate energy and momentum transport between different vertical layers, and understanding the extent of this vertical coupling is a key goal for EJSM's study of Jovian dynamics and circulation.

JGO-Earth occultations would occur only in the southern hemisphere, clustered at low and high latitudes. JEO-Earth occultations would cover low to mid-southern latitudes. Together, planned occultations by the two spacecraft cover nearly the entire range of latitudes on the planet and offer significant northern hemisphere coverage (Figure 4-46).

The much shorter spacecraft-to-spacecraft distance compared with spacecraft-to-earth distance would result in a significant increase in occultation signal-to-noise ratio (SNR). The increase varies from about one to three orders of magnitude, depending on the distance between the two spacecraft, with commensurate enhancement in measurement sensitivity and dynamic range. On-board capabilities required for spacecraft-to-spacecraft occultations (RF receivers) also enable comparable increases in measurement SNR of "uplink" Earth occultations conducted using transmission from the Earth (of RF power up to 20 kW, from one of many Deep Space Network stations) and reception on-board the spacecraft.

4.4.3.2 Dynamics and Vertical Structure of the Atmosphere

To fully understand the dynamics and vertical structure of the atmosphere we must study their evolution in time over many wavelengths and, if possible, viewing angles. Ground-based and spacecraft measurements usually rely on the cloud particles observed at different times to act as true tracers of the flow, and on the intrinsic nature of the particles themselves (their reflectivity, size and shape), to turn two-dimensional data into a four-dimensional

understanding. There are two distinct regimes of study under this category that could benefit from two spacecraft: atmospheric structure modeling and dynamical tracking.

For atmospheric structure modeling, it is typically necessary to observe the same cloud features as they appear at different emission angles. However, clouds are ever morphing into new configurations; coalescing, diffusing, and changing in the zonal wind shear. During the time elapsed between required multiple viewing geometries one cannot assume static atmospheric structure. In addition, structure modeling is dependent on *a priori* assumptions about cloud geometry and particle properties, and without enough data, some parameters are not uniquely retrieved. EJSM would provide a unique opportunity whereby two spacecraft could simultaneously view the same atmospheric feature from vastly different viewing geometries. For example, both narrow angle observations (e.g., looking in detail at the turbulence associated with a storm or plume) and contextual imaging could occur simultaneously, and such observations allow us to study the coupling between events over large horizontal distances. Ideally, with an identical instrument, or at least well cross-calibrated instruments, on each spacecraft, the same feature could be viewed in a sort of stereo, where one could produce a nadir view and the other at high emission angle. This would improve the accuracy of vertical cloud retrievals.

For dynamical studies, cloud motions are usually tracked either "intensely" with several time steps over 30 minutes to a few hours, or with separations of one Jovian rotation to allow a longer time base for motion to become apparent. Features evolve on timescales of minutes to days, however, showing divergence or convergence related to vertical motions, large-scale rotation, and lateral motions independent of the zonal flow field. With two

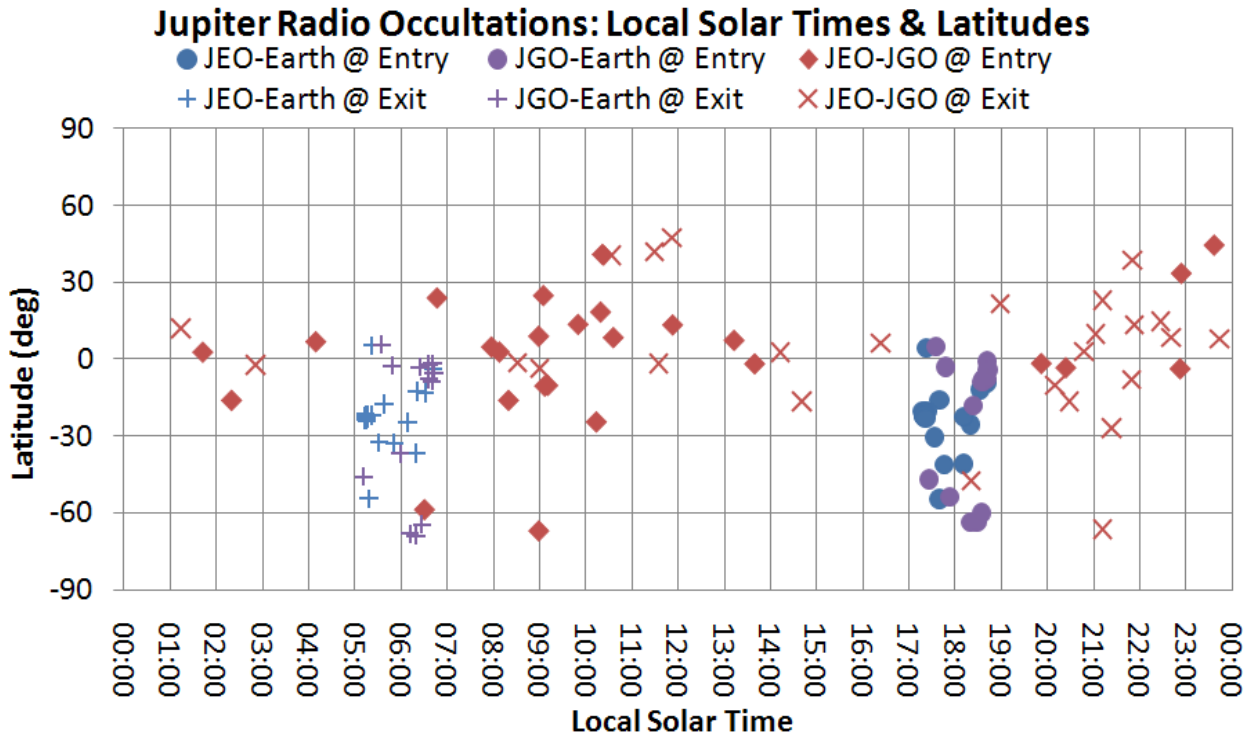

Figure 4-46. JEO-to-JGO communication would allow for radio occultations of Jupiter at latitudes and local solar times not possible with only spacecraft-to-Earth communication.

spacecraft, a cloud feature, such as a convective thunderstorm or vortex, could be observed much more thoroughly on short timescales and continuously tracked for longer periods to better measure three-dimensional flow. This is particularly true if we take Jupiter's ten-hour rotation into account: from a single spacecraft, a feature could only be tracked for a 5-hour period, with a 5-hour wait before it could be reacquired. The added flexibility of two orbiting platforms would allow regular wind and compositional measurements over much longer periods.

4.4.3.3 Global Atmospheric Circulation

Over the course of the mission, the two spacecraft would work together to sample the full phase angle coverage for scattering of Jovian clouds and hazes. By sampling the full phase curve (rather than the low phase angles that could be observed from Earth), we may break degeneracy in cloud structure retrievals to extract information on optical properties, such as scattering, particle shapes and sizes, optical depth and, ultimately, the composition of the Jovian clouds and hazes, which remain largely a mystery.

If different instruments on a single spacecraft were unable to operate together, for whatever reason (data rates, different fields of view, etc.), then the presence of similar instruments on the second spacecraft would provide added coverage. For example, visible imaging from one platform could complement thermal and compositional mapping from the second. As the troposphere and middle atmosphere (stratosphere, mesosphere) are expected to act as tightly coupled systems, the simultaneous study of both regimes would greatly increase the potential science return relative to either dataset in isolation. Similarly, detection of lightning activity by one spacecraft could be simultaneously monitored by remote sensing instruments on the other. Finally, the interaction of the Jovian atmosphere with the immediate planetary environment could also be studied if magnetospheric and plasma instruments on one spacecraft observe phenomena in the magnetodisc that have direct manifestations on the upper atmosphere being studied by the second spacecraft.

Lastly, JEO and JGO synergies could be found where the two spacecraft are dissimilar. The Jovian tour geometries are different for the two spacecraft (a product of the flybys necessary to reach their satellite targets), with JGO providing more opportunities for long-range continuous monitoring than JEO. The combination of EJSM elements working together would add considerable flexibility to the mission design while still meeting Jupiter science objectives. JGO and JEO could ultimately contribute different instruments to the mission (e.g., sub-mm instrumentation on JGO; thermal infrared instrumentation on JEO), which would work together to study Jupiter simultaneously across a broad wavelength range (from the radio to the UV) with a range of spatial and spectral resolutions.

5 SCIENCE IMPLEMENTATION

5.1 JEO Science Implementation

5.1.1 JEO Model Payload

To demonstrate that the science objectives of the JEO component of EJSM could be achieved with the types of instruments currently available, the JJSDT assembled a model payload consisting of ten instruments along with use of the spacecraft X-band and Ka-band telecommunications systems for radio science. While all instruments are assumed to be independent "standalone" instruments, mechanical integration of instrument electronics into a shared Science Electronics Chassis (SEC) is assumed here as a means to reduce radiation shielding mass and to facilitate efficient payload thermal management.

JEO's notional instrumentation consists of a Laser Altimeter, an Ice Penetrating Radar, a Visible-Infrared Spectrometer, an Ultraviolet Spectrometer, a Thermal Instrument, a Narrow-Angle Camera, a Camera Package containing medium-angle and wide-angle cameras, an Ion and Neutral Mass Spectrometer, a Magnetometer and a Particle and Plasma Instrument. The specifications for each instrument are discussed in the sections that follow. Table 5-1 and Table 5-2 summarize the instrument specifications and resource requirements of the model payload.

Table 5-1. JEO Model Payload Resource Requirements

Instrument	Acronym	Unshielded Mass (kg)	Shielding Mass (kg)	Total Mass (kg)	Operating Power (W)	Instantaneous Telemetry Bandwidth (kbps)	Science Electronics Chassis Board Count
Laser Altimeter	LA	5.0	4.7	9.7	15	2	2
Ice Penetrating Radar	IPR	26.0	5.0	31.0	45	140	6
VIS-IR Spectrometer	VIRIS	15.7	11.8	27.5	25	11,400	3
UV Spectrometer	UVS	6.4	3.1	9.5	5	10	1
Ion and Neutral Mass Spectrometer	INMS	13.0	2.1	15.1	33	2	2
Thermal Instrument	TI	3.7	1.3	5.0	5	15	1
Narrow-angle Camera	NAC	10.4	3.0	13.4	14	10,700	2
Camera Package (MAC + MAC)	WAC	2.3	1.5	3.8	6	213	1
	MAC	2.6	1.5	4.1	7	1,065	1
Magnetometer	MAG	3.2	0.0	3.2	4	4	1
Particle and Plasma Instrument	PPI	7.6	8.8	16.4	13	2	2
Science Electronics Chassis		10.0	16.6				
TOTAL ALL INSTRUMENTS		105.9	59.4	165.3	172		22
TOTAL ALL INSTRUMENTS + 30% contingency				214.9	224		

Note: Resource requirements for the Ultra-Stable Oscillator and the Ka-band Translator used for radio science are carried as part of the spacecraft telecommunications system.

Table 5-2. JEO Model Payload Specifications

Acronym	Characteristics	Similar Instruments
LA	**Time-of-Flight Laser Rangefinder** **Transmitter:** 1.064 μm laser **Detector:** Avalanche Photodiode **Resolution:** better than 1 m vertical **Spatial:** 50 m laser spot size, 26 Hz pulse rate	**NEAR NLR** **MESSENGER MLA** **LRO LOLA**
IPR	**Dual-Mode Radar Sounder** **Shallow Mode:** 50 MHz with 10 MHz bandwidth **Vertical Depth:** ~3 km **Vertical Resolution:** 10 meters **Deep Mode:** 5 or 50 MHz with 1 MHz bandwidth **Vertical Depth:** ~30 km **Vertical Resolution:** 100 meters	**Mar Express MARSIS** **MRO SHARAD**
VIRIS	**Pushbroom Imaging Spectrometer** **Detector:** two HgCdTe arrays **Spectral range:** 400 to > 5200 nm **Spectral resolution:** 5 nm from 400 to 2600 nm **Spectral resolution:** 10 nm from 2600 to 5200 nm **FOV:** 9.2 deg cross-track **IFOV:** 0.25 mrad **Spatial Resolution:** 25 m from 100 km orbit **Articulation:** Along-track scan mirror	**MRO CRISM** **Chandrayaan MMM**
UVS	**Grating Spectrometer + High-Speed Photometer** **Detector:** MCP + position sensitive anode **Format:** 1024 spectral × 64 spatial pixels **Spectral range:** 70–200 nm **Spectral Resolution:** 0.5 nm **Spatial Resolution:** 100 m from 100 km orbit **FOV:** 3.7 deg cross-track **IFOV:** 1 mrad **Articulation:** 1-D scan system for stellar occultations	**Cassini UVIS** **New Horizons Alice**
TI	**Temperature Sensing Thermopile Array** **Detector:** Thermopile array with filters **Detector Configuration:** 21 pixels cross-track, 6 bands **Spectral Bands:** 8-20 μ, 20-100 μ, 21 μ, 28 μ, 40 μ, 17 μ **Spatial Resolution:** 250 m **IFOV:** 2.5 mrad **Temperature Range:** >160K to 80K **Resolution:** 2K	**MRO MCS** **LRO Diviner**
NAC	**Pushbroom and Framing Imager** Panchromatic Pushbroom Imager + Color Framing Imager **FOV:** 1.2° **IFOV:** 0.01 mrad IFOV **Spatial Resolution:** 1 m from 100 km orbit **Detector:** CMOS array or CCD array + line array **Detector Size:** 2048 pixels wide **Color Bands:** 9 plus panchromatic **Mechanism:** Filter wheel	**New Horizons LORRI**

Acronym	Characteristics	Similar Instruments
WAC+MAC	**WAC - Pushbroom Imager with fixed color filters** **FOV:** 58° line scan, **IFOV:** 1 mrad **Spatial Resolution:** 100 m from 100 km orbit **Detector:** CMOS or CCD line arrays (4) **Detector Size:** 1024 pixel line arrays (4) **Color Bands:** <450 nm, 630-670 nm, >930 nm **MAC - Panchromatic Pushbroom Imager** **FOV:** 11.7 deg line scan **IFOV:** 0.1 mrad **Spatial Resolution:** 10 m from 100 km orbit **Detector:** CMOS or CCD line array **Detector Size:** 2048 pixels	**MRO MARCI** **MESSENGER MDIS** **New Horizons MVIC**
INMS	**Reflectron Time-of-Flight Mass Spectrometer** **Mass Range:** 1 to > 300 Daltons **Mass Resolution:** > 500 **Pressure Range:** 10^{-6} to 10^{-7} mbar **Sensitivity:** 10^{-4} A/torr **FOV:** 10 × 40 deg	**Rosetta ROSINA RTOF**
MAG	**Dual 3-axis Fluxgate Magnetometer** **Boom:** 10 m **Sensor Location:** 5-m and 10-m from S/C **Dynamic Range:** 3000 nT **Sensitivity:** 0.1 nT **Sampling Resolution**: 0.01 nT **Maximum sampling rate:** 32 Hz	**MESSENGER MAG** **Galileo MAG**
PPI	**Plasma: Top Hat Analyzer** **Energy Range:** 10 eV to 30 KeV electrons **Energy Range:** 10 eV to 30 KeV ions with composition **FOV:** 360° × 90° **Particles: Puck Analyzer** **Energy Range:** 30 KeV to 1 MeV electrons **Energy Range:** 30 KeV to 10's of MeV ions **FOV:** 120° × 20° **High Energy Electrons: Omnidirectional SSDs** **Energy Ranges:** >2 MeV, >4 MeV, >8 MeV, >16 MeV	**DS1 PEPE** **MESSENGER FIPS** **New Horizons PEPSSI** **Juno JEDI**
RS	**Ka-band Transponder** **Doppler Accuracy:** 0.01 mm/s **Integration Time:** 60 seconds for stated accuracy **Ultra Stable Oscillator** **Stability:** 2×10^{-13} **Timescales:** 1 to 100 seconds for stated stability	**Cassini** **Juno** **New Horizons** **GRAIL**

To determine the instrument specifications the SDT translated the JEO science requirements into measurement requirements (Foldout 1), which were further translated into specific sensitivity and resolution requirements. The instrument resource allocations were based on those of previous instruments with adjustments for radiation shielding and for partitioning of instrument electronics to make use of the Science Electronics Chassis.

5.1.1.1 Laser Altimeter

The notional JEO Laser Altimeter (LA) is a simple instrument tailored to measure topographic differences at cross-over points from globally distributed topographic profiles with better than or equal to 1 m vertical accuracy (1 m rms in range to the same spot). The LA concept would consist of a diode-pumped Cr:Nd:YAG Q-switched laser transmitting at 1.064 μm, a reflective receiver telescope, a linear-mode avalanche photodiode (APD) detector, and time-of-flight (TOF) sensing electronics. From a 100 km orbit with a 1300 m/s ground track rate, a 0.5 mrad beam expander produces a single 50 m laser spot while a 26 Hz laser pulse rate provides contiguous spots and 50 m along-track resolution. With each orbit crossing every previous orbit twice, in the course of 60 days over 1 million points are available for cross-over analysis.

Instrument performance and resource estimates for the notional LA are based on the laser transmitter subsystem of LRO LOLA and scaling of the receiver subsystem of NEAR NLR. A preliminary link analysis indicates that a 2.7 mJ transmitter (consistent with that of LRO LOLA) at a range of 200 km with a surface albedo of 67% at Europa requires an unobscured collecting area of ~100 cm^2 (modestly larger than NLR). With use of an Ultra-Stable Oscillator (USO) and radiation-hardened TOF ASICs, the LA range error budget is expected to be dominated by spacecraft orbit knowledge errors and spacecraft pointing angle uncertainty rather than instrument performance. The expected performance of the JEO spacecraft (0.25 m radial orbit knowledge (with Ka-band) and 0.10 mrad pointing uncertainty) allows the notional LA to meet the 1 m rms vertical accuracy requirement.

The laser transmitter and optical receiver are assumed to be located on the nadir-facing deck of the spacecraft and would be co-boresighted with the other JEO remote-sensing instruments. The laser transmitter power supply, TOF electronics, system controller, and spacecraft interface electronics are assumed to be packaged as two 6U cPCI boards located in the shielded Science Electronics Chassis.

The LA is assumed to have a single operating mode with a variable range gate used to accommodate changes in JEO orbit height. The notional APD detector is susceptible to background radiation, which could create transient signals larger than those produced by the optical return. Significant radiation shielding (*e.g.,* 1-cm Ta) to reduce flux and tight range gate selection to mask transients would be required for successful mitigation of transient radiation noise. The large number of orbital crossing points mitigates the impact of individual range measurements that may be corrupted despite robust shielding and range gating.

5.1.1.2 Ice Penetrating Radar

The notional JEO Ice Penetrating Radar (IPR) is conceived as a dual-frequency sounder. The higher-frequency band (nominally 50 MHz with 10 MHz bandwidth) is required to provide high spatial resolution (footprint and depth) for studying the subsurface above 3 km depth at high (10 m) vertical resolution. The low-frequency band (nominally 5 MHz with 1 MHz bandwidth) is required to search for the ice/ocean interface on Europa or the hypothesized transition between brittle and ductile ice in the deep subsurface at a depth of up to 30 km (and a vertical resolution of 100 m). This band mitigates the risks posed by the unknown subsurface structure both in terms of unknown attenuation due to volumetric scattering in the shallow subsurface and thermal/compositional boundaries that may be characterized by brine pockets. Additionally, the low-frequency band is less affected by surface roughness which could reduce the coherence of the reflected echo and potentially

increase the clutter noise. However, because the low-frequency band has to compete with the Jupiter noise within the radar band when operating on the Jovian side of the moon, it is necessary to increase the radiated power compared to the MARSIS and SHARAD radar sounders currently deployed for subsurface studies of Mars. The Jupiter noise should not impact the radar performance on the anti-jovian side of Europa and the noise is expected to be transient even in the Jovian side.

The notional IPR uses a dual antenna system consisting of a nadir-pointed 50 MHz dipole array with a backing element that also serves as a dipole antenna for the 5 MHz system. Because this instrument is a depth sounder operating at relatively low frequencies and using a dipole antenna, the field of view is very wide and there are no strict pointing requirements. A 30 m dipole similar to those used by MARSIS and SHARAD is baselined. Deployment releases the folded antenna elements in the nadir direction and is baselined for early in the mission before the magnetometer boom is deployed.

The IPR transmitters and matching network are located close to the antenna array on the nadir-facing deck of the spacecraft. The receivers, digital processing electronics, and power supplies are assumed to be packaged as six 6U cPCI boards located in the shielded Science Electronics Chassis.

The IPR is assumed to have three operating modes. The first is the raw data mode where a burst of unprocessed data is collected over a short orbit segment for high-resolution focused processing on the ground. Due to the high data rate, this mode would be used only for instrument check-out and calibration and over high-value science targets, using full power for several minutes at each target and producing up to 900 Mb of data. The second mode is the shallow investigation mode, in which the radar provides high-resolution (10 m) range data over short receive windows (less than 3 km depth targets). The third mode is the deep investigation mode, which has a relatively lower range resolution (100 m) but could investigate the subsurface to a depth of 30 km. Both the shallow investigation mode and the deep investigation mode employ onboard processing (a combination of range compression, pre-summing, Doppler filtering, data averaging, and resampling) internal to the IPR to reduce the output data rate.

5.1.1.3 VIS-IR Spectrometer

The notional JEO VIS-IR Spectrometer (VIRIS) is a pushbroom imaging spectrometer with broad wavelength coverage, high spectral and spatial resolution, and flexible internal processing modes to support a variety of surface composition objectives. Two primary modes of operation are baselined for VIRIS. The targeted mode uses target motion compensation (via a scan system) and the full spectral and spatial resolution of the instrument to generate high-resolution data products over limited, selected areas while in Europa orbit and during flybys. Full resolution is specified as 25 m (spatial) and 5 nm (spectral) and from 0.4- to 2.5-μm and 50 m (spatial) and 10 nm (spectral) and from 2.5- to 5.2-μm. The mapping mode employs data processing (spectral binning, spectral editing, spatial binning, and spatial editing, etc.) within the instrument to produce lower-resolution data products matched to the constraints upon JEO downlink telemetry bandwidth.

The notional VIRIS is a single optic, dual spectrometer, dual detector system with an along-track scan system that enables extended exposure times for high-resolution targeted observations. A 0.25 mrad IFOV meets the requirement for a 25-m pixel footprint from the 100-km Europa orbit for the short wavelength detector. Fast relay optics implementing a 2:1 focal reduction produce a

0.50 mrad IFOV and 50 m pixel footprint from the 100 km orbit for the long wavelength detector. The notional detectors are 640 × 480 HgCdTe arrays with cutoff wavelengths adjusted as required for each detector. Use of 640 cross-track pixels on the short-wavelength detector and 320 pixels on the long-wavelength detector results in a 9.2° instrument FOV. Spectral resolution of 5 nm from 0.4 to 2.6-μm requires the use of 440 columns on the short-wavelength detector, while spectral resolution of 10 nm from 2.6- to 5.2-μm requires the use of 260 columns on the long-wavelength detector.

The notional VIRIS is capable of a signal to noise ratio of greater than 50 at 5 μm for full resolution targeted observations assuming scan system enabled exposure times of ~150 ms, barring noise induced by transient radiation. While longer exposure times enabled by target motion compensation could be used to increase the SNR, longer exposure times also increase the vulnerability to noise induced by background radiation. Analysis indicates that the equivalent of 1-cm of Ta shielding is required to mitigate transient radiation noise to an acceptable level, creating a significant implementation challenge for VIRIS.

The VIRIS scan system, optics, spectrometers, detectors, and detector electronics are assumed to be located on the nadir-facing deck of the spacecraft. The field of regard of the scan system includes nadir, allowing observations while co-boresighted with the other JEO remote sensing instruments. A relatively large passive radiator on the anti-sunward side of the spacecraft is assumed for detector cooling (~80 K for the long-wavelength detector and ~160 K for the short-wavelength detector). Interface electronics, pixel processing and data compression electronics (for 2 detectors), system controller, scan system electronics and power supplies are assumed to be packaged as three 6U cPCI boards located in the shielded Science Electronics Chassis.

5.1.1.4 UV Spectrometer

The notional JEO Ultraviolet Spectrometer (UVS) would use stellar occultations to characterize the structure, composition, variability, and dynamics of Europa's tenuous sputter-induced atmosphere and investigates Ganymede's aurorae, Io's torus, and the sources and sinks of Io's crustal volatiles and atmosphere. UVS consists of a single far ultraviolet (FUV) imaging spectrometer stacked with a high-speed photometer (HSP) in a manner similar to that of the Cassini UVS. The notional imaging spectrometer has a detector format of 1024 spectral by 64 cross-track spatial pixels. A 1-mrad instantaneous field of view (IFOV) provides an instrument FOV of 3.7° cross-track. A slit change mechanism and commandable binning modes allow tradeoffs between spectral resolution, spatial resolution, and light collection capability. The notional high-speed photometer employs a telescope mirror approximately 10 times larger than that used in the imaging spectrometer, which enables high temporal resolution (integration times as short as 2 ms). An aperture stop limits the FOV to 6 mrad, minimizing background to improve the signal to noise ratio.

The notional detector for the imaging spectrometer is a two-dimensional imaging, photon-counting system consisting of a microchannel plate (MCP) with a position-sensitive anode and a solar-blind photocathode coating of CsI. A vacuum door mechanism protects the CsI photocathode against damage from exposure to moisture and contamination during ground operations, and when opened in flight allows detector response from 70 nm to 190 nm. Desired spectral resolution for stellar occultation is better than 0.5 nm with a signal to noise ratio greater than 5. The notional detector for the high-speed photometer is also an MCP with a CsI photocathode. A fixed

MgF_2 window protects the detector from contamination but limits response to a wavelength range of 115 nm to 190 nm.

Boresight of the stacked instrument is controlled by an instrument-provided single-axis scan system that allows both sensors to view a 90° field of regard from nadir (co-boresighted with the other remote-sensing instruments) to the spacecraft anti-ram axis. Analysis indicates that while in Europa orbit, multiple stellar occultations would be available per day within the notional 6-mrad wide high-speed photometer FOV. A given star would be available every orbit for a day or more, allowing longitude sampling at a single latitude for each star. The distribution of star's declinations allows latitude sampling.

The UVS optics, detector electronics, and high-voltage power supplies are assumed to be located on the anti-ram side of the nadir-facing deck of the spacecraft allowing a clear scan field of regard for stellar occultations. Electronics for mechanisms, photon processing, system control, and low-voltage power supply are assumed to be packaged on a 6U cPCI board located in the shielded Science Electronics Chassis.

5.1.1.5 Thermal Instrument

The notional JEO Thermal Instrument (TI) would map thermal emissions and measure thermal inertial of surface materials. The TI is a pushbroom imager employing six uncooled thermopile line arrays each with a fixed spectral filter. Two filter bands (8– to 20-μm and 20– to 100-μm) have been selected to achieve Europa surface temperature measure-ments over a range of 80 K to 160 K with better than 2K accuracy. Four filter bands (21.0 ± 3 μm, 28.2 ± 5 μm, 40.0 ± 5 μm, and 17.2 ± 3 μm) have been selected to allow retrieval of Jupiter atmospheric temperatures between 100- and 500-mbar and retrieval of para-H_2 from the spectral shapes associated with S(0) and S(1) transitions.

The notional TI has a 2.5-mrad wide IFOV to produce a 250 m/pixel footprint from the 100 km orbit. Six 21-element linear arrays of thermopile detectors are oriented to provide a 3.0° cross-track instrument FOV and a 5.25-km swath width from the 100 km orbit. For an orbital ground track speed of 1300 m/s in the 100 km orbit, 250 m spatial resolution requires a sampling interval of 192 ms. A nominal 10-Hz detector readout is assumed based on previous instruments using similar detector arrays. Preliminary analysis indicates a signal to noise ratio of ~25 could be achieved for Δ2 K at 80 K and a signal to noise ratio greater than 100 could be achieved for Δ2 K at 160 K. Of the four filter bands dedicated to Jupiter atmospheric science, the minimum estimated signal to noise ratio of ~70 is achieved by the 17.2 μm filter.

Two-point calibration is achieved with a motorized flip mirror providing frequent looks at deep space and a warm calibration flag or shutter providing a second temperature reference point. Given the relative insensitivity of thermopile arrays to focal plane temperature, only modest control of focal plane temperature is assumed.

The TI optics, detector readout electronics, and analog to digital converter are assumed to be located on the nadir-facing deck of the spacecraft and co-boresighted with the other JEO remote-sensing instruments. The system controller, mechanism electronics, and low-voltage power supply are assumed to be packaged on a 6U cPCI board located in the shielded Science Electronics Chassis.

A single mode of science data collection is assumed for TI with calibration events inserted into the operational timeline as needed.

5.1.1.6 Narrow Angle Camera

The notional JEO Narrow-Angle Camera (NAC) is a dual-mode instrument providing high-resolution panchromatic line-scan imagery of selected targets on the surface of Europa and high-resolution color framing imagery of objects in the Jovian system. Candidate observations using the NAC in the Jovian system include flyby imaging (and mosaic imaging) of satellites during both targeted and "non-targeted" encounters, and monitoring of the Jupiter atmosphere and Io.

Two approaches to meeting the requirement for both line-scan and framing modes have been identified. The first approach is development of a detector similar to that of the New Horizons Multispectral Visible Imaging Camera (MVIC), with multiple elements (zones) on a single substrate. This device could be either a charge coupled device (CCD) or a CMOS active pixel sensor (APS). One element would be a 2048-pixelwide line array for pushbroom operation while the other element would be a framing array use. The second approach is development of a CMOS APS that provides a region-of-interest readout zone which could be used to read a line or small number of lines for pushbroom operation or the full array for framing operation. With either approach, a motorized 10-position filter wheel would provide multi-color capability for framing mode and a clear passband for panchromatic line-scan mode. Preliminary NAC filter selections are shown in Table 5-3. The notional NAC has a 0.01-mrad IFOV to meet the requirement for a 1 m/pixel footprint from the 100 km Europa orbit. A 2048-pixel-wide image sensor results in an instrument FOV of ~1.17°. Acquisition of panchromatic images while in Europa orbit is complicated by limitations on exposure time required to minimize image smear. An exposure time of 770 μs results in 1 pixel of smear from the 100 km orbit. The notional optical system provides a signal to noise ratio of ~50 assuming 1 pixel of smear. Improvement in the signal to noise ratio or a reduction in image smear would require implementation of analog time-delay-and-integration (TDI) for a CCD based instrument or digital TDI for a CMOS APS based instrument. Background radiation noise is mitigated by these very short exposure times and is not considered to be significant issue for NAC.

The NAC telescope, detector, and detector electronics are assumed to be located on the nadir-facing deck with the optical axis co-boresighted with the other JEO remote sensing instruments. A passive radiator on the anti-sunward side of the spacecraft provides detector cooling. The NAC interface electronics, pixel processing and data compression electronics, system controller, mechanism electronics and power supplies are assumed to be packaged as two 6U cPCI boards located in the shielded Science Electronics Chassis.

5.1.1.7 Camera Package (Wide Angle Camera & Medium Angle Camera)

The notional JEO Camera Package consists of a Wide-angle Camera (WAC) and a Medium-angle Camera (MAC). The WAC would generate global color imagery and stereo topographic imagery from both the 200 km

Table 5-3. Narrow-Angle Camera Color Filters

Filter	Function	Bandpass (nm)	Center (nm)	Width (nm)
1	Violet	< 450		
2	Red	630–670	650	40
3	Near-IR	> 930		
4	Green	510–610	560	100
5	Methane #1	883–8898	890	15
6	Methane #2	903–918	910	15
7	Methane #3	913–928	920	15
8	Continuum	924–944	934	20
9	Continuum	725–775	750	50
10	Open			

and 100 km orbits at Europa. The MAC would generate context imagery near closest approach of targeted flyby satellite encounters.

Collection of a WAC global map with 100 m spatial resolution in 8 eurosols (~28 Earth days) while using only every other 100 km orbit requires an image swath-width greater than 60 km, resulting in a requirement for greater than 600 WAC pixels cross-track. The notional WAC is assumed to use a 1024-pixel-wide image sensor, which would allow ample cross-track swath overlap for stereo imaging. Combined with the 1-mrad IFOV required to produce a 100 m/pixel footprint from the 100 km orbit, the notional 1024-pixel wide detector results in a WAC FOV of ~58°. A digital elevation model (DEM) vertical resolution of 20 m is achieved at a stereo convergence angle of 60°, approximately the largest convergence angle available with WAC. Multiple passes (N) would improve vertical resolution by SQRT(N), extending the area at which 20 m resolution is achieved. Preliminary WAC color filter selections are shown in Table 5-4 and are selected to match filters in the notional JEO NAC. Given a 1300 m/s ground track rate in the 100 km orbit at Europa, the maximum exposure time for 1 pixel of smear is ~77 ms. The relatively long exposure times allow implementation of color capability using either multiple pushbroom line array detectors with fixed color filters or a single framing array detector with a motorized color filter wheel. The former reduced mass and potentially lower cost.

Table 5-4. Wide-Angle Camera Color Filters

Filter	Function	Bandpass (nm)	Center (nm)	Width (nm)
1	Violet	< 450		
2	Red	630–670	650	40
3	Near-IR	> 930		
4	Open			

The notional MAC has a 0.1-mrad IFOV to produce a 10 m pixel footprint from the 100 km orbit and a 2048-pixel-wide image sensor for an instrument FOV of ~11.7°. This combination allows context imaging at ten times the resolution of the notional JEO WAC and ten times the FOV of the notional JEO NAC. Panchromatic imaging is baselined and the ~7.7 ms exposure time for 1 pixel of smear in the 100 km orbit favors use of a pushbroom line array relative to a framing array.

While the relatively short exposure times tend to mitigate the impact of background radiation noise for the MAC, the longer exposure times required by the WAC are of concern on JEO. Longer exposure times would typically be required for the WAC due to its wide-angle small-aperture optics, which also present challenges for implementation of radiation shielding in the forward direction.

The telescope, detector, and detector electronics for both the WAC and the MAC are assumed to be located on the nadir-facing spacecraft deck with their optical axis co-boresighted with the other JEO remote sensing instruments. Passive radiators on the anti-sunward side of the spacecraft provide detector cooling. All other electronics are assumed to be packaged on two 6U cPCI boards located in the shielded Science Electronics Chassis. Two independent boards are assumed as a way of preventing a single-point failure that could cause the loss of both the WAC and the MAC. A higher degree of electronic integration could result in mass, power, and cost savings which must be weighed against the increased risk of losing both sensors.

5.1.1.8 Ion and Neutral Mass Spectrometer

The notional JEO Ion and Neutral Mass Spectrometer (INMS) would determine the elemental, isotropic, and molecular composition of Europa's atmosphere and ionosphere from orbit, and those of Io, Callisto, and

Ganymede during close flybys. Characterization of sputtered products (ions and neutral particles) from energetic particle bombardment of the surfaces requires an INMS with an extended mass range, high mass and energy resolution, and the ability to operate over a wide range of pressures. Notional specifications for the JEO INMS are mass range greater than 300 Da, mass resolution ($M/\Delta M$) better than or equal to 500, energy resolution better than 10%, and a pressure range from 10^{-6} to 10^{-17} mbar.

A reflectron time-of-flight mass spectrometer is adopted because of its ability to achieve the required mass range and mass resolution and because of its flight heritage. The detector typically used in this type of instrument is a micro-channel plate (MCP). MCPs are sensitive to transient radiation in proportion to their physical size and use of an MCP with a small active area (per Rosetta ROSINA RTOF) mitigates the sensitivity to radiation-induced noise. Further mitigation is achieved by the extremely short duration data acquisition using the MCP when an ion bunch is released towards the detector. Preliminary analysis indicates that an acceptable measurement noise floor could be achieved using these mitigation techniques.

The notional JEO INMS would require a clear field of view (approximately 30×30 degrees or more) in the spacecraft ram-facing direction for collection of ions and particles. The presence of the notional JEO Ice Penetrating Radar antenna and antenna storage container on the ram-facing side of the spacecraft present a possible a spacecraft accommodation concern for the JEO INMS.

Partitioning of INMS electronics for use in the JEO Science Electronics Chassis is another potential concern for the notional JEO INMS. Previous INMS instruments (Cassini, Rosetta) have packaged all instrument electronics within the instrument envelope, which on JEO would result in a significant mass penalty for radiation shielding. It is assumed that the detector data acquisition systems, interface electronics, system controller, and low-voltage power supplies are packaged as two 6U cPCI boards located in the shielded Science Electronics Chassis.

5.1.1.9 Magnetometer

The notional JEO Magnetometer (MAG) would measure the magnetic field at Europa with sufficient sensitivity to resolve the induction signal generated in Europa's ocean as a response to Jupiter's magnetic field. Operation in Europa orbit for an extended period allows sounding at multiple frequencies to determine ocean thickness and conductivity. Characterization of the magnetic environment at Europa to determine the induction response from the ocean requires a measurement rate of better than or equal to 8 vectors/second with a measurement sensitivity of better than 0.1 nT. Measurement of ion-cyclotron waves that relate to plasma-pickup and erosion require a measurement rate of better than or equal to 32 vectors/second, again with a measurement sensitivity of better than 0.1 nT.

The notional MAG would contain two sensors located on a spacecraft-provided 10-m boom with one sensor at the tip and the other at the halfway point. The dual magnetometer configuration could quantify and separate the spacecraft field from the background field, improving the overall sensitivity of the system and providing redundancy for in-flight calibrations performed to assess the spacecraft generated magnetic field. The expected magnetic field range over the full JEO mission is 0- to 3000-nT, with the upper limit set by the Io torus. Analysis indicates that the JEO spacecraft could achieve the level of magnetic field cleanliness (better than 0.1 nT with better than 0.03 nT variation) required for the MAG to

achieve the required sensitivity assuming use of a 10-m boom.

Fluxgate sensors suffer from small drifts in their zero levels that require periodic calibration. These calibrations could be achieved using the rotational nature of the interplanetary magnetic field during the cruise phase. However, slow spacecraft spins around two orthogonal axes would be required every 2 to 4 weeks once inside Jupiter's magnetosphere.

The notional MAG sensors would use three orthogonally mounted ring-core fluxgate sensors. Both analog fluxgate magnetometers and digital fluxgate magnetometers have been demonstrated to meet the JEO measurement requirements, and no significant issues are expected in radiation hardening of the instrument electronics. The MAG electronics are assumed to be packages as a single 6U cPCI board located in the shielded Science Electronics Chassis.

5.1.1.10 Particle and Plasma Instrument

The notional JEO Particle and Plasma Instrument (PPI) would consist of multiple sensor heads assumed to be integrated into a common central electronics unit. The concept represents the minimum measurement capability sufficient to achieve the JEO science requirements.

The first detection system in the notional PPI is a low-energy plasma sensor measuring the spectra and angular distribution of low-energy electrons and mass-resolved ions. The JEO PPI instrument would detect plasma for several reasons. In the Jovian system, plasma moments such as flow direction and electron temperature tell us about the ability of the magnetospheric system to maintain co-rotation and about the rate of impact ionization of the iogenic and other neutrals, respectively. Close to Europa, in addition to determining the plasma moments, we would attempt to determine the contribution of the plasma to the magnetic signal. This would help isolate that part of the magnetic field measurement due to inductive response. Plasma measurements should cover a minimum energy range of ~10 eV to ~30 keV with energy resolution ($\Delta E/E$) of better than 0.1 and angular resolution of better than 15 degrees. The JEO spacecraft is 3-axis stabilized (non-spinning) which makes a very wide field of view a requirement.

The second detection system in the notional PPI is a medium-energy charged particle sensor measuring the spectra and angular distribution of electrons and ions. Energetic particles are measured in the Jovian system for a number of reasons, including the study of the radiation environment of all of the satellites. Precipitating charged particle fluxes are used to connect optical detections of the surface with radiolytic weathering. Electrons and their secondary particles deposit energy into the surface, catalyze reactions, and create molecules such as peroxide. Energetic heavy ions sputter the surface, re-depositing volatiles from the high precipitation regions. In the magnetosphere itself, the presence of electron beams and their connection to auroral emissions, the rate and distribution of ion and electron injections, and other dynamic processes would be investigated. Particle measurements should cover a minimum energy range from tens of keV to ~1.5 MeV with energy resolution ($\Delta E/E$) of better than 0.1 and angular resolution of better than 15 degrees. As with the plasma sensor, a very wide field of view is desirable.

The third detection system is a set of omnidirectional integral electron detectors that measure the population of very energetic electrons. Energy bands for the notional PPI are >2 MeV, >4 MeV, >8 MeV, and >16 MeV.

The notional PPI would use solid state detectors and micro-channel plates (MCPs) in

its detection systems and shielding these detectors from background (penetrating) radiation is a significant challenge on JEO. Large detector areas typically result in improved instrument performance (geometry factor) but result in increased susceptibility to background radiation, requiring careful trade-off.

While previous plasma and particle instruments have typically co-located instrument electronics with the sensor heads, on JEO this would result in a significant mass penalty for radiation shielding. For the notional PPI it is assumed that time-of-flight electronics, data acquisition and event processing circuitry, spacecraft interface electronics, and low-voltage power supplies are packaged as two 6U cPCI boards located in the shielded Science Electronics Chassis.

5.1.1.11 Radio Subsystem

JEO radio science would make use of the JEO spacecraft telecommunications system. As an engineering-critical system, these elements are provided and accommodated by the JEO project.

The JEO telecommunications system would include redundant small deep-space transponders (SDSTs) that receive commands from Earth tracking stations at X-band and transmit data to Earth at Ka-band, a configuration used on the Deep Space 1 and Kepler projects. Redundant traveling-wave tube amplifiers (TWTAs) would provide amplification for the downlink channel. The SDST would also support X/Ka Doppler range, and delta-differential one-way range (ΔDOR) for orbit determination. The SDST-based Doppler measurement accuracy is better than 0.1 mm/s for 60-s integration time. Simulations show that these measurements could determine the radial component of the orbit about Europa to 2-m accuracy as well as making useful accuracies of gravity and tidal parameters.

To meet the better than 1-m radial orbit determination accuracy required for the Laser Altimeter instrument, and to provide higher-accuracy estimation of tidal and gravity parameters, the JEO spacecraft telecommunications subsystem would include a Ka-band Translator (KaT) that could receive a Ka-band signal from Earth and supports a Doppler measurement accuracy of 0.01 mm/s for 60-s integration times. The KaT is based on the Ka/Ka experiment performed with Cassini and planned for Juno with the same Doppler accuracy as specified for JEO.

To support radio occultation experiments, the telecommunications subsystem would include an ultrastable oscillator (USO) with stability better than 2×10^{-13} over time scales of 1- to 100-s. The notional USO is based on an oven-controlled crystal oscillator like those used on many missions, including the Galileo probe and more recently the GRAIL spacecraft planned for launch in 2011. The performance requirement for the USO is the same as that for the GRACE and GRAIL projects. For the Galileo probe, the USO was pre-conditioned with a 1-Mrad dose from a cobalt-60 source to make frequency stability less susceptible to radiation effects in the Jovian environment. Radiation dose rates of 1 rad/s could cause frequency drift of order 10^{-9}.

5.1.2 JEO Mission Constraints and Requirements imposed by Science

Measurements identified for JEO objectives and investigations place constraints on JEO (Table 5-5). Optimizing among the envelope of constraints has shaped the Europa Science phase. The nominal JEO mission would be 9 months at Europa. As a risk mitigation strategy, and to ensure sufficient time to follow up on discoveries, the primary science hypotheses would be addressed in the first 100 days in Europa orbit (≈ 28 eurosols ≈ 3 months). The desired orbit is nearly circular, with an orbital inclination of 80–85° (or the retrograde equivalent of ~95–100°). The

Table 5-5. Traceability from the EJSM Goal to Science Objectives to Science Investigations

Objective	Architecture and Orbit Constraints	Additional Mission Constraints
EA. EUROPA'S OCEAN: Characterize the extent of the ocean and its relationship to the deeper interior.	Gravity and Altimetry: Orbiter required, low altitude (~100-300 km), orbital inclination of ~40–85° (or retrograde equivalent) for broad coverage and crossovers. Ground-tracks should not exactly repeat (while near-repeat is acceptable), so that different regions are measured. Requires a mission duration of at least several eurosols to sample the time-variability of Europa's tidal cycle. Magnetometry, Particles and Plasma: Near-continuous measurements near Europa, globally distributed, at altitudes ≤500 km, for a duration of at least 1–3 months.	Gravity and Altimetry: Knowledge of the spacecraft's orbital position to high accuracy and precision (~meters radially) via two-way Doppler. Gravity: Long undisturbed data arcs are required (>12 hr periods without spacecraft thrusting), and momentum wheels to maintain spacecraft stability Magnetometry: Magnetic cleanliness of 0.1 nT at the sensor location, and knowledge of spacecraft orientation to 0.1°. Calibration requires slow spacecraft spins around two orthogonal axes each week to month.
EB. EUROPA'S ICE: Characterize the ice shell and any subsurface water, including their heterogeneity, and the nature of surface-ice-ocean exchange.	Radar Sounding: Low orbit (≤ 200 km) considering likely instrument power constraints. Near-repeat groundtracks are required to permit targeting of full-resolution observations of previous survey-mode locations. Close spacing of profiles requires a mission duration of months, and near-global coverage implies orbital inclination ≥80°.	Radar Sounding and Altimetry: Data sets need to be co-aligned, and highly desirable to be time-referenced to 10–30 ms accuracy. Radar Sounding: Raw full-resolution targeted radar data requires ≥900 Mb solid-state recorder. Early flyby of Europa for radar signal processing assessment.
EC. EUROPA'S COMPOSITION: Determine global composition, distribution, and evolution of surface materials, especially as related to habitability.	Infrared Spectroscopy: Solar phase angles of ≤45°, with orbital inclination ≥80° for near-global coverage. Near-circular orbit is desirable. Close spacing of profile-mode data implies a mission duration on the order of months. A near-repeat orbit is desired, to permit targeted observations to overlap previous profiling-mode observations. INMS: As low an orbit as feasible is desired, for direct detection of sputtered particles.	Optical remote sensing: Boresight co-alignment of all nadir-pointed imaging and profiling instruments is highly desirable.

Objective	Architecture and Orbit Constraints	Additional Mission Constraints
ED. EUROPA'S GEOLOGY: Understand the formation of surface features, including sites of recent or current activity, and identify and characterize candidate sites for future *in situ* exploration.	Optical Remote Sensing: Near-repeating orbits required to permit regional-scale coverage overlap, follow-up targeting, and stereo; close spacing of profile data implies a mission duration on the order of months; ≥80° orbital inclination to provide near-global coverage. Imaging: Solar incidence angles of 45–60° are best for morphological imaging, while a solar phase angle ≤45° is best for visible color imaging. Near sun-synchronous and near-circular orbit is highly desired to permit global coverage to be as uniform as practical. Beginning at a higher orbital altitude and reducing to a lower altitude would allow rapid initial areal coverage, followed by improved resolution coverage at low altitude. Thermal Mapping: Day-night repeat coverage required; afternoon orbit is desirable.	Optical Remote Sensing: Boresight co-alignment of all nadir-pointed imaging and profiling instruments is highly desirable, and also highly desirable to be time-referenced to 10–30 ms accuracy. Radar Sounding and Altimetry: Data sets need to be co-aligned, and highly desirable to be time-referenced to 10–30 ms accuracy. Magnetometry: Magnetic cleanliness of 0.1 nT at the sensor location, and knowledge of spacecraft orientation to 0.1°. Calibration requires slow spacecraft spins around two orthogonal axes each week to month. Ultraviolet Spectroscopy: Atmospheric emissions observations and stellar occultations require a view to the satellite's limb.
EE. EUROPA'S LOCAL ENVIRONMENT: Characterize the local environment and its interaction with the jovian magnetosphere.	Optical Remote Sensing: Near-repeating orbits required to permit regional-scale coverage overlap; close spacing of profile data implies a mission duration on the order of months; ≥80° orbital inclination to provide near-global coverage. INMS: As low an orbit as feasible is desired, for direct detection of sputtered particles. Magnetometry, Particles and Plasma: Near-continuous measurements near Europa, globally distributed, at altitudes ≤500 km.	Radio Subsystem: Inclusion of an ultra-stable oscillator (USO) is desirable. INMS: Requires observing in the ram direction. Ultraviolet Spectroscopy, Infrared Spectroscopy: Atmospheric emissions observations and stellar occultations require a view to the satellite's limb.
G. GANYMEDE: Characterize the extent of the ocean and its relation to the deeper interior; characterize the ice shell; characterize the local environment and its interaction with the jovian magnetosphere; understand the formation of surface features and search for past and present activity; determine global composition, distribution and evolution of surface materials.	At least five flybys of Ganymede (altitudes of < 1000 km with at least four with altitude < 200 km).	Optical Remote Sensing: Boresight co-alignment of all nadir-pointed imaging and profiling instruments is highly desirable. INMS: Requires observing in the ram direction.

Objective	Architecture and Orbit Constraints	Additional Mission Constraints
S. JOVIAN SATELLITE SYSTEM: Study Io's active dynamic processes; study Callisto as a witness of the early jovian system.	One to three flybys of Io, with one at low altitude over an active volcanic region; at least five Callisto flybys including one high latitude all with altitudes <1000 km; satellite closest approach points distributed globally in latitude and longitude. Imaging: Solar incidence angles of 45–60° are best for morphological imaging, while a solar phase angle ≤45° is best for visible color imaging. Radio Science: ≥10 radio occultation observations of the Galilean Satellites. INMS: Very close Io fly-bys (≤75 km altitude) strongly desired.	Optical Remote Sensing: Boresight co-alignment of all nadir-pointed imaging and profiling instruments is highly desirable. INMS: Requires observing in the ram direction. Radio Subsystem: Inclusion of an ultra-stable oscillator (USO) is desirable. INMS: Requires observing in the ram direction.
R. RINGS AND SMALL SATELLITES: Characterize the rings and small satellites.	Optical Remote Sensing: Geometry permitting high phase (greater than 170 degrees) observations of the rings from within Jupiter's shadow, at least 3 times. At least eight distinct phase angles on the rings, well distributed between 0 and 170 degrees. Imaging: Fly-by of an outer irregular satellite at a range sufficiently close to obtain at least 10 NAC pixels across the body's disk. Radio Science: At least 2 opportunities for dual-spacecraft ring occultation observations, covering radial limits of at least 122,000 to 130,000 km, at least one of which having opening angle less than 3 degrees and preferably smaller. Others occultations should be widely separated in time and should have opening angles less than 10 degrees.	Optical Remote Sensing: Boresight co-alignment of all nadir-pointed imaging and profiling instruments is highly desirable. Radio Subsystem: Requires capability for spacecraft-to-spacecraft communications.
M. JOVIAN MAGNETOSPHERE: Characterize the magnetosphere as a fast magnetic rotator, and as a giant accelerator; understand the moons as sources and sinks of magnetospheric plasma.	Magnetometry, Particles and Plasma, INMS: Near-continuous measurements throughout the Jovian tour; campaign to observe the Io torus; Broad distribution of Ganymede-magnetic latitude sampled on both leading and trailing hemispheres; near-continuous measurements near Europa during flybys, globally distributed, at altitudes ≤500 km.	Magnetometry: Magnetic cleanliness of 0.1 nT at the sensor location, and knowledge of spacecraft orientation to 0.1°. Calibration requires slow spacecraft spins around two orthogonal axes each week to month. Particles and plasma, and INMS: Require observing in the ram direction. Magnetometry: Magnetic cleanliness of 0.1 nT at the sensor location, and knowledge of spacecraft orientation to 0.1°. Calibration requires slow spacecraft spins around two orthogonal axes each week to month.

Objective	Architecture and Orbit Constraints	Additional Mission Constraints
J. JOVIAN ATMOSPHERE: Characterize the atmospheric dynamics and circulation, the atmospheric composition and chemistry, and the atmospheric vertical structure.	Optical Remote Sensing: Coordinated feature-track observations using the entire suite of remote sensing instruments; sufficient time and resources for dedicated campaigns covering at least 2 full Jupiter rotations; solar, stellar and radio occultations covering as wide a range of latitudes as possible. At least one shadow passage from long range; ≥3° inclination off of the ring plane.	Optical Remote Sensing: Boresight co-alignment of all imaging instruments is highly desirable. Radio Subsystem: Inclusion of an ulltra-stable oscillator (USO).

Table 5-1. Primary and Secondary Instruments Would Work Together to Address Science Investigations and Objectives

Objective		Science Investigation	RS	LA	IPR	VIRIS	UVS	INMS	WAC +MAC	NAC	TI	MAG	PPI
EA. OCEAN: Characterize the extent of the ocean and its relationship to the deeper interior.	EA.1.	Determine the amplitude and phase of the gravitational tides.	P	S									
	EA.2.	Determine the magnetic induction response from the ocean and characterize the influence of space plasma environment on this response.										P	S
	EA.3.	Characterize surface motion over the tidal cycle.	S	P									
	EA.4.	Determine the satellite's dynamical rotation state (forced libration, obliquity and nutation).	P	S					P	S			
	EA.5.	Investigate the core, rocky mantle, rock-ocean interface, and compensation of the ice shell	P	P	S							S	S
EB. ICE: Characterize the ice shell and any subsurface water, including heterogeneity, and the nature of surface-ice-ocean exchange.	EB.1.	Characterize the distribution of any shallow subsurface water and the structure of the icy shell including its subsurface properties.		S	P				S				
	EB.2.	Search for an ice-ocean interface.		S	P				S				
	EB.3.	Correlate surface features and subsurface structure to investigate processes governing material exchange among the surface, ice shell, and ocean.		S	P	P	S		S	S	P		
	EB.4.	Characterize regional and global heat flow variations.			P						S		

Objective		Science Investigation	RS	LA	IPR	VIRIS	UVS	INMS	WAC +MAC	NAC	TI	MAG	PPI
EC. CHEMISTRY: Determine global surface composi-tions and chemistry, especially as related to habitability.	EC.1.	Characterize surface organic and inorganic chemistry, including abundances and distributions of materials, with emphasis on indicators of habitability and potential biosignatures.				P	S	P					
	EC.2.	Relate compositions to geological processes, especially material exchange with the interior.		S	P	P	P	S	S	S	S	S	
	EC.3.	Investigate the effects of radiation on surface composition, including organics, and regional structure.				P	P	P		S	S	S	S
	EC.4.	Characterize the nature of exogenic materials.				P	S	P	S				P
	EC.5.	Determine volatile content to constrain satellite origin and evolution.				P	S	P					P
ED. GEOLOGY: Understand the formation of surface features, including sites of recent or current activity, and identify and characterize candidate sites for future *in situ* exploration.	ED.1.	Determine the formation history and three-dimensional characteristics of magmatic, tectonic, and impact landforms.		P	S	S	S		P	P	S		
	ED.2.	Determine sites of most recent geological activity, and evaluate future landing sites.				S	P		P	S	P		S
	ED.3.	Constrain global and regional surface ages.	S		S	S	S		P	P			
	ED.4.	Investigate processes of erosion and deposition and their effects on the physical properties of the surface.				S	S			P	P	S	S
EE. LOCAL ENVIRONMENT: Characterize the local environment and its interaction with the jovian magnetosphere.	EE.1.	Characterize the composition, structure, dynamics, and variability of the bound and escaping neutral atmosphere.	P			P	P				S		
	EE.2.	Characterize the composition, structure, dynamics, and variability of the ionosphere and local (within the Hill sphere) charged particle population.						P				S	P

P Primary S Secondary

optical remote sensing instruments are nadir-pointed and mutually boresighted. The initial orbital altitude is 200 km, which is reduced to 100 km altitude after several eurosols to meet the requirements of gravity, altimetry, magnetometry, and radar. The orbit is not quite sun-synchronous but precesses slowly, such that the orbit does not exactly repeat the same ground track but allows instrument fields of view to overlap with previous tracks. Thus, the orbit is near-repeating after several eurosols, within about 1° of longitude at the equator. The solar incidence angle is nominally 45° (2:30 p.m. orbit) on average, as the best compromise to the requirements of imaging and spectroscopic optical remote sensing measurements.

Significant Jupiter system science would be enabled by the Jovian tour, which lasts approximately two and a half years prior to Europa Orbit Insertion. Requirements and desires on the tour to accomplish Jupiter system science are also listed in Table 5-5. The model payload would provide the capability for meeting Jupiter system science objectives, tracking Jupiter and the other Galilean satellites to accomplish observations during the Jovian Tour phase (see §5.1.4.4). However, as a lower priority goal, Jupiter system science generally does not impose strong constraints on the spacecraft itself, with the exception of the addition of an Ultra-Stable Oscillator (USO) to derive the properties of the satellites' and Jupiter's atmospheres and ionospheres from radio occultations.

The EJSM science investigations are best accomplished through collaborative observations achieved by multiple instruments. Table 5-6 shows examples of how primary and secondary instruments work together to address each of the Europa science investigations and objectives. The fact that model instruments are primary to achieving at least one of the science investigations, and secondary to other demonstrates efficient use of resources and multiple paths to science success.

5.1.3 JEO Mission Concept: Overview and Instrument Accommodation

The JEO mission concept would encompass three major components summarized in Table 5-7, while key mission parameters are shown in Table 5-8. The baseline mission concept would include a single orbiter flight system that travels to Jupiter by means of a gravity assist trajectory and would reach Jupiter approximately 6 years after launch. The large

Table 5-7. JEO Reference Mission Components

Component	Description
Launch Vehicle	▪ Atlas V 551 ▪ Support and procurement provided by Launch Planning Office at KSC ▪ Launch mass capability of 5040 kg to C_3 of 12.8 km^2/s^2 for the February 2020 VEEGA opportunity
Flight System	▪ Single Orbiter ▪ Spacecraft ▪ MMRTG Power Source supplied by the Department of Energy ▪ Chemical Propulsion—dual mode Bi-propellant system ▪ X up/down and Ka-Band down Telecommunications (Ka-Band up/down link for gravity science) ▪ Launch Vehicle adapter ▪ Instruments selected via NASA Announcement of Opportunity
Ground System	▪ Ground Data System ▪ Flight Operations Team (engineering and science) ▪ Deep Space Network and related services

Table 5-8. Key JEO Baseline Mission Parameters

Parameter	Baseline Value	Notes
Instruments		
Number of instruments	11	Includes the on-board Ka-band uplink/downlink equipment for Radio Science in the baseline flight system.
Instrument mass	165 kg	Current Best Estimate. Includes 43 kg of radiation shielding for the detectors and 16.6 kg shielding for the instrument electronics that is carried by the spacecraft bus. Does not include Ka-band transponder (1.5 kg) and USO (1.5 kg) that are tracked in telecom.
Instrument power	71 W	Current Best Estimate, orbital average. This is the average power level over two consecutive Europa science orbits (one radar orbit and one optical remote sensing orbit). Does not include power for Ka-band transponder.
Science Accommodation		
Pointing accuracy	1 mrad (3 σ)	S/C body pointing control accuracy during nadir-oriented non-thrusting orbital period.
Pointing stability	10 μrad/s (3 σ)	For body-fixed instruments in science orbit during non-thrusting periods.
Minimum duration between reaction wheel orbit desaturations	24 hours	Minimum duration between desaturation thruster firings.
Science Data storage Tour/Europa Orbit	16 + 1 Gbits (tour), 1 Gbits (Europa orbit)	16 Gbits radiation tolerant SDRAM for tour. Radiation hardened, non-volatile, phase changing CRAM in baseline design for Europa orbit use.
Data volume	4.5 Tbits	Assumes 3 dB link margin, Ka band, 34 m stations, 90% weather, multiple data rates optimized for range, elevation, Jupiter presence, while in Europa orbit.
Spacecraft		
Available power at EOM	540 W	Power output from 5 MMRTGs at EOM
ΔV requirement	2260 m/s	Propellant mass is calculated assuming launch mass is equal to the launch vehicle capability (5040 kg).
Radiation design point	2.9 Mrad behind 100 mils of aluminum	Represents the reference design point without radiation design factor applied. Note that current trajectory. Results in a lower estimated dose.
Heliocentric operating range	0.7 to 5.5 AU	Minimum range defined by VEEGA trajectory.
Maximum Earth Range	6.5 AU	

main engine would place the flight system into orbit around Jupiter, followed by approximately 2.5 years of Jupiter System science, while the flight system would use repeated satellite gravity assists to lower its orbit until a final burn inserts it into orbit around Europa.

The flight system would use a gravity assist of Io on approach to Jupiter just prior to Jupiter Orbit Insertion (JOI). Then, using a series of Io, Ganymede, Europa, and Callisto flybys to lower its energy, most of the Jupiter System science objectives would be achieved over a

period of 2- to 3- years. Icy satellite flybys would allow for focused science measurements while distant monitoring of Jupiter's atmosphere, Io's activity, Jupiter's ring system, the magnetosphere, and other activities would fill in critical pieces of information regarding how the system interacts and operates. Once in Europa orbit and after a 5-day engineering assessment period, the Europa Campaigns 1 to 3 would span approximately 100 days (~28 eurosols) to address all Level 1 science measurements.

Key design drivers on the spacecraft are Jupiter's radiation environment, planetary protection, high propulsive needs to get into Europa orbit, the large distance from the sun and Earth and the accommodation of the instrument payload. The high-level constraints and assumptions on the JEO flight system design are contained in Table 5-9. Figure 5-1 depicts the operational configuration of the JEO Flight System.

All remote-sensing instruments in the model payload would nominally view in the nadir

Table 5-9. Constraints and Assumptions for Reference JEO Spacecraft Design

The flight system design shall employ technology that either exists already or is under development and is planned for qualification early in the JEO project lifecycle.
The mission reference radiation design dose (referenced to 100 mil aluminum shell) is 2.9 Mrad.
The required total ΔV is 2260 m/s.
Approximately 7.3 Gbits of science data is returned per Earth-day during the Europa Science phase and ~3.6 Gbits per Earth-day during the Jovian Tour phase.
Retransmission of downlinked data is not required while in Europa orbit.
34 m DSN antenna used during normal operations, with limited 70 m antenna use (or equivalent) for critical or emergency events.
Heliocentric operating range of 0.7 AU to 5.5 AU, with a maximum Earth range of 6.5 AU.

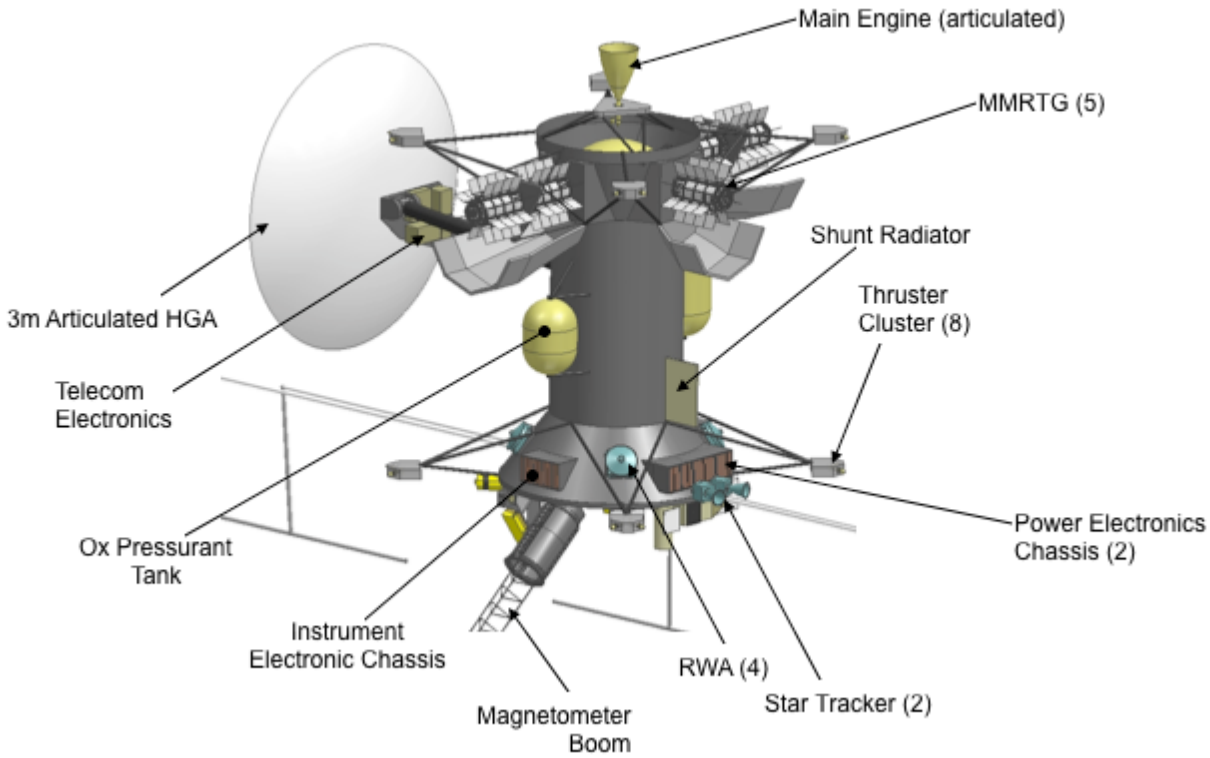

Figure 5-1. JEO Flight System Operational Configuration (Conceptual Design)

direction when in orbit around Europa, as shown in Figure 5-2. Because JJSDT analysis indicates that nominal nadir pointing of the remote sensing instruments can accomplish the science objectives, spacecraft-provided scan platforms are not assumed. It is envisioned that instruments requiring scan systems for target tracking or target motion compensation would need to provide such a system as an integral part of the instrument. Two notional instruments in the model payload, the UV Spectrometer (UVS) and the VIS-IR Spectrometer (VIRIS), assume such systems.

Adequate instrument mounting area for the science payload on the nadir-facing deck would be available. *In situ* instruments with wide fields of view, such as particle and plasma sensors, would be located to minimize obstructions in those fields of view. The high-gain antenna (HGA) would be deployed well clear of instrument fields of view and would be articulated on two axes to decouple instrument pointing from the telecom link to Earth. Instrument accommodation requirements are summarized in Table 5-10.

The JEO design calls for an orbit at Europa with 95° to 100° inclination. Orbit plane orientation would provide local time such that one side of the spacecraft is protected from the Sun and an ideal location for thermal radiators. The science payload is expected to contain instruments with detectors requiring cooling to as low as 80 K for proper operation while dissipating perhaps 300 mW of heat. Cooling to this level would be accomplished via passive radiators, mounted so their view is directed away from the Sun and away from Europa at all times. Jupiter would move across the radiator field of view (FOV) every 3.5 days, subtending a small portion of the radiator FOV and presenting a transient perturbation to instrument thermal system designs. Preliminary analysis indicates that a 0.25 m^2 radiator would be sufficient to achieve a detector temperature of 80 K with less than 5 K variation in detector temperature due to the effect of Jupiter.

The remote sensing instruments would require spacecraft pointing control to better than or equal to 1 mrad, stability to 10 µrad/s and reconstruction to 0.1 mrad. Pointing requirements are driven by the Narrow-angle Camera (NAC) with a 10 µrad pixel field of view and, while NAC exposure times in Europa orbit would be on order of 1 ms, longer

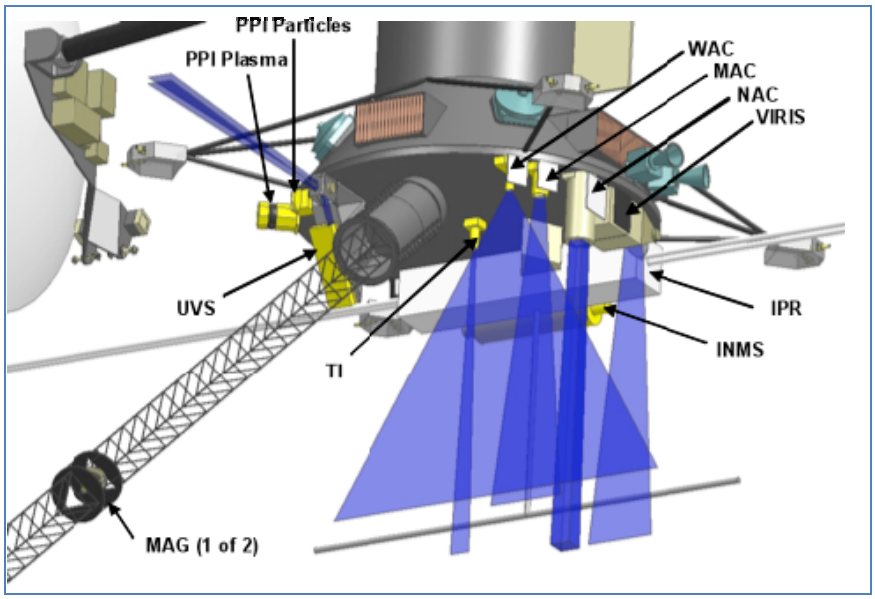

Figure 5-2. Spacecraft Nadir Deck (Conceptual Design)

Table 5-10. JEO Model Payload Resource Requirements and Accommodations

Instrument	Acro-nym	Unshielded Mass (kg)	Shield-ing Mass (kg)	Total Mass (kg)	Operat-ing Power (W)	Telemetry Interface	Science Chassis Board Count	Field of View
Laser Altimeter	LA	5.0	4.7	9.7	15	Mil-Std-1553	2	0.029° diameter spot
Ice Penetrating Radar	IPR	26.0	5.0	31.0	45	SpaceWire	6	5.7° swath width
VIS-IR Spectrometer	VIRIS	15.7	11.8	27.5	25	SpaceWire	3	9.17° × 0.014°
UV Spectrometer	UVS	6.4	3.1	9.5	5	Mil-Std-1553	1	3.67° × 0.057°
Ion and Neutral Mass Spectrometer	INMS	13.0	2.1	15.1	33	Mil-Std-1553	2	20° × 40°
Thermal Instrument	TI	3.7	1.3	5.0	5	Mil-Std-1553	1	3° × 0.14°
Narrow-angle Camera	NAC	10.4	3.0	13.4	14	SpaceWire	2	1.17° × 0.00057° Push 1.17° × 1.17° Framing
Wide-angle Camera and Medium-angle Camera	WAC	2.3	1.5	3.8	6	SpaceWire	1	58° × 0.057°
	MAC	2.6	1.5	4.1	7	SpaceWire	1	11.7° × 0.0057°
Magnetometer	MAG	3.2	0.0	3.2	4	Mil-Std-1553	1	N/A
Particle and Plasma Instrument	PPI	7.6	8.8	16.4	13	Mil-Std-1553	2	Plasma:360° × 90° torus Particles:160° × 12° fanbeam Onmi Electrons: 4π
Science Electronics Chassis		10.0	16.6					
TOTAL ALL INSTRU-MENTS		105.9	59.4	165.3	172		22	
TOTAL ALL INSTRU-MENTS + 30% contin-gency				214.9	224			

exposure times would be required during the tour phase of the mission. To achieve the Europa geophysical science objectives connected with characterizing the subsurface ocean and the overlying icy shell, the JEO orbit trajectory must be tracked to an accuracy of 2 m in the radial direction. To achieve this level of accuracy, adequate levels of Doppler

tracking would be required and with thruster firings restricted to not more than one per 24 hours.

The limited capacity of the spacecraft's solid state recorder (SSR), coupled with near-continuous collection and downlink of instrument data during Europa orbit, would require that high-data-rate instruments perform data reduction and data compression before sending the data to the SSR. Consideration is being given to a payload module that would have avionics that accommodate science payload power distribution and could perform science payload data compression. The notional model payload block diagram (Figure 5-3) assumes this data system architecture with SpaceWire interfaces baselined for the instruments having high data rates and Mil-Std-1553 interfaces assumed for those having low data rates.

Radiation

The severe radiation environment at Europa presents significant challenges for the science instruments, as does the need to meet the planetary protection requirements. These challenges have been addressed by a notional payload architecture that efficiently implements radiation shielding, the use of radiation hardened application specific integrated circuits (ASICs) throughout the payload, and by a thorough study of both radiation effects and the impact of planetary protection protocols on detectors by a Detector Working Group (DWG). The DWG developed a methodology for determining the required radiation shielding for successful instrument operation in the severe transient radiation environment at Europa, assessed degradation of detectors due to total dose and displacement damage effects, and assessed the compatibility of candidate detectors with the planetary protection protocols.

The mission radiation design point is 2.9 Mrad behind 100 mils of aluminum shielding without design margin. Therefore, sensors and supporting electronics would require significant shielding. The most mass-efficient approach to providing radiation shielding would be to centrally locate as much of the instrument electronics as possible, minimizing the electronics that must be co-located with the sensor portion of the instrument. The model payload design presented here assumes instrument partitioning in this manner and includes a science electronics chassis implemented using the industry-standard 6U Compact PCI form-factor. Space for 22 electronics boards is baselined, with radiation shielding sufficient to allow use of components hardened to 300 krad without additional spot shielding. The total radiation shielding mass for the science electronics chassis is estimated to be 16.6 kg. Internal partitioning of the science electronics is baselined to provide electrical isolation between instruments and to mitigate electromagnetic interference (EMI). Louvers would provide thermal control of the science electronics chassis in the same manner used for the spacecraft avionics systems.

The Detector Working Group (DWG), established as part of the study, was charged with assessing the existence of a feasible pathway for photonic detector technologies required by the JEO model payload. The DWG included experienced instrument, detector, and radiation environment experts from APL and JPL. The DWG used an empirical approach to determine worst-case estimates of the effects of electrons and protons incident on detectors. This information was used to assess the performance potential of existing detector technologies subjected to the end-of-mission total dose. Additionally, the impact of radiation-induced transient noise in each detector technology was evaluated for radiation flux levels encountered during Europa orbit as well as at mission peak flux during Io flybys. Finally, the tolerance of each

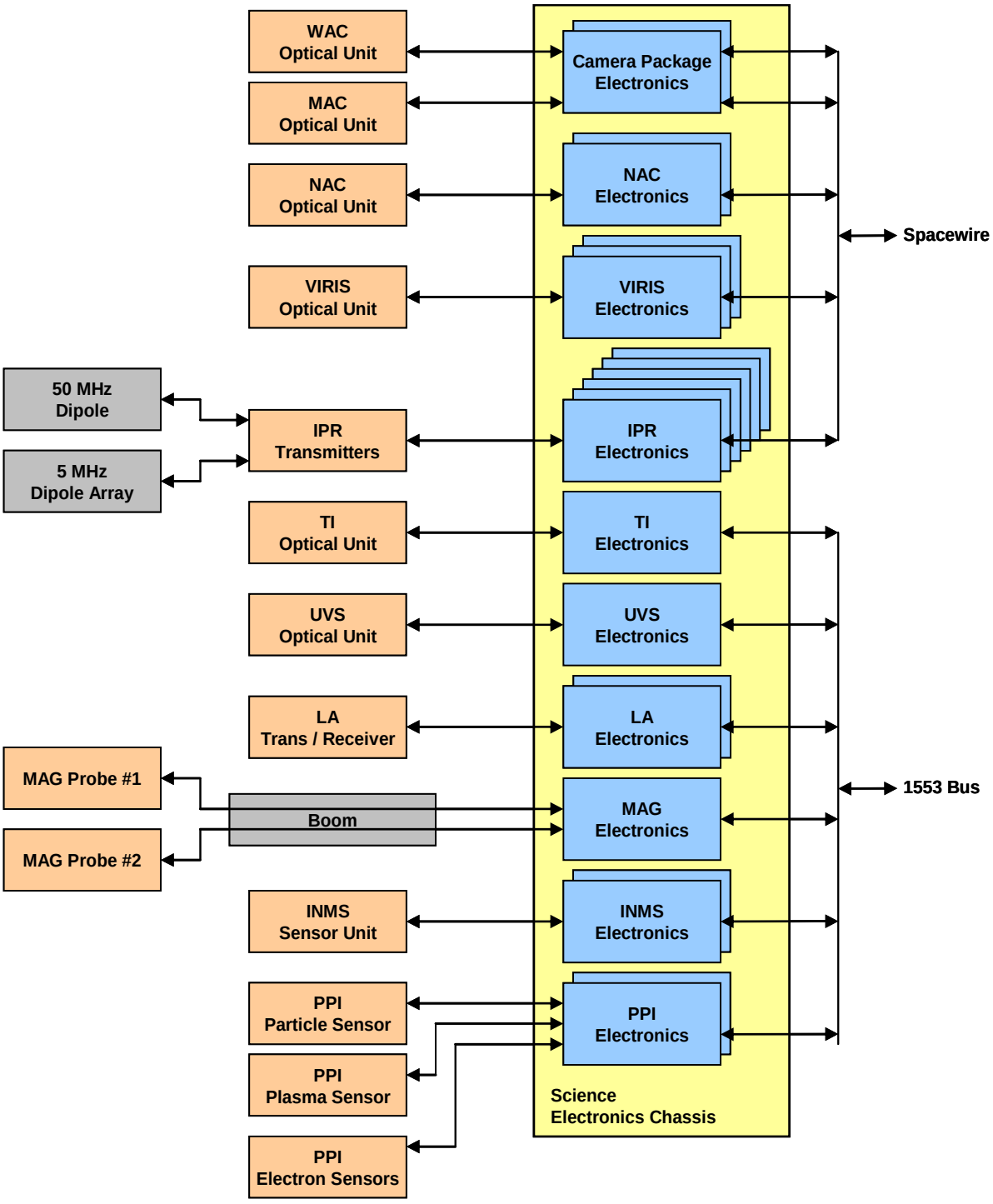

Figure 5-3. Payload Block Diagram

detector technology to dry heat microbial reduction (DHMR) for planetary protection was evaluated.

The DWG concluded that the radiation and planetary protection challenges facing the model payload are well understood. The question of detector survivability and science

data quality is not considered to be a significant risk provided appropriate shielding is allocated to reduce cumulative TID, DDD and instantaneous electron and proton flux at the detector, and early mitigation approaches are implemented. The full DWG assessment report may be found under separate cover [*Boldt et al. 2008, Yan et al. 2008*].

The impact of radiation-induced transient noise on detectors was analyzed by estimating the number of high-energy electrons and protons penetrating the radiation shield and assessing their effect on the detector material. The flux of incident electrons reaching the detector for different radiation shielding thicknesses T could be estimating by applying the cutoff energy E determined from E(MeV) = [T(gm/cm^2) + 0.106]/0.53 [*Zombeck 1982*] to the external integral electron flux. For 1 cm of Ta shielding, an estimated 4.3 × 10^5 electrons/cm^2 s would reach the detector while in orbit at Europa. During Io flybys, the flux of incident electrons would increase by approximately a factor of 8 to a rate of 3.5 × 10^6 electrons/cm^2 s. The flux of incident protons reaching the detector could be estimated by applying a 100-MeV cutoff energy to the external integral proton flux. For 1 cm of Ta shielding, about 50 protons/cm^2 s would reach the detector while in orbit at Europa. During Io flybys, the flux of incident protons would increase by approximately a factor of 18 to a rate of 920 protons/cm^2 s. The predominance of electrons in the Jovian environment is the determining factor for the detector radiation shielding analysis.

Planetary Protection

The approach to planetary protection compliance for the JEO mission could be summarized as pre-launch sterilization to control the bioburden for areas not sterilized in flight, and in-flight sterilization via radiation prior to Europa orbit insertion. The preferred method of sterilization is Dry Heat Microbial Reduction (DHMR). It is currently envisioned that system-level dry heat sterilization of the spacecraft would be invoked for planetary protection purposes. Current planetary protection protocols include a time vs. temperature profile ranging from 125°C for 5 hours to 110°C for 50 hours. It is anticipated that in some cases contamination control bake-out parameters could be modified to allow bioburden reduction credit. During assembly, test and launch operations it is assumed that cleanliness would be maintained (as for the Mars Exploration Rovers and the Mars Science Laboratory) to ensure that surface spore density would not exceed 300 spores/m^2, so that remaining surface spore bioburden would be sterilized via radiation during flight. To prevent recontamination after sterilization and to support cleaning operations during ATLO, high-efficiency particulate air (HEPA) filters and instrument aperture covers with biobarriers would be baselined.

5.1.4 JEO Operational Scenarios

Operations scenarios for JEO are driven by prioritized science objectives, in turn drive the operational use of the model payload and the design of the mission trajectory, and flight systems. [*Paczkowski 2008*]

The JEO mission design combines aspects of orbiting science missions (like MRO, Magellan, and MESSENGER) and previous outer planets flagship missions (Cassini and Galileo). The operations scenarios and the flight system design likewise incorporate the best features from both mission sets. In the Jovian Tour phase, JEO would have similar needs to those of Cassini and Galileo. For the Europa Science phase, JEO would need to perform similarly to MRO but with memory constraints more like those for Magellan. [*Strauss at al.* 2008]

The most stringent and driving operational requirements and constraints for JEO are derived from Europa Science needs. The

analysis presented here focuses on ensuring the system functionality and performance needed for operating in Europa orbit as well as exploring scenarios to demonstrate the ability to accomplish highly diverse objectives for Jupiter atmosphere and system science in the Jovian Tour phase. As an overview, Figure 5-4 provides a timeline of the science campaigns and satellite encounters from JOI through the end of the nominal mission that will be discussed in this section.

5.1.4.1 Summary of JEO Mission Phases

Launch and Cruise

After launching in February of 2020, the mission focus would be on the checkout and deployment of all flight systems. For the first month of operations, the mission would rely on continuous tracking with 34 m DSN stations. Using sequences validated prior to launch, the operations team would characterize the flight system.

The interplanetary cruise phase would include gravity assist flybys of Venus and Earth, which would be needed to add the necessary energy to the trajectory to reach Jupiter. Flybys offer the opportunity to check out and characterize the instruments, flyby operating processes, and tools. During quiet periods of cruise, the operations and supporting teams would be testing and training on the tools and processes to be used for the Jupiter system science and Europa science operations. Cruise sequences would last one to two months during quieter periods, and would last one to two weeks near the Venus and Earth flybys.

Starting in early 2025, the mission operations and science teams and operations centers would begin preparing for JOI and science in the Jupiter system and would deploy and test final flight and ground software. While all critical activities for JOI and science operations at Jupiter would have been tested pre-launch, updates based on post-launch experience and new capabilities would be deployed. Testing and training would be performed to assure mission readiness after the long cruise phase.

Jovian Tour

In the Jovian Tour phase, the flight system would make routine and frequent observations of Jupiter, its satellites, and its environment.

Many measurements supporting satellite specific objectives would be accomplished during the satellite flyby encounters. Flyby geometries are highly varied for latitude and

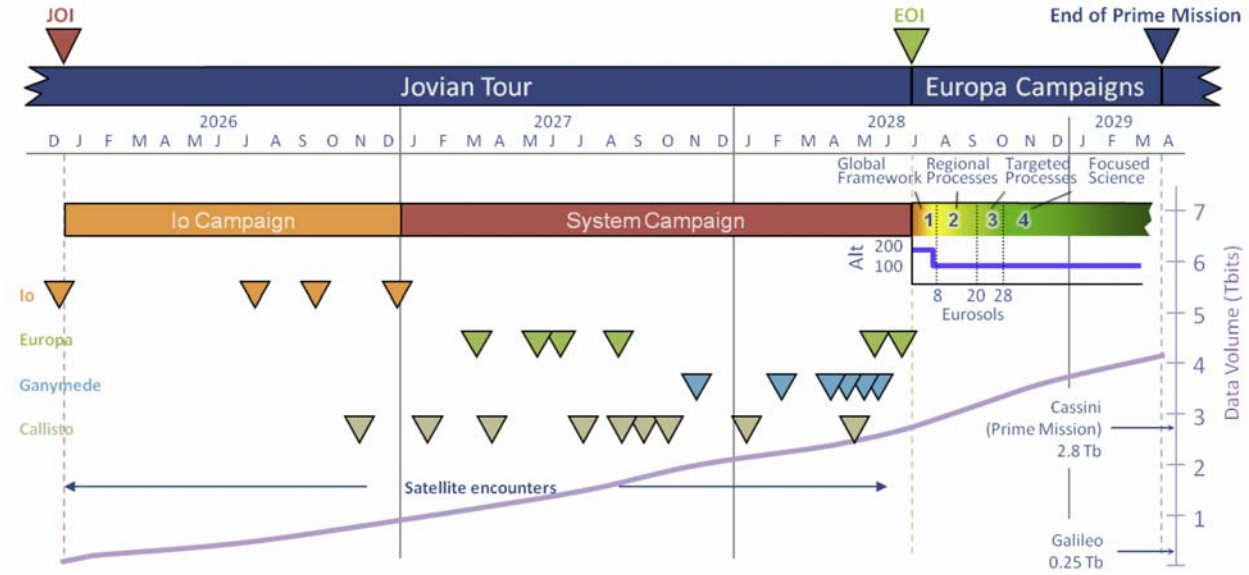

Figure 5-4. Notional JEO science mission timeline with campaigns

lighting but are opportunistic, as the trajectory would be optimized for meeting the science requirements along with duration, ΔV and radiation dose. The orbiter would be able to collect and return about 14 Gigabits of science data during the closest approach 1- to 2-hours for each encounter. This would enable NAC, MAC, and VIRIS observations, UVS observations, TI profiles, and (altitude permitting) laser altimeter profiles and IPR full and low rate profiles.

Monitoring of the Jupiter atmosphere and Io volcanic plumes would entail detailed observations and dynamic studies every week or two. Monitoring and measurement of the system plasma environment and magnetosphere would be accomplished through continuous data collection from the magnetometer and PPI instruments.

Complementary and synergistic science observations between JEO and JGO would add unique measurements and enhance the data return that either mission would be able to return separately.

Europa Science

The JEO Europa Science scenarios are designed to obtain Europa Science objectives in priority order. Data collection spans 4 major campaigns:

- Europa Campaign 1, Global Framework at 200 km orbit for 8 eurosols (~28 days),
- Europa Campaign 2, Regional Processes at 100 km orbit for 12 eurosols (~43 days),
- Europa Campaign 3, Targeted Processes at 100 km for 8 eurosols (~28 days), and
- Europa Campaign 4 Focused Science at 100 km for 46 eurosols (~165 days).

Europa Campaigns 1–3

The highest priority goals would be accomplished from 200 km altitude during Europa Campaign 1, including acquisition of two global maps, 1 to 2 degree global grids from the four profiling instruments, and several hundred targeted observations of high-interest sites using multiple instruments in their highest-resolution modes.

After the initial campaign, the orbit altitude would be lowered to 100 km, allowing acquisition of higher-resolution global maps, additional profile grids, and hundreds more coordinated target observations to answer regional process questions, based in large part upon Campaign 1 and Campaign 2 data. Europa Science Campaign 3 would be devoted almost entirely to acquiring coordinated targets to answer local-scale science questions. The fourth and final campaign would focus on addressing new questions arising from data collected in the first three campaigns.

To meet the mission's science objectives, the flight system would acquire and return an average 7.3 Gb per day. To balance power, mass, and data volume, continuous tracking by DSN 34 m stations (or equivalent) would be required.

For Europa Campaign 1 and 2, science data collection would be continuous and repetitive with continuous fields and particles, altimetry, and TI and VIRIS profile data collection, along with alternating orbit radar sounding and global imaging. This repetitive data collection represents about 2/3 of the daily average downlink data volume. Additional data volume would be devoted to targeted data acquisitions comprising either coordinated targets (IPR profiles, NAC, MAC and VIRIS images) or full-resolution IPR observations. Except for the low rate instruments, all observations would be taken when Earth is in view, enabling rapid downlink of high volume science data. Data sequences from repetitive mapping activities would be uplinked once per week. Lists of targets to be acquired via on-board targeting software would be developed

and uplinked to the flight system every few days. Quick-look data processing, mapping assessment, and target selection processes would all be rapid, needing about one day each. Data would be returned via continuous 34 m tracking through the end of Europa Campaign 3.

Europa Campaign 3 would have similar observing activities as the previous campaigns, but the emphasis would shift from global mapping with limited targeted observations to primarily targeted observations with limited profiling and gap-fill observations from the WAC.

Europa Campaign 4 would continue targeted observations, but would include new observation activities not permitted in the first three campaigns. These might include off-nadir imaging, Io and Jupiter monitoring, low-altitude observing with imagers and INMS, and other measurements responding to new questions arising from early observations.

5.1.4.2 Trajectory Characteristics

The Tour trajectory is designed to reduce orbit energy for EOI ΔV savings, avoid excessive radiation dose prior to Europa arrival, and to achieve science goals. Optimization of the tour trajectory to achieve all of the science goals, including JEO-JGO synergy and complementary science, was beyond the scope of this report but some example scenarios studied indicate considerable opportunities for high data volumes, efficient power profiles, and advantageous viewing geometries for a large variety of observing scenarios. The baseline trajectory achieves multiple flybys for all of the Galilean satellites, including high and low altitude and latitude flybys and varied lighting conditions, and a wide range of lighting conditions for Jupiter atmosphere and system science. Figure 5-5 shows the JEO range and Jupiter phase during the reference Tour phase. Opportunities to meet the key objectives for occultation experiments and high and low phase angles for dust and ring observations could be inferred from the phase and range plot. The range and phase space would offer frequent opportunities for sunlit viewing of

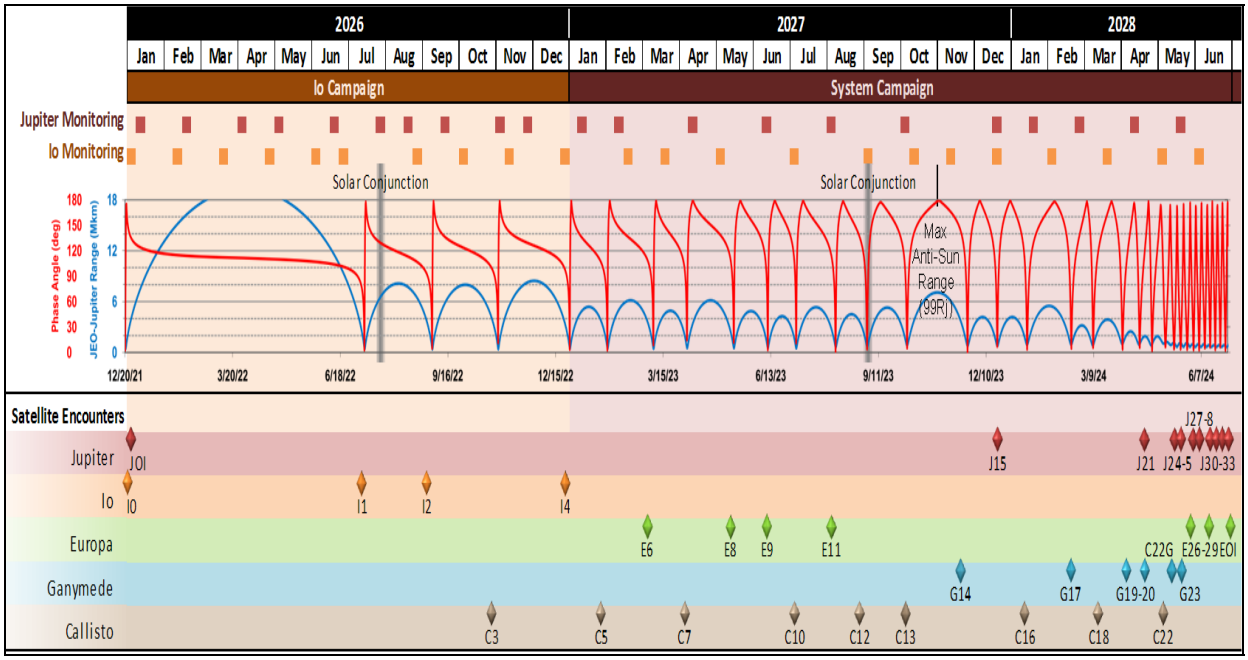

Figure 5-5. JEO reference Jovian Tour phase range to Jupiter, solar phase angle, and satellite flyby events versus time.

Jupiter's atmosphere.
The 33 orbits between JOI and EOI would include 3 Io flybys (after the first at JOI), 6 Europa, 6 Ganymede, and 9 Callisto flybys. Flybys would be 1- to 2-months apart early in the phase, becoming a week or less apart as the tour ends. Ten Jovian orbits have no targeted flybys, allowing comprehensive investigations of Jupiter's atmosphere, rings, dust and small bodies. The trajectory also allows for a large variation of range and sun angles for observing the magnetic and particle environment of the system. Distant viewing opportunities exist to observe Jupiter from less than 1 million kilometers, and Io, Europa, Ganymede, and Callisto from less than 500,000 km

To satisfy the science objectives, the science orbit at Europa would be low-altitude (~100- to 200-km), near-circular, high-inclination, and have consistent day-to-day lighting. Depending on altitude, there would be 10- to 11-orbits per day and ground-track speeds would be between 1.2 and 1.3 km per second. Because of the 2- to 4-p.m. local solar time orientation of the orbit, each orbit would be occulted from the Earth for 30% to 40% of the time. Twice each week Europa would be occulted and eclipsed by Jupiter from the Earth and Sun respectively for about 2 hours.

5.1.4.3 Flight System Operability

The model JEO flight system would consist of an orbiter and a model payload of 11 science instruments. Based on operations trade studies and analysis of operations lessons learned from previous missions, including Cassini, MRO, MESSENGER, and New Horizons, JEO has incorporated a comprehensive set of operability features. Key operability features of the model flight system include:

- Reaction wheels and coupled thrusters for greatly reduced trajectory perturbations (resulting in reduced coupling of observation pointing design, navigation predictions, and attitude control activities);
- Co-aligned remote sensing instruments and independent pointing of the communications system;
- On-board ephemeris-based pointing for rapid observation planning and updates;
- Independent sequencing for individual instruments and spacecraft activities (acquisition and return, health, etc.);
- File-based SSR and CCSDS protocols for file management and delivery;
- Autonomy for fault protection and science operations.

The Flight System would be capable of continuous pointing and operation of the science instruments while communicating with the Earth (via 2-axis HGA gimbal). In the Tour Science phase this is important for radio science (Doppler gravity and occultations) data collection while also collecting remote sensing data. In Europa orbit, this allows the payload to be nadir-pointed continuously and to monitor the local environment from a consistent attitude.

The JEO Solid State Recorder (SSR) would be a hybrid design using a 1 Gb, radiation hardened, CRAM-based partition for use in the Europa Science phase and a somewhat less radiation tolerant 16 Gb SDRAM partition for the Tour Science phase when higher data volume storage would be needed to meet science goals.

To meet orbit maintenance needs, the orbiter would be expected to perform orbit trim maneuvers one to two times per week while in Europa orbit. During the Tour Science phase, maneuvers would be less frequent except for the final pre-EOI orbits where a few maneuvers would be within days of each other.

Reaction wheel desaturations would be needed no more than every other day during all

mission phases. It is expected that this frequency would decrease significantly in the Interplanetary Cruise and Tour Science phases, during which gravity gradient torques are negligible.

Operational characteristics for the model payload have not been analyzed for operability issues but do have features deemed to be of concern by the JJSDT for accomplishing the science goals within the operations scenarios considered. The key operational characteristics for the model payload are shown in Table 5-11.

5.1.4.4 Jovian Tour Phase

The Jovian Tour phase is divided into two science campaigns: the Io Campaign and the System Campaign. The Jupiter system presents a rich and varied set of observing opportunities. The JEO thirty-month baseline tour trajectory would enable substantial Jupiter system science in four major themes: the Jovian satellite system, rings and small satellites, the Jovian magnetosphere, and the Jovian atmosphere.

While complete assessment of all potential Jovian Tour scenarios is beyond the scope of this analysis, preliminary scenarios for selected flybys and assessment of potential

Table 5-11. JEO Model Payload Operational Characteristics

Science Instruments	Operational Characteristics		200 km			100 km		
			Rate (Mb/s)	Mapping Duty Cycle	Data Redux Factor	Rate (Mb/s)	Mapping Duty Cycle	Data Redux Factor
LA	Continuous Operation		0.002	100%	1	0.002	100%	1
Telecom system	Ka-band uplink with Ka-band downlink, 8 hours/day X-band uplink with Ka-band downlink, 16 hours/day		2-way Doppler			2-way Doppler		
IPR	Alternating orbits for distributed global profiles. Modes for shallow water and deep ocean searches.	Shallow Profile Mode	0.28	35%	107	0.28	35%	107
		Deep Profile Mode	0.14	45%	215	0.14	45%	215
	Full resolution target mode	Target Mode	30	–	1	30	–	1
VIRIS	Point mode, every orbit, for distributed global profiles.	Point Mode	0.1	35%	2.5	0.1	35%	2.5
	Target mode for 10 km × 10 km full spectrum images.	Target Mode	30	–	2.5	30	–	2.5
UVS	Limb viewing for stellar occultations several times per day.	Point Mode	0.01	14%	2	0.01	14%	2
INMS	Sensitive to low gas concentrations.		0.002	50%	1	0.002	50%	1
TI	Narrow profiles every orbit, for distributed global profiles.		0.009	100%	3	0.009	100%	3
NAC	Used for targeted modes in framing or pushbroom modes.		13.5	–	4	32	–	4
WAC	Provides global color and stereo maps	Color	0.27	40%	4	0.64	40%	4
	Operates every other orbit.	Panchromatic	0.07	40%	4	0.16	40%	4
MAC	Used for targeted modes.		1.4	–	4	3.2	–	4
MAG	Dual magnetometers; 10 m boom.		0.004	100%	1	0.004	100%	1
PPI	Includes ion species.		0.002	100%	1	0.002	100%	1

imaging coverage and data usage for all of the satellite flybys are described in this section.

The events shown represent half of the available downlink data capability, leaving 50% of the downlink data volume as margin for future detailed considerations of the science objectives. While no data allocations have been made for these system science activities, the 14- to 28-Gb returned per week allow very large numbers of observations to be scheduled.

Tour Scenarios

During the tour, each satellite gravity assist flyby typically happens within a day of a perijove passage. Weeks containing perijove passages and flybys would have additional DSN tracking coverage scheduled. The tracking coverage supports the return of approximately 6- to 12-Gb per day. Non-perijove weeks would allow the return of 2- to 4-Gb per day. The SSR could support collection and return of 17 Gb/per flyby or major event. While a highly diverse set of observing scenarios is likely, a set of basic scenarios was examined to establish the feasibility of key scenario types during the Tour Phase.

Orbit 11 of the tour, about 2/3 through the tour phase, is a representative example of tour orbits and contains all of the observing opportunities to be illustrated by the example scenarios. The scenarios are described in Table 5-12 and Figure 5-6. The basic scenarios were developed to explore operations characteristics of all of the instrument types during the Jovian Tour phase. The examples include continuous observing with the MAG and the PPI with periodic MAG rolls, Jupiter atmosphere monitoring using remote sensing instruments, Io monitoring for volcanic plumes, UV star occultations, a Ganymede flyby, and a JEO-to-JGO radio occultation activity. Aggregate

Table 5-12. Basic Tour Scenarios Examined in Tour Orbit 11

Category	Observations of Interest	Cadence	Instruments / Mode	S/C Attitude	Ops Concept
F&P / Mag Observing	From spinning s/c	1/ 2 days	MAG PPI	Earth Point	Do during 8hr DSN passes. Spin the s/c 2-3 times in 2 orthogonal directions and re-orient.
Jupiter Monitoring	Atmospheric Feature Monitoring (e.g. brown band)	1/wk (4-5/orbit)	VIRIS (long wavelength) TI UVS NAC MAC	Jupiter Point	Want 20 hrs of monitoring --> every 10 deg longitude. For each observation, make movie (72 images).
Io Monitoring	Io in Jupiter shadow Io's dark side Io longitudinal grid	1/wk 1/wk 1-2/wk	NAC VIRIS UVS	Io Point	 Take image every ~5deg longitude (72 images) & look at limb.
JEO-JGO Synergy	S/C occultation	1-2/orbit	USO	JGO Point	Monitor for 1-2 hours before an event and 30 minutes after plus time to get back to Earth-pointed orientation.
Fly-By (Ganymede)	Areas not previously mapped by Galileo	~1/orbit	NAC WAC&MAC	Ganymede Point	
Other Observations	Galilean Moons		NAC, WAC&MAC		
	Small Moons		NAC, WAC&MAC		Jovian disc crossings desired?
	Rings				
	UV Stars		UVS		
	UV Aurora		UVS		

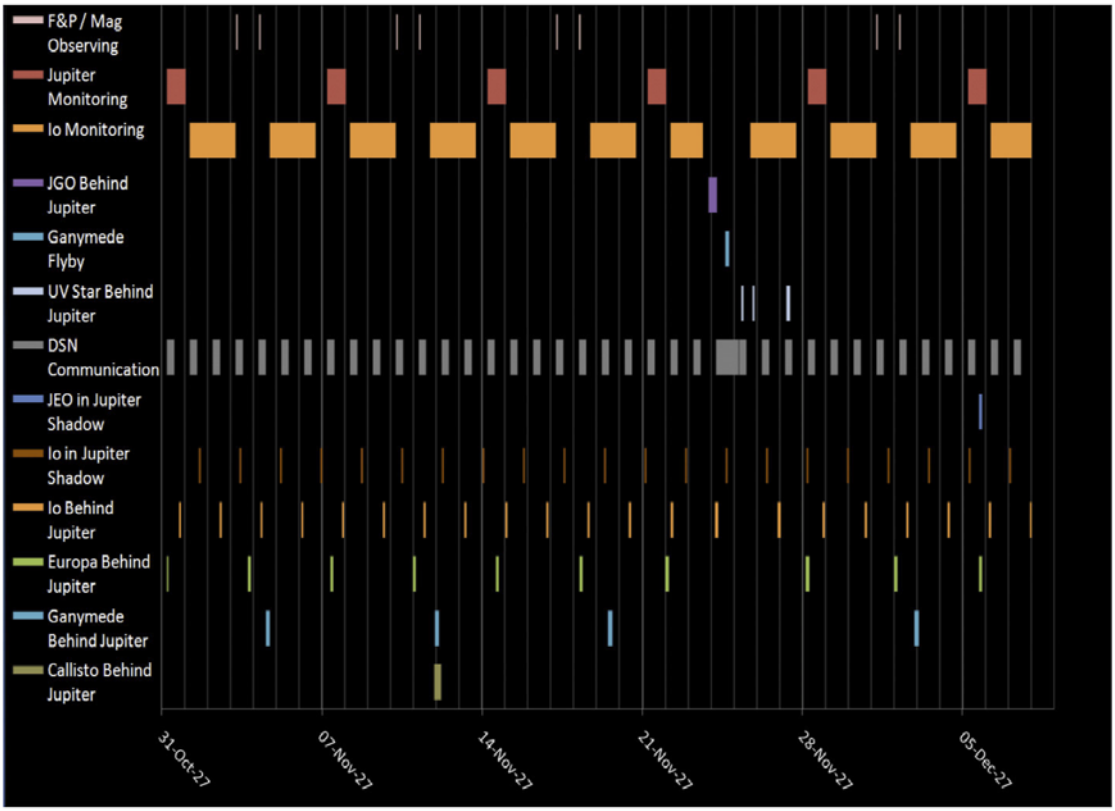

Figure 5-6. Timeline of scenario activities and geometries in Tour orbit 11.

effects of all flybys are shown on Cartesian maps of the satellites, including an example of the complementary imaging coverage available from both JEO and JGO. The spacecraft-to-spacecraft radio occultation opportunities are also shown in aggregate form that illustrates the ability to make measurements impossible from either spacecraft alone.

Flybys

The JEO planning payload is intended to collect data in a close near-circular orbit of Europa. Ground speeds, altitudes, and lighting conditions are consistent in Europa orbit but would vary drastically for flybys. Furthermore, to effectively use some of the instruments for flybys, flight system slews may be needed to provide the apparent ground motion (when the actual motion is too fast or too slow) needed by pushbroom style line-array detectors.

The flyby scenarios are exemplified by the low altitude Io flyby (I4) as shown on Figure 5-7. A sample observation profile is shown detailing the number and timing of observations for each of the instruments. The data volume plot shows the accumulation of data in the SSR and compares it to the maximum value of 17 Gb. A margin of 3 Gb is set aside (for such things as potential opnav images, UVS aurorae observations and unique observations of the Io torus) as a preload to the analysis. This is to accommodate data acquisition outside of the closest approach (C/A) ±30-minute timespan of the analysis. Also shown are the speed of the orbiter, the groundtrack speed, solar phase angle as viewed by the orbiter, and altitude above the surface.

The Io example represents a notional science sequence. Early observations collect global views at moderate to low resolution.

Observations near closest approach (C/A) have higher resolution but reduced extent. Because the period after the C/A is at high phase angles (in the dark) imaging observations are limited to the lit limb and thermal profiles. Within 10 minutes of C/A, ground speeds are too fast for most of the imaging instruments other than WAC and limited VIRIS observations. Near C/A the IPR would observe at full-uncompressed rates for 2 minutes to sample the subsurface. The LA would be operated as well for IPR processing context. WAC images would also be collected for topography context. Independently, the INMS would be operated to collect *in situ* samples of plume material near C/A. The fields and particles instruments (MAG and PPI) would operate continuously during the entire mission phase and would collect Io data during the flyby..

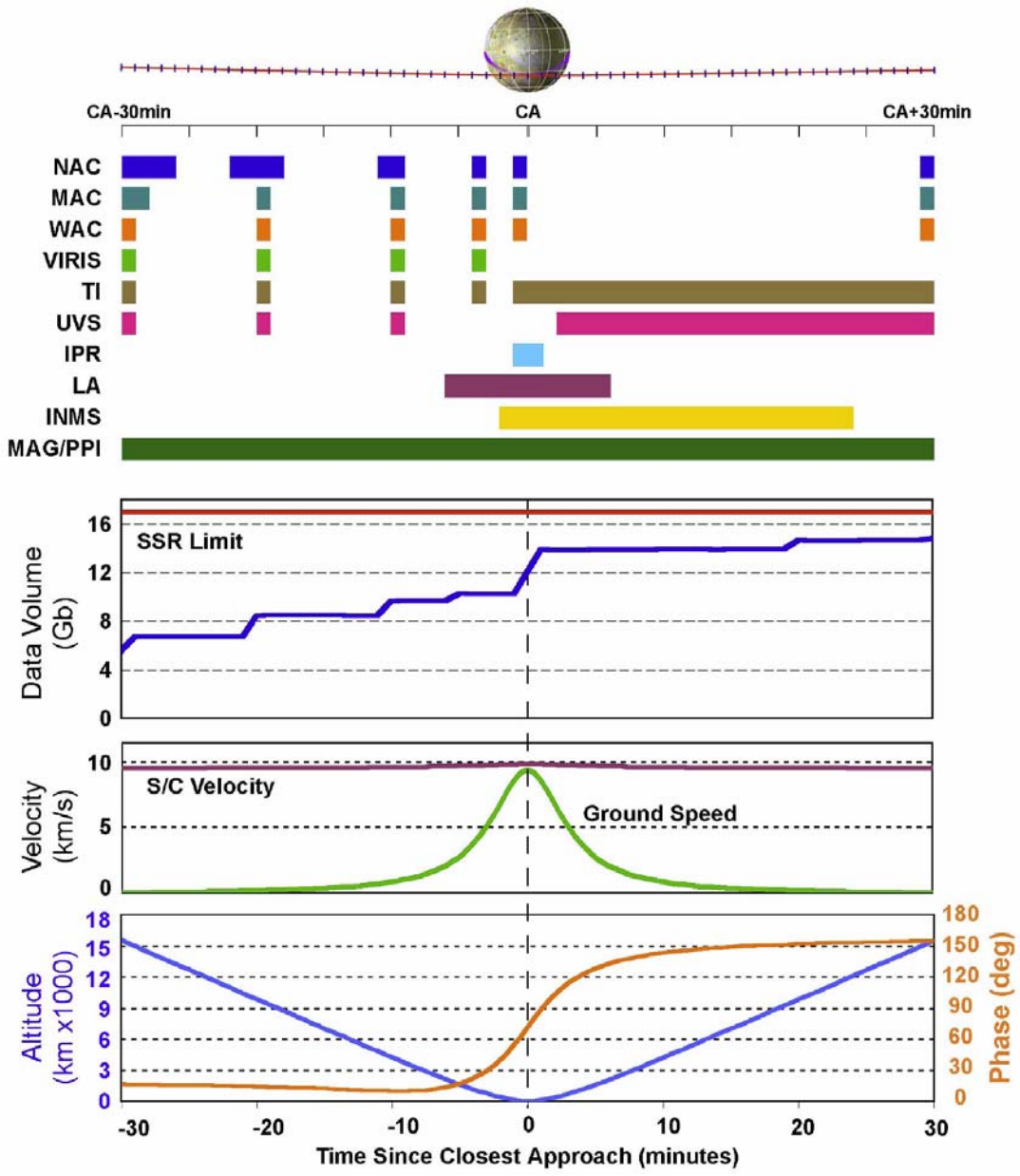

Figure 5-7. Io flybys, I4 shown here, have significant data volume available for intensive investigations by all instruments. Lighting, altitudes, and ground speeds are typical for all Io flybys and most early Tour flybys.

The flight system would be able to point the orbiter instrument deck to Io nadir and the INMS to the ram vector at closest approach using the relatively slow reaction wheels (this avoids contaminating the INMS measurements with hydrazine exhaust). As a consequence, the orbiter would have reduced pointing control in the along track direction during the central 10- to 15-minutes of the flyby (but be nadir pointed at C/A). This would result in a pointing lag with respect to the nadir tracking direction by less than 10 degrees. This constraint would only be present during the early flybys (mainly in the Io Campaign). After that the slew rate needs would be low enough for the orbiter to track nadir throughout the encounters.

Figure 5-8 through Figure 5-10 show Cartesian maps of the Galilean satellites with the flyby imaging observing performance from the current tour trajectory superimposed. Combined with lighting information, these indicate the extent and resolution to which the surfaces could be mapped by JEO in the baseline Tour. The fields of view and resolution contours indicate performance for nadir pointing opportunities.

Figure 5-8 shows image coverage for all of the Io flybys. The groundtrack for the first Io flyby (I0) is shown in dark gray. This flyby precedes JOI by just a few hours and would allow limited science and, for this analysis, is assumed to have no remote sensing contribution. The start and end longitudes are similar for all groundtracks. Global coverage would be collected mainly in one hemisphere (centered on 210° West). Imaging at resolutions better than 1000 m/pixel would be possible for over ~50% of Io's surface. Regional-scale coverage (better than 200 m/pixel) would be obtained for 25% of the surface while local-scale (better than 50 m/pixel) coverage could be achieved of 5% of the satellite. Very high resolution (better than 10 m/pixel) targeted observations could be obtained for <0.01% of Io due to the very high speeds and low durations at low altitudes needed for maximum resolutions. Two Io

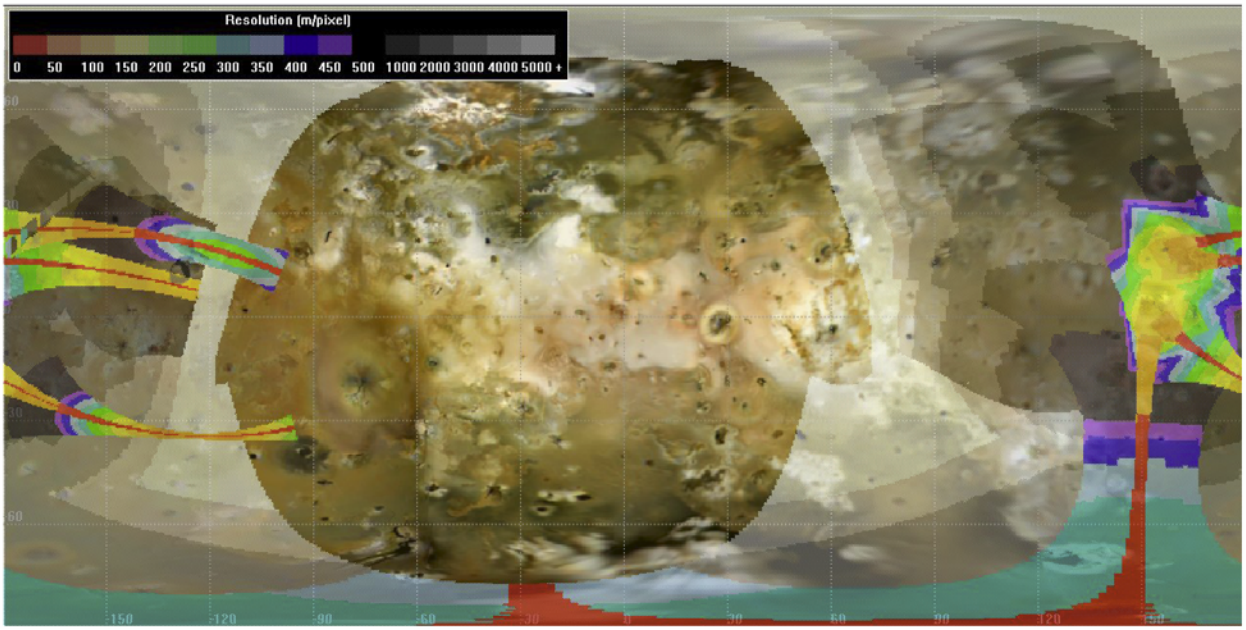

Figure 5-8. Io flyby geometry would allow excellent viewing of one hemisphere, the South Polar region, and *in situ* measurements of volcanic plumes. The figure shows the sunlit portions of the NAC, MAC, & WAC FOVs contoured with resolution (m/pixel) in accordance with the color key, assuming nadir-pointing.

flybys have closest approach altitudes less than 2000 km. This allows the collection of laser altimetry and IPR data (at altitudes <1000 km). Laser altimetry would be collected for 8000 km of total track length and IPR swaths would be collected for a total of 2 minutes for a total length of 1000 km. The IPR tracks would be shorter, due mainly to data volume allocation limits.

Europa, Callisto, and Ganymede have a higher diversity of flyby opportunities in altitudes and phase angles and would allow greater global coverage. Figure 5-9 shows the 6 Europa flyby groundtracks on a map of Europa. The Europa E11 flyby (not shown because it is in the dark) provides an opportunity for IPR calibration. The calibration requirements were for an altitude of less than 1000 km and a velocity of 7 km/s at a time at least 6 months prior to EOI (this flyby occurs 11 months prior to EOI). The closest approach is at 866 km and the ground speed is 4.4 km/s. As the closest approach is in the dark, imaging opportunities would largely be at the global scales near the beginning and end of the encounter. The IPR would use 4- to 6-Gb of the available data volume for calibration, thus leaving more than 10 Gb for global imaging, compositional studies and studies outside of the flyby closest approach period. Taken together, the 6 Europa flybys allow regional-scale (better than 200 m/pixel) coverage of 60% of Europa's surface and local-scale (better than 50m/pixel) of 15% of the satellite. Very high resolution (better than 10 m/pixel) targeted observations could be achieved for about 0.01% of the satellite. Throughout the tour phase, the IPR could collect a total of 6600 km of data profiles while the laser altimeter could return 19,000 km of altimetric information.

The 6 flybys of Ganymede are shown in Figure 5-11. The total regional-scale (better than 200 m/pixel) image coverage allowed by geometry and lighting constraints is 50%. At local scales (better than 50 m/pixel) data could be collected for 10% of Ganymede. At the very highest spatial scale (better than 10 m/pixel) about 0.02% surface coverage could be achieved. The long slow flybys near the end of the Tour (C22 and G23) allow excellent

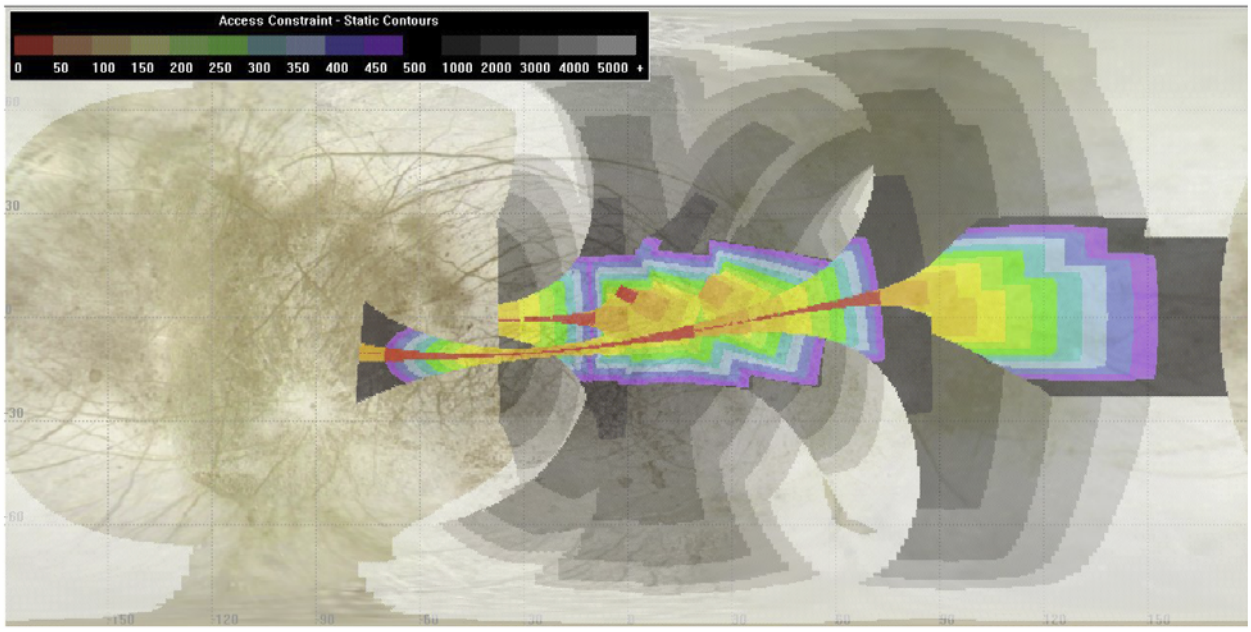

Figure 5-9. Europa flybys would allow excellent imaging and Ice Penetrating Radar observations to calibrate instruments and prepare for Europa mapping operations. The figure shows the sunlit portions of the NAC, MAC, & WAC FOVs contoured with resolution (m/pixel) in accordance with the color key, assuming nadir-pointing.

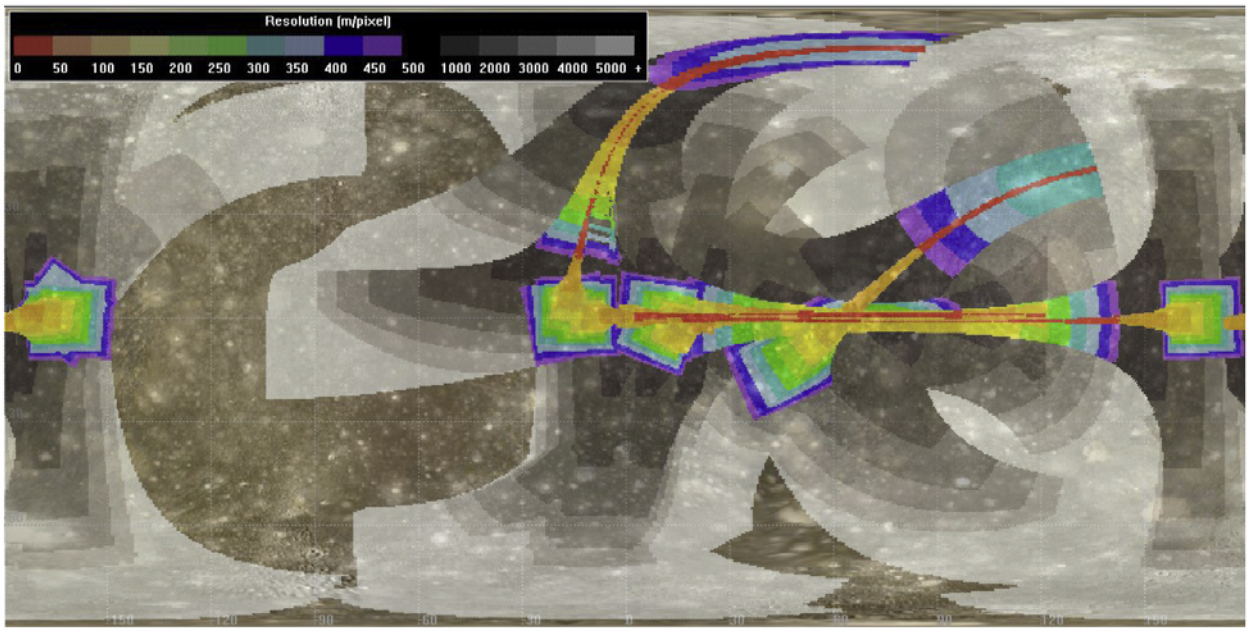

Figure 5-10. Callisto flybys would offer highly varied observation opportunities over most of the satellite's surface. The figure shows the sunlit portions of the NAC, MAC, & WAC FOVs contoured with resolution (m/pixel) in accordance with the color key, assuming nadir-pointing.

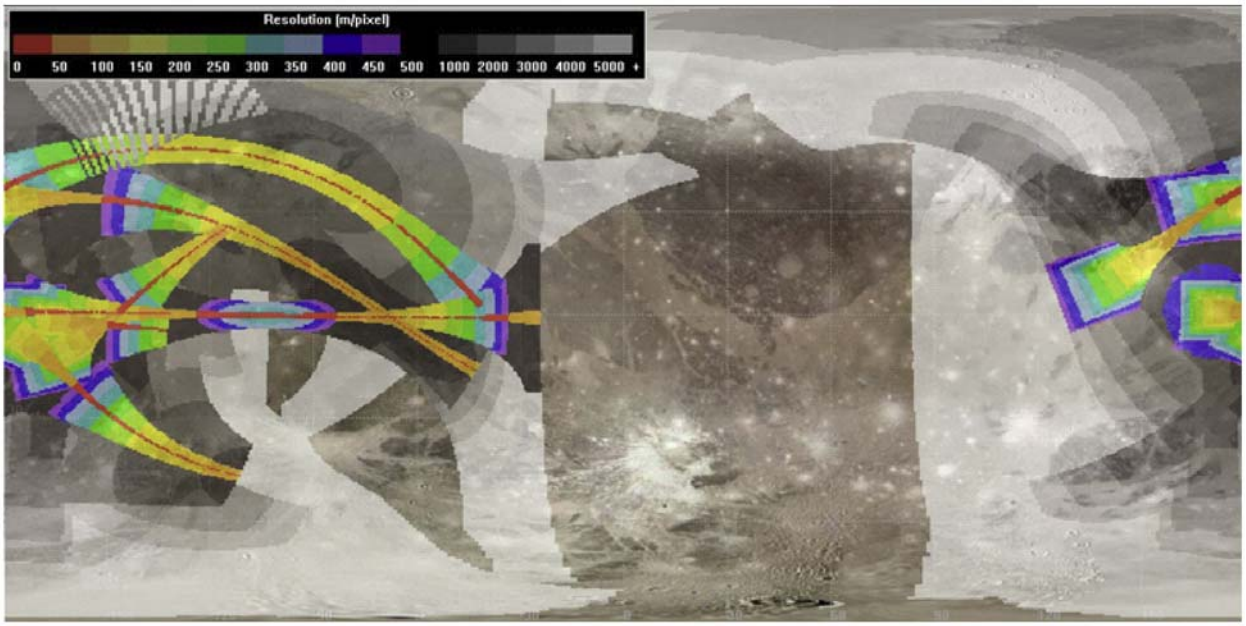

Figure 5-11. Ganymede flybys would offer excellent imaging, composition and IPR investigations over broad regions including examination of both polar regions and high resolution at low latitudes. The sunlit portions of the NAC, MAC, & WAC FOVs contoured with resolution (m/pixel) in accordance with the color key, assuming nadir-pointing. This figure shows coverage opportunity, not represent the coverage actually achieved when balanced with the other instruments and spacecraft resources.

high resolution imaging opportunities and views of both poles at incidence angles from 15° to 20°. The IPR could collect nearly 17,000 km of profiles at over a range of latitudes. The laser altimeter would be able to measure 28,000 km of topographic profiles.

With 9 flybys, Callisto has by far the most varied and complete set of opportunities. Shown in Figure 5-10, the Callisto flybys allow 85% of the surface to be imaged at better than 1000 m/pixel. Regional-scale (better than 200 m/pixel) coverage could be achieved for 75% of Callisto. Because many of the closest approaches are either in the dark or at higher altitudes (above 1000 km), only about 5% of the satellite could be imaged at local scales (better than 50 m/pixel). Like the other satellites, targeted very high-resolution (better than 10 m/pixel) observations could be achieved for only 0.01% of the surface. The IPR and laser altimeter could achieve 15,000 km of profiles and 30,000 km elevation data respectively. The C3 flyby includes a high latitude flyby of the north polar region to facilitate gravity measurements to assess the hydrostatic state of Callisto.

Jupiter Atmosphere and Io Monitoring

The tour phase would provide a significant number of opportunities to study the dynamics and structure of the Jovian atmosphere along with monitoring global-scale volcanic activity at Io.

A large number of monitoring images could be collected to support observations of Jupiter's atmosphere both globally with MAC, VIRIS, UVS, and TI and the periodic tracking of hundreds of features with the 9-color NAC.

Because the large capacity SSR would allow many observations to be collected over a short period of time, dynamic observations are possible (*e.g.,* movies) even in conjunction with other activities such as Io monitoring. Figure 5-12 shows an example analysis of Jupiter monitoring from a distance of 1.4 million km and a view of Jupiter near apoapsis (nighttime observations to monitor lightning events). The example shows that for ranges near perijove, observing conditions are very good for tracking dynamic features in Jupiter's atmosphere. Monitoring movies at longer ranges with longitude increments of 10 deg are achievable with manageable data volumes.

Io monitoring goals for each Jupiter orbit are to collect a wide variety of data types including global maps (once per orbit), plume inventories (roughly 5 deg longitude, once per

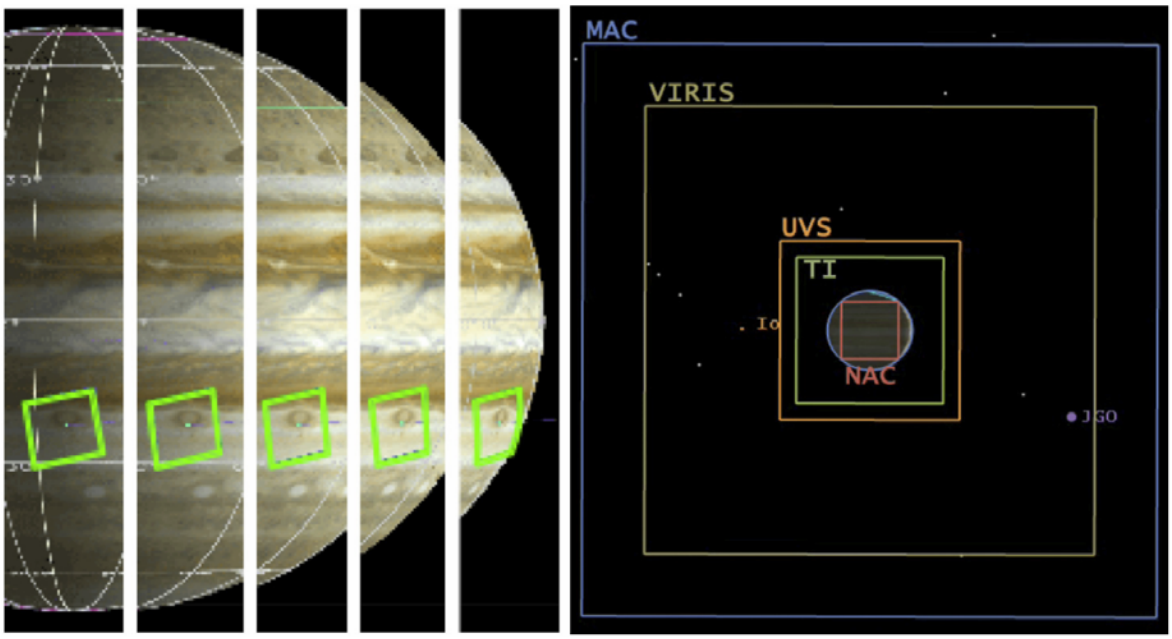

Figure 5-12. Jupiter monitoring example shows feature tracking near perijove and near apojove.

orbit), plume movies (30 to 40 frames) when plumes are on the limb, and images sampled over a wide variety of timescales. One full set of these images would occupy roughly a half of the capacity of the SSR and would be downlinked in a few days. Subsets of these would be collected each Jupiter orbit in combination with other activities.

Tour Data Return

The science data return strategy for the Jovian Tour phase is simple and repetitive. The 16+1 Gb hybrid SSR would allow rapid and long term data collection at faster rates than the downlink rate. Days of downlink could be stored allowing the possibility of data retransmission in the event of a missed DSN pass, weather outage, link noise or orbiter safing.

Data rates vary with Earth range, from 64- to 144-kb/s (see Figure 5-13) using standard link

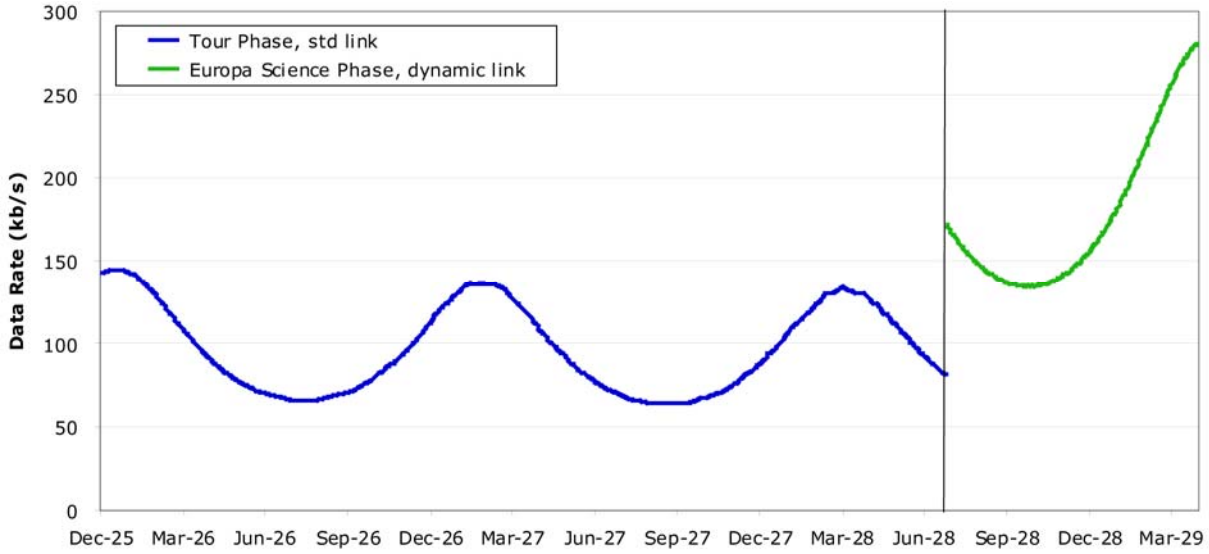

Figure 5-13. Average Data Rates for 34 m DSN Stations.

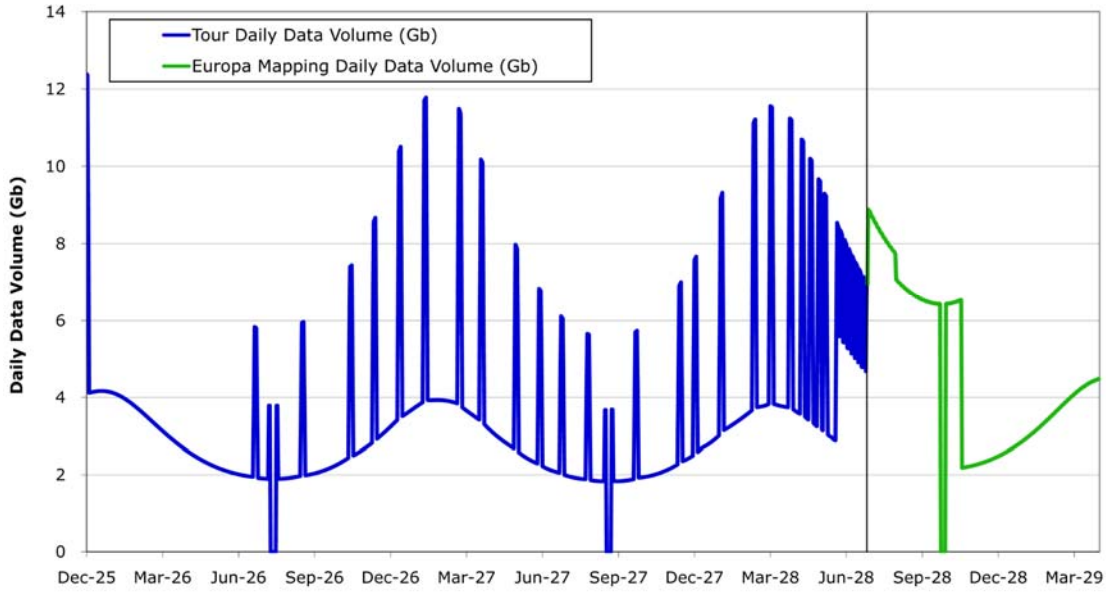

Figure 5-14. Daily Data Volumes. Sharp peaks are from increased DSN tracking for flyby events. Dropouts reflect Solar Conjunction.

design methods (90% weather, 20° station elevation, maximum Jupiter hot body noise). For routine daily downlinks in the tour, the standard method is the baseline to save complexity and cost.

Figure 5-14 shows the daily data volumes ranging from 2- to 4-Gb for the nominal 1 track per day DSN schedule. In weeks near perijove and the satellite flybys, tracking would be increased to 2- to 3-tracks per day increasing the returned data to 6- to 12-Gb per day. The additional tracks would be scheduled both just before the flyby to ensure large SSR capacity for the flyby and just after the flyby to empty the SSR and accommodate Jupiter and Io monitoring observations. The data gaps in the figure represent solar conjunction time periods where no data return is possible.

5.1.4.5 Europa Science Phase

The most challenging issues driving the design and operation of the JEO mission arise from the Europa science operations scenarios. This section describes the science data acquisition strategies and operations scenarios for the Europa Science phase. These scenarios are designed to balance the model payload and the flight system, ground system and mission design.

Europa Science Campaigns

During Europa Campaign 1, the flight system would orbit at 200 km altitude for 8 eurosols (28 days), and the mission's highest priority data would be acquired. During the first 4 eurosols (Phase 1A), gravity, altimetry, and magnetometry would provide a first-order characterization of the ocean. The WAC attains a global color map, and the IPR would search for shallow water. During the next 4 eurosols (Phase 1B), the WAC would acquire a stereo map, and the IPR would search the deep ocean. Profile-mode observations would be performed by the visible-infrared spectrometer and the thermal instrument. Coordinated targeted observations would be performed by the multiple optical remote sensing instruments. Target selection would use existing Galileo data and data obtained during the Jovian Tour flybys. Global maps obtained during this campaign would be used to select target observations in later campaigns.

Regional-scale processes are the science emphasis of Europa Campaign 2. Characterization of the gravity field during Europa Campaign 1 would allow a relatively stable orbit to be selected for Europa Campaign 2, where the flight system would move to a 100 km altitude orbit for the remainder of the mission. From this distance, optical remote sensing instruments would provide two times better spatial resolution but only half the longitudinal area coverage. The duration of the campaign would be expanded to 12 eurosols (43 days) to accomplish the global mapping and profile distribution goals. Gravity, altimetry, and magnetometry would improve characterization of the ocean. The first 6 eurosols (Phase 2A) would again concentrate on conducting a shallow-water search by the IPR and producing a global map with the WAC. The subsequent 6 eurosols (Phase 2B) would emphasize a deep ocean search by the IPR and stereo mapping by the WAC. Profile-mode observations by the visible-infrared spectrometer and the thermal instrument would continue at higher spatial resolution owing to the lower orbit. Global mapping at higher resolutions would generate higher data rates, leaving significantly less data volume per day for coordinated targeted observations.

Europa Campaign 3 emphasizes Targeted Processes. Targets of these synergistic observations would be specific high-priority features and terrains recognized from data obtained earlier in the mission. Most of the

downlink resource would be allocated to targeted observations.

The emphasis of Europa Campaign 4 is to focus on science discoveries achieved earlier in the mission. The principal priority would be to obtain "chains" of targeted observations that attack these new discoveries and newly established priorities based on previous observations. A list of potential observation scenarios includes:

- Create a finer global and regional grid of profiling observations (IPR, VIRIS, TI), particularly in discovery areas. This would be routine mapping data collected on particular orbits;
- Continue gravity and continuous laser altimetry and fields and particles measurements;
- Collect additional coordinated target sets to investigate new discoveries and priorities and to improve coverage and characterization of candidate future landing sites;
- Collect off-nadir NAC stereo images using left/right roll-only pointing;
- Propellant permitting, plan a campaign of lower altitude operations for improved measurements (altitude depends on propellant allocation and orbit stability analysis through Europa Campaign 3);
- Monitor Io and Jupiter for several orbits, 1 to 2 times per week. Date selection gives range of resolution, phase and longitude.

Europa Data Acquisition Scenarios

Except for coordinated targeted observations, most science data collection would be continuous and repetitive. Particles and magnetic field investigations (MAG and PPI) would operate continuously and the LA would profile the surface continuously for the entire mission phase. The TI would profile the surface continuously for Europa Campaigns 1 and 2 and then operate sporadically to monitor hotspots or other areas of interest. The VIRIS, in point mode, would profile the dayside of every other orbit. In every other orbit the WAC would collect a swath of moderately compressed imaging data over 80% of the dayside. On alternate orbits, the IPR would collect a data-reduced sounding profile over 90% of the dayside surface.

The WAC would image in two modes: full color (3 colors + panchromatic) and panchromatic-only modes for stereo mapping coverage (with a factor of 4 difference in data rate). The WAC data would be compressed with a slightly lossy factor of 4. At 100 km WAC data rates would be more than twice the rates from 200 km. The early portions of Europa Campaign 1 would produce global color images from the WAC. After completing the global map, stereo coverage at lower rates would be collected until the end of the campaign. Multiple images would allow improved stereo processing.

IPR data would be collected in two different modes. The shallow water search mode would be used in the first half of Europa Campaigns 1 and 2. The deep ocean search mode would be used in the second half of Europa Campaigns 1 and 2. The shallow mode would collect data at 280 kb/s and the deep mode would collect data at 140 kb/s.

Data volumes for the 2-orbit repetitive cycle would be allocated based on coverage extent needed. Precise timing is not specified, however. This would allow adjustment of the image or sounding start times to allow coverage of both polar regions. These allocations allow close spacing at high latitudes in both hemispheres providing planning margin for the WAC or for radar data processing advantages for the IPR.

Continuous and alternating orbit data collection activities represent about 2/3 of the daily average downlink data volume in Europa

Campaigns 1 and 2. The data would be collected at low enough rates that most of the data would be downlinked in near real-time, requiring very little of the 1 Gb SSR storage capacity. The continuously operating instruments would fill the SSR by about 15% during Earth occultations, which would be rapidly downlinked after occultation exit. This strategy would allow the remaining 1/3 of the daily data volume to be used for coordinated target observations over selected sites at Europa. Either imaging or IPR targets could be acquired at nearly any time in either orbit type.

Figure 5-15 shows the 2-orbit cumulative data volume usage for the instruments and the downlink for the beginning of Europa Campaign 1. The SSR state and limits are shown to highlight minute-by-minute usage. The simulation is per minute and does not account for latencies in data transfer, compression or encoding, which are assumed to be small. Estimates for occultation start/end times include orbit period, occultation durations, DSN lockup times and ephemeris timing errors.

The mission design includes two types of target data sets, coordinated target observations, and full resolution IPR. Coordinated target observations are: MAC monochromatic imaging (orange, 10 m/pixel), VIRIS imaging (green, 25 m/pixel, 700 wavelengths), NAC imaging (yellow, 1 m/pixel), and a low-data rate IPR profile (blue, 60 seconds of data at 140 kb/s). The laser altimeter would operate simultaneously in profiling mode. Full resolution IPR data sets would be based on 30 sec of data at 30 Mb/s, approaching the 1 Gb capacity of the SSR, and could not be taken at the same time as coordinated target observations.

Figure 5-16 shows a view of the coordinated target observations, with scales based on a 100 km orbiter altitude. Each coordinated image represents about 290 Mb of data collected in about 1 minutes' time. The SSR would hold this data until it could be downlinked (along with the other data collected). On average, less than one target per orbit would fit in the data stream. Two

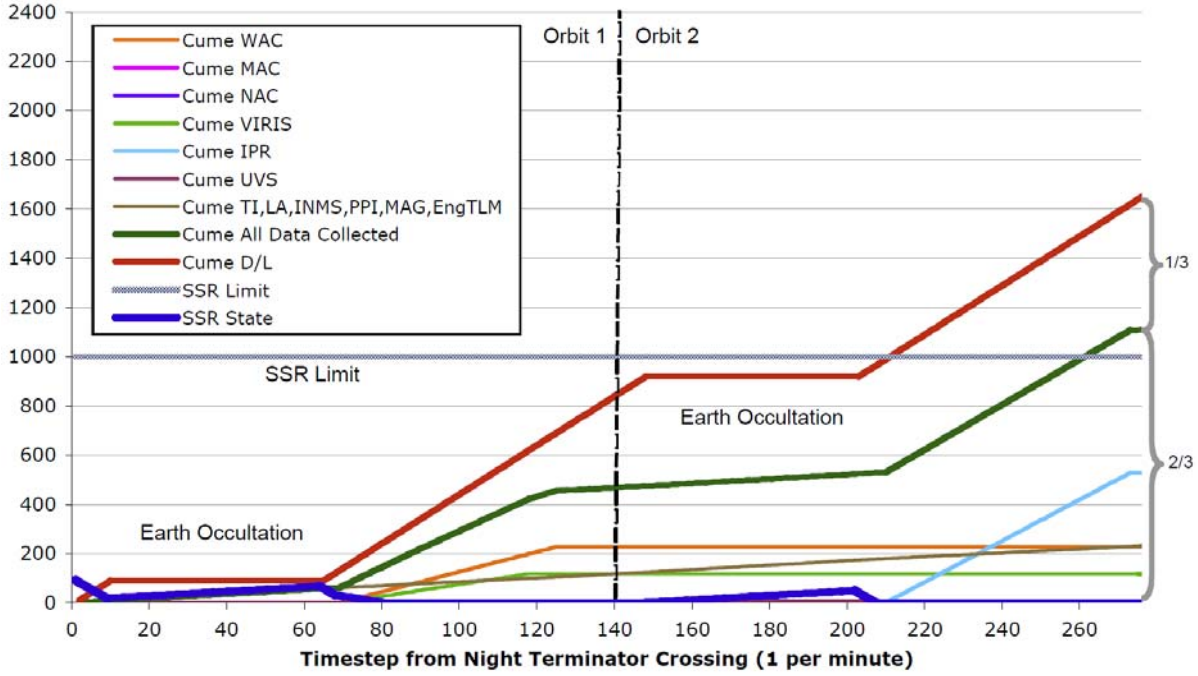

Figure 5-15. Cumulative data volume for a 2-orbit repeating cycle

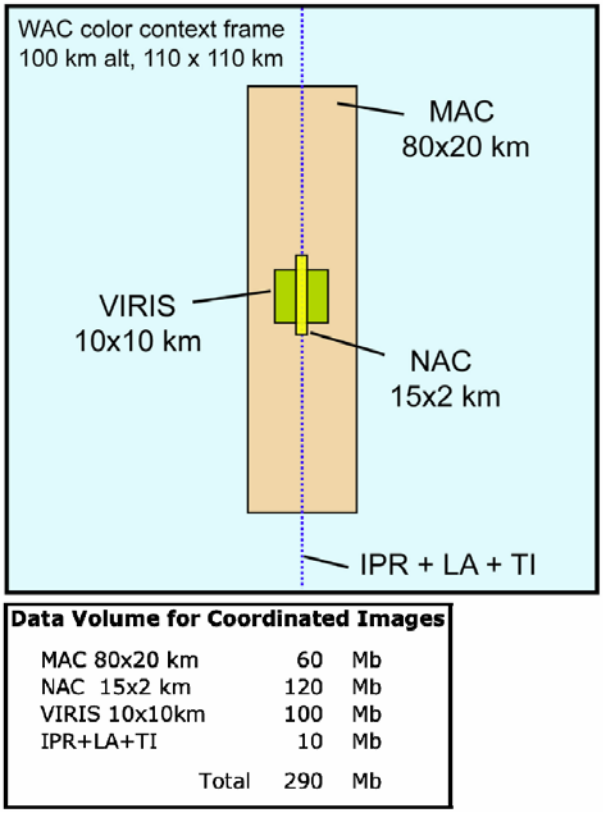

Data Volume for Coordinated Images		
MAC 80x20 km	60	Mb
NAC 15x2 km	120	Mb
VIRIS 10x10km	100	Mb
IPR+LA+TI	10	Mb
Total	290	Mb

Figure 5-16. Coordinated Targets

coordinated targets could be collected at a time for delayed downlink. The IPR full resolution targets are 900 Mb and only one of these could be collected at a time. More than 1900 targets of both types would be returned in the Europa Science phase. This would provide considerable margin over the 1000 targets required by the JJSDT.

Targets would be acquired via on-board, ephemeris driven software. The Flight System would have a shape model of Europa and an orbit ephemeris. Targeting software would calculate the precise time to image a selected site (lat, lon, elevation) as it passed into the instrument field of view. Updated ephemeris files would be uplinked to the flight system as needed to maintain the desired accuracy. Lists of targets to be acquired and corresponding imaging parameters would be developed and uplinked to the flight system every few days. To speed up the selection and file development process, targets could be selected by ground software using data volume modeling and priority based selection criteria.

Data reduction and compression strategies vary by instrument and by campaign. Table 5-11 shows payload operational characteristics, including the data rates, data reduction factors, and instrument duty cycles and data volume collected for the 2-orbit repetitive cycle and for the 200 km and 100 km orbits.

Mapping sequences would be updated and uplink products built and tested once per week. Data collection profiles and patterns (orbit repeat intervals, collection lengths, start locations, etc.) would be based on previous week's planning, reflecting the adjustment of pre-arrival plans. Collection profiles would be developed from activity template menus to reduce development and verification schedules. As mapping progressed, the short planning cycle would enable adjustment of data collection profiles to avoid redundant coverage or to recover observation opportunities lost due to telecom link outages, spacecraft engineering events (*e.g.,* OTMs), or safing events. Routine engineering activities such as OTMs, reaction wheel momentum desaturation, and health and safety activities would be planned and uplinked to the orbiter on a weekly basis, coinciding with mapping sequence uploads.

Coordinated target observations would be planned several times per week based on the remaining data volume resources from the weekly mapping sequences. A target database would be maintained with prioritized target locations (lat, lon, elevation, extent). Based on available data volume, SSR state, DSN schedule, ground track locations, and target priority, targets would be selected, by ground software, for one to two day planning cycles. Only targets predicted to pass under the nadir

track of the orbiter would be considered for selection. Target lists would be sent to the orbiter and executed via ephemeris driven on-board sequencing software. The short planning duration would be needed to accommodate large ephemeris errors based on poor gravity field knowledge early in the orbiting mission. The number of targets would vary with available data volume, but, on average, would be fewer than one target per orbit.

Europa Science Data Return

In the Europa Science phase, data acquired by the science instruments would either be stored on the SSR or transferred directly to Earth in the downlink stream. The C&DH would prepare and/or process the science data (compression and frame encoding) then route through the SDST for downlink. All acquired data would be transmitted to the DSN. For each week during the mission, data volume estimates would be provided to the operations teams based on the scheduled DSN tracking for the period. The data volume estimates would be used to verify the science activity plans and to determine data volume availability for target selection in the coming one week period.

The SSR would function as a short term buffer for data acquired while the flight system communications are occulted by the Earth or when data is collected at aggregate rates exceeding the downlink rate. The 16 Gb SDRAM partition of the SSR is assumed, for planning purposes, to have failed due to radiation effects, by start of the Europa Science phase. For most orbits, 10–15% of the 1 Gb CRAM SSR science partition would be needed for storing data from the continuously operating instruments while in occultation. Up to once or twice per orbit, a coordinated target observation would be collected and stored in the SSR. The target observation sizes are constrained to fit, with margin, into the SSR. The data would be queued with all other data for subsequent downlink. Buffer architectures and queuing schemes have not yet been considered. The small SSR could be used for longer-term storage of very small amounts of high priority data. For the most part, data collected would be downlinked in the order it was collected. No facility for re-transmission, data editing, or for accommodating long DSN gaps is possible or required. The science objectives are systematic and repetitive. Observations needed to achieve the science goals could be rescheduled in the event of lost downlink time. It is assumed that data transfers, compression, encoding, and other processing steps would not cause significant latencies in the data flow and, therefore, no congestion in the SSR.

The current telecom design provides 80 kb/s to a 34 m DSN antenna at a range of 5.7 AU (at 20 deg elevation and 90% weather). Using an operational technique demonstrated by MRO and Cassini to transmit at the best achievable rate after each orbit occultation, the system design takes advantage of increased elevation angles at DSN sites during a tracking pass as well as increasing rates when Europa is farthest away from Jupiter's hot body noise. These advantages increase the estimated average data rate to 170 kb/s at 5.7 AU with an orbit-to-orbit variation from 60 kb/s to 260 kb/s.

Europa Science Phase Performance

The distribution of data volume resources and targets acquired is shown in Table 5-13. 1.25 Tbits of science data would be collected along with nearly 1900 targeted observations, of which half would be before the end of Europa Campaign 3.

Table 5-13. Summary of Data Volumes and Targets Which Could be Acquired by Phase and Instrument

	Europa Campaign 1					Europa Campaign 2					Europa Campaign 3					Europa Campaign 4					All Europa Campaigns		
Reference S/C	Glob data per day (Gb)	Targ data per day (Gb)	% tot vol	Targ per day	C1 Tot Vol (Gb)	Glob data per day (Gb)	Targ data per day (Gb)	% tot vol	Targ per day	C2 Tot Vol (Gb)	Glob data per day (Gb)	Targ data per day (Gb)	% tot vol	Targ per day	C3 Tot Vol (Gb)	Glob data per day (Gb)	Targ data per day (Gb)	% tot vol	Targ per day	C4 Tot Vol (Gb)	Total Targets	% total vol	Total Vol (Gb)
Data Volume	6.1	2.3			238	6.0	0.9			294	2.0	4.5			184	0.4	2.6			499			1215
WAC	0.74		9%		21	0.62		9%		26	0.04		1%		1	0.01		0%		2		4%	51
MAC		0.39	5%	13 T	11	0.00	0.19	3%	6 T	8		0.78	12%	13 T	22		0.37	12%	6 T	61	1710 T	8%	103
NAC		0.78	9%	13 T	22	0.00	0.39	6%	6 T	17		1.56	24%	13 T	44		0.75	25%	6 T	122	1710 T	17%	205
IPR	3.53	0.45	47%	1 T	113	3.53	0.00	51%	0 T	150	0.91	0.90	28%	1 T	51	0.05	0.90	31%	1 T	155	207 T	39%	470
VIRIS	0.61	0.65	15%	13 T	36	0.62	0.32	14%	6 T	40	0.04	1.30	21%	13 T	38	0.01	0.62	21%	6 T	104	1710 T	18%	218
UVS	0.03		0%		1	0.02		0%		1	0.03		1%		1	0.01		0%		2		0%	5
TI	0.26		3%		7	0.26		4%		11	0.05		1%		2	0.02		1%		3		2%	23
LA	0.17		2%		5	0.17		3%		7	0.17		3%		5	0.06		2%		9		2%	27
INMS	0.09		1%		2	0.09		1%		4	0.02		0%		1	0.01		0%		1		1%	8
PPI	0.17		2%		5	0.17		3%		7	0.17		3%		5	0.06		2%		9		2%	27
MAG	0.35		4%		10	0.35		5%		15	0.35		5%		10	0.12		4%		19		4%	53
S/C TLM	0.17		2%		5	0.17		3%		7	0.17		3%		5	0.06		2%		9		2%	27

[1] MAC targets are 1 minute duration (71 km/min @200 km, 78 km/min @100 km)

[2] VIRIS targets are each 400x400 pixels, 100 Mb

[3] IPR targets are each 30 Mb/s x 30 s, 900 Mb

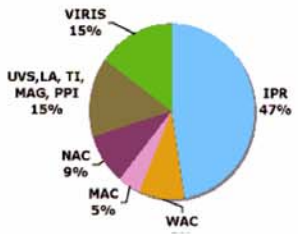

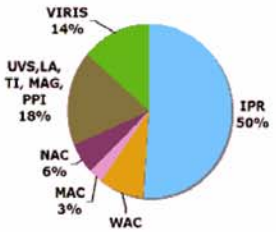

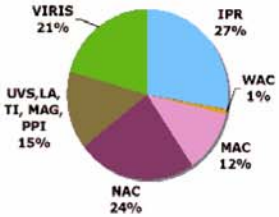

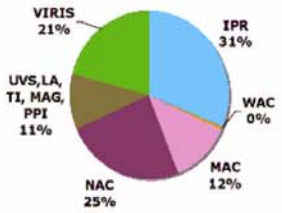

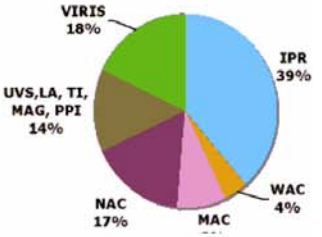

Figure 5-17 shows the coverage of Europa during Europa Campaign 1 from the 200 km orbit. Complete color WAC coverage would be obtained in the first 3 eurosols. Another complete WAC map (in panchromatic mode) to be used for stereo topography takes another 3 eurosols. Additional stereo coverage would be acquired during the two remaining eurosols to improve stereo products.

Figure 5-18 shows the coverage of Europa during Europa Campaign 2 from the 100 km orbit. Complete panchromatic coverage would be obtained in the first 7 eurosols. Because of the significant overlap in the first 7 eurosols, stereo coverage would be complete in another 4- to 5- eurosols.

Ground track coverage could be used as a proxy for the coverage of the profiling instruments. Figure 5-19 and Figure 5-20 show the buildup of ground tracks in Europa Campaign 1 and Europa Campaigns 1–3, respectively. The white box overlay is a 10×10 degree square with 1 degree tick marks to show that ground track coverage would be better than the 25 km spacing requirement at the equator by about a factor of

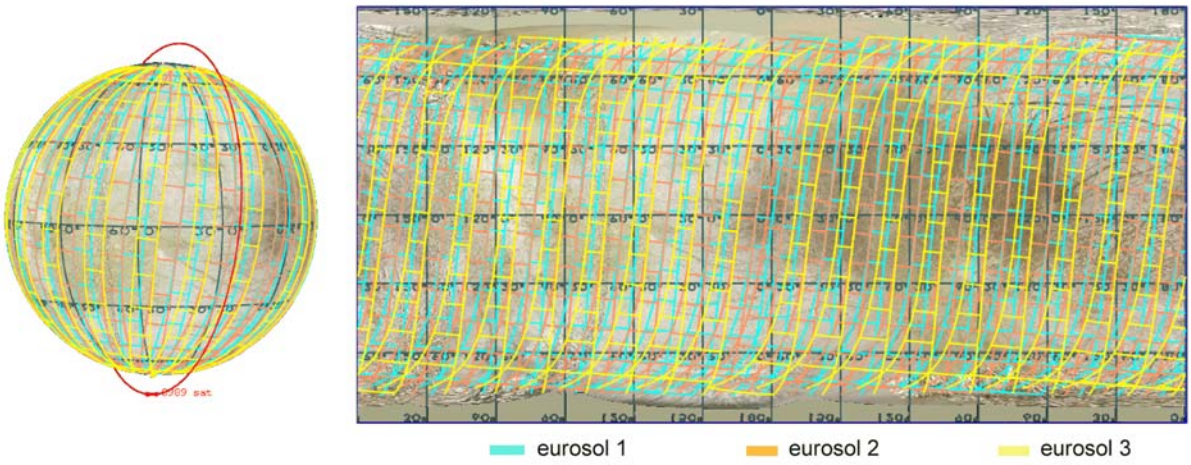

Figure 5-17. WAC coverage in Reference Europa Campaign 1

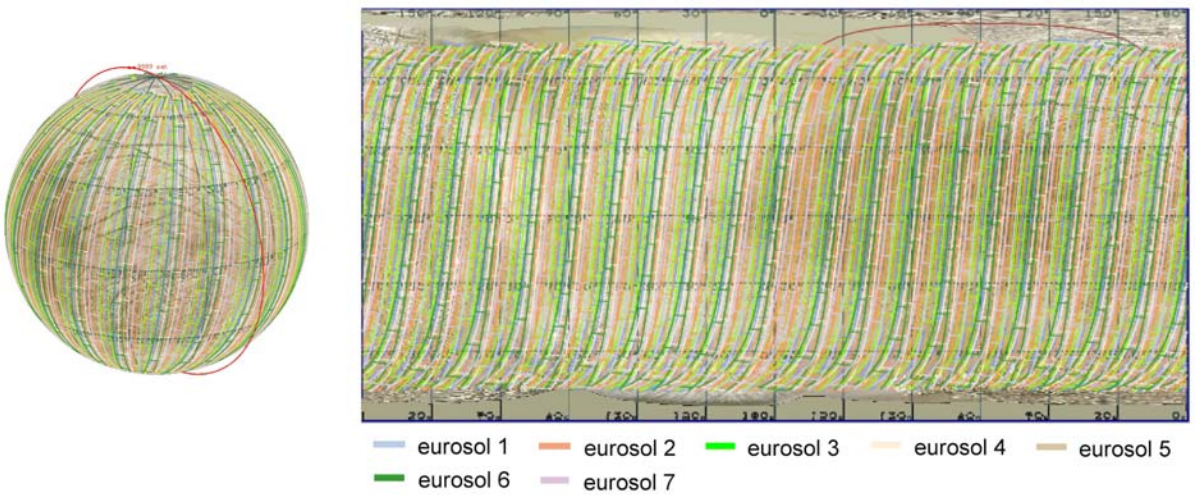

Figure 5-18. WAC coverage in Reference Europa Campaign 2

4 (1 deg = 27 km at equator). IPR profiles would have half the number of ground tracks due to the alternating orbit data collection strategy. IPR tracks would exceed requirements by a factor of 4 also.

The pie charts below Table 5-13 show the data volume fractions for each instrument by campaign.

The Jovian Tour phase would return over 3 Tb, similar to the Cassini mission data volume. The 1.25 Tb data volume returned in the primary Europa Science phase is sufficient to meet science objectives with significant margin for collecting more targets than required and with time to respond to discoveries and augmented science questions.

5.1.5 Summary

The JEO mission has developed operational scenarios for both the Jovian Tour and the Europa Science mission phases. The preliminary tour scenarios show robust data volume margins and frequent opportunities to conduct the science campaigns defined by the JJSDT. Europa science scenarios are robust to achieve the science objectives with the planning payload.

The long mission duration at Jupiter and

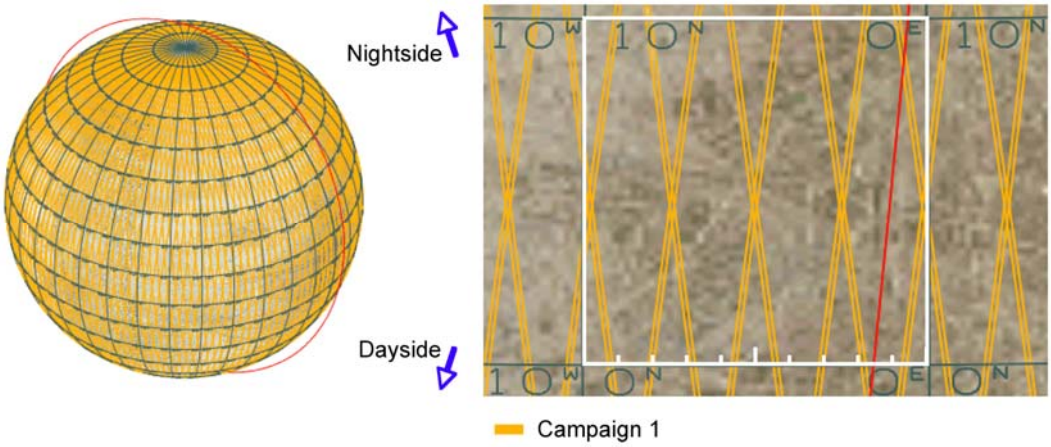

Figure 5-19. Ground Track coverage in Reference Europa Campaign 1

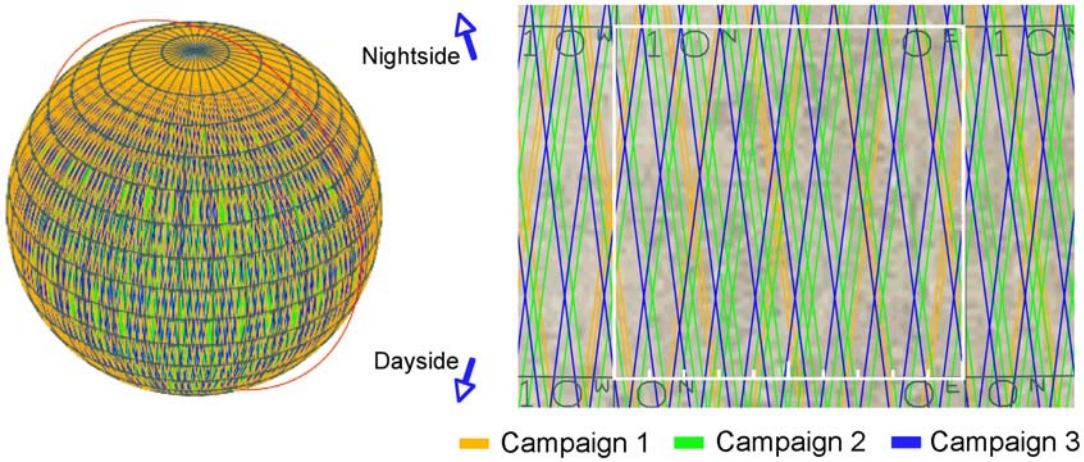

Figure 5-20. Ground Track coverage in Reference Europa Campaigns 1,2,3

especially at Europa enables significant flexibility of science scenarios to achieve mission science goals and cope with possible radiation based anomalies, and allowed a more diverse set of measurements and investigations in the final Europa science campaigns.

5.2 JGO Science Implementation

5.2.1 JGO Model Payload

To show that the science objectives of the JGO component of EJSM could be achieved, the JJSDT identified instrument types that are currently available to assemble a model payload. This set of notional instruments was put together prior to the ESA JGO industrial study phase. Instrument Declaration of Interest (DoI) studies that ran in parallel with industrial activities demonstrated sufficient maturity of the model payload. For most of the instruments the estimated TRL is 5-8.

The JGO model payload consists of 11 instruments and includes: a Laser Altimeter, a Radio Science Instrument, an Ice Penetrating Radar, a Visible Infrared Hyperspectral Imaging Spectrometer, an Ultraviolet Imaging Spectrometer, a Narrow Angle Camera, a Wide Angle Camera, a Magnetometer, a Plasma Instrument–Ion Neutral Mass Spectrometer, a Sub-millimeter Wave Instrument, and a Radio and Plasma Wave Instrument. The characteristics of each instrument are summarized in Table 5-14. To establish the instrument specifications, the JJSDT identified science measurement requirements (FO-1), which were used to determine sensitivity and resolution requirements. The instrument resource allocations (Table 5-15) were based on those of existing instruments with similar capability.

5.2.2 JGO Mission Concept and Phases

The configuration of the JGO spacecraft is driven by the long distance to Jupiter, the high Δv, the need to protect equipment from the intense radiation field, resulting in grouping of instrument and spacecraft hardware, and by the requirement of using solar electric power generation, resulting in a large area of solar arrays. Furthermore, to optimize the data downlink rate, a large high gain antenna is included in the baseline. Due to its remote sensing and *in situ* exploration requirements, a three-axis stabilized spacecraft is assumed.

The trajectory is achieved by using gravity assist maneuvers (Venus-Earth-Earth and Earth-Venus-Earth-Earth for baseline and backup launches, respectively), and following Jupiter Orbit Insertion (JOI), by using the two outer Galilean moons, Callisto and Ganymede for shaping the trajectory within the Jupiter system. Science observations are assumed to be carried out during the flybys of the Jovian moons. In addition to allow for an extended exploration of Callisto and allowing for extended exploration of the Jupiter magnetosphere in this key region, a series of resonant orbits with Callisto is assumed, which is designed such that at least 9 Callisto flybys would be performed.

Finally, the spacecraft would be transferred into an elliptical orbit around Ganymede, which would be circularized and reduced in altitude, until final deposition on Ganymede's surface.

The following phases of the mission could be identified:

- Launch and interplanetary trajectory (5.9 years, 7.1 years for the backup launch date);
- Jupiter orbit insertion, and energy reduction for transfer to Callisto (179 days);
- Callisto science phase (388 days);
- Transfer to Ganymede (240 days);
- Ganymede science phase (300 days).

Table 5-14. JGO Model Payload

Model Instrument	Acronym	Characteristics	Similar Instruments
Laser Altimeter	**LA**	Single Beam @ 1064 nm 20 m spot @ 200 km 20 to 90 Hz pulse rate	Bepi-Columbo BELA
Radio Science Instrument	**RST & USO**	2-way Doppler and ranging with Ka-Band transponder Ultra-Stable Oscillator	Cassini, BepiColombo, Juno
Ice Penetrating Radar	**IPR**	Single frequency: 20- to 50-MHz Along track resolution: 1 km Across track resolution: < 5 km Penetration depth: 3- to 9-km Vertical resolution: 10 m to 1% of target depth Dipole antenna: 10 m	Mars Express MARSIS; MRO SHARAD
Visible Infrared Hyperspectral Imaging Spectrometer	**VIRHIS**	Pushbroom imaging spectrometer with two channels and scan system 640 × 480 detector Spectral range: 400 to 5200 nm Spectral resolution: 2.3 nm @ <1.7μm Spectral resolution: 5.8 nm @ >1.7 μm IFOV: 0.125- to 0.250-mrad FOV: 3.4°	Cassini VIMS; Mars Express OMEGA; Rosetta and Venus Express VIRTIS
Ultraviolet Imaging Spectrometer	**UVIS**	EUV and FUV + MUV grating spectrometers 512 × 512 Detector Spectral range: 50- to 320-nm IFOV: 0.01 mrad FOV: 2°	BepiColumbo PHEBUS; Mars Express SPICAM; Venus Express SPICAV
Narrow Angle Camera	**NAC**	Pushbroom imaging in orbit around Ganymede; framing imager for distant targets. Color and multispectral imaging capability with filter wheels (12 colors); 1024 × 1024 detector FOV: 0.30°. Pixel IFOV: 0.005 mrad Spectral range: 350- to 1050-nm	Mars Express SRC; Dawn Camera; Exomars PanCam
Wide Angle Camera	**WAC**	Framing imager: 1024 × 1024 detector Spectral range: 350- to 1050-nm IFOV: 2 mrad FOV: 117 deg	Mars Express SRC
Magnetometer	**MAG**	Dual tri-axial fluxgate sensors; boom length to meet magnetic cleanliness requirements	Cassini & Venus Express Magnetometers
Particle and Plasma Instrument - Ion and Neutral Mass Spectrometer	**PPI - INMS**	<u>Plasma Analyzer:</u> Electrons: 1 eV to 20 keV Ions: 1 eV to 10 keV <u>Particle Analyzer:</u> Electrons: 15 keV to 1 MeV; Ions: 3 keV to 5 MeV, ENA: 10 eV to 100 eV	Mars Express and Venus Express/ASPERA; Rosetta/ROSINA
Sub-millimeter Wave Instrument	**SWI**	Spec. range, two bands: 550 & 230 μm Resolving power $\lambda/\Delta\lambda$: 10^7 FoV: 0.15° to 0.065°	Rosetta MIRO
Radio and Plasma Wave Instrument	**RPWI**	Plasma density ($0.001\text{-}10^6$ cm^{-3}) and temperature (0.01-20eV); Spacecraft potential (± 50V) Near Dc E-Field (up to 3 MHz), E (1kHz-45 MHz) and B (0.1-600 kHz) plasma and radio wave detectors	Cassini/RPWS

Table 5-15. JGO Model Payload Resources

Model Instrument	Mass (kg)	Power (W)	Data Rate (kb/s)
Laser Altimeter	11	24	30
Radio Science Instrument	2- to 2.5	26	very low, HK data only
Ice Penetrating Radar	10	20	300
Visible Infrared Hyperspectral Imaging Spectrometer	17	20	5000
Ultraviolet Imaging Spectrometer	6.5	20	30
Narrow Angle Camera	< 8	15 (incl. DPU)	75
Wide Angle Camera	1.5	3 (excl. DPU)	5000
Magnetometer	1.8	2 (excl. heaters)	7- to 70
Particle and Plasma Instrument – Ion Neutral Mass Spectrometer	17.5	50	2- to 25
Sub-millimeter Wave Instrument	9.7	39	10
Radio and Plasma Wave Instrument	11.5	7-32	0.05- to 6

5.2.2.1 Launch and Interplanetary Trajectory

Launch is foreseen on an Ariane 5 ECA with direct escape towards a Venus gravity assist. In the baseline mission, with a launch date in March 2020, a Venus-Earth-Earth gravity assist sequence is planned, leading to a JOI, preceded by a Ganymede gravity assist maneuver, in February 2026, after 5.9 years. The mass injected into the Earth escape trajectory would be 4172 kg, with a hyperbolic escape velocity of 3.38 km/s, which increases to 5.5 km/s after the last Earth swing-by. In this baseline transfer scenario, the launch declination is 0°, which is optimal for launch-to-orbit mass performance.

For the main backup launch that was considered during the study, an additional Earth gravity assist is required extending the transfer time to Jupiter by about 1 year. Due to the relative alignment of Venus and Earth, the Earth departure and Venus arrival conditions are different and are depending on the launch opportunity influencing the direct escape conditions. The declination needed for the direct escape to Venus is low (close to 0°) for 2020, and high (close to about 45°) for 2022 launch opportunities. As the performance of Ariane 5 quickly degrades for non-zero declination, an additional Earth swing-by was introduced allowing for a close to zero degree declination launch, resulting in an Earth-Venus-Earth-Earth sequence. Because of this additional initial Earth gravity assist, the launch mass is considerably increased, partly being used by higher propellant mass required for an additional deep space maneuver for targeting Earth, partly resulting in higher dry-mass. Table 5-16 provides a summary of the launcher performance for the primary and for the backup launch considered.

These launch dates were the best opportunities that were found and analyzed in detail for the purpose of this study. They are very similar in dry mass and the backup opportunity has a

Table 5-16. Summary of Launch Mass and Transfer Duration for JGO Primary and Backup Launch Dates

Launch Date	Launch Mass	Dry Mass	Propellant Mass	Transfer Duration
March 2020	4172 kg	1687 kg	2425 kg	5.9 yr
May 2022	4641 kg	1701 kg	2872 kg	7.1 yr

Note: For the purpose of this table the propellant mass is calculated based on an assumed I_{sp} of 312 s.

more than one year longer transfer duration. For the purpose of constraining the design of the JGO spacecraft, the worst cases of the two options were taken as the baseline for the spacecraft design: maximum allowed dry mass (including maturity margins) being 1687 kg, and the size of the propellant tanks such that the ΔV equivalent to the backup launch could be supported. The mission properties for operations in the Jupiter system are identical in both options. The total ΔV budget is 2465 and 2771 m/s for the 2020 and 2022 launch opportunities, respectively.

Additional launch opportunities could be found at the cost of either mass or extended interplanetary transfer duration. These were not studied in detail. It was however verified that no larger ΔV than for the nominal backup launch would be required.

5.2.2.2 Jupiter Orbit Insertion and Transfer to Callisto

The JOI would be the most critical maneuver of the mission. All other maneuvers are either without thrusting (Venus and Earth gravity assists), or occur while the spacecraft would be in a bound orbit around Jupiter, when sufficient repetitive opportunities for failure recovery exist. The JOI maneuver would require an operation of the main engine for almost 2 hours to deliver 874 m/s.

This Jupiter orbit insertion maneuver would be preceded by a Ganymede gravity assist. While from a purely kinetic energy point of view, it would be most efficient having a gravity assist as close as possible to Jupiter, this would significantly increase the encountered radiation dose, and it was therefore decided to limit the closest approach to about the Ganymede orbit (15 R_J). The Ganymede gravity assist foreseen prior to JOI reduces the required ΔV by about 300 m/s.

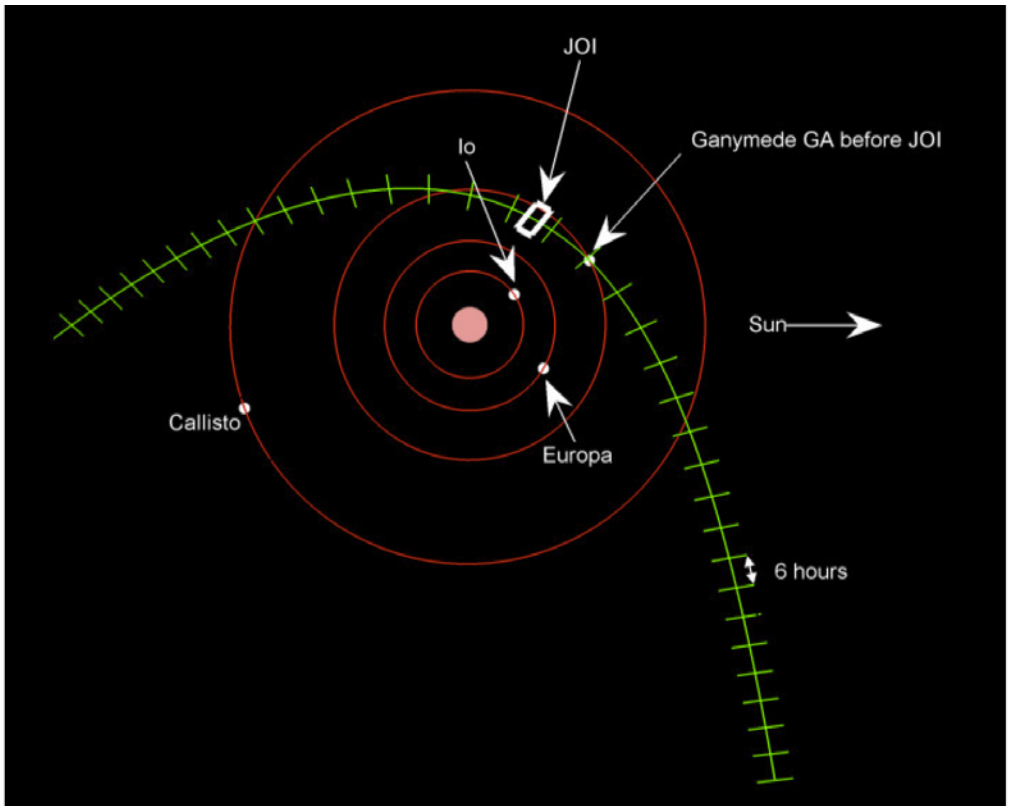

Figure 5-21. Reference JGO Trajectory showing Jupiter Orbit Insertion (JOI) together with the preceding Ganymede gravity assist.

The JOI maneuver would insert the spacecraft in a 13 × 243 R_J orbit, the perijove being defined by the orbit after Ganymede gravity assist, and the apojove being a consequence of the optimization for the following Ganymede gravity assist (this orbit is in 25:1 resonance with Ganymede). A perijove raising maneuver of 63 m/s would be performed at apojove to reduce the radiation dose upon the next Jupiter approach, and to reduce the relative velocity prior to the next Ganymede gravity assist. The geometry of this initial orbit around Jupiter is shown in Figure 5-21 and Figure 5-22, where the orbits of Callisto, Ganymede and Europa are also indicated. This single orbit would take 179 days.

The orbit would further be reduced by three more Ganymede gravity assists (7:1, 4:1, 3:1 resonances), and the inclination would be reduced from the initial value of –7.4° with respect to the Jupiter equatorial plane. The total required deep space ΔV is 23 m/s, and the final apojove and perijove are 50 R_J and 12.2 R_J, respectively (duration 120 days).

Finally the spacecraft would be brought into a Callisto resonant orbit through a sequence of Callisto-Ganymede-Ganymede-Callisto gravity assists, which takes 58 days.

The entire duration of this phase starting with the JOI and ending with the arrival at Callisto takes 357 days.

5.2.2.3 Callisto Science Phase

The exploration of Callisto would be achieved through a series of flybys. The spacecraft would be placed into a resonant orbit with Callisto, and 10 flybys are performed allowing

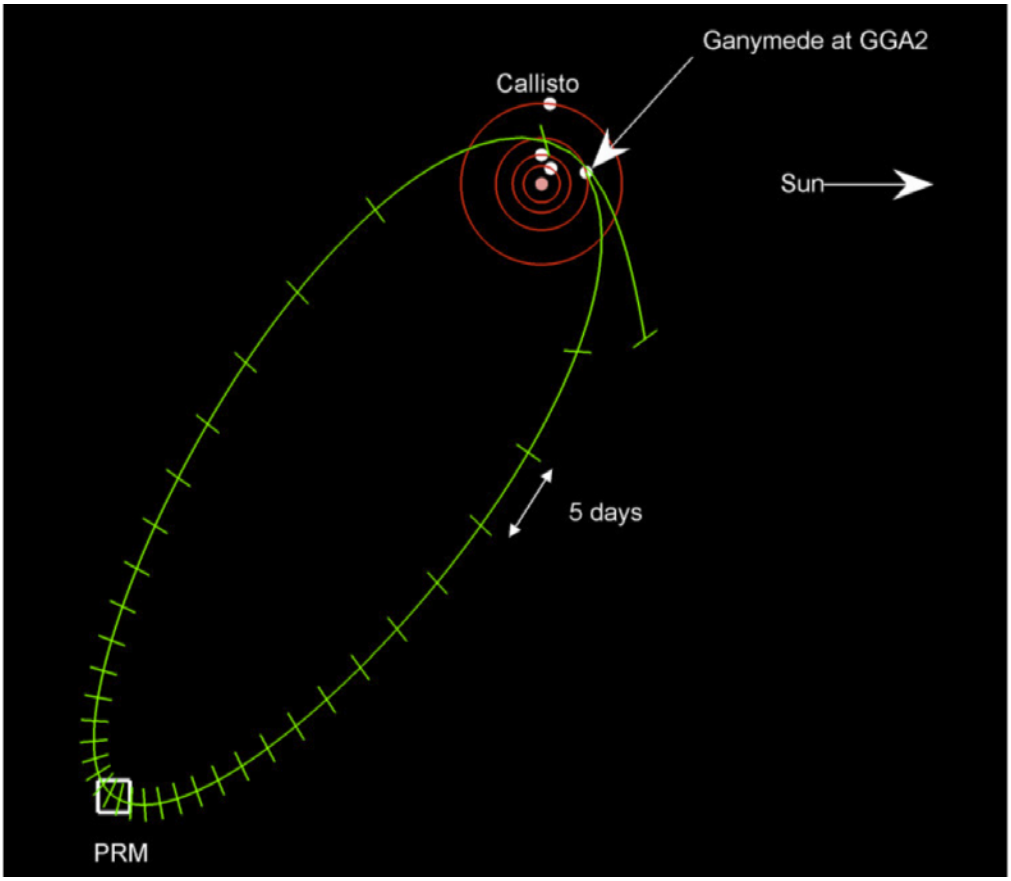

Figure 5-22. Trajectory of the first Jupiter orbit also showing the positions of Callisto, Ganymede, Europa, and Io.

to achieve the science objectives at Callisto. The flybys are arranged to allow for (a) studies of the interior structure through one polar and one equatorial flyby; (b) filling gaps from Galileo and Voyager surface observations; (c) remote sensing observations of special targets; (d) geology observations of the leading or trailing equatorial regions. All flybys are targeted at 200 km altitude, except the final one, which is constrained by the transfer to Ganymede and has a higher altitude (~1200 km). From the mission analysis point of view, it is also possible to achieve lower altitude flybys, but due to navigation uncertainty a conservative altitude of 200 km was assumed in this study. A lower flyby altitude may be considered during the last flybys, if navigation accuracy has improved, as it would allow performing *in situ* measurements deeper in Callisto's exosphere.

The orbit during this Callisto phase is shown in Figure 5-23 in Jupiter Solar Orbit (JSO) coordinates, where the sun is at the right. The apojove of most of the orbits with higher eccentricity is opposite to the Sun, which is advantageous for magnetospheric *in situ* measurements. A more detailed summary of the remote sensing opportunities is shown in Figure 5-24, where the ground tracks for each flyby are drawn on a cylindrical map of Callisto's surface. Local time and specific

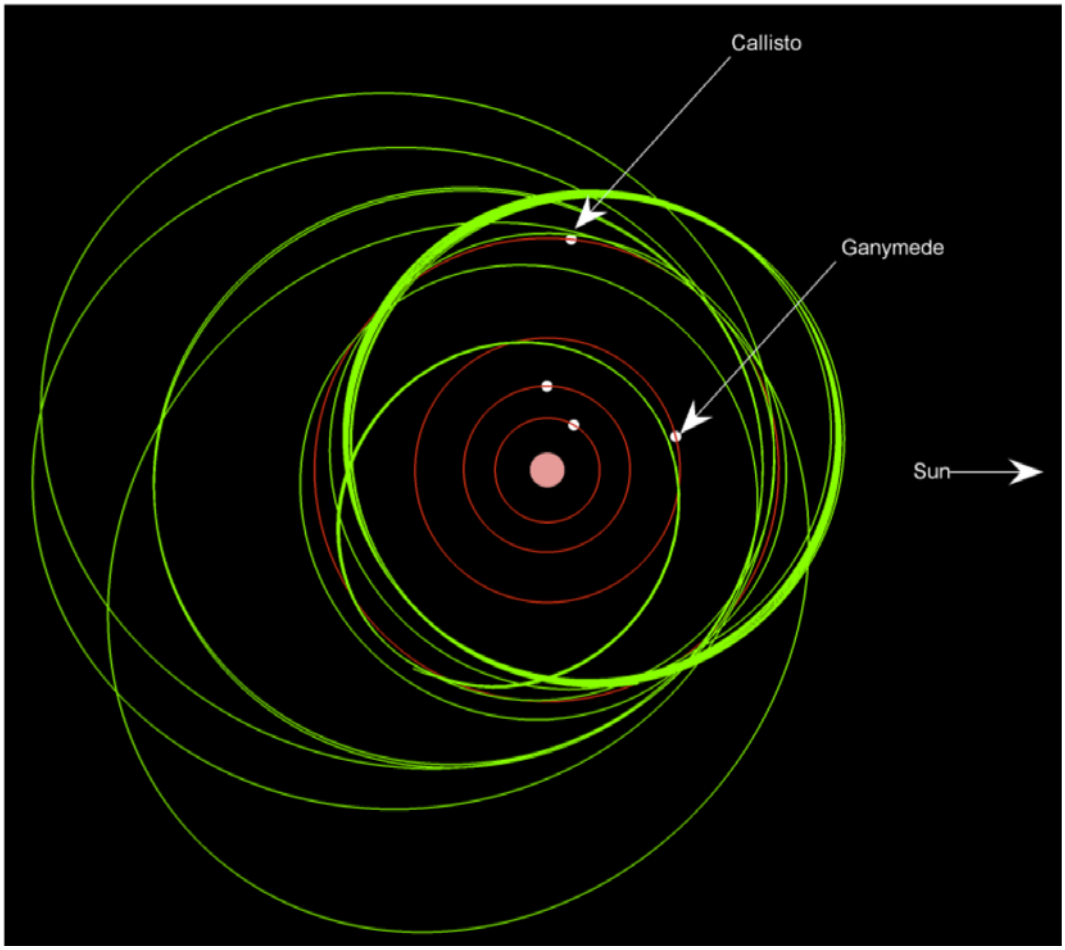

Figure 5-23. The spacecraft trajectory (green) during the reference Callisto phase in Jupiter Solar Orbital (JSO) coordinates: Jupiter is located at the center, as seen from the north celestial pole; the direction to the Sun is to the right; direction to dawn is up. The orbits of Callisto, Ganymede, Europa and Io are also indicated. This trajectory would include 10 targeted flybys.

areas and targets of interest are also indicated. The duration of this phase is 388 days.

For the Callisto flybys a ΔV budget of 10 m/s per flyby was allocated for navigation corrections. This is limiting the number of flybys that are considered in the baseline. Further navigation analysis would be carried out during the next phase to investigate among others, whether this average amount of ΔV could be reduced, thereby allowing for the number of flybys being increased. No changes to the implementation of the spacecraft would be required in this case.

5.2.2.4 Transfer to Ganymede

The transfer would be performed by using the moon resonance strategy, which significantly reduces the ΔV spent compared to the gravity assist strategy, at the cost of added transfer time, which however could be used for science observations, as the region between Callisto and Ganymede is particularly interesting for magnetospheric/plasma physics. The transfer takes 240 days and 92 m/s, and would be completed by the Ganymede orbit insertion maneuver, consuming 144 m/s.

5.2.2.5 Ganymede Science Phase

The Ganymede science phase would be composed of three different types of orbits, which are driven by the requirements of remote sensing at specific illumination conditions, magnetospheric sampling, and the constraint to avoid Ganymede eclipses that would require oversizing the solar panels. Obviously, the eclipse duration in Ganymede orbit is a consequence of the combination of spacecraft altitude and sun declination relative to the plane of its orbit (called β-angle), resulting at given altitude in longer eclipse durations for smaller sun declination values

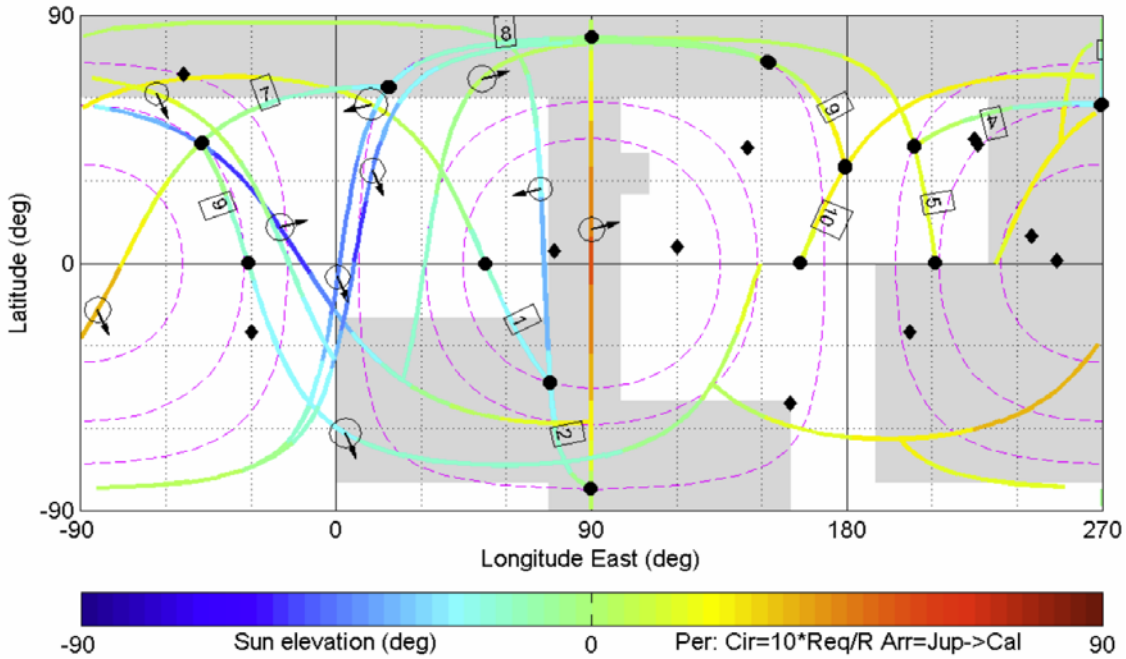

Figure 5-24. Ground track of the Callisto flybys for altitudes <5000 km. The color scale indicates local Sun elevation of the sub-nadir point in degrees (values <0° refer to local night). Numbers indicate the sequence of the flyby. The shaded areas correspond to the scientific target areas to fill gaps from Galileo and Voyager data. The black diamonds correspond to specific target locations. The black circles along each flyby trajectory correspond to the pericenter location (the size of the circle is linear with the pericenter altitude; the arrow gives the Jupiter-Callisto direction in the Jupiter equator of date).

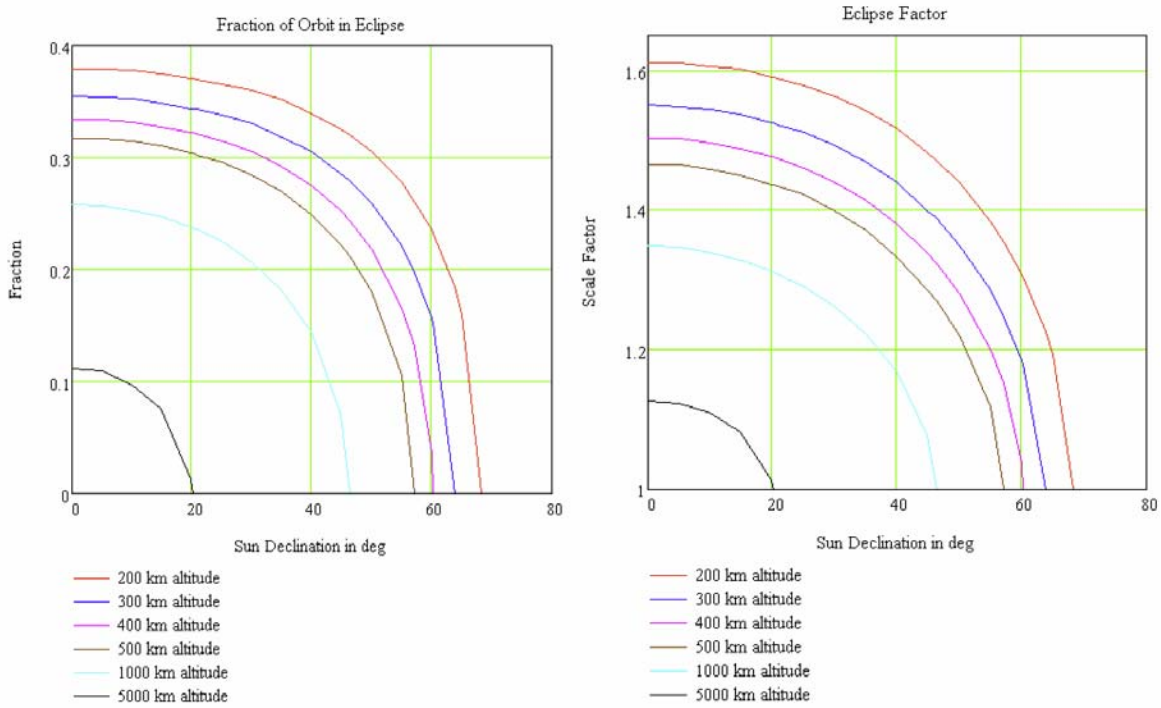

Figure 5-25. Influences of eclipses by Ganymede on the spacecraft design. Left: the fraction of time spent in eclipse as a function of Sun declination to the orbital plane for circular polar orbits with altitudes from 200 to 5000 km. Right: the scale factor of increase of the solar panel for additional power generation.

(see Figure 5-25). For close to polar Ganymede orbits, the orbital plane of the spacecraft would rotate around the pole as a function of inclination because of the influence of Ganymede's oblateness and Jupiter's attraction. This was used to design the orbit such that lower altitudes could be realized later during this phase, while still avoiding sun eclipses, allowing for a sequence of orbits with decreasing altitudes as summarized in Table 5-17. Because of the high apocenter of the elliptical orbit, perturbation by Jupiter is significant, and would cause the orbit to quickly evolve. The argument of pericenter was chosen such that this evolution leads to a circular orbit within about 20 days, where it would remain at an altitude of 5000 km, which would be maintained for about 80 days, and then the eccentricity would increase until a suitable point for injection into a 500 km altitude circular orbit is reached. The evolution of the most important parameters such as apocenter and pericenter altitudes, inclination, argument of pericenter, and sun declination are shown in Figure 5-26.

When a suitable altitude is reached, a maneuver of 480 m/s would be applied to

Table 5-17. Parameters of the orbits around Ganymede.

Phase	Altitude [km]	Sun Declination (β-angle) [deg]	Duration [days]
Elliptical*	200 × 10,000 to 5000 circular	40	120
High Circular	500	62	120
Low Circular	200	71	60
End	200	76	n/a

*Note that in this phase an elliptical orbit is only available for limited time.

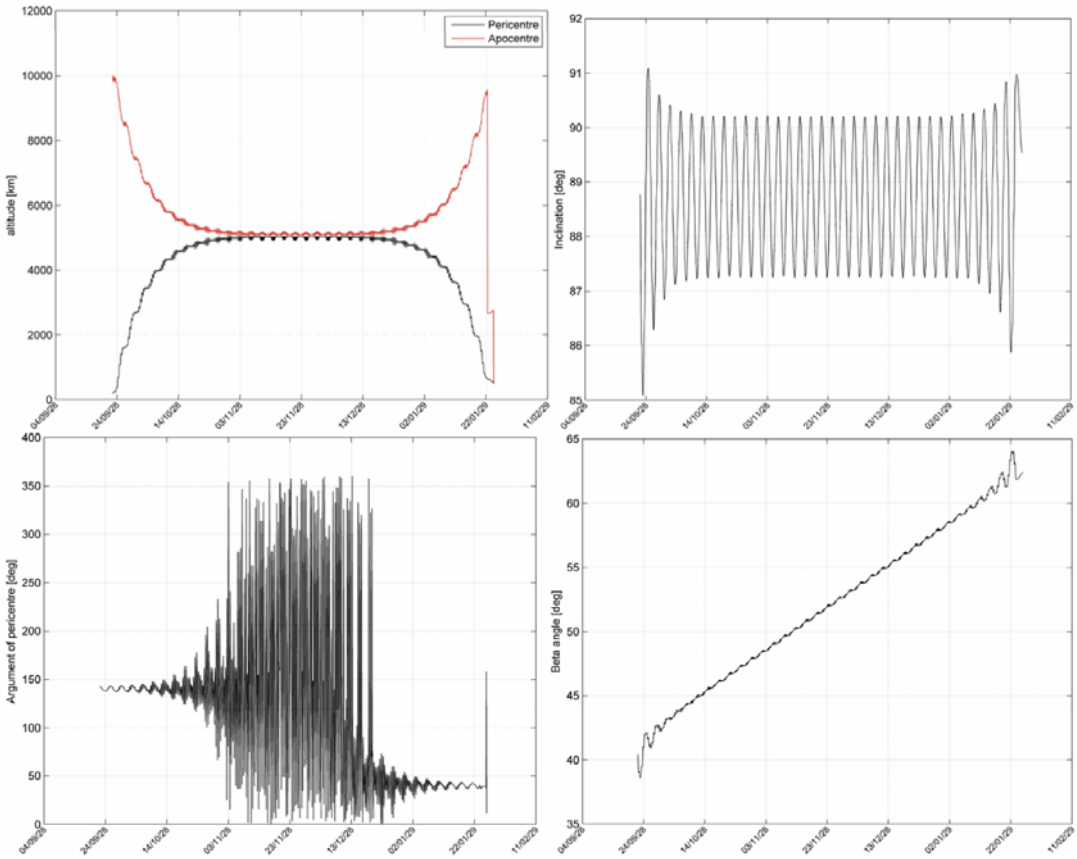

Figure 5-26. Evolution of the orbit during the Ganymede elliptical phase: apocenter and pericenter altitudes (top left); inclination (top right); argument of pericenter (bottom left); sun declination, called *β*-angle (bottom right).

arrive at a circular 500 km altitude orbit, where the spacecraft would operate for 120 days, and the final orbit of 200 km altitude would be obtained after a ΔV of 92 m/s. After nominal operations of at least 60 days, orbit maintenance would be discontinued, and the spacecraft would be left in an orbit with natural growth of eccentricity until disposition on Ganymede's surface. In this final phase the orbit would be very close to polar (deviation <1°), and its evolution of the sun declination is shown in Figure 5-27. Mission extension would be possible based on remaining consumables and spacecraft health.

5.2.3 Spacecraft Design

An ESA assessment study included an activity that involved three parallel industrial studies of JGO. The three designs of JGO that resulted are referred to as solution 1, solution 2, and solution 3.

5.2.3.1 Mission Drivers and Design Consequences

Deep Space, Solar Power, and Telemetry

The main mission drivers are related to the large distance to the Sun, the fact that the mission shall use solar power generation, and to Jupiter's specific radiation environment. The orbit insertions at Jupiter and Ganymede and the large number of flyby maneuvers (>25 gravity assists and flybys) lead to a rather high ΔV requirement, which translates into a high wet/dry mass ratio (about 2.6:1), which amplifies changes of the dry-mass. The large distance to Earth results in a signal round trip time of up to 1^h46^m requiring careful pre-planning and autonomous execution of

operations by the spacecraft. Additionally, a high gain antenna would be required for data downlink. The studies that were conducted aimed at maximizing the diameter of the high gain antenna for maximum science return. For the study purposes, a daily data volume of 1 Gb was assumed as being feasible.

The requirement of using solar array power generation in combination with the large distance from the Sun, providing a worst case solar constant of 46 W/m^2, results in large area solar arrays, of typically about 60–75 m^2. This is a constraining item, which is also correlating the maximum available power with the allowed launch mass.

From the detailed analysis of the mission phases, the Ganymede circular phase was identified as the most challenging phase, which was therefore used as the reference for system sizing.

During this phase, the largest amount of scientific data would be generated. For the baseline, it was assumed that data downlink would occur every time the spacecraft is visible from the single ground station, and would last for the entire pass, possibly only interrupted, by Jupiter or Ganymede occultations. To maximize the data return, more power would be provided to the telemetry system, and very limited instrument operations would be performed during downlink periods. Consequently the need for a steerable high gain antenna was ruled out, allowing for mass optimization and avoiding losses by the radio-frequency chain because of flexible joints. Furthermore, for orbits, during which the spacecraft would be in eclipse, an increase of the required solar array area (and therefore mass) was found as a function of eclipse duration, already requiring significantly more area even for short eclipse durations Figure 5-25. It was therefore decided to avoid orbits around Ganymede, which would cause the spacecraft flying through regular Sun eclipses.

The power generation was further optimized

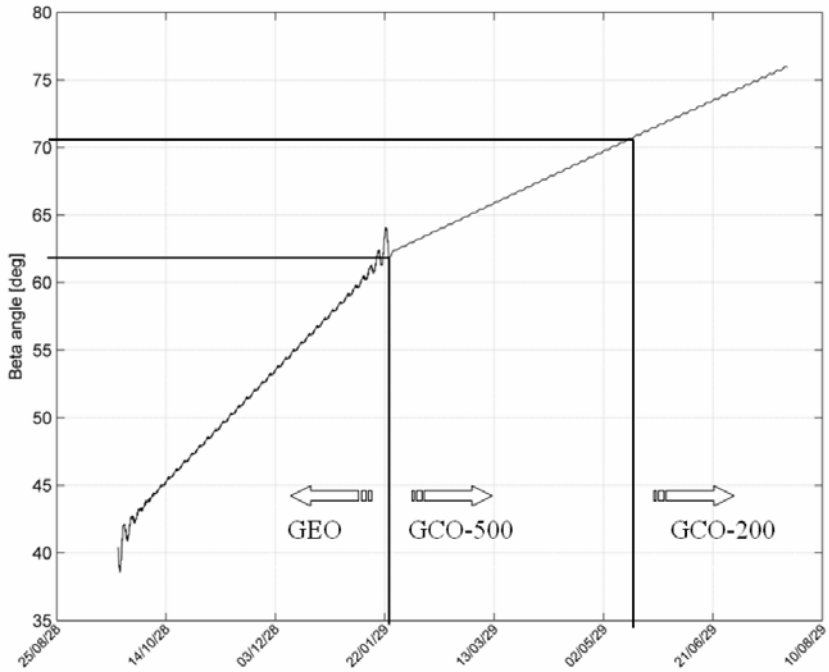

Figure 5-27. Evolution of the orbit during the Ganymede elliptical phase: apocenter and pericenter altitudes (top left); inclination (top right); argument of pericenter (bottom left); sun declination, called *β*-angle (bottom right).

Table 5-18. Definition of Five Generic Model Instrument Observation Scenarios

Obs1 Remote Sensing	Obs2 *In situ*, WAC, LA	Obs3 Radar + *in situ*	Obs4 Radio Science & downlink	Obs5 Jupiter obs., others
VIRHIS	WAC	IPR	RST &	SWI
NAC	LA	RPWI	USO	VIRHIS
UVIS	MAG	MAG		NAC
MAG	RPWI	PPI-INMS		WAC
LA	PPI-INMS			UVIS

Note: Observing scenarios Obs1 to Obs5 were grouped such that one scenario would operate for an entire orbit.

by keeping the solar arrays close to normal to the Sun direction. This would be achieved by a combination of the rotation of the solar arrays around their mounting axis and a spacecraft rotation around the nadir direction. Such a rotation of the spacecraft (yaw steering) would be performed during baseline operations. It is however foreseen to be able to halt this yaw steering for a limited period of time, *e.g.,* for high resolution imaging. This case was however not considered as a design driver, and would therefore only be allowed in combination with power saving measures.

Payload Operations Scenarios

To arrive at a realistic sizing of the spacecraft power subsystem, the mass memory and the telemetry subsystem, a generic baseline operations scenario of the model instruments was compiled. Instruments that would likely be operated together were combined in one scenario, and a schedule of a generic operations sequence was compiled. The Ganymede orbit phase was considered as the reference for this specification, as it is generating the highest volume of science data. The grouping of instruments that would operate in a combined manner on a per orbit basis is summarized in Table 5-18.

Observation scenarios Obs1 and Obs2 would mainly be used during flights over the dayside of Ganymede. In the baseline assumption, these modes would be used alternating and all instruments listed in these groups would be operational. Observation mode Obs3 would be the baseline operation mode during night side observations. The mode Obs4 would either be used in parallel to the data downlink, or for the radio-link to the JEO spacecraft for radio-occultation sounding of Jupiter's atmosphere. The mode Obs5 is intended for remote observations of Jupiter and the other Galilean moons. All these scenarios would not be limited to the Ganymede phase, but would also be used in the other mission phases. It is emphasized that these are example scenarios designed for sizing of the spacecraft resources. Detailed science operations would be developed in the future, in collaboration with the instrument PIs.

Model Payload Accommodation Considerations

Several instrument accommodation requirements appear to be competing for similar locations, which makes the configuration complex. The model instruments include a large number of sensors that would need to be mounted on booms, and which have specific requirements on their orientation on the spacecraft and relative to the spacecraft's velocity vector. In addition there is a set of remote sensing instruments, which would require unobstructed fields of view. And also some particle instruments require as close as possible to 4 π unobstructed field of view. This becomes even more challenging, due to a number of surfaces of the spacecraft already being occupied by platform subsystems, such as: solar panels (2 surfaces), high gain antenna (1 surface), main engine and launcher interface (1 surface). Therefore a compromise in sharing the surfaces had to be found for the accommodation of instruments with specific

orientation requirements, such as facing nadir, anti-nadir, velocity, and anti-velocity. A set of different configurations derived as consequences of these constraints are being presented in the following sections.

To reduce the number of booms and antennae, thereby simplifying the accommodation and reducing the complexity for deployment, sharing of booms and antennae by more than one instrument is recommended. The magnetometer boom and the radar antenna may lend themselves as obvious examples for accommodation of additional sensors, provided the interface requirements are compatible, *e.g.,* on electromagnetic fields.

Because of the large number of fields and particles measurements to be performed, strict limits on the electromagnetic compatibility of the spacecraft subsystems was included as goals, which need more analysis during the next study phase. The electric charging of the surface of the spacecraft shall remain within a few Volts, at least in the vicinity of the electric field sensors and the low energy plasma spectrometers; the DC magnetic field shall remain <2 nT, with a stability of <0.1 nT over the range 0 to 64 Hz (at least during magnetometer measurements), and the electric stray field shall remain <50 dB μV/m within the frequency range below 45 MHz.

5.2.3.2 Spacecraft Design – Solution 1

Configuration

The configuration of this solution is dominated by the accommodation of the tanks of the bi-propellant system being stacked on top of each other within a central tube (derived from Spacebus; see Figure 5-28). All platform and instrument equipment would be accommodated on panels around this central tube, including a vault-type structure serving as radiation shield in the middle that would contain the majority of the units. The large solar arrays (2×32 m^2) would be attached to the side of the spacecraft structure, and consist of four panels each, two of which would be deployed sideways so as to reduce the total length and moment of inertia. The solar arrays would include one drive mechanism each for rotating the solar panels around the spacecraft Y-axis. The high gain antenna would be fixed

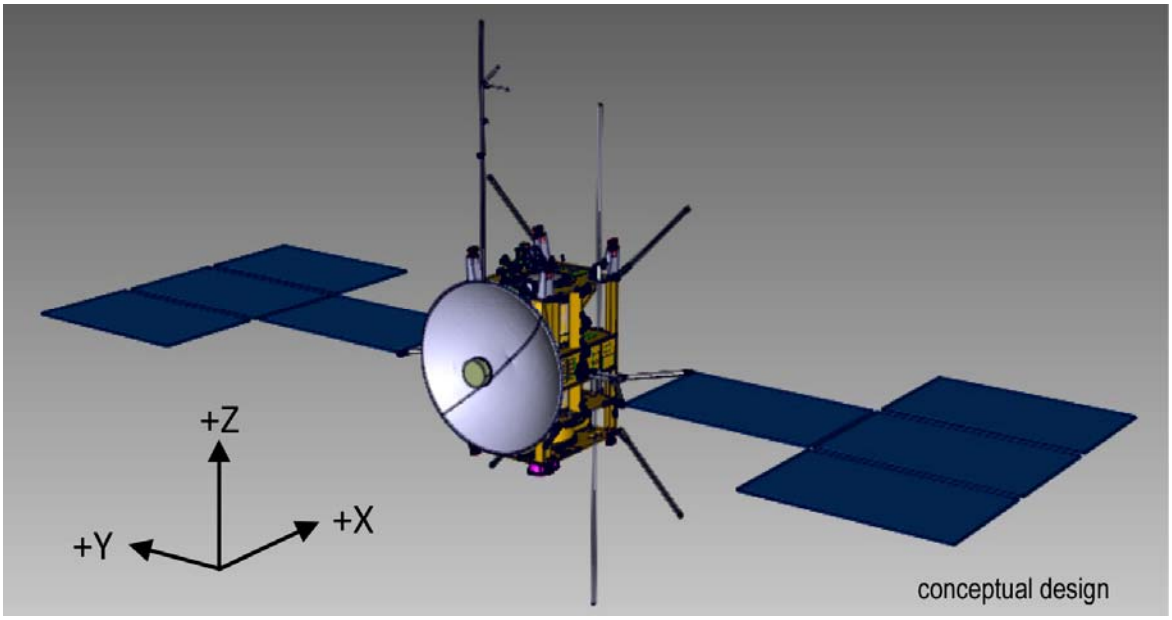

Figure 5-28. Spacecraft configuration of solution 1 shown with the side panels removed. The main engines and the launcher interface would be at the bottom (–Z), the remote sensing and *in situ* instruments, which required access to the velocity direction would be located the back of this view (+X). The cold plate would be at the top (+Z).

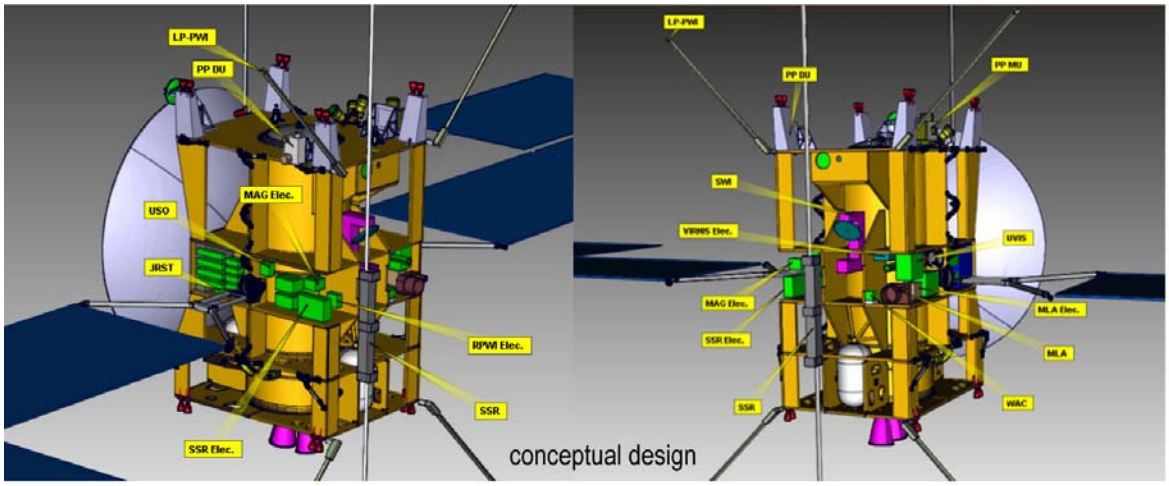

Figure 5-29. Accommodation of the model instruments in spacecraft solution 1.

and mounted to the side of the main tube, where it would be recessed in the main structure so as to maximize its diameter (3.2 m), while still respecting the limits of the launcher fairing. Most of the booms would be extended parallel to the Z axis so as to reduce frequency coupling during thrusting. The size of the spacecraft body ($x \times y \times z$) would be 2.25 m × 1.70 m × 3.13 m, and the extent of the unfolded solar arrays, from the edge of the spacecraft's body is 9.214 m, with a maximum of 7.038 m across.

The main remote sensing and *in situ* instruments would be mounted on the +X panel (see Figure 5-28). The spacecraft orientation with respect to the nadir and velocity directions would be changed per observation scenario. During remote sensing operations, the +X panel would be oriented to the target and the main component of the velocity vector would be parallel to the spacecraft Y axis. During the Ganymede phase, the spacecraft would perform a rotation maneuver around the X-axis (yaw steering) with amplitude depending on the latitude, so as to allow for optimum illumination of the solar panels by the Sun. For *in situ* measurements, the spacecraft would be turned such that the +X direction is parallel to the main component of the velocity, and thus the instruments mounted on the +X panel could be exposed to the incoming plasma particles. In this configuration the Y-axis would be towards the nadir direction, and the spacecraft would perform a roll operation around the X-axis for optimization of solar panel illumination. During data downlink and radio-science measurements, the spacecraft would be inertial pointing with its high gain antenna oriented to the Earth.

Attitude and Orbit Control System

A careful trade-off optimizing the effective total mass required for reaction wheels (including solar array mass for producing the required power) resulted in three large momentum wheels (plus one backup) with maximum capacity 68 N·m·s, rotating at low speed. The system is designed to support the necessary yaw-steering in the Ganymede orbit (up to 28 N·m·s), and nadir tracking during Callisto flybys (200 km altitude, v_∞ = 2.1 km/s) in the worst configuration (solar panels along track) requiring a capacity of 26 N·m·s. The thruster configuration would be pure torque for support of wheels unloading without parasitic ΔV. AOCS sensors include a mini-Sun sensor. The IMU includes ring laser gyro and an accelerometer with sub-mg precision, sufficient for monitoring the ΔV changes due to the impulse firing.

Communications

Data downlink would be provided by a fixed 3.2 m high gain antenna (HGA), which is capable for X and Ka-band transmission. The antenna geometry and feeds are optimized for interplanetary Ka-band. According to the baseline assumption, housekeeping data would be transmitted in X-band during the early parts and during the late parts of the pass above the single ground-station, when the ground station antenna elevation is low. The science data would be transmitted in Ka-band at higher ground-station antenna elevations. Transmission from the spacecraft would take place with 100 W_{RF}. In addition, to optimize the total downloaded data volume, the downlink data rate would be adjusted as a function of elevation from the ground station. A single ground station was assumed, with a data link being established during each pass (once per day). Initial estimates confirm that the assumed data volume of 1 Gb per day could be met with margin. Command uplink would be performed in X-band. Provisions for the integration of the radio-science experiment and the link to JEO would also be included in the telemetry subsystem.

A two-axis steerable medium gain antenna (MGA) would be provided to allow for communications during the path of the inner solar system (when the HGA is being used as a thermal shield). Furthermore, for distances >2 AU during the interplanetary phase, and during the Jupiter phase, the MGA would be used for Earth search during safe mode recovery.

Payload Accommodation

The majority of the scientific equipment would be accommodated within a main and a smaller secondary compartment (see Figure 5-31). These compartments provide the possibility of additional wall shielding. The main compartment would be located at the center of the spacecraft providing accommodation volumes at the inside of the ±Y panels, and the +X panel (nadir direction). The sensor heads would be accommodated in the +X panel, and electronic units on the ±Y panels, which also allow for additional radiator surfaces. The second instrument compartment would be located on the corner of the +X and the +Z panels, close to the coldest radiator. Instruments requiring high cooling power, and/or high stability mounting would be included, such as the high resolution camera and the visible near infra-red hyperspectral imager. *In situ* particle and plasma sensors would be accommodated on the +X panel, the +Z panel for access to the anti-nadir/anti-velocity directions, or on booms, as required.

Mechanisms

The solar array deployment for achieving the configuration with side-panels is being used on telecommunications satellites, and is therefore not considered new. One axis solar array drive mechanisms would be needed. The main force would occur during the periods of the main engine thrusting. For stability the solar arrays would be rotated such that they are aligned with the plane of the thrust vector. All other booms and appendices are accommodated such that they are extending parallel to the thrust vector so as to reduce vibration loads.

The medium gain antenna would include two rotation mechanisms, the elevation with a stroke of 100°, and the azimuth with a stroke of 360°. Such mechanism would be employed on the BepiColombo mission.

In support of the instruments, a 5 m boom is baselined for the magnetometer, four 3 m booms for RPWI probes, and two 5 m sub-surface radar booms.

5.2.3.3 Spacecraft Design – Solution 2

Configuration

The spacecraft design is based on a cube structure, which would include four main propulsion tanks and the propulsion system.

The platform electronic units and the instruments would be accommodated outside of this structure in separate compartments on the +X and –X panels (see Figure 5-30). The size of the main structure ($x \times y \times z$), without solar arrays and high gain antenna, would be 1.56 m × 1.56 m × 2.68 m. A 3.5 m diameter high gain antenna would be fixed to the body of the spacecraft on the +Z panel and could be accommodated inside the launcher fairing with margin. The diameter of the high gain antenna was derived from a combination of mass optimization, data transmission capability and pointing performance. Large solar arrays consisting of seven panels each would be mounted on either side of the spacecraft body yielding a total area of 72 m^2. The solar arrays could only be rotated about the Y-axis of the spacecraft. The instrument booms would be extended in the ±X directions, avoiding conflicts with the solar panels and with the high gain antenna.

The remote sensing and the *in situ* instruments would be mounted on opposing faces of the spacecraft and consequently the *in situ* measurements and the remote sensing measurements would be performed using different orientations of the spacecraft with respect to nadir and to the flight direction. During remote sensing the +X panel would be facing the surface, and the main component of the velocity vector would be parallel to the spacecraft Y-axis. In the baseline, during the Ganymede phase, the spacecraft would perform a rotation around the nadir direction (yaw steering) optimizing the illumination of the solar panels. During *in situ* observations, the spacecraft would be oriented such that the solar arrays (Y axis) are aligned with the nadir/anti-nadir direction, pointing the –X panel to the anti-velocity direction. In this orientation illumination of the solar arrays would be optimized by rotations around the velocity vector (roll). During both modes the rotations could be stopped for limited duration, so as to allow for observations with a stable instrument platform. Radio science measurements would be performed in parallel to science data download, when the spacecraft would be held using inertial pointing with the high gain antenna pointing to the Earth.

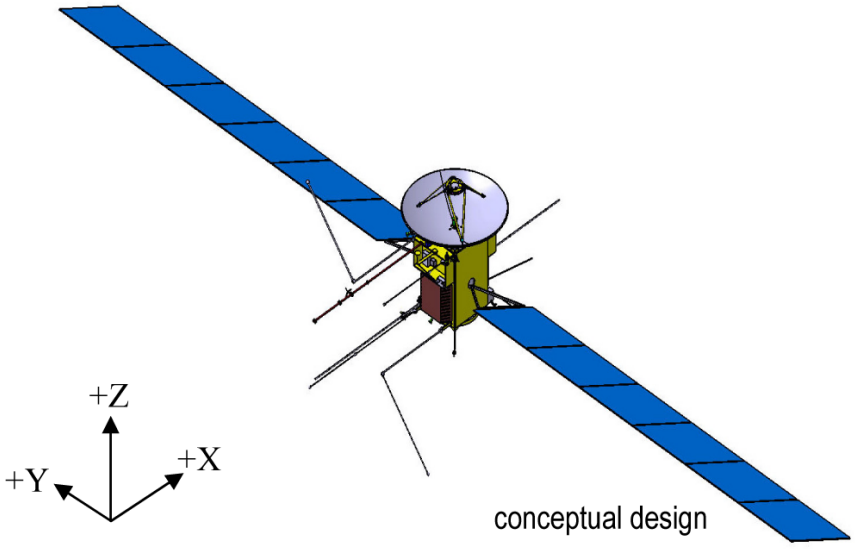

Figure 5-30. Spacecraft configuration of solution 2. The main engine and the launcher interface is at the bottom (–Z), the remote sensing instruments are located the back of this view (+X), and the *in situ* instruments, which require access to the velocity direction are mounted on the –X panel. The high gain antenna is at the top (+Z).

Attitude and Orbit Control System

The sizing of the reaction wheels for the required momentum storage was based on careful mass optimizations taking the mass of the wheels and their required power including solar generator mass into account. A baseline with three wheels plus one redundant was selected, with a slightly asymmetric configuration accounting for different angular momentum needs. The maximum required capacity of 50 N·m·s was driven by the Callisto flyby scenario, allowing full flexibility of the orientation of the spacecraft during the flyby. The required yaw rotation around Ganymede was not considered as a driver during the study, as it was calculated that the reduction of the power generation due to a minor off-pointing of the solar arrays during the short period of peak rotation (around the equator) would be negligible (0.5% power loss). The thruster configuration is enabling pure torque and pure force in all directions, resulting in 12 thrusters being mounted on three corners of the spacecraft. Two additional thrusters are foreseen for control of the main engine torques. The star tracker would utilize a three head system (Hydra). The sensors would also include a redundant inertial measurement unit and two redundant Sun sensors.

A redundant navigation camera with a field of view of 1.5° and optimized for extended object recognition would be provided in support of navigation at the Jupiter system.

To reduce the risk of failure due to the extended required operational lifetime of the reaction wheels and gyros, a hibernation mode for transfer to Jupiter would be implemented, which would be similar to the near Sun hibernation mode of Rosetta.

Communications

The spacecraft would provide a 3.5 m HGA which is fixed to the body, and which would provide 60 W_{RF} output power in either X- or Ka-band. The initial comparison on the maximum of the achievable downlink data volume per telemetry band indicated a critical dependency on the spacecraft pointing performance (assumed between 0.1° and 0.05°). Therefore the studied design of the telecommunications system is compatible with either band for data downlink, which would be revisited during later study phases when a more accurate assessment of the pointing performance would be available. In either case, would the specified data volume of 1 Gb per day be obtainable with margin.

A one-axis steerable medium gain antenna would be provided for communications during

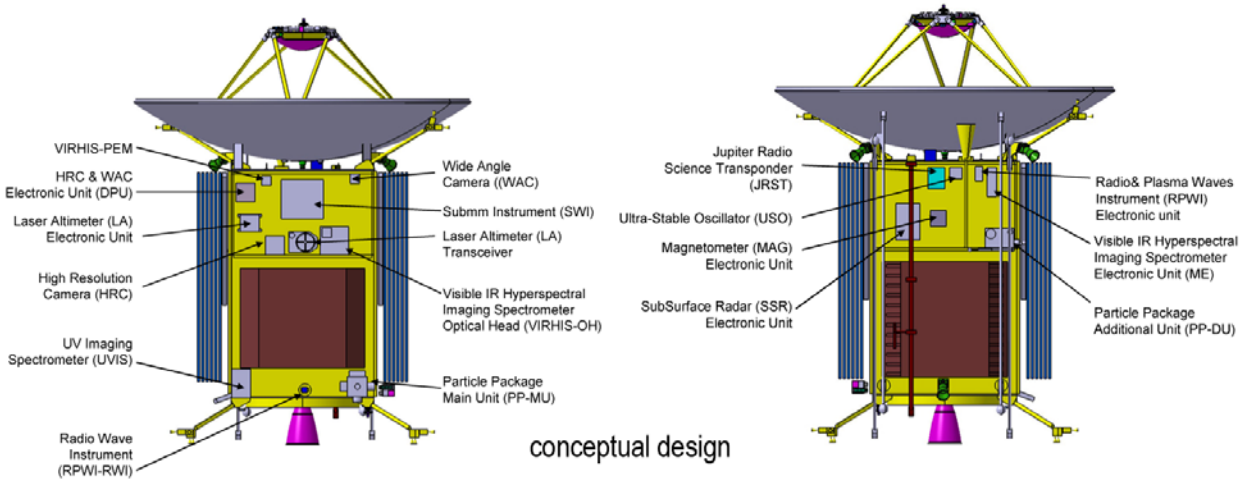

Figure 5-31. Accommodation of the model instruments in spacecraft solution 2. Platform equipment would be accommodated within the volumes which is indicated by brown covers in this drawing.

the Venus gravity assist, and when the omni-directional low gain antenna is out of reach from the ground station.

Payload Accommodation

The science instruments would be accommodated on the upper parts (+Z side) of the +X and –X panels (see Figure 5-31). All remote sensing instruments would be co-aligned and would be mounted on the +X platform, and *in situ* instruments and the sub-surface radar would be located on the –X platform. Electronic units, which are part of the instruments could be accommodated within either side, depending on instruments requirements and space available and could be used for balancing the thermal dissipation.

The instrument compartments are based on a U-shaped structure, in which variable conductance loop heat pipes would be included, which would connect the X-panels to both radiators on the +Y and –Y sides.

Mechanisms

The solar array deployment would be similar to Rosetta, which has a comparable solar array size. The solar array drive mechanisms would have one axis of rotation (around Y-axis) and would be compatible with the forces acted upon during main engine operations.

Based on a comparison of requirements with previous spacecraft, several feasible options for a magnetometer and Langmuir probe booms were identified. The booms are oriented in orthogonal direction to the major extent of the solar arrays so as to minimize interference during deployment and operations (EMC).

The medium gain antenna would be supported by a one degree of freedom pointing mechanism.

5.2.3.4 Spacecraft Design – Solution 3

This design solution was studied in less detail than the solutions described above, and consequently some divergent values may be derived. The solution is nevertheless presented here, discussing interesting options.

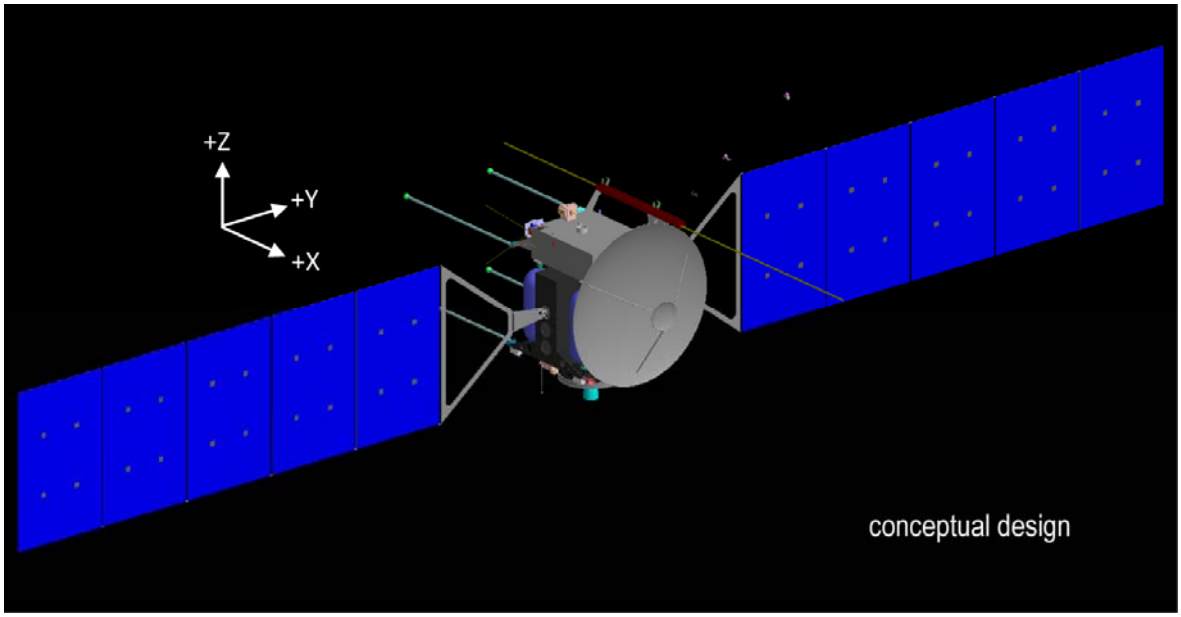

Figure 5-32. Spacecraft configuration of solution 3. The main engine and the launcher interface is at the –Z side. The nadir direction is at the +Z side (up), and main component of the velocity remains parallel to the –X direction for all observing modes.

Configuration

The structure would be divided into two parts separately supporting the propellant tanks and the platform and instrument units. The single MON tank would be accommodated inside a short central tube, with the four MMH tanks around it. In addition two helium tanks would be included. The main engine would be placed on the –Z panel (see Figure 5-32). The compartment for the platform and instrument equipment would be located in a separate box-shaped structure at the +Z side. The inclusion of the majority of the equipment in a single compartment allows for a high unit density, good shielding optimization and short harness lengths. A 3.2 m fixed high gain antenna would be mounted to the side of the spacecraft body. The solar panels would be mounted on the ±Y panels and would each provide 32 m^2 with of five panels and with a single axis drive mechanism around the Y-axis. The size of the spacecraft ($x \times y \times z$) would be 3.52 m × 2.76 m × 3.47 m and the total wing span after deployed solar arrays 27.5 m.

With the exception of one group of sensors requiring access to the anti-nadir direction, all instruments would be included in the main compartment at the +Z panel. The remote sensing instruments would be co-aligned with the field-of-views towards nadir, and all *in situ* instruments would be accommodated at the –X panel of the main compartment. No change of orientation of the spacecraft with respect to the flight direction has to be performed for changing between remote sensing and *in situ* observations. As with the other solutions, the illumination of the solar panels would be optimized by rotation around the nadir direction (yaw). Inertial pointing would be used for data downlink to point the high gain antenna to the Earth.

Attitude and Orbit Control System

Four wheels with maximum capacity of 68 N·m·s would be used, which would allow for 16 hours continuous operations without off-loading during the Ganymede orbit phase. Two star trackers based on STAR1000 would be placed close to the high gain antenna so as to minimize pointing errors. In addition a navigation camera is foreseen for assistance in targeting the moons during the flybys with a wide field of view, which would be located at the outside of the main compartment, at its –X panel. Furthermore, a redundant set of IMU and Sun sensors would be provided.

Communications

The telemetry system would use redundant X and Ka transponders for telemetry reception and transmission. The amplifiers would be based on redundant 65 W_{RF} Ka travelling wave tube amplifiers for Ka-band, and 75 W_{RF} for X-band, respectively. The downlink of the science telemetry would be in either X-band, or Ka-band, or with both systems simultaneously, meeting the baseline data volume of 1 Gb per 24 hours with margin. The high gain antenna would be fixed with a diameter of 3.2 m. A medium gain antenna would be based on a horn antenna with an opening angle of the 20°, which covers the maximum angular distance of the Earth when seen from Jupiter, and would therefore allow the MGA to be Sun-pointed during safe mode.

Payload Accommodation

The main compartment at the +Z panel would be split into two parts, where the lower part (closer to the propulsion module) would be reserved for platform equipment, and the volume closer to the surface be reserved for instruments. The accommodation of the instruments in the main compartment is illustrated in Figure 5-33. The remote sensing instruments would have access through the +Z panel, and the *in situ* instruments would have access through the –X panel, which would be parallel to the main component of the velocity direction. The PP-DU sensor requires access to the anti-nadir direction and would therefore be

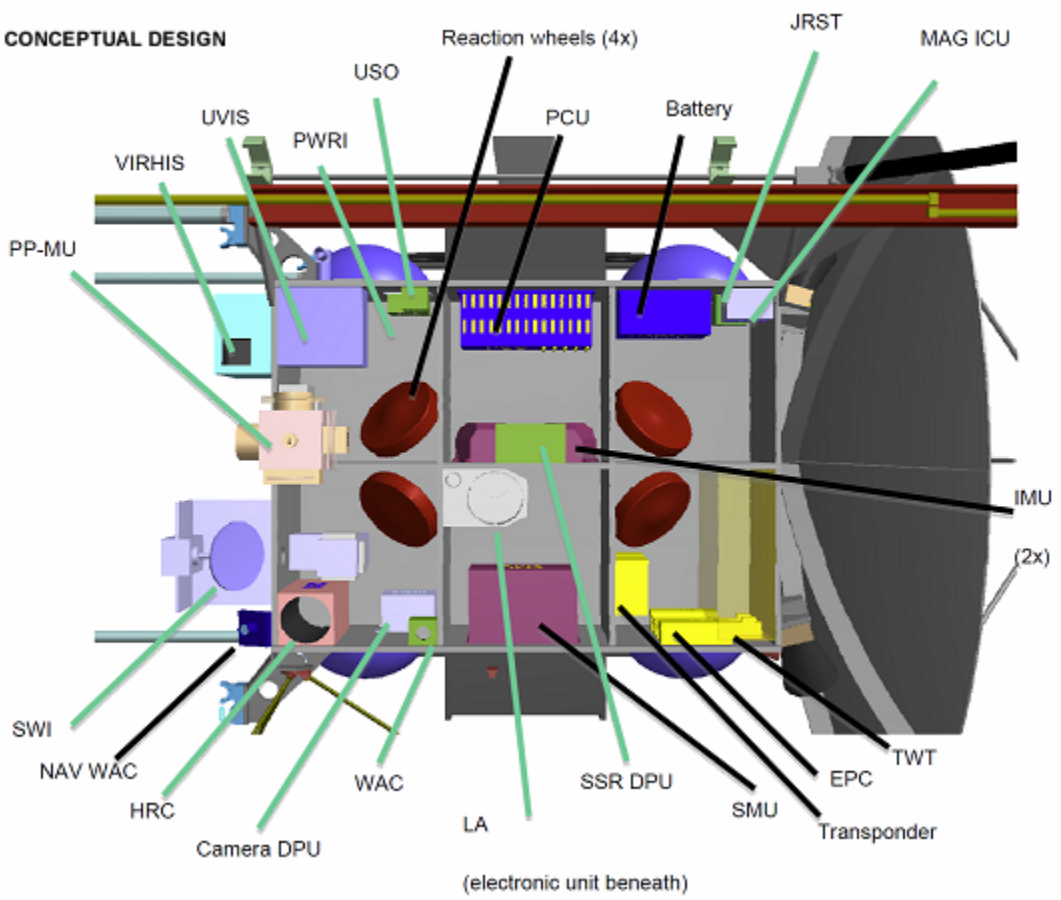

Figure 5-33. Accommodation of the platform units and model instruments in spacecraft solution 3.

accommodated outside the main compartment, close to the –Z panel.

Mechanisms

Standard deployment mechanisms would be used for the deployment of the solar array panels. The drive mechanisms would be single axis rotations around the spacecraft Y-axis.

All appendices are mounted on the main compartment, except the RPWI booms, which are mounted on the corners of the –X panel, such that the sensors are oriented towards the velocity direction (ahead of the spacecraft).

A 5 m magnetometer boom is foreseen and would consist of two elements, which would be deployed towards the nadir direction but pointing slightly aside such that interference with the field of view of the remote sensing instruments is avoided. The structural support for the magnetometer boom would be shared with the sub-surface radar boom The sub-surface radar boom (2×5 m) would be deployed with segments of 2.5 m length each being based on the MARSIS antenna design, and would be mounted asymmetrically, so as not to interfere with the accommodation requirements of the RPWI sensors (the extent of the radar boom in the –X direction would be equal to the length of the RPWI booms). The RPWI sensors would be mounted on four 3 m booms in the –X panel.

5.2.3.5 Mass Budgets

Table 5-19 summarizes the mass budget for the solutions studied. On a subsystem level, mass margins have been applied according to Technology Readiness Level (TRL) status and in addition a 20% system margin has been

applied. All solutions are compatible with the launch requirements with spare mass.

5.2.4 JGO Mission Constraints and Risk Mitigation

The operation of the JGO spacecraft in the Jovian environment would provide for a variety of unique challenges for flight system implementation. In this section, we discuss a number of these challenges and the strategies for the mitigation of the risk that they pose.

Table 5-19. Mass Budgets for the Spacecraft Solutions Studied

Baseline 2020 Item	Solution 1 [kg]	Solution 2 [kg]	Solution 3 [kg]
S/C			
Total Dry	1639.3	1711.7	1323.0
Structure	238.1	281.5	139.1
Shielding	88.2	156.0	54.9
Thermal CS	66.6	38.3	38.5
Mechanisms	40.2	25.4	48.4
Communications	79.8	99.7	56.3
Data Handling	22.8	26.3	40.5
Power	371.0	325.3	336.5
AOCS	52.1	50.5	48.6
Propulsion	212.0	235.4	219.9
Harness	85.0	72.0	0.0
Instruments	110.4	116.0	119.6
Propellant	2502.9	2447.0	2367.0
Adapter	190.0	190.0	165.0
S/C wet	4332.1	4348.7	3855.0
Max launch	4362.0	4362.0	4365.0
launch margin	29.9	13.3	510.0

Note: All values are including margin, and a system margin is also included. Differences in instrument masses are due to different accounting for antennae, etc.

5.2.4.1 Radiation Environment

The mission radiation environment is dominated by the properties of the plasma at Jupiter. The radiation dose contribution during the interplanetary phase is less than 1% of the total dose, about 34% is accumulated during the tour in the Jupiter system, and about 63% is obtained during the final phases at Ganymede. The radiation environment is dominated by electrons, which have an energy spectrum with significant densities up to 1 GeV. These high energies mean that the penetration depth is greater than for typical geostationary applications (assuming about 10 years lifetime), for instance. At lower energies, where the density is significantly higher, the interactions with the surface layers will dominate, causing local surface charging effects, if not properly mitigated, e.g. by shielding and conductive layers. The design solutions assumed below consider the accommodation of instrument and platform equipment in reasonable close vicinity and within compartments, taking advantage of shielding by neighboring units. In addition, the amount of extra shielding applied to the compartments (also called the "vault") was derived from first order radiation transport calculations. Because the radiation spectrum is dominated by electrons, shielding by high Z materials, such as tantalum or tungsten (or alloys with e.g. copper) are very efficient. Charged particle transport simulations show that a reduction of about 35% in shielding mass could be possible when using high Z materials, as compared to shielding by aluminum. This could be used as shielding material for the vault, and for spot shielding of specific items with lower radiation tolerance.

5.2.4.2 Electromagnetic Compatibility

For the sensitivity of the plasma and electromagnetic field measurements, strict limits on the electromagnetic compatibility of the spacecraft subsystems would be required and were included as goals in the studies: The electric charging of the surface of the spacecraft shall remain within a few Volt, at least in the vicinity of the electric field sensors and the low energy plasma spectrometers; the DC magnetic field shall remain <2 nT, with a stability of <0.1 nT over the range 0 to 64 Hz (at least during magnetometer measurements), and the electric stray field shall remain <50 dB μV/m in the frequency range below 45 MHz. Initial evaluations of these requirements indicated that some options would be available for meeting these goals. More specific measures would be discussed in the next study phase, and would also include instrument teams.

5.2.4.3 Planetary Protection

Currently Ganymede is a Planetary Protection Category II target ("significant interest relative to the process of chemical evolution and the origin of life, but only a remote chance that contamination by spacecraft could compromise future investigations"); however, the COSPAR working group on *Outer Planets and Satellites* has identified the need for additional requirements [*Rummel et al. 2010*]. These requirements related to the technical mission implementation could be grouped in two categories:

Collateral contamination of alternative critical bodies, such as Europa shall or Mars (including any part of the launch vehicle within 50 years) shall be smaller than 10^{-4} and 10^{-2}, respectively.

Control and limiting the bio-burden brought to Ganymede shall be such that the likelihood of one active organism reaching the Ganymede sub-surface ocean shall be $<10^{-4}$.

Contamination avoidance of Europa could easily be demonstrated based on mission analysis, as the energy of the spacecraft in Jupiter orbit is too high to reach Europa within reasonable timescale. Similarly, as Mars is at very unfavorable position for gravity assists, and it could be demonstrated that neither the spacecraft nor any part of the launcher would impact Mars within reasonable timescale.

The likelihood of bringing a surviving organism to the Ganymede sub-surface ocean is largely reduced by the low probability of the burial mechanism (10^{-4}) and by the low likelihood of landing in an active region (2×10^{-3}). Further factors, such as the estimated cruise survival fraction (10^{-1}), sterilization through radiation (10^{-1}), and probability of survival (10^{-2}), bring the total likelihood to 2×10^{-11}. Assuming a typical bioburden at launch around 10^6 organisms, the requirement would be met by a factor of 5.

Consequently the bioburden would be monitored during the mission implementation, by break down and allocation of allowed budgets to each hardware supplier, including payload. Monitoring would be achieved through essays taken at regular intervals.

5.2.4.4 Critical Elements and Drivers

Significant heritage exists from ESA planetary missions with high radiation environments such as BepiColombo, or a deep space mission such as Rosetta.

The main JGO mission challenge is due to the high intensity radiation environment. This requires careful modelling and increasing level of detail of transport simulations, such that the spacecraft configuration could efficiently be optimized early in the design. The expected total mission low energy electron fluence is actually lower than a typical exposure for 10-year geostationary mission. At such energies electrons are predominantly being absorbed at the surface, and therefore heritage is available on materials withstanding such doses. At high energies, the electron fluence is more enhanced for the JGO mission, causing charge deposition at deeper layers. Electrons could however very effectively be shielded, and thereby the optimization of shielding material by careful simulations and design appears feasible. Because detailed designs are not available for all units, large margins for shielding mass were considered in the spacecraft solutions. The uncertainties of the model were taken into account by assuming the worst cases of a combination of available models. In addition early estimates indicated that the shielding by Ganymede during the final mission phases would reduce the radiation fluence at Ganymede by 40–50%, which was not taken into account yet, due to the uncertainties of the model predictions.

Existing GaAs based triple junction solar cells showed a lower than expected efficiency at the combination of low temperature and low intensity. ESA is currently developing the technology for producing reliable high efficiency solar cells. Results from prototypes confirmed the feasibility of such cells, and an ongoing activity is focusing on increasing the yield with a larger production base. As a backup, it was assumed during the studies that a careful selection of cells at low temperature would provide cells with equivalent efficiency.

Mass is a critical parameter for any high ΔV mission. Increases of equipment masses resulting in a higher dry mass would be amplified by about a factor of 2.6 for the JGO mission. Risk of mass increase comes primarily from more radiation shielding required, payload mass excursions, and higher system power requirements due to higher stand-by power of instruments, or higher equipment power consumption in general, resulting in increased size of the solar arrays. Additionally larger solar array area could also be caused by solar cell underperformance. Mitigation options of mass increases exist by using the higher performance of the launcher, as currently a more powerful launching capability is being developed in Europe than the nominal ECA version, which was assumed for this Ariane-5 study. Alternatively the mission profile could be changed mainly resulting in a longer interplanetary transfer to Jupiter by adding an additional Earth gravity assist before the Venus gravity assist (as is the baseline for the backup launch). This increase of available dry mass could be obtained, at the cost of about 1 year longer transfer time and is similar to the difference of dry-mass between the baseline and backup launches considered during this study phase. Furthermore the reduction of the total consumed power would directly result in a reduced solar array size. As a last resort the power reduction could be achieved by reductions of the telemetry downlink durations, which are one of the drivers of the power consumption.

The insertion of an additional Earth gravity assist would also provide a larger spread of launch opportunities, with at least a yearly repetition of similar launch capabilities.

5.2.4.5 Mitigation of Technical Risk

Prior to the start of the recent spacecraft Assessment Phase, ESA had initiated an effort for modeling of the Jupiter radiation environment (JOREM). The study is now being concluded and initial results were used during the assessment study phase as reported in the ESA Assessment Study Report (ESA/SRE 2011), albeit with conservative margins on the predicted fluences.

The availability of solar cells operating under LILT conditions and providing the assumed performance (28% at end-of-life) is critical to this mission. ESA started a development two years ago, which provided promising results. A following phase has been initiated, to determine the achievable uniformity, reliability and yield during manufacturing of the promising updated technology of triple-junction GaAs cells. This development is planned to be concluded within two years.

The majority of the remaining technical development activities are related to validation components for the high radiation environment. Investigating the limits of radiation tolerance of electronic components provides more accuracy of shielding calculations. The following validations are being pursued:

- Survey of critical components for power converters;
- Radiation characterization of radiation tolerant optocouplers, sensors and detectors;
- Characterization of radiation resistant materials;

- Characterization of charging effect in materials under extreme conditions;
- Latch-up protection for commercial of the shelf items;
- Evaluation of star tracker performance under extreme conditions;
- Demonstration of LEON2 in harsh environment.

In addition specific components are being developed for enhancing capabilities:

- Development and qualification of analogue/mixed signal readout ASIC;
- Development and qualification of front-end readout ASIC;
- Low mass SpaceWire;
- Development of radiation tolerant flash memory.

It is emphasized that backup options exist for these developments by using conventional components possibly in combination with more shielding. A more detailed evaluation of the combination of radiation tolerance and shielding mass needs to be performed during the definition phase.

5.2.5 Summary

The JGO mission has developed a robust strategy for both the Jovian Tour and the Ganymede science mission phase. Our analysis shows adequate flight system capability and tour observation opportunities to perform the science campaigns defined by the JJSDT. The Ganymede observation strategy would provide a means to achieve the science objectives with the planning payload. The mission phases, both at Jupiter and in Ganymede orbit, would enable science scenarios to achieve mission science goals.

5.3 Science Value

Science value is necessarily subjective, and impossible to accurately quantify. Nonetheless, the JJSDT has worked to estimate science value rating for each example measurement in the EJSM Traceability Matrix (Foldout 1). The science value ratings are shown in the colored columns at the right of the Traceability Matrix and reflect an assessment of the individual contributions by JEO and JGO respectively.

Rating criteria are:

	Significant contribution or achieves the measurement (75% to 100%)
	Major contribution to achieving the measurement (50% to 75%)
	Moderate contribution to achieving the measurement (25% to 50%)
	Little or no contribution to achieving the measurenent (less than 25%)
	Tour trajectory does not provide a suitable opportunity to make observations
	Example instrument not in model payload

For measurements made by JEO during the orbital Europa Campaign, science value ratings are for the end of Campaign 3. Similarly, for JGO science at Ganymede, the value is for the orbit phase. Most measurements for investigations pertinent to Jupiter System science are primarily obtained during the Jovian tour, i.e., prior to EOI and GOI.

In constructing the Traceability Matrix, the JJSDT has identified example measurements that the group believes would make the largest advancement in achieving the objectives and investigations. The model payload was selected to address the highest priority measurements, without overly stressing each spacecraft's resources (cost, mass, power, and risk). By taking this approach, the JJSDT acknowledges that not all measurements are fully addressed by the model payload—in fact, a few measurements are not at all addressed. This conservative strategy was taken intentionally, for several reasons:

- it allows those with innovative or proprietary ideas to propose more capable instruments;

- it balances the development risk and science value given publicly available information;
- it demonstrates that the targets and mission are scientifically rich, leaving room for innovative concepts;
- it highlights how JEO also provides direct benefit to the complementary and synergistic JGO science;
- for JEO, it provides NASA Headquarters with information to best evaluate the cost vs. risk posture once the instruments are actually proposed via the Announcement of Opportunity process.

References

Abramov, O. and J. Spencer 2008. Numerical modeling of endogenic thermal anomalies on Europa. *Icarus* **195**, 378–385.

Alexander, C., R. Carlson, G. Consolmagno, R. Greeley, and D. Morrison 2009, The exploration history of Europa. *Europa* (R.T. Pappalardo, W.B. McKinnon, and K.K. Khurana, Eds.), Univ. of Arizona Press, Tucson, 3–26.

Anderson, J.D., R.A. Jacobson, E.L. Lau, W.B. Moore, and G. Schubert 2001. Io's gravity field and interior structure. *J. Geophys. Res.* **106**, 32,963–32,970.

Anderson, J.D., E.L. Lau, W.L. Sjogren, G. Schubert, and W.B. Moore 1996. Gravitational constraints on the internal structure of Ganymede. *Nature* **384**, 541–543.

Anderson, J.D., G. Schubert, R.A. Jacobson, E.L. Lau, W.B. Moore et al. 2004. Discovery of mass anomalies on Ganymede. *Science* **305**, 989–991.

Anderson, J.D., G. Schubert, R. A. Jacobson, E.L. Lau, W.B. Moore et al. 1998a. Europa's differentiated internal structure: Inferences from four Galileo encounters. *Science* **281**, 2019–2022.

Anderson, J.D., G. Schubert, R.A. Jacobson, E.L. Lau, W.B. Moore, and W.L. Sjogren 1998b. Distribution of rock, metals, and ices on Callisto. *Science* **280**, 1573–1576.

Atreya, S., P. Mahaffy, H. Niemann, M. Wong, and T. Owen 2003. Composition and origin of the atmosphere of Jupiter: An update, and implications for the extrasolar giant planets. *Planetary and Space Science* **51**, 105–112.

Ball, A.J., J.R.C. Garry, R.D. Lorenz, and V.V. Kerzhanovich 2007. *Planetary Landers and Entry Probes*, Cambridge Univ. Press.

Barr, A.C. and A.P. Showman 2009. Heat transfer in Europa's icy shell. *Europa* (R.T. Pappalardo, W.B. McKinnon, and K.K. Khurana, Eds.), Univ. of Arizona Press, Tucson, 405–430.

Barriot, J.P, V. Dehant, W. Folkner, J. Cerisier, A. Ribes et al. 2001. The NetLander Ionosphere and Geodesy Experiment, *Adv. Space Res.* **28**, 1237–1249.

Barth, C., C. Hord, A. Stewart, W. Pryor, K. Simmons 1997. Galileo ultraviolet spectrometer observations of atomic hydrogen in the atmosphere of Ganymede. *Geophy. Res. Lett.* **24**, 2147–2150.

Bell, J.F. 1992. Charge-coupled device imaging spectroscopy of Mars 2: Results and implications for Martian ferric mineralogy. *Icarus* **100**, 575–597.

Bibring, J., Y. Langevin, A. Gendrin, B. Gondet, F. Poulet et al. 2005. Mars surface diversity as revealed by the OMEGA/Mars express observations. *Science* **307**, 1576–1581.

Bierhaus, E.B., K. Zahnle, and C.R. Chapman 2009. Europa's crater distributions and surface ages. *Europa* (R.T. Pappalardo, W.B. McKinnon, and K.K. Khurana, Eds.), Univ. of Arizona Press, Tucson, 161–180.

Billings, S.E. and S.A. Kattenhorn 2005, The great thickness debate: Ice shell thickness models for Europa and comparisons with estimates based on flexure at ridges. *Icarus* **177**, 397–412.

Bills, B.G. 2005. Free and forced obliquities of the Galilean satellites of Jupiter. *Icarus* **175**, 233–247.

Bills, B.G. and F.G. Lemoine 1995. Gravitational and topography isotropy of the Earth, Moon, Mars, and Venus. *J. Geophys. Res*. **100**, 26,275–26,295.

Bills, B.G. and F. Nimmo 2008. Forced obliquity and moment of inertia of Titan. *Icarus* **196**, 293–297.

Bills, B.G., F. Nimmo, Ö. Karatekin, T. Van Hoolst, N. Rambaux et al. 2009. Rotational dynamics of Europa. *Europa* (R.T. Pappalardo, W.B. McKinnon, and K.K.

Khurana, Eds.), Univ. of Arizona Press, Tucson, 119–136.

Blanc, M. and the LAPLACE Consortium. 2007. Laplace: A Mission to Europa and the Jupiter system for ESA's Cosmic Vision Programme. http://jupiter-europa.cesr.fr.

Blankenship, D.D., D.A. Young, W.B. Moore, and J.C. Moore 2009. Radar sounding of Europa's subsurface properties and processes: The view from Earth. *Europa* (R.T. Pappalardo, W.B. McKinnon, and K.K. Khurana, Eds.), Univ. of Arizona Press, Tucson, 631–654.

Boldt, J., J.W. Alexander, H. Becker, E. Blazejewski, E.H. Darlington et al. 2008, Assessment of Radiation Effects on Science and Engineering Detectors for the JEO Mission Study, JPL D-48256.

Brown, M.E. 2001. Potassium in Europa's atmosphere. *Icarus* **151**, 190–195.

Brown, M.E. and R.E. Hill 1996. Discovery of an extended sodium atmosphere around Europa. *Nature* **380**, 229–231.

Brunetto, R., G. Baratta, M. Domingo, and G. Strazzulla et al. 2005. Reflectance and transmittance spectra (2.2–2.4μm) of ion irradiated frozen methanol. *Icarus* **175**, 226–232.

Burns, J.A., M.R. Showalter, D.P. Hamilton, P.D. Nicholson, I. de Pater et al. 1999. The formation of Jupiter's faint rings. *Science* **284**, 1146–1150.

Burns, J.A., D.P. Simonelli, M.R. Showalter, D.P. Hamilton, C.C. Porco et al. 2004. Jupiter's ring-moon system. *Jupiter: The Planet, Satellites, and Magnetosphere* (F. Bagenal, T.E. Dowling, and W.B. McKinnon, Eds.), pp. 241–262, Cambridge Univ. Press, Cambridge.

Canup R.M. and W.R. Ward 2002. Formation of the Galilean satellites: Conditions of accretion. *The Astronomical J.* **124**, 3404–3423.

Carlson, R.W. 1999. A tenuous carbon dioxide atmosphere on Jupiter's moon Callisto. *Science* **283**, 820–821.

Carlson, R.W. 2001. Spatial distribution of carbon dioxide, hydrogen peroxide, and sulfuric acid on Europa. *Bull. Am. Astron. Soc.* **33**, 1125.

Carlson, R.W., M.S. Anderson, R.E. Johnson, W.D. Smythe, A.R. Hendrix et al. 1999a. Hydrogen peroxide on the surface of Europa. Science 283, 2062–2064.

Carlson, R.W., M. Anderson, R. Johnson, M. Schulman, and A. Yavrouian 2002. Sulfuric acid production on Europa: The radiolysis of sulfur in water ice. *Icarus* **157**, 456–463.

Carlson, R.W., M. Anderson, R. Mehlman, and R. Johnson 2005. Distribution of hydrated sulfuric acid on Europa. *Icarus* **177**, 461–471.

Carlson, R.W., W. M. Calvin, J.B. Dalton, G.B. Hansen, R.L. Hudson et al. 2009, Europa's Surface Composition, *Europa*, R.T. Pappalardo, W.B. McKinnon, K.K. Khurana, eds., University of Arizona Press, 283–328.

Carlson, R.W., R.E. Johnson, and M.S. Anderson 1999b. Sulfuric acid on Europa and the radiolytic sulfur cycle. *Science* **286**, 97–99.

Carr, M.H., M.J.S. Belton, C.R. Chapman, A.S. Davies, P. Geissler et al. 1998a. Evidence for a subsurface ocean on Europa. *Nature* **391**, 363–365.

Carr, M.H., A.S. McEwen, K.A. Howard, F.C. Chuang, P. Thomas, P. Schuster et al. 1998b. Mountains and calderas on Io: Possible implications for lithosphere structure and magma generation. *Icarus* **135**, 146–165.

Cassidy, T., R. Johnson, M. McGrath, M. Wong, and J. Cooper 2007. The spatial morphology of Europa's near-surface O_2 atmosphere. *Icarus* **191**, 755–764.

Cassidy, T., R. Johnson, P. Geissler, and F. Leblanc 2008. Simulation of Na D emission near Europa during eclipse. *J. Geophys. Res.* **113**, doi: 10.1029/2007 JE002955.

Cheng, A.F., A.A. Simon-Miller, H.A. Weaver, K.H. Baines, G.S. Orton et al. 2008. Changing characteristics of Jupiter's little red spot. *Astro. J.* **135**, 2446–2452.

Cheng, K., C. Ho, and M. Ruderman 1986. Energetic radiation from rapidly spinning pulsars: 1. Outer magnetosphere gaps. *Astrophys. J.* **300**, 500–521.

Christensen, P.R., J.L. Bandfield, V.E. Hamilton, S.W. Ruff, H.H. Kieffer et al. 2001. Mars Global Surveyor thermal emission spectrometer experiment: Investigation description and surface science results. *J. Geophys. Res.* **106**, 23,823–23, 871.

Chyba, C.F. and K.P. Hand 2005. Astrobiology: The study of the living universe. *Ann. Rev. Astron. Astrophys*. **43**, 31–74.

Chyba, C.F. and C.B. Phillips 2001. Possible ecosystems and the search for life on Europa. *Proc. National Acad. Sci.* **98**, 801–804.

Chyba, C.F., S.J. Ostro, and B.C. Edwards 1998. Radar detectability of a subsurface ocean on Europa. *Icarus* **134**, 292–302.

Clark, K., R. Greeley, R. Pappalardo, and C. Jones 2007a. *2007 Europa Explorer Mission Study: Final Report*, JPL Internal Document D–38502.

Clark, K., R. Greeley, R. Pappalardo, C. Jones 2007b. *2007 Europa Explorer Mission Study Report: Final Report*, JPL Internal Document D–41283.

Clark, R., F. Fanale, and A. Zent, 1983. Frost grain size metamorphism: Implications for remote sensing of planetary surfaces. *Icarus* **56**, 233–245.

Clark, R. and T. McCord 1980. The Galilean satellites: New near-infrared spectral reflectance measurements (0.65–25μm) and a 0.325–5 μm summary. *Icarus* **41**, 323.

Clark, R.N. R.H. Brown, R. Jaumann, D.P. Cruikshank, R.M. Nelson et al. 2005. Compositional maps of Saturn's moon Phoebe from imaging spectroscopy. *Nature* **435**, 66–69.

Collins, G. and F. Nimmo 2009. Chaotic terrain on Europa. *Europa* (R.T. Pappalardo, W.B. McKinnon, and K.K. Khurana, Eds.), Univ. of Arizona Press, Tucson, 259–282.

Comstock, R.L., and B.G. Bills 2003. A solar system survey of forced librations in longitude. *J. Geophys. Res.* **108**, doi: 10.1029/ 2003JE002100.

Constable, S. and C. Constable 2004. Observing geomagnetic induction in magnetic satellite measurements and associated implications for mantle conductivity. *Geochemistry, Geophysics, Geosystems* **5**, doi: 10.1029/ 2003GC000634.

Cooper, J.F. R.E. Johnson, B.H. Mauk, H.B. Garrett, and N. Gehrels 2001. Energetic ion and electron irradiation of the icy Galilean satellites. *Icarus* **149**, 133–159.

Crowley, J.K. 1991. Visible and near-infrared (0.4–2.5μm) reflectance spectra of playa evaporite minerals. *J. Geophys. Res.* **96**, 16,231–16,240.

Cruikshank, D.P., J. Dalton, C. Dalle Ore, J. Bauer, K. Stephan et al. 2007. Surface composition of Hyperion. *Nature* **448**, 54–56.

Dalton, J.B. 2000. Constraints on the surface composition of Jupiter's moon Europa based on laboratory and spacecraft data. Ph.D. dissertation, Univ. of Colorado, Boulder.

Dalton, J.B. 2007. Linear mixture modeling of Europa's non-ice material using cryogenic laboratory spectroscopy. *Geophys. Res. Lett.* **34**, 21,205.

Dalton, J.B., R. Mogul, H. Kagawa, S. Chan, and C. Jamieson 2003. Near-infrared detection of potential evidence for microscopic organisms on Europa. *Astrobiology* **3**, 505–529.

Dalton, J.B., O. Prieto- Ballesteros, J. Kargel, C. Jamieson, J. Jolivet, and R. Quinn 2005. Spectral comparison of heavily hydrated salts to disrupted terrains on Europa. *Icarus* **177**, 472–490.

Dalton, J.B. and R.N. Clark 1998. Laboratory spectra of Europa candidate materials at

cryogenic temperatures. *Bull. Am. Astron. Soc.* **30**, 1081.

Dalton, J.B. and R.N. Clark 1999. Observational constraints on Europa's surface composition from Galileo NIMS data. *Proc. Lunar Planet. Sci. Conf. XXX*, 2064.

Daud, T. and E. Shalom, *Long Life Design Guidelines*, JPL Internal Document D–48271

Dehant, V., P. Lognonne, and C. Sotin 2004. Network science, NetLander: A European mission to study the planet Mars. *Planet. Space Sci.* **52**, 977–985.

Delitsky, M.L. and A.L. Lane 1997. Chemical schemes for surface modification of icy satellites: A road map. *J. Geophys. Res.* **102**, 16,385–16,390.

Delitsky, M.L. and A.L. Lane 1998. Ice chemistry on the Galilean satellites. *J. Geophys. Res.* **103**, 31,391–31,403.

Doggett, T., R. Greeley, P. Figueredo, and K. Tanaka 2009. Geologic stratigraphy and evolution of Europa's surface. *Europa* (R.T. Pappalardo, W.B. McKinnon, and K.K. Khurana, Eds.), Univ. of Arizona Press, Tucson, 137–160.

Ehlmann, B., J. Mustard, C. Fassett, S. Schon, J. Head III et al. 2008. Clay minerals in delta deposits and organic preservation potential on Mars. *Nature Geoscience* **1**, 355.

Ellery, A. and D. Wynn-Williams 2003. Why Raman spectroscopy on Mars? A case of the right tool for the right job. *Astrobiology* **3**, 565–579.

Eluszkiewicz, J. 2004. Dim prospects for radar detection of Europa's ocean. *Icarus* **170**, 234–236.

ESA/SRE 2011. *EJSM-Laplace: Assessment Study Report*, ESA, in press.

ESA 2005, *Cosmic Vision: Space Science for Europe 2015–2025*, ESA Brochure BR-247, ESA Publ. Div., ESTEC, Noordwijk, The Netherlands.

Fanale, F.P., J.C. Granahan, T.B. McCord, G. Hansen, C.A. Hibbitts et al. (1999). Galileo's multiinstrument spectral view of Europa's surface composition. *Icarus* **139**, 179–188.

Figueredo, P.H., R. Greeley, S. Neuer, L. Irwin, and D. Schulze-Makuch 2003. Locating potential biosignatures on Europa from surface geology observations. *Astrobiology* **3**, 851–4861.

Figueredo, P.H. and R. Greeley 2004. Resurfacing history of Europa from pole-to-pole geological mapping. *Icarus* **167**, 287–312.

Fink, U. and G.T. Sill 1982. The infrared spectral properties of frozen volatiles. *Comets* (L.L. Wilkening, Ed.), Univ. of Arizona Press, Tucson, 164–202.

Fukazawa, K., T. Ogino, and R.J. Walker (2005), Dynamics of the Jovian magnetosphere for northward interplanetary magnetic field (IMF), *Geophys. Res. Lett*., 32, L03202, doi:10.1029/2004GL021392.

Gaidos, E. and F. Nimmo 2000. Tectonics and water on Europa. *Nature* **405**, 637.

Geissler, P.E., R. Greenberg, G. Hoppa, A. McEwen, R. Tufts et al. 1998. Evolution of lineaments on Europa: Clues from Galileo multispectral imaging observations. *Icarus* **135**, 107–126.

Gierasch, P., A. Ingersoll, D. Banfield, S. Ewald, P. Helfenstein et al. 2000. Observation of moist convection in Jupiter's atmosphere. *Nature* **403**, 628–630.

Giese, B., R. Pappalardo, J. Head III, and G. Neukum 2001. Topographic features of bright and dark terrains on Ganymede: Implications from Galileo-G28 stereo images. *Bull. Am. Astro. Soc.* **33**, 1100.

Greeley, R., P.H. Figueredo, D.A. Williams, F.C. Chuang, J.E. Klemaszewski et al. 2000. Geologic mapping of Europa. *J. Geophys. Res*. **105**, 22,559–22,578.

Greeley, R., C. Chyba, J. Head, T. McCord, W. McKinnon et al. 2004. Geology of Europa. *Jupiter: The Planet, Satellites, and Magnetosphere* (F. Bagenal, T.E. Dowling, and W.B. McKinnon, Eds.), pp. 329–362, Cambridge Univ. Press, Cambridge.

Greenberg, R., G.V. Hoppa, B.R. Tufts, P. Geissler, J. Riley et al. 1999. Chaos on Europa. *Icarus* **141**, 263–286.

Grundy, W., B. Buratti, A. Cheng, J. Emery, A. Lunsford et al. 2007. New horizons mapping of Europa and Ganymede. *Science* **318**, 234.

Hall, D.T., D.F. Strobel, P.D. Feldman, M.A. McGrath, and H.A. Weaver 1995. Detection of an oxygen atmosphere on Jupiter's moon Europa. *Nature* **373**, 677–679.

Hamilton, D. and H. Krüger 2008. The sculpting of Jupiter's gossamer rings by its shadow. *Nature* **453**, 72.

Hand, K.P. 2007. On the physics and chemistry of the ice shell and sub-surface ocean of Europa. Ph.D. dissertation, Stanford Univ.

Hand, K.P. and C.F. Chyba 2007. Empirical constraints on the salinity of the europan ocean and implications for a thin ice shell. *Icarus* **189**, 424–438.

Hand, K.P., C.F. Chyba, J.C. Priscu, R.W. Carlson, and K.H. Nealson 2009. Astrobiology and the potential for life on Europa. *Europa* (R.T. Pappalardo, W.B. McKinnon, and K.K. Khurana, Eds.), Univ. of Arizona Press, Tucson , 589–630.

Hansen, C.J., L. Esposito, A. Stewart, J. Colwell, A. Hendrix et al. 2006. Enceladus' water vapor plume. *Science* **311**, 1422–1425.

Hansen, G. and T.B. McCord 2004. Amorphous and crystalline ice on the Galilean satellites: A balance between thermal and radiolytic processes. *J. Geophys. Res*. **109**, E1, E01012, 0148-0227.

Hansen, G. and T.B. McCord 2008. Widespread CO_2 and other non-ice compounds on the anti-jovian and trailing sides of Europa from Galileo/NIMS observations. *Geophys. Res. Lett.*, **35**, L01202.

Hartle, R.E. and R. Killen 2006. Measuring pickup ions to characterize the surfaces and exospheres of planetary bodies: Applications to the Moon. *Geophys. Res. Lett.* **33**, 5201.

Head, J., R. Pappalardo, G. Collins, M. Belton, B. Giese et al. 2002. Evidence for Europa-like tectonic resurfacing styles on Ganymede. *Geophy. Res. Lett.* **29**, 2151.

Head, J., R. Pappalardo, J. Kay, G. Collins, I. Prockter et al. 1998. Cryovolcanism on Ganymede: Evidence in bright terrain from Galileo solid state imaging data. *Lunar and Planetary Science XXIX, Proc. 29th Lunar and Planetary Science Conference, Mar. 16–20 1998, Houston, Texas*.

Hendrix, A., C. Barth, C. Hord, and A. Lane, 1998. Europa: disk-resolved ultraviolet measurements using the Galileo ultraviolet spectrometer. *Icarus* **135**, 79–94.

Hendrix, A.R., C. Barth, and C. Hord 1999. Ganymede's ozone-like absorber: Observations by the Galileo ultraviolet spectrometer. *J. Geophys. Res*. **104**, 14,169–14,178.

Herzberg, G. 1991. *Molecular Spectra and Molecular Structure: Infrared and Raman of Polyatomic Molecules*, Krieger Pub. Co.

Hibbitts, C.A., J.E. Klemaszewski, T.B. McCord, G.B. Hansen, and R. Greeley 2002. CO_2-rich impact craters on Callisto. *J. Geophys. Res.*, **107**, 14-1–14-12.

Hibbitts, C.A., R.T. Pappalardo, G.B. Hansen, and T.B. McCord 2003. Carbon dioxide on Ganymede. *J. Geophys. Res.* **108**, 5036.

Hopf, T. et al. 2010. Shock protection of penetrator-based instrumentation via a sublimation approach. *Adv. Space Sci*. **45**, 460-467.

Hoppa, G.V. et al. 1999. Formation of cycloidal features on Europa. *Science* **285**, 1899–1902.

Horanyi, M., G. Morfill, and E. Grün 1993. Mechanism for the acceleration and ejection of dust grains from Jupiter's magnetosphere. *Nature* **363**, 144–146.

Hussman, H. and T. Spohn 2004. Thermal-orbital evolution of Io and Europa, *Icarus* **171**, 391–410.

Ingersoll, A.P., T.E. Dowling, P.J. Gierasch, G.S. Orton, P.L. Read et al. 2004. Dynamics

of Jupiter's atmosphere. *Jupiter: The Planet, Satellites and Magnetosphere* (F. Bagenal, T. Dowling, and W. McKinnon, Eds.), pp. 105–128, Cambridge Univ. Press, Cambridge.

Jaeger, W.L., E.P. Turtle, L.P. Keszthelyi, J. Radebaugh, A.S. McEwen et al. 2003. Orogenic tectonism on Io. *J. Geophys. Res.* **108**, doi: 10.1029/2002JE001946.

Jia, X., R. J. Walker, M. G. Kivelson, K. K. Khurana, and J. A. Linker, (2008), Three-dimensional MHD simulations of Ganymede.'s magnetosphere, *J. Geophys*. Res., 113, A06212, doi:10.1029/2007JA012 748.

Johnson, R.E., M.H. Burger, T.A. Cassidy, F. Leblanc, M. Marconi et al. 2009. Composition and detection of Europa's sputter-induced atmosphere. *Europa* (R.T. Pappalardo, W.B. McKinnon, and K.K. Khurana, Eds.), Univ. of Arizona Press, Tucson, 507–528.

Johnson, R.E., R.W. Carlson, J.F. Cooper, C. Paranicas, M.H. Moore et al. 2004. Radiation effects on the surfaces of the galilean satellites. *Jupiter: The Planet, Satellites and Magnetosphere* (F. Bagenal, W.B. McKinnon, and T.E. Dowling, Eds.), pp. 485–512, Cambridge Univ. Press, Cambridge.

Johnson, R.E., R.M. Killen, J.H. Waite, and W.S. Lewis 1998. Europa's surface composition and sputter-produced iono–sphere. *Geophys. Res. Lett.* **25**, 3257–3260.

Johnson, R.E., F. Leblanc, B.V. Yakshinskiy, and T.E. Madey 2002. Energy distributions for desorption of sodium and potassium from ice: The Na/K ratio at Europa. *Icarus* **156**, 136–142.

Johnson, R.E. and T.I. Quickenden 1997. Radiolysis and photolysis of low-temperature ice. *J. Geophys. Res.* **102**, 10,985–10,996.

Joyce, G.F. 1994. Foreward. *Origins of Life: The Central Concepts* (Deamer, D.W. and G.R. Fleischaker), Jones and Bartlett, Boston.

Kargel, J.S., J.Z. Kaye, J.W. Head, III, G.M. Marion, R. Sassen et al. 2000. Europa's crust and ocean: Origin, composition, and the prospects for life. *Icarus* **148**, 226–265.

Keszthelyi, L., W. Jaeger, E. Turtle, M. Milazzo, and J. Radebaugh 2004. A post-Galileo view of Io's interior. *Icarus* **169**, 271–286.

Kattenhorn, S.A. and T. Hurford 2009. Tectonics of Europa. *Europa* (R.T. Pappalardo, W.B. McKinnon, and K.K. Khurana, Eds.), Univ. of Arizona Press, Tucson, 199–236.

Khurana, K., R.T. Pappalardo, N. Murphy, and T. Denk 2007. The origin of Ganymede's polar caps. *Icarus* **191**, 193–202.

Khurana, K.K., M. Kivelson, D. Stevenson, G. Schubert, C. Russell et al. 1998. Induced magnetic fields as evidence for subsurface oceans in Europa and Callisto. *Nature* **395**, 777–780.

Khurana, K.K., M.G. Kivelson, K.P. Hand, and C.T. Russell 2009. Electromagnetic induction from Europa's ocean and the deep interior, *Europa* (R.T. Pappalardo, W.B. McKinnon, and K.K. Khurana, Eds.), Univ. of Arizona Press, Tucson, 571–588.

Kirk, R. and D. Stevenson 1987. Thermal evolution of a differentiated Ganymede and implications for surface features. *Icarus* **69**, 91–134.

Kivelson, M.G., F. Bagenal, W.S. Kurth, F.M. Neubauer, C. Paranicas, and J. Saur 2004. Magnetospheric interactions with satellites. *Jupiter: The Planet, Satellites and Magnetosphere* (F. Bagenal, W. B. McKinnon, and T. E. Dowling Eds.), pp. 513–536, Cambridge Univ. Press, Cambridge.

Kivelson, M.G., K.K. Khurana, C.T. Russell, M. Volwerk, R.J. Walker et al. 2000. Galileo magnetometer measurements: A stronger case for a subsurface ocean at Europa. *Science* **289**, 1340–1343.

Kivelson, M.G., K.K. Khurana, C.T. Russell, R.J. Walker, J. Warnecke et al. 1996. Discovery of Ganymede's magnetic field by the Galileo spacecraft. *Nature* **384**, 537.

Kivelson, M.G., K.K. Khurana, D.J. Stevenson, L. Bennett, S. Joy et al. 1999. Europa and Callisto: induced or intrinsic fields in a periodically varying plasma environment. *J. Geophys. Res.* **104**, 4609–4625.

Kivelson, M.G., K.K. Khurana, and M. Volwerk 2009. Europa's Interaction with the Jovian Magnetosphere. *Europa* (R.T. Pappalardo, W.B. McKinnon, and K.K. Khurana, Eds.), Univ. of Arizona Press, Tucson, 545–570.

Kliore, A.J., A. Anabtawi, R.G. Herrera, S.W. Asmar, A.F. Nagy et al. 2002. Ionosphere of Callisto from Galileo radio occultation observations. *J. Geophys. Res. (Space Physics)* **107**, SIA 19–1 SIA 19-7.

Kliore, A.J., A. Anabtawi, and A.F. Nagy 2001a. The ionospheres of Europa, Ganymede, and Callisto. *Eos Trans. AGU*, Abstract #P12B-0506.

Kliore, A.J., A. Anabtawi, A.F. Nagy, and Galileo Radio Propagation Science Team 2001b. The ionospheres of Ganymede and Callisto from Galileo radio occultations. *BAAS* **33**, 1084.

Kliore, A.J., D.P. Hinson, F.M. Flasar, A.F. Nagy, and T.E. Cravens 1997. The ionosphere of Europa from Galileo radio occultations. *Science* **277**, 355–358.

Konopliv, A.S., C.F. Yoder, E.M. Standish, D-N. Yuan, and W.L. Sjogren 2006. A global solution for the Mars static and seasonal gravity, Mars orientation, Phobos and Deimos masses, and Mars ephemeris. *Icarus* **182**, 23–50.

Kovach, R.L. and C.F. Chyba 2001. Seismic detectability of a subsurface ocean on Europa. *Icarus* **150**, 279-287.

Kuiper, G.P. 1957. Infrared observations of planets and satellites. *Astro. J.* **62**, 295.

Kwok, J., L. Prockter, D. Senske, and C. Jones 2007. *Jupiter System Observer Mission Study: Final Report*, JPL Internal Document D-41284.

Lane, A.L., R. Nelson, and D. Matson 1981. Evidence for sulphur implantation in Europa's UV absorption band. *Nature* **292**, 38–39.

Leblanc, F., R.E. Johnson, M.E. Brown 2002. Europa's sodium atmosphere: An ocean source? *Icarus* **159**, 132–144.

LeBlanc, F., A. Potter, R. Killen, and R. Johnson 2005. Origins of Europa Na cloud and torus. *Icarus* **178**, 367–385.

Lee, S., R.T. Pappalardo, and N.C. Makris 2005. Mechanics of tidally driven fractures in Europa's ice shell. *Icarus* **177**, 367–379.

Leighton, T.G., D. Finfer, and P. White 2008. The problems with acoustics on a small planet. *Icarus* **193**, 649-652.

Leovy, C.B., A.J. Friedson, and G.S. Orton 1991. The quasiquadrennial oscillation of Jupiter's equatorial stratosphere. *Nature* **354**, 380–382.

Liang, M.-C., B.F. Lane, R.T. Pappalardo, M. Allen, and Y.L. Yung 2005. Atmosphere of Callisto. *J. Geophys. Res.* **110,** doi: 10.1029/2004JE002322.

Linkin, V., A. Harri, A. Lipatov, K. Belostotskaja, B. Derbunovich et al. 1998. A sophisticated lander for scientific exploration of Mars: Scientific objectives and implementation of the Mars-96 Small Station. *Planetary and Space Science* **46**, 717–737.

Little, B., C.D. Anger, A.P. Ingersoll, A.R. Vasavada, D.A. Senske et al. 1999. Galileo images of lightning on Jupiter. *Icarus* **142**, 306–323.

Lognonné, P., T. Spohn, D. Mimoun, S. Ulamec, and J. Biele, 2005. GEP: A piggyback package for deploying geophysics and environment observatories on Mars. *Am. Geophys. Union, Fall Meeting 2005*, abstract P41A-0919.

Lopes, R.M. and J.R. Spencer 2007. *Io After Galileo: A New View of Jupiter's Volcanic Moon*, Cambridge Univ. Press, Cambridge.

Lopes, R.M.C. and D.A. Williams 2005. Io after Galileo. *Reports on Progress in Physics* **68**, 303–340.

Lorenz, R. 2000. Post-Cassini exploration of Titan: Science rationale and mission concepts. *J. British Interplanetary Soc.*, **53**, 218–234.

Lorenz, R.D., J. Moersch, J. Stone, A. Ron Morgan Jr, and S. Smrekar 2000. Penetration tests on the DS-2 Mars microprobes: Penetration depth and impact accelerometry. *Planet. Space Sci*. **48**, 419–436.

Lorenz, R.D. 2006. Thermal interaction of the Huygens Probe with the Titan environment: Surface wind speed constraint. *Icarus* **182**, 559–566.

Lunine, J., A. Coradini, D. Gautier, T. Owen, and G. Wuchterl 2004. The origin of Jupiter. *Jupiter: The Planet, Satellites, and Magnetosphere* (F. Bagenal, T.E. Dowling, and W.B. McKinnon, Eds.), pp. 19–34, Cambridge Univ. Press, Cambridge.

Luthcke, S.B., C. Carabajal, and D. Rowlands 2002. Enhanced geolocation of spaceborne laser altimeter surface returns: Parameter calibration from the simultaneous reduction of altimeter range and navigation tracking data. *J. Geodynamics* **34**, 447–475.

Luthcke, S.B., D. Rowlands, T. Williams, and M. Sirota 2005. Reduction of ICES at systematic geolocation errors and the impact on ice sheet elevation change detection. *Geophys. Res. Lett.* **32**, L21S05.

Luttrell, K. and D. Sandwell 2006. Strength of the lithosphere of the Galilean satellites. *Icarus* **183**, 159–167.

Marchis, F., I. de Pater, A. Davies, H. Roe, T. Fusco et al., 2002. High-resolution Keck adaptive optics imaging of violent volcanic activity on Io. *Icarus* **160**, 124–131.

Matson, D. and R. Brown 1989. Solid-state greenhouse and their implications for icy satellites. *Icarus* **77**, 67–81.

Mauk, B.H., D.G. Mitchell, S.M. Krimigis, E.C. Roelof, and C. Paranicas 2003. Energetic neutral atoms form a trans-Europa gas torus at Jupiter. *Nature* **421**, 920–922.

McCord, T.B. 2000. Surface composition reveals icy Galilean satellites' past. *Eos Trans. Am. Geophys. Union* **81**, 209.

McCord, T.B., R.W. Carlson, W.D. Smythe, G.B. Hansen, R.N. Clark et al. 1997. Organics and other molecules in the surfaces of Callisto and Ganymede. *Science* **278**, 271–275.

McCord, T.B., G.B. Hansen, F.P. Fanale, R.W. Carlson, D.L. Matson et al. 1998a. Salts on Europa's surface detected by Galileo's near infrared mapping spectrometer. *Science* **280**, 1242.

McCord, T.B., G.B. Hansen, and C.A. Hibbitts 2001a. Hydrated salt minerals on Ganymede's surface: Evidence of an ocean below, *Science* **292**, 1523–1525.

McCord, T.B., G.B. Hansen, R.N. Clark, P.D. Martin, C.A. Hibbitts et al. 1998b. Non-water-ice constituents in the surface material of the icy Galilean satellites from the Galileo near-infrared mapping spectrometer investigation. *J. Geophys. Res.* **103**, 8603–8626.

McCord, T.B., G.B. Hansen, D.L. Matson, T.V. Johnson, J.K. Crowley et al. 1999. Hydrated salt minerals on Europa's surface from the Galileo near-infrared mapping spectrometer (NIMS) investigation. *J. Geophys. Res.* **104**, 11,827–11,851.

McCord, T.B., T.M. Orlando, G. Teeter, G.B. Hansen, M.T. Sieger et al. 2001b. Thermal and radiation stability of the hydrated salt minerals epsomite, mirabilite, and natron under Europa environmental conditions. *J. Geophys. Res*. **106**, 3311–3320.

McCord, T.B., G. Teeter, G.B. Hansen, M.T. Sieger, and T.M. Orlando 2002. Brines exposed to Europa surface conditions. *J. Geophys. Res.* **107**, 4-1–4-6.

McCord, T.B., G.B. Hansen, and C.A. Hibbitts 2001a. Hydrated salt minerals on

Ganymede's surface: Evidence of an ocean below. *Science* **292**, 1523–1525.

McEwen, A.S., L.P. Keszthelyi, R. Lopes, P.M. Schenk, J.R. Spencer 2004. The lithosphere and surface of Io. *Jupiter: The Planet, Satellites, and Magnetosphere* (F. Bagenal, T.E. Dowling, and W.B. McKinnon, Eds.), pp. 307–328, Cambridge Univ. Press, Cambridge.

McGrath, M. 2009. Galilean satellite atmospheres and aurora. *Eos Trans Am. Geophys. Union* **1**, 05.

McGrath, M.A., C.J. Hansen, and A.R. Hendrix 2009. Observations of Europa's tenuous atmosphere. *Europa* (R.T. Pappalardo, W.B. McKinnon, and K.K. Khurana, Eds.), Univ. of Arizona Press, Tucson, 485–506.

McGrath, M.A., E. Lellouch, D.F. Strobel, P.D. Feldman, and R.E. Johnson 2004. Satellite atmospheres. *Jupiter: The Planet, Satellites, and Magnetosphere* (F. Bagenal, T.E. Dowling, and W.B. McKinnon, Eds.), pp. 457–483, Cambridge Univ. Press, Cambridge.

McKay, C.P. 2004. What is life and how do we search for it in other worlds. *PLoS Biol.* **2**, 1260-1263.

McKinnon, W. and H. Melosh 1980. Evolution of planetary lithospheres: Evidence from multiringed structures on Ganymede and Callisto. *Icarus* **44**, 454–471.

McKinnon, W.B. 2005. Radar sounding of convecting ice shells in the presence of convection: Application to Europa, Ganymede, and Callisto. *LPI Workshop on Radar Investigations of Planetary and Terrestrial Environments, Feb. 7–10, 2005, Houston, Texas,* abstract no. 6039.

McKinnon, W.B. and E.M. Parmentier 1986. Ganymede and Callisto. *Satellites of Jupiter* (D. Morrison, Ed.), pp. 718–763, Univ. of Arizona Press, Tucson.

McKinnon, W.B. and M.E. Zolensky 2003. Sulfate content of Europa's ocean and shell: Evolutionary considerations and some geological and astrobiological implications. *Astrobiology* **3**, 879–897.

Menvielle, M., G. Musmann, F. Kuhnke, J. Berthelier, K. Glassmeier et al. 2000. Contribution of magnetic measurements onboard NetLander to Mars exploration. *Planetary and Space Science* **48**, 1231–1247.

Moersch, J., J. Bell III, L. Carter, T. Hayward, P. Nicholson et al. 1997. What happened to Cerberus? Telescopically observed thermo-physical properties of the Martian surface. *Mars Telescopic Observations Workshop II, Lunar and Planetary Science* Technical Report 97–03.

Moore, J. 2000. Models of radar absorption in Europan ice. *Icarus* **147**, 292–300.

Moore, J.C., A.P. Reid, and J. Kipfstuhl 1994. Microphysical and electrical properties of marine ice and its relationship to meteoric and sea ice. *J. Geophys. Res.* **99**, 5171–5180.

Moore, J.M., E. Asphaug, M. Belton, B. Bierhaus, H. Breneman et al. 2001. Impact features on Europa: Results of the Galileo Europa Mission (GEM). *Icarus* **151**, 93–111.

Moore, J.M., C. Chapman, E. Bierhaus, R. Greeley, F. Chuang et al. 2004. Callisto. Jupiter: The Planet, Satellites, and Magnetosphere (F. Bagenal, T.E. Dowling, and W.B. McKinnon, Eds.), pp. 397–426, Cambridge Univ. Press, Cambridge.

Moore, J.M., G. Black, B. Buratti, C.B. Phillips, J. Spencer, and R. Sullivan 2009. Surface properties, regolith, and landscape degradation. *Europa* (R.T. Pappalardo, W.B. McKinnon, and K.K. Khurana, Eds.), Univ. of Arizona Press, Tucson, 329–352.

Moore, J.M. and R.T. Pappalardo 2008. Titan: Callisto with weather? *Am. Geophysi. Union, Fall Meeting 2008,* abstract P11D-06.

Moore, W.B. 2001. The thermal state of Io. *Icarus* **154**, 548–550.

Moore, W.B. and H. Hussmann 2009. Thermal evolution of Europa's silicate interior. *Europa* (R.T. Pappalardo, W.B. McKinnon, and K.K. Khurana, Eds.), Univ. of Arizona Press, Tucson, 369–380.

Moore, W.B. and G. Schubert 2000. The tidal response of Europa. *Icarus* **147**, 317–319.

Moroz, V.I. 1965. Infrared spectrophotometry of the Moon and the Galilean satellites of Jupiter. *Soviet Astro.* **9**, 999.

Moses, J.I., T. Fouchet, R.V. Yelle, A.J. Friedson, S.G. Orton et al. 2004. The stratosphere of Jupiter. *Jupiter: The Planet, Satellites, and Magnetosphere* (F. Bagenal, T.E. Dowling, and W.B. McKinnon, Eds.), pp. 129–158, Cambridge Univ. Press, Cambridge.

Mosqueira, I. and P.R. Estrada 2003. Formation of the regular satellites of giant planets in an extended gaseous nebula I: Subnebula model and accretion of satellites. *Icarus* **163**, 198–231.

Mousis, O., Y. Alibert 2006. Modeling the Jovian subnebula. II. Composition of regular satellite ices. *Astro. and Astrophy.* **448**, 771-778.

Mousis, O., J.I. Lunine, J.H. Waite, B. Magee, W.S. Lewis et al. 2009. Formation conditions of Enceladus and origin of its methane reservoir. *Astrophysical J.* **701**, L39-L42.

Mustard, J., S. Murchie, S. Pelkey, B. Ehlmann, R. Milliken et al. 2008. Hydrated silicate minerals on Mars observed by the Mars Reconnaissance Orbiter CRISM instrument. *Nature* **454**, 305.

NASA 2006. *Solar System Exploration Roadmap.* NASA Science Mission Directorate, http://solarsystem.nasa.gov/multimedia/downloads/SSE_RoadMap_2006_Report_FC-A_med.pdf.

Nash, D. and R. Howell 1989. Hydrogen Sulfide on Io: Evidence from telescopic and laboratory infrared spectra. *Science* **244**, 454–457.

Neumann, G.A. D. Rowlands, F. Lemoine, D. Smith, and M. Zuber 2001. Crossover analysis of Mars Orbiter Laser altimeter data. *J. Geophys. Res.* **106**, 23,753–23,768.

Nimmo, F., B. Giese, and R.T. Pappalardo 2003. Estimates of Europa's ice shell thickness from elastically supported topography. *Geophys. Res. Lett.* **30**, 1233.

Nimmo, F. and M. Manga 2009. Geodynamics of Europa's icy shell. *Europa* (R.T. Pappalardo, W.B. McKinnon, and K.K. Khurana, Eds.), Univ. of Arizona Press, Tucson, 381–404.

Nimmo, F., R. Pappalardo, and J. Cuzzi 2007a. Observational and theoretical constraints on plume activity at Europa. *Am. Geophys. Union, Fall Meeting 2007*, abstract P51E-05.

Nimmo, F. and P. Schenk 2006. Normal faulting on Europa: Implications for ice shell properties. *J. Structural Geology* **28**, 2194–2203.

Noll, K., R. Johnson, A. Lane, D. Domingue, and H. Weaver 1996. Detection of ozone on Ganymede. *Science* **273**, 341.

Noll, K.S., H.A. Weaver, and A.M. Gonnella 1995. The albedo spectrum of Europa from 2200 to 3300. *J. Geophys. Res.* **100**, 19,057–19,060.

Ojakangas, G.W., D.J. Stevenson 1989. Thermal state of an ice shell on Europa. *Icarus* **81**, 220–241.

O'Reilly, T.C. and G.F. Davies 1981. Magma transport of heat on Io—A mechanism allowing a thick lithosphere. *Geophys. Res. Lett.* **8**, 313–316.

Orlando, T.M., T.B. McCord, and G.A. Grieves 2005. The chemical nature of Europa surface material and the relation to a sub-surface ocean. *Icarus* **177**, 528–533.

Owen, T. and H.B. Niemann 2009. The origin of Titan's atmosphère: Some recent advances. *Phil. Trans. Series A* **367**, 607–615.

Paczkowski, B. 2008. *Outer Planets Flagship Mission Science Operations Concept Study Report*, JPL Internal Document D–46870.

Palguta, J., J.D. Anderson, G. Schubert, and W.B. Moore 2006. Mass anomalies on Ganymede. *Icarus* **180**, 428–441.

Panning, M., V. Lekic, M. Manga, and B. Romanowicz 2006. Long-period seismology on Europa: 2. Predicted seismic response. *J. Geophys. Res.* **111**, doi: 10.1029/ 2006JE002712.

Pappalardo, R. and R. Sullivan 1996. Evidence for separation across a gray band on Europa. *Icarus* **123**, 557–567.

Pappalardo, R.T. et al. 1998a. Geological evidence for solid-state convection in Europa's ice shell. *Nature* **391**, 365.

Pappalardo, R.T., J. Head, G. Collins, R. Kirk, G. Neukum et al. 1998b. Grooved terrain on Ganymede: First results from Galileo high-resolution imaging. *Icarus* **135**, 276-302.

Pappalardo, R.T., J.W. Head, R. Greeley, R.J. Sullivan, C. Pilcher et al. 1999. Does Europa have a subsurface ocean? Evaluation of the geological evidence. *J. Geophys. Res.* **104**, 24,015–24,056.

Pappalardo, R.T. and A.C. Barr 2004. Origin of domes on Europa: The role of thermally induced compositional buoyancy. *Geophys. Res. Lett.* **31**, L01701.

Pappalardo, R.T., G.C. Collins, J.W. Head III, P. Helfenstein, T.B. McCord, J.M. Moore, L.M. Procktor, P.M. Schenk, and J.R. Spencer 2004. Geology of Ganymede. *Jupiter: The Planet, Satellites, and Magnetosphere* (F. Bagenal, T.E. Dowling, and W.B. McKinnon, Eds.), pp. 363–396, Cambridge Univ. Press, Cambridge.

Paranicas, C., J.F. Cooper, H.B. Garrett, R.E. Johnson, and S.J. Sturner 2009. Europa's radiation environment and its effects on the surface. *Europa* (R.T. Pappalardo, W.B. McKinnon, and K.K. Khurana, Eds.), Univ. of Arizona Press, Tucson, 529–544.

Paranicas, C., B.H. Mauk, K. Khurana, I. Jun, H. Garrett et al. 2007. Europa's near-surface radiation environment. *Geophys. Res. Lett.* **34**, L15103.

Paranicas, C., B. Mauk, J. Ratliff, C. Cohen, and R. Johnson 2002. The ion environment near Europa and its role in surface energetics. *Geophys. Res. Lett.* **29**, 18–1.

Parmentier, E.M., S.W. Squyres, J.W. Head, and M.L. Allison 1982. The tectonics of Ganymede. *Nature* **295**, 290–293.

Passey, Q. and E. Shoemaker 1982. Craters and basins on Ganymede and Callisto: Morphological indicators of crustal evolution. *Satellites of Jupiter* **1**, 379–434.

Peale, S.J. 1976. Orbital resonances in the solar system. *Ann. Rev. Astron. Astrophys.* **14**, 215–246.

Peters, K.E., C. C. Walters , J. M. Moldowan 2005. *The Biomarker Guide*, Cambridge Univ. Press, Cambridge.

Pilcher, C.B., S.T. Ridgway, and T.B. McCord 1972. Galilean satellites. *J. Geophys. Res.* **103**, 31,391–31,403.

Pinçon, J., M. Menvielle, and L. Szarka 2000. Geomagnetic induction study using the NetLander network of magnetometers. *Planetary and Space Science* **48**, 1261–1270.

Porco, C.C., P. Helfenstein, P.C.T. Thomas, A.P. Ingersoll, J. Wisdom et al. 2006. Cassini observes the active south pole of Enceladus. *Science* **311**, 1393–1401.

Prockter, L. and R. Pappalardo 2000. Folds on Europa: Implications for crustal cycling and accommodation of extension. *Science* **289**, 941–943.

Prockter, L.M., J.W. Head, R.T. Pappalardo, D.A. Senske, G. Neukum et al. 1998. Dark terrain on Ganymede: Geological mapping and interpretation of Galileo Regio at high resolution. *Icarus* **135**, 317–344.

Prockter, L.M., J.W. Head, R.T. Pappalardo, R.J. Sullivan, A.E. Clifton et al. 2002. Morphology of Europan bands at high resolution: A mid-ocean ridge-type rift mechanism, *J. Geophys. Res.* **107**, 4-1–4-28. doi:10.1029/2000JE001458.

Prockter, L.M. and G.W. Patterson 2009. Morphology and evolution of Europa's ridges and bands. *Europa* (R.T. Pappalardo, W.B. McKinnon, and K.K. Khurana, Eds.), Univ. of Arizona Press, Tucson, 237–258.

Riley, J., G.V. Hoppa, R. Greenberg, B.R. Tufts, and P. Geissler 2000. Distribution of

chaotic terrain on Europa. *J. Geophys. Res.* **105**, 22,599–22,616.

Rogers, J. 1995. *The giant planet Jupiter*. Cambridge Univ. Press, Cambridge.

Rothschild, L. and R. Mancinelli 2001. Life in extreme environments. *Nature* **409**, 1092–1101.

Rowlands, D.D., D. Pavlis, F. Lemoine, G. Neumann, and S. Luthcke 1999. The use of laser altimetry in the orbit and attitude determination of Mars Global Surveyor. *Geophys. Res. Lett.* **26**, 1191–1194.

Rudolph, M. and M. Manga 2009. Fracture penetration in planetary ice shells. *Icarus* **199**, 536–541.

Rummel, J., F. Raulin, and P. Ehrenfreund *eds.* 2010. COSPAR Workshop on Planetary Protection for Titan and Ganymede. COSPAR, Paris, 29 pp.

Salyk, C., A.P. Ingersoll, J. Lorre, A. Vasavada, and A.D. Del Genio 2006. Interaction between eddies and mean flow in Jupiter's atmosphere: Analysis of Cassini imaging data. *Icarus* **185**, 430–442.

Sanchez-Lavega, A., G. Orton, R. Hueso, E. García-Melendo, S. Pérez-Hoyos et al. 2008. Depth of a strong Jovian jet from a planetary-scale disturbance driven by storms. *Nature* **451**, 437–440.

Sandwell, D.P., P. Rosen, W. Moore, and E. Gurrola 2004. Radar interferometry for measuring tidal strains across cracks on Europa. *J. Geophys. Res.* **109**, doi: 10.1029/2004JE002276.

Sarid, A.R., R. Greenberg, G.V. Hoppa, T.A. Hurford, B.R. Tufts et al. 2002. Polar wander and surface convergence of Europa's ice shell: Evidence from a survey of strike-slip displacement. *Icarus* **158**, 24–41.

Schenk, P. 2009. Slope characteristics of Europa: Constraints for landers and radar sounding. *Geophy. Res. Lett.* **36**, L15204.

Schenk, P. and R. Pappalardo 2004. Topographic variations in chaos on Europa: Implications for diapiric formation. *Geophys. Res. Lett.* **31**, L16703 1–5.

Schenk, P., W. McKinnon, D. Gwynn, and J. Moore 2001. Flooding of Ganymede's bright terrains by low-viscosity water-ice lavas. *Nature* **410**, 57–60.

Schenk, P.M. and M.H. Bulmer 1998. Origin of mountains on Io by thrust faulting and large-scale mass movements. *Science* **279**, 1514.

Schenk, P.M., C.R. Chapman, K. Zahnle, J.M. Moore 2004. Ages and interiors: The cratering record of the Galilean satellites. *Jupiter: The Planet, Satellites, and Magnetosphere* (F. Bagenal, T.E. Dowling, and W.B. McKinnon, Eds.), pp. 427–457, Cambridge Univ. Press, Cambridge.

Schenk, P.M., and E.P. Turtle 2009. Europa's impact craters: Probes of the icy shell. *Europa* (R.T. Pappalardo, W.B. McKinnon, and K.K. Khurana, Eds.), Univ. of Arizona Press, Tucson, 181–198.

Schilling, N., F.M. Neubauer, and J. Saur, J. 2007. Time-varying interaction of Europa with the Jovian magnetosphere: Constraints on the Conductivity of Europa's subsurface ocean. *Icarus* **192**, 41–55.

Schubert, G., F. Sohl, and H. Hussmann 2009. Interior of Europa. *Europa* (R.T. Pappalardo, W.B. McKinnon, and K.K. Khurana, Eds.), Univ. of Arizona Press, Tucson, 353–368.

Schubert, G., K. Zhang, M.G. Kivelson, and J.D. Anderson 1996. The magnetic field and internal structure of Ganymede. *Nature* **384**, 544–545.

Shirley, J.H., J.B. Dalton III, L.M. Prockter, and L.W. Kamp 2010. Europa's ridged plains and smooth low albedo plains: Distinctive compositions and compositional gradients at the leading side–trailing side boundary. *Icarus* **210**, 358–384.

Shoemaker E.M., B.K. Lucchitta, J.B. Plescia, S.W. Squyres, and D.E. Wilhelms 1982. The geology of Ganymede. *Satellites of Jupiter* (D. Morrison, Ed.), pp. 435–520, Univ. of Arizona Press, Tucson.

Showalter, M., I. de Pater, G. Verbanac, D. Hamilton, and J. Burns, 2008. Properties and

dynamics of Jupiter's gossamer rings from Galileo, Voyager, Hubble and Keck images. *Icarus* **195**, 361–377.

Showalter, M.R., A.F. Cheng, H.A. Weaver, S.A. Stern, J.R. Spencer et al. 2007. Clump detections and limits on moons in Jupiter's ring system. *Science* **318**, 232–234.

Showman, A.P. and R. Malhotra 1999. The Galilean satellites. *Science* **286**, 77–84.

Showman, A.P. and D.M.R. Stevenson 1997. Coupled orbital and thermal evolution of Ganymede. *Icarus* **129**, 367–383.

Simon-Miller, A.A., N.L. Chanover, G.S. Orton, M. Sussman, and E. Karkoschka 2006. Jupiter's white oval turns red. *Icarus* **185**, 558–562.

Smythe, W.D., R. Carlson, A. Ocampo, D. Matson, and T. McCord 1998. Galileo NIMS measurements of the absorption bands at 4.03 and 4.25 microns in distant observations of Europa. *Amer. Astronom. Soc.* **30**, 1448.

Smyth, W.H. and M.L. Marconi 2006. Europa's atmosphere, gas tori, and magnetospheric implications. *Icarus* **181**, 510–526.

Smrekar, S., R.D. Lorenz, and M. Urquhart, M. 2001, The Deep-Space-2 Penetrator Design and Its Use for Accelerometry and Estimation of Thermal Conductivity, In Kömle, N.I., Kargl, G., Ball, A.J. and Lorenz, R.D. (eds), pp. 109–124. *Penetrometry in the Solar System*. Austrian Academy of Sciences Press, Vienna

Sotin, C., G. Tobie, J. Wahr, and W.B. McKinnon 2009. Tides and tidal heating on Europa. *Europa* (R.T. Pappalardo, W.B. McKinnon, and K.K. Khurana, Eds.), Univ. of Arizona Press, Tucson, 85–118.

Spencer, J. 1987. Thermal segregation of water ice on the Galilean satellites. *Icarus* **69**, 297–313.

Spencer J.R., E. Lellouch, M. Richter, M. López-Valverde, K. Lea Jessup et al. 2005. Mid-infrared detection of large longitudinal asymmetries in Io's SO_2 atmosphere. *Icarus* **176**, 283–304.

Spencer, J.R. and W.M. Calvin 2002. Condensed O_2 on Europa and Callisto. *Astron. J.* **124**, 3400–3403.

Spencer, J.R., L.K. Tamppari, T.Z. Martin, and L.D. Travis 1999. Temperatures on Europa from Galileo PPR: Nighttime thermal anomalies. *Science* **284**, 1514–1516.

SSB 1999. *A Science Strategy for the Exploration of Europa*, Space Studies Board, National Research Council, National Academies Press, Washington, D.C.

SSB 2003. *New Frontiers in the Solar System: an Integrated Exploration Strategy*, Space Studies Board, National Research Council, National Academies Press, Washington, D.C.

Stephan, K., C. Hibbitts, G. Hansen, R. Wagner, and R. Jaumann 2006. Close up view of the spectral properties of Ganymede at mid-latitudes with respect to geological surface features. *Bull. Am. Astron. Soc.* **38**, 1298.

Stephan, K., C. Hibbitts, R. Wagner, R. Jaumann, and G. Hansen 2009. Ganymede's spectral properties: Implications for further investigations in a future mission to Jupiter and its satellites. In *European Planetary Science Congress 2009, vol. 1, Sept. 14–18, Potsdam, Germany*, p. 633.

Strauss, K., D. Sheldon, and S. McClure**,** *Memory Investigation for Jupiter Europa Orbiter Mission 2008*, JPL Internal Document D–48262.

Strobel, D.F., J. Saur, P.D. Feldman, and M.A. McGrath 2002. Hubble Space Telescope space telescope imaging spectrograph search for an atmosphere on Callisto: A Jovian unipolar inductor. *Astrophys. J.* **581**, L51–L54.

Sullivan, R., R. Greeley, K. Homan, J. Klemaszewski, M.J.S. Belton et al. 1998. Episodic plate separation and fracture infill on the surface of Europa. *Nature* **391**, 371–373.

Summons, R., P. Albrecht, G. McDonald, and J. Moldowan 2008. Molecular biosignatures. *Space Science Rev.* **135**, 133–159.

Taylor, F.W., S.K. Atreya, T. Encrenaz, D.M. Hunten, P.J.G. Irwin et al. 2004. The composition of the atmosphere of Jupiter. *Jupiter: The Planet, Satellites, and Magnetosphere* (F. Bagenal, T.E. Dowling, and W.B. McKinnon, Eds.), pp. 59–78, Cambridge Univ. Press, Cambridge.

Tufts, B.R., R. Greenberg, G. Hoppa, and P. Geissler 2000. Lithospheric dilation on Europa. *Icarus* **146**, 75–97.

Turtle, E.P. 2001. Mountains on Io: High-resolution Galileo observations, initial interpretations, and formation models, *J. Geophys Res.* **106**, 33,175–33,200.

Tyler, G., E. Marouf, and G. Wood 1981. Radio occultation of Jupiter's ring: Bounds on optical depth and particle size and a comparison with infrared and optical results. *J. Geophys. Res.* **86**, 8699–8703.

Tyler, R.H., S. Maus, and H. Luhr 2003. Satellite observations of magnetic fields due to ocean tidal flow. *Science* **299**, 239–241.

Van Cleve, J., R. Pappalardo, and J. Spencer 1999. Thermal palimpsests on Europa: How to detect sites of current activity. *30th Ann. Lunar and Planetary Science Conf., March 15–29, 1999, Houston, Texas*. [Abstract]

Vasavada, A.R. and A. Showman 2005. Jovian atmospheric dynamics: An update after Galileo and Cassini. *Reports on Progress in Physics* **68**, 1935–1996.

Veeder, G.J., D.L. Matson, T.V. Johnson, A.G. Davies, and D.L. Blaney 2004. The polar contribution to the heat flow of Io. *Icarus* **169**, 264–270.

Volwerk, M., K. Khurana, and M. Kivelson 2001. Wave activity in Europa's wake: Implications for ion pickup. *J. Geophys. Res.* **106**, 26,033–26,048.

Wahr, J.M., M. Zuber, D. Smith, and J. Lunine 2006. Tides on Europa, and the thickness of Europa's icy shell. *J. Geophys. Res.* **111**, doi: 10.1029/2006JE002729.

Waite, J.H., M. Combi, W. Ip, T. Cravens, R. McNutt et al. 2006. Cassini ion neutral mass spectrometer: Encleadus plume composition and structure. *Science* **311**, 1419–1422.

Waite, J.H., W.S. Lewis, B.A. Magee, J.I. Lunine, W.B. McKinnon et al. 2009. Liquid water on Enceladus from observations of ammonia and ^{40}Ar in the plume. *Nature*, **460**, 487–490.

Ward, W.R. 1975. Past orientation of the lunar spin axis. *Science* **189**, 377–379.

Weber, R.C., B.G. Bills, and C.L. Johnson 2009. Constraints on deep moonquake focal mechanisms through analysis of tidal stress. *J. Geophys. Res.* **114**, doi: 10.1029/2008JE003286.

West, R.A., K.H. Baines, A.J. Friedson, D. Banfield, B. Ragent et al. 2004. Jovian clouds and haze. *Jupiter: The Planet, Satellites, and Magnetosphere* (F. Bagenal, T.E. Dowling, and W.B. McKinnon, Eds.), pp. 79–104, Cambridge Univ. Press, Cambridge.

Wienbruch, U. and T. Spohn 1995. A Self–Sustained Magnetic Field on Io? *Planetary and Space Science* **43**, 1045–1057.

Wu, X.P., Y. Bar-Sever, W. Folkner, J. Williams, and J. Zumberge 2001. Probing Europa's hidden ocean from tidal effects on orbital dynamics. *Geophys. Res. Lett.* **28**, 2245–2248.

Wynn-Williams, D., H. Edwards, and F. Garcia-Pichel 1999. Functional biomolecules of Antarctic stromatolitic and endolithic cyanobacterial communities. *European J. Phycology*, **34**, 381–391.

Yan, T-Y. et al. 2008. *Risk Mitigation Plan: Radiation and Planetary Protection*, JPL Internal Document D–47928.

Yelle, R.V. and S. Miller 2004. Jupiter's thermosphere and ionosphere. *Jupiter: The Planet, Satellites, and Magnetosphere* (F. Bagenal, T.E. Dowling, and W.B. McKinnon, Eds.), pp. 185–218, Cambridge Univ. Press, Cambridge.

Yoder, C.F. and S. Peale 1981. Tidal variations of Earth rotation. *J. Geophys. Res.* **86**, 881–891.

Yoder, C.F. and S.J. Peale 1981. The tides of Io. *Icarus* **47,** 1–35.

Zahnle, K., L. Dones, and H.F. Levison 1998. Cratering rates in the Galilean satellites. *Icarus* **136**, 202–222.

Zahnle, K., P. Schenk, H. Levison, and L. Dones, 2003. Cratering rates in the outer solar system. *Icarus* **163**, 263–289.

Zimmer, C., K.K. Khurana, and M. Kivelson 2000. Subsurface oceans on Europa and Callisto: Constraints from Galileo magnetometer observations. *Icarus* **147**, 329–347.

Zolotov, M.Y. and J.S. Kargel 2009. On the Chemical Composition of Europa's Icy Shell, Ocean, and Underlying Rocks. *Europa* (R.T. Pappalardo, W.B. McKinnon, and K.K. Khurana, Eds.), Univ. of Arizona Press, Tucson, 431–458.

Zombeck, M., 1982. *Handbook of Space Astronomy and Astrophysics*, Cambridge Univ. Press, Cambridge.

Zuber, M.T., D. Smith, S. Solomon, D. Muhleman, J. Head 1992. The Mars Observer Laser Altimeter investigation. *J. Geophys. Res.* **97**, 7781–7797.

APPENDIX A. SURFACE ELEMENT EVALUATION

Working Group members:

Co-Chairs:
Bruce G. Bills , JPL/Caltech, USA
Angioletta Coradini, IFSI-INAF, Italy

Members:
Andrew J. Coates, MSSL-UCL, UK
Olivier Grasset, University of Nantes, France
Kevin P. Hand, JPL/Caltech, USA
Hauke Hussmann, DLR, Germany
Ralph D. Lorenz, APL, USA
Olga Prieto-Ballesteros, CAB-INTA-CSIC, Spain
Christophe Sotin, JPL/Caltech, USA

JEO support:
Louise Prockter, APL, USA

JGO support:
Christian Erd, ESTEC, NL
Jean-Pierre Lebreton, ESTEC, NL

A.1. Introduction

In April 2010, a working group was convened to consider the potential scientific merit of placing a small payload, comprising only a few kg of instrument mass, on the surface of Europa, as an augmentation to the Europa Jupiter System Mission (EJSM).

We had neither the time nor the resources available to conduct detailed, independent studies of this problem, but instead relied upon extensive previous work on small planetary surface payloads, and also the Jupiter Icy Moons Orbiter (JIMO) mission surface component.

In addition, there are two currently active studies which are especially relevant. The UK Penetrator Consortium had been examining the possibility of a surface element on Ganymede, as part of the Jupiter Ganymede Orbiter (JGO) mission, and has recently changed the focus of that study to consider a Europa surface element, to be carried by the Jupiter Europa Orbiter (JEO). A group at JPL has also been examining options for configuration, delivery, and operation of a modest payload on the surface of Europa.

The Europa surface element working group had a series of weekly teleconferences, and two face-to-face meetings; one at Imperial College in London, UK and another at ESTEC in Noordwijk, Netherlands.

This document presents the primary conclusions and recommendations of the surface element working group, along with some supporting background material.

A.2. Conclusions

We conclude that important and unique science could result from placing a small payload on the surface of Europa, and operating it there for a short period of time. The criteria we used, in evaluating potential science investigations, are that they each must:

- address an important science question relevant to the EJSM and JEO mission objectives,
- plausibly be achievable with the stringent constraints of delivery to, and operation on, the surface of Europa, and
- not be achievable from the JEO orbital platform.

The nominal recommended payload consists of three components. In order of decreasing priority they are:

1) a complex chemistry investigation, such as a mass spectrometer,
2) a geophysics investigation, consisting of a seismometer, and
3) a suite of engineering instruments to characterize the physical environment at

the Europan surface, including such things as acceleration history during landing, ionizing radiation dose rate, and temperature.

If additional resources are available, augmentations to the nominal payload should consist of, in order of decreasing priority:

- a surface characterization camera, to provide a landing site panorama for a surface lander, or a microscope for a penetrator,
- additional capability for the complex chemistry investigation,
- additional geophysics, including a more capable seismometer, a magnetometer, a tiltmeter, and a tracking beacon
- enhanced surface lifetime, and
- a descent camera.

Though the science that could potentially be achieved by a surface element would be extremely valuable, we agree with an earlier assessment of the JEO science definition team that no aspect of the currently envisioned surface element has a higher priority, relative to the overall JEO mission objectives, than any of the baseline payload investigations on the orbiter. As a result, we strongly recommend that the surface element, if it is further considered at all, should be placed very high on the mission descope list.

In addition, since a major component of the cost of the surface element, as presently conceived, is basic infrastructure such as the delivery system, power supply, and telecommunication system, it appears that there are no viable descopes of the surface element duration or modest instrument complement described hereafter. Thus, the most prudent descope option would not be at the instrument or investigation level, but would amount to complete removal of the surface element. It appears that the cost of delivery, to the surface of Europa, of an un-instrumented system, comprised solely of a telecommunication system and power source would be similar to that for delivery and operation of the nominal payload discussed here.

Current uncertainties regarding both the performance of the delivery system and operational capabilities on the surface have made a detailed assessment of the plausibility of some potential science instruments very difficult. We thus strongly urge continuation of present studies of those issues, including (but not limited to) the UK penetrator consortium study, to address aspects including access to material outside the penetrator, as well as the JPL surface element study.

We also recommend that, if a surface element is to be further pursued as part of JEO, then a science definition team should be assembled to give this matter further study. As noted above, many of the science feasibility issues are strongly coupled to the implementation strategy selected, such as a penetrator versus a semi-hard lander. Until such issues are further clarified, a science payload cannot be fully defined. The integrated nature of the system and payload may lend itself to a PI-led model of implementation.

A.3. Logistical Background

In this section we briefly summarize some of the logistical issues which challenge the delivery and operation of a surface element on Europa. While some logistical considerations depend upon details of implementation strategy, many are quite generic. Broadly speaking, the main challenges are: getting to the surface, communicating with the Jupiter Europa Orbiter, and surviving on the surface. Table A-1 lists the topics and corresponding lead authors.

Table A-1. Logistics Section Leads

Topic	Lead(s)
Getting to the surface	Bills, Lorenz
Communicating	Bills
Surviving on the surface	Bills
Data volumes	Lorenz

A.3.1 Getting to the Surface

To change the vehicle state from orbital speed at an altitude above Europa to near zero speed near the surface requires a total velocity change on the order of 1500 m/s. The basic physics of the rocket equation, combined with the relatively low specific impulse (Newtons of thrust per kilogram of mass) of available chemical propellants, therefore dictate that from a nominal 100 km altitude circular orbit, most of the allocated mass must be propellant in order to deliver any mass to the surface of Europa. Moreover, much of the remainder must be infrastructure such as fuel tanks, rocket nozzles, and some sort of guidance, navigation, and control system.

The principal design degree of freedom is whether the impact velocity with the surface should be controlled propulsively to a small value (as in a conventional soft-lander like Surveyor or Apollo), a modest value (a semi-hard lander like Luna-9 or Pathfinder), or allowed to be as high as 200-300 m/s, which could be dissipated by penetration into Europa's surface. A wide solution space to this landing problem exists [*Ball et al. 2007*].

The solution with the minimum velocity change, and thus minimal propellant, is the penetrator, with a high velocity at impact with the surface. Typical impact velocities contemplated for Europa penetrators are roughly 200 m/s, which then imply deceleration at a mean rate of 20,000 m/s^2 (2000 g) to stop at a depth of 1 m. Very few existing instruments could survive that level of acceleration and continue to operate. Instruments requiring direct access to the penetrator's exterior, either through an open port or a transparent window, place further constraints on the system architecture.

Most de-orbiting strategies relevant to a Europa surface element comprise variations on a simple theme. The surface package is first gently moved away from the orbiter and then two propulsive events are used to deliver it to the surface. The first propulsive event makes a transition from a circular orbit to an eccentric orbit with periapse closer to the surface. The second propulsive event is executed half an orbit later, at the next periapse, and stops the along-track motion. The surface element then drops to the surface.

Table A-2 shows relevant parameters for a range of such "stop and drop" delivery scenarios. The parameters are: drop height, change in velocity at the two propulsive maneuvers, and the resulting impact speed. The total propulsive cost of a gentle landing is not appreciably higher than that for a 200 m/s penetrator. However, the complexity of the required guidance, navigation, and control (GNC) systems may be higher, in order to perform the function of re-orienting the lander before and after the required second burn. It may be that some intermediate solutions offer superior performance. For example, the original Ranger seismic capsules and the

Table A-2. Surface Delivery Parameters.

Drop height	ΔV1	ΔV2	Total	Impact speed
Km	m/s	m/s	m/s	m/s
0	22	1455	1476	0
10	19	1448	1467	162
20	17	1441	1458	228
30	15	1434	1449	278
40	13	1427	1440	320
50	11	1421	1431	357
60	8	1414	1423	390
70	6	1408	1414	420
80	4	1406	1406	447
90	2	1395	1397	473
100	0	1389	1389	497

Luna-9 lander were both delivered by descent systems close to the surface at modest velocity. Studies of the stop-and-drop architecture at JPL, and the European penetrator study, indicate that the accuracy of the GNC system and the dispersions in velocity following the second burn are key factors determining the impact conditions.

An additional consideration is that a penetrator could only be delivered successfully if its angle of attack (orientation of the vehicle with respect to its velocity) and angle of incidence (angle between the velocity and the target surface normal) are below certain limits (approximately 30 degrees total). The Europa surface has surface slopes that exceed this value over ~10% of the terrain [*Schenk 2009*], making Europa is considerably rougher than Mars, so a certain probability of mission failure would accompany any individual penetrator delivery, regardless of how good its GNC system is at orienting the vehicle correctly with respect to its velocity. It is possible that JEO might be able to identify regions on Europa that are large enough to target reliably, but have local roughness less than cited above, but this cannot be guaranteed a priori.

A.3.2 Communicating with the Orbiter

Mass and power constraints on the surface element telecommunications package imply that the only feasible means of returning data to Earth is via a radio-frequency link to the orbiter, which would then relay the data to Earth. Communication with the orbiter would be limited to the short intervals of time when it is visible above the horizon, as seen from the surface element. Depending upon currently unknown details, such as Europa's topography and surface roughness at the surface element location, and telecommunication effective beam width, the orbiter may need to be well above the horizon for communication to occur, which would further restrict the available times.

Figure A-1 and Figure A-2 illustrate the most favorable case, in which the surface is flat and the orbiter passes directly over the surface element. For a 100 km altitude circular orbit, the maximum possible communication time per orbit is just under 14 minutes. Figure A-2 illustrates the ground track pattern for a 100 km altitude circular orbit, with inclination of 95 degrees, as seen from the north or south pole. The availability of the orbiter on passes subsequent to delivery of the surface element is much better for surface element locations nearer to the poles.

Though the cadence of orbiter contact times would depend on implementation details, the basic scenario is as follows. Immediately upon landing, the orbiter may be visible from the surface, but would only remain visible for a few minutes. The next opportunity would be one JEO orbital period (roughly 2 hours) later, and would also be only a few minutes in duration. At sufficiently high latitudes, the orbiter would continue to be visible for a few minutes on all subsequent orbits. At lower latitudes, there would be only a few orbits of consecutive visibility, separated by "black-

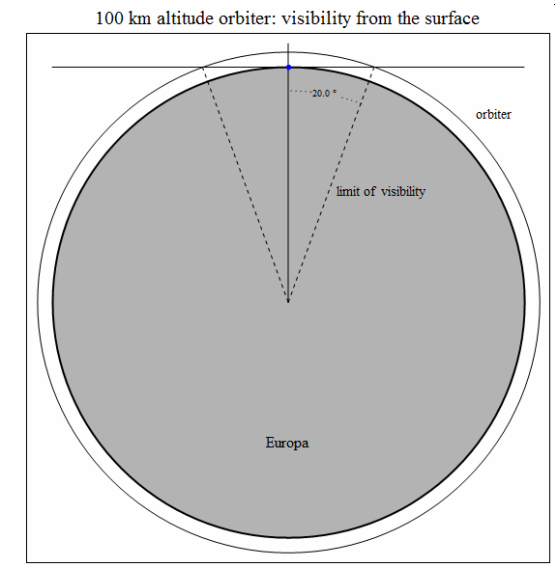

Figure A-1. Visibility of orbiter from the surface, global view.

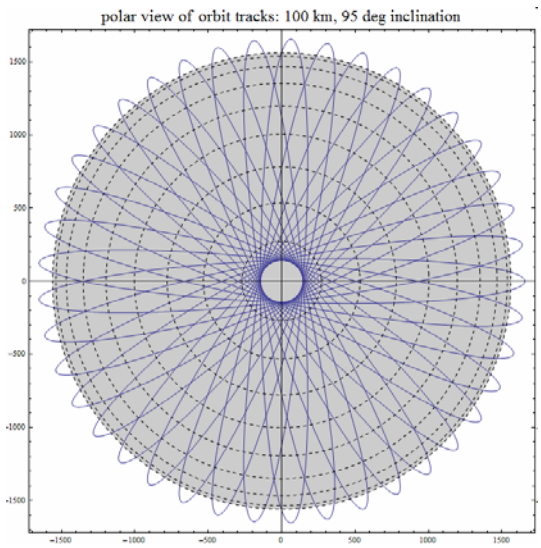

Figure A-2. Polar view of orbiter ground tracks.

out" periods of half a Europa day.

A.3.3 Surviving on the Surface

After a 5.5 year trip from Earth to Jupiter, and a 30 month cruise phase within the Jupiter system, and some (as yet unknown) fraction of the prime Europa orbital mission phase, the surface element package would be delivered to the surface of Europa, and there it would need to operate long enough to collect and transmit its data back to the orbiter. From the perspective of minimizing radiation-induced damage, it would be desirable to have the surface element deployed as soon after orbit insertion at Europa, as possible.

It is envisioned that much of the complex chemistry experiment could be conducted within a few tens of minutes. Due to orbiter access issues, as described above, the surface element would need to continue operating for at least two hours after arrival on the surface in order to transmit back the complex chemistry data it has collected. The surface properties measurements could likely be completed within minutes after arrival.

High latitudes are best for communications with the orbiter.

The seismic experiment would take longer to complete. If there is sufficient seismic activity, at the time and place of surface landing, then the first order question (is Europa seismically active at the present time?) could also be answered within a few minutes or hours. If the seismic activity level is relatively low, or below the detection threshold, then quantifying the level would take longer. Answering the next question, concerning how the seismic activity level correlates with tidal forcing, would require at least half of a 3.55 day (85 hour) tidal cycle, and would benefit from an even longer duration.

The chief factors likely to limit the surface operation lifetime are batteries and thermal control. The batteries must have sufficient capacity to perform their roles during deployment and continue powering the science instruments and telecommunications system. When the batteries are drained, the surface element operation would cease.

If we assume that the surface element accommodation on the orbiter is such that it is not significantly protected from ionizing radiation prior to deployment, then the radiation dose on the surface would not likely be much of an increment. However, that is one of many technical issues that require further study.

If the surface element were deployed to a high latitude region to increase communication access time to the orbiter, then the ambient temperatures, even during daytime, would be very low. Although in general one could link energy requirements to data return (see next section), emplacement in a cold material by a penetrator either requires tolerance of low temperatures (which many electronic systems could do, but batteries typically cannot), isolation from the environment by a vacuum bottle, or other insulation.

The thermal challenges are much less severe for low-latitude Martian environments or the Moon, to which most penetrator mission studies have been directed to date. On the other hand, a semi-hard lander (a vehicle where the impact velocity is higher than is typical for a propulsive soft-lander, but where the impact energy is absorbed on-board by a crushable material, rather than by the planetary surface material) would be more likely to have a hemispheric view of the sky, and so conventional radiative thermal control could be accomplished more easily.

The coupled delivery and thermal design problem is beyond the scope of this report. Insofar as some scientific investigations require contact with surface or subsurface material, a penetrator solution might notionally be simpler, but this depends on the details of the implementation.

A.3.4 Data Volume Capabilities

An empirical relationship links the energy budget of small *in situ* planetary spacecraft and the data volume they could return to Earth: about 1 bit per Joule [*Lorenz 2000*] although this could be exceeded by an order of magnitude or more. Inspection of the characteristics of proposed or flown penetrator missions [DS-2, Lunar-A, Mars-96 - see, e.g. *Ball et al. 2006*] suggests that typical characteristics of such vehicles are battery mass of 1-3 kg, installed energies of hundreds to thousands of W-hr and downlink capabilities of a few kbit/s with total data return of the order of 10 Mbit. However, for Europa, the installed energy may well be driven more by thermal considerations (and thus the choice of penetrator vs semi-hard lander) than downlink data requirements.

A.4. Investigation Descriptions

The following sections give supporting information for the main investigation areas. For this purpose, the working group was divided into smaller subgroups, each with a focus on a particular investigation. The topics and group leads are listed in Table A-3.

Table A-3. Instrument Section Leads

Topic	Lead(s)
astrobiology	Hand, Prieto-Ballesteros
geophysics	Grasset, Hussmann
surface properties	Lorenz
geology	Prockter

A.4.1 Astrobiology

The objective of the surface element astrobiology investigation is to characterize surface organic and inorganic chemistry, with emphasis on complex organic chemistry, indicators of habitability, and potential biosignatures. Critical advantages of *in situ* analysis include providing ground truth of orbital measurements and providing enhanced concentration sensitivity—and thereby greater detection limits—for surface chemistry. These advantages are of great utility to astrobiology because they: 1) resolve compositional ambiguities that arise when limited to remote sensing observations, and 2) enable detection of trace non-ice materials that improve our ability to assess the habitability of Europa.

To develop a notional instrument payload to service the above investigation we use the lessons learned from the Viking Landers as a guide [*SSB 1999*, *Chyba and Phillips 2001*]. Specific recommendations from that analysis include:

1) If the payload permits, conduct experiments that assume contrasting definitions for life [see e.g. *Joyce 1994*, *Chyba and Hand 2005*],
2) Given limited payload, the biochemical definition deserves priority,
3) Establishing the geological and chemical context of the environment is critical,
4) Life-detection experiments should provide valuable information regardless of the biology results.

On the surface of Europa, the search for potential biosignatures would largely take the form of a biochemical search, i.e. a search for chemical and molecular species associated with the structures of life and biological processes. Given the harsh surface conditions, we would not anticipate finding viable life forms on the surface, and thus metabolic or even genetic definitions would prove challenging.

The utility of molecular and compound complexity, as a tool for astrobiology, is rooted in the simple fact that in life "an enormous diversity of large molecules are built from a relatively small subset of universal precursors" [*Summons et al. 2008*], namely, the nucleobases of DNA and RNA (uracil, thymine, adenine, guanine, and cytosine), 20 amino acids, and two lipid building blocks (acetyl and isopentenyl diphosphate precursors). Alone, such compounds are ambiguous, but in polymer form the structure and complexity help to build the case for a biogenic origin.

Coupled with the structural subunits is the selectivity and order in which they are polymerized. This largely refers to chiral preference for subunits (e.g. biological proteins are constructed only from L-amino-acids). The construction of complex molecules from subunits brings with it the capacity for a large number of permutations, leading to various branches and functional group arrangements of the same molecule. This amounts to a compounded chirality, because with each addition new chiral centers are created, making it possible for a larger pool of possible variations on the same molecule. This is referred to as isomerism and a given spatial arrangement for a specific compound is referred to as a diastereomer [*Summons et al. 2008*]. Biological processes not only preferentially select subunits of a specific chirality, but they also synthesize compounds with a diastereomeric preference.

Lipid biomarkers have arguably been the most robust window into the early history of life on Earth and may serve astrobiology well as we look for carbon-based life forms on other worlds. These molecules are derivatives of lipids found in the cellular membranes of Bacteria, Eukaryotes, and Archaea. The acetogenic lipids occur in units of methylene and consequently yield gas chromatograph mass spectrometer (GCMS) results patterned in a series of even numbered carbon compounds. The lipids constructed from isopentenyl diphosphate result in lipids of linked isoprene units. These are commonly referred to as terpenoids and this family of lipids consists of complex arrangements of linear and ring structures built from the isoprene subunit. It is largely the survival of terpenoid compounds (specifically hopanes and steranes) that have permitted exploration of the history of life in the terrestrial Archaean rock record. The harsh radiation environment of Europa would cause concentration of any lipid biomarkers to decrease through time, unless buried under the surface [*Hand et al. 2009*].

The technological solutions to achieve the above investigation are manifold [*Peters et al., 2005*], but one solution, mass spectrometry, is the clear favorite for both assessing complex chemistry associated with life as we know it, and for providing highly complementary information to the orbital science payload.

Geographic Considerations

Investigating indicators of habitability and searching for potential biosignatures would be facilitated by selecting a region with a compelling compositional and geological context, much of which could be supplied from orbit. The Galileo mission provided a useful basis for this context and *Figueredo et al.* [*2003*] established several geological

criteria to help guide the search for biosignatures, including a prioritization of regions that show: 1) evidence for high material mobility, 2) concentration of non-ice components, 3) relative youth, 4) textural roughness (providing a possible shield from the degrading effects of radiation), and 5) evidence for stable or gradually changing environments.

The trailing hemisphere is a region heavily processed by radiolytic chemistry [e.g. *Paranicas et al. 2001*]; thus, the dark material in that region is unlikely to reveal potential biosignatures. The leading hemisphere likely contains an enhanced exogenous organic inventory from micrometeorites, which could serve to mask any existing endogenous organic chemistry. For these reasons, astrobiology investigations should target non-ice material on the sub- or anti-jovian hemisphere. Furthermore, targeting of young endogenous material is highly desirable in the search for potential biosignatures. A chaos region on the sub- or anti-jovian hemisphere, some of which are tens of kilometers in extent, serves as a useful notional target for this investigation. There are no latitudinal constraints other than to optimize for young, endogenous material.

Technological Considerations

Though this report is focused on science, some attention to specific instrument constraints and potential technology limitations is warranted. Foremost among the unique challenges posed by a "stop and drop" surface element is the high-g impact load. All instrumentation would likely need to survive several thousand to tens of thousands of g's. Thus, moving parts and fragile components are highly undesirable. Given the complexity of some instrumentation utilized for astrobiology, there is a need to consider potential science return as a function of instrument complexity.

While a mass spectrometer was noted above as the premier instrument for achieving the desired astrobiology investigation, here we provide a short list of instruments in decreasing science priority that would surpass the threshold for astrobiology science while simultaneously decreasing instrument complexity. The list below should not be interpreted as comprehensive or distilled from a list of thoroughly vetted instruments; it is merely representative.

An additional consideration, which must be addressed in further detail if a surface element is to be developed, is that of active or passive sampling. Active sampling here refers to using moving parts (e.g. a drill) to collect a surface sample for molecular analysis. Passive sampling refers to the collection of photons passed through a window on the surface element or entry of molecules into the surface element via thermal or sputtering enhanced diffusion. Though mass spectrometry is typically considered to require active sampling, the irradiated surface environment of Europa may be conducive to passive sampling of large and complex compounds. Further work must be done to explore this possibility.

Mass Spectrometer

As a tool for detecting life as we know it, mass spectrometry serves two key roles: 1) detecting organics, and 2) providing information on the complexity of organics. The first yields a binary answer (or an upper limit) that informs further investigation. The second yields information that may serve to distinguish abiotic organic chemistry from biologically generated organics. *McKay* [*2004*] has argued that the spectrometric distinction could be characterized as the 'Lego Principle': biology preferentially uses specific organic subunits to build larger compounds while abiotic organic chemistry proceeds randomly. According to the "Lego Principle," mass spectra associated with life are punctuated by peaks indicative of the subunit preferences while those associated with abiotic chemistry have a broad Gaussian

spread of peaks with no obvious structure. There are many caveats to this rule, but it provides a useful guide for analysis of complex chemistry.

A gas chromatography column is not necessary to supply the size distribution needed. This simplifies the instrumentation and removes many of the more complex components of the system. Also of importance is the fact that high mass resolution is unnecessary, as the key parameter of interest is the size of the compounds, not their isotopic composition. A mass range of 0-500 amu would reveal both large molecules and help refine our understanding of Europa's sulfur and ion chemistry.

Finally, mass spectrometry serves as a very useful and complementary technique to the UV/Vis/IR spectroscopic techniques employed from orbit (which could provide functional group and some backbone information, but little indication of size). Thus, while astrobiology may serve as the motivating science for a lander package, a mass spectrometer would provide useful information independent of any potential biosignature results.

Raman Spectrometer

Raman spectroscopy has long been acknowledged as an important tool for *in situ* astrobiology [*Wynn-Williams et al. 1999, Ellery and Wynn-Williams 2003*] as some laser wavelengths probe a "fingerprint" region that is of great utility for both geochemistry and biochemistry. A critical advantage of utilizing Raman on Europa is that water ice is a weak scatterer, permitting high sensitivity to sulfur and biological compounds. Raman could reveal highly complementary information to orbital compositional measurements and, though the size distribution capabilities are not as good as a mass spectrometer, a variety of vibration modes observables in Raman permit investigation of molecular structure, abundance, and complexity.

Raman could be employed with a window that allows the laser light to exit the surface element and permits the scattered photons to return into the surface element where they are collected with a detector. Raman instruments are currently in development for future Mars missions, but there is no flight heritage for such an instrument at this time.

Tunable Diode Laser

Absorption spectroscopy using tunable diode lasers provides a simplified system for investigating specific, predetermined absorption features of interest. This is one of the few instruments of any kind that has been designed for a high-g impact and flown on a planetary science mission. As part of its science payload, the Deep Space 2 mission had a tunable diode laser absorption spectrometer for detecting water in the soil of Mars. The instrument was designed to survive over 30,000 g's. The entire science payload for that mission was contained in a 670 g forebody that was 10.6 cm long and 3.9 cm in diameter. A comparable, though much more complex, version is planned to fly as the Tunable Laser Spectrometer on the Mars Science Laboratory.

Typical diode band-passes for terrestrial applications of trace gases fall in the 0.9-2.5 μm range and permit parts per million detection of species such as methane, sulfide, HCN, and ammonia. A system for Europa astrobiology could be tuned for carbon, nitrogen, and sulfur features in either the 2-2.4 μm or 6-6.5 μm region. The issue of sample ingestion would need to be considered in detail, but it is conceivable that this technique could be employed through a window**.**

Additional Payload Augmentation

If chemical analyses are addressed by one or more of the above instruments, then the addition of imagery, either of the surface

environment near the spacecraft or microscopy of surface samples, provides an important morphological context for assessing biosignatures. Landscape imagery could reveal the endogenous nature of the immediate surroundings and microscopy could reveal structures or microfossils related to life if it exists in the near subsurface. Both types of imagery are desirable but are highly dependent on the spacecraft configuration (e.g. a hard lander or a subsurface penetrator).

A.4.2 Geophysics

The highest priority geophysical investigation for JEO is characterization of the tidal response of Europa, in terms of gravitational, topographic, and magnetic signatures. All three aspects are indicative of internal structure and processes, and should be very well captured by instruments on the orbiter. The primary geophysical objective of a surface element is the determination of the level of seismic activity driven by tidal flexing of the ice shell.

The long-term response of Europa to imposed tidal and rotational potentials is a static departure from spherical symmetry of over 1 km, with elongation toward Jupiter, and shortening along the rotation axis. This effect is principally diagnostic of internal density structure, and would be well sensed, both topographically and gravitationally, by JEO.

Spatial Pattern of Tidal Deformation

In addition, over the course of each 3.55 day tidal cycle, the surface moves up and down, with a well known spatial pattern (Figure A-3) and amplitude that depends upon both orbital forcing and internal structure. As the orbital forcing is well known, the tidal amplitude is diagnostic of internal structure. In this case, it depends both upon density and strength, or effective elastic rigidity, and thus is a potential indicator of a global ocean. The peak amplitude is predicted to be roughly 30 m, if a global ocean exists, but closer to 1 m if the interior is solid throughout [*Moore and Schubert 2000*].

However, the correlation to seismicity is uncertain. The majority of this tidal cycle flexing occurs either elastically within the ice shell, or fluidly within the underlying ocean. Only a small fraction of the displacement, on each tidal cycle, is associated with fracturing of the ice [*Sandwell et al. 2004, Lee et al. 2005, Nimmo and Schenk 2006, Rudolph and Manga 2009*]. Because the orbital eccentricity and obliquety of the spin pole, which control the forcing of the tides, vary on a wide range of time scales [*Bills 2005*], it is conceivable that Europa is presently in a non-seismic state, despite the abundant evidence of past surface fracturing [*Greeley et al. 2000*]. The primary objective of the seismic experiment is to measure the present rate of seismogenic fracturing. A secondary objective is to determine how that rate of fracturing varies over a tidal cycle. A tertiary objective would be to characterize internal structure within, and possibly even below, the ice shell [*Kovach and Chyba 2001, Lee et al. 2003, Cammarano et al. 2006, Panning et al. 2006, Leighton et al. 2008*].

Seismometer

A relatively simple seismometer, comparable to those envisioned for deployment on Mars [*Linkin et al. 1998, Lognonne 2005*] and suitably protected against damage upon delivery [*Hopf et al. 2010*], could answer the question of seismic activity in a short period of time. An affirmative answer could, in principle, be obtained within a few hours. Initial characterization of tidal cycle modulation of seismic activity would require at least half of the 3.55 day (85 hour) orbital period.

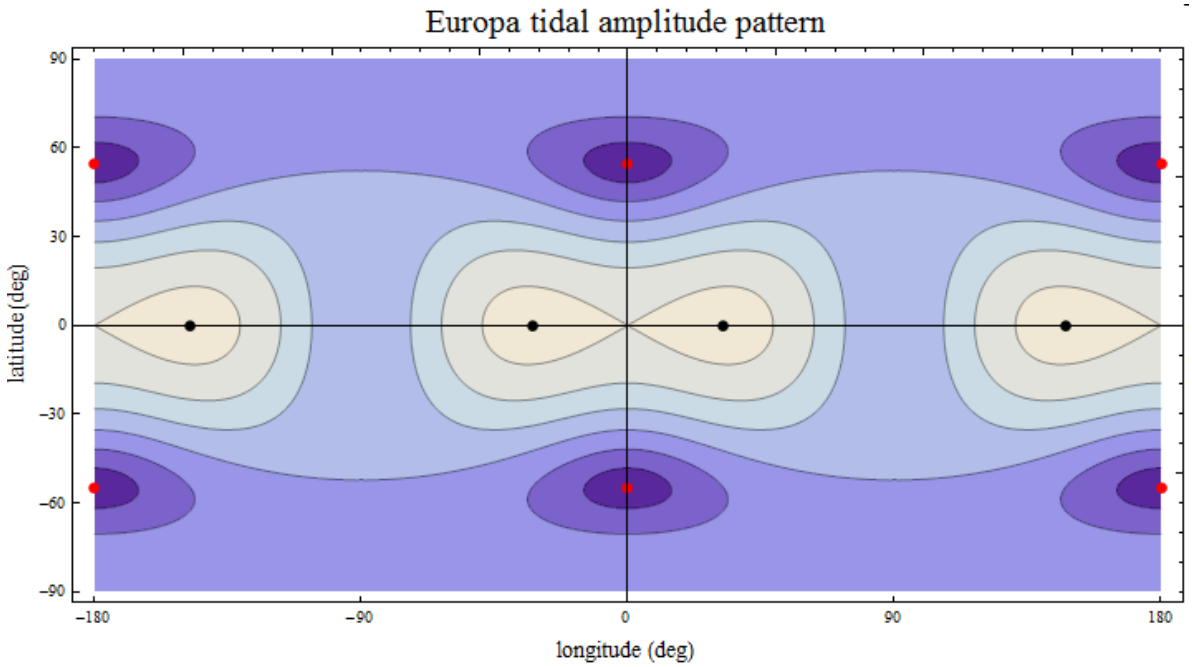

Figure A-3. Pattern of radial tidal displacement on Europa. Black dots are locations of maxima, and red dots are local minima. In the thin shell case, the contour interval is roughly 5 m.

However, it is possible that the tempo of seismic activity on Europa is somewhat similar to that seen on the Moon [*Weber et al. 2009*]. In the lunar case, there is strong tidal modulation of the seismic activity level, but the locations of maximum activity have no simple correlation with maximum tidal displacement, and there is considerable variation, from month to month, in the level of seismic activity. The time required for internal structure determination depends strongly upon the level, and nature, of seismic activity.

Potential desirable locations for a Europa surface element, from the perspective of the seismic investigation alone, would be at one of the 4 equatorial maxima of the tidal amplitude pattern (Figure A-3). They are symmetrically located ±32.3 deg either side of the sub- and anti-jovian points. However, as discussed earlier in this report, communications with the orbiter strongly favors a high latitude location. Potential places to avoid, from a seismic perspective, are the 4 high latitude minima, at ±54.7 deg latitude, along the sub- and anti-jovian meridians (red dots in Figure A-3). At sufficiently high latitude, the tidal amplitude varies little with longitude. Right at the poles, the amplitude is 46.8% of the equatorial maxima.

Other Instruments

A wide range of other instruments could be envisioned for geophysical investigation of Europa. The Mars NetLander program [*Dehant et al. 2004*] proposed several instruments which might be relevant to Europa. Notably, a magnetometer [*Menvielle et al. 2000*] would complement those on the orbiter, and an electromagnetic induction experiment [*Pincon et al. 2000*] would provide information about resistivity, and hence composition and structure, within the interior. Extremely relevant to determination of the deeper internal structure would be monitoring of spin pole direction [*Bills 2005*] and forced librations in longitude [*Comstock and Bills 2003*] via a geodetic package similar to NEIGE [*Barriot et al. 2001*]. Unfortunately, most of these investigations would require more time on the surface than appears likely for a Europa surface element.

A.4.3 Surface Properties

Compared with the geophysical and astrobiological objectives, the goal of measuring surface properties is of intrinsically lower priority, but certain physical measurements are required to properly interpret the geophysical and astrobiological investigations. Thus, a limited set of physical properties measurements are included in the desired payload.

First, it is vital to know the depth at which any astrobiological composition measurement is made. This is readily accomplished via double-integration of an impact accelerometer signal. The impact accelerometer investigation on DS-2 used an off-the-shelf accelerometer (volume < 1 cm^3, mass ~2g) sampling at 25 kHz [*Smrekar et al. 2001, Lorenz et al. 2000*]. The impact event is contained in only ~30 kbit of data per axis. A 3-axis measurement is preferred, but a single axis could be tolerated with some reduced confidence in the depth result. In addition to yielding penetration depth, the accelerometer record provides a measure of the penetration resistance (i.e. crush strength) of the surface material, which relates (though non-uniquely) to the porosity and degree of sintering of a regolith. Surface inhomogeneities (layers, voids, rocks) may also be inferred.

In addition to the penetration depth, the attitude of the vehicle should be known. This is done via fluid-vial tilt sensors (as flown, e.g. on Huygens) or more likely with a small (separate) 2- or 3-axis accelerometer (again < 1 cm^3) The relevant devices are used in some consumer electronic devices to determine orientation relative to the gravity field.

Depending on the thermal design of a penetrator, the walls of the vehicle would probably be well coupled to the regolith. The decay of any difference in temperature between the walls and the regolith would be a function largely of the thermal diffusivity of the regolith. Thus, it would be scientifically useful to measure the wall temperature, both to constrain the diffusivity, and to estimate the local regolith temperature. It is likely that several temperature measurements would need to be made, in any case, to document the thermal behavior of the vehicle for engineering reasons: attention should be paid to the number, location, mounting, span and resolution of the sensors to ensure scientific utility.

As a cautionary note, several engineering sensors on the Huygens probe would have given important insights into the Titan environment, but did not read low enough temperatures [*Lorenz 2006*]. Sensor range should span ~40 K to room temperature conditions (to facilitate integrated testing) with a resolution of 0.1 K or better. Measurements should be recorded rapidly (~seconds, depending on the thermal mass of the mounting) to document the decay of initial conditions (including possible frictional heating), but could relax to a slower rate (minutes/hours) to document any diurnal changes. For a suite of 8 sensors recording with 12 bit accuracy, a total data volume for initial and diurnal monitoring of ~100 kbit would be adequate.

It is unlikely to be a practical goal to measure geothermal heat flow, in that over vehicle length scales (~0.3m) the temperature differences from expected heat flows (~30 mW/m^2) would be only ~0.01 K. This small temperature different would likely be overwhelmed by uncertainties, such as the perturbations induced by the vehicle itself. However, measuring the local temperature (desirably at the top and bottom of the vehicle) still would be useful to constrain effects such as the proposed “solid state greenhouse” [*Matson and Brown 1989*]. For such measurements, some sensors should desirably be isolated from the vehicle to the extent

possible (e.g. by mounting in insulating recesses). Adequate documentation of the vehicle thermal behavior (e.g. constructed heat capacities of elements, dissipation histories within them, and the conductances between them) should be available for the scientific interpretation of temperature data.

Possible illumination of the subsurface is important to understand the deposition of energy into the regolith. The penetration of visible light into the regolith is of astrobiological interest. Also light penetration may be correlated with the penetration of ionizing radiation, as well as the thermal opacity. Light intensity measurement should desirably sample a range of azimuths, elevations and wavelengths (including UV) to properly understand the scattering and absorption in the regolith (of order 10 filtered photodiodes would be reasonably comprehensive). Around ~100 measurements per Europa day are necessary, amounting to ~10 kbit.

Characterizing the penetration of energetic particles into the regolith is vital to understanding the possible direct radiation processing of organic and inorganic material, as well as the generation of oxidants by radiolysis of water ice. Such materials may in turn affect non-ice material, and could serve as an energy source for Europan biota.

The proper design of a radiation measurement suite would require some modeling of likely fluxes and attenuation by regolith. Although total dose sensors (e.g. RadFETs) could make a useful measurement starting from zero dose, it seems likely that the vehicle would accumulate a substantial dose before delivery to Europa's surface; thus, the incremental dose over one Europan day would be difficult to discriminate. Instead, direct counting of particles is likely to be the best approach, for example using diode detectors.

It would be desirable to record the radiation fluxes over a Europan day at intervals that are short compared with a Jovian day. A dataset of some tens of kilobits (e.g. summarizing accumulated count rates at 10-minute intervals) should be adequate.

In summary, the physical property measurements could be accomplished with sensors that are individually very small, but which could be distributed about the body of a surface element and intimately connected with its structure. The mass cost of making these measurements would likely be dominated by the harness (and indirectly, the battery energy cost of the heat leaks introduced by the harness), rather than by the sensors themselves. Thus, they are more properly considered as part of the vehicle than as a separately provided instrument. The ideal dataset would comprise a few hundred kbit as discussed above, although intelligent on-board processing could yield key summary results (e.g. peak deceleration) transmitted in a lower data volume.

A.4.4 Geology

Here we discuss geological investigations focused on geomorphology, while investigations of surface composition and other related properties which are relevant to geology are covered in other sections of this report. Geological investigations are generally addressed with some type of imaging system and fall into the following categories:

- Context imaging for a landed element
- Characterization of surface processes at large and small scales
- Characterization of future landing sites

Context Imaging

Knowledge of context is vitally important for a landed element. Descent images could meet this objective and could be useful for characterizing the landing site of a surface

element. For example for the Huygens probe, high-resolution imaging of the surface by Cassini was not possible because of the atmosphere, and descent images provided invaluable context. However, it is expected that JEO would acquire images from orbit at resolutions of up to 1 m/pixel, which should amply satisfy the requirement for regional and local context. Thus, there is no obvious added benefit of descent imaging, and its accommodation would place unnecessary burdens on the delivery vehicle.

Characterization of Surface Processes

The highest priority geology science investigations for Europa involve characterizing regional-scale processes such as tectonism and cryovolcanism. These investigations are best achieved with imaging at regional to local scales (hundreds of meters to tens of meters), which would be accomplished by JEO from orbit.

Geomorphology objectives that are best achieved by landed imaging involve the investigation of erosion and deposition processes at local and small scales. Evidence of weathering processes involving the atmosphere or liquid has been observed in surface images of Venus, Titan, and Mars, by the Venera landers, the Huygens probe, and various Mars landers, respectively. These images have provided a wealth of information as to how surface materials are eroded, transported, and deposited. Images of the lunar surface have provided critical information about impact and regolith processes.

Because Europa has an extremely tenuous atmosphere, very few impacts, and surface deformation likely on a large scale of hundreds of meters to kilometers, it is expected that only small-scale regolith processes (centimeters to meters) could be usefully studied from the surface, analogous to those processes observed on our Moon and the martian moons, and on asteroids Eros and Itokawa. Furthermore, since Europa's surface is relatively young, it may have developed very little regolith, and it may also be difficult to separate the effects of micrometeoroid bombardment from sublimation or sputtering processes on the surface simply by imaging it.

Overall, regolith processes are of lower priority than other Europa geology objectives, and a soft lander would be needed for the camera to view the surrounding terrain. It is not clear that it would be worth the necessary resources to use imaging to study regolith processes alone, although much would be gained by associated measurements of ice rheology and composition.

Characterization of Future Landing Sites

One objective for EJSM is to characterize surface roughness in order to select future landing sites. This objective could be accomplished by descent imaging (e.g., the Huygens probe Venera landers [Figure A-4]) and/or imaging with a panoramic camera mounted on a surface element (e.g., the Mars rovers). However, given the high-resolution images expected from JEO, this objective would also likely be met from orbit.

Recommendation

Although the EPO value of surface images cannot be underestimated, it is arguable whether any truly groundbreaking science would result from them. In the case of the Mars Rovers, Pancam images have proven invaluable for planning future traverses and determining potential hazards, but no such value would be added for a static lander on Europa's surface. The expectation that the Europan surface is principally shaped by regolith processes at the meter scale and below suggests that surface imaging may not yield dramatic scientific insights.

In general, because high-resolution imaging and spectroscopic measurements are expected to be acquired from orbit by JEO, geological

investigations would be best served by other experiments on a lander, such as seismic or compositional investigations. Thus, a dedicated geology instrument (i.e., a camera) would not have a high priority on a landed payload.

A.5. Summary

Despite the considerable technical challenges associated with delivery and operation of a surface element on Europa, it appears to provide a unique opportunity to achieve significant science, which would complement that anticipated from the JEO orbital instruments.

The highest priority science objectives for a surface element would be to:

- Characterize the complex chemistry at the surface, in a region expected to be in communication with the deeper interior, and
- Characterize the seismic activity level, and its modulation by the tidal cycle.

Performance of the delivery system and operational capabilities on the surface are currently not well understood. This makes a detailed assessment of the plausibility of some potential science instruments very difficult. We thus strongly urge continuation of present studies of those issues.

We also recommend that, if a surface element is to be further pursued as part of JEO, then a science definition team should be assembled to give this matter further study. Many of the science feasibility issues are strongly coupled to the implementation strategy selected, such as a penetrator versus a semi-hard lander. Until such issues are further clarified, a science payload cannot be fully defined.

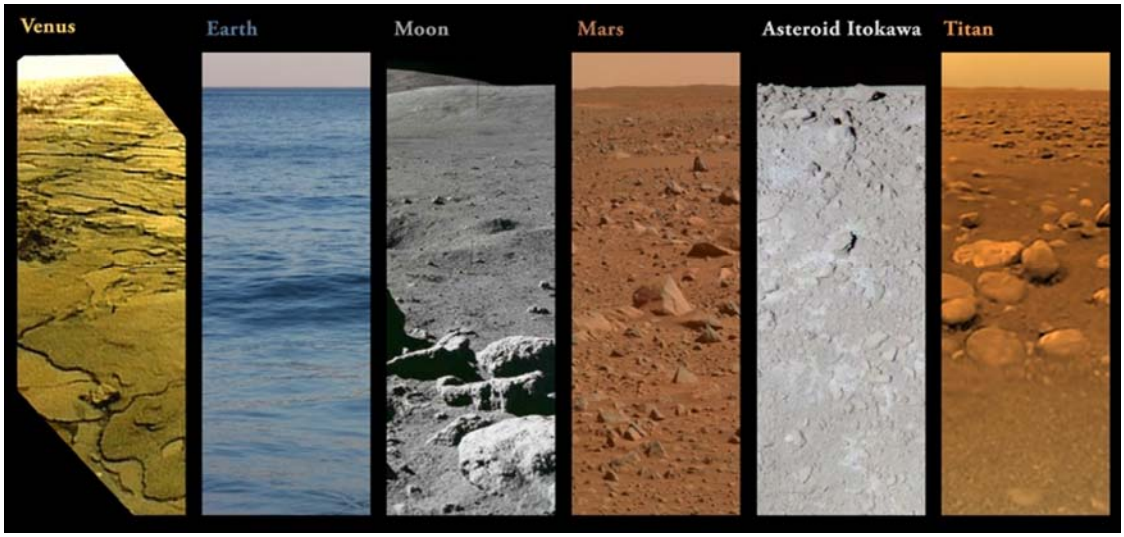

Figure A-4. Representative surface views. Courtesy Mike Malaska.

APPENDIX B. ACRONYMS

Acronym	Definition
AOCS	Attitude and Orbit Control System
APD	Avalanche Photodiode Detector
APL	Applied Physics Laboratory
APS	Active Pixel Sensor
ARTEMIS	Africa Real Time Environmental Monitoring Information System
ASIC	Application Specific Integrated Circuits
ATLO	Assembly, Test, and Launch Operations
C&DH	Command & Data Handling
C/A	Closest Approach
CCD	Charge Coupled Device
CCSDS	Consultative Committee for Space Data Systems
COSPAR	Committee on Space Research
CRAM	Chalcogenide Random Access Memory
CRISM	Compact Reconnaissance Imaging Spectrometer for Mars
DEM	Digital Elevation Model
DHMR	Dry Heat Microbial Reduction
DLR	German Center for Aerospace
DOR	Differenced One-way Ranging
DS1	Deep Space 1
DS-2	Deep Space 2
DSN	Deep Space Network
EOI	Europa Orbit Insertion
EOS-MLS	Earth Observing System Microwave Limb Sounder
EPO	Education and Public Outreach
EPSC	European Planetary Science Congress
ESA	European Space Agency
ESTEC	European Space Research and Technology Center
EUV	Extreme Ultraviolet
FIPS	Fast Imaging Plasma Spectrometer
FUV	Far Ultraviolet
FWHM	Full Width at Half Maximum
GAP	Gravity Advanced Package
GCMS	Gas Chromatograph Mass Spectrometer
GNC	Guidance, Navigation, and Control
GOI	Ganymede Orbit Insertion
GRACE	Gravity Recovery and Climate Experiment
GRAIL	Gravity Recovery and Interior Laboratory
HEPA	High Efficiency Particulate Air
HGA	High Gain Antenna
HSP	High Speed Photometer
HST	Hubble Space Telescope
IFOV	Instantaneous Field Of View

Acronym	Definition
IMU	Inertial Measurement Unit
INMS	Ion and Neutral Mass Spectrometer
IPR	Ice Penetrating Radar
IR	Infrared
JEDI	Jupiter Energetic-particle Detector Instrument
JEO	Jupiter Europa Orbiter
JGO	Jupiter Ganymede Orbiter
JIMO	Jupiter Icy Moons Orbiter
JJSDT	Joint Jupiter Science Definition Team
JOREM	Jovian Radiation Environment
JPL	Jet Propulsion Laboratory
JSO	Jupiter Solar Orbit
LA	Laser Altimeter
LILT	Low Intensity Low Temperature
LOLA	Lunar Orbiter Laser Altimeter
LORRI	Long Range Reconnaissance Imager
LRO	Lunar Reconnaissance Orbiter
M3	Moon Mineralogy Mapper
MAC	Medium Angle Camera
MAG	Magnetometer
MARCI	Mars Color Imager
MARSIS	Mars Advanced Radar for Subsurface and Ionosphere Sounding
MCP	Microchannel Plate
MCS	Mars Climate Sounder
MDIS	Mercury Dual Imaging System
MGA	Medium Gain Antenna
MIRO	Microwave Instrument for Rosetta Orbiter
MLA	Mercury Laser Altimeter
MMH	Monomethylhydrazine
MMM	Moon Mineral Mapper
MOLA	Mar Orbiter Laser Altimeter
MON	Mixed Oxides of Nitrogen
MR2	Satellite Mass and Mean Radius
MRO	Mar Reconnaissance Orbiter
MVIC	Multispectral Visible Imaging Camera
NAC	Narrow Angle Camera
NASA	National Aeronautics and Space Administration
NEAR	Near Earth Asteroid Rendezvous
NEIGE	NetLander Ionosphere and Geodesy Experiment
NIMS	Near Infrared Mapping Spectrometer
NIR	Near Infrared
NLR	NEAR Laser Rangefinder
NRC	National Research Council
NUV	Near Ultraviolet
OMEGA	Observatoire pour la Minéralogie, l'Eau, les Glaces et l'Activité

Acronym	Definition
OTM	Orbit Trim Maneuver
PCI	Peripheral Component Interconnect
PEPE	Plasma Experiment for Planetary Exploration
PEPSSI	Pluto Energetic Particle Spectrometer Science Investigation
PP-DU	Particle Package Data processing and power control Unit
PPI	Particle and Plasma Instrument
QQO	Quasi-quadrennial Oscillation
RNA	Ribonucleic acid
ROSINA	Rosetta Orbiter Spectrometer for Ion and Neutral Analysis
RPWI	Radio and Plasma Wave Instrument
RS	Radio Science
RTOF	Reflectron type Time-of-Flight
SDRAM	Synchronous Dynamic Random Access Memory
SDST	Small Deep Space Transponders
SDT	Science Definition Team
SEC	Science Electronics Chassis
SETI	Search for Extra-Terrestrial Intelligence
SHARAD	Shallow Subsurface Radar
SMALL	
SNR	Signal to Noise Ratio
SQRT	Square Root
SSB	Space Studies Board
SSDs	Solid State Detectors
SSR	Solid State Recorder
TDI	Time-Delay-and-Integration
TI	Thermal Instrument
TID	Total Ionizing Dose
TOF	Time-of-Flight
TRL	Technology Readiness Level
TWTA	Travelling Wave Tube Amplifier
USO	Ultra-Stable Oscillator
UV	Ultraviolet
UVIS	Ultraviolet Imaging Spectrometer
UVS	Ultraviolet Spectrometer
VIMS	Visual and Infrared Mapping Spectrometer
VIR	Visible-Infrared
VIRIS	Visible and Infrared Imagine Spectrometer
VIRTIS	Visible and Infrared Thermal Imaging Spectrometer
VIS/NIR	Visible/Near-Infrared
VIS-IR	Visible and Infrared
WAC	Wide Angle Camera
YAG	Yttrium Aluminum Garnet